Title 40 CFR Part 191
Compliance Certification
Application
for the
Waste Isolation Pilot Plant

Appendix DVR

United States Department of Energy
Waste Isolation Pilot Plant

Carlsbad Area Office
Carlsbad, New Mexico

Design Validation Report

U.S. DEPARTMENT OF ENERGY

DOE-WIPP-86-010

WASTE ISOLATION PILOT PLANT

DESIGN VALIDATION
FINAL REPORT

JOB 12484

OCTOBER 1986

BECHTEL NATIONAL, INC.
SAN FRANCISCO, CALIFORNIA

NOTICE

FOREWORD

The reference design for the underground facilities at the Waste Isolation Pilot Plant was developed using the best criteria available at initiation of the detailed design effort. These design criteria are contained in the U.S. Department of Energy document titled Design Criteria, Waste Isolation Pilot Plant (WIPP), Revised Mission Concept-IIA (RMC-IIA), Rev. 4, dated February 1984. The validation process described in the Design Validation Final Report has resulted in validation of the reference design of the underground openings based on these criteria. Future changes may necessitate modification of the Design Criteria document and/or the reference design. Validation of the reference design as presented in this report permits the consideration of future design or design criteria modifications necessitated by these changes or by experience gained at the WIPP. Any future modifications to the design criteria and/or the reference design will be governed by a DOE Standard Operation Procedure (SOP) covering underground design changes. This procedure will explain the process to be followed in describing, evaluating and approving the change.

The Department of Energy wishes to acknowledge the following for their contributions to the design validation program:

Bechtel National, Inc.
International Technology Corporation
Sandia National Laboratories
Peer Review Panel
- Neville G. W. Cook
- Francois E. Heuze
- Hamish D. S. Miller
- Robert L. Thoms

CONTENTS

CONTENTS (continued)

CONTENTS (continued)

CONTENTS (continued)

CONTENTS (continued)

APPENDICES

TABLES

TABLES (continued)

TABLES (continued)

FIGURES

FIGURES (continued)

FIGURES (continued)

FIGURES (continued)

FIGURES (continued) .

FIGURES (continued)

FIGURES (continued)

FIGURES (continued)

WASTE ISOLATION PILOT PLANT
DESIGN VALIDATION
EXECUTIVE SUMMARY

INTRODUCTION

The Waste Isolation Pilot Plant (WIPP) is being developed by the U.S. Department of Energy (DOE) as a research and development facility to demonstrate the safe disposal of radioactive waste from U.S. defense programs. The facility is located in southeastern New Mexico, about 25 miles east of the city of Carlsbad. Underground development is at a depth of about 2,150 feet in thick deposits of bedded salt. The facility operation will include in situ experiments addressing technical issues for defense waste programs and storage of defense related contact-handled (CH) and remote-handled (RH) transuranic (TRU) waste.

In 1979, the DOE established a Site and Preliminary Design Validation (SPDV) Program to provide additional confidence in the siting and design of the WIPP facility. On July 1, 1981, the DOE entered into an agreement with the State of New Mexico whereby the DOE would perform certain work to validate the reference design of the WIPP underground openings. The results of the site validation portion of the program are presented in the report titled Results of Site Validation Experiments, Volumes I and II, TME document 3177, dated March 1983. The results of the preliminary design validation portion of the program are presented in the report titled Waste Isolation Pilot Plant Preliminary Design Validation Report, dated March 30, 1983.

Design validation of the WIPP is defined as the process by which the reference design of the underground openings is confirmed by determining the compatibility of the design criteria, design bases and reference design configurations using site specific information. The design validation process consists of an assessment of the condition and behavior of shafts, drifts and a full-sized, four-room test panel

excavated during the SPDV Program and full WIPP construction. Based on this assessment of these excavations, and on predictions of their future behavior, any modifications to the design criteria, design bases or design configurations required to achieve a validated reference design will be developed. In addition, the validated reference design may be modified in the future as still more data and experience are gained during a 5-year demonstration period (period during which all waste must be retrievable) and permanent storage operations.

The WIPP Preliminary Design Validation Report was an interim report prepared as part of the overall validation of the WIPP underground opening reference design. The WIPP Design Validation Final Report contains additional information gathered after completion of the SPDV Program. This information has been analyzed and evaluated to complete the design validation process for the WIPP.

Four types of information were gathered for the WIPP Design Validation Final Report:

(1) observations of the behavior of the underground openings;

(2) descriptions of the geologic conditions encountered during underground construction;

(3) descriptions of core samples from instrumentation and other holes in the roof and floor of the underground openings; and

(4) data from installed geomechanical instrumentation.

The design validation process provides for the collection, analysis and evaluation of in situ data. This process is designed to permit determination of the need to modify elements of the underground opening reference design so that construction and operation of the full facility can proceed in a timely, safe, environmentally acceptable and cost effective manner. Observation and instrumentation data have been

collected and evaluated for each of the underground design elements. Tables I through VI at the end of this summary present the evaluation results for the design criteria, design bases and design configurations of the shafts and horizontal openings.

BACKGROUND OF UNDERGROUND DESIGN

Geologic characterization of the site began with a literature review and continued with the collection of field data. Special emphasis was placed on correlating data obtained from seismic reflection and resistivity surveys and borehole drilling. Design information regarding site stratigraphy from the ground surface to about 250 feet below the underground facility level was developed from geologic data obtained from drill holes ERDA-9, WIPP-12 and DOE-1, and from the SPDV exploratory and ventilation shafts.

The engineering designs for the WIPP surface and underground facilities began with the conceptual design, initiated in 1975 and completed in 1977. The conceptual design provided the basis for the development of the preliminary design of both the surface and underground facilities, which was completed in January 1980. The preliminary design incorporated the conventional room and pillar method for underground development.

Design of the WIPP provided for the access and storage openings to remain stable and provide minimum clearance for equipment during waste emplacement and the 5-year demonstration period, even though these openings will eventually close due to salt creep. Modeling techniques were used to estimate the geomechanical behavior and structural stability of the openings. The preliminary design included numerical modeling of the selected underground opening configurations. These models were used to predict opening closures and augmented other conventional mining industry methods of stability evaluation.

UNDERGROUND FACILITIES

Seven stratigraphic horizons were identified in 1979 as potential locations for the facility level. These horizons were chosen from examinations of available geotechnical data and on horizon selection criteria established by the WIPP project participants. Selection of the final underground development level was made by the DOE following the recommendation of WIPP project participants.

The WIPP facility is composed of three shafts connected to a single underground facility level. The C & SH shaft provides the principal means of access and also serves as the primary air intake opening. The waste shaft is designed to permit the transport of radioactive waste between the surface waste-handling facilities and the underground storage area. The exhaust shaft is the primary opening for exhaust air from the underground facility. All three shafts have three principle constituents: a lined section penetrating the rock overburden; an unlined section penetrating the salt; and a key at the rock/salt contact to act as a transition from the lined section to the unlined section.

The storage level contains all of the underground facilities for waste handling, waste storage, operations and maintenance. All of the underground horizontal openings are rectangular in cross section. The drift configurations range from 8 feet to 12 feet high and 12 feet to 25 feet wide.

Underground construction was accomplished in two phases. The initial (SPDV) phase was conducted from May 1981 through March 1983. The second phase, full construction, was accomplished from October 1983 through February 1985. Both phases included the excavation and outfitting of shafts, drifts and rooms.

SUPPORTING VALIDATION DOCUMENTS

The primary documents supporting design validation are the WIPP Preliminary Design Validation Report and quarterly geotechnical field data reports (GFDR).

The objective of preliminary design validation was to provide initial evaluation of the design criteria and design bases, and initial confirmation of the underground reference design. Geologic mapping, core drilling and logging, and geomechanical instrumentation data were assimilated to provide an early, short-term evaluation. The preliminary conclusions presented in the WIPP Preliminary Design Validation Report stated that the shafts and underground openings were performing as expected and were stable. In addition, gas had not been encountered in any significant quantity during excavation and no brine pockets had been encountered.

The GFDRs were initiated by the DOE to provide data from the SPDV Program and full construction in a timely manner. The GFDRs were intended to present in situ data on the geomechanical behavior of the strata surrounding the underground openings along with visual observations of opening behavior and analyses of selected underground design elements.

METHODOLOGY

Design validation is accomplished by determining the compatibility of the design criteria, design bases and reference design using site specific information. The design validation process consists of three major steps: data collection; analysis and evaluation; and prediction of future behavior.

The data collection program was designed to provide information on the geologic conditions encountered throughout the underground facility and on the structural behavior of the underground openings. The program

included geologic mapping, core drilling and logging, laboratory testing, visual inspections, and geomechanical instrumentation measurements. The data collected from these activities were analyzed and evaluated to determine the behavior of the various components of the underground facility and predict their future behavior by projecting the results of both finite element model and regression analyses.

The geomechanical instrumentation measurements provided in situ data on the behavior of the underground openings. These data were then used in empirical equations relating time and closure. Laboratory test results were used to calculate the salt creep and elastic parameters. Salt creep parameters were also determined by the regression analysis of in situ data. Long-term behavior of the underground openings was predicted by extrapolation of the results of the regression analysis.

GEOLOGIC CHARACTERIZATION

Geologic characterization of the WIPP underground openings began in June 1981. Data collection activities included geologic mapping, core drilling and logging, and fluid measurements. The SPDV exploratory shaft was mapped prior to selecting the storage horizon. The waste shaft was mapped, first as the SPDV ventilation shaft and again after it was enlarged to its final diameter. Geologic mapping was also conducted in the exhaust shaft.

Geologic mapping of the horizontal openings was conducted during design validation. This mapping was performed primarily to determine stratigraphic continuity. Mapping was conducted along one wall of the drifts to the northern extent of the facility and along the full length of the south exploratory drift. Geologic mapping was also conducted to the east and west facility boundaries in the experimental area and in the test rooms.

Geologic mapping confirmed the continuity of the stratigraphy within the horizontal openings to the facility boundaries. Core drilling and logging confirmed this stratigraphic continuity for a distance of 50 feet above and below the facility level. The geologic mapping and core logging did not detect any significant geologic structures. Data from the core holes were also used to establish the WIPP reference stratigraphy.

Fluid inflow measurements were obtained by various activities designed to characterize the two water-bearing dolomite members of the Rustler formation and the potential for the occurrence of gas and brine at the facility level. Measurements in the three shafts showed that water inflow from the Rustler formation is essentially negligible due to liner and seal performance.

Small amounts of pressurized gas have been encountered by some underground core holes. Brine has also been encountered in small quantities and is sometimes associated with gas occurrences. There has been no occurrence of gas or brine in quantities significant enough to jeopardize the stability or safety of the facility. Two programs, the brine testing program and the gas testing program, are being conducted to further characterize these occurrences. Neither program is associated with design validation.

Subsidence monuments have been installed on the surface over the shaft pillar area. The design criteria require that subsidence due to underground excavation not exceed 1 inch within a 500-foot radius of the waste shaft. It is not possible at this time to determine actual subsidence; this will occur over the next 25 years. Subsidence calculations used in the reference design indicate that the criteria limits will not be exceeded.

C & SH SHAFT

The C & SH shaft consists of a lined section, a shaft key, an unlined section and a shaft station. The shaft liner is made of structural steel that increases in thickness with depth to withstand increasing hydrostatic pressure. The reinforced concrete shaft key serves as a transition between the lined and unlined sections of the shaft. Chemical water seals behind the concrete key are designed to prevent ground water from flowing behind the key, into the unlined section of the shaft. The shaft station is excavated near the bottom of the unlined section.

Validation of the C & SH shaft reference design was accomplished by acquiring a variety of geotechnical data for analysis, evaluation and prediction of future behavior. The condition of the shaft liner and key are monitored by geomechanical instrumentation and visual inspections. Convergence points measure diametric closure; piezometers monitor ground-water pressures; strain gauges and pressure cells monitor the effect of salt creep on the concrete key. Telltale pipes in the shaft key provide information on the effectiveness of the chemical water seals. The unlined section of the shaft is monitored by extensometers and convergence points and is visually inspected for fracturing and rock slabbing. The shaft station has an extensive geomechanical instrumentation monitoring system and is inspected regularly.

The design basis hydrostatic pressure is suitable. Piezometer measurements indicate that the hydrostatic pressure is currently much less than the design pressure. Analysis of the shaft key indicates that lateral pressure on the key at the end of the operating period will be much less than the design basis lateral pressure requirement. Diametric closure of the key will be minimal. Computational analyses of stresses and strains indicate that the shaft will be stable and remain within the required safety limits during its operating life. Analysis of computed diametric closure near the bottom of the shaft

indicated that, while the closure will be within the design criteria and design basis limits, the lower buntons will be impacted.

The shaft design complies with the design criteria requirements for ground-water control. Regular inspections of shaft conditions show no signs of deterioration or instability.

The C & SH shaft station exhibits the highest degree of deterioration in the underground facility. The fracturing and separation observed has been stabilized, but will continue to develop. Closure during the 25-year operating life of the station will be on the order of 8 feet vertically and 5 feet horizontally. These conditions will require maintenance to ensure safety and to maintain the required minimum clearances for equipment and operations.

WASTE SHAFT

The waste shaft also consists of a lined section, a key, an unlined section and a shaft station. The shaft is lined with unreinforced concrete from the surface to the top of the Salado formation. The shaft liner terminates with a reinforced concrete key at the Rustler/Salado formation contact. The shaft is unlined, except for wire mesh, from the key to the bottom of the shaft.

Data collection activities in the waste shaft have consisted of geologic mapping, ground-water inflow measurements, geomechanical instrumentation measurements and periodic visual inspections. Except for convergence points, the geomechanical instruments are monitored remotely by the datalogger.

The waste shaft data was analyzed with respect to design parameters for each component of the shaft. As part of the engineering analysis, predictions of future behavior were made for each of the components.

Stability of the shaft liner has been confirmed. The water pressure exerted on it is significantly below the design hydrostatic pressure. If the pressure should reach the design hydrostatic pressure, the liner will still be stable. The shrinkage cracks in the liner do not present a structural problem.

The shaft key was designed to withstand a lateral pressure due to salt creep equivalent to 50 percent of the vertical overburden pressure. A numerical analysis was utilized to simulate the long-term effect of salt creep on the concrete key. It showed that the computed lateral pressure at the end of the operating period will be slightly higher than the design lateral pressure, but well below the total lateral pressure capacity of the key.

Observations of the waste shaft key have determined that only one minor seep occurs in the key and that no water seepage is occurring from the base of the key. This supports the conclusion that the water seals are functioning, that no water is seeping along the concrete/salt contact, and that salt dissolution is not occurring behind the key.

The design criteria require that no uncontrolled ground water reach the facility level through the shafts. Although minor amounts of fly water do reach the facility, this water has a negligible impact on operations and does not affect validation of this criterion.

The unlined section of the shaft was designed to be stable and maintain a diameter adequate for the operating life of the facility. The structural behavior of this section was analyzed using a finite element model and creep parameters determined from the C & SH shaft in situ data. The results indicate that the maximum stress occurred immediately after excavation and will decrease with time. Stress behavior will not cause a stability problem. Diametric closure due to salt creep will not exceed the design limits.

The design of the waste shaft station is based primarily on operational parameters. The closure and stability of the station was evaluated using in situ data from the C & SH shaft station. The estimated vertical closure rate will result in a total closure of over 7 feet during the 25 year operating life of the station. Actual closure may be less, but remedial work will still be required to maintain the proper clearances.

EXHAUST SHAFT

The exhaust shaft is constructed similarly to the waste shaft. It consists of a concrete lined section, a shaft key and an unlined section. The lined section is constructed of unreinforced concrete and the shaft key of reinforced concrete. The unlined section contains only rock bolts and wire mesh.

Data collection in the exhaust shaft has been on a much smaller scale than in the other two shafts. Geomechanical instrumentation was not required by the original shaft design because geologic and structural conditions were assumed to be similar to the other two nearby shafts. However, remotely monitored instrumentation has been installed to provide shaft-specific information for use in the sealing program. Geologic mapping and visual inspections have confirmed that the geologic and geohydrologic environment is similar to that of the other two shafts. Data from these two shafts have been used to predict the future performance of the exhaust shaft.

Geohydrologic and geomechanical data from the C & SH shaft and the waste shaft have been compared to model simulations for each section of the exhaust shaft. These models, field observations and instrumentation data confirm that the exhaust shaft reference design is suitable for its 25 year operating life.

The shaft liner is stable and has a water pressure against it that is less than the design basis hydrostatic pressure. If the pressure

increases, the liner will remain stable. Shrinkage cracks will not result in structural instability.

As with the waste shaft, an analysis of the exhaust shaft key indicates that the lateral pressure calculated for 25 years will slightly exceed the design lateral pressure, but will be well below the maximum allowable lateral pressure. Computational analyses of the stresses and strains indicate that the unlined section of the shaft will be stable and remain within safety limits during its operating life. The computed diametric closure will be within design criteria and design basis limits.

Water is entering the exhaust shaft through cracks and construction joints in the concrete liner. A small amount of water still reaches the shaft even after a remedial grouting program. When the exhaust fans are on, this water evaporates before reaching the facility. The water seals in the key appear to be functioning and there is no evidence of salt dissolution behind the key.

DRIFTS

The discussion of drifts contained in this section pertains to all horizontal underground openings except the shaft stations, test rooms, and storage area rooms and their associated drifts. The drifts were designed in accordance with the design criteria and design bases. The largest drifts were initially excavated 8 feet high and 25 feet wide. These drifts have been or will be enlarged to 12 feet high. This drift height is dictated by the minimum 11-foot operating clearance required for the waste storage equipment.

A variety of geotechnical activities were conducted to evaluate the behavior of the excavated drifts. These activities included geologic mapping, core drilling and logging, visual inspections, and geomechanical instrumentation measurements.

Visual inspections consisted of qualitative observations and documentation of various aspects of drift behavior. These observations are divided into four categories: roof and wall spalling; pillar fracturing; roof displacements and separations; and floor fracturing, displacements and separations.

Deformational behavior consisting of spalling from the roof and walls of the drifts and fracturing and spalling at pillar corners has occurred. Separations and lateral displacements have been detected in the halite above the roof, primarily at clay seams. These types of behavior are expected and will continue to occur, but can be controlled by scaling and rock bolting.

Fracturing has occurred in marker bed 139 (MB-139) and in the overlying halite beneath the floor of the drifts. The fracturing is not well developed and occurs primarily beneath large intersections. Based on experience in local potash mines, this fracturing is not expected to cause stability or operational problems.

The comparison of measured closure behavior in drifts with different dimensions indicates that the maximum closure and closure rate will occur in 12 x 25-foot drifts. The closure rates are affected by the presence of nearby parallel drifts and crosscuts as well as differences in salt properties. Based on available measurement data and the results of modeling analyses, the closure rate in the 13 x 25-foot storage area drifts may be 30 percent greater than that of a single, infinitely long drift with the same dimensions.

Analyses of salt behavior around the 25-foot wide drifts has determined both the redistribution of stresses due to creep and the locations of effective creep strain concentrations. The stresses which develop immediately after excavation relax with time due to creep behavior and will not cause future stability problems. The strain will remain within the limit required for structural stability with respect to catastrophic failure.

The evaluation of field observations and analytical results have shown that the design criteria were appropriate for design of the horizontal openings. The criteria identified as requiring specific evaluation were determined to be suitable. The reference design for the horizontal openings is therefore validated.

Based on the results of design validation of the drifts, it is recommended that all drifts be inspected frequently for operational clearance and safety. If the clearance is insufficient, the drifts must be trimmed to the required dimensions. Scaling and rock bolting should be performed where necessary for safety purposes.

TEST ROOMS

The test rooms comprise a panel of four rooms having a similar configuration as the planned storage rooms. They have been instrumented, observed and analyzed to evaluate the behavior of the future storage rooms. Data collection activities have consisted of geologic mapping, core drilling and logging, visual inspections and geomechanical instrumentation measurements. The instrumentation includes borehole extensometers, inclinometers, convergence points, convergence meters and rigid-inclusion, vibrating-wire stressmeters.

Room deterioration has been minimal and consists of spalling from the roof and walls, vertical fracturing in the pillars, minor displacements and separations above the roof and beneath the floor, and fracturing beneath the floor. Areas of drummy rock detected by roof and wall inspections immediately following excavation were scaled and rock bolted. These areas have not increased noticeably in size since the test rooms were excavated, over 3 years ago.

Subhorizontal fracturing has developed beneath the test room floors. Separations and fractures are on a small scale except for one isolated location beneath Test Room 3. Fracturing in this area is well developed and occurs in two distinct zones. Studies have not shown

fracturing of this magnitude to occur anywhere else within the underground WIPP facility.

The analysis of closure of the test rooms using creep constants derived from laboratory data underestimate actual closure. The design criteria closure of 12 inches in 5 years has been exceeded within 3 years. Strains measured in the test rooms compare well with strains computed by numerical modeling.

STORAGE AREA

The storage area rooms and drifts are designed to permit the permanent storage of defense-related CH and RH TRU waste. The storage area is composed of eight panels consisting of seven rooms each. Each room is 13 feet high, 33 feet wide and 300 feet long. The storage area, including all rooms and drifts, is designed to provide storage space for 6,330,000 cubic feet of CH TRU waste and 1,000 canisters of RH TRU waste.

Validation of the storage room reference design depends primarily on the analysis of data from the four test rooms. Evaluation of the storage rooms was based on the results of a finite element model analysis using creep parameters determined from the test room analyses. The results of this analysis provided determinations of horizontal and vertical stresses, effective stresses, effective creep strains, principal stresses, room deformation and closure, and intersection closure.

The analyses show that the stress arch around the opening migrates away with time. The maximum stress occurs immediately after excavation and is reduced as the opening deforms over time due to salt creep. These stresses will therefore not cause a stability problem in the future. However, MB-139, the anhydrite bed approximately 4 feet below the floor, is expected to be subjected to gradually increasing stress and may exhibit local failure.

Effective creep strains will intensify and concentrate at some locations around the opening. While minor spalls and failures are expected to occur on the excavation surfaces, the rooms will remain structurally stable.

The storage room reference design of 13 feet high and 33 feet wide was based on calculations using laboratory-derived average creep parameters. This design allowed for 12 inches of vertical closure and 9 inches of horizontal closure 5 years after excavation. This accommodates the design bases requirements for a minimum of 16 inches of ventilation space above the stored waste and a 12-foot minimum height for storage equipment. The current predicted vertical closure at 5 years is about 22 inches. For permanent storage, the additional 10 inches of closure can be accommodated by excavating the storage rooms to a height of 13 feet 10 inches.

If a decision is made to retrieve the stored waste, the design criteria assumed, using a one-shift-per-day basis, that a room may be as much as 15 years old before removal of all of the waste is completed. A 15-year old room has a predicted vertical closure of 54 inches. This closure is 14 inches greater than the maximum acceptable closure and would result in crushing and possible breaching of the waste containers. Because this is not in compliance with the design criteria, other alternatives must be considered.

A 10 year maximum for retrieval is conservative. If three shifts per day were utilized, no room would be older than 7 years by the time its waste was removed. A 7 year old room would have 28 inches of vertical closure. Additional closure benefits can be gained by excavating a room to is maximum dimensions and then trimming the room to those maximum dimensions after 1 year of closure. This will allow the room to close at the rate determined by secondary creep and will result in 21 inches of vertical closure 7 years after trimming. This will meet the design criteria requirements.

The design bases provide for 9 inches of horizontal closure in the first 5 years after room excavation. The current prediction, based on in situ data, is 15 inches of closure in the 33- to 34-foot wide rooms. If the rooms are excavated 34-feet wide and backfilled with loose salt, this closure will be suitable for permanent storage.

For retrieval, the horizontal closure 15 years after excavation will be approximately 36 inches. This closure will result in some crushing and possible breaching of the waste containers. Even if retrieval is effected within 7 years, some containers may still be crushed and breached.

The timing of retrieval operations and two-stage excavation can be used to reduce wall-to-wall closure. Using a three-shift-per-day basis, a 7 year old room would close approximately 20 inches. If a first in/first out storage and retrieval operations is utilized, and waste is removed before a room reaches an age of 6 years, horizontal closure will be reduced to 18 inches. Both these changes would decrease the possiblity of crushing or breaching the containers. If a 34-foot wide room is trimmed after 1 year to its initial full dimensions, the horizontal closure at 7 years will be about 14 inches. This will further minimize crushing or breaching of the containers. The extent to which crushing will be minimized is unknown. This is because the space between the waste canisters and the room wall will be filled with loose salt. The load transferring capabilities of the backfill is not known at the present time.

The reference design also provides for permanent waste storage in all of the storage area drifts. Fifteen years after excavation a 13 x 25-foot drift is predicted to have a vertical closure of about 25 inches and a horizontal closure of about 20 inches. This is suitable for waste storage but trimming will be required for equipment clearance.

The storage area entry drifts will contain plugs for the isolation of the storage panels. The final design of these plugs is not yet

complete. However, the conceptual design envisions a multiple-component plug approximately 100 feet long.

The reference design for the storage rooms will be considered to be validated when any of the following recommended alternative modifications, or combination of these modifications, are incorporated:

(1) Maintain the reference design storage room dimensions of 13 to 14 feet high and 33 to 34 feet wide and maintain the salt backfill, but reduce the volume of waste to be stored and modify the container stacking configuration for the 5-year demonstration period. Revise the design criteria to require that waste be retrieved before a room exceeds an age of 7 years. This will meet the criteria that the waste containers not be crushed or breached, but it will require a significant number of additional storage rooms.

(2) Maintain the reference design storage room dimensions and maintain the planned waste volume. Revise the design criteria to delete the requirement for salt backfill and to require that waste be retrieved before a room exceeds an age of 7 years. This will meet the criteria that the waste containers not be crushed or breached without requiring additional storage rooms.

(3) Maintain the reference design storage room dimensions, planned waste volume, and salt backfill requirement. Revise the storage operations so that the first-emplaced waste is the first-retrieved waste with retrieval effected before the room exceeds 6 years of age. Excavate the room to 14 x 34 feet, then, 1 year later, trim the room to its initial 14 X 34 foot dimensions. This will minimize container crushing and breaching. More storage rooms will be utilized during the 5-year demonstration period, but the total number of rooms will remain the same as provided by the reference

design. This modification will require changing the design criteria to allow crushing and breaching of the CH waste containers prior to retrieval and to require a demonstration of the retrieval and handling of crushed and breached containers.

(4) Reduce the reference design storage room width from 33 feet to 28 feet, maintain the room height at 13 to 14 feet, and reduce the pillar width to 84 feet. Maintain the first room for RH waste emplacement at the original reference design dimensions. Reduce the planned waste volume and maintain the salt backfill requirement. Excavate the rooms to 14 x 28 feet, then trim them to this dimension after 1 year. Use a first-in/first-out storage operation. This will reduce the creep to approximately that of a 13 x 25-foot drift. Stability will be enhanced and crushing and breaching will be minimized. The volume of excavation will be approximately the same as for the reference design storage rooms, but with the advantage of a lower creep rate. If this alternative is selected, additional engineering evaluation will be required.

(5) Maintain the reference design storage room dimensions, the planned waste volume, the salt backfill requirement, and the reference design optimized excavation and storage plan. Revise the design criteria, as in alternative number 3, to allow crushing and breaching of the CH waste containers prior to their retrieval. Require a demonstration of the retrieval and handling of crushed and breached containers prior to the receipt of waste. This will not only demonstrate the safe retrieval of waste during the 5-year demonstration period, but also during permanent storage.

In addition to these recommended alternative modifications, the following modifications are recommended:

(6) The drifts used for storage will require maintenance and trimming to accommodate the required equipment and storage clearances. Their closure rates are not critical for storage because they will be used only for permanent storage near the end of the permanent storage period.

(7) Add additional rooms to compensate for the space occupied by the plugs in the storage area entry drifts.

(8) Install instrumentation in the storage rooms to obtain in situ data to monitor storage room behavior.

Table I

EVALUATION RESULTS FOR ABRIDGED DESIGN CRITERIA

ELEMENT	RESULT AND CHAPTER REFERENCE
(1) Facility design	
a. Designed for an operating life of 25 years.	*
b. Underground facilities and equipmentshall be designed to be compatible with retrieval operations for all contact-handled (CH) and remote-handled (RH) TRU waste, with a retrieval decision to be made within 5 years after the intial emplacement of each species.	Suitable 12.3.3
c. The facility will be decommissioned after it has fulfilled its intended purposes. This will include backfilling the underground facilities, sealing the shafts and decommissioning the surface facilities.	*
(2) CH TRU waste **	
a. Estimated annual volume is 500,000 cubic feet.	*
b. Estimated volume at the end of the 5 year retrieval decision period is 1,410,000 cubic feet.	*
c. Estimated total storage capacity is 6,330,000 cubic feet.	*
d. Heat generated from the waste is negligible; it will be less than 10 milliwatts for average drums, less than 20 milliwatts for average boxes, and 10 watts for few drums containing heat source plutonium.	*

* Indicates element for which evaluation is not required.
** See Foreword.

Table I (continued)

EVALUATION RESULTS FOR ABRIDGED DESIGN CRITERIA

ELEMENT	RESULT AND CHAPTER REFERENCE
e. Estimated annual quantities are 9,616 six-packs and 2,404 modular steel boxes.	*
f. Estimated total quantities are 121,700 six-packs and 30,430 modular steel boxes.	*
g. Underground facilities and equipment shall be designed to provide for a determination to effect retrieval of waste stored for a period up to 5 years after the initial emplacement and for a target of 5 to 10 years to reach the waste and retrieve it after the decision is made.	Suitable 12.6.1 12.6.2
(3) RH TRU waste **	
a. Assumed total receipt of 1,000 cansisters.	*
b. Assumed maximum receipt rate of two canisters per day and 250 canisters per year.	*
c. If assumed quantities are insufficient, additional RH waste storage will be accommodated within existing storage rooms.	*
d. Heat generated from the waste is on the order of 60 watts per canister.	*
e. Access shall be available to all emplacement positions throughout the retrievability period.	Suitable 12.3.3

Table I (continued)

EVALUATION RESULTS FOR ABRIDGED DESIGN CRITERIA

ELEMENT	RESULT AND CHAPTER REFERENCE
f. When both CH and RH waste are scheduled for the same room, the RH waste shall be emplaced first. After the 5 year retrievability period has terminated, CH waste may be emplaced in that room.	*
(4) Shaft design	
a. Shafts shall be designed to be structurally stable throughout the operating life of the underground facility and the decommissioning period.	Suitable 7.4.1 8.4.1 9.4.1
b. Time-dependent closure of shafts due to salt creep shall be considered. Shafts shall be designed so that minimum dimensions required for shaft functions are maintained during design life.	Suitable 7.4.1 8.4.1 9.4.1
c. Ground-water flow into the shafts shall be controlled so that no uncontrolled ground water reaches the storage horizon via the shafts.	Suitable 7.4.1 8.4.1 9.4.1
(5) Shaft liner design	
a. Help ensure that dimensions remain within limits required for shaft functions.	*
b. Prevent ground-water flow into the shaft.	Suitable 7.4.1 8.4.1 9.4.1
c. Protect wall rock from deterioration.	*

Table I (continued)

EVALUATION RESULTS FOR ABRIDGED DESIGN CRITERIA

ELEMENT	RESULT AND CHAPTER REFERENCE
d. Preclude risk of rock fall from shaft wall.	*
(6) Mine design	
a. The underground openings shall be designed so that deformation of excavations and pillars will remain within limits required for structural function, ventilation and safety.	Suitable 7.4.1 8.4.1 10.4.1
b. Rock bolts shall be used where necessary to provide positive support of roof and walls.	*
c. Surface subsidence resulting from underground excavation shall not exceed 1 inch within a 500-foot radius of the waste shaft.	Suitable 6.5
d. Excavations and pillars shall be located and dimensioned to avoid geologic discontinuities. If discontinuities are encountered, remedial action shall be engineered to correct the problem.	Suitable 3.4 6.3.1.2 6.3.3
e. Design shall be based on established mining procedures.	*
f. Predicted behavior of the salt shall be verified by in situ testing (SPDV) before proceeding with construction of the storage area.	*
g. Designed to accommodate creep closure and maintain the minimum dimensions required for the operating life of the opening.	Suitable 10.4.1 12.6.1

Table I (continued)

EVALUATION RESULTS FOR ABRIDGED DESIGN CRITERIA

ELEMENT	RESULT AND CHAPTER REFERENCE
h. Creep closure rates used for design shall be confirmed by instrument observations in the excavations.	Suitable 11.3.2 12.3.2
i. Excavation dimensions shall include allowance for creep closure sufficient to prevent container breaching by creep-induced stresses during the retrievability period.	Suitable 12.6.1 12.6.2
j. Minimize the potential for repository rock fracturing.	Suitable 11.4.1
k. Underground waste storage procedures shall include a designed backfill plan for fire protection. The backfill thickness shall be 1 to 2 feet.	Suitable 12.6.1
l. Permit isolation of panels of rooms with plugs after storage and backfilling are completed.	Suitable 12.6.1
m. Air locks, dampers, regulators and doors shall be designed and installed in such a manner that they can accommodate creep without impairment to their ability to maintain ventilation separation.	*
(7) Emplacement criteria	
a. The underground storage rooms and access drifts shall be designed to be compatible with the waste transport vehicle, with waste container sizes, shapes, weights and stacking configurations, and with waste emplacement equipment.	Suitable 12.6.1

Table I (continued)

EVALUATION RESULTS FOR ABRIDGED DESIGN CRITERIA

ELEMENT	RESULT AND CHAPTER REFERENCE
b. Provisions shall be made to accommodate backfilling over and around CH waste containers.	Suitable 12.6.1
c. Each storage panel shall have provisions for being isolated from other panels upon completion of storage operations in that panel.	Suitable 12.6.1
(8) Retrievability	
a. All wastes placed into the WIPP are retrievable, with retrievability to be demonstrated, until such time as the pilot plant is converted to an operational repository for permanent disposal of wastes.	Suitable 12.6.1 12.6.2
b. Each storage room shall allow for salt creep and shall be sized to minimize breaching of the CH waste containers for a period of 10 years.	Suitable 12.6.1 12.6.2
(9) Underground excavation and haulage	
a. Mining shall be performed with continuous miners or equivalent machine type devices. Drill and blast-type mining shall be prohibited except where authorized.	*
b. Underground design shall provide maximum stability for excavated rooms and entries.	Suitable 7.4.1 8.4.1 10.4.1 11.4.1 12.6.1

Table I (continued)

EVALUATION RESULTS FOR ABRIDGED DESIGN CRITERIA

ELEMENT	RESULT AND CHAPTER REFERENCE
c. Meet or exceed the intent of the applicable requirements of the MSHA in 30 CFR 57.9 and the New Mexico Mine Safety Code for All Mines.	*

Table II

EVALUATION RESULTS FOR C & SH SHAFT DESIGN BASES

ELEMENT	RESULT AND CHAPTER REFERENCE
(1) Shaft liner	
a. Hydrostatic pressure is considered to start 250 feet below the ground surface and extend to the top of the key.	Suitable 7.4.1
b. Water shall be prevented from flowing down the unlined shaft from behind the liner.	Suitable 7.4.1
(2) Shaft key	
a. Key shall be designed to resist the lateral pressure from the salt. (Assumed to be 75 percent of the overburden pressure.)	Suitable 7.4.1
b. Key shall be designed to resist the hydrostatic pressure from above the salt.	Suitable 7.4.1
(3) Unlined section	
Provide 11-foot 8-inch diameter to allow for future salt creep deformation.	Suitable 7.4.1

Table III

EVALUATION RESULTS FOR WASTE SHAFT DESIGN BASES

ELEMENT	RESULT AND CHAPTER REFERENCE
(1) Shaft liner	
Hydrostatic pressure is considered to start 250 feet below the ground surface and extend to the top of the key.	Suitable 8.4.1
(2) Shaft key	
Design lateral pressure shall be 50 percent of the vertical pressure due to soil, rock and salt overburden.	Suitable 8.4.1
(3) Unlined section	
Provide 20-foot diameter to allow for future salt creep deformation.	Suitable 8.4.1

Table IV

EVALUATION RESULTS FOR EXHAUST SHAFT DESIGN BASES

ELEMENT	RESULT AND CHAPTER REFERENCE
(1) Shaft liner	
Hydrostatic pressure is considered to start 250 feet below the ground surface and extend to the top of the key.	Suitable 9.4.1
(2) Shaft key	
Design lateral pressure shall be 50 percent of the vertical pressure due to soil, rock and salt overburden.	Suitable 9.4.1
(3) Unlined section	
Provide 15-foot diameter to allow for future salt creep deformation.	Suitable 9.4.1

Table V

EVALUATION RESULTS FOR STORAGE AREA DESIGN BASES

ELEMENT	RESULT AND CHAPTER REFERENCE
(1) Operational requirements	
a. The storage area rooms, drifts and crosscuts shall be designed to allow for retrieval of all CH and RH waste stored for a period of up to 5 years after the initial emplacement of each waste species.	Suitable 12.6.1 12.6.2
b. Excavation dimensions in the waste storage area shall be to a uniform height of 13 feet.	Suitable 12.6.1 12.6.2
(2) Essential features	
Provide 1 foot vertical and 9 inches horizontal allowance for creep closure to maintain the minimum design dimensions up to 5 years after initial emplacement.	Suitable 12.6.1 12.6.2
(3) Safety design requirements	
A minimum opening of 16 inches shall be left at the top of the rooms and drifts for air passage above the waste and backfill.	Suitable 12.6.1 12.6.2

Table VI

EVALUATION RESULTS FOR DESIGN CONFIGURATIONS

ELEMENT	RESULT AND CHAPTER REFERENCE
(1) C & SH shaft	
a. Provide 5/8 to 1 1/2-inch thick and 10-foot I.D. stiffened steel liner in upper 846 feet.	Suitable 7.3.2.1 7.3.3.1
b. Provide 30-inch thick, 10-foot I.D. and 39-foot long concrete key at rock/salt interface.	Suitable 7.3.2.2 7.3.3.2
c. Provide 11-foot 10-inch diameter unlined shaft below the key.	Suitable 7.3.2.3 7.3.3.3
d. Provide 17-foot high and 32-foot wide station.	Suitable 7.3.2.4 7.3.3.4
(2) Waste shaft	
a. Provide 10 to 20-inch thick and 19-foot I.D. concrete liner in upper 837 feet.	Suitable 8.3.2.1 8.3.3.1
b. Provide 51-inch thick, 19-foot I.D. and 63-foot long concrete key at rock/salt interface.	Suitable 8.3.2.2 8.3.3.2
c. Provide 20-foot diameter unlined shaft below the key.	Suitable 8.3.2.3 8.3.3.3
d. Provide 17-foot high and 30-foot wide station.	Suitable 8.3.2.4 8.3.3.4
(3) Exhaust shaft	
a. Provide 10 to 16-inch thick and 14-foot I.D. concrete liner in upper 844 feet.	Suitable 9.3.2.1 9.3.3.1

Table VI (continued)

EVALUATION RESULTS FOR DESIGN CONFIGURATIONS

ELEMENT	RESULT AND CHAPTER REFERENCE
b. Provide 42-inch thick, 14-foot I.D. and 63-foot long concrete key at rock/salt interface.	Suitable 9.3.2.2 9.3.3.2
c. Provide 15-foot diameter unlined shaft below the key.	Suitable 9.3.2.3 9.3.3.3
(4) Storage area	
a. Provide 13-foot high and 25-foot wide or smaller drifts.	Suitable 12.6.1 12.6.2
b. Provide 13-foot high and 33-foot wide storage rooms.	Suitable 12.6.1 12.6.2

CHAPTER 1
INTRODUCTION

1.1 PURPOSE

This report presents the results of validation of the underground opening reference design for the Waste Isolation Pilot Plant (WIPP). The basis for the report is defined in the Design Validation Plan (ref. 1-1) which, in part, includes certain data requirements defined in the Stipulated Agreement (ref. 1-2) reached between the U.S. Department of Energy (DOE) and the State of New Mexico on July 1, 1981.

Design validation of the WIPP is defined as the process by which the reference design of the underground openings is confirmed by determining the compatibility of the design criteria, design bases and reference design configurations using site specific information. The design validation process consists of an assessment of the condition and behavior of shafts, drifts and a full-sized, four-room test panel excavated during an initial stage known as the Site and Preliminary Design Validation (SPDV) Program and during full WIPP construction. Based on this assessment of these excavations, and on predictions of their future behavior, any modifications to the design criteria, design bases or design configurations required to achieve a validated reference design will be developed. In addition, the validated reference design may be modified in the future as still more data and experience are gained during a 5-year demonstration period (period during which all waste must be retrievable) and permanent storage operations.

In fulfilling the data requirements for design validation, this report provides documentation of actual underground conditions encountered as they relate to the design criteria, design bases and design configurations for the reference design of the underground openings. The contents of this report include all relevant data and field observations acquired for design validation. The underground openings excavated to date provide a firm basis for evaluation of the current and expected future behavior of the underground development.

The purpose of design validation is to:

- o validate the underground reference design, thus providing confidence in the safety and stability of the WIPP underground openings;

- o confirm the suitability of the design criteria, design bases and design configurations established specifically for the reference design of the underground openings;

- o re-confirm and expand upon the conclusions of the SPDV Program; and

- o comply with the DOE agreement with the State of New Mexico to validate the reference design of the WIPP underground openings.

This process was initially described in the WIPP Preliminary Design Validation Report (ref. 1-3) issued in March 1983. That report presented the results of a preliminary evaluation of the underground opening reference design based on activities conducted during the SPDV phase of underground development. That initial report was prepared in response to conditions contained in the Stipulated Agreement (Appendix A) between the DOE and the State of New Mexico which permitted a preliminary evaluation of design considerations at an early stage in underground development and allowed for any reference design modifications deemed necessary for full WIPP construction. The WIPP Design Validation Final Report (this report) is an extension of the preliminary report and presents further confirmation of the reference design based on additional data collected since completion of the SPDV Program in both old and new areas of underground excavation.

The WIPP Design Validation Final Report presents:

- o a summary of the background and development of the WIPP reference design;

- the design criteria and design bases used to develop the reference design for the underground openings;

- geologic characterizations of the shafts, drifts and test rooms;

- the methodology used for data collection, its analysis and evaluation, and the predictions of future behavior of the underground openings;

- the description of data collection activities in the shafts, drifts and test rooms;

- analyses and evaluations of the geologic behavior of the rock strata surrounding the shafts, drifts and test rooms based on visual inspections and geomechanical instrumentation measurements;

- predictions of expected future conditions of the underground openings based on model simulations using in situ data;

- an assessment of the suitability of the design criteria and design bases and validation of the reference design configurations, with recommendations for design modifications, if any;

- recommendations for operation and maintenance of the underground facility as they pertain to design validation; and

- all data and reference sources that support design validation.

1.2 SCOPE

Design validation of the WIPP underground openings has been accomplished through an assessment of their safety, stability and predicted future behavior. Observation and instrumentation data consistent with the Design Validation Plan objectives have been

collected and evaluated for each of the major design elements: shafts, drifts and test rooms.

Initial analyses and evaluations of the underground data obtained for design validation were provided in the WIPP Preliminary Design Validation Report. The WIPP Design Validation Final Report presents the results of activities whose objectives are outlined in the Design Validation Plan. These activities included field data collection and analyses of these data to determine the validity of the reference design.

Basically, four types of information were gathered for design validation. These are:

(1) observations of the behavior of the underground openings;

(2) descriptions of the geologic conditions encountered during underground construction;

(3) descriptions of core samples from instrumentation and other holes in the roof and floor of the underground openings; and

(4) data from installed geomechanical instrumentation.

Field tasks performed to gather this information included the following:

- establishment of survey control for underground excavations and reference points for geologic mapping;

- development of procedures and standards for activities such as geologic mapping/logging of underground excavations;

- geologic mapping in the shafts and horizontal openings;

- examination and logging of rock cores from boreholes to obtain geologic information;

- observation and measurement of ground-water flow into the shafts;

- measurement of hydrostatic and lateral pressures on the shaft liner and shaft key;

- monitoring the floor height of horizontal openings above the top of marker bed 139 (MB-139) and the height of clay seams above the roofs using core hole data;

- measurement of closure in the shafts and horizontal openings;

- determination of the presence of gases and fluids;

- survey of shaft verticality; and

- examination of all surfaces of underground openings for displacement of clay seams, fracturing, roof sagging, floor heaving, or other occurrences that may indicate unstable conditions.

1.3 HISTORICAL BACKGROUND

The WIPP is being developed by the DOE as a research and development (R & D) facility to demonstrate the safe disposal of radioactive waste from U.S. defense programs. The facility is located in southeastern New Mexico, about 25 miles east of the city of Carlsbad (Figure 1-1). The underground development level is at a depth of approximately 2,150 feet in thick deposits of bedded salt. The facility will include space for the permanent storage of defense related transuranic (TRU) waste and for in situ experiments addressing technical issues for high-level defense waste programs. The WIPP's phased design and construction resulted in initial confirmation of the underground opening reference design through the SPDV Program. Design

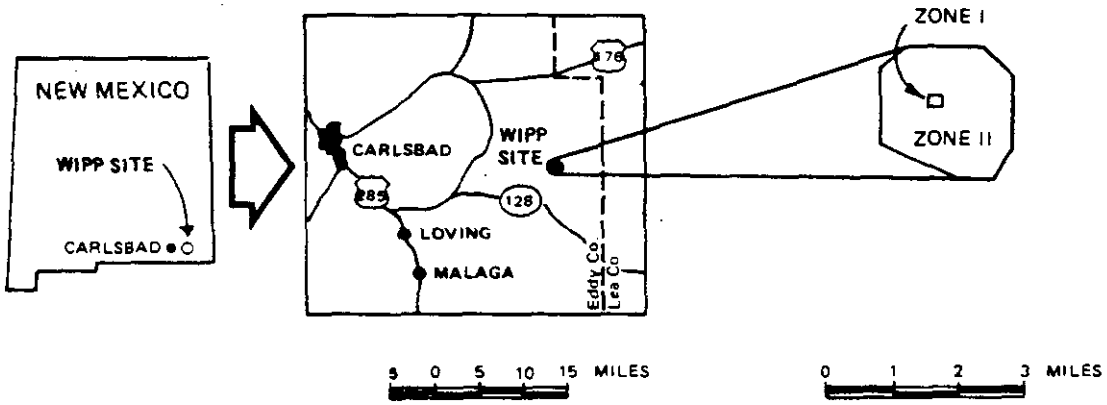

ZONE DESCRIPTION

ZONE I Surface Facilities Area
ZONE II Underground Storage Limits

M

Figure 1-1

LOCATION OF THE WIPP

validation will provide confirmation of the decision to continue facility construction with subsequent in situ experiments and defense TRU waste storage.

The WIPP project is the result of waste management program efforts that were started by the U.S. government as long ago as 1955 when the U.S. Atomic Energy Commission (AEC) requested that the National Academy of Sciences (NAS) evaluate methods for disposing of radioactive waste in geologic formations. The NAS recommended bedded salt as the geologic formation providing the highest confidence for long-term isolation of waste from the biosphere. As a result of these efforts, the DOE (formerly the AEC) initiated the WIPP program in 1975. The major accomplishments of the program are listed in Table 1-1.

Assessments that pertain to design of the WIPP include extensive analyses of the impact of the facility on present and future environments. A Final Environmental Impact Statement (FEIS) (ref. 1-4) was prepared which provides information about the environmental and safety consequences of the WIPP project. A Safety Analysis Report (SAR) (ref. 1-5) was also prepared to support construction and operation of the WIPP. The SAR addresses all aspects of industrial and nuclear safety of the project and is updated periodically.

The WIPP is being developed in phases. At the time this report was prepared, most of the site characterization, design and supporting technological development had been done. The engineering design of the underground openings began with a conceptual design followed by a preliminary design and finally a detailed reference design. Facility development at the site began with the SPDV Program which allowed direct observation of the underground facility geology through two shafts and associated underground drifts. This program provided data for preliminary evaluation and confirmation of the reference design of the proposed underground excavations. Design and construction of the surface facilities have proceeded virtually independent of the underground opening design validation and are not addressed in this report.

Table 1-1

MAJOR ACCOMPLISHMENTS OF THE WIPP PROGRAM

	ITEM	DATE STARTED	DATE COMPLETED
(1)	National Academy of Sciences recommends salt as best geologic formation for disposal of nuclear waste.	-	1957
(2)	Salt deposit studies conducted in New Mexico by U.S. Geological Survey and Sandia National Laboratories.	1972	1975
(3)	Conceptual design of the WIPP.	1975	1977
(4)	Characterization of the WIPP site.	1975	1983
(5)	Public law authorizes capital funding for the WIPP.	-	1977
(6)	Title I - Preliminary design of the WIPP.	1/78	1/80
(7)	Safety Analysis Report issued for the WIPP.	-	2/80
(8)	Final Environmental Impact Statement issued for the WIPP.	-	10/80
(9)	SPDV Preliminary Design Validation Program.	7/79	3/83
(10)	Detailed design for Site and Preliminary Design Validation (SPDV).	7/79	10/80
(11)	SPDV Site Validation Experiments Program.	8/80	3/83
(12)	Title II - Detailed design of the WIPP.	2/81	2/84
(13)	Construction of SPDV shafts.	5/81	3/82
(14)	Design validation.	4/81	10/86
(15)	SPDV shaft outfitting and test room development.	10/81	7/83
(16)	Authorization for full WIPP construction.	-	7/83

1.4 THE WIPP MISSION

The authorized mission for the WIPP emphasizes its role as an R & D facility to demonstrate safe disposal of radioactive waste from U.S. defense programs. Its mission is also to provide information from site characterization, laboratory experiments, geomechanical instrumentation and in situ tests which can be used to develop performance-assessment models for technological applications. Figure 1-2 shows the underground layout of the three R & D areas at the WIPP.

The WIPP R & D Program consists of three major program areas:

(1) site characterization and evaluation;

(2) repository development and operation; and

(3) waste package interactions.

In addition to providing for the permanent storage of defense related TRU waste, these program areas include technology development in waste isolation, in situ tests without radioactive material, and in situ tests with radioactive material. The WIPP will also serve as a laboratory for experiments with high-level defense waste. All high-level wastes will be removed from the WIPP at the conclusion of the testing period. These in situ waste experiments and associated activities are not part of design validation and, therefore, are not discussed in this report. An initial description of the in situ testing plan for the WIPP R & D Program was provided in Sandia National Laboratories' (SNL) Report 2628 (ref. 1-6).

1.5 DESIGN VALIDATION PROGRAM

Validation of the WIPP facility underground reference design is based on a strategy consisting of a detailed plan and approach for validating major reference design elements. A description of this strategy is

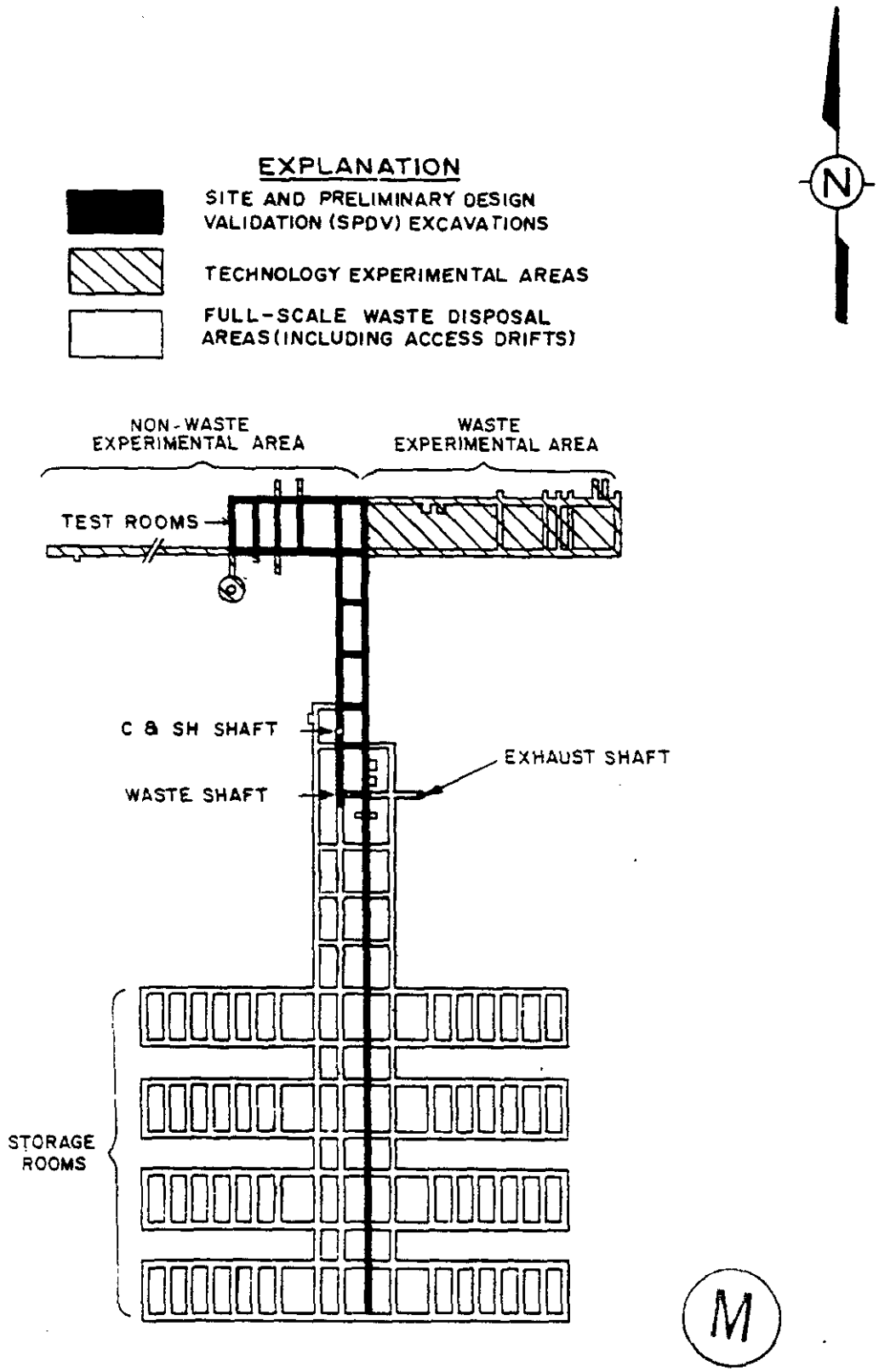

Figure 1-2

PLAN VIEW OF UNDERGROUND FACILITY

contained in the document titled Design Validation Strategy (ref. 1-7). The elements comprising the strategy for design validation are:

(1) Identify the design approaches and construction activities for the underground openings.

(2) Identify the design criteria, design bases and design configurations to be validated.

(3) Develop the methodology for validation.

(4) Acquire data on the underground development level from core samples, geologic mapping, laboratory tests, in situ tests, visual observations and mines in similar geologic formations.

(5) Synthesize the data obtained from the activities in element 4 to define the geologic environment of the facility level.

(6) Evaluate in situ geomechanical instrument measurements and visual observations to determine the response of the geologic materials to changes resulting from excavation or other disturbances.

(7) Predict the future behavior of the underground openings and salt surrounding the openings based on current in situ measurements, visual observations and computational analyses.

(8) Provide for comparisons of predicted and existing conditions at regular time intervals.

(9) Document design validation results and conclusions.

(10) Provide recommended design modifications as required.

(11) Provide data and reference sources to support the performance of the above activities.

Design validation efforts for the WIPP began with the SPDV Program. This program involved the excavation of underground openings, shafts, drifts and test rooms, representative of the full WIPP facility. These underground openings permitted the direct examination of geologic features and material behavior at the facility level. Additional observations and geomechanical instrumentation measurements were obtained following completion of the SPDV Program to complete the design validation program. A brief description of the design validation program is presented in the following subsections.

1.5.1 Site and Preliminary Design Validation (SPDV)

The SPDV Program was designed to further characterize and validate the WIPP site geology and provide preliminary validation of the underground opening reference design. The SPDV Program was composed of two integrated parts:

(1) site validation (ref. 1-8) to increase confidence in the process of site characterization and qualification; and

(2) preliminary design validation to assess the condition and behavior of excavated shafts, drifts and a full-sized, four-room test panel similar to those planned for the waste storage area.

The general SPDV underground layout is shown on Figure 1-3. The underground development level is located in Zone II, a WIPP site control zone that delineates the limits of underground storage. A preliminary design validation report was issued on March 30, 1983. This report presented the results of early observations and analyses of the condition and behavior of the SPDV excavations and is discussed in Chapter 4.

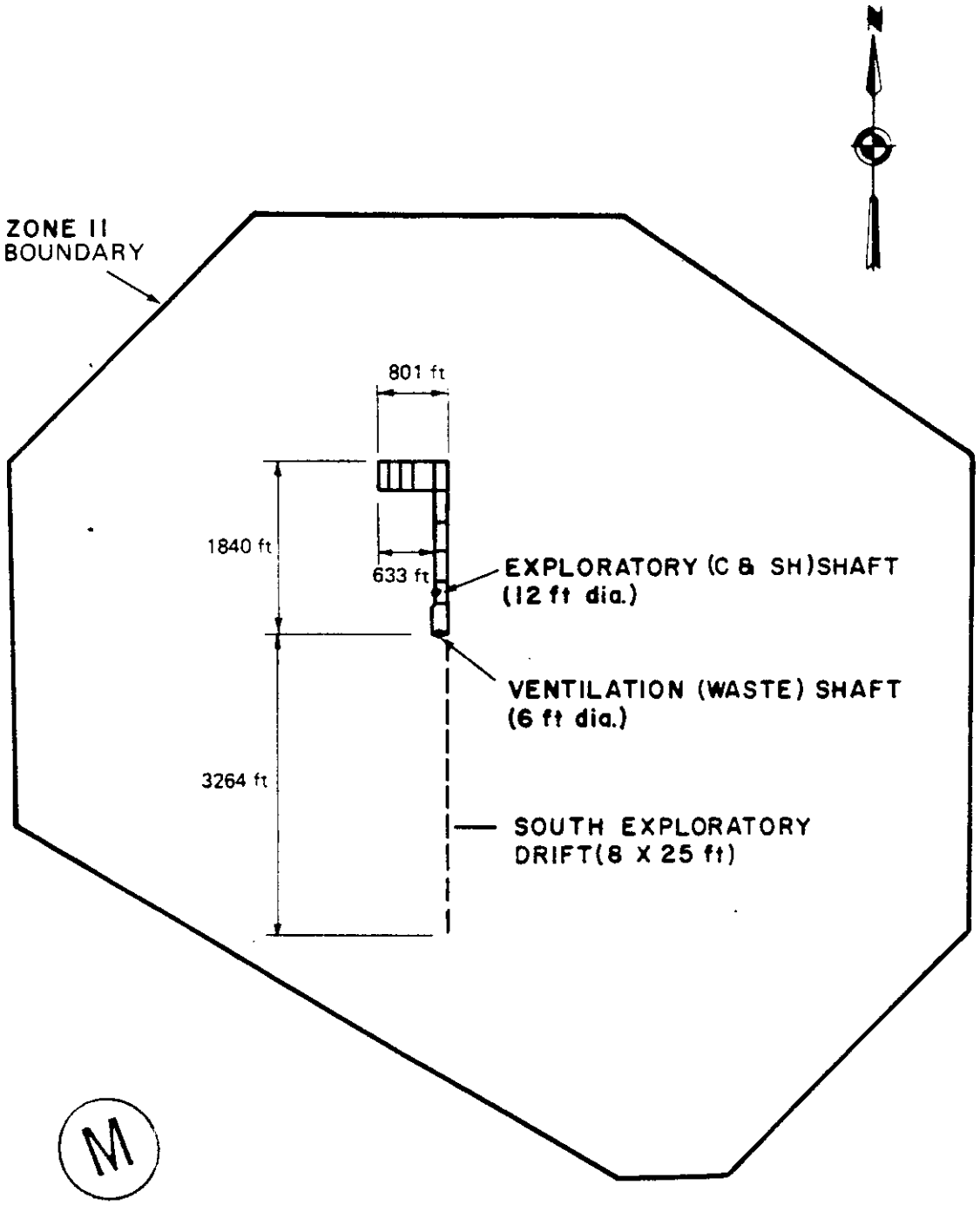

Figure 1-3

THE SPDV UNDERGROUND LAYOUT

1.5.2 Design Validation

Major activities related to design validation are cited in Table 1-2. As indicated by this table, field data collection activities that began with the SPDV Program were continued beyond the end of the program to provide additional data for design validation. The design validation process includes the evaluation and analysis of data obtained by these activities. The results of these evaluations and analyses have been presented in quarterly geotechnical field data reports (GFDR), each of which presents a discussion of different selected elements of the WIPP underground development. These reports provide supporting documentation for the WIPP Design Validation Final Report and are discussed in Chapter 4.

Some of the field data collection activities shown in Table 1-2 will continue after submittal of the WIPP Design Validation Final Report and beyond the completion of full WIPP construction. Collection of this data will provide additional information on the behavior of the underground openings through the 5-year demonstration period and through permanent storage operations. The data will also permit continuous monitoring of the safety of the openings. Underground facility reference design modifications will be made as required by an evaluation and analysis of these data. The data obtained will be periodically distributed to the project participants, the State of New Mexico, and will be placed in WIPP public reading rooms.

Table 1-2

DESIGN VALIDATION ACTIVITY SCHEDULE

	ACTIVITY	RESPONSIBILITY	SCHEDULE
(1)	Prepare and issue Design Validation Plan	B/DOE	7/82 - 1/83
(2)	Field data collection:		
	a. Geologic mapping of vertical and horizontal underground excavations	TSC/B	3/82 - 3/83
	b. Geomechanical instrumentation measurements and visual observations in shafts, drifts, and test rooms	TSC/B	4/82 - 3/83
	c. Log core from holes in horizontal underground openings	TSC/B	10/82 - 3/83
	d. Fluid inflow measurements	TSC/B	9/81 - 3/83
	e. Shaft verticality surveys	DOE/TSC	1/82 - 3/83
(3)	Evaluate field data; prepare Preliminary Design Validation Report	B	10/82 - 3/83
(4)	Issue Preliminary Design Validation Report	DOE	3/83
(5)	Continue with (2a), (2b), (2c), and (2d) above	TSC/B	3/83 - 7/86
(6)	Evaluate/analyze field data; prepare Design Validation Final Report	B	3/83 - 5/86
(7)	Design Validation Final Report review by Peer Review Panel	B	5/86 - 6/86
(8)	Issue Design Validation Final Report	DOE	10/86

B = Bechtel National, Inc.; DOE = U.S. Department of Energy; TSC = Technical Support Contractor (Westinghouse Electric Corp.)

CHAPTER 2
BACKGROUND OF UNDERGROUND DESIGN

2.1 SITE CHARACTERIZATION AND EVALUATION

WIPP site characterization programs have consisted of geologic and hydrologic studies as well as biologic, meteorologic and economic studies. Geologic and geohydrologic characterization of the site, which started with surveys of literature and existing data, continued with the collection of new data and had the greatest degree of influence on design of the underground facility. Special emphasis was placed on correlating data obtained by geophysical techniques and borehole drilling. The geophysical techniques most widely used were seismic reflection and resistivity. Borehole drilling programs included holes drilled primarily for stratigraphic information on or near the site and holes drilled at the edge of, or away from, the site to study salt dissolution. Three holes, WIPP-11, WIPP-12 and DOE-1, were drilled through the Salado formation to acquire geologic data on deeper strata outside the Zone II boundaries of the site (refs. 2-1, 2-2 and 2-3). Within Zone II, the drilling of deep exploratory holes, i.e., to the depth of the WIPP facility level, was restricted by siting criteria. Prior to the drilling of the SPDV exploratory and ventilation shafts (subsequently known as the C & SH and waste shafts, respectively), ERDA-9 was the only borehole within Zone II that extended below the facility level.

The generalized stratigraphic relationship of the geologic formations of interest beneath the WIPP site is shown on Figure 2-1. Siltstone and fine-grained sandstone are the main rock types forming the Dewey Lake red beds. The Rustler formation, composed primarily of anhydrite and fine-grained sandstone, siltstone and mudstone, contains two water-bearing dolomite beds. Saline water is found in these beds, the Magenta and Culebra members, and at the contact between the Rustler and Salado formations. The Salado formation consists largely of halite containing thin beds of anhydrite and polyhalite with occassional thin clay seams. The Castile is a thick anhydrite and halite formation

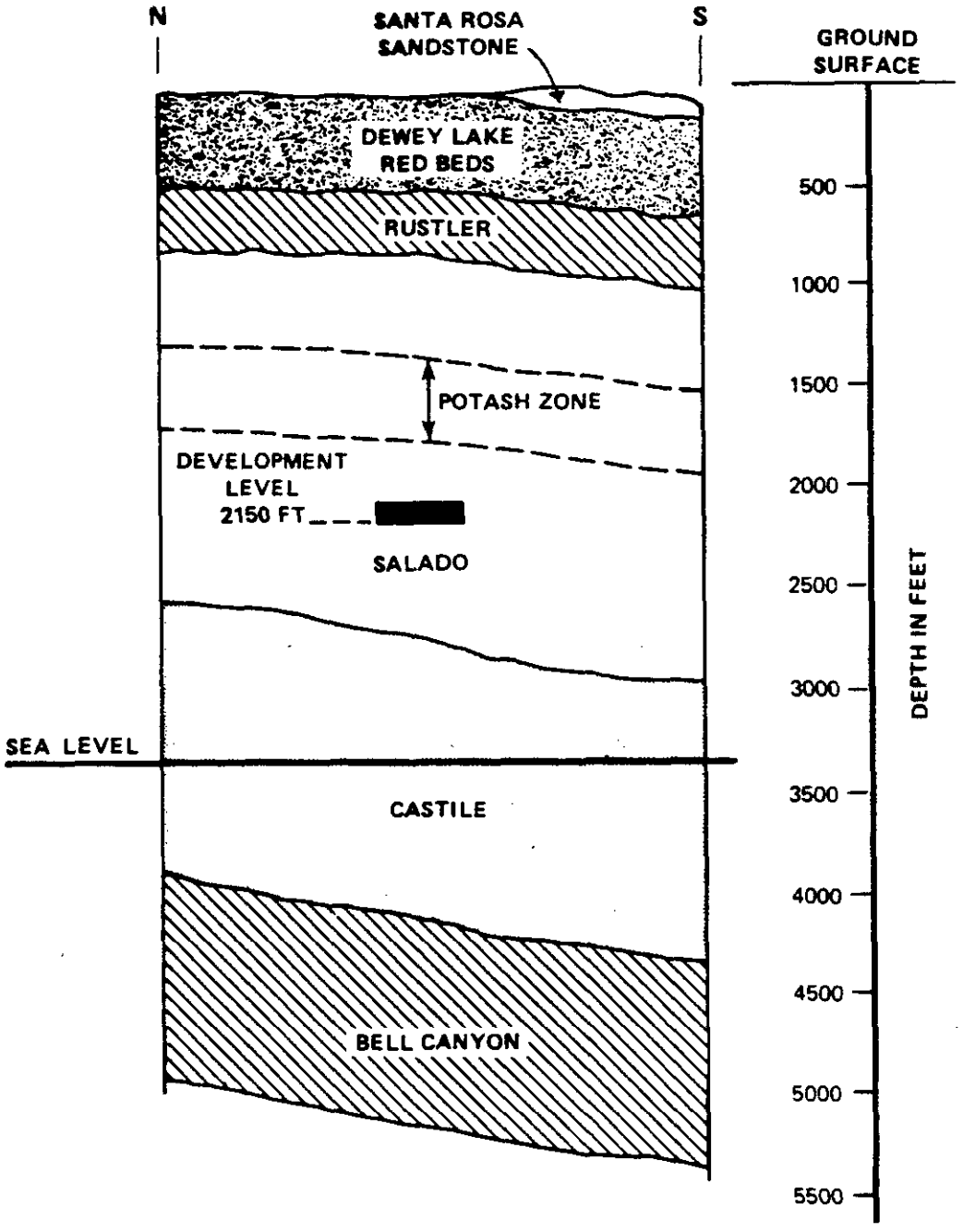

Figure 2-1

GENERAL SITE STRATIGRAPHY

M

underlying the Salado. The Bell Canyon formation consists primarily of sandstone, limestone and shale. No aquifers are present in the Salado or Castile formations beneath the site.

Site stratigraphy from the ground surface to about 250 feet below the underground facility level is presented in Appendix B, Figure B-1, Sheets 1 through 5. The stratigraphy shown is based on geologic data obtained from boreholes WIPP-12, ERDA-9 and DOE-1, and from the C & SH and waste shafts. An analysis of these data shows a strong correlation of the stratigraphy between the boreholes and shafts from the ground surface to below the underground facility level. This correlation is based primarily on the geophysical logs because core sample logging or "hands-on" mapping was not always carried out through the entire interval. Where possible, graphic lithologic descriptions based on logging or mapping of the rock strata have been included on Figure B-1 in Appendix B. This helps to more fully define the stratigraphic relationships shown by the geophysical logs.

The analysis between boreholes WIPP-12 to the north and DOE-1 to the south resulted in correlation of the major formation contacts and most marker beds in the Salado formation. Due to a lack of distinctive stratigraphic changes, the Dewey Lake red beds exhibit a relatively uniform profile in both the lithologic and geophysical logs. The Rustler formation, however, exhibits a much greater fluctuation in its geophysical profile as a result of the anhydrite, dolomite and fine-grained clastic beds it contains. Figure B-1 in Appendix B shows that the Rustler thickens slightly to the north with a slight rise in formation contacts occurring in the area of the WIPP facility.

Correlation of the Salado formation stratigraphy between WIPP-12 and DOE-1 verifies the consistency of most of the marker beds. The geophysical logs shows distinct breaks where polyhalite and anhydrite beds occur in the largely halitic rock strata. The major stratigraphic occurrence, in that portion of the Salado formation shown on Figure B-1 in Appendix B, is a thinning of strata to the north. This thinning

becomes apparent below marker bed 124 (MB-124) and is relatively well pronounced in the underground facility horizon. The effect of this thinning is to produce a reversal in the direction of dip of the strata above and below MB-124 between WIPP-12 and DOE-1. Above this marker bed the strata dip to the north, while below the marker bed the strata dip to the south. This thinning of strata controls the slope of the facility level excavation because the excavation must avoid encroachment on any stratigraphic horizons that could affect the stability or safety of the underground openings.

The figures in Appendix B show the continuity of rock strata across the WIPP site and in the area of underground excavation. These figures are intended to show that the major design assumptions which were made based on data from boreholes ERDA-9 and WIPP-12 remain valid, based on additional data obtained from geologic mapping of the underground openings and logging of underground core holes. Therefore, correlation of the site stratigraphy from the ground surface to below the underground facility level confirms the macroscopic continuity of stratigraphy beneath the WIPP site. Geologic characterization at the WIPP underground facility level is presented in Chapter 6.

Geohydrologic data pertaining to the site were obtained from conventional and special-purpose tests in many boreholes (ref. 1-5). Geophysical logging of these holes provided hydrogeologic information on the rock strata encountered. Pressure measurements, fluid samples and ranges of rock permeability were obtained for selected formations. Also, potentiometric surfaces of major aquifer systems were contoured by using measured water level elevations in boreholes.

Evaluation of data obtained from early site selection studies indicated that the current WIPP site was a suitable candidate for the establishment of a facility to demonstrate the safe disposal of radioactive waste. Additional studies have resulted in the issuance of numerous reports regarding the suitability of the WIPP site, including the Geological Characterization Report, Waste Isolation Pilot Plant

(WIPP) Site, Southeastern New Mexico (ref. 2-4), Final Environmental Impact Statement: Waste Isolation Pilot Plant (ref. 1-4), and the Waste Isolation Pilot Plant Safety Analysis Report (ref. 1-5). Final site validation was achieved in 1983 by an evaluation of the data contained in a report titled Results of Site Validation Experiments, Waste Isolation Pilot Plant (WIPP) Project, Southeastern New Mexico (ref. 2-5) which presented the results of studies performed to fully satisfy all site qualification criteria. This report was followed by a confirmation of overall site suitability in a report titled Summary Evaluation of the Waste Isolation Pilot Plant (WIPP) Site Suitability (ref. 2-6).

2.2 DESIGN CRITERIA

The Design Criteria, Waste Isolation Pilot Plant (WIPP), Site and Preliminary Design Validation (SPDV) (ref. 2-7), and the Design Criteria, Waste Isolation Pilot Plant (WIPP), Revised Mission Concept-IIA (RMC-IIA) (ref. 2-8) were used as guides by the Architect-Engineer (Bechtel National, Inc.) in developing the reference design for the WIPP underground openings. The documents contain general requirements which were addressed in the reference design. The Design Criteria, RMC-IIA, is the highest level design document for the project. All other design documents, such as design bases, drawings and specifications, were required to be in compliance with this document.

The design criteria also stipulate the type and estimated or assumed rate of waste to be received at the WIPP. The majority of the criteria presented in the RMC-IIA document are requirements which do not need evaluation as to their suitability and have no impact on validation considerations for the underground opening reference design. The major criteria that governed development of the reference design are presented in Table 2-1. Although some of the criteria in this table are elements which cannot be evaluated, they are included because of their influence on the reference design configurations. Those criteria that can be evaluated are discussed in later chapters of this report as

Table 2-1

ABRIDGED WIPP DESIGN CRITERIA

(1) Facility design

a. Designed for an operating life of 25 years.

b. Underground facilities and equipment shall be designed to be compatible with retrieval operations for all contact-handled (CH) and remote-handled (RH) TRU waste, with a retrieval decision to be made within 5 years after the initial emplacement of each species. (Chapter 12)

c. The facility will be decommissioned after it has fulfilled its intended purposes. This will include backfilling the underground facilities, sealing the shafts and decommissioning the surface facilities.

(2) CH TRU waste *

a. Estimated annual volume is 500,000 cubic feet.

b. Estimated volume at the end of the 5 year retrieval decision period is 1,410,000 cubic feet.

c. Estimated total storage capacity is 6,330,000 cubic feet.

d. Heat generated from the waste is negligible; it will be less than 10 milliwatts for average drums, less than 20 milliwatts for average boxes, and 10 watts for few drums containing heat source plutonium.

e. Estimated annual quantities are 9,616 six-packs and 2,404 modular steel boxes.

f. Estimated total quantities are 121,700 six-packs and 30,430 modular steel boxes.

g. Underground facilities and equipment shall be designed to provide for a determination to effect retrieval of waste stored for a period up to 5 years after the initial emplacement and for a target of 5 to 10 years to reach the waste and retrieve it after the decision is made. (Chapter 12)

(3) RH TRU waste *

a. Assumed total receipt of 1,000 canisters.

b. Assumed maximum receipt rate of two canisters per day and 250 canisters per year.

* See Foreword.

Table 2-1 (continued)

ABRIDGED WIPP DESIGN CRITERIA

c. If assumed quantities are insufficient, additional RH waste storage will be accommodated within existing storage rooms.

d. Heat generated from the waste is on the order of 60 watts per canister.

e. Access shall be available to all emplacement positions throughout the retrievability period. (Chapter 12)

f. When both CH and RH waste are scheduled for the same room, the RH waste shall be emplaced first. After the 5 year retrievability period has terminated, CH waste may be emplaced in that room.

(4) Shaft design (Chapters 7, 8 and 9)

a. Shafts shall be designed to be structurally stable throughout the operating life of the underground facility and the decommissioning period.

b. Time-dependent closure of shafts due to salt creep shall be considered. Shafts shall be designed so that minimum dimensions required for shaft functions are maintained during design life.

c. Ground-water flow into the shafts shall be controlled so that no uncontrolled ground water reaches the storage horizon via the shafts.

(5) Shaft liner design

a. Help ensure that dimensions remain within limits required for shaft functions.

b. Prevent ground-water flow into the shaft. (Chapters 7, 8 and 9)

c. Protect wall rock from deterioration.

d. Preclude risk of rock fall from shaft wall.

(6) Mine design

a. The underground openings shall be designed so that deformation of excavations and pillars will remain within limits required for structural function, ventilation and safety. (Chapters 7, 8 and 10)

Table 2-1 (continued)

ABRIDGED WIPP DESIGN CRITERIA

b. Rock bolts shall be used where necessary to provide positive support of roofs and walls.

c. Surface subsidence resulting from underground excavation shall not exceed 1 inch within a 500-foot radius of the waste shaft. (Chapter 6)

d. Excavations and pillars shall be located and dimensioned to avoid geologic discontinuities. If discontinuities are encountered, remedial action shall be engineered to correct the problem. (Chapters 3 and 6)

e. Design shall be based on established mining procedures.

f. Predicted behavior of the salt shall be verified by in situ testing (SPDV) before proceeding with construction of the storage area.

g. Designed to accommodate creep closure and maintain the minimum dimensions required for the operating life of the opening. (Chapters 10 and 12)

h. Creep closure rates used for design shall be confirmed by instrument observations in the excavations. (Chapters 11 and 12)

i. Excavation dimensions shall include allowance for creep closure sufficient to prevent container breaching by creep-induced stresses during the retrievability period. (Chapter 12)

j. Minimize the potential for repository rock fracturing. (Chapter 11)

k. Underground waste storage procedures shall include a designed backfill plan for fire protection. The backfill thickness shall be 1 to 2 feet. (Chapter 12)

l. Permit isolation of panels of rooms with plugs after storage and backfilling are completed. (Chapter 12)

m. Air locks, dampers, regulators and doors shall be designed and installed in such a manner that they can accommodate creep without impairment to their ability to maintain ventilation separation.

Table 2-1 (continued)

ABRIDGED WIPP DESIGN CRITERIA

(7) Emplacement criteria

a. The underground storage rooms and access drifts shall be designed to be compatible with the waste transport vehicle, with waste container sizes, shapes, weights and stacking configurations, and with waste emplacement equipment. (Chapter 12)

b. Provisions shall be made to accommodate backfilling over and around CH waste containers. (Chapter 12)

c. Each storage panel shall have provisions for being isolated from other panels upon completion of storage operations in that panel. (Chapter 12)

(8) Retrievability

a. All wastes placed into the WIPP are retrievable, with retrievability to be demonstrated, until such time as the pilot plant is converted to an operational repository for permanent disposal of wastes. (Chapter 12)

b. Each storage room shall allow for salt creep and shall be sized to minimize breaching of the CH waste containers for a period of 10 years. (Chapter 12)

(9) Underground excavation and haulage

a. Mining shall be performed with continuous miners or equivalent machine type devices. Drill and blast-type mining shall be prohibited except where authorized.

b. Underground design shall provide maximum stability for excavated rooms and entries. (Chapters 7, 8, 10, 11 and 12)

c. Meet or exceed the intent of the applicable requirements of the MSHA in 30 CFR 57.9 and the New Mexico Mine Safety Code for All Mines.

indicated in the table.

2.3 DESIGN BASES

The design bases identify the detailed design requirements for the WIPP underground facilities. They are derived from the more general concepts presented in the design criteria. The design bases cover all aspects of the design and facility operations. Design bases applicable to design validation are listed in references 2-9 through 2-20. The essential elements of the design bases pertaining to design validation of the C & SH shaft, waste shaft, exhaust shaft, drifts and storage area are discussed in Chapters 7 through 10 and Chapter 12. The discussions cover only those bases that require evaluation. All other bases are requirements determined during design reviews and need not be evaluated for their suitability.

2.4 DESIGN CONFIGURATIONS

The reference design configurations are the engineered facilities designed to comply with the design criteria and design bases. They are described in various contract drawings and specifications. The essential elements of the design configurations are discussed in Chapters 3 and 12.

2.5 DESIGN DEVELOPMENT

Design of the WIPP surface and underground facilities consisted of three stages:

(1) the conceptual design;

(2) the preliminary design; and

(3) the detailed design, including the underground opening reference design.

At both the conceptual and preliminary design stages, an extensive, independent review of the underground layout and design was made by the

DOE and its consultants, SNL and Westinghouse Electric Corporation. The review included assessment of the underground design concept and consultation with Carlsbad area potash mine operators to obtain information from their experience. The preliminary design was also reviewed by other Federal agencies, the State of New Mexico and the NAS.

From these reviews and consultations, the DOE concluded that the detailed design, based on the current state of the art, was sound. However, for further confirmation, it was decided that the impact of site-specific geologic conditions on the underground opening reference design should be verified by direct observation. Consequently, the DOE initiated the SPDV Program described in Chapter 1. The SPDV Program provided in situ data on the local geology and on the geomechanical response of the strata to the underground openings.

2.5.1 Conceptual Design

Design of the WIPP surface and underground facilities began with the conceptual design, initiated in 1975 and completed in 1977 (ref. 2-21). The conceptual design provided the basis for development of the preliminary design of both the surface and underground facilities.

2.5.2 Preliminary Design

The WIPP preliminary design was begun in 1978 and completed in 1980 (ref. 2-22). The preliminary design (Figure 2-2) was based on empirical methods and local mining practices, incorporating the conventional room and pillar method for underground development. It included analytical evaluations of underground openings in bedded salt using the finite element method and laboratory test data (refs. 2-23 and 2-24). The roof and floor of the rooms and entries were checked for stability by methods described in the SME Mining Engineering Handbook (ref. 2-25). In addition to Bechtel, SNL performed confirming numerical analyses (refs. 2-26 and 2-27). These analyses predicted short- and long-term stress distributions around the selected openings as well as elastic and creep deformations.

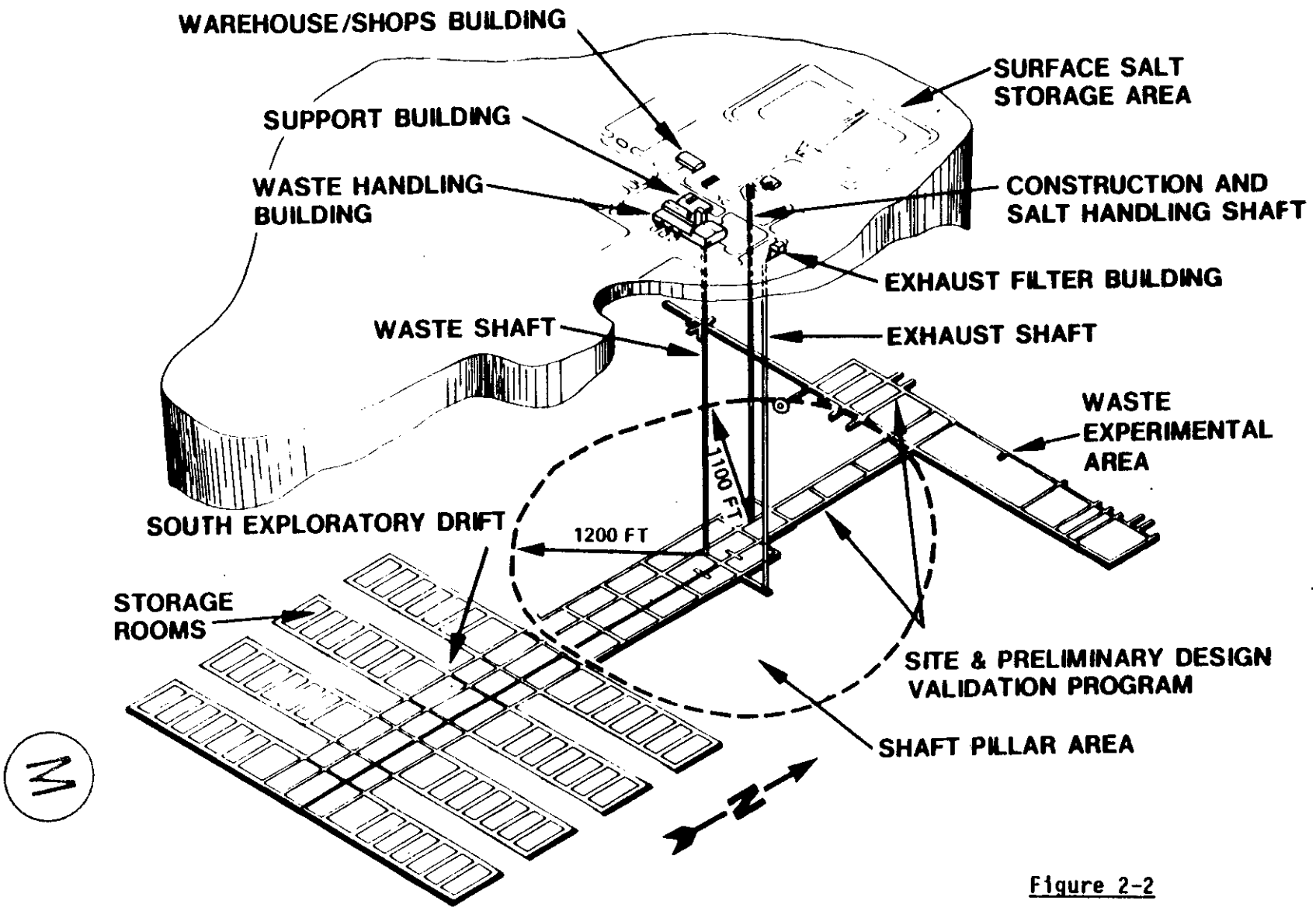

Figure 2-2

PERSPECTIVE VIEW OF THE WIPP

2.5.3 Detailed Design

Detailed design of the WIPP, begun in 1981 and completed in 1984, included design of the surface and underground facilities and the reference design for the underground openings. This was based on an extensive amount of data derived from the site characterization, including information from boreholes, surface geophysical measurements and laboratory tests. These data were used to establish the facility level and the design parameters. The number of holes drilled to the proposed facility level was restricted in order to retain its isolation from the surface. The layout and configuration of the underground openings were based mainly on empirical data which incorporates the room and pillar concept utilized in existing potash mines in Carlsbad and other mining areas, and on storage efficiency. The design was also based on mining and engineering standards universally applied to underground projects.

Analyses were performed to evaluate the stability of underground openings using material properties obtained from laboratory tests of core samples (ref. 2-28). Validation of the underground opening reference design with respect to the actual underground environment requires direct observation of geologic conditions at the facility level and the behavior of the underground openings. This interaction between observation of underground excavation and development of design is consistent with engineering practice for underground construction and with achieving the most cost-effective facility configuration.

Detailed design of the WIPP had sufficient flexibility to allow the incorporation of initial information obtained from excavation during the SPDV Program. This design flexibility was necessary for construction of the underground facilities. Calculations that applied material properties and analytical models developed from laboratory tests were performed to evaluate the behavior of the underground openings. Information obtained from the design validation program was used to confirm, refine, or alter the underground opening reference design as required to accommodate in situ conditions. The detailed

design included the development of construction details for the experimental areas and the full-scale waste storage area. It also included design of the surface facilities but this is not included in the design validation program.

2.6 DESIGN METHODS

Practical experience in the safe construction of salt and potash mines extends over many years. Empirical knowledge on the safe sizes of openings and pillars has been documented (ref. 2-29) and performance records of openings in salt are available. Different methods of analysis are required to determine the stability of openings in salt for different conditions of potential failure. The normal safety concepts of engineering, which relate a factor of safety to loads or stresses, cannot be transferred directly to the analysis of underground openings in salt. Therefore, postulated failure conditions were analyzed by other appropriate methods. In general, an opening in salt can be considered stable when the following two basic requirements are satisfied:

(1) the deformation of the opening conforms to the clearance envelope allowed for safe operation of the workings during design life; and

(2) the load bearing capacity of the salt around the opening is adequate to prevent sudden structural failure of the opening.

Subsections 2.6.1 through 2.6.3 discuss the empirical methods, closed form solutions and model simulations used for the reference design of the WIPP underground openings.

2.6.1 Empirical Method

Most of the seven potash mines in the Carlsbad area were visited by project participants on several occasions as the design evolved. The preliminary room and pillar configurations, including the width and

spacing of the rooms, drifts and pillars, were based primarily on experiences gained from general mining practices in those mines in areas with similar geology. The extraction ratio at the WIPP facility horizon is significantly less than that used in potash mines of similar depth in the Carlsbad area and in other parts of North America.

2.6.2 Closed Form Solutions

Closed form solutions in the SME Mining Engineering Handbook were used to check the design of the room-and-pillar system, including room dimensions, room spacing, pillar stresses and pillar width-to-height ratios. These types of solutions were also used to check room stability, including the stresses on the roof beams, and to estimate surface subsidence (ref. 2-30). Closed form solutions for steel and concrete structural design were used for design of the shaft liners and keys.

2.6.3 Model Simulation

To determine the geomechanical and structural behavior around the underground openings, mathematical models of the openings were generated and preliminary finite element analyses were performed to simulate this behavior. These analyses used material properties obtained from laboratory tests of drill core samples to estimate closure of the openings. In order to maintain the operational capability of the underground facility during its design life, allowances for roof, floor and wall closures were added to the operational clearance envelope of the underground openings. The design criteria require confirmation or modification of the estimated closure based on geomechanical instrument measurements obtained in the excavations.

Preliminary analyses were only considered parametric studies since important feedback from the design validation program observations and geomechanical instrument measurements was required to complete the understanding of the mechanism of creep deformation in the salt at the WIPP site.

CHAPTER 3
UNDERGROUND FACILITIES

3.1 INTRODUCTION

This chapter presents a brief history of the underground development level selection process. It also describes the configurations of the WIPP shafts, drifts and rooms, and summarizes their excavation history. The discussion of excavation history includes those details pertaining to the "as-built" openings which are considered significant with respect to the reference design. The reference design of the underground openings was based on requirements contained in the Design Criteria (refs. 2-7 and 2-8) and Design Bases (refs. 2-9 through 2-20) documents.

The WIPP underground facility is divided into three general areas (Figure 3-1). The northern portion is the experimental area containing the design validation test rooms and technology experiments. The central area is the shaft pillar. The number of drifts in this area is restricted to minimize subsidence around the shafts. This portion of the facility will primarily contain shops and personnel areas. The southern portion of the facility is the waste storage area. Although some mining has been conducted in this area, it remains largely unexcavated at the time of publication of this report.

3.2 SELECTION OF THE UNDERGROUND DEVELOPMENT LEVEL

Selection of the WIPP underground development level evolved over several years and various facility design concepts. Seven stratigraphic horizons were identified in 1979 as potential locations for the facility level and ranked in order of their preference. These seven horizons were chosen based on an examination of available borehole data, primarily geologic and geophysical logs from borehole ERDA-9, and on horizon selection criteria established by the WIPP project participants. The selection criteria consisted of recommended distances between the underground opening surfaces and the nearest overlying or underlying clay seams or partings.

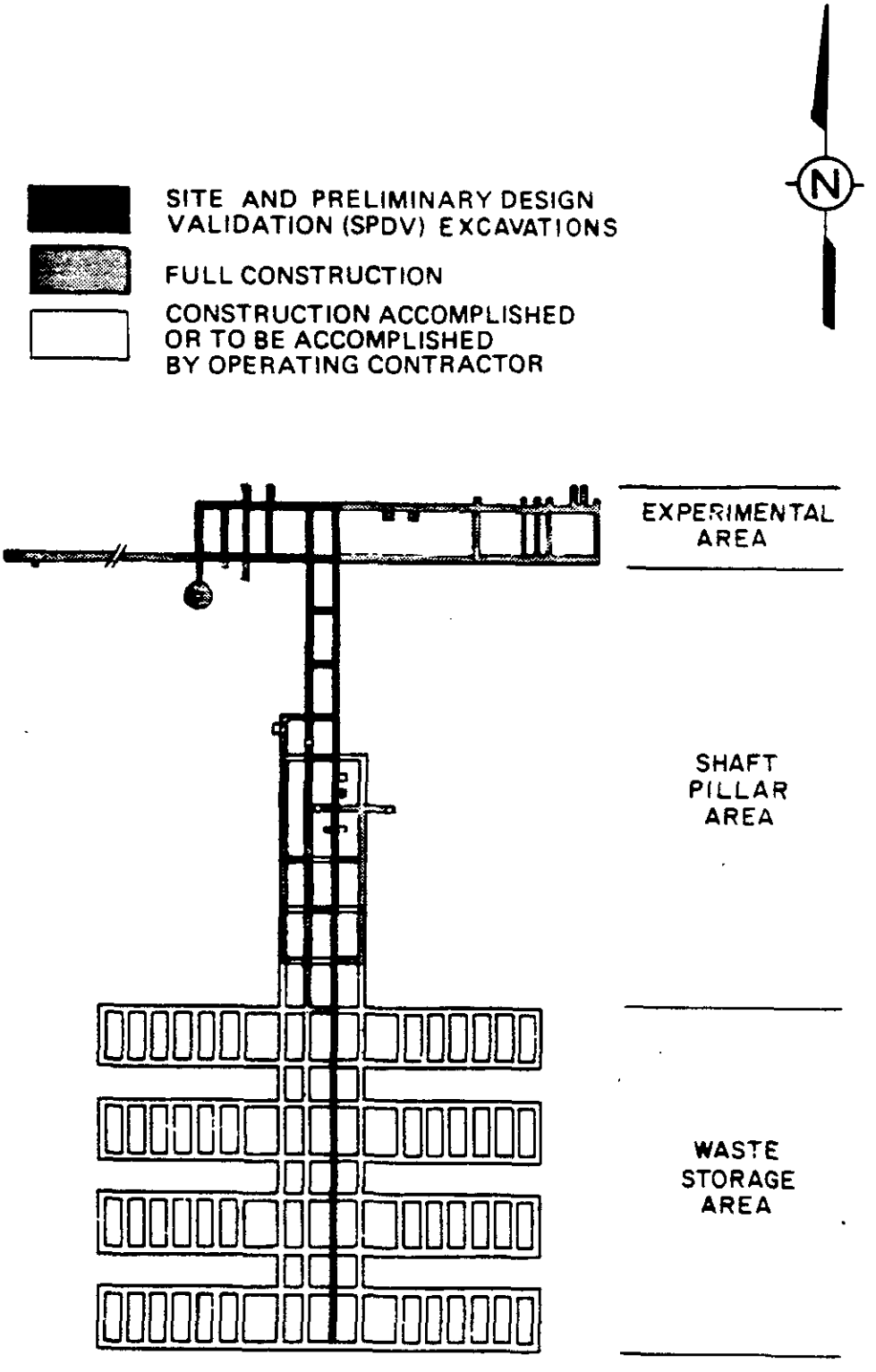

Figure 3-1

FUNCTIONAL AREAS OF THE UNDERGROUND FACILITY

Geologic mapping of the SPDV exploratory shaft in April and May 1982 permitted an assessment of the suitability of those intervals in the area of MB-139 preferred for the location of the facility level. This assessment included an evaluation of the intervals of interest against a modified version of the 1979 horizon selection criteria. These modified criteria were a result of changes to the initial WIPP facility concept, consisting of a reduction from two levels to one and alterations in the room size. The modified criteria were as follows:

(1) The rock comprising the underground facility horizon should contain no significant dissolution features, faults, or fractures. If any such features are noted, a detailed investigation must be conducted. (This element was not explicitly stated in the 1979 criteria.)

(2) There should be a minimum 4-foot thickness of halite between the top of MB-139 and the facility floor. The undulatory upper contact of MB-139 shall be considered in the selection of the facility floor level. (The 1979 criteria required a 5-foot thickness between the facility floor and the first underlying clay seam or parting.)

(3) There should be a minimum 14 1/2-foot section of halite for construction of nominal 13-foot high rooms. Minor impurities, such as argillaceous halite and polyhalite, may be acceptable. (The facility design in 1979 called for 12-foot high rooms.)

(4) There should be a minimum of 5 feet of halite between the facility roof and the first overlying clay seam (defined as 1/4 inch thick or greater) for purposes of roof stability. (This criterion was adjusted at the site to a 5- to 10-foot thickness at the verbal request of SNL personnel.)

(5) Horizons containing substantial amounts of polyhalite should be avoided. The minimum thickness of halite defined in the

third criterion listed above was increased from 14 1/2 feet to 17 feet or more to accommodate the 17-foot high SPDV exploratory shaft station.

Selection of the final underground development level was made following a series of meetings in which the interval ranked first was evaluated for its ability to satisfy these criteria. The selection was based primarily on the results of detailed geologic shaft mapping from a depth of 2,080 feet to 2,185 feet. A meeting, attended by representatives from the DOE, Westinghouse, SNL and Bechtel, was held on May 2, 1982, to discuss the results of the selection process and to present a recommendation for the facility level location to the DOE. The final level selected for the facility floor was at a preliminary depth of 2,149 feet (elev. 1258.4 feet). The recommendation was accepted by the DOE and later reviewed and concurred in by a representative of the New Mexico Environmental Evaluation Group (EEG).

Geologic mapping of the SPDV exploratory shaft and subsequent evaluation by the project participants showed that, as anticipated, the geology was similar to that encountered in borehole ERDA-9. One exception was the discovery of an additional anhydrite bed, anhydrite "b", and its underlying clay seam. Figures 3-2 and 3-3 show the preliminary design (pre-SPDV) of the shaft station and storage rooms. This preliminary design was based on the stratigraphy at the first-ranked alternative horizon. Figures 3-2 and 3-3 show that only one anhydrite layer and clay seam were expected above the facility level at this horizon, based on the interpretation of ERDA-9 core. This would have produced 12 feet of uninterrupted halite above the shaft station and 16 feet above the storage rooms. However, shaft mapping revealed an intermediate bed, anhydrite "b", approximately 7 feet below the known bed, anhydrite "a". This reduced the uninterrupted halite thickness above the facility level roof to 3.5 to 5 feet at the shaft station and 7 to 8.5 feet in the waste storage area. Despite this finding, the underground facility horizon chosen was judged to adequately meet all of the established criteria.

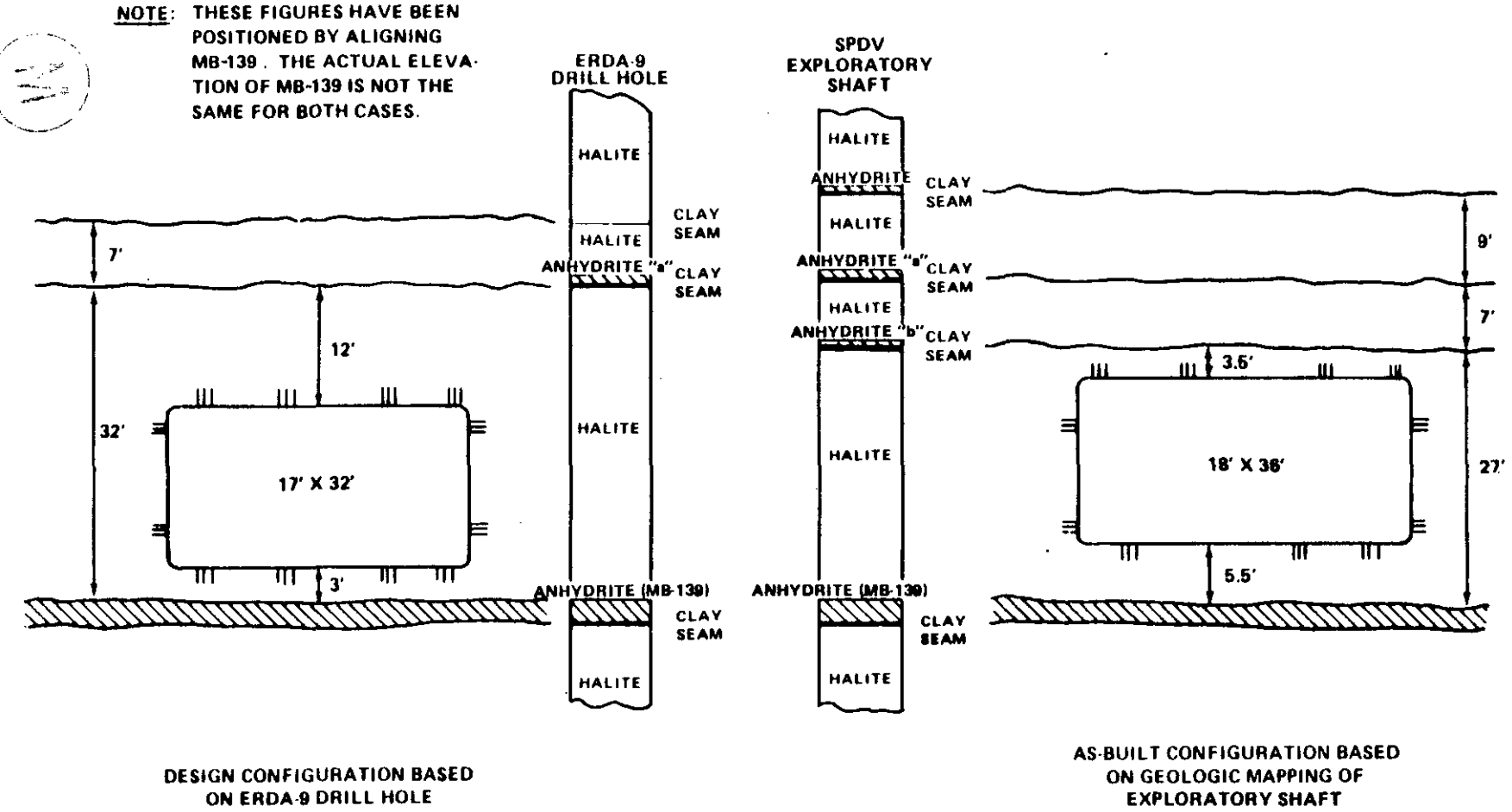

Figure 3-2

SPDV EXPLORATORY SHAFT STATION
DESIGN VERSUS AS-BUILT CONFIGURATION

NOTE: THESE FIGURES HAVE BEEN POSITIONED BY ALIGNING MB-139. THE ACTUAL ELEVATION OF MB-139 IS NOT THE SAME FOR BOTH CASES.

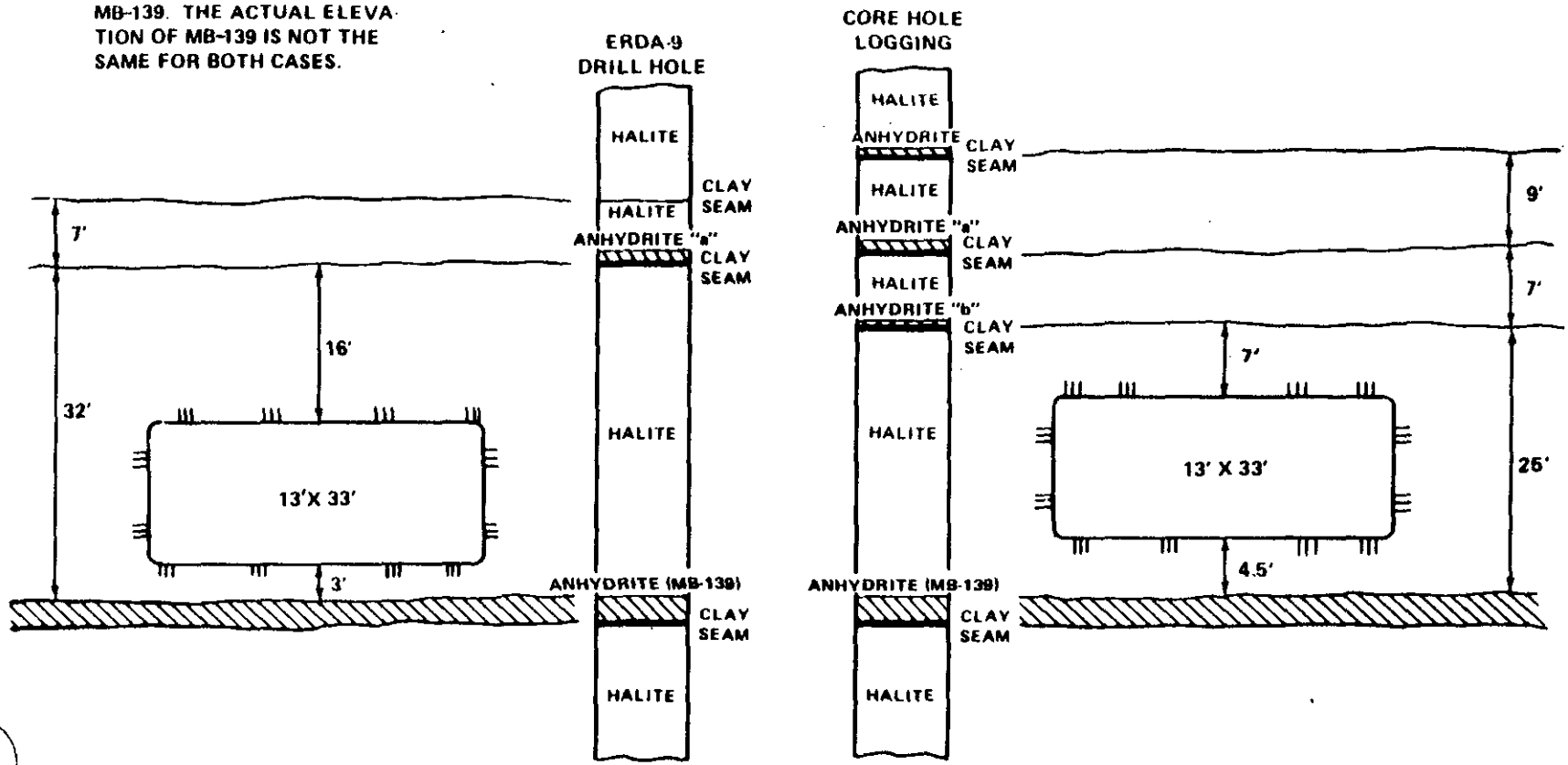

DESIGN CONFIGURATION BASED ON ERDA-9 DRILL HOLE

REVISED CONFIGURATION BASED ON CORE HOLE DATA

Figure 3-3

STORAGE ROOM
DESIGN VERSUS REVISED CONFIGURATION

At a meeting held on February 13, 1986, consideration was given to the desirability of relocating the facility level to a different stratigraphic horizon (ref. 3-2). The discussion was prompted by the following observations of the behavior of the underground openings:

(1) The effect of excavation on the strata surrounding the underground openings are being investigated by gas permeability testing. These tests indicate that zones of increased permeability due to fracturing, and proportional to the size of the opening, have developed between the floor of the openings and the base of MB-139 in the test rooms. These zones have also developed at intersections and other locations in the N1420 drift. Increased permeability has also been detected within anhydrite "b" above the roof of the test rooms. (Additional permeability testing is being conducted by SNL. The final results from this program are not yet available.)

(2) Fracturing has been encountered both within and above MB-139. It is especially well developed in the southern half of Test Room 3 (Room T). This fracturing is discussed in Chapter 10, subsection 10.3.2.1, and in Chapter 11, subsection 11.3.2.1.

(3) Both horizontal displacements and vertical separations have been observed above the roof of the underground openings. These occur primarily at anhydrite "b" and are associated with the underlying clay seam. This is discussed in Chapter 10, subsection 10.3.2.1, and in Chapter 11, subsection 11.3.2.1.

(4) In situ closure rates are almost three times greater than the rates originally predicted from laboratory test data. This is discussed in Chapters 10, 11 and 12.

The underground opening behavior occurring at the WIPP is similar to that of other openings excavated in areas with similar geologic formations. The conditions are understood and any problems encountered can be adequately mitigated using standard mining engineering procedures. The behavior experienced at the present facility level is likely to occur to some extent at any alternate horizon selected. These conclusions, and the fact that the behavioral characteristics and geologic environment at the existing level are known, resulted in a decision by the WIPP project participants to keep the facility level at its present location. Studies of the behavior of the rooms and drifts will continue beyond design validation as discussed in Chapter 1, subsection 1.5.2.

3.3 DESCRIPTION OF UNDERGROUND FACILITIES

3.3.1 C & SH Shaft

The construction and salt handling (C & SH) shaft is the principal means of access to the underground WIPP facility and is the primary fresh-air intake for the underground ventilation system. It was originally designated the exploratory shaft during the SPDV Program. The shaft provides a means of access for personnel and materials to and from the facility, and for the removal of excavated salt. Geomechanical instrumentation installed in the shaft provides important data for monitoring the behavior of the liner and key, the salt strata surrounding the shaft. and ground-water pressures.

The shaft is lined with steel casing having a 10-foot inside diameter from the ground surface to a depth of 846 feet. The 10-foot diameter extends through the concrete shaft key to a depth of 880 feet. From the key to the bottom of the shaft at 2,298 feet the shaft is a nominal 12 feet in diameter and is unlined.

The steel liner was designed to retain the rock formations above the salt and to prevent water seepage into the shaft. The liner was designed for both construction and permanent loads. The construction load was considered to be the hydrostatic pressure exerted on the liner

by the fluid used to "float" it into place for installation. The permanent load is the hydrostatic pressure exerted on the liner by ground water under artesian conditions in the water-bearing zones. Rock pressure was not used in design due to the controlling influence of the hydrostatic pressure. Since hydrostatic pressure increased with depth, the steel liner thickness was also increased. The liner is 5/8 inch thick at the top and increases to 1 1/2 inches thick at the bottom. The liner is held in place with cement grout.

The C & SH shaft key is a 37 1/2-foot long reinforced-concrete structure at the base of the steel liner. The key serves two important functions. First, it provides a transition from the lined to the unlined sections of the shaft. Second, as an integral part of the liner, it prevents ground water from the upper water-bearing members from dissolving the salt around and beneath the key. This water movement is obstructed primarily by two water seals installed behind the concrete. A third seal, installed at the interface of the steel liner and concrete key, prevents water from flowing out at the interface and down the inner surface of the key. A gravel-filled trench was constructed behind the concrete above the lower of the two seals to intercept water migration past the upper seal. This water is drained through four pipes, called "telltales", to the key surface and into a water collection ring at the base of the key.

The shaft is unlined below the concrete key. Excavation by the rotary drilling method has resulted in shaft walls that are smooth and undamaged. No support or protective wire mesh was required.

3.3.2 Waste Shaft

The waste shaft serves to connect the waste handling building on the ground surface with the WIPP underground facility. The shaft's primary function is to permit the transfer of radioactive waste from the surface to the underground storage area. It will also serve as an intake shaft for small volumes of air during storage operations and as an emergency escape route. The waste shaft was initially excavated as

a 6-foot diameter ventilation shaft, which was the primary exhaust route during the SPDV phase of construction. As in the C & SH shaft, geomechanical instruments installed in the waste shaft provide important geotechnical data with which to monitor the behavior of the shaft and its surrounding geologic environment.

The waste shaft is lined with unreinforced concrete from the ground surface to the top of the key at a depth of 837 feet. The purpose of the liner is to retain the surrounding rock and to prevent ground water from entering the shaft. The lined section of the shaft has a finished inside diameter of 19 feet. The liner thickness increases with depth from 10 inches at the surface to 20 inches at the key. A water collection ring was incorporated into the liner immediately beneath both the Magenta and Culebra water-bearing members. These rings are connected to another ring at the base of the key.

The waste shaft key is similar in construction to the C & SH shaft key. It serves as a transition from the concrete-lined section to the exposed salt section of the shaft and it prevents ground water from reaching the salt via the shaft opening. The key is 63 feet long, 4 1/4 feet thick and constructed of reinforced concrete. The bottom of the key is at a depth of 900 feet. In contrast to the C & SH shaft key, the waste shaft key has only two water seals.

A water collection ring at the base of the key collects water trickling down the surface of the key and conducts it, as well as water from the two upper rings, to the shaft station via a 2-inch diameter PVC pipe. Two guide pipes, consisting of 2-inch diameter polyvinyl chloride (PVC) pipe, were also installed in the concrete key at a depth of 843 feet at the request of SNL to serve as guides for drilling test holes across the contact of the Rustler formation with the Salado formation.

The section of the shaft below the key is 20 feet in diameter and consists of exposed salt lined with wire mesh anchored by rock bolts. The 20-foot diameter shaft enlarges to 23 feet just above the waste

shaft station. This 23-foot diameter extends to the bottom of the shaft, approximately 122 feet below the facility level.

3.3.3 Exhaust Shaft

The exhaust shaft is the primary ventilation exhaust for the underground facilities. It is designed as a duct to remove air from the underground areas up through the exhaust filter building at the ground surface. In addition, the exhaust shaft will serve as a backup escape route during emergencies. This shaft is also used to carry an auxiliary 15 kV power cable and signal cables underground. These redundant cables serve as emergency alternates should the primary cables in the C & SH shaft become inoperative. The exhaust shaft, like the C & SH and waste shafts, contains a suite of geomechanical instruments.

The exhaust shaft is lined with unreinforced concrete from the ground surface to the top of the shaft key at a depth of 844 feet. The purpose of the liner is the same as that in the other two shafts. The liner has an inside diameter of 14 feet. The liner thickness increases from 10 to 16 inches with depth.

The exhaust shaft key serves the same function as the keys in the other two shafts. It is a transition element between the concrete liner in the upper section of the shaft and the exposed salt in the lower section. It is also designed to prevent ground water in the upper water-bearing members from reaching the salt section of the shaft. The key is 63 feet long and 3 1/2 feet thick. The key contains eight telltale drains at a depth of 857 feet and nine drains each at 855 feet and 870 ft. The key also contains two water seals, a water collection ring, and two guide pipes for drilling test holes. The bottom of the key is at a depth of 907 feet.

The exhaust shaft below the key is 15 feet in diameter. It is lined with wire mesh anchored by rock bolts. The exhaust shaft terminates at the facility level; there is no shaft sump.

3.3.4 Drifts

The underground shaft stations and drifts have been designed to facilitate the handling and transport of radioactive waste. They also provide access for construction operations and experimental activities. The drifts are designed to provide adequate ventilation supply and exhaust for all areas of the underground facility.

All drifts are rectangular in cross section with typical dimensions that range from about 8 to 12 feet high and 14 to 25 feet wide. Access drifts serve as the main haulageways between the shafts and the experimental and waste storage areas. Cross-cut drifts (crosscuts) are designed to accommodate equipment, shops and traffic flow. The crosscuts are generally smaller in cross-sectional dimensions than the access drifts. The excavated dimensions of major drifts and rooms are presented in Table 3-1. The horizontal underground openings are oriented either north-south or east-west and are labeled based on a grid system having the centerline of the C & SH shaft as its origin. For example, the E0 drift runs north-south in line with the C & SH shaft and the N1100 drift is an east-west drift 1100 feet north of the C & SH shaft.

The northern part of the facility contains the experimental areas. Four test rooms were excavated west of the E0 drift as part of the SPDV Program. These rooms are discussed in subsection 3.3.5. The remaining experimental areas have been excavated for long-term experimental programs to be conducted under the direction of SNL. These experiments are not part of design validation and are addressed in this report only when necessary to clarify the discussion.

The shaft pillar area (Figure 3-1) is designed to protect the surface structures and shafts from settlement resulting from the natural closure of underground openings. The shaft pillar dimensions were derived in accordance with standard analyses developed by the U.S. Bureau of Mines (ref. 2-30). Excavation within the shaft pillar area was designed to maintain an extraction ratio of less than 15 percent.

Table 3-1

FACILITY LEVEL CONFIGURATIONS
NOMINAL EXCAVATED DIMENSIONS OF MAJOR DRIFTS AND ROOMS

Drift or Room					Width (ft)	Height (ft)
E0	From	N35	To	N1420	25	12
E140	From	N140	To	N1420	14	8
E140	From	N140	To	S2210	25	12
E140	From	S2210	To	S3264 (Exploratory Drift)	25	8
E300	From	S90	To	S1980	14	12
W30	From	S90	To	S700	20	12
W30	From	S700	To	S1950	14	12
W170	From	N140	To	S1300	14	12
N140	From	E0	To	E140	12	12/19
N140	From	E0	To	W170	12	12/19
N460	From	E0	To	E140 (Conference Room)	20	8
N780	From	E0	To	E140	12	12
N1100	From	E0	To	E1546	14	9
N1100	From	E0	To	W667	20	12
N1100	From	W667	To	W1800 (Room G Entry Drift)	20	9
N1100	From	W1800	To	W2990 (Room G)	20	10
N1420	From	E140	To	E1546	14	12
N1420	From	E140	To	W647	20	12
S90	From	E0	To	E140	12	12
S90	From	E140	To	E300	14	12
S400	From	E60	To	E140	20	12
S400	From	E140	To	E300	14/18	12/17
S400	From	E300	To	E500	20	12
S700	From	W170	To	W30	20/25	12
S700	From	W30	To	E140	20	12
S700	From	E140	To	E300	20/35	12
S1000	From	W170	To	W30	20	12
S1000	From	W30	To	E140	25	12
S1000	From	E140	To	E300	20	12
S1300	From	W170	To	W30	20	12
S1300	From	W30	To	E140	20	12
S1300	From	E140	To	E300	20	12
S1600	From	W170	To	W30	20	12
S1600	From	W30	To	E140	20	12
S1600	From	E140	To	E300	20	12
S1600	From	E300	To	E520	14	12
S1950	From	W30	To	E140	14	12
S1950	From	E140	To	E300	20	12
S2180	From	E140	To	E300	14	12

Table 3-1 (continued)

FACILITY LEVEL CONFIGURATIONS
NOMINAL EXCAVATED DIMENSIONS OF MAJOR DRIFTS AND ROOMS

Drift or Room	Width (ft)	Height (ft)
Test Rooms 1, 2, 3 & 4 (300 feet long)	33	13
Experimental Rooms A1, A2, A3, B & D (306 feet long)	18	18
Alcove I1 (43 feet long)	24	12
Alcoves I2, I3, I4, I5, I6 & I7 (33 feet long)	33	12
Rooms C1 & C2 (98 and 102 feet long)	18	18
Room J (98 feet long)	33	12
Rooms L1 & L2 (98 feet long)	33	12
Room H Entry	12	10
Room H (outside radius = 54 feet)	36	10

A geomechanical instrumentation program was implemented to gather geotechnical data from the underground drifts. The program was designed to monitor the stability of the openings, to assess deformational characteristics of the salt, and to measure closure rates of typical drifts, rooms and intersections. In addition, an extensive program of geologic mapping, core drilling, laboratory testing and visual observations has been conducted. The methodology used and the results of these programs are discussed in other chapters of this report.

3.3.5 Test Rooms

Four test rooms were excavated in the northern section of the facility during the SPDV phase of construction. These rooms represent full-scale models of the future waste storage rooms and have the same dimensions, 13 feet high, 33 feet wide and 300 feet long, as the planned storage rooms.

The test rooms are designed to permit an assessment of deformation and closure rates due to salt creep as well as the stability of the future storage rooms. This has been accomplished by evaluations and analyses of geotechnical data gathered from geomechanical instruments installed in each room and the results of geologic mapping, core drilling, laboratory testing of samples from the surrounding strata, and qualitative visual observations by project geotechnical personnel. The results of these evaluations and analyses are presented in Chapters 11 and 12.

3.3.6 Waste Storage Area

The waste storage area will be developed in the southern portion of the facility (Figure 3-1). The reference design for this area includes a series of eight panels with seven storage rooms in each panel. The room dimensions are 13 feet high, 33 feet wide and 300 feet long. The width of the pillars between rooms is 100 feet. This configuration results in a storage area extraction ratio of less than 25 percent based on a line 100 feet beyond the storage area excavation neat line.

Full development of the waste storage area will eventually encompass about 140 acres. The reference design is based on the assumption that the storage rooms and panels will be excavated in stages coordinated with the scheduled arrival of waste. Waste storage is designed not only for the rooms but also for all drifts and crosscuts in the waste storage area (south of the S1600 drift).

3.4 UNDERGROUND CONSTRUCTION

The existing WIPP underground facility was constructed in two phases. The first phase, SPDV (Figure 3-1), was conducted from 1981 to 1983 and consisted of the excavation of the exploratory and ventilation shafts as well as several drifts and a panel of four test rooms. SPDV accomplished two objectives: (1) it permitted the completion of experiments and geotechnical activities required for the Site Validation Program (ref. 2-5); and (2) it provided for the initial in situ confirmation of the underground facility reference design. This allowed construction of the underground facility to proceed in a timely and cost-effective manner.

Excavation associated with the second phase of underground construction was accomplished from October 1983 through February 1985 and is designated as full construction on Figure 3-1. This excavation included enlarging the ventilation shaft for its conversion to the waste handling shaft, constructing the exhaust shaft, and mining additional underground drifts and test rooms for conducting R & D experiments. The operational name of the exploratory shaft changed to the C & SH shaft during this period. Design validation has been an integral part of this construction activity.

A third phase of underground construction is currently in progress. This is the initial operations phase during which excavation of the storage rooms will occur concurrently with waste emplacement. Mining for this phase started in June 1985 with the excavation of crosscuts for the installation of shops in the shaft piller area. Partial excavation of some storage rooms will follow. However, initial waste

emplacement is currently not scheduled to begin until late 1988. No discussion of the operations phase is presented in this report, although it will be strongly affected by the design validation results presented herein.

3.4.1 C & SH Shaft

C & SH shaft construction was performed during 1981 and 1982. Construction started in May 1981 with the excavation of a 98-foot deep pilot hole. The pilot hole was augered using a crane-mounted drilling unit. Steel surface casing with an interior diameter of 12 feet was grouted into place to a depth of 93.4 feet.

Shaft drilling started on July 4, 1981, and was completed 112 days later. The drilling was performed using a jacknife derrick with draw works capable of supporting a suspended load of 500 tons. The drilling method used consisted of air-lifted reverse circulation performed through double-walled drill pipe. The drilling fluid (brine) was maintained at a relatively constant level above the drill bit. The drill bit consisted of a 142-inch diameter full-face rolling cutter head. Shaft drilling was completed to a depth of 2,298 feet on October 24, 1981. Table 3-2 contains an abridged history of the C & SH shaft drilling program.

Liner installation began on November 12, 1981, and was completed on December 3, 1981. A steel liner was installed in 20- and 40-foot sections in the shaft above the salt formation. The steel sections were connected during installation using full-penetration bevel welds. Nondestructive radiographic examination was performed on each welded section. The liner was partially floated into place by filling the shaft with brine and adding brine to the inside of the liner to overcome the effect of buoyancy. Additional support for installation was provided by the drilling derrick and draw works. After the liner was in place, the annular space was grouted by the tremmie method. The grouting was completed on December 8, 1981.

Table 3-2

C & SH SHAFT - ABRIDGED DRILLING HISTORY

Location:		Eddy County, New Mexico; New Mexico Grid Coordinates X 666894.89, Y 499687.23
Elevation:		Ground Surface = 3410.5 ft MSL
Drilling Contractors/Rig Types:		Meredith Drilling Company/Auger (11.0 ft to 97.5 ft*); Challenger Drilling Company/ National 125 Jacknife Rotary (97.5 ft to 2,298 ft)
Drilling Data	Augered:	May 18 to June 17, 1981
	Spudded:	July 4, 1981
	Completed:	October 24, 1981
	Casing:	180-in. corrugated metal pipe, ground surface to 11 ft; 144-in. steel casing, ground surface to 93.4 ft; 120-in. steel liner, ground surface to 846 ft
	Drill Hole:	142-in. (nominal) diameter uncased borehole to a total depth of 2,298 ft
	Drilling Fluid:	Brine
Directional Survey Contractor:		Sperry-Sun (Gyroscopic Multishot Surveys)
Bottom Hole Coordinates:		X 666893.45, Y 499686.56 at 2,276 ft
Horizontal Displacement:		1.59 ft S 65.03° W at 2,276 ft

Table 3-2 (continued)

C & SH SHAFT - ABRIDGED DRILLING HISTORY

Geophysical Logging Contractors:	Birdwell(B) and Dresser Atlas(D)
Geophysical Logs:	October 16 to December 17, 1981
Fluid Density (D)	1,200 ft to 550 ft
Fluid Density (B)	750 ft to 20 ft
Density (B)	2,294 ft to 50 ft
Caliper (3-diameter/aver.) (B)	2,294 ft to 50 ft
Epithermal Neutron (B)	2,294 ft to 50 ft
Gamma Ray (B)	2,300 ft to 0 ft
Fluid Density (B)	400 ft to 100 ft
Nuclear Cement Top Locator (NCTL) (B)	827 ft to 0 ft
Nuclear Annulus Investigation Log (NAIL) (B)	839 ft to 0 ft
Fluid Density (D)	2,250 ft to 2,003 ft

* All depths measured from ground surface.

A key was constructed at the base of the steel liner during March and April 1982. The key is 37 1/2 feet long and constructed of reinforced concrete. Key construction required additional excavation in the salt below the liner to enlarge the shaft diameter. After the installation of reinforcing steel, drains, geomechanical instruments, grout pipes and block-outs for the injection of chemical seals, concrete was placed in several lifts from the bottom of the key to the bottom of the liner. Finally, the chemical seals were placed by injection.

3.4.2 Waste Shaft

Drilling of the SPDV ventilation shaft started on December 24, 1981, and was completed to a depth of 2,196 feet on March 10, 1982. The drilling operation was performed with the same drill rig used to drill the C & SH shaft. The drill bit was a 72-inch diameter full-face rolling cutter head. An abridged history of the shaft drilling is presented in Table 3-3. Except for a 97-foot long surface casing, the ventilation shaft was unlined. The ventilation shaft, and later the waste shaft, served as the exhaust for the underground facility until excavation of the permanent exhaust shaft was completed.

Enlargement of the SPDV ventilation shaft to become the waste shaft began in October 1983 (Table 3-3). This enlargement was performed from the top to the bottom of the shaft using the smooth-wall drill and blast method. The blasting was accomplished in 10-foot rounds that permitted the muck to fall down the 6-foot diameter shaft to the facility level. The muck was removed from the waste shaft station and hauled to the surface via the salt-handling skip in the C & SH shaft.

Construction of the unreinforced concrete liner closely followed this excavation. Typically, the shaft crew would take out three rounds (30 feet) of rock before placing one 24-foot section of concrete. This arrangement normally left no more than 6 feet of unlined shaft below the concrete.

Table 3-3

WASTE SHAFT - ABRIDGED CONSTRUCTION HISTORY

Location:		Eddy County, New Mexico; New Mexico Grid Coordinates X 666920.76, Y 499286.92
Elevation:		Ground Surface = 3407.5 ft MSL Shaft Collar = 3407.9 ft MSL (ventilation shaft) Shaft Collar = 3409.0 ft MSL (waste shaft)
Ventilation Shaft		
Drilling Contractors/Rig Types:		Meredith Drilling Company/Auger (8.0 ft to 98.2 ft*); Challenger Drilling Company/ National 125 Jacknife Rotary (98.2 ft to 2,196 ft)
Drilling Data	Augered:	June 13 to 17, 1981
	Spudded:	December 24, 1981
	Completed:	March 10, 1982
	Casing:	108-in. corrugated metal pipe, ground surface to 8 ft; 74-in. steel casing, 0.5 ft above ground surface to 96.9 ft
	Drill Hole:	72-in. (nominal) diameter uncased borehole to a total depth of 2,196 ft
	Drilling Fluid:	Brine
Directional Survey Contractor:		Sperry-Sun (Gyroscopic Multishot Surveys)
	Bottom Hole Coordinates:	X 666918.81, Y 499285.81 at 2,177 ft
	Horizontal Displacement:	2.25 ft S 60.2° W at 2,177 ft

Table 3-3 (continued)

WASTE SHAFT - ABRIDGED CONSTRUCTION HISTORY

Shaft Survey Contractor:	Cementation West, Inc.
Horizontal Displacement:	1.37 ft SW at 2,150 ft
Geophysical Logging Contractor:	Birdwell
Geophysical Logs:	March 8 to 10, 1982
Caliper (3-diameter/aver.)	2,190 ft to 0 ft
Epithermal Neutron	2,190 ft to 0 ft
Density	2,190 ft to 0 ft
Gamma Ray	2,100 ft to 0 ft
Fluid Density	2,191 ft to 1,800 ft

Waste Shaft

Excavation Contractor:	Ohbayashi Corporation
Excavation Method:	Smooth-wall drill and blast
Finished Shaft Diameter:	Lined = 19 ft Unlined = 20 ft minimum
Shaft Collar Excavation Began:	October 11, 1983
Liner Plate and Concrete Backfill Completed:	November 12, 1983
Collar Pads and Sinking Headframe Foundations Poured:	November 14, 1983
Concrete Liner Constructed: (including key)	November 30, 1983, to April 3, 1984
Liner Plate at Magenta Dolomite Grouted:	March 8 to 10, 1984
Liner Plate at Culebra Dolomite Grouted:	April 3 to 5, 1984
Salt Section Excavated:	April 7 to June 11, 1984
Sump Excavated:	June 20 to August 8, 1984
Liner Grouted:	August 11 to 25, 1984

* All depths measured from ground surface.

As part of the shaft design, both the Magenta and Culebra dolomite members of the Rustler formation were overexcavated and covered with steel liner plate prior to concrete placement. The space between the liner plate and the rock provided room for water from these water-bearing zones to accumulate. This allowed the concrete liner to reach full strength without damage from hydrostatic pressure buildup. After the concrete liner had reached full strength, this annular space was grouted with Portland cement grout at a 1:1 cement-to-water ratio.

Construction of the waste shaft key was nearly identical with that of the C & SH shaft key. The key is 63-feet long and composed of reinforced concrete. The shaft was overexcavated and the reinforcing steel, drainpipes, geomechanical instruments and chemical seal blockouts were installed. Unlike in the C & SH shaft, the chemical seals were placed between lifts of concrete. Concrete was placed from the bottom of the key to the top in several lifts, with construction joints at the top of each lift and at each chemical seal blockout. At the chemical seal locations the seal material was placed into the blockout prior to placing the next lift of concrete. Construction of the shaft liner and key was completed on April 3, 1984.

Excavation of the shaft to its 20-foot finished diameter below the key began on April 7, 1984. This section of the shaft is lined with wire mesh anchored by 3-foot long rock bolts. Mesh installation, like liner installation, was accomplished concurrently with excavation. The shaft enlargement reached the facility level on June 11, 1984. The shaft sump was excavated between June 30 and August 8, 1984. The sump extends approximately 122 feet below the facility level.

The concrete liner and grouting at both water-bearing zones did not completely prevent water from entering the shaft. Water seeped through the liner at construction joints and some cracks from a depth of about 560 feet to 835 feet. A grouting program was undertaken to seal these leaks in August 1984. A total of 628 bags of Portland Type V cement, 103 bags of MC-500 microfine cement, and 76 gallons of Scotch-brand

5600 foam chemical grout were injected into 293 drilled holes (ref. 3-3). The grouting significantly reduced, but did not eliminate, water seepage through the concrete liner.

3.4.3 Exhaust Shaft

The exhaust shaft was constructed in two phases over a 16 month period. The first phase was the excavation of a 6-foot diameter pilot shaft using upreaming techniques. The second phase consisted of enlargement of this shaft by conventional drill and blast methods and lining of the upper 907 feet. The construction history is summarized in Table 3-4.

Shaft excavation began on September 22, 1983, with the drilling of a pilot hole. The pilot hole was a 7 7/8-inch diameter hole drilled from the ground surface to intersect with the S400 drift at a depth of about 2,150 feet. Therefore, directional control of the hole was critical. The upper 80 feet of the pilot hole was augered, then lined with a surface casing. Drilling progressed to a depth of 744 feet using a tri-cone roller bit and compressed air. A "Dynadrill" was then used to correct hole alignment from 735 to 1,183 feet based on the results of gyroscopic hole surveys. The circulating medium was also changed at this time from air to brine. The tri-cone bit was used to complete the pilot hole. The hole diameter was then reamed to 11 inches from the surface to the facility level, again using a tri-cone roller bit. Pilot hole drilling was completed on December 16, 1983.

Excavation of the pilot shaft was performed by reaming the 11-inch diameter pilot hole to a diameter of 6 feet. This was accomplished by the raise-bore method. Reaming was performed from the facility level to the ground surface. The raise-boring operation was conducted from December 31, 1983, to February 10, 1984, using a Robbins series 61R1131 raise-bore machine. This machine utilizes a full-face rolling cutter head pulled to the surface with hydraulic jacks. Drill cuttings fell to the facility level and were hauled to the surface via the C & SH shaft.

Table 3-4

EXHAUST SHAFT - ABRIDGED CONSTRUCTION HISTORY

Location:	Eddy County, New Mexico; New Mexico Grid Coordinates X 667370.39, Y 499287.23
Elevation:	Shaft Collar = 3411.5 ft MSL Shaft Reference = 3409.0 ft MSL
Excavation Contractor:	Ohbayashi Corporation
Excavation Method:	Raise-bore 6-ft diameter pilot shaft; smooth-wall drill and blast to final dimensions
Subcontractors for Raise-Bore Excavation:	Raisebore, Inc., and J. S. Redpath Co.
Finished Shaft Diameter:	Lined = 14 ft Unlined = 15 ft
Pilot Hole Drilled:	September 22 to December 16, 1983
Raise-Bore Excavation:	December 31, 1983, to February 10, 1984
Shaft Collar Excavation Began:	July 15, 1984
Liner Plate and Concrete Backfill Completed:	July 17, 1984
Concrete Liner Constructed: (including key)	July 18 to November 29, 1984
Liner Plate at Culebra Dolomite Grouted:	December 2 to 4, 1984
Liner Plate at Magenta Dolomite Grouted:	December 4 to 5, 1984
Salt Section Excavated:	December 7, 1984, to January 17, 1985
Liner Grouted:	June 1 to July 31, 1985

Enlargement of the pilot shaft from 6 feet to the final exhaust shaft diameter of 15 feet began on July 15, 1984, and was accomplished by drilling and blasting in 10-foot rounds. Excavation was performed from the ground surface to the facility level. The rock was blasted into the open pilot shaft so that it fell to the facility level where it could be removed and hauled to the surface via the C & SH shaft.

The upper 844 feet of the exhaust shaft is lined with unreinforced concrete. As in the waste shaft, construction of the exhaust shaft liner occurred concurrent with the drill and blast excavation. Concrete placement for the liner was completed on November 29, 1984. The two water-bearing zones in the Rustler formation, the Magenta and Culebra dolomites, received the same special treatment that was performed in the waste shaft. Each zone was overexcavated and covered with steel liner plate prior to placing the concrete liner. After the liner had cured, grout was injected behind the liner plates.

Exhaust shaft key construction, similar to that in the waste shaft, was performed in November 1984. The key consists of reinforced concrete and extends from a depth of 844 to 907 feet. It initially contained 2 chemical seals, 8 telltale drains, 2 guide pipes for test hole drilling, and geomechanical instrumentation. Placement of the concrete and chemical seal material was identical to that performed in the waste shaft. Two additional sets of telltale drains were installed in the key by drilling after its construction. Each set contains nine drains. One set was installed above and one set below the initial eight-drain set.

The exhaust shaft is 15 feet in diameter from the bottom of the key to the facility level. For safety, the walls are covered with wire mesh anchored by rock bolts. Excavation of the shaft to its final dimensions was completed on January 17, 1985.

As in the waste shaft, water began seeping through the exhaust shaft liner at construction joints and small cracks. Total water inflow

through the liner was measured at 0.35 gallons per minute in January 1985. A grouting program, using Portland cement and chemical grout, was conducted from June 1 through July 31, 1985, to seal these leaks and to ensure that the integrity of the shaft key was maintained. A total of 164 bags of Class C cement and 826.9 gallons of Terragel 5531 chemical grout were used. The total water inflow was reduced by this grouting to an essentially non-measureable quantity.

3.4.4 Drifts

The exploratory (C & SH) shaft station was the first underground horizontal opening excavated after completion of the SPDV exploratory and ventilation shafts. The initial shaft station excavation was performed from May 2 to June 3, 1982, using the drill and blast method. The station was trimmed to its final dimensions using the Dosco continuous mining machine discussed later in this subsection. The station area north of the shaft is 32 feet long, 32 to 35 feet wide and 12 feet high. South of the shaft, the station is 90 feet long and 32 to 38 feet wide. The height of the station south of the shaft is 18 feet for a distance of 54 feet and 14 feet for the remaining 36 feet. Cartridge water-gel explosives detonated by electric detonators were used for the drill and blast excavation. A detailed description of the SPDV exploratory shaft station excavation is presented in the WIPP Preliminary Design Validation Report (ref. 1-3).

Following the initial excavation of this station, the drill and blast method was used to excavate a drift southward to provide a connection between the two shafts so ventilation could be established. This drift was approximately 310 feet long, 18 feet wide and 9 feet high. Excavation of the drift was accomplished from June 3 to June 13, 1982.

The only other major use of the drill and blast method at the facility level was for construction of the loading pocket in the SPDV exploratory shaft. This pocket was constructed from June 1 through 30, 1982, on the north side of the shaft below the facility floor level.

It was later outfitted with a steel hopper and other equipment associated with the salt handling system.

The initial (SPDV) underground construction phase was conducted by Cementation West, Inc., of Tucson, Arizona. A British-made Dosco LH 1300, boom-type continuous mining machine was mobilized underground to the SPDV exploratory shaft station during late summer of 1982. This machine was used to excavate the remaining horizontal underground openings during the SPDV Program. The Dosco was capable of excavation rates of 1,000 to 1,200 tons per 24 hours (excavation was conducted on a three-shifts-per-day, seven-days-per-week basis). However, the excavation rate was often much less due to numerous construction and engineering related constraints. The mining machine was demobilized in May 1983 at the completion of the SPDV Program.

A second underground construction contract for full WIPP construction was awarded to Ohbayashi Corporation of South San Franicsco, California. During this phase of construction, two Japanese Mitsui Miike, boom-type continuous mining machines were used for excavation of the underground horizontal openings. Each of these machines excavated at a rate of 300 to 400 tons per 24 hours. These machines were mobilized to the underground facility in October 1983 and demobilized in April 1985.

A summary of the excavation sequence for the underground horizontal openings is presented on Figure 3-4. This figure shows the mining progress on a daily basis from October 14, 1982, through March 31, 1986. The underground mining operation was performed in the same manner during both construction phases regardless of the type of mining machine being used. The rotating head on the boom of the mining machine cut the salt away from the working face. The "muck" was pulled through the machine on a conveyor and deposited in one of several types of haul vehicles. Typically, the haul vehicles were underground trucks capable of carrying about 5 tons of muck. Other vehicles used included LHDs (Load-Haul-Dump, a type of front-end loader) and a telescoping-bed haul truck. The trucks carried the muck to the C & SH shaft station

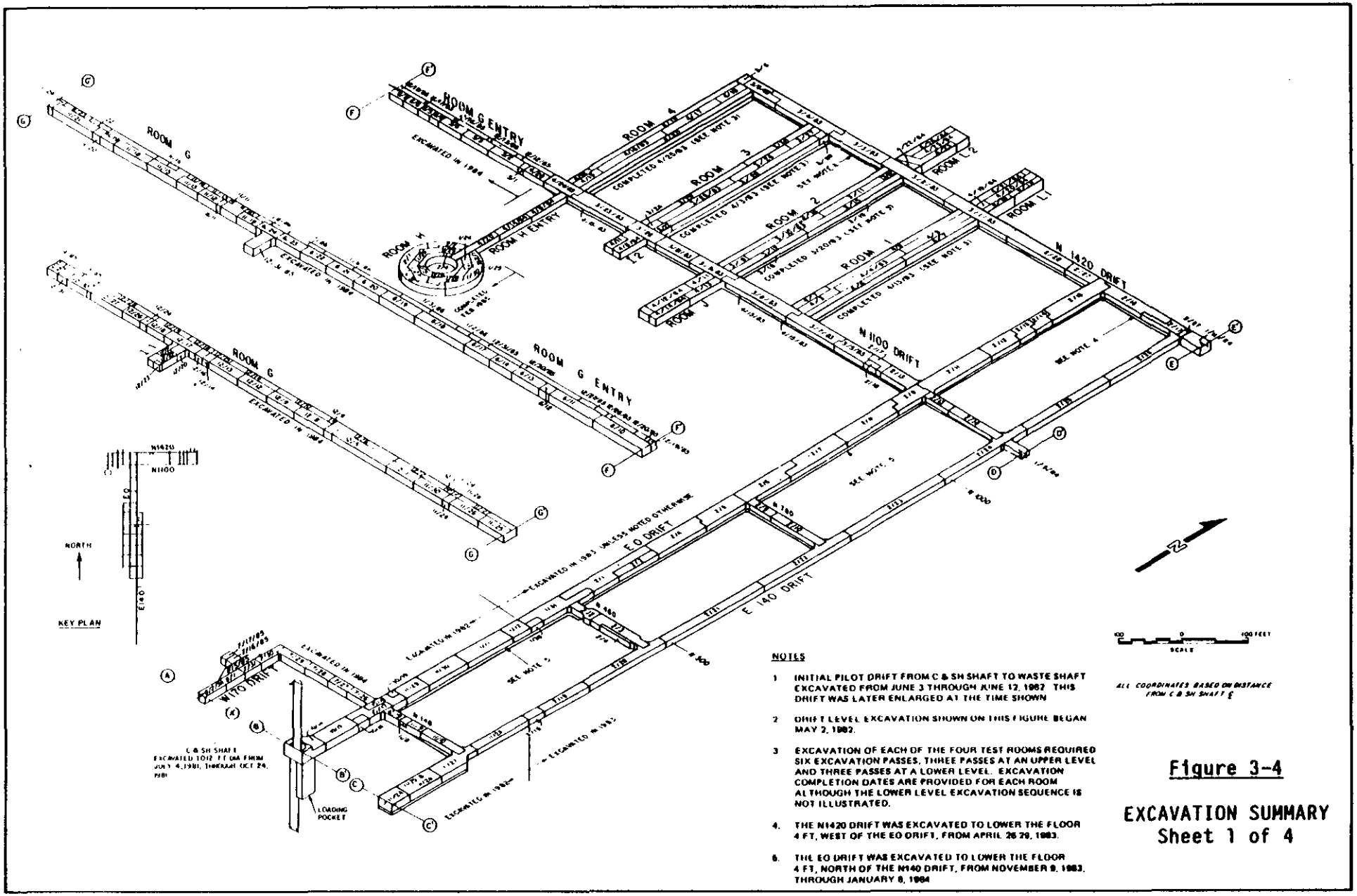

NOTES

1. INITIAL PILOT DRIFT FROM C & SH SHAFT TO WASTE SHAFT EXCAVATED FROM JUNE 3 THROUGH JUNE 12, 1982. THIS DRIFT WAS LATER ENLARGED AT THE TIME SHOWN.
2. DRIFT LEVEL EXCAVATION SHOWN ON THIS FIGURE BEGAN MAY 2, 1982.
3. EXCAVATION OF EACH OF THE FOUR TEST ROOMS REQUIRED SIX EXCAVATION PASSES, THREE PASSES AT AN UPPER LEVEL AND THREE PASSES AT A LOWER LEVEL. EXCAVATION COMPLETION DATES ARE PROVIDED FOR EACH ROOM ALTHOUGH THE LOWER LEVEL EXCAVATION SEQUENCE IS NOT ILLUSTRATED.
4. THE N1420 DRIFT WAS EXCAVATED TO LOWER THE FLOOR 4 FT, WEST OF THE E0 DRIFT, FROM APRIL 26 TO 29, 1983.
5. THE E0 DRIFT WAS EXCAVATED TO LOWER THE FLOOR 4 FT, NORTH OF THE N140 DRIFT, FROM NOVEMBER 9, 1983, THROUGH JANUARY 6, 1984.

ALL COORDINATES BASED ON DISTANCE FROM C & SH SHAFT ℄

Figure 3-4

EXCAVATION SUMMARY
Sheet 1 of 4

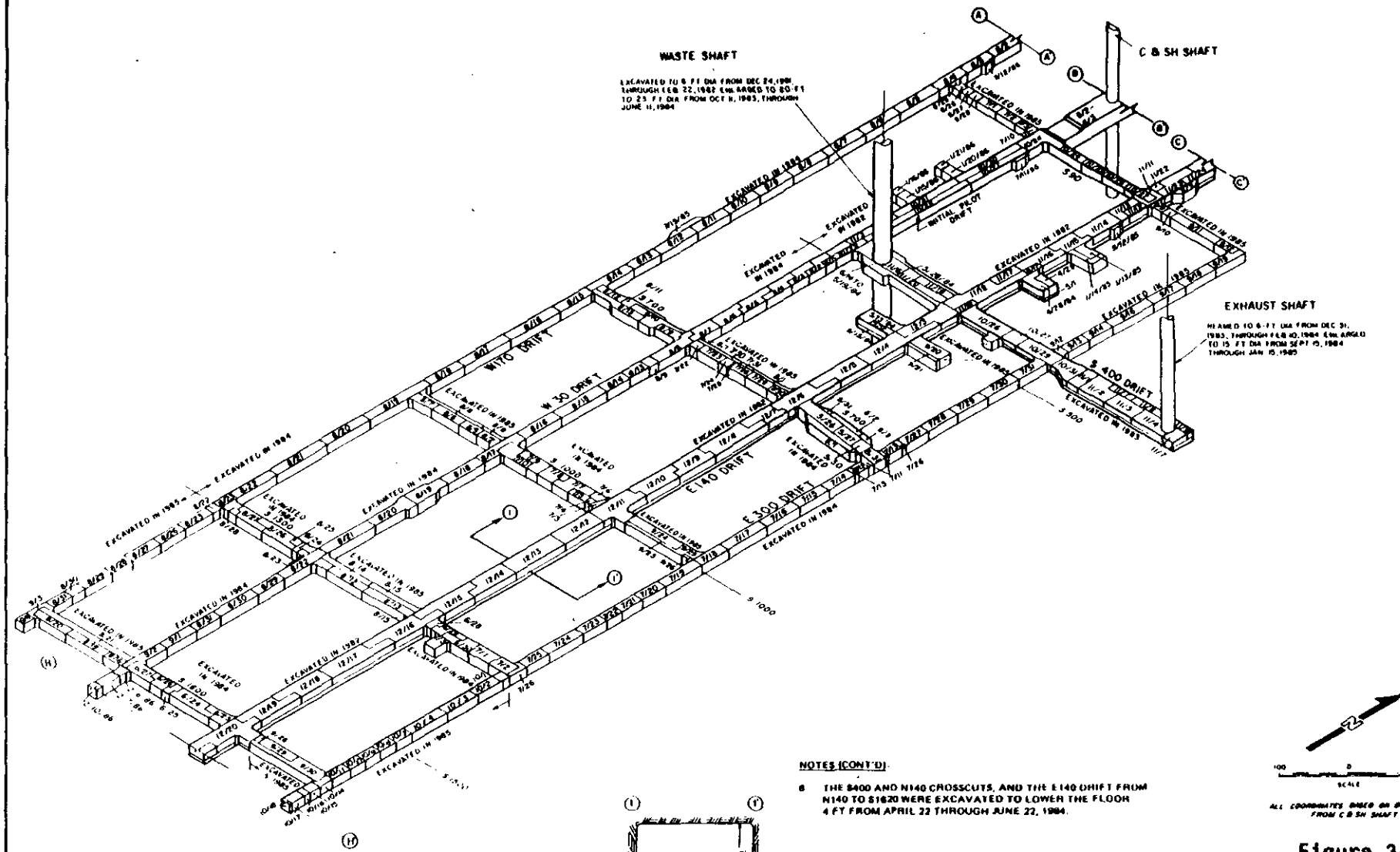

SOUTH EXPLORATORY DRIFT
SECTION 1-1'

NOTES (CONT'D):

8. THE S400 AND N140 CROSSCUTS, AND THE E140 DRIFT FROM N140 TO S1620 WERE EXCAVATED TO LOWER THE FLOOR 4 FT FROM APRIL 22 THROUGH JUNE 22, 1984.

Figure 3-4

EXCAVATION SUMMARY
Sheet 2 of 4

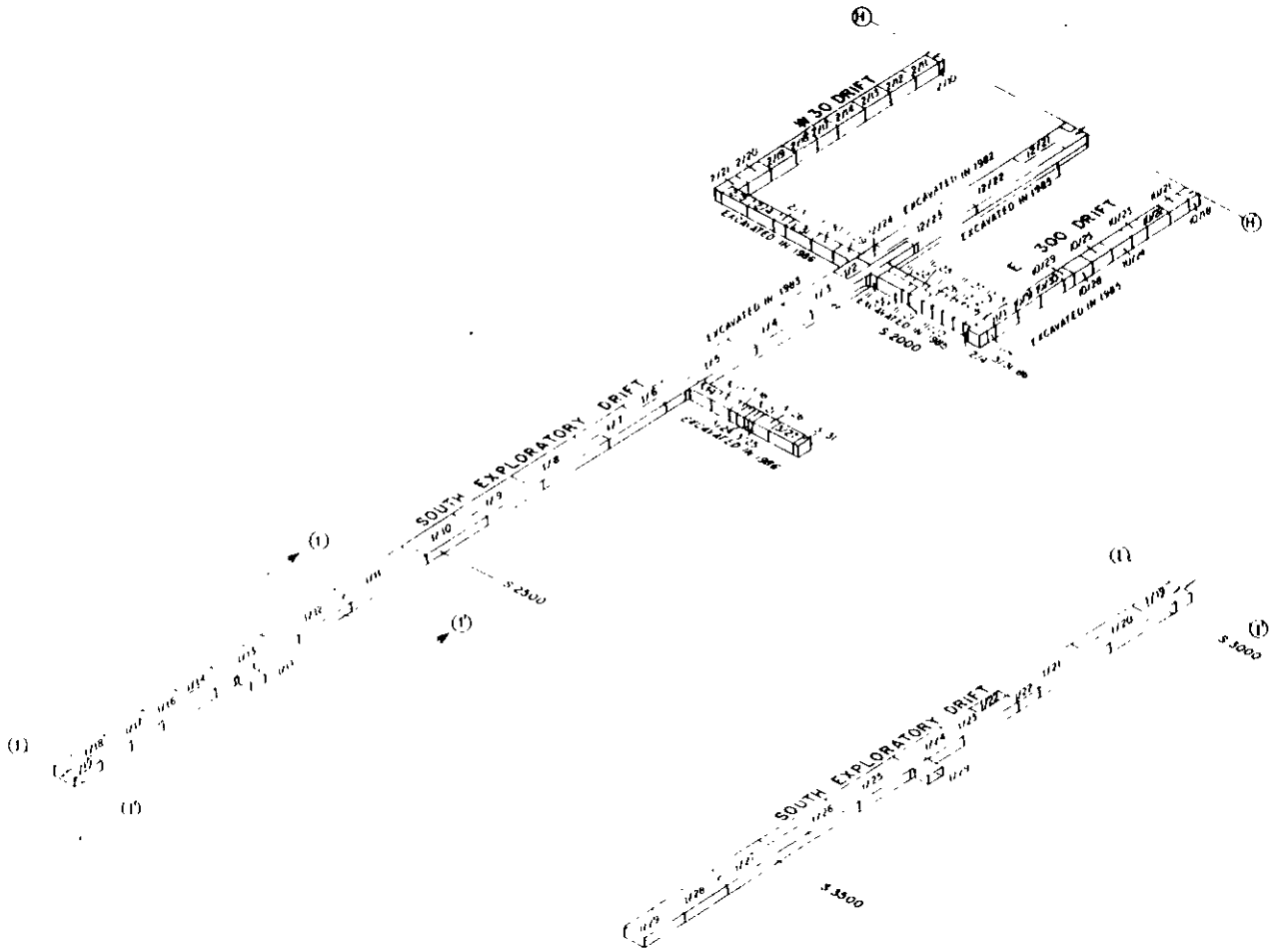

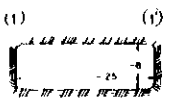

SOUTH EXPLORATORY DRIFT
SECTION I-I'

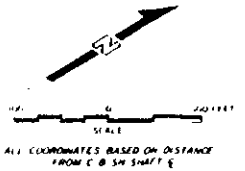

Figure 3-4

EXCAVATION SUMMARY
Sheet 3 of 4

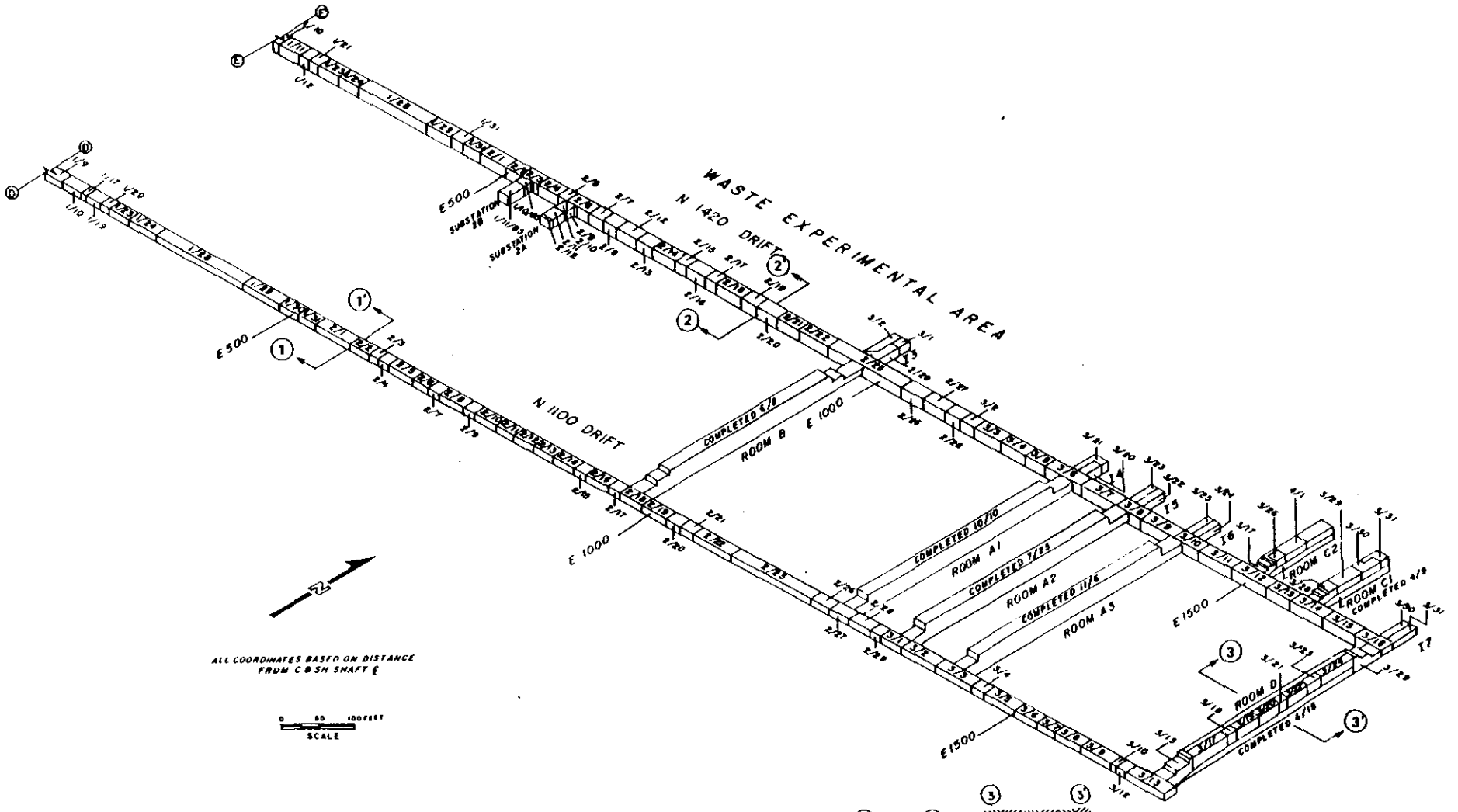

NOTES:

1. EXCAVATION SUMMARY FOR ROOMS A1, A2, A3, AND B ARE NOT PRESENTED
2. ALL EXCAVATIONS SHOWN ON THIS SHEET WERE MADE IN 1984, EXCEPT FOR SUBSTATION 2B

Figure 3-4

EXCAVATION SUMMARY
Sheet 4 of 4

and dumped it into the loading pocket. From there, the muck was carried to the surface in 7- to 8-ton loads in the skip. The skip dumped the muck at the surface into 50-ton Caterpillar or Euclid haul trucks which then carried the muck to the surface salt storage area.

During and immediately after excavation, a sounding survey of the roofs in the horizontal openings was made using a scaling bar to identify areas of drummy or slabby rock which could pose safety or stability problems. Remedial work was performed immediately after sounding in any areas identified as potentially unstable. This work consisted of hand-scaling thin drummy areas, removing larger drummy areas up to 18 inches thick with the mining machine, or rock bolting. In addition, two follow-up surveys were made of the roofs in all of the horizontal openings excavated at the time of the survey. The first survey was completed in July 1983 and the second in November 1984. Remedial work was performed on problem areas identified during these surveys. This work consisted of scaling, excavation, or rock bolting. It should be noted that the drummy areas identified during the July 1983 survey were sounded again in the November 1984 survey and did not show any noticeable enlargement.

Rock bolts are used selectively throughout the underground drifts for both remedial work and safety. The roofs of many high-traffic personnel areas are pattern bolted and covered with wire mesh as an additional safety precaution.

The C & SH shaft station has presented the majority of problems associated with roof stability. Due to its initial excavation by the drill and blast method, and the proximity of overlying clay seams, the roof in the station has required support by a large number of rock bolts. The method of rock bolting has evolved through several phases due to the effect of salt creep on roof separation along the clay seams.

Rock bolts were initially installed in the C & SH shaft station roof

from May 9 to June 20, 1982. These bolts were 1 inch in diameter, 8, 10 or 12 feet in length, and made of grade 60 steel. They were anchored using resin cartridges.

These resin-anchor bolts began failing at the head assemblies shortly after their installation was completed. The failed bolts were replaced with 8-foot long, 5/8-inch diameter mechanical-anchor bolts with 2 x 12 x 12-inch wooden blocks installed between the steel head assembly plate and the salt. A total of over 400 resin-anchor and mechanical-anchor bolts were installed in the shaft station roof through April 1983.

During December 1983 and January 1984, 146 additional mechanical-anchor bolts, 5/8 inch in diameter and 8 feet long, were installed in the C & SH shaft station roof. In May 1984, another 91 similar anchor bolts were installed. After the mechanical-anchor bolts were installed, the nut and head assembly plate were cut off those older resin-anchor bolts showing evidence of excessive deformation. This was to prevent injury to personnel from falling nuts and plates should these resin-anchor bolts fail.

From mid-April through early August 1985, approximately 133 3/4-inch diameter mechanical-anchor bolts, 6 and 8 feet long, were installed in the station roof on approximately 3 1/2-foot centers. In addition, 245 resin-anchor bolts, 1 inch in diameter, were anchored above anhydrite "b" and across anhydrite "a". These bolts were 12 and 14 feet in length. The entire station roof was covered at this time with wire mesh secured with 2-foot long, 5/8-inch diameter mechanical-anchor bolts. Approximately 750 of the 2-foot long bolts were installed.

Although some resin-anchor bolts were used in the SPDV drifts and test rooms excavated in 1982 and 1983, mechanical-anchor bolts have been used in all subsequently excavated areas. Bolt lengths vary from 2 to 8 feet in the drifts and rooms. Wire mesh secured by 2-foot long mechanical-anchor bolts has been installed on the roofs of all high-traffic personnel areas. This includes instrument-shed and

electrical alcoves, many of the shop areas, and some of the brows above the entries to the waste experimental rooms. Rock bolts and wire mesh have also been installed in the roof of the N140 crosscut.

Rock bolts and wire mesh have been installed for roof support in the waste shaft station waste transfer area. The bolts, 3/4 inch in diameter and 12 feet long, are mechanical-anchor steel bolts set on nominal 4-foot centers.

3.4.5 Test Rooms

As part of the SPDV Program, four test rooms were excavated at the north end of the underground facility (Figure 3-4) by Cementation West, Inc., using the Dosco mining machine. The test room excavation was conducted from March 9 to April 25, 1983. Test Room 2 was excavated first, followed by Test Rooms 3, 1 and 4, in that order. Each room was excavated in a series of six passes along its longitudual axis (Figure 3-5). The first pass was the largest in cross section and was conducted down the center of the planned room along its roof. This pass was approximately 15 feet wide and 8 feet high. The second and third passes were conducted on either side of the first pass. Each of these passes were about 9 feet wide and 8 feet high. The last three passes lowered the floor 5 feet to complete the room excavation to its design height and width of 13 x 33 feet.

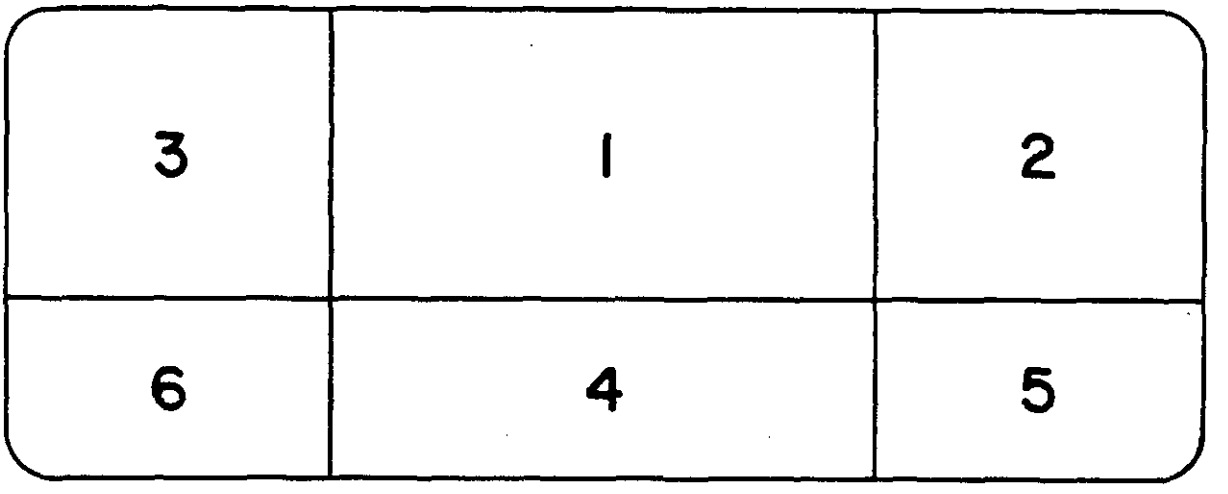

Figure 3-5

TEST ROOM EXCAVATION SEQUENCE

CHAPTER 4
SUPPORTING VALIDATION DOCUMENTS

4.1 INTRODUCTION

This chapter discusses the principle documents containing information used to support design validation. These documents are the Waste Isolation Pilot Plant Preliminary Design Validation Report (ref. 1-3) and geotechnical field data reports (refs. 4-1 thru 4-19). These documents contain all of the data which has been collected, analyzed and evaluated for design validation since site construction activities began in July 1981. Other documents pertaining to design and site characterization are referenced throughout this report. However, they are considered peripheral documents not directly related to the design validation process and, therefore, are not described in this report. Because these other reports are public documents, they are available to anyone interested in obtaining additional background information or detailed data on the WIPP project.

4.2 PRELIMINARY DESIGN VALIDATION REPORT

The following subsections present a summary of the WIPP Preliminary Design Validation Report produced for the SPDV Program described in Chapter 1.

4.2.1 Purpose and Objectives

The purpose of the WIPP Preliminary Design Validation Report was to provide documentation on the behavior of the initial underground openings. Four types of information were gathered for this purpose:

(1) observations of the behavior of the underground openings;

(2) descriptions of the geologic conditions encountered during SPDV underground construction;

(3) descriptions of core samples from instrumentation and exploratory holes in the roof and floor of the underground openings; and

(4) data from installed geomechanical instrumentation.

The objective of the report was to provide initial evaluations of the suitability of the design criteria and design bases and initial confirmation of the underground opening reference design in order to permit full facility construction. This initial confirmation was based on data obtained from geologic field activities and geomechanical instrumentation which were subjected to preliminary analysis and evaluation.

4.2.2 Data Acquisition Program

The preliminary design validation data acquisition program consisted of geologic field activities which provided information for initial validation of the WIPP underground opening reference design. Data was obtained from three principal activities:

(1) geologic mapping;

(2) vertical core hole logging; and

(3) geomechanical instrument measurements.

All of the data collected was verified at the site field office, then sent to the DOE/Technical Support Contractor (TSC) offices in Albuquerque, New Mexico, for preparation and inclusion into the GFDRs and other reports. Due to the qualitative nature of the geologic mapping and core hole data, efforts for preparation of this material generally required only limited evaluation, editing and drafting. The geomechanical instrumentation data, however, required more extensive preparation and analysis due to its applications to various aspects of underground opening behavior and the calculation of in situ salt properties.

4.2.3 Geomechanical Instrumentation

The SPDV geomechanical instrumentation program for the WIPP was designed to provide empirical data on the behavior of the salt around the underground openings and on the pressure developed behind the exploratory shaft liner and key by ground water and salt creep. The objective of the geomechanical instrumentation program for SPDV was to provide:

(1) short-term in situ measurements for assessment of the preliminary design performance of the underground openings;

(2) early detection of conditions that could affect the safety of personnel during construction; and

(3) data on adverse ground conditions that may be developing, in order to identify potential problems and plan and implement remedial measures.

Instruments were initially installed in the SPDV exploratory shaft, exploratory shaft station, ventilation shaft station, the E0, E140 and N1100 drifts, and the S90 crosscut to provide data input for the WIPP Preliminary Design Validation Report. The exploratory drift extending south of the ventilation shaft was added to the SPDV Program to provide additional information on the geology in the area proposed for excavation of the waste storage rooms. Geomechanical instruments were installed at several locations in this drift.

For the WIPP Preliminary Design Validation Report, borehole extensometer and convergence point data from the SPDV exploratory shaft, as well as data from the ventilation shaft station and drifts, were insufficient to estimate long-term closure rates. Most drift extensometers and convergence points had been installed only a relatively short time before the report was prepared. A period of 1 year or more was thought to be required before a relatively steady closure rate could be established. The data were useful in

demonstrating short-term stability of the excavations and for developing cumulative closure amounts. Instruments with the most extensive data typically showed a maximum of only 3 or 4 months of regular monitoring since installation.

4.2.4 Preliminary Conclusions

Preliminary conclusions presented in the WIPP Preliminary Design Validation Report were:

(1) The walls of the finished shafts are stable, both in the overburden and salt formations. The mapped shaft stratigraphy is generally comparable to the stratigraphy used in the design. Ground-water control is satisfactory. The shaft liner and shaft key are performing as expected. No major revision of design elements or parameters is foreseen for future WIPP shafts as a result of the findings of preliminary design validation.

(2) The underground horizontal openings are also stable. After excavation, repeated inspections of the exploratory and ventilation shaft stations, entry drifts, crosscuts and the south exploratory drift revealed essentially no deterioration in rock stability. The underground drifts and shaft stations are stable and provide safe working conditions.

(3) Encounters of gas were expected and are typical of nearby potash mines. The small amount of gas encountered is well below the limit permitted in the underground facility by MSHA regulations. No brine pockets have been encountered or detected during excavation of the shafts and underground openings.

4.3 GEOTECHNICAL FIELD DATA REPORTS

4.3.1 Background

The compilation of GFDRs was initiated by the DOE to provide geotechnical and related information from the WIPP underground activities to interested persons or groups in a timely manner. These reports provided data from the two major phases of WIPP development: SPDV and full construction. As discussed previously, SPDV was established as an early construction phase to permit validation of the WIPP site and preliminary validation of the reference design of the underground openings. The full construction phase following SPDV was utilized to continue visual inspections of the underground openings, monitoring and interpretation of data from geomechanical instruments, and evaluations and computational analyses of the behavior of the underground openings for design validation.

The GFDRs were eventually produced on a quarterly basis. These quarterly reports contain an evaluation of selected aspects of the WIPP underground environment based on preliminary interpretation and analyses of data collected from the above activities. The analyses and evaluations contained in the GFDRs provide the supporting documentation required for design validation.

4.3.2 Objectives

As stated in the GFDRs, the geomechanical instrumentation program for SPDV and design validation was designed and implemented to provide in situ data on the behavior of the rock (primarily salt) around the shafts and horizontal underground openings. More specifically, the instrumentation program was designed to provide:

(1) early detection of conditions that could affect operational safety;

(2) monitoring of closure rates to allow evaluation of waste storage and retrievability;

(3) a greater understanding of the in situ behavior of bedded salt by comparison of observed response with current facility reference design calculations; and

(4) measurements of salt deformation and stresses to confirm or indicate the necessity for revisions to the opening configuration and the parameters used in underground facility design based on clearance requirements.

4.3.3 Geomechanical Instrumentation

An extensive geomechanical instrumentation program was implemented to provide in situ data on the shafts and horizontal underground openings as part of the investigations performed at the WIPP site. These instruments have been providing data on deformation, pressure, loads and stress on a regular basis for analysis and evaluation. Instruments for measuring the geomechanical response of the shafts and horizontal underground openings include convergence points, convergence meters, multiple-point and single-point borehole extensometers, load cells, pressure cells, stressmeters, strain gauges, inclinometers, piezometers and lateral movement gauges.

Data from these geomechanical instruments are read remotely by an automatic datalogger system and/or collected manually. All data obtained are entered on magnetic tape for data reduction, tabulation, analysis and archiving. Data collected from the geomechanical instruments have been documented in the GFDRs. These data are the basis for analysis and evaluation by the project participants and other interested groups. The geomechanical instruments provide data for the analysis and evaluation of several phenomena at various locations, including strain in the C & SH shaft key, water pressure behind the C & SH and waste shaft liners, radial closure of shafts, pressures between shaft keys and wall rock, roof-to-floor and wall-to-wall closure in the shaft stations, drifts and rooms, and displacements at depth into the walls, roof and floor of shaft stations, drifts and rooms.

The frequency of data collection is determined on a per instrument basis and is dependent upon instrument location, method of instrument reading (manual or datalogger), and the number of days elapsed since excavation at the instrument location. After installation, the instrument is read frequently, but with time this reading frequency is decreased since the rate at which the salt mass responds following excavation also decreases with time.

The geomechanical instrumentation data are presented graphically in the GFDRs and represent readings collected from the WIPP site since April 1982. The data plots in the reports are grouped by areas within the underground facility and also by instrument type. The data plots are updated as new data become available. Summary tables of the instruments, with the latest readings and the operating histories, are also presented in the reports.

4.3.4 Geologic Data

Geologic data presented in the GFDRs have included the results of geologic mapping activities, core hole logging, and observations of the condition and behavior of underground opening surfaces. Geologic maps of the shafts and representative horizontal opening surfaces have been presented periodically in the GFDRs or in topical reports issued separately. Geologic logs containing descriptions of core samples obtained from core holes in the underground openings were presented in the GFDRs as they became available.

Frequent observations by project geotechnical personnel have provided qualitative determinations of the condition of the underground openings. These assessments were presented in the GFDRs to document changes in the condition of the underground openings and in salt behavior on a regular basis. Observations such as the condition of the roof and rock bolts in shaft stations, fractures in pillar corners at drift intersections and in the salt surrounding the drifts and rooms, behavior of the roof and walls of the drifts and rooms, and horizontal displacements, vertical separations and fracturing detected in open

boreholes were documented. This information has provided important input for design evaluation and safety assessments.

4.3.5 Geomechanical/Structural Analyses

The quarterly GFDRs contain sections on both geotechnical and computational analyses. These sections present analyses of various elements of the underground excavations. The analyses are updated periodically to include the most current data available at the time the reports are published. They have provided a significant amount of information related to the geomechanical and structural behavior of the underground openings.

CHAPTER 5
METHODOLOGY

5.1 INTRODUCTION

Design validation of the WIPP underground openings is accomplished by determining the compatibility of the design criteria, design bases and reference design configurations using site specific information. Design validation also allows for the development of recommendations to improve or optimize the reference design. The methods used to validate the reference design may also be used to validate any recommended design modifications. Mathematical models containing the modifications can be generated and analyses performed to predict the future behavior of the modified reference design.

The design validation process consists of three major steps:

(1) data collection;

(2) analysis and evaluation; and

(3) prediction of future behavior.

Sections 5.2 through 5.4 present the methods used for data collection, analysis and evaluation, and prediction of future behavior.

5.2 DATA COLLECTION

One of the principal areas of effort in support of design validation was the compilation of geotechnical data. This data formed the basis for later analysis and evaluation and for predictive modeling. Data collected from geologic mapping, core drilling and logging, laboratory testing, geomechanical instrumentation and field observations have provided information for validation of the underground opening reference design. These data can be categorized based on their relationship to observations of geologic conditions or to structural behavior. Geologic observations include an assessment of the rock

characteristics; stability of the openings in rock; reaction of the rock to excavation; and movements along clay seams. Structural behavior is the development or modification of stresses and strains in the salt created by excavation of the underground openings, and the pressures occurring at rock/structure interfaces.

5.2.1 Geologic Mapping

Geologic mapping of the shafts, drifts and test rooms was conducted by site geologists. The objectives of the mapping were:

(1) provide confirmation and documentation of the continuity of the stratigraphy, lithology and structure above and below the facility horizon;

(2) evaluate any geologic conditions which may affect the excavation, stability, or safety of the horizontal openings;

(3) support field adjustments and modifications to the reference design based on the geologic conditions encountered; and

(4) finalize geomechanical instrument locations.

5.2.2 Core Drilling and Logging

Information on stratigraphy and lithology was obtained from core holes drilled into the floor and roof of the underground openings. The objectives of the core drilling program were:

(1) confirm the thickness, lateral extent, mineralogy and stratigraphic continuity of the host rock beyond the limits of the excavations;

(2) confirm the continuity of the geologic structure and the absence of any unusual features within the immediate zone of influence of the excavations; and

(3) obtain stratigraphic information in order to determine extensometer anchor depths.

Details of the core drilling program are discussed in Chapter 6.

5.2.3 Laboratory Testing

Initial laboratory tests were performed on core samples of evaporite minerals and clay from exploratory boreholes AEC-7 and ERDA-9. These tests were performed by RE/SPEC, Inc., of Rapid City, South Dakota, and by SNL (refs. 5-1 and 5-2). The evaporite samples were tested in triaxial vessels at both room and elevated temperatures. Quasi-static compression tests were performed under different constant confining pressures and variable axial loads in steps, each load step being maintained for about 10 minutes. Quasi-static compression tests were considered as constant stress-rate tests for all practical purposes. Direct shear tests were performed on samples of clay to determine the coefficient of sliding friction.

5.2.4 Geomechanical Instrumentation

Geomechanical instruments in the WIPP underground facility provide data on deformation, pressure, loads and stress. Instruments for measuring the geomechanical response of the shafts and other underground openings include convergence points, convergence meters, multiple-point and single-point borehole extensometers, load cells, pressure cells, stressmeters, strain gauges, inclinometers, piezometers and lateral movement gauges. Data from the geomechanical instruments are collected manually as well as read remotely by an automatic datalogger system at the surface. All data are entered on magnetic tape for data reduction, tabulation, analysis and archiving. These data are a basis for the analysis and evaluation of underground opening behavior.

The geomechanical instrumentation program for design validation was designed and implemented to provide in situ data on the behavior of the

rock (primarily salt) around the shafts and underground openings. More specifically, the instrumentation program was designed to provide:

(1) early detection of conditions that could affect construction and operational safety;

(2) closure monitoring for evaluation of the ability of the underground openings to permit waste storage and retrieval;

(3) a greater understanding of the in situ behavior of bedded salt by a comparison of the observed responses with underground opening reference design calculations; and

(4) measurements of salt deformation to permit confirmation or revision of the opening configurations and the parameters used in the underground opening reference design based on clearance requirements.

Tables 5-1 through 5-5 present information on the distribution of geomechanical instruments installed at the WIPP. The instruments provide data for the evaluation and analyses of several phenomena at various locations, including strain in the C & SH shaft key, water pressure behind the C & SH and waste shaft liners, radial closure of the shafts, pressures between the concrete shaft keys and wall rock, roof-to-floor and wall-to-wall closure in the shaft stations, drifts and rooms, and displacements at depth into the walls, roof and floor of shaft stations, drifts and rooms.

Data from the geomechanical instruments are collected manually or read remotely by an automatic datalogger system. The datalogger is a computer system that automatically collects and records output from instruments at specified polling times. The signals from the instruments are first sent to local termination cabinets (LTC) where the signal is digitized and then transmitted to the datalogger for disk storage. Manual readings are manually entered into the computer system. Changes from initial readings and rates of change are

Table 5-1

C & SH SHAFT
INSTRUMENTS

Location and Type	Purpose
Lined Section	
Convergence points	Measure wall-to-wall closure of shaft
Piezometer	Measures fluid pressure buildup behind liner due to water accumulation
Key	
Piezometer	Measures fluid pressure buildup behind key due to water accumulation
Pressure cell	Measures contact pressure buildup between concrete key and wall rock
Welded strain gauge	Measures strain in reinforcing steel of shaft key
Embedment strain gauge	Measures strain in concrete of shaft key
Unlined Section	
Multiple-point extensometer	Measures salt creep deformation
Convergence points	Measure wall-to-wall closure of shaft
Station	
Convergence points (includes permanent and temporary convergence points and wall shortening points)	Measure roof-to-floor and wall-to-wall closure of openings and pillar shortening
Extensometer (single-point and multiple-point)	Measures salt creep deformation in roof, floor and walls
Rock bolt load cell	Measures tensile loads on rock bolts
Lateral movement gauge	Measures lateral movement in roof

Table 5-2

WASTE SHAFT
INSTRUMENTS

Location and Type	Purpose
Lined Section	
Piezometer	Measures fluid pressure buildup behind liner due to water accumulation
Key	
Piezometer	Measures fluid pressure buildup behind key due to water accumulation
Pressure cell	Measures contact pressure buildup between concrete key and wall rock
Unlined Section	
Convergence points	Measure wall-to-wall closure of shaft
Multiple-point extensometer	Measures salt creep deformation
Station	
Convergence points (includes permanent and temporary points)	Measure roof-to-floor and wall-to-wall closure of openings
Multiple-point extensometer	Measures salt creep deformation in roof, floor and walls

Table 5-3

EXHAUST SHAFT
INSTRUMENTS

Location and Type	Purpose
Lined Section	
Piezometer	Measures fluid pressure buildup behind liner due to water accumulation
Key	
Piezometer	Measures fluid pressure buildup behind key due to water accumulation
Pressure cell	Measures contact pressure buildup between concrete key and wall rock
Unlined Section	
Multiple-point extensometer	Measures salt creep deformation

Table 5-4

DRIFTS
INSTRUMENTS

Location and Type	Purpose
Convergence points (includes permanent and temporary convergence points and wall shortening points)	Measure roof-to-floor and wall-to-wall closure of openings and pillar shortening
Extensometer (single- and multiple-point)	Measures salt creep deformation in roof, floor and walls of openings

Table 5-5

TEST ROOMS
INSTRUMENTS

Location and Type	Purpose
Convergence points	Measure roof-to-floor and wall-to-wall closure
Multiple-point extensometer	Measures salt creep deformation in roof, floor and walls
Inclinometer	Measures direction and amount of salt movement above the roof, below the floor, and in the walls
Rigid-inclusion stressmeter	Monitors changes in stress within anhydrite
Convergence meter	Measures vertical closure

calculated and stored in the computer. The data is transferred monthly to magnetic tapes which are made available to project participants.

Instruments connected to the datalogger include extensometers, piezometers, strain gauges, pressure cells, convergence meters and stressmeters. All convergence points, inclinometers, rock bolt load cells, lateral movement gauges and some extensometers must be read manually. Strain gauges, piezometers and pressure cells have been read manually at times.

The frequency of data collection is determined on a per instrument basis and is dependent upon instrument location, method of instrument reading (manual or datalogger). and the number of days elapsed since excavation at the instrument location. After installation the instrument is read frequently, but with time this reading frequency is decreased since the rate at which the salt mass responds following excavation also decreases with time.

The frequency of readings has been influenced by access limitations caused by construction operations and by the volume of data to be collected. At a few convergence point stations in newly excavated areas, readings were taken frequently to record the early rock response. Monitoring periods in these instances were typically every 4 to 12 hours for 24 hours, then once daily. Most manually read instruments were initially read weekly, then once every 2 weeks, and then once every month. Instruments connected to the datalogger were initially read at 24-hour intervals, then several times per week, and then once every 2 weeks. The current schedule for obtaining readings is shown in Table 5-6. Each instrument's range, sensitivity, resolution and precision are also presented in this table. These parameters are important when interpreting and evaluating the data, especially those readings which reflect changes that are close to the resolution, sensitivity, or precision limits of the instrument.

Table 5-6

GEOMECHANICAL INSTRUMENTATION SPECIFICATION SUMMARY

Location	Instrument Type	Phenomenon Monitored	Parameters to be Evaluated	Scheduled Frequency of Readings as of this Report	Instrument Specifications: Range (R), Sensitivity (S) Resolution (E), Precision (P)
C&SH shaft	Borehole extensometers	Deformation	$\Sigma\delta^*$, $\frac{\Delta L^{**}}{\Delta t}$	Weekly (D)	(R): 0-2 in. (P): 0.001 in. (E): 0.001 in.
C&SH shaft key	Strain gauges	Strain	Σ Strain*	As accessible (M)	(R): 0-3000 μin./in.-embedded (R): 0-2500 μin./in.-spot welded (S): 1 μin./in.
C&SH shaft key	Pressure cells	Pressure	Σ Pressure*	As accessible (M)	(R): 0-1000 psi (S): 1 psi
C&SH shaft liner & key	Piezometers	Water pressure	Σ Pressure*	Monthly (M)	(R): 0-500 psig (E): ±0.5 psi
C&SH shaft	Convergence points	Deformation	$\Sigma\delta^*$, $\frac{\Delta L^{**}}{\Delta t}$	As accessible (M)	(R): 2-50 ft (P): ±0.005 in.
Waste shaft	Borehole extensometers	Deformation	$\Sigma\delta^*$, $\frac{\Delta L^{**}}{\Delta t}$	As accessible (D)	(R): 0-2 in. (P): 0.001 in. (E): 0.001 in.
Waste shaft Key	Pressure cells	Pressure	Σ Pressure*	Weekly (D)	(R): 0-1000 psi (S): 1 psi
Waste shaft liner & key	Piezometers	Water Pressure	Σ Pressure*	Weekly (D)	(R): 0-500 psig (E): ±0.5 psi
Waste shaft	Convergence points	Deformation	$\Sigma\delta^*$, $\frac{\Delta L^{**}}{\Delta t}$	As accessible (M)	(R): 2-50 ft (P): ±0.005 in.
Exhaust shaft	Borehole extensometers	Deformation	$\Sigma\delta^*$, $\frac{\Delta L^{**}}{\Delta t}$	Weekly (D)	(R): 0-2 in. (P): 0.001 in. (E): 0.001 in.
Exhaust shaft liner & key	Piezometers	Water pressure	Σ Pressure*	Monthly (M)	(R): 0-500 psig (E): ±0.5 psi
Exhaust shaft key	Pressure cells	Pressure	Σ Pressure*	As accessible (M)	(R): 0-1000 psi (S): 1 psi
Drifts	Rockbolt load cells	Load	Σ Load*, $\frac{\Delta p^{**}}{\Delta t}$	Monthly (M)	(R): 0-300 kips (S): 16 lb
Drifts	Borehole extensometers	Deformation	$\Sigma\delta^*$, $\frac{\Delta L^{**}}{\Delta t}$	Weekly (D)/ Monthly (M)	(R): 0-2 in. (P): 0.001 in. (E): 0.001 in.
Drifts	Convergence points	Deformation	$\Sigma\delta^*$, $\frac{\Delta L^{**}}{\Delta t}$	Monthly to every 2 months (M)(1)	(R): 2-50 ft (P): ±0.005 in.
Drifts	Lateral movement gauges	Deformation	$\Sigma\delta$	No longer read	(R): 0-5 in. (E): 1/64 in. (P): ±1/64 in.
Test rooms	Vertical inclinometers	ϕ_x, ϕ_y	$\Sigma\delta_x^*$, $\Sigma\delta_y^*$, $\Sigma\delta_{xy}^*$, Azimuth*, $\frac{\Delta\Sigma w_x}{\Delta t}$, $\frac{\Delta\Sigma w_y}{\Delta t}$, $\frac{\Delta\Sigma\delta_{xy}}{\Delta t}$	Every 2 months (M)	(R): 0-30° (P): ±0.3 in./100 ft of casing (E): ±0.001 in./2 ft of casing (S): ±0.001 ft/2 ft of casing
Test rooms	Horizontal inclinometers	ϕ_z	$\Sigma\delta w_z^*$, $\frac{\Delta\Sigma w_z}{\Delta t}$	Every 2 months (M)	(R): 0-30° (P): ±0.3 in./100 ft of casing (E): ±0.001 in./2 ft of casing (S): ±0.001 ft/2 ft of casing
Test rooms	Vibrating wire stressmeters	Stress	ΣS^*, $\frac{\Delta S^*}{\Delta t}$	Weekly (D, M)	(R): 12,000-44,000 psi wire stress
Test rooms	Convergence meters	Deformation	$\Sigma\delta^*$, $\frac{\Delta L^{**}}{\Delta t}$	Weekly (D)	(R): Approximately 2.5 ft (S): ±0.001 in.
Test rooms	Convergence points	Deformation	$\Sigma\delta^*$, $\frac{\Delta L^{**}}{\Delta t}$	Monthly (M)	(R): 2-50 ft (P): 0.005 in.
Test rooms	Borehole extensometers	Deformation	$\Sigma\delta^*$, $\frac{\Delta L^{*}}{\Delta t}$	Weekly (D)	(R): 0-2 in. (P): 0.001 in. (E): 0.001 in.

Notes:

(D) = read through datalogger
(M) = read manually
$\Sigma\delta$ = total change from t = 0
ϕ = angle
ΔL = change from last reading
Δt = elapsed time since last reading

(1) New convergence points are read weekly for the first month after installation.
*Design/validation parameter
**Safety/operational parameter

M

5.2.5 Field Observations

The determination of underground conditions includes a qualitative assessment based on frequent observations by WIPP site geotechnical personnel. Changes in rock conditions and in the behavior of the underground openings have been observed and documented on a regular basis in the GFDRs. In addition, quarterly inspections have been made by Bechtel home office design engineering personnel. These inspections augmented the site geologists' observations and helped highlight those changes which occurred so slowly that they were difficult to detect on a daily basis.

Periodic inspections of the C & SH shaft have been made since the shaft was completed. Conditions of the shaft walls, liner and key have been observed in addition to any water flow into the shaft. Similar inspections of the waste and exhaust shafts have also been made but less frequently due to limited accessibility.

Observations of the horizontal openings include such items as the condition of their roofs and walls; fracturing in pillar corners at drift and room intersections and in roofs and floors; and horizontal displacements and vertical separations measured in open boreholes. This information has provided important input for design and safety evaluations.

5.3 ANALYSIS AND EVALUATION

Data collected at the WIPP site have been analyzed and evaluated by qualified engineers and scientists. Engineering experience and judgement were used in the evaluation of field observed conditions. Laboratory tests were performed on core samples to determine the constitutive equations for the host rocks. Theoretical and applied aspects of measurements, statistics and physics were utilized to analyze and evaluate geomechanical instrument data.

5.3.1 Observations

The observations of geologic conditions documented during visual inspections are used to evaluate the performance of the underground openings. These evaluations are made in conjunction with the analytical techniques. The evaluations are qualitative, however, and are subjective assessments of the behavior of the salt surrounding the excavations.

5.3.2 Laboratory Tests

The results of the laboratory testing described in subsection 5.2.3 on samples of halite, argillaceous halite, anhydrite, polyhalite and clay from the facility level were evaluated and statistically analyzed to determine elastic and creep constants. Constitutive equations for each of these materials were established and their material property constants were determined (ref. 5-3). The material property constants based on the laboratory test results are presented in Chapter 6.

5.3.3 In Situ Measurements

Statistical and numerical methods were used to analyze in situ data and to evaluate the physical behavior of salt. Numerical models were used to compute creep parameters from the in situ data.

In situ measurement data from selected geomechanical instruments in the drifts and test rooms were fitted with analytical equations using regression procedures. Since early data are lacking for most of the instruments, one approach was to calculate the closure rates and fit an equation to the closure rate versus elapsed time relationship. An estimate of the early closure not measured by the instruments was independently derived.

5.4 PREDICTION OF FUTURE BEHAVIOR

Validation of the underground opening reference design requires predicting the future behavior of the openings. This was achieved by collecting in situ data consisting of field observations and

geomechanical instrument measurements. Statistical methods were then used to extrapolate the data obtained from the geomechanical instruments. Selected in situ data were fitted to analytical curves and predictions were made based on the extrapolated results. Closed form solutions and engineering experience were also utilized to substantiate the adequacy of the facility. A model simulation method was used to verify the creep model of salt based on creep constants derived from data obtained from laboratory material tests. After the determination of creep parameters using a statistical technique, the numerical model for simulating the facility was also utilized to predict and evaluate future behavior. This includes the closures, strain distributions and stress distributions over the operating life of the facility.

Design reviews were performed as required during design of the WIPP underground facility. Experience and judgment were an important adjunct in predicting the future behavior of the underground openings. More than 3 years of continuous data collection and analysis and evaluation have provided an adequate data base for predicting future behavior.

Subsections 5.4.1 through 5.4.3 describe the methods used for predicting the future behavior of the underground openings.

5.4.1 Extrapolation of In Situ Data

Selected in situ closure data were analyzed and fitted by analytical curves for extrapolation of future responses. Regression analyses by the Gauss-Newton or Marquardt compromise techniques were performed to determine the regression parameters. These regression parameters were assumed to be valid for the future behavior of the opening, and the equations were used to predict the future closure rate. To estimate the additional closure that could occur, the equation was integrated over the required time interval.

5.4.2 Closed Form Solutions

Closed form solutions provided in the SME Mining Engineering Handbook (ref. 2-25) were used to evaluate the selected room and pillar sizes and their stability. Closed form solutions for steel and concrete structural design were also used to substantiate the adequacy of the shaft liners and keys (refs. 5-4 thru 5-7).

5.4.3 Model Simulations

Numerical analyses were performed to compute the predicted responses of the underground openings. The constitutive laws discussed in Appendix C were used in these analyses. However, yield or failure criteria developed for halite and non-halitic materials based on the results of laboratory tests were not incorporated in the numerical modeling. Due to the idealization of the real system in a mathematical model, the uncertainty of in situ auxiliary conditions corresponding to the mathematical model, and deviations in the material properties obtained from the laboratory tests, analyses using laboratory test data did not provide suitable results for design validation. Therefore, an engineering approach using curve fitting methods was employed. Creep parameters computed by the following procedure were used for the analyses. Additional information pertaining to material property deviations based on laboratory tests is presented in Chapter 6.

Numerical models were generated for the locations of specific instruments to simulate the instrument response and compute the creep parameters.

After generating the numerical models for these locations, their creep parameters were computed and the structural behavior was simulated by performing an analysis using the statistical method presented in Appendix C and the following procedures:

(1) At the initial stage, the surface of the openings were restrained to simulate the unexcavated condition.

(2) An internal stress was applied at each element to represent the initial lithostatic stress state, which is defined as:

$$\delta_{xx} = \delta_{yy} = \delta_{zz} = -\int_0^y pgdy \qquad (5\text{-}1)$$

where: p is the rock mass per unit volume;
g is the gravitational constant; and
y is the depth.

(3) The overburden and support pressures at the boundaries and the weight of the rock were applied to compute the static solution.

(4) The restraints at the surface of the openings were then removed to simulate the excavation.

(5) The structural responses were computed using a time step integration scheme. Normalized time steps were used throughout the analysis. At the first time step, the time increment was calculated by an iterative scheme using a predetermined initial time increment.

(6) In subsequent time steps, the time increment for each time step was calculated based upon the previous time steps and the specified maximum tolerances of stress and strain increments at the previous and current time steps. The structural responses were computed at each normalized time step.

CHAPTER 6
GEOLOGIC CHARACTERIZATION

6.1 INTRODUCTION

Geologic characterization of the underground excavations for design validation of the WIPP began in June 1981. Initial characterization activities consisted of monitoring the drilling and geophysical logging of the SPDV exploratory shaft. As shaft outfitting and underground excavation progressed, the geologic work evolved into mapping of the shafts and underground horizontal openings, performing ground-water inflow tests, monitoring geomechanical instrumentation installations and taking subsequent readings or measurements, logging underground core hole samples, and performing other tasks related to defining the geologic integrity of the WIPP site. Data from these activities were evaluated in conjunction with information from previous site studies to more accurately define site geologic conditions as they related to design validation of the WIPP underground facility.

6.2 DATA COLLECTION ACTIVITIES

6.2.1 Geologic Mapping

An important aspect of validating the WIPP underground opening reference design included geologic mapping of the shafts and drifts. The objectives of this mapping were discussed in Chapter 5.

6.2.1.1 C & SH Shaft

Geologic characterization of the C & SH shaft began in late June 1981 with the drilling of the SPDV exploratory shaft (see Chapter 3, subsection 3.3.1, for an explanation of the two shaft names). The initial activity conducted to develop this characterization consisted of logging the drill cuttings at periodic intervals to permit a determination of rock types and to provide a description of the geologic formations penetrated (Appendix D, Figure D-1). These formations included, in descending order, the Dewey Lake red beds, the Rustler formation and the Salado formation.

After completion of the drilling operation, geophysical logging was performed in the shaft to determine the condition of the shaft wall and to more accurately define the stratigraphy penetrated. These logs were the caliper, gamma ray, density and epithermal neutron. The logs were analyzed to better determine the depths to various stratigraphic horizons and correlate them with those found in holes drilled during previous site investigation phases (Appendix B, Figure B-1).

Reconnaissance and detailed geologic mapping of the C & SH shaft was performed between March 31, 1982, and May 2, 1982, from a depth of about 846 feet (elev. 2564 feet) near the Rustler/Salado formation contact to a depth of 2,193 feet (elev. 1217 feet). Mapping above the 846-foot depth could not be performed due to the presence of the permanent steel liner, while drilling fluid and muck prevented mapping below the 2,193-foot depth. The results of this mapping, combined with criteria established as a result of previous site investigations, were used to select the final depth for the underground development level (Chapter 3, Section 3.2). The mapping results are shown in Appendix D, Figures D-2 through D-4. A detailed discussion of the mapping is contained in reference 3-1.

Vertical control for the shaft mapping was established by tape measure from a known elevation provided by the SPDV underground excavation contractor at the shaft collar. The scope of work and methodology for the shaft geotechnical activities are contained in reference 6-1.

Reconnaissance geologic mapping of the shaft from a depth of about 920 feet (elev. 2490 feet) to 2,083 feet (elev. 1327 feet) was accomplished after construction of the shaft key. The mapped area was limited to a strip 1 to 5 feet wide along the south side of the shaft. One interval from about 1,832 feet (elev. 1578 feet) to 1,892 feet (elev. 1518 feet) was not mapped due to the interference of shaft outfitting activities.

Detailed circumferential geologic mapping was performed in the key area from the base of the steel liner to a depth of about 920 feet.

Detailed mapping was also performed from a depth of about 2,083 feet to about 2,193 feet. Detailed mapping was carried out through this interval to obtain sufficient geologic information for use in making the final facility level selection. The facility level selection mapping was performed by several teams of geologists working over a 3-day period from April 30 to May 2, 1982. The detailed mapping was generally performed independently of shaft outfitting activities to permit better observation and interpretation of the shaft geologic characteristics.

Representative samples of the geologic strata surrounding the shaft were obtained during mapping for later, more detailed classification. Photographs were taken at various locations along the shaft wall for verification of the mapping results and record-keeping purposes. As mapping progressed, observations of the shaft wall were also made to determine the condition of the salt as a result of its behavior following excavation.

Based on the data obtained from the above activities, characterizations were made of the geologic formations penetrated by the C & SH shaft. The characterizations consisted primarily of descriptions of the stratigraphy, lithology and structure of the formations. Other detailed data were included, where relevant, to more accurately characterize the salt strata in areas of primary concern to the design of the WIPP underground facility.

The C & SH shaft geologic activities served to further refine and confirm the data obtained from previous site investigations. The geologic conditions observed in the C & SH shaft within the mapped interval corresponded to the conditions expected from previous investigations. Borehole ERDA-9, in particular, showed conditions similar to the C & SH shaft. Although some variation was observed, it was attributed to core loss in ERDA-9 which prevented the early detection of these conditions.

Only minor modifications to the reference design of the C & SH shaft key structure and the geomechanical instrumentation levels were made to accommodate the observed geology.

6.2.1.2 Waste Shaft

Drilling of the initial 6-foot diameter SPDV ventilation shaft (later to be enlarged to the waste shaft) was conducted from December 1981 to February 1982. Samples of the drill cuttings were obtained at periodic intervals from the drilling fluid to permit monitoring of the stratigraphy being penetrated. After the drilling was completed, a set of geophysical logs was run to determine the shaft wall conditions and to further define the boundaries of the rock strata penetrated.

Geologic mapping of the 6-foot diameter shaft began in July 1982 in conjunction with the initiation of shaft outfitting. Initially, five areas of weaker rock which had been washed out by the drilling operation were mapped between July and September 1982 before steel liner plate was placed over these areas for safety purposes. Geologic mapping of the SPDV ventilation shaft from the bottom of the steel surface casing at 97 feet (elev. 3312 feet) to the bottom of MB-139 was conducted during September and October 1982.

Both reconnaissance and detailed geologic mapping were performed in the 6-foot diameter shaft. The mapping extended from a depth of 97 feet below the ground surface to a depth of about 2,170 feet (elev. 1239 feet). The results of this mapping are shown in Appendix E, Figures E-1 through E-6. In addition, a lithologic log, based on the geologic mapping, and a geophysical density log are shown in Appendix B, Figure B-1, for correlation with the C & SH shaft and boreholes WIPP-12, ERDA-9 and DOE-1. A detailed description of the SPDV ventilation shaft geotechnical activities is contained in reference 4-3.

Mapping of the SPDV ventilation shaft was generally performed by a team of two geologists. Depth control was maintained by hanging a tape down the shaft wall at 100- to 200-foot intervals from the top of the

surface casing. Orientation in the shaft was maintained by following a steel guide installed on the southwest wall to control movement of the work platform used in the shaft. Most of the shaft was mapped in a strip about 2 to 3 feet wide along the steel guide. Although only a portion of the shaft wall was mapped, visual examination was made of the entire wall to determine if any geologic abnormalities existed. Below a depth of about 1,180 feet (elev. 2229 feet), mapping was performed on a limited basis due to salt incrustation on the shaft wall. This crust was apparently the result of dust from the facility level that was exhausting through the shaft and depositing on the wet shaft wall. Representative samples of the rock strata were collected to permit a more detailed description. Photographs were taken at various locations along the shaft wall for verification of the mapping results and record-keeping purposes. In addition to providing a description of the rock strata, observations of the shaft wall were made to determine, where possible, the reaction of the rock to excavation.

Detailed mapping around the full circumference of the 6-foot diameter shaft was performed at the following five intervals:

(1) Magenta dolomite member,
(2) Culebra dolomite member,
(3) Rustler formation fracture zone;
(4) Rustler/Salado formation contact; and
(5) MB-139.

Because of salt incrustation on the shaft wall immediately above the facility level, detailed circumferential mapping could not be performed in this area. However, two opposing strips about 1 foot wide were cut through the crust to permit mapping of the shaft wall for a distance of about 50 feet above the facility level. Depths in the facility level area were verified by a separate survey utilizing elevation points established in the C & SH shaft station.

The enlargement of the SPDV ventilation shaft into the waste shaft began in October 1983 and was completed in August 1984. Additional geologic mapping and visual inspections were conducted concurrently with this excavation. Mapping was conducted from December 9, 1983, to August 10, 1984. Visual inspections of the shaft surface were performed throughout the shaft enlargement operations. The lithology of the exposed shaft stratigraphy was described and compared with the description of the same stratigraphic interval mapped in the SPDV ventilation shaft. Any differences or additional detail were noted and the SPDV ventilation shaft geologic map was modified accordingly.

In the lined section of the waste shaft, the depth to the base of each successive concrete segment was provided by the shaft excavation contractor. Vertical control for mapping was then established from the base of the previous segment. During enlargement of the unlined section of the shaft, vertical control was established from occasional survey control points installed by the contractor and from the previously mapped SPDV ventilation shaft geology. In the shaft sump, vertical control was based on a contractor survey point installed at a depth of 2,167 feet (elev. 1242 feet).

Detailed, full circumference geologic mapping was performed in areas of specific geologic interest. These areas were selected because of their poor exposure in the SPDV ventilation shaft, the possible occurrence of dissolutioning, or their hydrologic significance. These areas of detailed mapping were:

(1) the Forty-niner member claystone;
(2) the Magenta dolomite member;
(3) the Tamarisk member claystone;
(4) the Culebra dolomite member;
(5) the upper portion of the unnamed lower member of the Rustler formation; and
(6) the Rustler/Salado formation contact and key area.

The detailed mapping in the waste shaft was generally conducted as outlined in reference 6-1. Mapping was conducted by teams of four to six people. Once vertical control was established by the contractor from the base of the previous concrete segment, a 5 x 5-foot grid was painted on the shaft surface around its circumference to permit the accurate location of any lithologic contacts and geologic features.

Reconnaissance geologic mapping was performed in the waste shaft sump. A vertical strip, approximately 5 feet wide, was cleaned and mapped along the entire length of the sump.

A detailed description of the geotechnical activities conducted in the waste shaft is contained in reference 6-2. The results of the mapping are shown in Appendix E, Figure E-1.

The geologic mapping and visual inspections of the SPDV ventilation/waste shaft has provided additional documentation of the strata above and below the WIPP underground development level. Based on the data obtained from the shaft mapping activities, a general characterization of the stratigraphy, lithology and structure of the geologic formations penetrated by the waste shaft was made.

The waste shaft penetrates five formations. In descending order, they are the Gatuna formation of Quaternary age, the Santa Rosa sandstone of Triassic age, and the Dewey Lake redbeds, Rustler formation and Salado formation, all of Permian age. In addition, the waste shaft also penetrates thin surficial Quaternary dune sands and the Mescalero caliche. In the WIPP site area, the Santa Rosa sandstone and the Gatuna formation are represented by thin layers of sandstone (ref. 6-3). They were not mapped in the waste shaft due to installation of the shaft collar facilities.

The results of the geologic mapping of the waste shaft correlate well with the SPDV ventilation shaft mapping results. The stratigraphic units penetrated by the waste shaft are the same as those encountered by the C & SH shaft.

Post-depositional dissolution features were not observed in any stratigraphic horizons in the waste shaft. Several zones previously identified as containing dissolution residues in borehole ERDA-9 are now considered to contain pronounced primary sedimentary features.

6.2.1.3 Exhaust Shaft

The exhaust shaft was enlarged from a 6-foot diameter raise-bored shaft to its finished 14- to 15-foot diameter using conventional drill and blast methods from July 1984 to January 1985. Geologic mapping of the shaft wall was conducted concurrently with excavation and construction activities.

Reconnaissance geologic mapping was performed along the entire length of the shaft with the exception of selected areas where detailed mapping was performed. A vertical strip, approximately 5 feet wide, was cleaned and mapped. The procedures used for the reconnaissance mapping are contained in reference 6-1.

Detailed circumferential mapping of specific areas of geologic interest was also performed. These areas included those previously described in the C & SH and waste shafts and four additional areas within the Dewey Lake redbeds, three of which contain gypsum filled fractures. The areas of detailed mapping in the exhaust shaft were:

(1) gypsum-filled fractures at a depth of 195.0 to 210.0 feet;
(2) gypsum-filled fractures at a depth of 269.0 to 280.5 feet;
(3) gypsum-filled fractures at a depth of 353.5 to 375.0 feet;
(4) the Dewey Lake/Rustler formation contact (546.4 feet);
(5) the Forty-niner member claystone (575.5 to 586.5 feet);
(6) the Magenta dolomite member (602.5 to 627.0 feet);
(7) the Tamarisk member claystone (689.0 to 695.5 feet);
(8) the Culebra dolomite member (713.5 to 736.0 feet);
(9) the upper portion of the unnamed lower member (736.0 to 800.0 feet); and
(10) the Rustler/Salado formation contact and key (845.0 to 912.0 feet).

The detailed geologic mapping was performed in a manner similar to that in the waste shaft, using a 5 x 5-foot grid. Vertical survey control was provided by the shaft excavation contractor. As the shaft liner was constructed, the depth to the base of each successive concrete segment was provided by the contractor. Vertical control for mapping was then established from the base of the previous segment. During excavation of the unlined section of the shaft, vertical control was established with survey chains suspended from contractor-installed survey control points.

The results of the exhaust shaft mapping are shown in Appendix F, Figure F-1. A detailed description of the geotechnical activities in the exhaust shaft are included in the report titled Geotechnical Activities in the Exhaust Shaft (ref. 6-4).

In general, the exhaust shaft mapping results correlate well with the results from the waste shaft. Slight lateral variations in the geology produce minor exceptions. The exhaust shaft geologic mapping activities have produced additional confirmation of data obtained from previous site investigations. This mapping confirms the suitability of the shaft reference design, with some minor modifications, based on the original design parameters.

6.2.1.4 Drifts and Test Rooms

Geologic mapping of the drifts and test rooms was performed to characterize the facility level geology, demonstrate its continuity, and provide permanent documentation of the geology exposed in the underground excavations. Those drifts and rooms that were not mapped were visually inspected by site geologists to verify that the stratigraphy is laterally continuous and similar to that exposed in the mapped areas of the facility. No unusual geologic features were observed.

Geologic mapping was conducted in accordance with the procedures established in reference 6-1. A horizontal level-line referenced to

the C & SH shaft station floor elevation was established in the drifts and rooms using an engineer's tripod level. All stratigraphic contacts and geologic features were referenced to this level-line datum. Horizontal distances were measured with an engineer's tape using the C & SH shaft centerline as the zero reference point. Detailed mapping was performed at 10-foot intervals along one wall of the drifts. Between these intervals, the continuity of the stratigraphic contacts and the nature of the individual units were observed and noted on the map. The mapped drifts were the E140 drift, the E0 drift, the N1100 drift and the N1420 drift. Selected figures showing the megascopic results of this mapping are contained in Appendix B.

Geologic Mapping in the test rooms consisted of describing a 6- to 10-foot wide strip surrounding the instrument array in the center of each room. Both walls and the roof in each room were mapped. The remainder of the room was carefully inspected to confirm lateral continuity of the stratigraphic units. The strip maps from the test rooms are presented in Appendix G, Figures G-1 through G-4.

6.2.2 Core Drilling

6.2.2.1 Purpose

Vertical core holes were drilled into the floor and roof of the underground openings to provide geologic information for design validation. The objectives of the vertical core holes are described in Supporting Document 3 of reference 2-5. The purpose of the program was discussed in Chapter 5 of this report.

6.2.2.2 Summary of Drilling

A total of 124 vertical core holes have been drilled and logged in the underground drifts and in the SPDV test rooms, excluding those drilled as part of SNL's in situ tests. This number includes 16 holes drilled to replace holes that had poor core recovery and four holes drilled to obtain information on non-cored sections in the original holes. The

holes were generally drilled in pairs, one hole drilled vertically into the roof and one hole drilled vertically into the floor. Core was obtained in each hole to a nominal depth of 50 feet. Table 6-1 presents a summary of the core hole data. A map showing the core hole locations is presented on Figure 6-1. Geologic cross sections at selected core hole locations in the drifts are contained in Appendix H. Geologic drill logs of all of the core holes are contained in Appendix I.

Drilling was performed by the underground excavation contractor. The drill rig was set up by the driller and the attitude of the core hole was checked by site geotechnical personnel. Logging and handling of the core were performed by geotechnical personnel in conformance with the procedures outlined in Supporting Document 3 of reference 2-5.

All core holes were drilled using rotary equipment and compressed air or saturated brine as the circulating medium. The holes were drilled with a diamond impregnated bit which produced 2-inch or 2 3/8-inch diameter core. A 5-foot long double-tube or split double-tube core barrel was used to retain the core.

The core was logged underground as it was removed from the core barrel or after the drilling of the hole was completed. Logging was generally performed by the same geologist to maintain consistency in the descriptions of the geologic materials. The following data are recorded on each log:

(1) location of core hole and direction of drilling (up or down);
(2) beginning and completion dates of drilling;
(3) length and number of core run;
(4) amount and percentage of core recovery;
(5) stratigraphic and lithologic descriptions (color descriptions are based on the Geological Society of America (GSA) Rock-Color Chart);
(6) graphic lithologic profile; and

Table 6-1

SUMMARY OF CORE HOLE DATA

Core Hole No.	Direction	Collar Elevation (ft-MSL)	Approximate Station (ft)		Facility Coordinates (ft)		Depth/ Penetration (ft)	Instrument Designation
MB-139-1	Down	1264.1	N79	W6	N9766	E6888	10.0	None
MB-139-2	Down	1251.2	S410	E150	N9277	E7044	15.7	None
MB-139-3	Down	1260.5	S101	E157	N9586	E7051	16.0	None
MB-139-4	Down	1258.7	S99	W17	N9588	E6877	16.2	None
DH-01	Up	1318.2	N1424	E439.5	N11110.9	E7335.5	50.8	None
DH-02(1)	Down		N1424	E440	N11110.9	E7336.06	50.2	None
DH-02A(1)	Down		N1424	E435	N11110.9	E7331.29	49.2	None
DH-02B	Down	1306.3	N1424	E442	N11110.9	E7331.29	53.0	None
DH-03	Up	1318.1	N1112	E444	N10799.2	E7335.4	48.8	None
DH-03A	Up	1317.4	N1112	E450.5	N10779.2	E7341.92	49.9	None
DH-04	Down	1309.6	N1112.5	E444	N10799.2	E7335.4	45.8	None
DH-04A(1)	Down	1309.6	N1113	E446			11.2	None
DH-04B	Down	1309.7	N1112	E450.5	N10799.70	E7341.85	51.4	None
DH-05	Up	1329.9	N1463	E972	N11149.6	E7865.0	51.0	None
DH-06	Down	1317.9	N1463	E972	N11149.7	E7864.9	49.75	None
DH-07	Up	1326.7	N1112	E976.5	N10799.3	E7870.8	49.8	None
DH-08	Down	1318.8	N1112	E976.5	N10799.4	E7870.9	38.3	None
DH-08A(1)	Down	1318.7	N1112	E975			50.7	None
DH-08B	Down	1318.0	N1112	E979.5	N10799.47	E7866.66	51.4	None
DH-09	Up	1324.5	N1432	E1332.5	N11108.71	E8227.11	51.1	None
DH-10	Down	1312.1	N1432	E1332.5	N11106.70	E8227.09	52.0	None
DH-11	Up	1320.5	N1112	E1332.5	N10799.8	E8227.3	50.9	None
DH-12	Down	1311.1	N1112	E1332.5	N10799.4	E8227.2	51.3	None
DH-13	Up	1311.4	N1424	E1690	N11112	E8585	13.8	None
DH-13A	Up	1311.5	N1424.5	E1691	N11112	E8586	49.0	None
DH-13B	Up	1311.4	N1425	E1695	N11112.6	E8590.1	21.0	None
DH-14	Down	1299.5	N1425	E1695	N11112.6	E8590.1	49.1	None
DH-15	Up	1308.9	N1104	E1688.5	N10793.26	E8589.96	51.0	None
DH-16	Down	1300.3	N1104	E1688	N10792.89	E8589.39	51.0	None
DH-17	Up	1316.5	N1427	E178	N11114.2	E7071.8	52.0	None
DH-18	Down	1305.1	N1429	E181	N11114.2	E7071.8	50.8	None
DH-19	Up	1314.7	N1107	E206.5	N10794.2	E7101.7	51.6	None
DH-20	Down	1306.2	N1109	E206	N10794.2	E7101.7	51.1	None
DH-21	Up	1331.0	N1421	E786	N11109.1	E7680.9	50.4	None
DH-22	Down	1318.8	N1421.5	E785.5	N11109.2	E7680.9	51.0	None
DH-23	Up	1328.0	N1112	E781	N10799.2	E7679.9	51.0	None
DH-24	Down	1319.5	N1112	E781	N10799.2	E7679.8	49.4	None
DH-24A	Down	1319.5	N1112	E780	N10799.08	E7678.59	50.4	None
DH-25	Up	1318.8	N1422	E1510	N11109.7	E8403.8	51.8	None
DH-26	Down	1307.2	N1427	E1510	N11114.3	E8403.8	53.0	None
DH-27	Up	1300.8	N1107	W682	N10793.7	E6218.4	50.5	None
DH-28	Down	1289.9	N1107	W682	N10793.8	E6218.3	50.5	None
DH-29	Up	1298.3	N1099	W982	N10785.4	E5932.4	50.4	None
DH-29A	Up	1298.1	N1099	W987	N10786.1	E5927.3	35.0	None
DH-30	Down	1289.2	N1099	W982	N10785.5	E5932.2	50.1	None
DH-31	Up	1298.5	N1099	W1282	N10784.9	E5632.3	50.5	None
DH-31A	Up	1298.5	N1099	W1280	N10784.8	E5630.5	49.2	None
DH-31B	Up	1298.5±	N1099	W1261	N10786.7	E5652.2	4.9	None
DH-32	Down	1289.6	N1099	W1282	N10784.9	E5632.2	50.0	None
DH-32A	Down	1289.5	N1099	W1261	N10786.7	E5652.2	5.5	None
DH-33	Up	1298.6	N1099	W1582	N10786.0	E5331.1	50.5	None
DH-33A	Up	1297.4	N1099	W1570	N10786.8	E5342.0	4.1	None
DH-34	Down	1289.4	N1099	W1582	N10786.5	E5331.7	51.5	None
DH-34A	Down	1289.2	N1099	W1570	N10786.8	E5341.9	3.6	None
DH-35	Up	1294.4	N1102	W1882	N10789.4	E5032.2	52.0	None
DH-36	Down	1284.6	N1102	W1882	N10789.4	E5032.2	51.5	None
DH-37	Up	1297.4	N1101	W2182	N10788.9	E4732.0	51.5	None
DH-38	Down	1287.0	N1101	W2182	N10788.8	E4731.9	47.5	None
DH-39	Up	1296.0	N1101	W2482	N10789.2	E4430.7	50.7	None
DH-40	Down	1286.1	N1101	W2482	N10789.2	E4431.0	51.0	None
DH-41	Up	1295.8	N1101	W2782	N10789.0	E4132.6	49.9	None
DH-42	Down	1285.9	N1101	W2782	N10789.0	E4132.4	51.2	None
DH-42A	Down	1285.7	N1101	W2789	N10789.2	E4125.5	40.5	None

(1) Survey data not available.

Table 6-1 (continued)

SUMMARY OF CORE HOLE DATA

Core Hole No.	Direction	Collar Elevation (ft-MSL)	Approximate Station (ft)		Facility Coordinates (ft)		Depth/ Penetration (ft)	Instrument Designation
DH-207	Up	1259.8	S697	E155	N8989.7	E7049.1	53.0	GE-246
DH-208	Down	1251.6	S698	E150	N8988.8	E7044.0	49.2	None
DH-211	Up	1270.5	S1320	E163	N8366.5	E7057.1	50.0	None
DH-212	Down	1261.7	S1320	E163	N8366.5	E7057.1	52.1	None
DH-215	Up	1272.0	S1960	E153	N7727.2	E7046.9	52.0	GE-247
DH-216	Down	1262.6	S1960	E153	N7727.2	E7046.9	54.2	GE-248
DH-219	Up	1266.3	S2422	E162	N7264.9	E7056.6	51.0	None
DH-219A	Up	1266.1	S2418	E162	N7268.5	E7056.2	11.3	None
DH-220	Down	1257.4	S2421	E162	N7265.5	E7055.9	51.8	None
DH-223	Up	1255.1	S3079	E154	N6607.2	E7048.5	52.6	GE-249
DH-224	Down	1246.6	S3079	E154	N6607.5	E7048.5	52.5	None
DH-227	Up	1247.0	S3656	E147	N6030.7	E7041.2	51.7	None
DH-228	Down	1237.8	S3656	E147	N6030.7	E7041.2	50.4	None
DH-301	Up	1276.9	N150	W170	N9830.5	E6724.5	50.75	None
DH-302	Down	1264.9	N150	W170	N9830.5	E6724.5	50.6	None
DH-303	Up	1267.2	S400	W170	N9282.3	E6726.1	51.4	None
DH-304	Down	1254.3	S400	W170	N9282.5	E6726.1	50.5	None
DH-306	Down	1244.1	S400	E140	N9287.3	E7049.9	52.0	None
DH-306A	Down	1244.0	S400	E125	N9287.9	E7034.6	8.5	None
DH-307	Up	1262.6	S400	E300	N9286.7	E7194.2	52.0	GE-263
DH-309	Up	1259.8	S700	E220	N8987.1	E7123.0	52.3	GE-265
DH-311	Up	1264.4	S1000	E300	N8686.3	E7194.9	52.0	GE-264
DH-313	Up	1270.6	S1300	E300	N8385.9	E7190.6	19.6	None
DH-313A	Up	1270.9	S1300	E299	N8386.6	E7189.5	50.2	None
DH-314	Down	1258.3	S1300	E300	N8386.5	E7189.5	50.75	None
DH-315	Up	1272.1	S1300	W170	N8387.3	E6725.5	50.3	None
DH-316	Down	1259.9	S1300	W170	N8387.2	E6725.3	50.1	None
DH-317	Up	1271.3	S1600	W33	N8077.4	E6875.9	50.1	None
DH-317A	Up	1271.2	S1600	W30	N8077.5	E6879.5	5.0	None
DH-317B	Up	1271.2	S1597	W30	N8080.3	E6881.0	51.0	None
DH-318	Down	1258.5	S1600	W30	N8077.3	E6876.1	50.0	None
DH-319	Up	1260.0	S700	E300	N8988.1	E7191.6	51.05	None
DH-321	Up	1261.4	S400	E0	N9792.0	E6891.8	52.0	GE-268
DH-323	Up	1261.2	S400	E55	N9291.7	E6952.5	52.5	GE-267
DO-45	Up	1285.5	N254	E147	N9941.0	E7041.3	52.4	GE-230
DO-46	Down	1276.5±	N254	E147	N9941.0	E7041.3	51.5	None
DO-52	Up	1280.4	N146	W4	N9832.5	E6890.5	51.6	GE-226
DO-53	Down	1266.6	N146	W4	N9832.5	E6890.5	49.2	None
DO-56	Up	1296.8	N621	E0	N10311.8	E6892.3	52.1	GE-234
DO-57	Down	1288.1	N621	E0	N10311.8	E6892.4	52.1	None
DO-63	Up	1310.6	N1110	E0	N10796.0	E6891.9	52.8	GE-243
DO-64	Down	1301.5	N1110	E0	N10796.0	E6891.6	52.8	GE-221
DO-67	Down	1296.8	N1265	W231.5	N10952.1	E6662.9	51.7	GE-220
DO-69	Up	1310.1	N1265	W231.5	N10951.9	E6662.5	51.4	GE-218
DO-77	Down	1294.6	N1270	W364.5	N10962.5	E6529.6	53.4	GE-216
DO-79	Up	1307.7	N1270	W364.5	N10962.6	E6529.5	51.8	GE-214
DO-88	Up	1305.9	N1265	W497.5	N10952.8	E6396.5	52.7	GE-212
DO-90	Down	1292.1	N1265	W497.5	N10952.6	E6396.4	53.6	GE-210
DO-91	Down	1292.1	N1275	W630.5	N10961.5	E6263.9	51.8	GE-209
DO-93	Up	1304.9	N1275	W630.5	N10961.1	E6263.9	52.0	GE-207
DO-201	Up	1262.2	S406	W19	N9280.6	E6874.9	51.7	None
DO-202	Down	1248.6	S406	W19	N9280.6	E6874.9	51.4	None
DO-203	Up	1298.2	N624	E140	N10308.6	E7041.7	52.0	GE-235
DO-204	Down	1290.5	N640	E140	N10308.5	E7041.5	51.6	None
DO-205	Up	1316.5	N1410	E0	N11095	E6892	50.7	None
DO-206	Down	1308.0	N1410	E0	N11095	E6892	50.6	None
DO-229	Up	1259.8	S401	E153	N9287	E7049	50.6	None
OH-9	Up	1310	N1433	W231.5	N11125.6	E6662.9	15.4	None
OH-11	Up	1308	N1433	W364.5	N11125.6	E6529.6	19.7	None
OH-13	Down	1298	N1433	W231.5	N11125.6	E6662.9	9.5	None
OH-14	Down	1296	N1433	W364.5	N11125.6	E6529.6	9.7	None

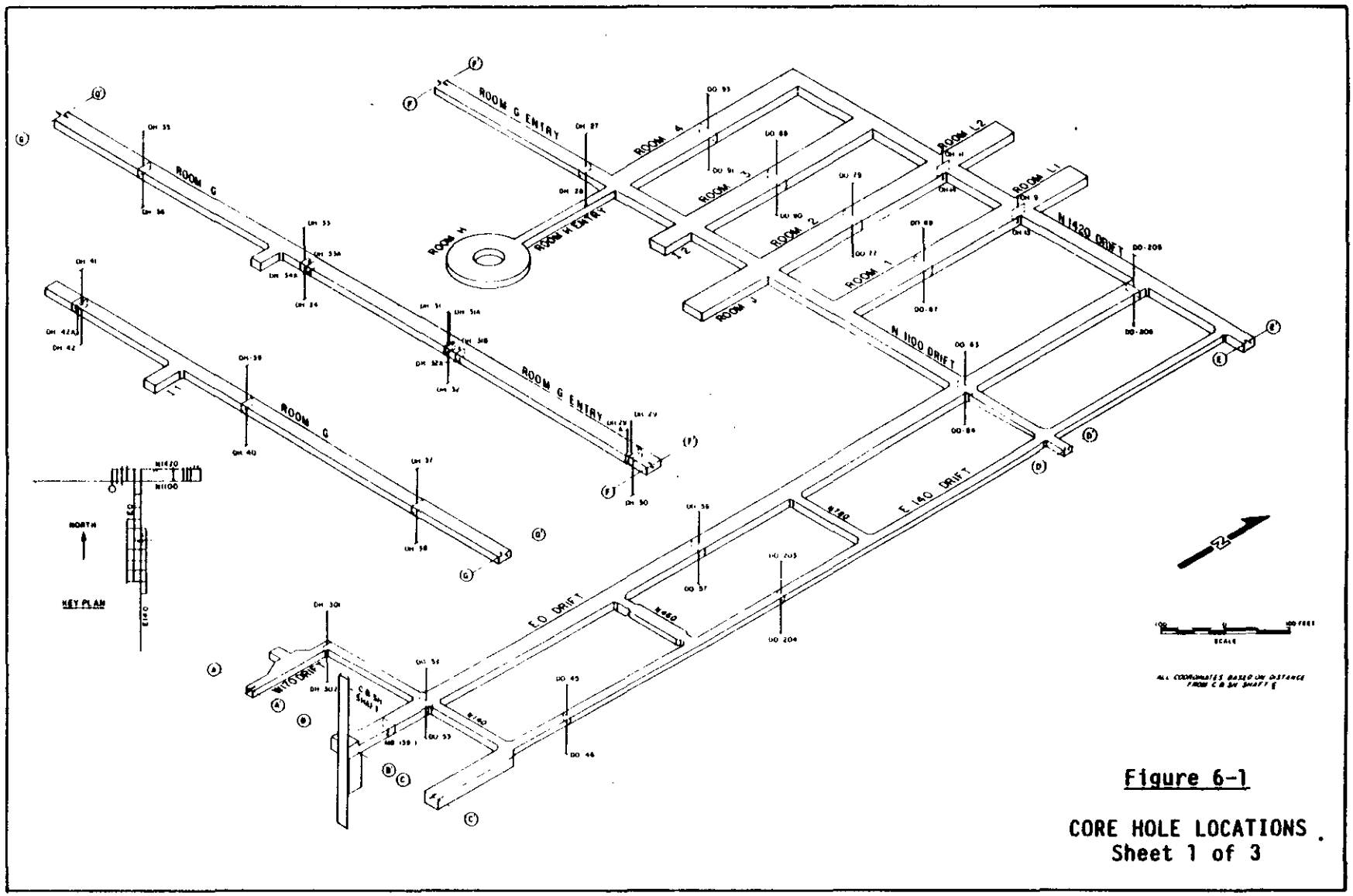

Figure 6-1

CORE HOLE LOCATIONS
Sheet 1 of 3

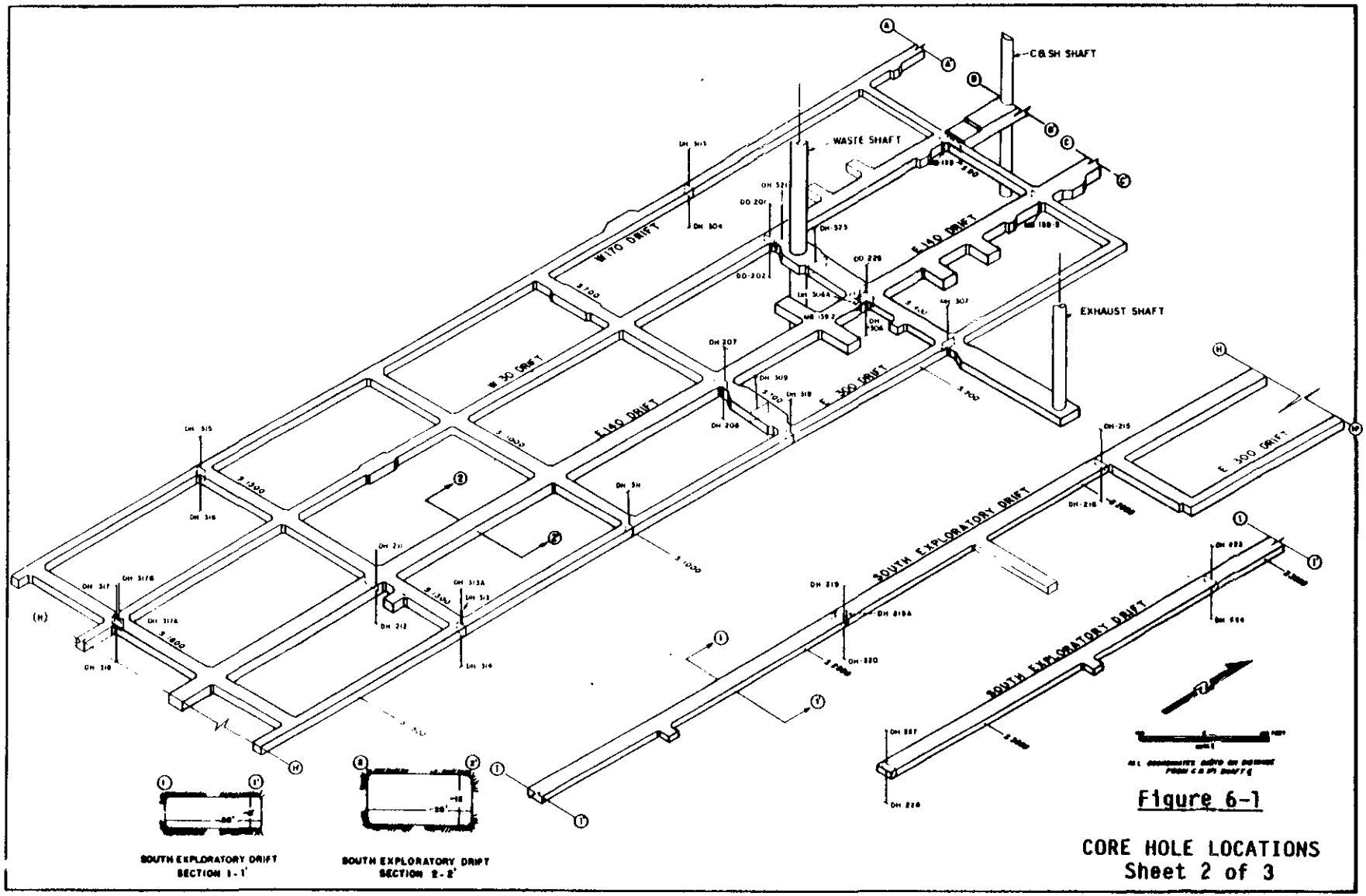

Figure 6-1

CORE HOLE LOCATIONS
Sheet 2 of 3

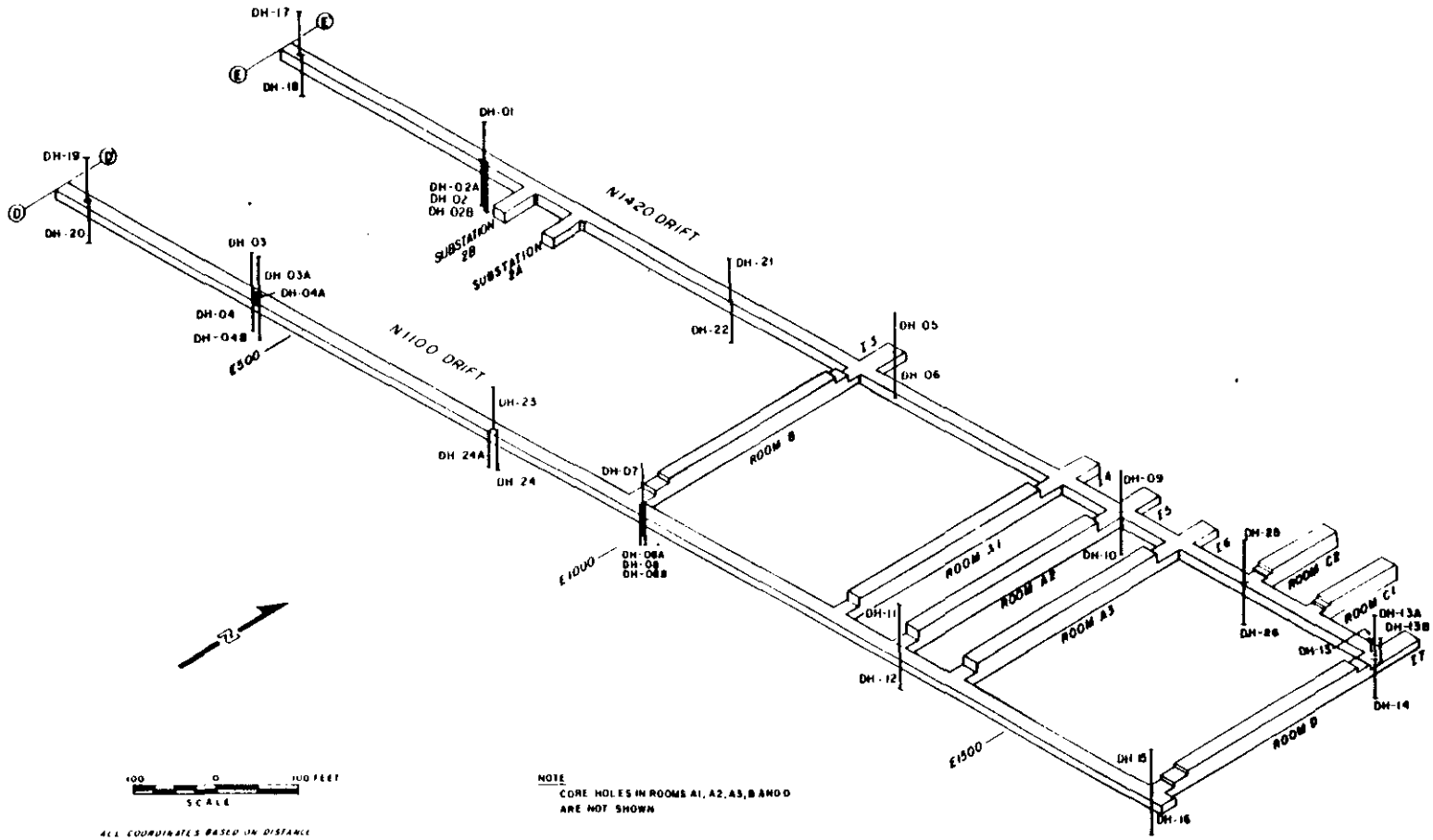

Figure 6-1

CORE HOLE LOCATIONS
Sheet 3 of 3

(7) other pertinent information related to core conditions and observations made during drilling.

Included on the logs of many of the core holes is a core sample reference number for each distinguishable stratigraphic unit (except anhydrite). This number (in some cases several numbers) is shown in brackets at the end of the unit description. The number identifies a specific core sample that has undergone a laboratory analysis to determine its percentage of insolubles (clay/polyhalite). A listing of the reference core samples and their laboratory test results for insoluble residues are presented in Table 6-2. The reference sample system was used to provide uniformity in the logging of the core and to facilitate the comparison of unit descriptions with samples having a known insoluble content. The sample number or numbers which appear on the log are those which are visually most similar to the overall unit. The crystal size in the reference samples may not be the same as in the units with which they are correlated.

Each box of core was photographed and then stored in the WIPP core library. After data from several of the core holes was collected, correlations between the holes were developed.

6.2.2.3 Summary of Results

The underground core drilling program has demonstrated the lateral continuity of stratigraphy throughout the underground facility horizon. Three anhydrite units were identified in the upholes and two anhydrite units were identified in the downholes. These units are consistently underlain by clay seams. In addition, a clay seam designated clay I was found in most of the upholes and a clay seam designated clay D was found in many of the downholes. Anhydrite is commonly associated with these two seams. The remaining units consist of halite with varying amounts of argillaceous material and polyhalite. Individual units vary slightly from hole to hole in thickness, crystal size, and the percentage of accessory constituents such as argillaceous material and polyhalite. The stratigraphy

Table 6-2

INSOLUBLE RESIDUES OF REFERENCE CORE SAMPLES
SANDIA NATIONAL LABORATORIES

Reference Sample Number	Hole Number	Depth Interval (feet)	Water-Insoluble			EDTA-Insoluble (1)		
			Sample Weight (grams)	Residue Weight (grams)	Percent Weight	Sample Weight (grams)	Residue Weight (grams)	Percent Weight
1	DO-52	9.0 - 9.7	451.09	0.03	0.01			
2	DO-52	39.4 - 40.0	336.10	0.11	0.03			
3	DO-52	14.3 - 15.0	415.57	2.15	0.52	1.61	0.72	44.72
4	DO-53	14.1 - 14.5	251.72	0.40	0.16	0.36	0.14	38.89(2)
5	DO-53	4.0 - 4.3	206.53	1.28	0.62	0.80	0.28	35.00(2)
6	DO-53	23.7 - 24.1	155.36	1.26	0.81	0.96	0.59	61.46
7(3)	DH-48	18.0 - 18.35			0.22			
8	DO-52	2.0 - 2.75	436.67	2.16	0.49	1.32	0.91	68.94
9(3)	DH-12	28.15- 28.6			0.75			57.1
10(3)	DH-11	46.5 - 46.9			3.85			39.2
11(3)	DH-12	50.05- 50.4						
12(3)	DH-11	32.8 - 33.35			2.36			50.0
13	DO-53	36.1 - 36.7	364.13	1.89	0.52	1.47	1.17	79.59
14	DO-52	42.6 - 43.5	543.62	17.97	3.31	5.13	4.58	89.28
15	DO-52	33.8 - 34.7	538.73	20.28	3.76	5.05	3.98	78.81
16	DO-52	48.7 - 49.2	315.06	16.59	5.27	5.31	4.33	81.54
17(3)	DH-10	43.3 - 43.6			0.52			49.2

Notes:

(1) For description of sample preparation see Results of Site Validation Experiments, Waste Isolation Pilot Plant (WIPP) Project, Southeastern New Mexico, Section 5.4 (ref. 2-5).

(2) Small sample volume may have produced inaccurate result.

(3) Reference sample used for visual comparison is identical to the sample tested in the laboratory, but is from different interval within the same unit.

encountered in the core holes was used to prepare the reference stratigraphic column discussed in subsection 6.3.1.3.

The presence of any gas or brine detected during drilling is recorded on the drill logs. Usually within 2 weeks of completing an air-drilled uphole, brine weeps or moisture halos appear at the collar of the hole. Brine has also collected in some downholes which were dry during drilling. Observations of gas and brine occurrences are discussed in the following subsection.

6.2.3 Fluid Measurements

6.2.3.1 General Description

Ground-water inflow measurements were taken in both the SPDV exploratory and ventilation shafts as part of the geologic field activities for the SPDV Program. In addition, measurements in the waste shaft and exhaust shaft were taken as part of design validation. Gas and brine have been encountered in boreholes and at excavation faces in the facility level drifts and rooms. Studies are being performed by other WIPP project participants to further investigate and evaluate these occurrences.

6.2.3.2 C & SH Shaft

Measurements of fluid inflow were taken during the SPDV exploratory shaft drilling operation when the drill tools were out of the hole for a bit change. The measurements were taken by monitoring changes in the drilling fluid level over a period of several hours. These data were then used to estimate approximate ground-water flow rates into the shaft.

6.2.3.3 Waste Shaft

Ground-water inflow measurements were taken in the 6-foot diameter SPDV ventilation shaft during shaft outfitting. These measurements were taken in the shaft sump and at the base of the Rustler formation. The measurements in the shaft sump were used to determine total flow into

the shaft from all ground-water sources penetrated. Periodic measurements to determine water level rise with respect to a known point at the top of the sump were obtained during test intervals ranging from about 1.5 to 90 hours. The data obtained from these measurements were used to calculate approximate ground-water flow rates into the shaft ranging from 0.3 to 0.9 gallons per minute (gpm). The average flow rate was determined to be about 0.6 gpm.

An attempt to measure ground-water inflow from the rock strata above the Salado formation was only partially successful. A collection system to retain ground-water inflow was constructed at the base of the Rustler formation by placing plastic sheeting across the shaft and attaching it to the wall. The quantity of water collected in the sheeting and drained into a graduated container was calculated to accumulate at a rate of approximately 0.3 to 0.4 gpm from all sources above the Salado formation.

No direct inflow from the Magenta or Culebra dolomite members or at the Rustler/Salado formation contact was measured. The Magenta dolomite did not exhibit measurable flow. Ground water from this member resulted in the wetting of the wall below the dolomite for a distance of about 20 feet. Below this distance the shaft wall was essentially dry. Therefore, it was concluded that the Magenta was making no contribution to the collection system at the base of the Rustler formation. Visual inspection of the Rustler/Salado formation contact, and shaft wall conditions immediately above and below this contact, suggested that the zone was making little, if any, contribution to the water accumulating in the sump. Based on these results, it was concluded that the Culebra dolomite member was contributing the majority of ground water reaching the SPDV ventilation shaft sump.

The 6-foot diameter SPDV ventilation shaft was later enlarged to become the waste shaft for the WIPP facility. Of the three formations observed during geologic mapping activities in the enlarged shaft, only the Magenta and Culebra dolomite members of the Rustler formation were

obvious fluid-bearing zones. The Magenta exhibited only a few weeps and generally produced very little water. The entire Culebra section, however, was wet, but no obvious local concentrations of water inflow were observed. Wherever a ledge was present, a steady dripping of water occurred. The Rustler/Salado formation contact, often considered a fluid-producing zone, did not contain any observable fluid except for some dampness around rock bolts.

After the waste shaft liner was constructed, ground water was observed seeping through cracks and construction joints in it. These observations are discussed in Chapter 8, subsection 8.3.1.1.

6.2.3.4 Exhaust Shaft

A water inflow measurement of approximately 0.4 gpm into the 7 7/8-inch diameter pilot hole for the exhaust shaft was taken on December 1, 1983. On December 21, 1983, a water inflow of 0.47 gpm was measured after the pilot hole was enlarged to 11 inches in diameter.

After the shaft was excavated to its finished dimensions, water inflow through cracks and construction joints in the liner was measured. Measurement was made from the 2-inch drainpipe that connects the three water collection rings in the shaft. The measured flow was 0.35 gpm in January 1985. A grouting program, conducted in June and July 1985 within the lined section of the shaft, reduced this inflow to a non-measurable quantity.

6.2.3.5 Drifts and Test Rooms

Small amounts of gas under pressure have been encountered by some underground boreholes and at the working face of underground horizontal excavations. Brine is observed to weep locally from walls and into some boreholes. The brine occurrences are visible during or immediately after excavation or drilling and remain moist or produce fluid for a period of from several weeks to more than 3 years. The formation of salt blisters on walls and salt straws and precipitate at

hole collars are common. Salt incrustations forming on the roof are being monitored at three locations: W30/S1600, E140/S2190 and E140/S2740.

The gas occurrences encounterd by boreholes are indicated on the geologic drill logs. Pressure transient testing and gas sampling were performed in several holes in the roof and floor of the facility as reported in reference 4-11. Only two occurrences of gas at the working face were documented prior to the end of December 1985. In both cases, degassing could be heard at the face for short periods of time.

The locations of major weeps occurring on walls that were geologically mapped are indicated on the maps and a discussion of their occurrence and structure is presented in reference 4-10. Sampling of brine from weeps for chemical analysis is currently being conducted. A preliminary inventory of brine occurrences at accessible locations is presented in reference 4-15.

The flow of gas from monitored holes has been low and erratic. It appears to be associated with clay seams or a result of fracture permeability in anhydrite beds. The spatial distribution of brine occurrences is also undefined. Although very few weeps have been observed on the roof surface, boreholes in the roof sometimes weep brine. The amount and duration of flow from boreholes and wall areas varies considerably. Based on observations made during preliminary gas testing, the brine appears to be associated primarily with anhydrite beds and their underlying clay seams. However, brine can also weep directly from halitic units, as observed on the walls and roof of drifts and in the drum durability test pit in Room J.

Two program plans have been developed to investigate gas and brine occurrences in the WIPP underground facility. The programs will investigate the origin, migration, volume and composition of the occurrences. Work on the Brine Testing Program (BTP) is presently

being conducted and will continue through 1987. The Gas Testing Program (GTP) is also currently in progress.

As part of the BTP, 36 accessible boreholes containing brine have been monitored. These holes include the shallow holes for the Material Interface-Interactions Test (MIIT) in Room J, inclinometer holes in Test Rooms 1 and 2 (51X-IG-00201 and 51X-IG-00202), an abandoned stressmeter hole (51X-NG-00252) in Test Room 2, hole L1-X00 in Room L1, nine stratigraphic core holes in Room G (DH-35 through DH-42A), and eight stratigraphic core holes in experimental Rooms A1, A2, A3 and B (A1X01, A1X02, A2X01, A2X02, A3X01, A3X02, BX01 and BX02). The static level of any brine in the holes is measured and recorded on a regular basis. The brine is then evacuated from the hole and its volume measured.

The BTP monitoring of brine occurrences in the MIIT holes in Room J was suspended at the end of April 1985 due to interference with experimental activities in the room. Monitoring of the remainder of the boreholes listed above continues. As new monitoring locations for the BTP are identified, they will be added to the program.

An inventory of all boreholes drilled in the underground facility has been assembled. Data contained in the inventory include hole location, diameter, depth, present status, drilling fluid used, and any observations on the occurrence of gas or brine. Over 1400 holes are presently listed, most of which contain geomechanical instruments or are otherwise inaccessible. The list will be used to locate accessible boreholes that may be suitable for use in the gas and brine testing programs.

6.3 DESCRIPTION OF FACILITY GEOLOGY

6.3.1 Stratigraphy

The stratigraphy within the WIPP underground facility horizon has been determined through vertical core hole drilling and geologic mapping of

the excavation walls. A description of the generalized stratigraphy and evidence for stratigraphic continuity is presented in the following subsections. Figures showing the stratigraphy within the WIPP underground facility horizon are presented in Appendix B.

6.3.1.1 Generalized Stratigraphy

The WIPP underground facility horizon consists primarily of halite containing varying amounts of polyhalite and clay. This halite is interrupted by 5 anhydrite beds, 12 clay seams and 6 argillaceous layers. Figure 6-2 contains a generalized stratigraphic column showing the relationship of these materials. Detailed descriptions of the individual units (except clay seams) are presented in Table 6-3. Figure 6-3 shows the individual clay seams and their descriptions.

Because of the difference in the behavior of halite and anhydrite, the five anhydrite beds represent significant boundaries above and below the horizontal underground openings. Three of the beds, abouth 1 1/2 to 12 inches thick, occur approximately 7, 14 and 35 feet above the roof of the storage level drifts and rooms. The remaining two beds occur beneath the floor of the drifts and rooms. The most significant of these two beds is MB-139 which occurs approximately 3 1/2 to 4 1/2 feet below the floor of the storage level and varies from 2.5 to 4 feet in thickness. The remaining bed occurs about 32 feet below the storage level and is approximately 4 inches thick. Thin clay seams underlie all of the anhydrite beds.

Fifteen lithologic units have been identified during geologic mapping within the facility level drifts, rooms and waste experimental area. The majority of these units are halite containing varying amounts of polyhalite and argillaceous material, usually less than 2 percent. The remaining units consist of 2 anhydrite beds, 2 argillaceious halite units and 1 polyhalitic halite unit. Each of the 15 mapped units has been assigned a numerical designation as shown on Figure 6-2 and contained in Table 6-3.

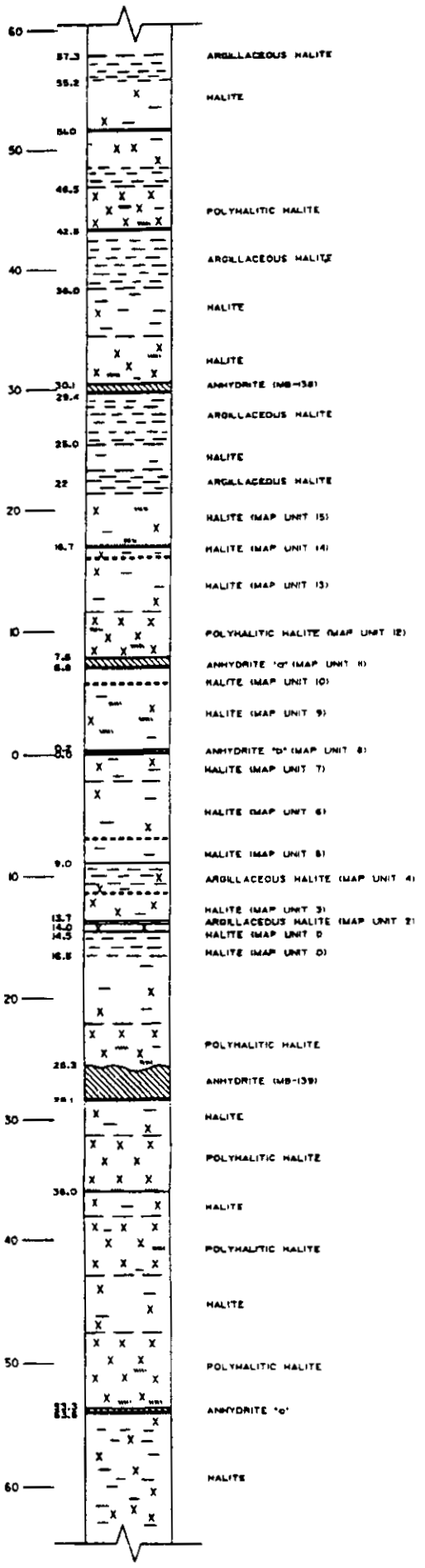

(SEE TABLE 6-3 FOR DETAILED DESCRIPTIONS OF UNITS)

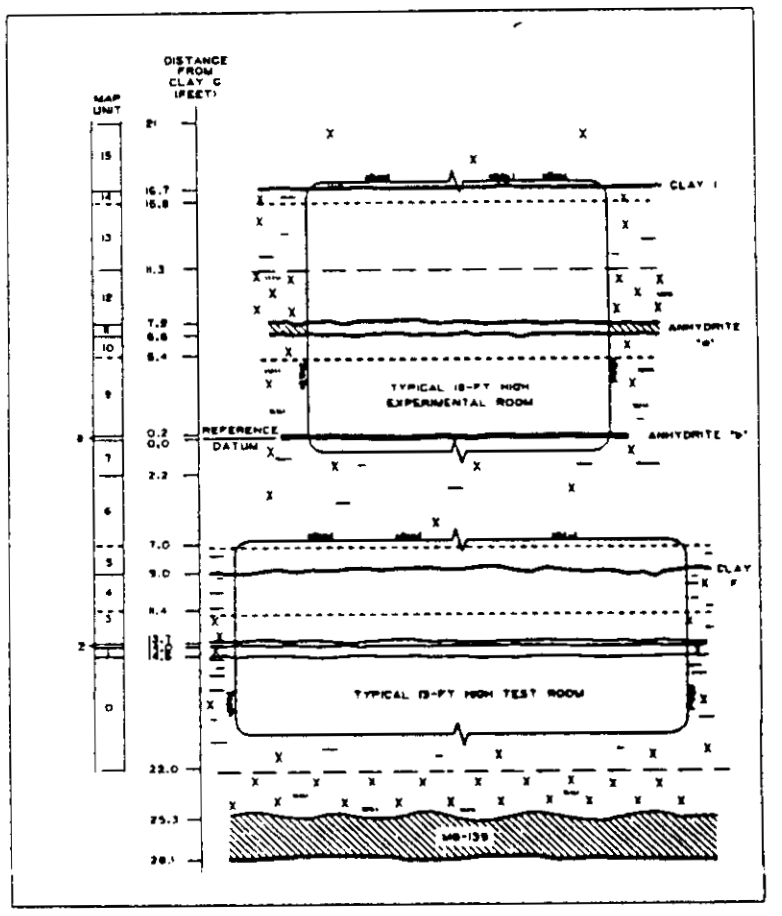

EXPLANATION

ROCK TYPE

HALITE | ANHYDRITE | POLYHALITIC HALITE | ARGILLACEOUS HALITE

ACCESSORY CONSTITUENTS

LAMINAR FEATURES

POLYHALITE | CLAY SEAM

ARGILLACEOUS MATERIAL

ANHYDRITE STRINGERS

LITHOLOGIC CONTACTS

SHARP (IDENTIFIABLE WITHIN 0.05 FT.) | GRADATIONAL (IDENTIFIABLE WITHIN 0.05 TO 0.2 FT.) | DIFFUSE (IDENTIFIABLE WITHIN 0.2 TO 0.6 FT.)

NOTES:

1. DISTANCES ARE MEASURED FROM THE BASE OF ANHYDRITE 'b' (CLAY G) AND ARE AVERAGED FROM REPRESENTATIVE CORE HOLE LOGS, SHAFT AND TEST ROOM MAPPING. ACTUAL DISTANCES AND UNIT THICKNESSES MAY VARY LOCALLY FROM THOSE SHOWN.
2. DESCRIPTIONS OF UNITS ARE BASED ON CORE HOLE DATA, SHAFT MAPPING AND VISUAL INSPECTION OF EXPOSURES IN UNDERGROUND DRIFTS AND ROOMS.
3. DETAILED DESCRIPTIONS OF CLAY SEAMS ARE PRESENTED ON FIGURE 6-4.
4. PERCENTAGES OF ARGILLACEOUS MATERIAL AND POLYHALITE ARE BASED ON VISUAL ESTIMATES FROM EXAMINATION OF DRILL CORE AND EXPOSURES IN THE UNDERGROUND EXCAVATIONS. SANDIA NATIONAL LABORATORIES' MEASUREMENTS OF INSOLUBLES FROM SELECTED CORE WERE USED AS A POINT OF REFERENCE.

Figure 6-2

WIPP GENERALIZED STRATIGRAPHIC COLUMN

Table 6-3

DESCRIPTION OF GENERALIZED STRATIGRAPHY

Approximate Distance From Clay G (Ft)	Stratigraphic Unit	Description*
55.2 to 57.3	Argillaceous halite	Clear to moderate brown, medium to coarsely crystalline. <1 to 3% brown clay. Intercrystalline and discontinuous breaks. In one core hole, consists of a 1 in. thick clay seam. Unit can vary up to 4 ft thickness. Contact with lower unit is gradational.
46.5 to 55.2	Halite	Clear to moderate reddish orange and moderate brown, coarsely crystalline, some medium. ≤1% brown clay, locally argillaceous (clays M-1 and M-2). Scattered anhydrite stringers locally.
42.8 to 46.5	Polyhalitic halite	Clear to moderate reddish orange, some moderate brown, coarsely crystalline. <1 to 3% polyhalite. None to 1% brown and some gray clay. Scattered anhydrite locally. Contact with unit below is fairly sharp.
38.0 to 42.8	Argillaceous halite	Clear to moderate brown, medium to coarsely crystalline, some fine. <1 to 5% brown clay. Locally contains 10% clay. Intercrystalline and scattered breaks. Locally contains partings and seams. Contact with lower unit is gradational based on increased clay content. Average range of unit is 38.0 to 42.8 ft above clay G but does vary from 33.8 to 46 ft.
34.0 to 38.0	Halite	Clear to moderate brown, some moderate reddish brown, coarsely crystalline, some fine and medium. ≤1% brown clay, trace gray clay locally. Scattered breaks. Locally argillaceous. <1% polyhalite. Contact with unit below is gradational based on clay and polyhalite content.
30.1 to 34.0	Halite	Clear to moderate reddish orange, coarsely crystalline. <1 to 3% polyhalite. Commonly polyhalitic. Scattered anhydrite stringers with anhydrite layers up to 1/2 in. thick locally. Scattered brown clay locally. Contact with MB-138 below is sharp.
29.4 to 30.1	Anhydrite (MB-138)	Light to medium gray, microcrystalline. Partly laminated. Scattered halite growths. Clays seam K found at base of unit.
25.0 to 29.4	Argillaceous halite	Clear to moderate brown, some light moderate reddish orange. Medium to coarsely crystalline. <1 to 3% brown clay, some gray. Locally up to 5% clay. Clay is intercrystalline with scattered breaks and partings present. < 1/2% dispersed polyhalite. Contact with lower unit is gradational based on clay content. Upper contact is sharp with clay K.
23.0 to 25.0	Halite	Clear, some light moderate brown, coarsely crystalline. <1/2% brown clay. Contact with clay J below varies from sharp to gradational depending if clay J is a distinct seam or merely an argillaceous zone.
21.0 to 23.0	Argillaceous halite	Usually consists of scattered breaks or argillaceous zone containing <1 to 3% brown clay. In C & SH shaft, it is a 1/2 in. thick brown clay seam.
16.7 to 21.0	Halite (Map Unit 15)	Clear, coarsely crystalline, scattered medium. None to <1% dispersed polyhalite and brown clay. Scattered anhydrite. Lower contact is sharp with clay I.
15.8 to 16.7	Halite (Map Unit 14)	Clear to grayish orange-pink, coarsely crystalline, some medium. <1/2% dispersed polyhalite. Scattered discontinuous gray clay stringers. Clay I is along upper contact. Contact with lower unit is diffuse.
11.5 to 15.8	Halite (Map Unit 13)	Clear to moderate reddish orange and moderate brown, medium to coarsely crystalline, some fine. ≤1% brown clay, locally up to 3%. Trace of gray clay. Scattered discontinuous breaks. <1% dispersed polyhalite and polyhalite blebs. Contact with unit below is gradational based on clay and polyhalite content.

Table 6-3 (continued)

DESCRIPTION OF GENERALIZED STRATIGRAPHY

Approximate Distance From Clay G (Ft)	Stratigraphic Unit	Description*
7.5 to 11.5	Polyhalitic halite (Map Unit 12)	Clear to moderate reddish orange, coarsely crystalline. <1 to 3% dispersed polyhalite and polyhalite blebs. Scattered anhydrite stringers. Contact is sharp with unit below.
6.8 to 7.5	Anhydrite "a" (Map Unit 11)	Light to medium gray, light brownish gray and sometimes light moderate reddish orange. Microcrystalline. Halite growths within. Partly laminated. Clear, coarsely crystalline halite layer, up to 2 in. wide, found within exposures in waste experimental area. Thin gray clay seam H at base of unit.
5.5 to 6.8	Halite (Map Unit 10)	Clear to moderate reddish orange/brown, fine to coarsely crystalline. <1% brown and/or gray clay and dispersed polyhalite. Discontinuous clay stringers locally. Contact with lower unit is diffuse based on crystal size and varying amounts of clay and polyhalite.
0.2 to 5.5	Halite (Map Unit 9)	Clear to light moderately reddish orange, coarsely crystalline, some medium. None to <1% polyhalite. Trace of gray clay locally. Scattered anhydrite stringers. Contact with unit below is sharp.
0.0 to 0.2	Anhydrite "b" (Map Unit 8)	Light to medium gray, microcrystalline anhydrite. Scattered halite growths. Thin gray clay seam G at base of unit.
0.0 to -2.2	Halite (Map Unit 7)	Clean to light/medium gray, some moderate reddish orange/brown. Coarsely crystalline, some fine and medium. <1 brown and gray clay. Locally up to 2% clay. <1% dispersed polyhalite. Upper contact is sharp with clay G. Contact with lower unit is gradational.
-2.2 to -7.0	Halite (Map Unit 6)	Clear, some moderate reddish orange, coarsely crystalline, some fine to medium locally. <1/2% gray clay and polyhalite. Contact with lower unit gradational and/or diffuse.
-7.0 to -9.0	Halite (Map Unit 5)	Clear coarsely crystalline. <1/2% gray clay. Contact with lower unit is usually sharp with clay F.
-9.0 to -11.4	Argillaceous halite (Map Unit 4)	Clear to moderate brown and moderate reddish brown, coarsely crystalline. <1% polyhalite. <1 to 5% argillaceous material; predominantly brown, some gray, locally. Intercrystalline and discontinuous breaks and partings common in upper part of unit. Decreasing argillaceous content downward. Contact with lower unit is gradational.
-11.4 to -13.7	Halite (Map Unit 3)	Clear to moderate reddish orange, coarsely crystalline. <1% dispersed polyhalite and polyhalite blebs. Locally polyhalitic. Scattered gray clay locally. Contact with lower unit is sharp.
-13.7 to -14.0	Argillaceous halite (Map Unit 2)	Moderate reddish brown to medium gray, medium to coarsely crystalline. <1 to 3% argillaceous material. Contact with lower unit is usually sharp.
-14.0 to -14.5	Halite (Map Unit 1)	Light reddish orange to moderate reddish orange, medium to coarsely crystalline. <1% dispersed polyhalite. Contact with lower unit is sharp.
-14.5 to -22.0	Halite (Map Unit 0)	Clear to moderate reddish orange/brown, moderate brown and grayish brown. Medium to coarsely crystalline. <1 to 5% argillaceous material. Predominantly brown, some gray, intercrystalline argillaceous material and discontinuous breaks and partings. Upper two feet of unit is argillaceous halite decreasing in argillaceous material content downward. None to <1% polyhalite. Contact with lower unit is gradational based on polyhalite content.

Table 6-3 (continued)

DESCRIPTION OF GENERALIZED STRATIGRAPHY

Approximate Distance From Clay G (Ft)	Stratigraphic Unit	Description*
-22.0 to -25.3	Polyhalitic halite	Clear to moderate reddish orange. Coarsely crystalline, some medium locally. <1 to 3% polyhalite. Scattered anhydrite. Scattered gray clay locally. Contact with lower unit (MB-139) is sharp, but commonly irregular and undulating. Trace of gray locally present along this contact.
-25.3 to -28.1	Anhydrite (MB-139)	Moderate reddish orange/brown to light and medium gray, microcrystalline anhydrite. "Swallowtail" pattern, consisting of halite growths within anhydrite, common in upper part of unit. Locally, hairline, clay-filled, low-angle fractures found in lower part of unit. Thin halite layer common close to lower contact. Clay seam E found at base of unit. Upper contact is irregular, undulating and sometimes contains <1/16 in. gray clay.
-28.1 to -31.2	Halite	Clear to moderate reddish orange, and light gray. Coarsely crystalline, some fine and medium. ≤1% polyhalite and intercrystalline gray clay. Contact with lower unit is gradational based on increased polyhalite content.
-31.2 to -36.0	Polyhalitic halite	Clear to moderate reddish orange, coarsely crystalline. < 1 to 3% polyhalite. Contact with lower unit is usually sharp along clay D.
-36.0 to -37.8	Halite	Clear to moderate reddish orange, some light gray. Medium to coarsely crystalline. ≤1% polyhalite and gray clay. Contact with lower unit is gradational based on increased polyhalite content.
-37.8 to -42.7	Polyhalitic halite	Clear to moderate reddish orange/brown, coarsely crystalline. < 1 to 3% polyhalite. Trace of clay locally. Scattered anhydrite locally. Contact with lower unit is gradational, based on decreased polyhalite content.
-42.7 to -47.3	Halite	Clear to moderate reddish orange, medium to coarsely crystalline. < 1% dispersed polyhalite. < 1% brown and/or gray clay. Contact with lower init is gradational and/or diffuse.
-47.3 to -53.3	Polyhalitic halite	Clear to moderate reddish orange. Coarsely crystalline with some medium sometimes present close to lower contact. <1 to 3% polyhalite. Scattered anhydrite especially common close to anhydrite "c". Lower contact is sharp with anhydrite "c".
-53.3 to -53.5	Anhydrite "c"	Light to medium gray, microcrystalline anhydrite. Scattered halite growths. Faintly laminated locally. Clay seam B found at base of unit.
-53.5 to -65.7	Halite	Clear to medium gray and moderate brown. Medium to coarsely crystalline, some fine locally. ≤1% polyhalite, locally polyhalitic. <1 to 3% clay, both brown and gray. Intercrystalline clay with discontinuous breaks and partings. Zones of argillaceous halite found within unit. Seams of clay mixed with halite crystals present locally. Upper contact of this unit is sharp with clay B.

* Descriptions are based on examination of drill core and exposures of units in shafts and other underground openings.

Map units 1 through 6 occur within the storage level drifts and rooms. Unit 1 is a distinct, relatively thin, orange-colored unit commonly referred to as the "orange marker bed". This unit is continuous throughout the facility level excavations. During excavation, it was used as a marker to help keep the underground openings within the proper stratigraphy. The descriptions for map units 7 through 15 represent the lithology most frequently encountered in the drifts and rooms in the waste experimental area. Minor variations in these lithologies occur at various locations but they are not of sufficient difference to justify their inclusion in the generalized descriptions.

6.3.1.2 Stratigraphic Continuity

The results of geologic mapping and core hole drilling in the underground facility have confirmed the lateral extent and stratigraphic continuity of the geologic units within the underground facility horizon. Strata exposed in the drifts have been traced continuously for 4,500 feet in an east-west direction and more than 5,000 feet in a north-south direction. North-south and east-west correlations between the vertical core holes have also demonstrated the continuity of the stratigraphic units above and below the facility level. Figures B-4 through B-9 in Appendix B show the correlations of stratigraphic horizons that have been made based on core hole data. These figures also demonstrate the slight southern dip of the units. Figure B-5 shows a slight thinning of units to the south by about 5 percent. Figures B-1 and B-2 show a larger correlation of stratigraphic horizons between boreholes WIPP-12 to the north and DOE-1 to the south. The five anhydrite beds shown on Figure 6-2 are laterally continuous across the WIPP site.

Although the general character of each stratigraphic unit remains constant throughout the underground facility horizon, minor variations occur. Some thin clay seams are discontinuous and some halite units thin locally or pinch out. The disruptions of some of these units are localized phenomena thought to result from syndepositional processes. Both lateral and vertical variations in the argillaceous and polyhalite

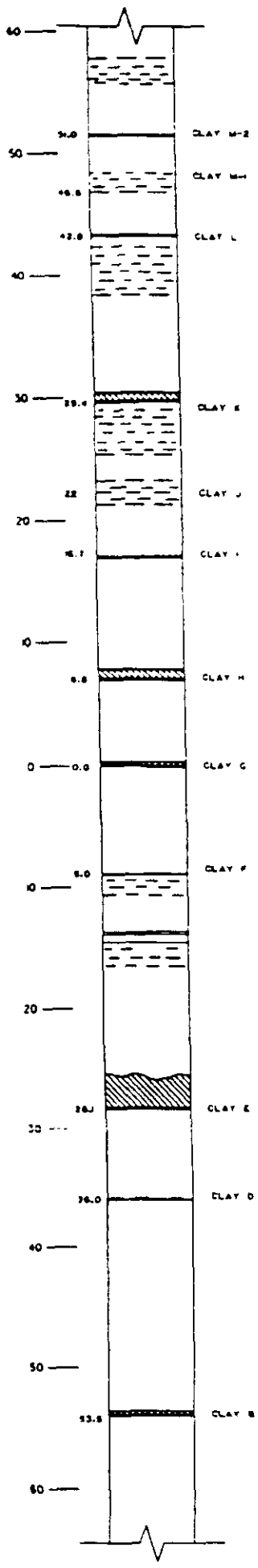

VARIES FROM AN ARGILLACEOUS HALITE ZONE CONTAINING <1 TO 3% BROWN CLAY TO A CLAY/HALITE SEAM UP TO 3 1/2 INCHES THICK.

COMMONLY FOUND AS AN ARGILLACEOUS HALITE ZONE CONTAINING <1 TO 3% BROWN CLAY OR MERELY A BROWN, SOMETIMES GRAY, CLAY PARTING. LOCALLY FOUND AS A SEAM UP TO 1/2-INCH THICK.

IN C & SH SHAFT, IT IS A 2-INCH THICK BROWN CLAY SEAM. MOST COMMONLY IT IS FOUND AS THE UPPER CONTACT OF THE ARGILLACEOUS ZONE BELOW.

USUALLY BROWN CLAY BUT SOMETIMES GRAY TO GRAY-BROWN. IN CORE, MOST COMMONLY FOUND AS 1/4 TO 1 1/4-INCH HARD, BROWN CLAY SEAM. IN THE C & SH SHAFT, IT IS UP TO 1 1/2 INCHES THICK. USUALLY IT IS A LOW ANGLE CONTACT.

IN C & SH SHAFT, CONSISTS OF A REDDISH BROWN CLAY SEAM UP TO 1/2-INCH THICK. IN CORE HOLES, FOUND AS SCATTERED BREAKS OR ARGILLACEOUS HALITE CONTAINING <1 TO 3% CLAY.

1/4 TO 5/8-INCH THICK CLAY. COMMONLY BROWN OR BROWNISH GRAY IN CORE BUT GRAY WHERE EXPOSED IN EXPERIMENTAL TEST ROOMS. COMMONLY ASSOCIATED WITH THIN ANHYDRITE ABOVE. EXPOSURES IN EXPERIMENTAL TEST ROOMS SHOW IT TO BE FAIRLY REGULAR WITH UNDULATIONS USUALLY LESS THAN 1 INCH AMPLITUDE. SOME SCATTERED HALITE GROWTHS LOCALLY WITHIN CLAY.

AVERAGES <1/4-INCH THICK CLAY BUT VARIES FROM TRACE UP TO 1/2 INCH. USUALLY GRAY COLOR BUT BROWN IN SEVERAL CORE HOLES. CLAY H IS EXPOSED IN THE WASTE EXPERIMENTAL AREA. HERE IT IS A GRAY, IRREGULAR SEAM WITH UNDULATIONS OF 1 TO 3 INCHES AMPLITUDE.

TRACE UP TO 3/8-INCH THICK GRAY CLAY. USUALLY A LOW ANGLE CONTACT IN CORE. EXPOSED IN WASTE EXPERIMENTAL AREA WHERE IT IS A GRAY, FAIRLY REGULAR SEAM WITH UNDULATIONS AVERAGING <2 INCHES AMPLITUDE. LOCALLY, MOISTURE IS NOTED ALONG THIS SEAM. EXPOSED ALONG THE WALLS OF MANY OF THE FACILITY LEVEL DRIFTS AND ROOMS ALONG THE UPPER CONTACT OF MAPPING UNIT 4, VERY IRREGULAR.

GRAY TO BROWN SEAM 1/8 TO 1/2-INCH THICK. HALITE IS COMMONLY MIXED WITH CLAY AND SILT. SOMETIMES BIFURCATES INTO TWO SEAMS. LOCALLY DISCONTINUOUS. UNDULATIONS OF 2 TO 8 INCHES AMPLITUDE.

1/8 TO 1 1/2-INCH GRAY CLAY SEAM. MOISTURE PRESENT IN SOME LOCATIONS. LOCALLY IRREGULAR WITH UNDULATIONS UP TO 4 INCHES AMPLITUDE.

VARIES FROM A ZONE OF CLAY BREAKS UP TO A 3/4-INCH, GRAY CLAY SEAM. SOMETIMES THIN ANHYDRITE IS ASSOCIATED ABOVE. NEAR HORIZONTAL IN CORE.

GENERALLY 1/8 TO 1/4-INCH GRAY CLAY SEAM BUT LOCALLY UP TO 1 1/4 INCHES. USUALLY LOW ANGLE AND SLIGHTLY IRREGULAR IN CORE.

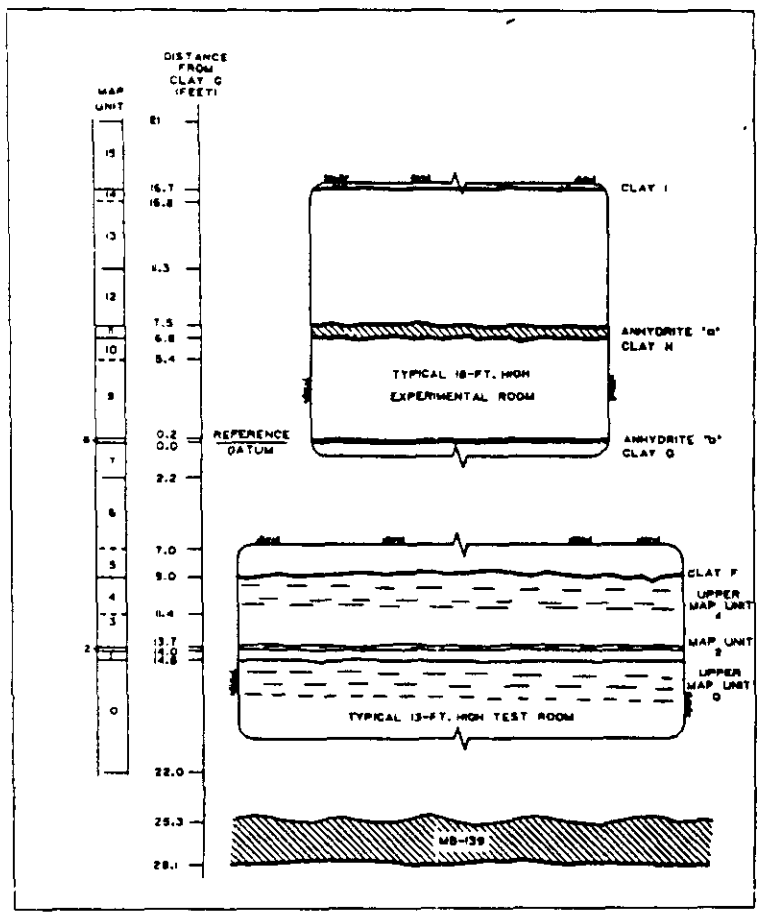

EXPLANATION

ROCK TYPE

ANHYDRITE

ARGILLACEOUS HALITE

ACCESSORY CONSTITUENTS

LAMINAR FEATURES

ANHYDRITE STRINGERS

CLAY SEAM X/4 IN. THICK

LITHOLOGIC CONTACTS

SHARP

IDENTIFIABLE WITHIN 0.05 FT.

NOTES:

1. DISTANCES ARE MEASURED FROM CLAY G AND ARE AVERAGED FROM REPRESENTATIVE CORE HOLE LOGS AND SHAFT MAPPING.
2. DESCRIPTIONS OF CLAY SEAMS ARE BASED ON CORE HOLE DATA, SHAFT MAPPING AND VISUAL INSPECTION OF EXPOSURES IN UNDERGROUND DRIFTS AND ROOMS.
3. ONLY CLAY SEAMS ARE SHOWN ON THIS FIGURE. ALL OTHER UNITS ARE SHOWN ON FIGURE 6-2 AND DESCRIBED IN TABLE 6-3.

Figure 6-3

CLAY SEAMS

content of the halite units are common. The size of halite crystals varies from fine to coarse both laterally and vertically within inidvidual units. Although the anhydrite is microcrystalline, the beds vary laterally in color, thickness and polyhalite or halite content. The upper surface of MB-139 is undulatory with amplitudes of up to 12 inches.

The halite around the underground openings exhibits slightly varied behavior in response to excavation at different locations. This may be due to minor variations in crystal size or clay content. The clear halite in the roof of the E140 drift south of the waste shaft exhibits more spalling than is apparent in similar halite in other areas of the underground openings. Spalling along the upper portion of map unit 4 occurs in many of the facility level drifts and rooms. In the locations where this unit contains abundant argillaceous material, the spalling appears to be more pronounced. This behavior is discussed in Chapters 10 and 11.

6.3.1.3 Reference Stratigraphy

A meeting was held on November 15, 1979, to determine a reference stratigraphy for the WIPP site. This was titled the "November '79 Reference Stratigraphy" and was based on data obtained from exploratory boreholes. The purpose of the reference stratigraphy was to provide input data for thermal/structural analyses of shafts, drifts and rooms at the WIPP that could be referenced by all structural analysts and updated as more data became available.

The "November '79 Reference Stratigraphy" was revised in July 1981 and again in September 1983 as more data were collected from construction activities and underground core holes. The 1983 revision was titled "September '83 Reference Stratigraphy". This revision was based on the evaluation of 39 core hole logs and the geologic mapping performed in the SPDV exploratory and ventilation shafts.

The evaluation determined that the strata are fairly horizontal but dip slightly to the south. Based on a statistical analysis, the entire stratigraphic section was found to vary in elevation in a regular manner, but individual unit thicknesses and the relative separation between units were found to have no statistically significant variation between the northern and southern limits of the underground facility horizon (ref. 5-3).

Figure 6-4 shows the reference stratigraphy developed by this statistical analysis. This stratigraphy consists of 1 polyhalite bed, 2 argillaceous halite units, 7 anhydrite beds, 12 clay seams, and halite as the remaining constituent. This reference stratigraphy extends approximately 165 feet above and below the facility level. The location and thickness of the various units were adjusted by averaging values determined from the core holes. Geologic maps of the SPDV exploratory and ventilation shafts and the log of borehole ERDA-9 were used for units outside the WIPP underground facility horizon. The uniformity of the rock in the core holes and shafts, the lack of a statistically significant variation in unit thicknesses and elevation, and the expected small influence of any differences on structural behavior resulted in a decision to use the same reference stratigraphy throughout the site.

Subsequent to the development of the September 1983 reference stratigraphy, additional core holes were drilled and logged, the ventilation shaft was enlarged to the waste shaft, the exhaust shaft was completed, and both of these shafts were geologically mapped. Based on additional data from these activities, a generalized stratigraphic column of the underground facility horizon was developed (Figure 6-2 and Table 6-3). This stratigraphic column does not vary significantly from the earlier 1983 reference stratigraphy. Therefore, the 1983 reference stratigraphy continued to be used for model calculations.

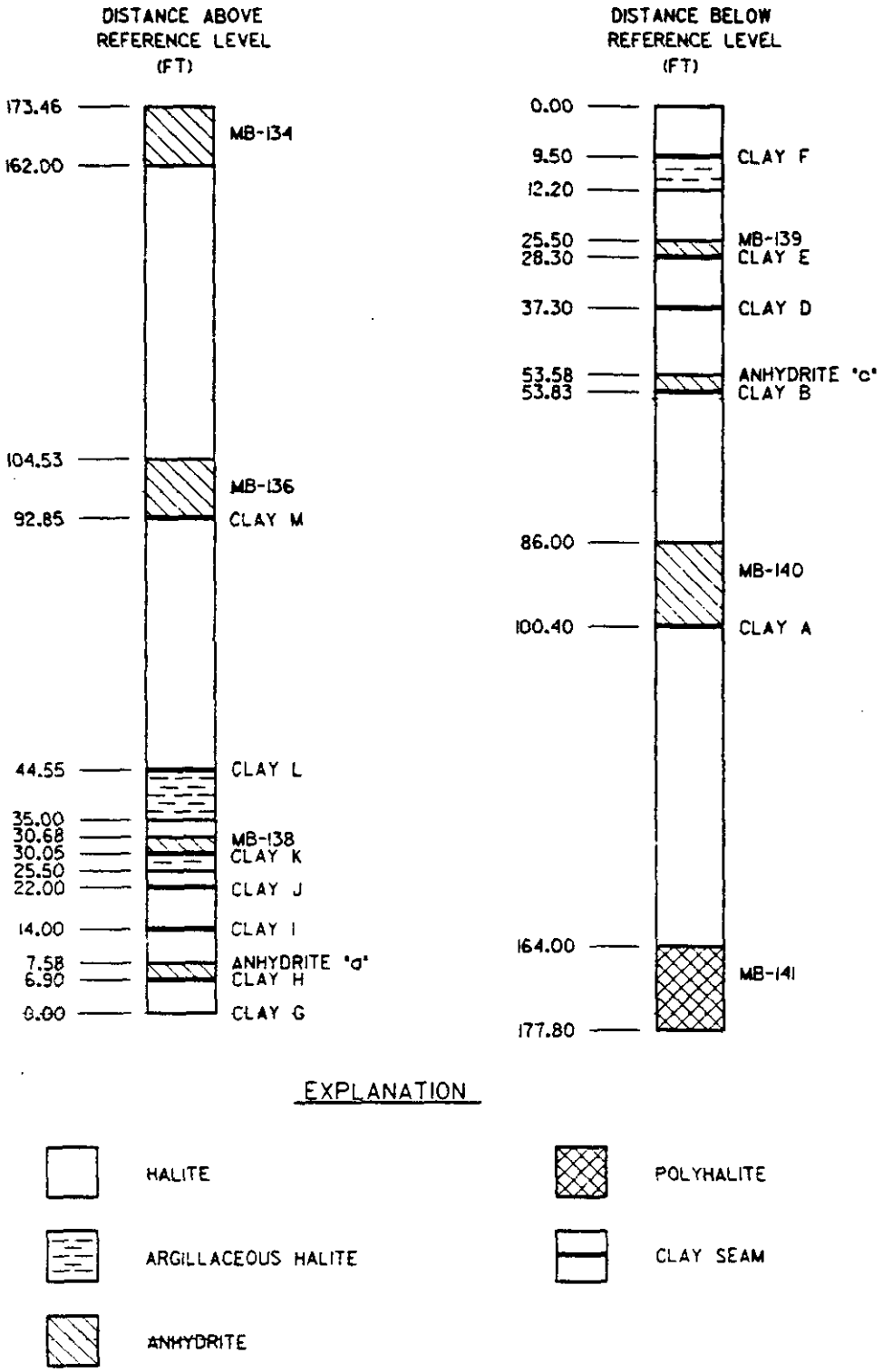

Figure 6-4

REFERENCE STRATIGRAPHY

6.3.2 Lithology

The Salado formation is predominantly halite, but other evaporite minerals and argillaceous materials are present that may locally compose up to 50 percent of the salt. Anhydrite, an early-precipitated evaporite mineral, is found in beds (usually less than 5 feet thick) which are typically underlain by a clay seam (1/16 to 3/4 inch thick). Polyhalite, a late-forming evaporite mineral, is commonly found as an accessory mineral in the Salado formation. Clay and silt may be found disseminated through the halite or in thin seams, partings, or breaks. Following is a description of the major lithologies occurring within the underground facility horizon.

Clear Halite. These units consist of halite with only trace amounts of impurities. The halite is predominantly medium to coarsely crystalline and clear to very light gray or moderate reddish orange. Less commonly, it occurs as finely crystalline, opaque, very light gray halite with a sucrose texture. Trace impurities of clay and/or polyhalite are generally dispersed in the halite. Scattered very light gray to white anhydrite or magnesite stringers may be present.

Polyhalitic Halite. These units are composed mainly of medium to coarsely crystalline halite with accessory amounts of polyhalite. As the polyhalite content increases, the color of the rock changes from transparent light orange-pink to translucent moderately reddish orange/brown or dark reddish brown. The polyhalite occurs primarily as interstitial blebs or patches and, less commonly, in stringers about 1/4 to 3/4 inch thick.

Argillaceous Halite. Six argillaceous halite units, three above and three below clay G, occur within the underground facility horizon. Generally, these units consist of medium to coarsely crystalline and some finely crystalline halite with from less than 1 to as much as 5 percent silty clay. The clay is predominantly brown in color with some gray. It is commonly intercrystalline or forms scattered breaks or partings. Discontinuous clay seams are present locally. The percent

of clay is a visual estimate; laboratory measurements of insolubles (ref. 6-5) were used as a reference.

The contacts between these units and the surrounding materials vary from gradational to distinct. Clays F, K and L occur at the upper contact of three of these argillaceous units. The three units below clay G are exposed in the underground drifts and rooms. These are geologic map units 2 and 4 and the upper portion of map unit O (Figure 6-2). They are exposed continuously throughout the openings except in the waste experimental area which is stratigraphically higher. Map unit 2 is very thin and absent in places.

No significant moisture is associated with these argillaceous halite layers. Commonly, they are slightly moist immediately after excavation and locally develop brine blisters on the walls of the underground openings.

Anhydrite. These beds range in thickness from a few inches to a few feet. Because they are readily identified, the anhydrite beds in the vicinity of the facility level have served as reference units.

Three anhydrite beds, 0.15 to 1.05 feet thick, are present above and two beds, 0.3 and 2.5 to 4 feet thick, are present below the facility level (Figure 6-2). All of the beds are laterally continuous and each is underlain by a thin clay seam. Locally, very thin anhydrite seams are associated with identified clay seams and scattered anhydrite stringers are common in several of the halite units. The anhydrite is microcrystalline and commonly ranges from a very light gray to medium gray-green color, although it is sometimes a moderate reddish to pinkish color. Halite growths are common, especially within MB-139. Anhydrite "a" commonly contains a clear halite seam up to 1 1/2 inches thick.

MB-139 is the thickest anhydrite unit within the underground facility horizon and is the most variable in color and composition. It is

described here in detail because of its importance in the deformational behavior of the underground openings, particularly the test rooms (Chapter 11).

MB-139 ranges from 2.5 to 4 feet thick. For mapping purposes, it has been divided into two subunits (Appendix G, Figures G-10 through G-34). Subunit A corresponds to Zones I, II and III described in reference 6-6. This subunit consists predominantly of reddish polyhalitic anhydrite and anhydrite mixed with light to medium gray anhydrite. Pods, lenses and seams of light to very light gray anhydrite are commonly scattered throughout the subunit. Irregular halite growths, ranging from less than 1/16 to more than 25 square inches, are common, especially in the upper half of subunit A. Commonly, a 1- to 2-inch thick seam of moderately reddish-orange to gray polyhalitic anhydrite with scattered halite and polyhalitic halite growths occurs along the upper contact. This corresponds to Zone I described in reference 6-6. Swallowtail growth patterns and hopper crystals are occasionally present in the upper 12 inches of subunit A, commonly within an upward undulation of the marker bed. Halite-filled fractures are found in places within the undulations. Scattered within the reddish polyhalitic anhydrite is an irregular and sometimes discontinuous layering of light gray anhydrite, which varies from less than 1/8 inch to 1/2 inch thick. Pods and lenses of gray anhydrite are often faintly aligned, although discontinuously, with the general trend of the layering. These pods and lenses are most prevalent in the lower half of subunit A.

Subunit B corresponds to Zones IV and V in reference 6-6. Its contact with subunit A is diffuse and based mainly on a change in color. Subunit B consists of light to medium gray anhydrite. Some core samples exhibit layering which faintly follows the general trend of the layering in subunit A. Halite growths are present, but to a much lesser degree than in subunit A. Usually the lower 4 to 8 inches of the subunit is faintly laminated and contains a few halite growths. A subhorizontal halite layer, usually less than 1/8 inch thick, is occassionally present close to the lower contact.

The upper contact of MB-139 is undulatory. The lower contact is underlain by clay E. This clay ranges from 1/4 inch to 1 1/2 inches thick. It is often slightly moist and sometimes wet.

Clay Seams. Characteristics of the clay seams within the underground facility horizon are shown on Figure 6-3 and summarized in Table 6-4. These include qualitative and/or quantitative characterizations and descriptions of the clay seams in terms of the following:

(1) color;
(2) thickness;
(3) moisture;
(4) grain size;
(5) consistency/plasticity;
(6) planar trend; and
(7) continuity/uniformity.

This information has been gathered through a review of core hole logs, geologic mapping and inspection of existing exposures.

The clay seams underlying anhydrite beds usually vary from less than 1/8 inch to 3/4 inch in thickness but may range up to 1 1/2 inches thick, as is common for clay E. The other, less continuous seams are usually less than 3/4 inch thick but may be as much as 2 inches thick, as is clay L in the C & SH shaft. Clay M-1 was as much as 3 1/2 inches thick in one hole but it consisted of a mixture of clay and halite crystals at this location.

Generally, the seams consist of clay with some silt. The clay varies from gray to brown in color. Only field classifications of the clay in core and underground exposures have been performed. These classifications indicate that the seams generally consist of soft to hard, medium plastic material. Locally, fine to coarse halite crystals are present in some of the seams. Clays F and M-1 commonly contain

Table 6-4

CLAY SEAM CHARACTERISTICS

Seam	Rating[1]	Color	Thickness	Moisture	Grain Size	Consistency/ Plasticity	Planar Trend	Continuity/ Uniformity	Occurrence
B	1	Gray	< 1/8 to 1/4 in. average; locally up to 1 1/4 in.	Dry to slightly moist.	Passes #200 sieve.	Generally hard.	Slightly irregular; generally low angle in core but locally up to 35°.	Continuous.	Present in core holes and C & SH and waste shaft mapping.
D	2	Gray	≤3/4 in.	Dry except hole DD-57 where clay is moist; hole drilled with fluid.	Passes #200 sieve.	Hard to medium soft; medium to highly plastic.	Near horizontal in core.	Varies from zone of breaks to seam with associated anhydrite.	Present in many core holes and in C & SH shaft mapping
E	1	Gray	1/4 to 1 1/2 in.	Locally moist to wet.	Passes #200 sieve.	Soft to hard; medium plastic	---	Continuous.	Present in many core holes and in C & SH and waste shaft mapping.
F	2	Gray, sometimes brown.	<1/8 to 1/2 in.	Slight.	Passes #200 sieve. Commonly mixed with halite crystals.	Slightly plastic.	Very irregular; undulations of 2-in. to 8-in. amplitude.	This is at the upper contact of map unit 4; locally discontinuous; sometimes bifurcates into two seams.	Exposed along walls of many of the facility level drifts and rooms.
G	1	Gray	Trace up to 3/8 in.	Slightly to moderately moist; weeps along exposures in underground excavations.	Passes #200 sieve.	Soft to hard; medium plastic.	Fairly regular; undulations average <2-in. amplitude.	Continuous.	Found in most core holes, shaft mapping and underground waste experimental area excavation.
H	1	Gray; brown in several core holes.	Average ≤1/4 in. but ranges from trace up to 1/2 in.	Slightly to moderately moist.	Passes #200 sieve.	Medium plastic.	Fairly irregular; undulations of 1-in. to 3-in. amplitude.	Continuous.	Found in most core holes, shaft mapping and underground waste experimental area excavation.

Table 6-4 (continued)

CLAY SEAM CHARACTERISTICS

Seam	Rating (1)	Color	Thickness	Moisture	Grain Size	Consistency/ Plasticity	Planar Trend	Continuity/ Uniformity	Occurrence
I	1	Brown-brownish gray in core; gray where exposed in waste experimental rooms.	<1/4 to 5/8 in.	Slightly moist.	Passes #200 sieve; some scattered halite crystals locally.	Hard in some core holes; medium plastic.	Regular; undulations generally <1-in. amplitude.	Fairly continuous.	Commonly found in core holes, C & SH and exhaust shafts; also exposed in waste experimental room excavation.
J	3	Reddish-brown	1/2 in. in C & SH Shaft only.	---	Passes #200 sieve; trace silt, trace to some halite crystals.	---	---	Generally found as scattered breaks or localized argillaceous zone.	Found in C & SH shaft as 1/2 in. seam; not found in other shafts; in core holes, found as scattered breaks or localized argillaceous zone; absent in many core holes.
K	1	Brown, sometimes gray to gray-brown.	3/4 to 1 1/2 in.	Dry to moist; locally wet.	Passes #200 sieve; claystone in exhaust shaft.	Hard to medium hard; medium plastic.	Generally low angle contact in core; fairly regular.	Continuous.	Present in many core holes and shafts.
L	3	Brown	Up to 2 in. in C & SH shaft; usually found only as top of argillaceous unit.	---	Passes #200 sieve; some halite crystals.	---	---	Not a continuous seam; it is found generally as the top of argillaceous zone throughout core holes and shafts.	Exposed in C & SH shaft as seam; otherwise only noted as top of argillaceous unit.

Table 6-4 (continued)

CLAY SEAM CHARACTERISTICS

Seam	Rating[1]	Color	Thickness	Moisture	Grain Size	Consistency/ Plasticity	Planar Trend	Continuity/ Uniformity	Occurrence
M-1	4	Brown	<1/16 to 1/2 in.	Dry	Passes #200 sieve.	---	---	Unknown.	These two layers found in core holes in waste experimental area; not noted in shaft mapping.
M-2	4	Brown	Up to 3 1/2 in.	Dry	Clay mixed with halite crystals.	---	---	Unknown.	

Notes:

(1) Key to "Rating": 1 - continuous throughout facility level;
2 - generally continuous, but varies in character and regularity;
3 - discontinuous and not always well developed;
4 - continuity unknown.

(2) Clays B, E, G, H and K are sometimes noted as only a trace or not at all on core logs. This is usually because core grinding or washing during drilling removed evidence of clay.

(3) Some core logs note clay layers are moist. In holes drilled with brine, this may be due to drilling fluid. Many layers are dry in holes drilled with air. These may actually be slightly moist in the in situ state, but dried out by the drilling process.

(4) Clays B, E, G, H and K always underly continuous anhydrite layers. Clays I and D are commonly associated with thin anhydrite layers.

(5) Plasticity and consistency based on evaluation of in situ condition.

more halite mixed with the clay/silt fraction. Clay F also appears to be more silty and less plastic than the other seams.

Generally, the clay seams are slightly moist in their in situ state. However, some of the seams are wet and exhibit some brine weeping in places. This was observed for clays E, G, H and K in some core holes. The clay seams in some of the holes where brine was used as a drilling fluid were observed to be moist. This was probably due in part to the drilling fluid. In contrast, clay seams were observed to be dry in many of the core holes drilled using air circulation. It is expected that, in the in situ state, these seams contain a slight amount of moisture which was evaporated as a result of the drilling method. Some moisture can be seen along exposures of clay H and clay G in the waste experimental area. More moisture is evident along clay G and some salt blisters have accumulated locally along this seam. The clay seams exposed in the underground openings are generally slightly moist during and immediately after excavation. Some seams have continued to expel moisture long after excavation. Often, however, they dry out at the surface within a few days after their exposure.

Clays G, H and I, exposed in the waste experimental area, commonly contain white specks which may be salt resulting from the air drying of the clay. The clay usually has a slightly salty taste. These white specks are soft, can be easily crushed between the fingers, and have a slightly bitter taste.

The consistency of the clay encountered in the core holes and excavations is related to its moisture content. When wet or moist, the clay is generally soft to medium stiff and can be picked out with the fingers and molded into a ball in the hand. When the clay is only slightly moist or dry, it is stiff to hard and is difficult to work in the hand.

6.3.3 Structure

Geologic mapping of the underground openings has not identified any faults, joints, significant folds, or other structural disruptions that could affect the suitability of the WIPP facility for storing radioactive waste. Very small scale (approximately 1 foot), localized disruptions of the bedding have been encountered. These are attributed to penecontemporaneous processes.

Detailed correlations between vertical core holes, combined with the results of geologic mapping in the drifts and test rooms, indicate that the strata within the underground facility horizon are deformed slightly into a sinusoidal shape. Figure B-4 in Appendix B depicts this shape, but greatly exaggerates the amplitude of the deformation. The amplitude of the fold is approximately 10 to 15 feet and its wavelength is approximately 2,000 to 3,000 feet. The fold is superimposed on a gentle southward dip.

The deformation of the strata is post-depositional in origin. While undulations of depositional surfaces are common, all of the strata in the interval from 50 feet above to 50 feet below the facility level exhibit parallel undulations. This consistency in folding over a relatively large interval containing numerous depositional sequences suggests that the beds were deformed after deposition. The folding is a minor feature which does not adversely affect the suitability of the facility for waste storage.

6.4 PROPERTIES OF HOST ROCKS

As discussed in subsection 6.3.2, the underground facility horizon is composed of halite containing beds of argillaceous halite, anhydrite, polyhalite and thin clay seams. Laboratory tests were performed to determine the constitutive equations and material property constants for these host rocks (ref. 5-3). Subsections 6.4.1 and 6.4.2 present the properties of the host rocks based on laboratory and in situ data. In situ closure measurments were also used to "back calculate" the creep parameters for halite.

6.4.1 Laboratory Tests

Laboratory tests were performed on core samples from surface boreholes at the WIPP site prior to the initiation of underground excavation (ref. 5-3). Material property constants determined from the laboratory tests are presented in Tables 6-5 through 6-7. Table 6-5 shows the elastic constants for halite, argillaceous halite, anhydrite and polyhalite.

The failure criteria for both anhydrite and polyhalite were defined based on the results of the laboratory tests. One such criterion is Mohr-Coulomb, which defines failure in terms of friction and cohesion. Failure means that the material is unable to hold a deviatoric stress beyond a certain value. Once this value is reached, the material starts yielding. However, the Mohr-Coulomb criterion ignores the effect of intermediate principal stress on failure. In terms of principal stresses at failure,

$$(\sigma_3 - \sigma_1) = 2\Theta_o \cos\beta - (\sigma_3 + \sigma_1) \sin\beta \qquad (6\text{-}1)$$

where: Θ_o and β are Mohr-Coulomb parameters; and

σ_1 and σ_3 are principal stresses that are positive in tension.

Because the process of yield must be independent of the choice of axes, the failure criterion must be independent of the choice of axes and should be expressed in terms of stress invariants. The Drucker-Prager yield criterion is expressed as follows:

$$\sqrt{J_2'} = c - aJ_1 \qquad (6\text{-}2)$$

where: $\sqrt{J_2'}$ is the second stress invariant and is equal to $\bar{\sigma}/\sqrt{3}$; and

J_1 is the first stress invariant:

$$J_1 = \sigma_1 + \sigma_2 + \sigma_3 \qquad (6\text{-}3)$$

$$\bar{\sigma} = \frac{1}{\sqrt{2}} [(\sigma_1 - \sigma_2)^2 + (\sigma_2 - \sigma_3)^2 + (\sigma_3 - \sigma_1)^2]^{1/2} \qquad (6\text{-}4)$$

Table 6-5

ELASTIC CONSTANTS DETERMINED FROM LABORATORY TESTS

MATERIAL	E (ksf)	υ
Halite	647,450.	0.25
Argillaceous halite	647,450.	0.25
Anhydrite	1,568,500.	0.35
Polyhalite	1,155,000.	0.36

Note:

E = elastic modulus

υ = Poisson's ratio

Table 6-6

FAILURE CONSTANTS DETERMINED FROM LABORATORY TESTS

	ULTIMATE				YIELD			
MATERIAL	Θ_o (ksf)	β (^{o})	a	c (ksf)	Θ_o (ksf)	β (^{o})	a	c (ksf)
Anhydrite	627.	37.0	0.279	752.	564.	29.0	0.226	689.
Polyhalite	395.	51.0	0.395	414.	359.	46.5	0.361	403.

Table 6-7

CREEP CONSTANTS DETERMINED FROM LABORATORY TESTS

MATERIAL	PRIMARY CONSTANTS A	B	$\dot{\varepsilon}^*$ (sec^{-1})	SECONDARY CONSTANTS D ($ksf^{-4.9}$ sec^{-1})	n	Q (kcal/mole)
Halite	4.56	127	5.39×10^{-8}	4.96×10^{-13}	4.9	12.0
Standard Error				1.05×10^{-13}	0.27	0.65
Argillaceous Halite	4.56	127	5.39×10^{-8}	1.49×10^{-12}	4.9	12.0

For anhydrite, however, the ultimate strength decreases somewhat with the change in strain rate. That is, a 10 percent decrease occurs as the strain rate is decreased from 10^{-4} sec^{-1} to 10^{-6} sec^{-1}. For polyhalite, the ultimate strength is assumed to be independent of the strain rate. Table 6-6 shows the failure constants for anhydrite and polyhalite.

Table 6-7 shows the creep constants for halite and argillaceous halite. Although the data for most individual creep tests are internally consistent, steady-state creep rates obtained from different specimens tested under the nominally same conditions may scatter by an order of magnitude. Nevertheless, statistical analysis has resulted in a "best fit" to the data. Table 6-7 also shows the deviation of the secondary creep constants for halite. It was concluded that when such large deviations or uncertainty exist, calculations using mean values are apt to be meaningless and the design process requires considerable judgement (ref. 6-7).

Based on laboratory tests, the failure criterion of halite can be described using a failure function ø, such that when ø becomes positive, halite no longer supports any deviatoric stress. The function ø is assumed to be:

$$\phi = \bar{\varepsilon} - 0.023 - f(p) \qquad (6\text{-}5)$$

where: $\bar{\varepsilon}$ is the effective creep strain (see Appendix C) and the function f(p) is expressed as:

$$f(p) = \begin{cases} 0.132 & \text{for } p \geq 125.26 \text{ ksf} \\ p(a - bp) & \text{for } p \leq 125.26 \text{ ksf} \end{cases} \qquad (6\text{-}6)$$

where: p, the pressure in ksf, is expressed as

$$p = - \frac{\sigma_1 + \sigma_2 + \sigma_3}{3} \qquad (6\text{-}7)$$

and is positive in compression; and

a and b are equal to 2.122×10^{-3} ksf^{-1} and 8.487×10^{-6} ksf^{-2}, respectively (ref. 5-3).

Equation 6-5 indicates that if $\bar{\epsilon} \geq 0.023 + f(p)$ at any point in the halite, yielding will be initiated at that point. For p greater than 120 ksf, the failure effective strain is about 0.16.

Laboratory test results have also shown that a clay seam will be active for a frictional coefficient of 0.4, and that clay seam separation is unlikely unless the seam is very near the opening.

The average unit weight of the salt within the reference stratigraphy interval was determined to be 143.6 pounds per cubic foot (pcf) (ref. 5-3).

6.4.2 In Situ Data

In situ data was gathered from geomechanical instruments at various underground locations. The creep law shown by equation C.4-1 in Appendix C was used to fit the in situ data and to determine the creep parameters. The MARC General Purpose Finite Element Program (ref. 6-8) was used for the numerical computation based on the theory discussed in Appendix C. Table 6-8 shows the primary and secondary creep parameters determined from test room in situ data. Chapter 11 presents a more detailed discussion of the procedures used for computing these parameters.

Secondary creep parameters were also computed using in situ data from the C & SH shaft. The secondary creep parameters computed from horizontal deformations in the C & SH shaft and in the test rooms are reasonably close. The parameter based on test room wall-to-wall

Table 6-8

CREEP PARAMETERS DETERMINED FROM IN SITU DATA

MATERIAL	PRIMARY PARAMETERS A	PRIMARY PARAMETERS z (sec^{-1})	SECONDARY PARAMETER C ($ksf^{-4.9}$ sec^{-1})
Halite			
Roof-to-Floor	1.774	5.573×10^{-8}	2.588×10^{-21}
Wall-to-Wall	1.618	4.757×10^{-8}	1.361×10^{-21}

closure is 1.36×10^{-21} $ksf^{-4.9}$ sec^{-1} while the parameter based on extensometer measurements in the C & SH shaft is 1.30×10^{-21} $ksf^{-4.9}$ sec^{-1}.

6.5 SURFACE SUBSIDENCE MONITORING

The design criteria state that subsidence due to underground excavation shall not exceed 1 inch within a 500-foot radius of the waste shaft. The layout of the underground excavation and the extraction ratio requirements were established to comply with this criteria. Subsidence monuments have been installed on the ground surface above the shaft pillar area (Chapter 2, Figure 2-2). Additional subsidence monuments are scheduled to be installed above the storage area in mid-1986. These monuments will be used to determine surface subsidence during the 25-year facility operating life.

Because the storage area has not yet been excavated, actual subsidence cannot be measured. This subsidence will occur over the next 25 years. The calculations used for the reference design indicate that subsidence is not likely to exceed the criteria limit. Therefore, the reference design subsidence criteria is considered validated on a computational basis rather than on actual measurement data. A review of this conclusion may be required later when a history of actual subsidence is available.

CHAPTER 7
C & SH SHAFT

7.1 INTRODUCTION

This chapter presents the results of the design validation program for the C & SH shaft. Included are discussions of the design criteria, design bases and design configurations pertaining to the C & SH shaft. This is followed by information and data from the design validation process including the data collected, its analysis and evaluation, and predictions regarding future behavior of the shaft liner and key and the rock strata surrounding the shaft. Conclusions and recommendations are presented based on a comparison of the results of the design validation process with the reference design.

7.2 DESIGN

This section presents the design criteria and design bases used to develop the reference design for the C & SH shaft. The configuration of the shaft is discussed in Chapter 3, subsection 3.3.1.

7.2.1 Design Criteria

The Design Criteria document (ref. 2-8) contains the general concepts that were used as a guide for design of the WIPP underground openings. Table 2-1 summarizes those design criteria elements that are to be evaluated by the design validation process. The following discussion provides a summary of the elements that pertain to validation of the C & SH shaft reference design.

The design criteria specify that all shafts shall be designed for structural stability over an operating life of 25 years. The design shall also consider the requirements for shaft decommissioning and sealing. Shaft design shall prevent wall deformations which would interfere with shaft functions or affect the safety of operations within the shafts. Rock support shall be used as required to limit rock deformations and to prevent loosening and fallout of wall rock.

The time-dependent diametric closure of the shafts due to creep shall be considered in their design. The shafts shall be designed so that the minimum dimensions required for shaft functions are maintained throughout the operating life of the facility. Provisions for instruments to measure closure shall be included in the design.

Ground-water flow into the shafts shall be controlled so that no uncontrolled ground water reaches the facility level via the shafts. Ground-water pressures and inflows shall be measured throughout the construction period and operating life of the shaft.

Shaft design shall consider the requirements of decommissioning and backfilling upon termination of operations. The design shall accommodate the need to ultimately seal potential pathways between the storage facility and the biosphere.

The shaft liner shall be designed to help ensure that the shaft dimensions remain within the limits required for shaft functions, prevent ground-water flow into the shaft, protect wall rock from deterioration, and preclude the risk of rockfall from the shaft walls.

The shaft stations shall be designed to provide structurally stable excavations and pillars. Deformations of excavations and pillars shall remain within the limits required for structural functions, ventilation and safety. The excavation design shall maintain the minimum dimensions required for the operating life of the opening by accommodating closure. Closure rates used for design shall be confirmed or modified by instrument observations in the excavations. Rock bolts shall be used where necessary to provide support of the roof and walls.

7.2.2 Design Bases

The Design Basis, Exploratory Shaft (ref. 2-10) and the Design Basis, Exploratory Shaft Geomechanical Instrumentation (ref. 2-12) were the primary documents used as a basis for design of the C & SH shaft. These documents, described in Chapter 2, provided the detailed design

requirements for the C & SH shaft. Table 7-1 summarizes those design basis elements which are to be evaluated by the design validation process. The following discussion provides a summary of the major design bases for the C & SH shaft. Not all of these bases require evaluation as seen by comparing the discussion with Table 7-1.

The design bases specify that the C & SH shaft shall be designed to provide access for personnel and equipment to excavate and operate the underground facility and to provide a means by which the excavated salt can be transported to the surface. It shall also serve as the ventilation intake shaft.

The shaft liner shall be made of structural steel and have an inside diameter of 10 feet. The remainder of the shaft shall be unlined and have an approximate diameter of 11 feet 8 inches. The steel liner shall extend from 1 foot above the ground surface to the top of the salt formation at a depth of approximately 850 feet. The primary materials used to line the shaft shall be cement grout, steel casing, corrugated metal pipe, structural steel and reinforced concrete.

The liner shall protect against sloughing, fallout and deterioration of the rock formations and shall prevent water seepage into the shaft. It shall have a smooth inner surface to reduce air friction. The liner shall be designed for temporary installation loads and permanent loads. The permanent load shall consist of a hydrostatic lateral pressure starting 250 feet below the ground surface and extending to approximately 837 feet below the surface. Rock pressure shall not be used as a factor in the design analysis. Installation loads to be considered shall be the compressive and tensile forces resulting from lateral pressure due to unequal heights of drilling fluid during the various stages of installation.

During shaft drilling, ground-water flow into the shaft shall be determined. If the amount of ground water entering the shaft is determined to be unacceptable by the DOE Contracting Officer, approved

Table 7-1

VALIDATION ELEMENTS OF C & SH SHAFT DESIGN BASES

(1) Shaft Liner

a. Hydrostatic pressure is considered to start 250 feet below the ground surface and extend to the top of the key.

b. Water shall be prevented from flowing down the unlined shaft from behind the liner.

(2) Shaft Key

a. Key shall be designed to resist the lateral pressure from the salt. (Assumed to be 75 percent of the overburden pressure.)

b. Key shall be designed to resist the hydrostatic pressure from above the salt.

(3) Unlined Section

Provide 11-foot 8-inch diameter to allow for future salt creep deformation.

corrective action shall be taken to control the water inflow. The basis for determining if the amount of ground water flowing into the shaft is unacceptable shall be if the inflow exceeds an amount which can be tolerated without appreciably altering the drilling fluid characteristics as approved by the DOE Contracting Officer.

The shaft key shall be constructed using reinforced concrete and will serve as the transition element between the lined and the unlined sections of the shaft. It shall retain the rock formation and shall be provided with chemical water seals and a water collection ring with drains to prevent water from flowing from behind the liner down the unlined shaft. The key shall be designed to resist lateral pressure generated by salt creep, rock and soil overburden, and by hydrostatic pressure from above the salt. The design lateral pressure was selected as 75 percent of the overburden pressure based on the configuration of mine shafts in the vicinity of the WIPP. These shafts generally have a concrete liner that is thinner and that extends to a greater depth than the shaft key at the WIPP. Most of these shafts are at least 25 years old and show no significant deterioration or structural instability.

No liner or wire mesh is planned for the section of the shaft in the Salado formation. However, if field conditions require, rock bolts and wire mesh may be installed in zones of fractured salt.

The shaft station excavation shall be the minimum required to meet the operational and safety requirements in the shaft pillar area of the waste storage level. Supports of underground workings shall comply with Federal and New Mexico codes. The use of rock bolts and wire mesh in specific areas shall be determined by excavation conditions and code requirements. The roof, walls and floor shall be checked periodically for loose salt in accordance with applicable codes.

The bottom of the shaft shall extend below the facility level to accommodate the salt handling equipment and a sump to collect water that might enter the shaft. Should the stratigraphy of the facility

level be unsuitable for waste storage, the shaft bottom may be lowered to reach a more suitable stratigraphy.

Geomechanical instruments shall be provided to measure radial convergence (closure) of the shaft, water pressure behind the liner, salt creep, forces on the concrete key, and the variation of load on rock bolts. The type of instruments installed shall be strain gauges, pressure cells, piezometers, stressmeters, extensometers, load cells and radial convergence points.

The shaft liner, key, unlined section and furnishings shall be inspected at approximately 1 month intervals, or lesser intervals as required, to detect cracking, corrosion, deterioration and water intrusion.

7.3 DESIGN VALIDATION PROCESS

The design validation process for the C & SH shaft consists of data collection, analysis and evaluation, and predictions of future behavior. The following discussions of each of these activities have been divided into four sections: the lined section of the shaft; the shaft key; the unlined section; and the shaft station. This division is based on the different in situ and design conditions in each of these areas.

7.3.1 Data Collection

Data collection in the C & SH shaft has consisted of geologic mapping, visual inspections and geomechanical instrument measurements. The results of shaft mapping have been discussed in Chapter 6. Field observations and the geomechanical instrumentation program are discussed in the following subsections.

7.3.1.1 Lined Section

Field Observations. The C & SH shaft has been inspected on a regular basis since its construction. During the facility level construction

phase, the mining contractors conducted weekly shaft inspections for safety and shaft maintenance. These weekly inspections are being continued by the facility operator.

Site geologists inspect the shaft at approximately 6-month intervals. These inspections provide geotechnical evaluations of the condition of the shaft, and of instrument conditions and their performance. Shaft inspections were performed on the following dates: August 29, October 1, October 5, October 22, November 19 and December 3, 1983; June 2, June 21, October 13 and November 12, 1984; and April 9 and December 9, 1985. The results of these inspections are presented in the GFDRs.

Geomechanical Instrumentation. Nine sets of radial convergence points were installed in the C & SH shaft between July 7 and 17, 1982. Two additional sets were installed on October 8, 1982. Five of these 11 sets were installed in the lined section of the shaft (Figure 7-1). Plots of the convergence point data from the lined section are presented in Appendix J, Figures J-205 through J-209.

Ten piezometers were installed in the lined section of the C & SH shaft above the shaft key between July 10 and 17, 1982 (Figure 7-1). Two piezometers each are at elevations of 2830, 2790, 2719, 2684 and 2608 feet. All of these piezometers are in the Rustler formation. The piezometers at elevations of 2790 and 2684 feet are in the water-bearing dolomite members, the Magenta and Culebra, respectively. Graphic plots of piezometer data are presented in Appendix J, Figures J-34 through J-44. The piezometers are dual-component instruments containing a vibrating-wire gauge and a pneumatic gauge. The vibrating-wire gauge is the principal instrument used to measure water pressure. The pneumatic gauge is used for initial calibration and periodic performance checks on the vibrating-wire units. The vibrating-wire piezometers were connected to the datalogger on October 30, 1982. The pneumatic units can only be read manually at the instrument location; however, most of the pneumatic units are no longer functioning.

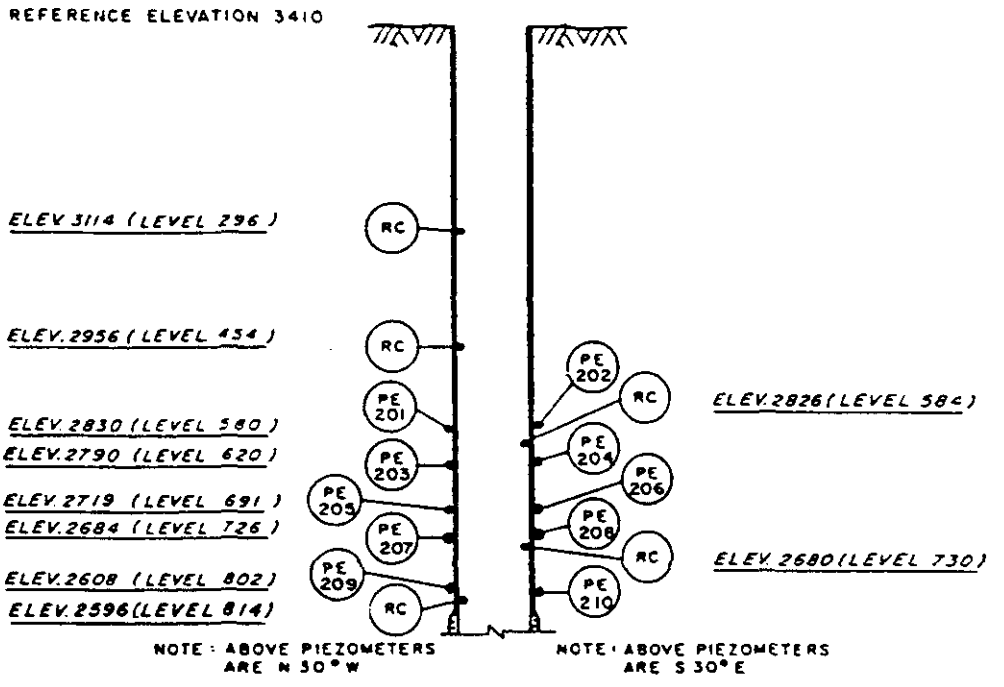

LEGEND

- PE — PIEZOMETER
- RC — RADIAL CONVERGENCE POINTS
- GE — EXTENSOMETER

NOT TO SCALE

NOTES

1. RC'S AT EACH LEVEL CONSIST OF FOUR POINTS.
2. THE TERM "LEVEL" IS AN APPROXIMATE DEPTH IN FEET FROM THE TOP OF THE SHAFT BUNTON AT ELEVATION OF 3410.0 FT MSL. ELEVATIONS ARE FROM CEMENTATION WEST, INC., 1983, WIPP SHAFT AND STATION SURVEY.

Figure 7-1

C & SH SHAFT LINER INSTRUMENTATION

The shaft instrumentation has had a history of damage. Convergence points and especially piezometers are susceptible to damage from falling objects and construction activities. Damage in the lined section of the shaft has generally consisted of sheared data cables, sheared or bent convergence points, broken junction boxes and water damage.

Water intrusion has been a major problem with most of the shaft instruments and control systems. One water source has been the holes drilled into the steel liner for piezometer installation. The bushing in the liner through which the piezometer was installed did not have tapered threads, making it difficult to seal the hole in the liner. Leakage through these holes has generally occurred at some time in their history. It was especially difficult to effect a seal when a piezometer was reinstalled after being repaired due to other damage.

Water trickling down the liner from around these bushings has sometimes entered damaged fiberglass junction boxes and terminal boxes through cracks. Water has also seeped into the conduit connecting piezometers with the nearest junction box. This water has corroded terminal blocks and seeped down cables connecting lower terminal boxes.

A second water source has been rainfall. During periods of heavy rain, water runs down the shaft along the surface of the liner. This water can enter terminal boxes broken by impact or construction activities. Once in the boxes, it causes corrosion and cable damage.

A great deal of effort has been exerted correcting these problems. Shields were placed over boxes, cables were replaced and rerouted, and piezometers were repaired and sealed as well as possible. These measures improved performance somewhat, but problems still exist. The data acquired from the instruments is considered valid, but must be interpreted in light of the various interruptions in data monitoring. The specific details of instrument damage are updated in every GFDR, particularly in the tables of operating histories.

7.3.1.2 Shaft Key

Field Observations. The shaft inspections conducted on October 1 and November 19, 1983, June 2 and October 13, 1984, and April 3 and December 9, 1985, paid particular attention to the shaft key. The design of the key provides a means to determine if any water from the water-bearing zones in the Rustler formation is flowing behind the key. This situation, if it existed, could cause dissolution of the salt around the key resulting in eventual structural instability.

During inspection of the shaft key, the condition of four telltale drains that connect to a French drain behind the key is observed. Any moisture in the drains is noted. Similarly, other capped pipes (those for possible future injection of grout and those originally used for chemical seal injection) are checked for accumulated water. The interface between the salt and the bottom of the key receives particular attention.

The latest geotechnical inspection of the shaft key was made on December 9, 1985. The four telltale drains at the key were inspected and cleaned. Only the hole on the northwest side of the shaft was weeping, resulting in salt accumulation on the terminal box below. After chipping off this salt, a small amount of liquified chemical seal material began oozing out of the telltale. Inspection of the bottom of the key showed no evidence of seepage below the concrete.

Geomechanical Instrumentation. Twenty-four embedment strain gauges, 16 spot-welded strain gauges, and 4 pressure cells were installed in the C & SH shaft key from April 11 to 17, 1982. Two piezometers were installed in the shaft key on July 10, 1982. The locations of these instruments are shown on Figure 7-2. All instruments were read manually until they were connected to the datalogger system on October 30, 1982. Appendix J contains plots of the data from these instruments. Piezometer data are presented on Figures J-44 and J-45. Figures J-54 through J-57 present pressure cell data. The strain gauge data are presented on Figures J-58 through J-97.

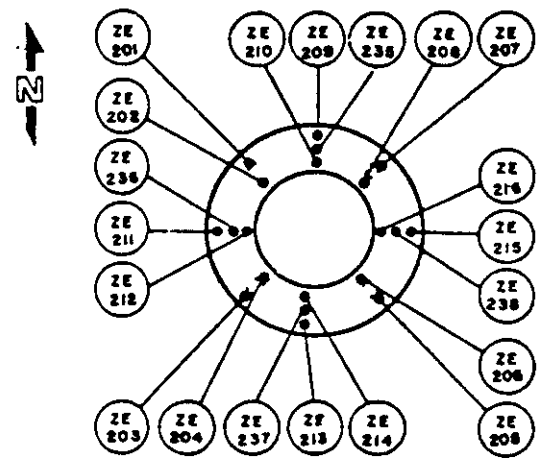

STRAIN GAUGE LOCATIONS
AT ELEV. 2553.7 FT (LEVEL 856.3 FT)

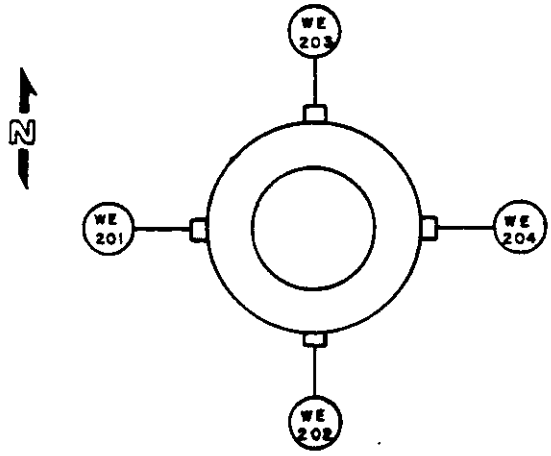

PRESSURE CELL LOCATIONS
AT ELEV. 2550.0 FT (LEVEL 860.0 FT)

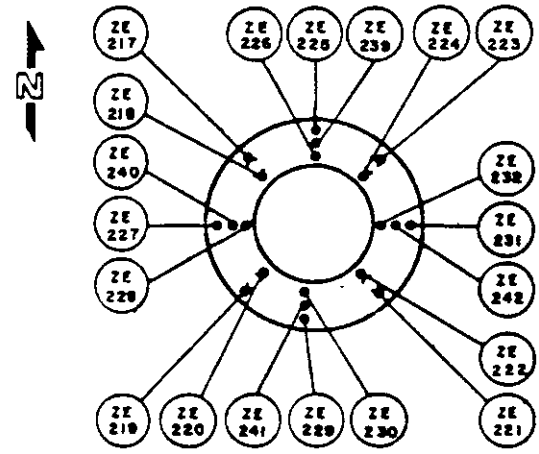

STRAIN GAUGE LOCATIONS
AT ELEV. 2547.6 FT (LEVEL 862.4 FT)

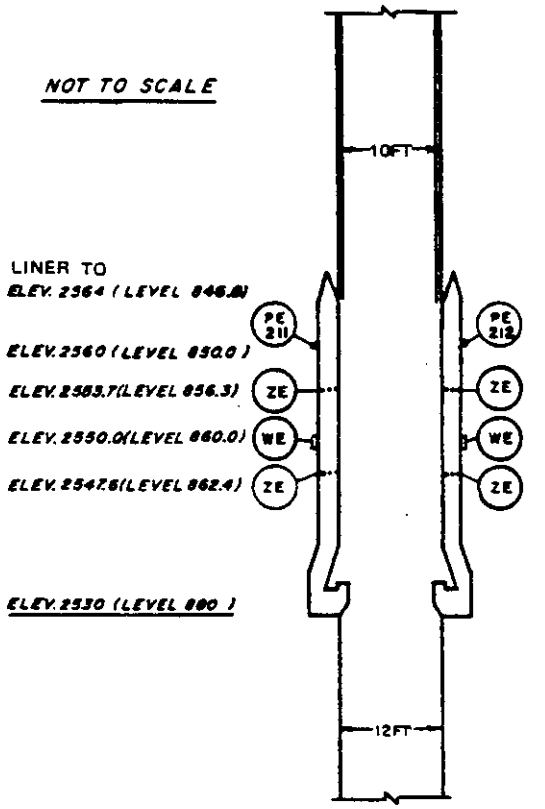

SHAFT KEY (PROFILE)

LEGEND

- ZE STRAIN GAUGE
- WE PRESSURE CELL
- PE PIEZOMETER

NOTES:

1. THE TERM "LEVEL" IS AN APPROXIMATE DEPTH FROM THE TOP OF THE SHAFT BUNTON AT AN ELEVATION OF 3410.0 FT MSL. ELEVATIONS ARE FROM CEMENTATION WEST, INC., 1983, WIPP SHAFT AND STATION SURVEY.
2. STRAIN GAUGES ARE ORIENTED HORIZONTALLY AND TANGENTIAL TO SHAFT CIRCUMFERENCE.
3. STRAIN GAUGES SHOWN AS ⊕ ARE SPOT WELDED TO REINFORCING STEEL.

M

Figure 7-2

C & SH SHAFT KEY
INSTRUMENTATION

The instruments for monitoring the shaft key, and especially their electrical boxes and cables, have had the same performance problems as the piezometers and convergence points in the lined section above. The two key piezometers have been damaged and repaired repeatedly.

The major problem in the key has been water damage inside the various electrical boxes. The worst damage was in termination cabinet LTC-1. Water seeping down inside cables connected to water-damaged boxes in the lined section of the shaft corroded the terminals in the LTC. LTC-1 links the piezometers, strain gauges and pressure cells to the surface datalogger. Several attempts were made to repair the LTC components. The components were permanently removed in October 1984 in order to avoid further damage. The shaft instrumentation system is scheduled for an overhaul during a future construction contract. Meanwhile, all LTC-1-controlled instruments are read manually during shaft inspections.

The terminal boxes for the pressure cells and strain gauges have also been damaged. Initial damage was to the fiberglass boxes and data cables as they were struck by falling objects and construction materials traveling on the shaft conveyance. Subsequent damage was by water seeping into the boxes. The boxes and cables have been repaired numerous times.

Detailed accounts of instrument damage are presented in the GFDRs, particularly in the tables of operating histories. The GFDRs also discuss data collection, data plots and interpretative problems with the C & SH shaft key instruments.

7.3.1.3 Unlined Section

Field Observations. Shaft inspections include observations of the unlined section of the C & SH shaft. This section of the shaft consists of exposed salt forming a smooth wall. The inspections consist primarily of determining if any spalling or fracturing of the salt is occurring.

The unlined section was inspected to a depth of 2,057 feet (elev. 1353 feet) on December 9, 1985. One near-vertical fracture was observed on the west side of the shaft between a depth of 1,021 feet and 1,043 feet (elev. 2389 feet and 2367 feet). It ranged from closed to less than 1/4-inch wide at the wall surface and extended about 10 feet in length. It did not appear on the east side of the shaft. Previous shaft mapping showed the presence of halite-filled vertical fractures in anhydrite from a depth of approximately 1,023 feet to 1,038 feet (elev. 2387 feet to 2372 feet). The fracture observed appears to be one of those previously mapped. Salt blisters and precipitate were noted in various areas commonly associated with clay layers. The most notable area was a 4-foot zone around the entire shaft circumference from a depth of approximately 1,038 feet to 1,042 feet (elev. 2372 feet to 2368 feet).

Geomechanical Instrumentation. Nine borehole extensometers were installed in the unlined section of the C & SH shaft between July 6 and 8, 1982. These extensometers are arranged in three-instrument arrays at elevations of 2337 feet, 1846 feet and 1353 feet (Figure 7-3). Readings were taken manually until the extensometers were connected to the datalogger system in October 1982.

The extensometers are the multiple-point, sonic-probe type consisting of four anchors. The anchors for each extensometer were set at depths of 4, 9, 18 and 36 feet. The collar of the extensometers was recessed 1 foot into the salt. Data plots for the extensometers are presented in Appendix J, Figures J-116 through J-124.

The extensometers have not been damaged as much as the other instruments in the shaft. Their operating histories rarely show any interruption in the data. This lack of damage is a result of several factors. The diameter of the unlined shaft is 2 feet greater than that of the key or lined section. The instruments are recessed and therefore not susceptible to damage from falling objects. The extensometers are connected to LTC-2 and LTC-3, which are not directly

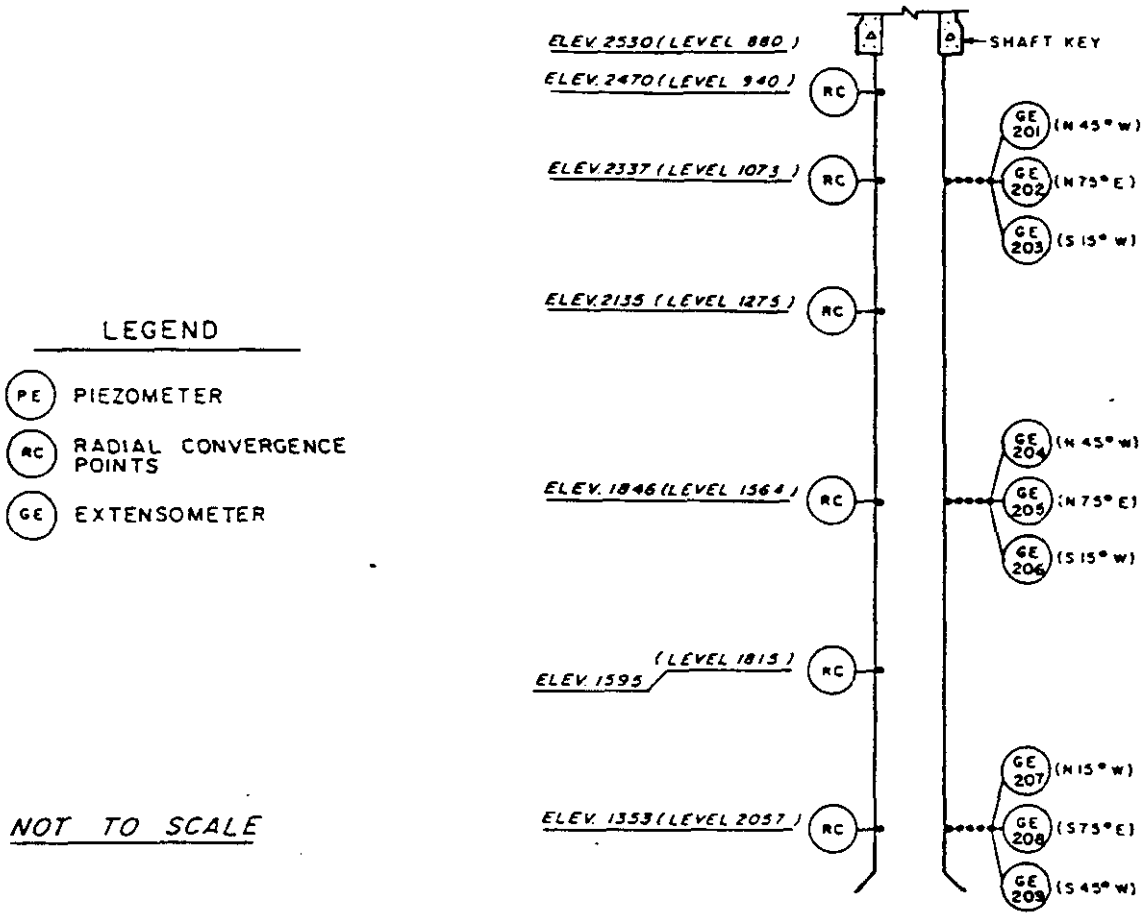

NOTES

1. RC'S AT EACH LEVEL CONSIST OF FOUR POINTS.
2. THE TERM "LEVEL" IS AN APPROXIMATE DEPTH IN FEET FROM THE TOP OF THE SHAFT BUNTON AT ELEVATION OF 3410.0 FT MSL. ELEVATIONS ARE FROM CEMENTATION WEST, INC., 1983, WIPP SHAFT AND STATION SURVEY.

M

Figure 7-3

C & SH SHAFT UNLINED SECTION
INSTRUMENTATION

linked to LTC-1 and the piezometers. Thus, water damage has not been a problem.

Six sets of radial convergence points are located in the unlined section of the shaft. These points have a history of damage and replacement similar to that of the other convergence points. This history is discussed in the GFDRs. Plots of the convergence point data from the unlined section are presented in Appendix J, Figures J-210 through J-214. Only five plots are presented since damage to the set of points at elevation 1595 feet prevented the obtaining of reliable readings.

7.3.1.4 Shaft Station

Field Observations. Site geologists monitor the deformational behavior of the C & SH shaft station on a regular basis. Particular attention is given to four aspects of movement or failure: roof and wall spalling; fracturing at pillar corners; roof displacements and separations; and floor displacements, separations and fracturing. The observations are recorded at least every 3 months and have been published in each GFDR since the February 1984 issue.

A description of the C & SH shaft station excavation and roof support methods were presented in Chapter 3. The failure of resin-anchored rock bolts installed initially in the shaft station roof has been attributed to a combination of the following factors:

(1) the resin firmly held the bolt shank in place and salt creep caused failure at the first weak point;

(2) improper bolt installation resulted in damage to the threaded section of the bolt (improper torque and lack of beveled or spherical washers); and

(3) contributing factors such as corrosion and hydrogen embrittlement.

Rock bolts installed to replace the failed bolts, and subsequent bolt installations, used mechanical anchors. As the load on these bolts increases due to salt creep, the anchor yields by slipping in the hole. Although this slipping is not desirable for the roof support of underground openings in hard rock, it provides more control than rigid anchors that do not yield but instead produce sudden bolt failure as a result of the stress created by creeping salt. The slipping reduces the load on the bolt, thus reducing the potential for bolt failure, but allows continued roof support and prevents sudden roof falls. Each mechanical-anchor rock bolt supports a load that is less than its capacity, but the aggregate support provided by all of the rock bolts in a pattern is more than adequate for positive ground control. The experience at WIPP shows that the mechanical-anchor rock bolts perform well in creeping salt if periodically inspected and maintained.

The station roof and walls have exhibited continual slabbing and spalling which has required periodic scaling. Wire mesh has been installed over the entire station roof to contain any small, loose salt fragments.

Vertical fractures have developed in the pillar corners at the S90 crosscut. The condition of these fractures has been monitored and the results reported on a regular basis in the GFDRs. A discussion of fracturing at pillar corners is presented in Chapters 10 and 11.

Displacements, separations and fractures have been detected in boreholes drilled into the station roof and minor separations have been detected in some holes drilled into the station floor. Separations and fracturing at clay G and in the underlying halite were detected shortly after the initial station excavation. Horizontal displacements have been observed in various boreholes during the past 2 years.

In May and June 1986, 20 boreholes were drilled in four arrays in the shaft station to further investigate the extent of separations and fracturing in the roof and floor. This drilling was conducted as part

of a program to characterize excavation effects in the salt surrounding the openings and particularly in MB-139. This program is discussed more fully in Chapters 10 and 11.

The new boreholes were inspected for the existence of separations and fractures. Existing holes were inspected for horizontal displacements. The probe used for this inspection consisted of an aluminum rod with a 1/16-inch thick nail attached perpendicular to one end. When applying moderate pressure, the nail snags on the borehole wall if a separation, fracture, or clay seam is encountered. The separation is considered to be less than 1/16 inch wide if the nail catches on, but does not penetrate the hole wall. If the separation at the wall surface is at least the nail width (approximately 1/16 inch) there will be a slight penetration. If the separation is larger, the nail penetrates its entire 1/2-inch length into the wall. When the probe catches on the hole wall, the feature is probed on all sides of the hole. This ensures that it is a continuous feature and not a clay pocket or an imperfection caused by the drilling.

Fracture zones, anhydrite beds, or clay seams were sometimes identified by picking out pieces of the material with the probe nail. An estimate of their vertical dimension was made by moving the probe rod up and down within the limits of the feature. Occassionally a slight penetration occurred at the clay seams due to a very small separation or penetration into the softer clay.

In the array of holes drilled north of the shaft, no separations or fractures were detected in the roof. In the two arrays drilled south of the shaft, multiple separations and fractures, ranging from approximately 1/16 inch to 4 inches wide, were found in most of the roof holes within the halite below clay G. Many of the fractures occur within 3 feet of the roof. Some separation and fracturing appears to be associated with clay G based on data from other holes in the station area and from the central roof holes in the two arrays, but no significant occurrence appears to have developed in the holes closest

to the station walls. A separation, less than 1/16 inch wide was detected in only one roof hole beyond a depth of 4 feet.

Only a few separations or fractures, less than 1/8 inch wide, were detected in the central floor hole of the hole array drilled north of the shaft. Some separations and fractures, less than 1/16 inch to 1 inch wide, were detected in the two floor hole arrays drilled south of the shaft. These occurrences were in MB-139 and the overlying halite. Essentially no separation was encountered at clay E at the base of MB-139. Holes drilled around the edge of the electrical substation concrete base slab foundation to investigate a potential source of its tilting encountered only small scattered separations. The total accumulated vertical separation is estimated to be less than 1/2 inch.

Geomechanical Instrumentation. As in other areas of the underground facility, a suite of geomechanical instruments was installed in the C & SH shaft station (Figure 7-4). The original instrumentation design consisted of 6 rock bolt load cells, 3 borehole extensometers, and 2 sets of convergence points. These instruments were installed between June 30 and November 16, 1982. Subsequently, 4 extensometers, 4 lateral movement gauges, 3 convergence point sets, and 1 set of wall shortening points were installed between January 8 and February 3, 1983. The purpose of this second suite of instruments was primarily to monitor any vertical or lateral movement of the immediate roof in the C & SH shaft station. The immediate station roof consists of a "beam" of salt resulting from separation along the thin clay seam beneath anhydrite "a". South of the shaft this beam is about 3 to 4 1/2 feet thick, while north of the shaft it is about 7 feet thick. Chapter 3, Section 3.2, presents a brief discussion of the underground facility horizon selection and the resulting location of the station with respect to overlying and underlying clay seams and anhydrite layers.

The data plots for the C & SH shaft station are presented in Appendix J. Figures J-146, J-147, J-163, and J-170 through J-173 show

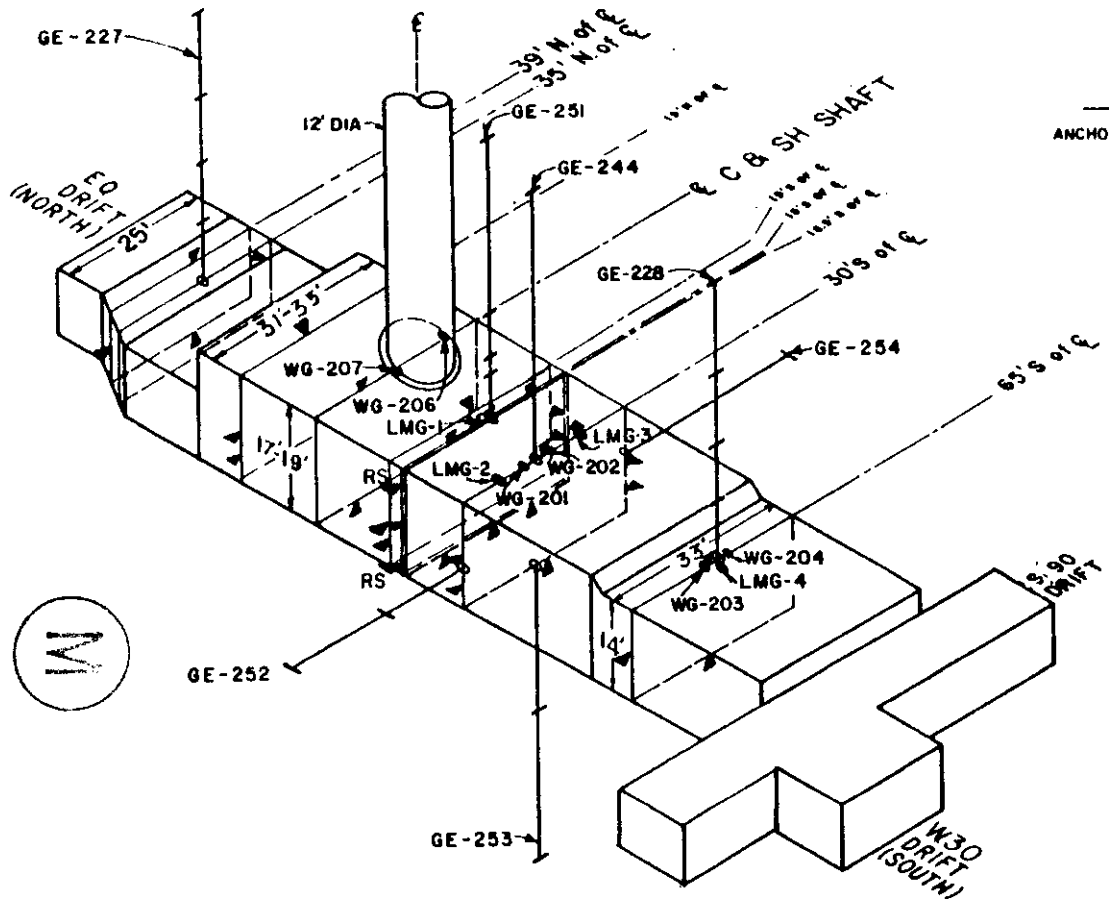

LEGEND

ANCHOR COLLAR

GE EXTENSOMETER

RC CONVERGENCE POINT

RS WALL SHORTENING POINT

WG ROCKBOLT LOAD CELL

LMG LATERAL MOVEMENT GAUGE

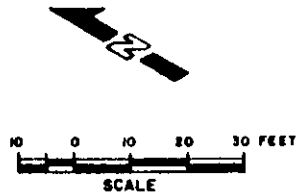

Figure 7-4

C & SH SHAFT STATION INSTRUMENTATION

the extensometer data. Convergence point data are presented on Figures J-188 through J-194 and rock bolt load cell data are shown on Figures J-192 through J-197.

Four lateral movement gauges were installed in the roof of the station. These were intended to measure lateral displacement of the salt above anhydrite "b". However, the lateral movement measurements were distorted by the vertical movement of the roof and a meaningful trend or pattern in the relative direction of horizontal movement did not develop. Therefore, reading of the lateral movement gauges was discontinued and the data are not presented in this report.

7.3.2 Analysis and Evaluation

The data collected from the C & SH shaft have been reviewed and subjected to statistical analysis, closed form solution and model simulation techniques for evaluation against the reference design parameters. The following subsections present discussions of these analyses and evaluations for the four sections of the shaft.

7.3.2.1 Lined Section

Observed Conditions. Observations of the steel liner during shaft inspections have detected no signs of deterioration. There is no indication of any liner instability due to shaft deformation. Water seepage has occurred only through the previously discussed piezometer bushings.

Structural Analysis. As a result of increasing hydrostatic pressure with depth, the thickness of the C & SH shaft steel liner and the size and spacing of its stiffener rings vary accordingly. The stiffener rings are 3-inch thick steel rings welded to the outer face of the liner. The thickness of the liner and the width and spacing of the stiffener rings for various depths are:

Depth (feet)	Plate Thickness (inches)	Stiffener Width (inches)	Stiffener Spacing (feet)
0.00 to 182.45	5/8	7-1/2	10
182.45 to 362.45	1	12	10
362.45 to 542.45	1	11	5
542.45 to 642.45	1-1/4	10-1/2	5
642.45 to 742.45	1-3/8	9	4
742.45 to 842.45	1-1/2	10-1/2	4

A structural analysis was performed for the shaft liner based on these depths and dimensions. The liner and stiffeners were made of A-441 steel fabricated into 20-foot sections by full penetration bevel welds between the liner sections and by fillet welds between the liner and the stiffeners. Radiographic acceptance examinations were performed on all welds in accordance with the American Welding Society (AWS) (ref. 7-1) and the ASME Boiler and Pressure Vessel Code, Sections VIII and IX (ref. 7-2).

A computer program was used to design the steel liner against elastic buckling between the stiffeners, elastic buckling of the combined liner and stiffener, and the yielding of the liner. This program was developed jointly by Fenix & Scisson and Southwest Research Institute and was based on Theory of Plates and Shells by S. P. Timoshenko and S. Woinowsky-Krieger (ref. 7-3).

The computational results of the analysis of the liner, based on the depths and dimensions presented above, show that the external pressure capacities and corresponding closure limits (maximum diametric changes) at the midpoint of a stiffener and at the midpoint between stiffeners are:

Depth (feet)	Pressure Capacity (psi)	Closure Limit at Stiffener (inches)	Closure Limit Between Stiffeners (inches)
0.00 to 182.45	139	0.007	0.054
182.45 to 362.45	281	0.010	0.069
362.45 to 542.45	434	0.019	0.108
542.45 to 642.45	518	0.030	0.104
642.45 to 742.45	595	0.043	0.112
742.45 to 842.45	684	0.043	0.118

In situ hydrostatic pressures determined from piezometer readings at elevations of 2830, 2790, 2719, 2684 and 2608 feet (Figure 7-1) were compared with design pressures and the pressure capacity of the liner as discussed below.

Measured Water Pressure. Piezometers are used to monitor the hydrostatic pressure exerted on the steel liner by water from the two water-bearing zones in the Rustler formation. Selected water pressure measurements are presented in Table 7-2. Because of the piezometer history of damage and leakage, the data must be used with caution. However, as expected, the data show a general trend of increasing pressure (Figure 7-5). The exceptions, 37X-PE-00211 and 37X-PE-00212, are discussed in the next subsection.

As indicated in Table 7-1, the design basis hydrostatic pressure is assumed to begin at a depth of 250 feet below ground level. This corresponds to the potentiometric surface of the water-bearing members in the Rustler formation. The hydrostatic design pressure gradient of the liner in the Rustler formation is shown on Figure 7-5. Piezometer reading data from June 1986 indicate pressures significantly less than the design hydrostatic pressure. This can be explained by a combination of the following conditions:

(1) drawdown of the potentiometric surface in the vicinity of the shafts;

Table 7-2

C & SH SHAFT LINER AND KEY
SUMMARY OF MEASURED WATER PRESSURES (psi)

Date of Reading	PIEZOMETER NO. 37X-PE-00											
	201	202	203	204	205	206	207	208	209	210	211	212
	Elev. 2830		Elev. 2790		Elev. 2719		Elev. 2684		Elev. 2608		Elev. 2560	
Pressure capacity of liner	518		518		595		595		684			
Jun. 20,'83	112	111	108	108	86	86	110	104	140	142	6	12
Dec. 3,'83	96	96	100	101	84	84	98	100	137	139	13	9
Jun. 5,'84	90	93	-	-	79	-	90	96	127	129	5	1
Dec. 27,'84	93	95	119	119	102	100	105	116	-	152	3	0
Feb. 8,'85	98	100	131	130	109	105	107	117	-	157	10	7
May 21,'85	90	93	84	81	61	44*	105	-**	146*	137*	5	6
Jun. 29,'85	89	92	91	-**	97	-**	104	-**	-**	-**	4	7
Dec. 9,'85	90	91	108	104	100	-**	108	-**	-**	-**	-1	-1
Mar. 24, '86	101	102	-	134	107	-**	104	-**	-**	-**	-2	-4
Jun. 02, '86	89	91	104	-	100	-**	108	-**	-**	-**	-	-2

NOTE: All piezometers have leaked or suffered damage at one time or another.

* Piezometer leaking.

** Piezometer removed for repair.

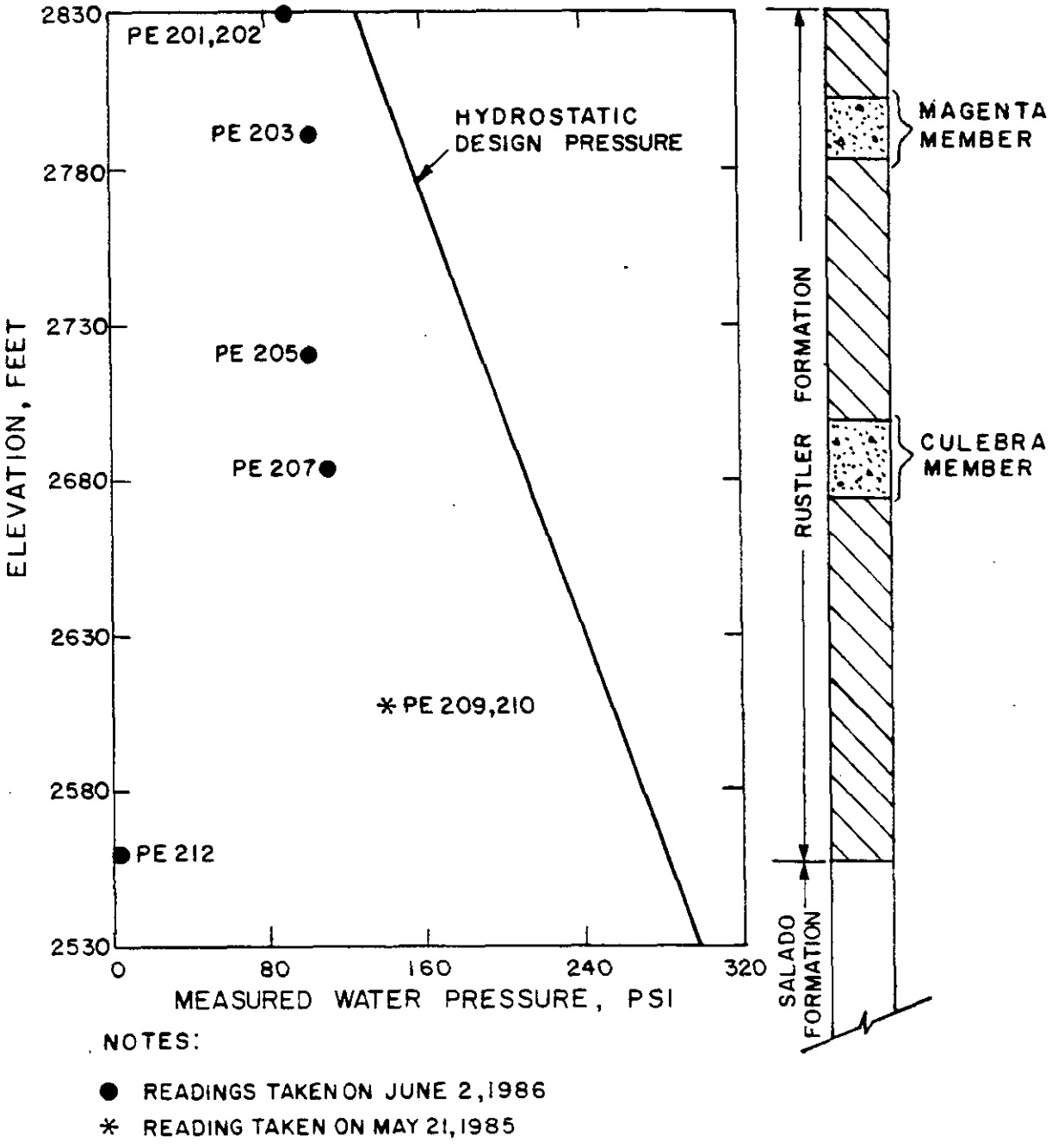

Figure 7-5

C & SH SHAFT LINER AND KEY
WATER PRESSURE DISTRIBUTION

(2) incomplete hydraulic continuity behind the liner;

(3) water leakage through the piezometer bushings and telltales; and

(4) partial plugging of the piezometer filters.

Lowering of the potentiometric surface is primarily the result of water flowing into the unlined SPDV ventilation shaft and later through cracks in both the waste and exhaust shaft liners. Hydrologic testing at the site by SNL has also contributed to lowering the potentiometric surface.

The annular space between the steel liner and the rock was filled with grout during liner installation (Chapter 3). In addition to supporting the liner, the grout was intended to help prevent water in the water-bearing zones from contacting the salt in the key area. The variations in water pressure at the different piezometer elevations, and especially the lack of a linear increase with depth, suggests that this objective has been at least partially achieved. The absence of hydraulic continuity along the rock/liner interface could prevent the water at individual piezometer elevations from achieving the anticipated pressures.

Most of the piezometers have developed leaks at some time in their history. This leakage would result in a drop in water pressure at the affected piezometer. The piezometer would then measure a water pressure that is lower than anticipated. The influence of the leaks on piezometer readings is considered to be minor because, as individual piezometers are repaired or bushings are sealed, the data plots do not show a significant change from the normal variation within the data.

The fourth cause of variation in the pressure readings could be a result of partially-plugged filters. Each piezometer contains a stainless steel, porous stone filter. It has been noted during their

repair that some filters are partially covered with salt deposits and corrosion. It is not clear how much of an effect this may have on the piezometer readings. It is possible that there is no effect if the corrosion and salt deposition occurred after the filter was exposed to the atmosphere during piezometer removal.

Closure. Closure data show the in situ diametric changes in the liner based on radial convergence point measurements at elevations of 3114, 2956, 2826 and 2680 feet (Figure 7-1). These data are considered a lower bound because the in situ readings represent only relative closures since the first readings were taken 329 days after excavation. In addition to the effect of hydrostatic pressure, the closure data are also affected by variables such as temperature and lithostatic pressure.

Radial convergence point measurements in the lined section of the shaft indicate that the maximum diametric closure is less than 0.10 inch. Since the shaft is used for ventilation purposes and is open to the atmosphere, changes in ambient temperature from around 0°F in the winter to over 100°F in the summer may affect the diametric closure by approximately 0.075 inch. Consequently, only closure data recorded at approximately the same temperature should be used for analysis.

7.3.2.2 Shaft Key

Observed Conditions. Shaft key inspections indicate that the key is stable. Certain observations, however, dictate that continuous monitoring of the key will be required. The telltale drains, connected to a French drain behind the key, drip intermittently. Several other capped pipes typically produce small amounts of water when opened after being closed for several weeks.

No water has been observed bypassing the lower chemical water seal. During the June 2, 1984, inspection, liquified chemical seal material was observed in two chemical seal injection pipes. It is likely that chemical seal material is migrating behind the key since small amounts

were observed dripping from the northwest telltale drain and from piezometer 37X-PE-00211. These fluid observations do not present any immediate cause for concern. However, the key should be monitored on a regular basis and appropriate actions taken if required to mitigate any significant increase in fluid discharge.

Inspection of the bottom of the key has revealed no evidence of seepage below the concrete. Some salt stalactites have been observed hanging from the concrete but these originate from brine dripping from the leaking piezometers or telltale drains above.

Model Simulation. The long-term impact of C & SH shaft salt creep on the concrete key was evaluated by a nonlinear computational analysis using the finite element method (ref. 7-4). The objective of the analysis was to determine the structural adequacy of the shaft key based on the appropriate ACI Codes (ref. 7-5). Site stratigraphy was considered in the analysis. The creep behavior of the salt was incorporated into the material properties used in the finite element model. The shrinkage of the concrete during initial curing was also simulated in the computation (ref. 7-6).

From the shaft geologic mapping, it was determined that the stratigraphy in the shaft key area consists of horizontal layers of halite, argillaceous halite, anhydrite and siltstone, with clay seams between some of these layers (Figure 7-6). This stratigraphy was used as the basis in modeling.

The properties for the host rock are based on laboratory test results (refs. 5-3 and 7-7) as described in Appendix C. Because the analysis was performed early in design validation, before the methods of computing primary creep and using in situ material properties were developed (ref. 5-1), the analysis included only the secondary creep of salt based on laboratory test data.

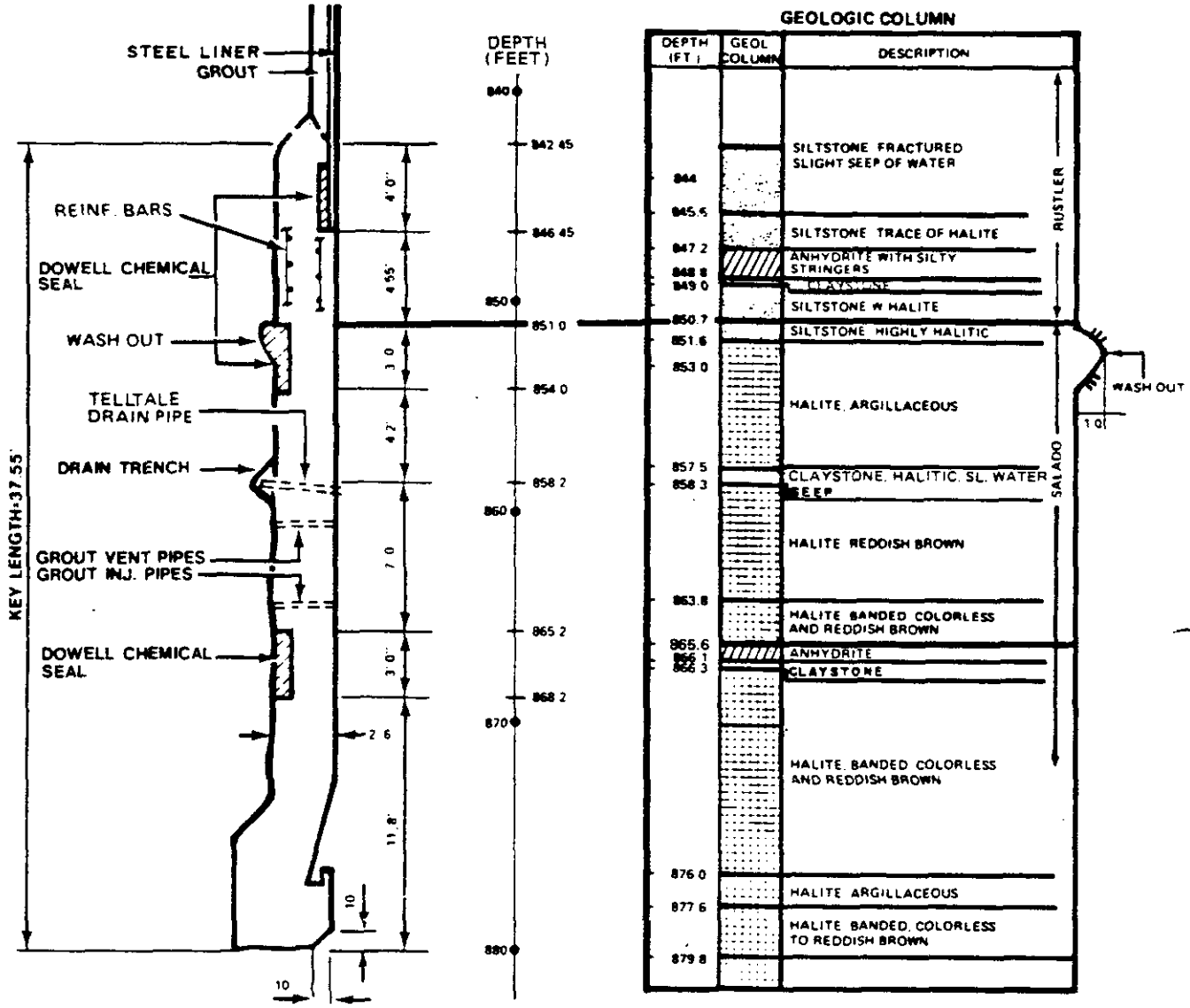

Figure 7-6

C & SH SHAFT KEY
STRATIGRAPHY

The relationship for concrete shrinkage (ref. 7-8) can be expressed as:

$$\varepsilon_{sh} = \frac{t}{35 + t} \varepsilon_{shu} C_{the} C_h C_s C_{cem} C_{fa} \quad (7\text{-}1)$$

for t in days, or:

$$\varepsilon_{sh} = \frac{t}{3{,}024{,}000 + t} \varepsilon_{shu} C_{the} C_h C_s C_{cem} C_{fa} \quad (7\text{-}2)$$

where: t is the shrinkage time in seconds;

ε_{shu} is the ultimate shrinkage strain, taken to be 0.0008;

C_{the} is the correction factor for thickness (1.17 - 0.029T);

C_h is the correction factor for humidity (1.40 - 0.010H);

C_s is the correction factor for slump (0.89 + 0.041S);

C_{cem} is the correction factor for cement content (0.75 + 0.034B); and

C_{fa} is the correction factor for percent fines and air content, taken to be 1.0.

The thickness T of the key wall is 30 inches; the humidity H is very low in the region of the key and is assumed to be 50 percent; the slump S of 4 inches is taken as the average value for 5,000 psi concrete; and B is the number of sacks of cement per cubic yard of concrete, considered to be equal to seven. The values of the correction factors C_{the}, C_h, C_s and C_{cem}, as calculated from the equations above, are 0.3, 0.90, 1.05 and 0.99, respectively.

Figure 7-7 shows the finite element model for the creep analysis. Since the structure is symmetrical about the centerline of the shaft, the shaft key and the area around it were modeled using 196 quadrilateral ring finite elements representing 18 distinct geologic layers. The MARC General Purpose Finite Element Analysis Program (ref. 6-8) was used for the analysis. To reduce the computation time, the stress and strain were computed at the centroid of each element. Four clay seams, at depths of 848.9, 857.9, 866.2 and 900.9 feet, were considered as active slip planes, represented by 25 friction and gap link elements with a coefficient of friction equal to 0.4. The outside

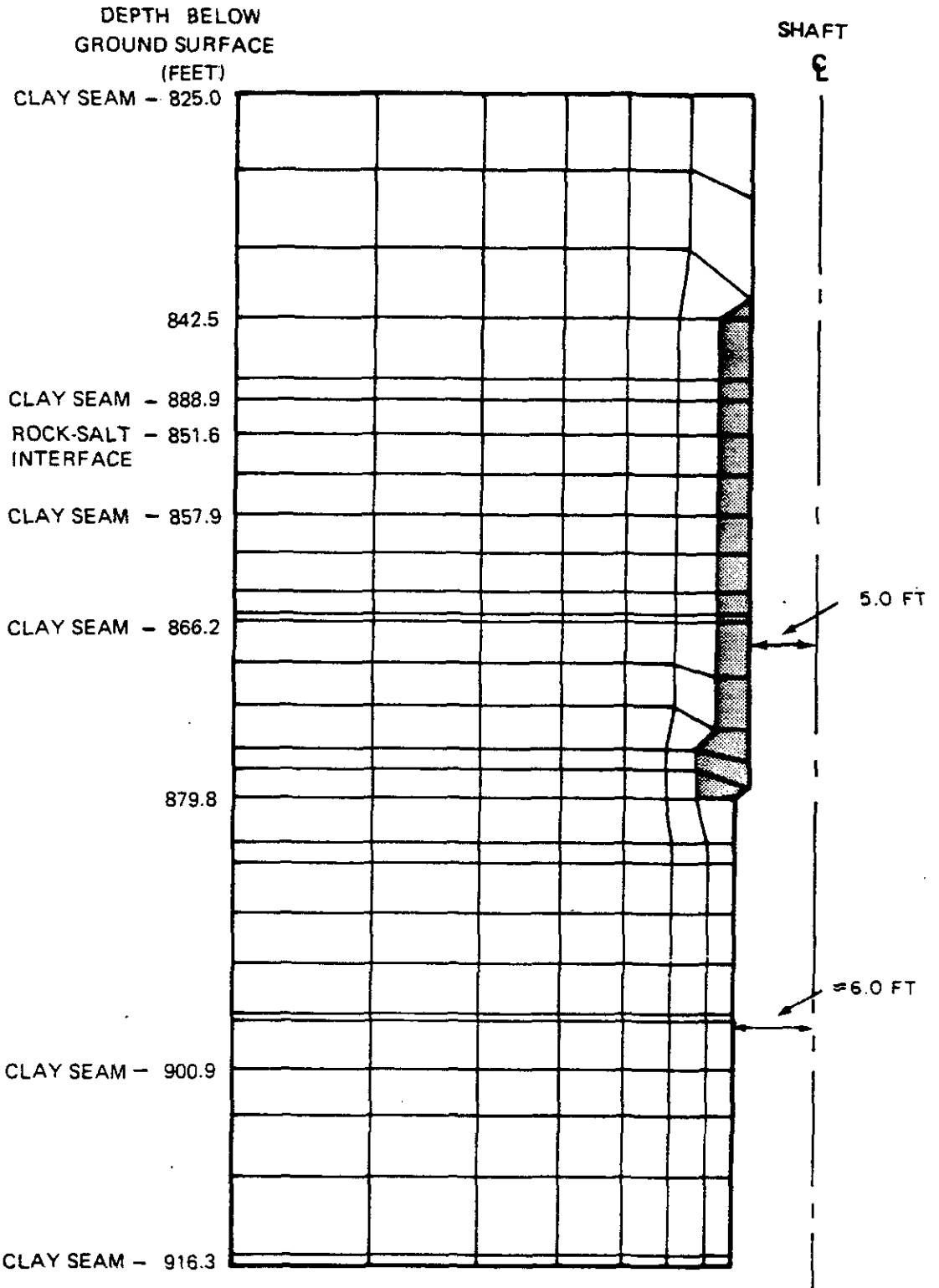

Figure 7-7

C & SH SHAFT KEY
FINITE ELEMENT MODEL

M

vertical boundary had zero horizontal displacement and the bottom boundary had zero vertical displacement. The boundary conditions at the top of the model were uniform calculated pressures based on the mass density of the geologic formation from the ground surface to the elevation of the boundaries. The lithostatic stress state was defined as described in Chapter 5, equation 5-1.

Creep analysis was performed on the mathematical model by using the procedures described in Chapter 5. The analysis was carried out for a 5-year interval without the key and a comparison was made of the corresponding radial deformations to determine the time when creeping salt would come into contact with the shrinking concrete key. The times computed for various layers behind the key were between 1.6 and 3.9 years with an average value of 2.7 years after excavation of the shaft (or 2 years after construction of the shaft key). To simulate contact of the shaft wall with the concrete key, the elements of the key were tied to the proper locations on the shaft wall and the analysis was continued for a total of 27 years (refs. 7-4 and 7-6).

Deformation. Readings from the strain gauges embedded in the concrete key show a range of strains from approximately 0.00014 in compression to 0.00021 in tension with an average compressive strain of 0.00004 through December 9, 1985. The readings from the strain gauges welded to the reinforcing steel show a range of approximately 0.00031 in compression to 0.00054 in tension with an average tensile strain of 0.00006.

Table 7-3 summarizes the changes in readings of the embedment and welded gauges at a depth of 856 feet (elev. 2554 feet) since April 22, 1982, immediately after concrete was placed for the shaft key. The trend of the change in strain readings indicates that the salt had not made contact with the key by June 1985.

Water Pressure. Figure 7-5 shows water pressure readings from piezometers 37X-PE-00211 and 37X-PE-00212. These piezometers have

Table 7-3

C & SH SHAFT KEY
SUMMARY OF STRAIN GAUGE READINGS AT ELEVATION 2554 FEET

Strain Gauge No.	Change in strain x 10^{-6} since April 22, 1982 Jun. 5, 1984	Feb. 8, 1985	Jun. 29, 1985	Dec. 9, 1985	Remarks
37X-ZE-209	-63	-59	-81	-9.5	Embedment
211	-23	-16	-34	-51	strain gauges
213	-133	-104	-139	-144	14.5 inches
215	-82	-67	-99	-111	from inner surface
235	-12	16	-23	-47	Embedment
236	56	88	37	16	strain gauges
237	-18	35	-23	-8	9 inches from
238	-63	-23	-81	-99	inner surface
210	-110	-71	-123	-154	Embedment
212	178	272	201	215	strain gauges
214	58	128	65	79	3.5 inches
216	-53*	-7	-61	-76	from inner surface
201	-93	-100	-102	-138	Strain gauges
203	-	-	444*	-	welded to the
205	-235	-286	-352	-371	outer rein-
207	-102	-127	-142	-95	forcing bar
202	-43	-	-61	-58	Strain gauges
204	443	2066	1056	541	welded to the
206	-193	-147	-230	-246	inner rein-
208	-	-	-1659**	-	forcing bar

NOTE: Negative strain change indicates compression.

• Reading taken on May 3, 1984.
** Reading taken on Dec 30, 1982.

shown a range of readings from a maximum of 30 psi in 1982 to a current reading of 2 psi. As shown on the figure and in Table 7-2, the readings of these two piezometers are consistently lower than the readings from the upper piezometers. These lower piezometers are at a depth of 850 feet (elev. of 2560 feet), just above the chemical water seal at a depth of 851 feet (elev. 2559 feet). It appears that this seal may be breached and that water is able to bypass it and exit through the French drain and telltales. Piezometers 37X-PE-00211 and 37X-PE-00212 may also be isolated from the upper piezometers by the grout that was injected behind the steel liner at a depth of 843 feet (elev. 2567 feet).

The assumption that the chemical water seal just below the piezometers may be breached is based on observations of piezometer behavior during the October 1983 inspection. As discussed in subsection 7.3.1.2, several capped pipes in the key were found to contain small amounts of water during this inspection and were drained. Prior to this, piezometers 37X-PE-00211 and 37X-PE-00212 indicated pressures of around 6 to 8 psi. After draining the pipes, both piezometers showed a drop to 2 psi within 2 days. This indicates a hydraulic connection across the water seal.

It is unlikely that water in the key originates from higher in the shaft. Detailed mapping in the shaft key noted weeps from claystone and siltstone beds at depths of 842. 846 and 858 feet. This is probably the source of the water seen in the French drain telltales and other pipes in the key. The fact that the key piezometers have had consistently lower readings than the upper piezometers indicates that there is probably no hydraulic connection with the water-bearing members higher in the shaft. The draining of water from the grout pipes influenced only those piezometers in the key; none of the upper piezometers showed any pressure drop. The existence of a source of water in the key area provides a better explanation of the dripping from the telltales and the performance of the key piezometers than does the migration of water from the water-bearing members higher in the shaft.

Salt Pressure. The four earth pressure cells installed between the concrete of the shaft key and the salt have a combined average reading of less than 10 psi in compression. These four cells, located 90 degrees apart at elevation 2550 feet (Figure 7-2), are intended to register changes in lateral pressures on the shaft key exerted by the creeping salt. Table 7-4 shows that the pressure cells have not registered any significant change in readings for a period of over 3 years since construction of the concrete key.

If we assume that the pressure cells are functioning properly, then the halite between a depth of 858 feet and 863 feet (elev. 2552 feet and 2547 feet) had not made contact with the pressure cell diaphragms as of December 9, 1985. According to the results of computational analyses, the contact between the salt and concrete will be reestablished at different elevations at different times between 1984 and 1986.

7.3.2.3 Unlined Section

Observed Conditions. The unlined section of the shaft appears to be stable with no evidence of rock spalling, wall deterioration, or dissolution by water.

Closure. Figure 7-8 compares average diametric closure readings at six elevations on December 9, 1985. The readings reflect only relative closure since the initial readings were taken nearly 1 year after completion of shaft excavation. Thus, the maximum diametric closure at a depth of 2,057 feet (elev. 1353 feet), near the bottom of the shaft, will be more than 1.0 inch. At higher elevations in the shaft, the actual diametric closure over the same period will, likewise, be higher than those shown on the figure.

Deformation. The radial deformation of salt behind an opening can be determined from the measurements of movements of borehole extensometers with multiple anchor points.

Table 7-4

C & SH SHAFT KEY
PERFORMANCE HISTORY OF PRESSURE CELLS

Description	Pressure Cell Reading (psi) WE-201	WE-202	WE-203	WE-204	Date of Reading
Initial Irad Gage Co calibration	+1	+2	+6	+13	Feb. 3,'82
Initial SRI calibration	+8	+7	+8	+8	Feb. 16,'82
Site received, inspection	-1	+1	0	-2	Mar. 30,'82
Pre-installation, surface	-1	+1	-5	-2	Apr. 4,'82
Pre-installation, in shaft	0	-1	-2	-2	Apr. 15,'82
After plaster of paris	-2	-2	0	-2	Apr. 15,'82
After concrete placement	0	0	0	0	Apr. 15,'82
Initial installed reading	0	0	0	0	Apr. 16,'82
Time after installation:					
7 days	+2	-1	+2	+17	Apr. 22,'82
107 days	-1	-3	-2	0	Jul. 31,'82
529 days	-2	-5	-31	+1	Sep. 26,'83
530 days	+1	-3	0	-2	Sep. 27,'83
544 days	-4	-8	-32	-3	Oct. 11,'83
597 days	-4	-7	-	0	Dec. 3,'83
797 days	-1	-7	-38	0	Jun. 20,'84
938 days	-12	-11	-27	0	Nov. 8,'84
1030 days	-12	-30	-	-2	Feb. 8,'85
1140 days	-6	-10	-25	+3	May 21,'85
1179 days	-6	-11	-25	+5	Jun. 29,'85
1342 days	-14	-10	-25	-2	Dec. 9,'85

NOTE: Negative sign indicates tension.

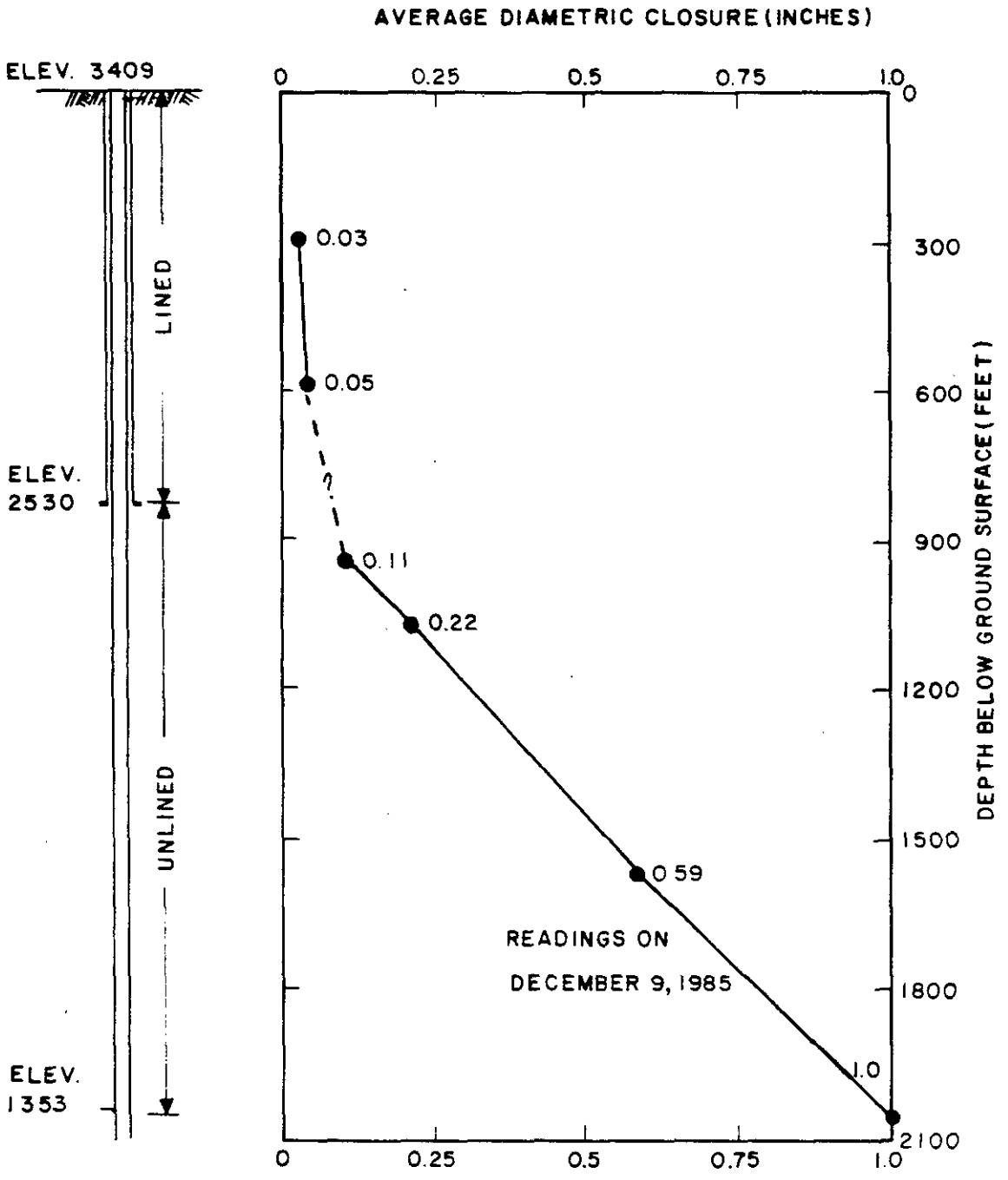

NOTES:

1. SHAFT WAS EXCAVATED FROM JULY THROUGH OCTOBER 1981
2. CONVERGENCE POINTS WERE INSTALLED FROM JULY THROUGH OCTOBER 1982.

Figure 7-8

C & SH SHAFT UNLINED SECTION
AVERAGE DIAMETRIC CLOSURE

According to extensometer readings on September 16, 1985, the total average collar displacements at elevations 1846 feet and 1353 feet (Figure 7-3) were 0.19 inches and 0.235 inches, respectively. However, the extensometers were installed nearly 7 1/2 months after the completion of shaft excavation.

Figure 7-9 shows the collar movement time histories for multiple-point borehole extensometers 37X-GE-00202, 37X-GE-00205 and 37X-GE-00208 relative to their deepest anchor. The undulating shape of the curves appears to reflect the influence of seasonal temperature changes on the extensometers. The effect of temperature changes is more pronounced on the instrument behavior than on the salt surrounding the instrument. Figure 7-10 shows the change in calculated rates of collar movement with time for the extensometer time histories on Figure 7-9. The maximum rates coincide with the hottest months while during mid-winter the rates are close to, or slightly less than, zero. Because the time interval chosen for calculating the rate of collar movement is much less than the total observation period of 2 years, these rates are probably very close to the actual rates.

Comparison of the extensometer collar movements with convergence point readings suggests that the salt in the vicinity of the deepest anchor may also be moving. Thus collar movement does not reflect the true radial closure of the shaft. The amount of movement of the deepest anchor for any extensometer of given length can be estimated so that the collar displacement provides absolute radial closure. The diametric closure can be computed by model simulation as described below, by curve fitting as described in reference 4-19, or by closed form solution, also described in reference 4-19. Based on this analysis, the absolute movements of the collar and intermediate anchors for the 36-foot long shaft extensometers will deviate from the measured values by only 0.03 inch.

Model Simulation. The structural behavior of the unlined section of the C & SH shaft was analyzed by a nonlinear creep analysis using the

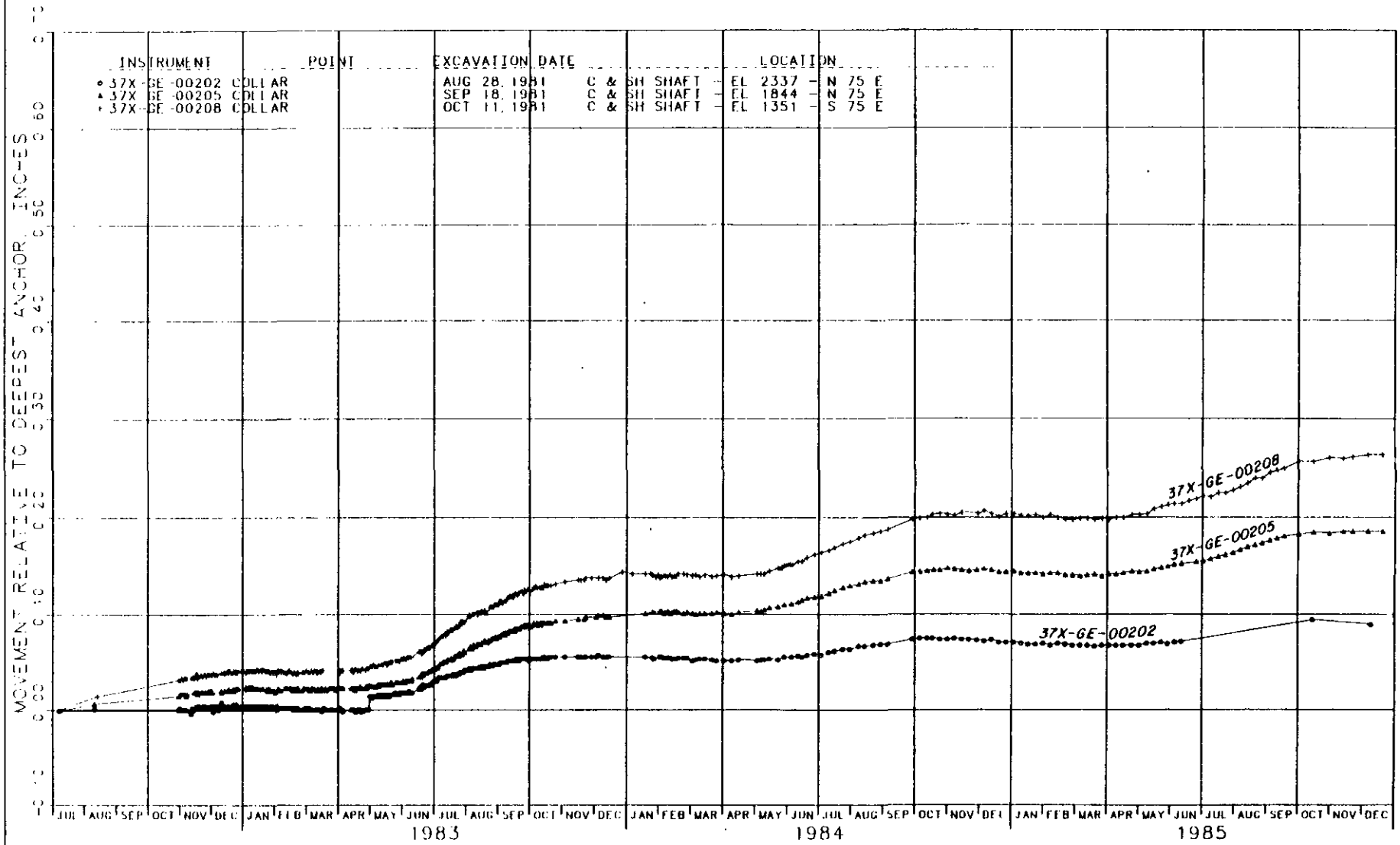

Figure 7-9

C & SH SHAFT UNLINED SECTION
COLLAR MOVEMENT TIME HISTORY

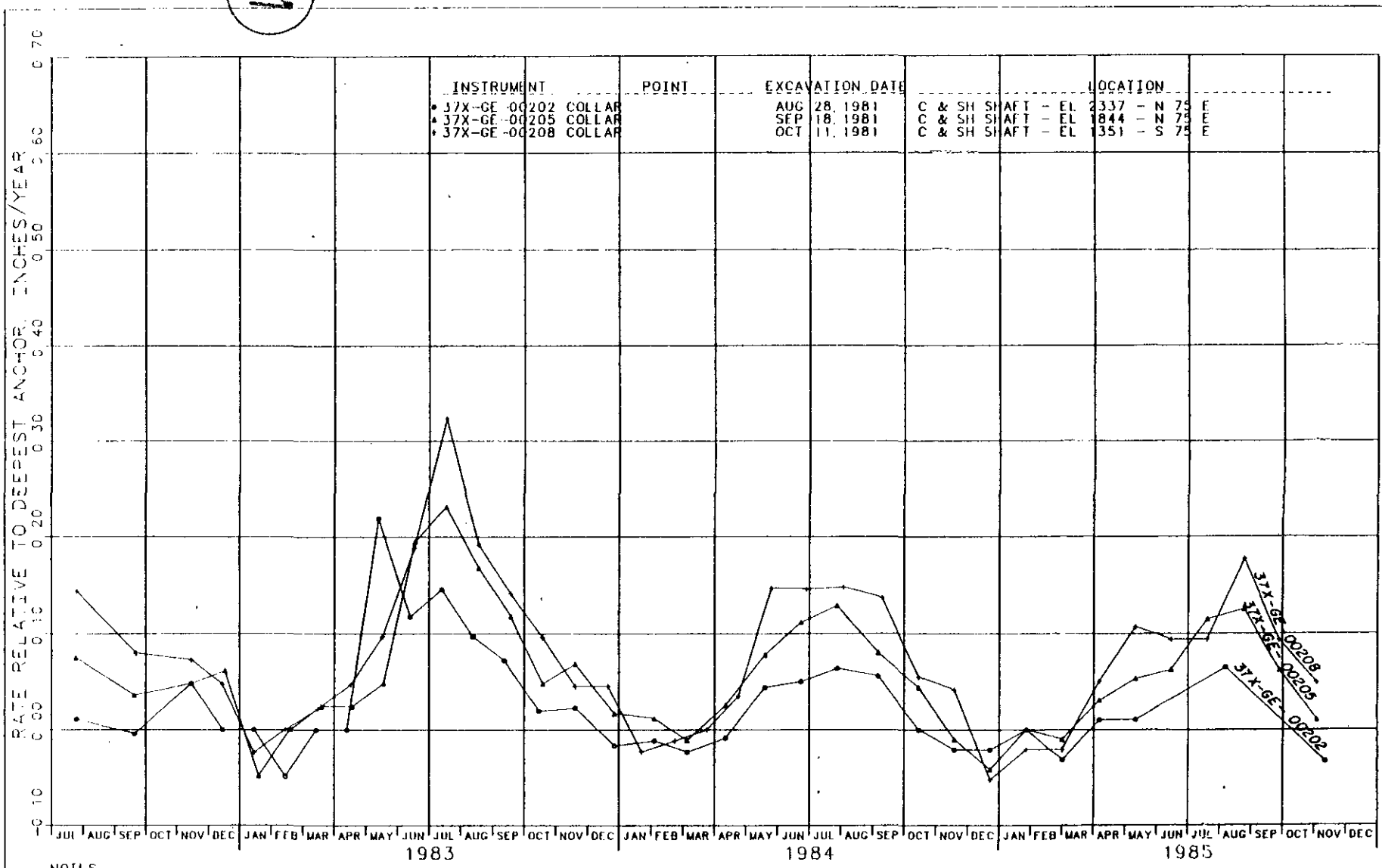

NOTES

1 RATE CALCULATED FOR MINIMUM INTERVALS OF 30 DAYS

Figure 7-10

C & SH SHAFT UNLINED SECTION
RATE OF COLLAR MOVEMENT VERSUS TIME

MARC General Purpose Finite Element Program (ref. 6-8). The objective of the analysis was to compute actual structural behavior by utilizing available in situ data, thereby verifying the design adequacy of the unlined section of the shaft.

The finite element model used for the analysis utilizes a single horizontal plane of quadrilateral ring elements with the upper and lower horizontal boundaries restrained against vertical displacement. This model is shown on Figure 7-11. The outside vertical boundary was given a constant uniform pressure based upon the lithostatic stress state defined in Chapter 5, equation 5-1. The inside boundary was also given a uniform pressure based upon the same lithostatic stress assumption; however, the pressure was removed in a step-wise fashion over a period of approximately 1 day. This was done to simulate the excavation of the drilled shaft, which results in a gradual relief of overburden pressure on the shaft interior and affects structural behavior in the early stage of excavation.

The secondary creep parameter C in Chapter 6, Table 6-8, was determined based on extensometer data at a depth of 2,057 feet (elev. 1353 feet). The value of C can be computed for each extensometer location using the analytical results and in situ data from the extensometer. Because C, determined from each extensometer, may vary, predicted diametric closures along each extensometer will vary accordingly. Using the diametric closures predicted at different directions on the horizontal plane, the principal directions of the strain on the horizontal plane can be determined. Consequently, closure along two horizontal principal directions can be predicted. Based on the predicted diametric closures at a depth of 2,057 feet in the N15°W, S75°E and S45°W directions, the major axis was found to be N17°40'W and the minor axis N72°20'E.

Closure predictions were made for two principal directions on the horizontal plane. Because the stress and strain distributions are not sensitive to the value of the secondary creep parameter, except during

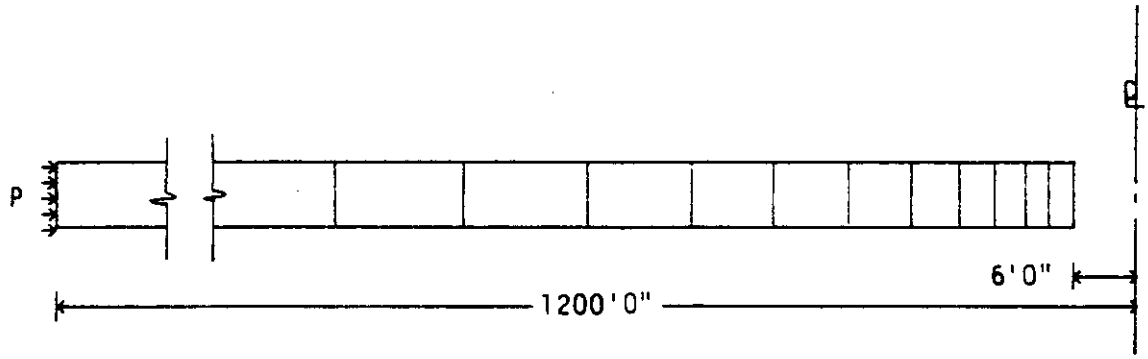

Figure 7-11

C & SH SHAFT UNLINED SECTION
FINITE ELEMENT MODEL

the initial stages of creep, the stress and strain distributions were computed based on the average values of the creep parameter C determined from three different directions.

7.3.2.4 Shaft Station

Observed Conditions. The C & SH shaft station exhibits spalling from both the roof and wall surfaces that requires continual routine maintenance. Displacements, separations and fracturing occuring above the roof at clay G and in the underlying halite were expected.

Data from the Excavation Effects Program indicate that the halite from 4 to 10 feet above the roof contains essentially no separations or fracturing. Floor heave is evident at the electrical substation where the concrete base slab has tilted several degrees, but holes drilled into the station floor encountered only minor separations and fracturing. Extensometer 51X-GE-00253, in the station floor, does not show any significant increase in collar movement that would be expected if floor heave and fracturing is occurring. Although the C & SH shaft station is the oldest and largest horizontal opening, the extent of separations and fracturing beneath the floor is very small relative to the fracturing found in the floor beneath Test Room 3 (Chapter 11).

The observed behavior in the station is apparently due in large part to its initial excavation by blasting. No other underground area has exhibited the degree of spalling that has occurred in the station. The blasting is thought to have accelerated separations at clay G and in the underlying halite in the main station area south of the shaft. However, the extensive rock bolting in the roof appears to have effectively controlled these separations.

Fracturing in the pillar corners at the S90 crosscut has continued to evolve as the salt responds to stresses produced by the station excavation. Changes in the fracturing are exhibited primarily by the appearance of new vertical fractures and by the elongation and widening of existing fractures. Minor spalling has also occurred, particularly

at the roof and wall intersection in the upper portion of geologic map unit 4.

Closure. Figure 7-12 shows closure rates calculated from the readings of roof-to-floor convergence points. The maximum rate appears to have occurred during the early part of August 1984.

The closure rates shown on Figure 7-12 cannot be directly compared without considering the differences in dimensions at the locations shown, as well as differences in the thickness of the roof beam below clay G, and the number of rock bolts in the vicinity of the respective convergence measurement stations.

Figure 7-13 compares the central vertical closure readings at stations S18.5 and N39. Although the closure measurements are very close at both stations, actual total closure at the S18.5 station will be greater since the initial reading at this station was taken nearly 261 days after the completion of excavation, compared to only 35 days at the N39 station. In addition, the larger opening dimensions at the S18.5 station will also result in more rapid closure. Even though the density of rock bolts is greater south of the C & SH shaft than north of it, the roof-to-floor closure is greater to the south. This is probably because the roof beam below clay G is thinner and longer to the south.

Figure 7-14 shows the collar movements of multiple-point borehole extensometers 51X-GE-00227 and 51X-GE-00228 in the station roof, 35 feet north and 65 feet south of the C & SH shaft, respectively. The average collar movement rate of 51X-GE-00228 is higher than that of 51X-GE-00227, as determined from Figure 7-14. The roof closure rate south of the shaft is currently more than the rate north of the shaft.

A double-point borehole extensometer (51X-GE-00253) was installed in the floor of the C & SH shaft station. The initial reading from this extensometer was taken nearly 238 days after the completion of

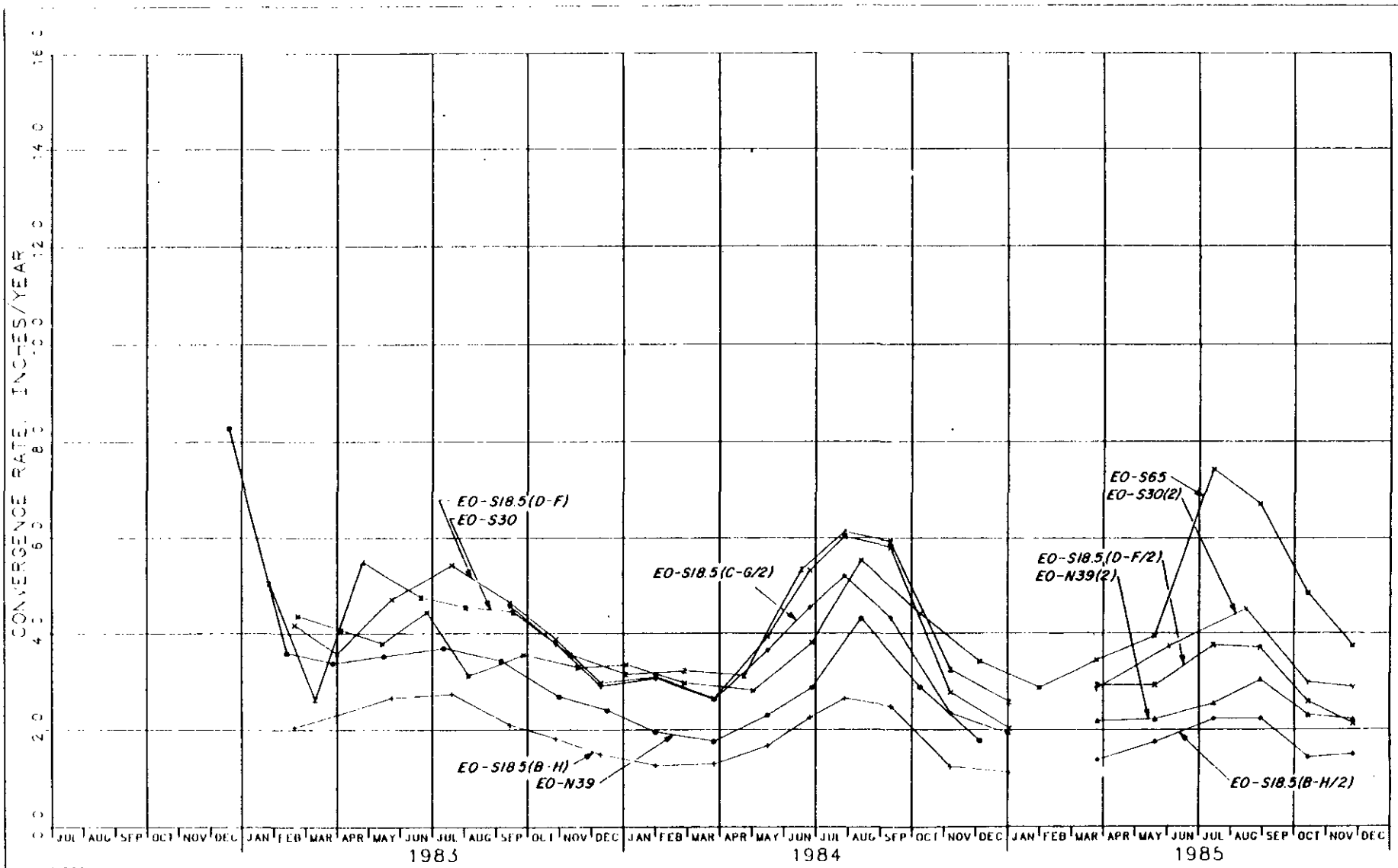

NOTES

1. RATE CALCULATED FOR MINIMUM INTERVALS OF 30 DAYS

Figure 7-12

C & SH SHAFT STATION
CALCULATED ROOF-TO-FLOOR CLOSURE RATES

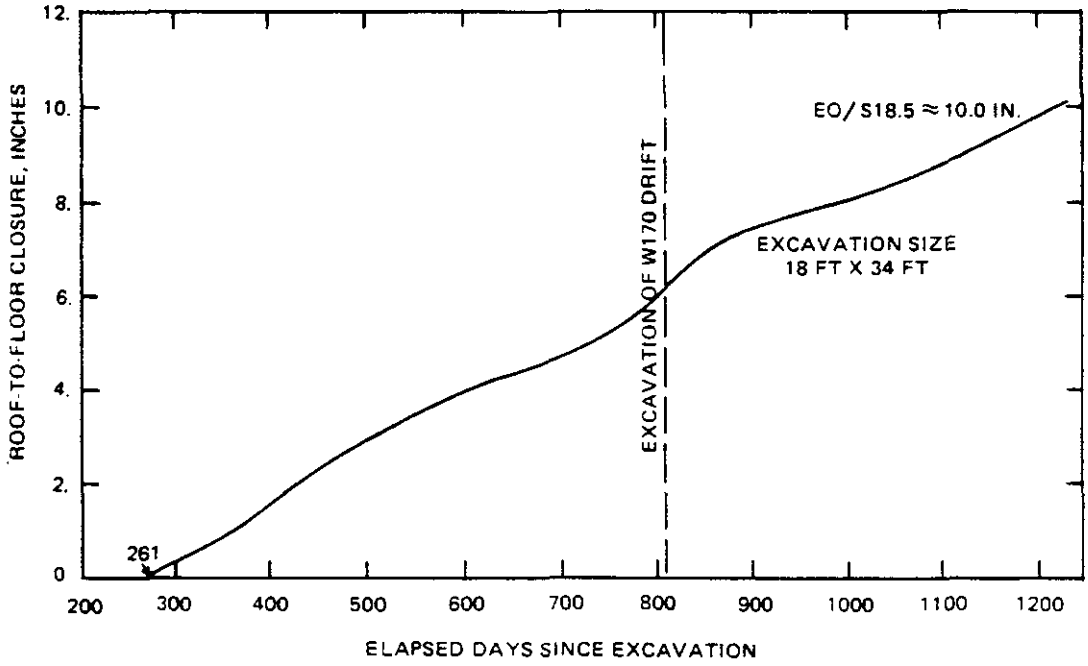

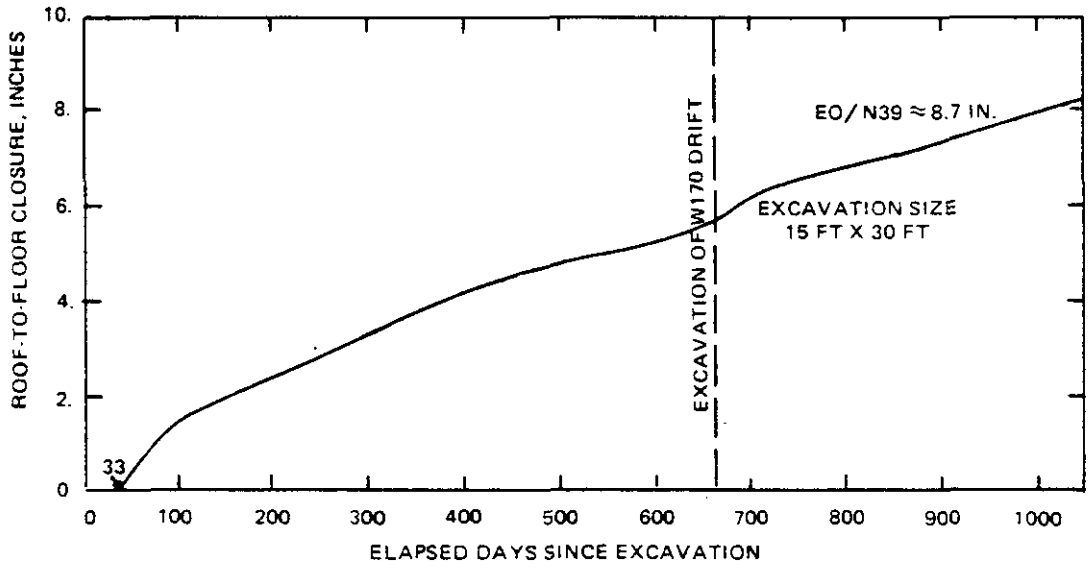

Figure 7-13

C & SH SHAFT STATION
TYPICAL ROOF-TO-FLOOR CLOSURE HISTORY

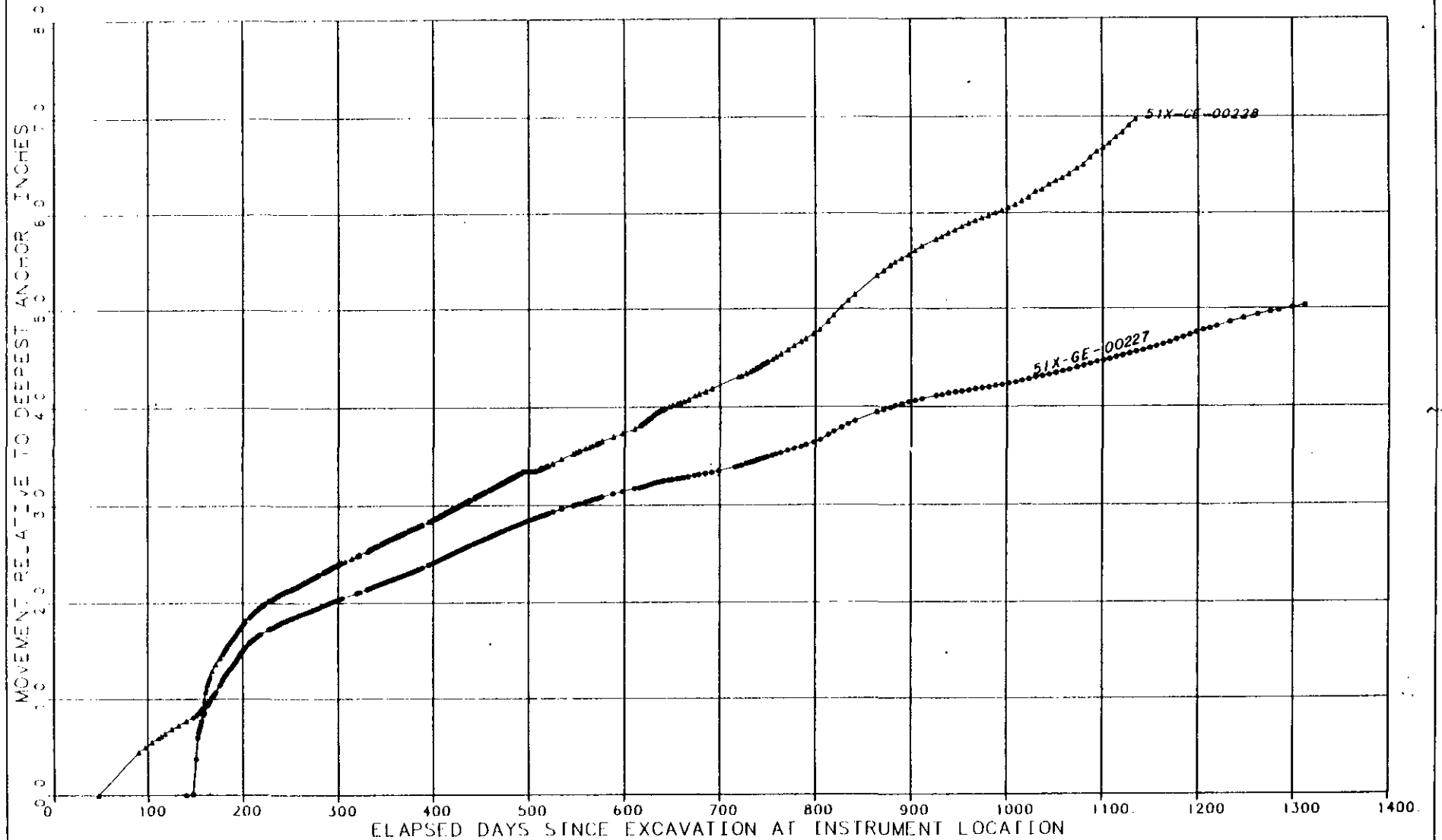

Figure 7-14

C & SH SHAFT STATION
HISTORY OF COLLAR MOVEMENTS - ROOF EXTENSOMETERS

excavation at the instrument location (Appendix J, Figure J-172). The measured collar movement relative to the deepest anchor was 3.26 inches on December 20, 1985. Actual floor heave will be higher as a result of the time-lag between the end of excavation and the initial reading date. There was a slight increase in the collar movement rate due to excavation of the nearby W170 drift, but the rate has since become steady.

Roof Stability. Figure 7-15 shows the distribution of measured movements along roof extensometer 51X-GE-00251, 18 1/2 feet south of the C & SH shaft, for the readings taken on September 18, 1985. The magnitudes shown are cumulative between the initial reading date of January 11, 1983, and September 18, 1985. The movements are also expressed as percentages of the collar reading. Sixty-one percent of the relative movement has taken place between the collar and anchor A. This has remained practically constant since December 1983 and is an indirect indication that there is no accelerating trend in the rate of opening at clay G in the vicinity of this extensometer. For comparison, the distribution of measured movement along roof extensometer 51X-GE-00227, 35 feet north of the C & SH shaft, is shown on Figure 7-16. The relative movement between the collar and anchor A has remained constant at 52 percent through December 1985. Based on these measurements, there is no indication that clay G is parting at an accelerating rate either north or south of the shaft.

7.3.3 Prediction of Future Behavior

This subsection presents the results of the analysis and evaluation of the finite element modeling and the data collected in the C & SH shaft. These results are presented in the form of predictions for future behavior of the constructed shaft elements (liner and key) and of the salt surrounding the unlined section of the shaft and the shaft station.

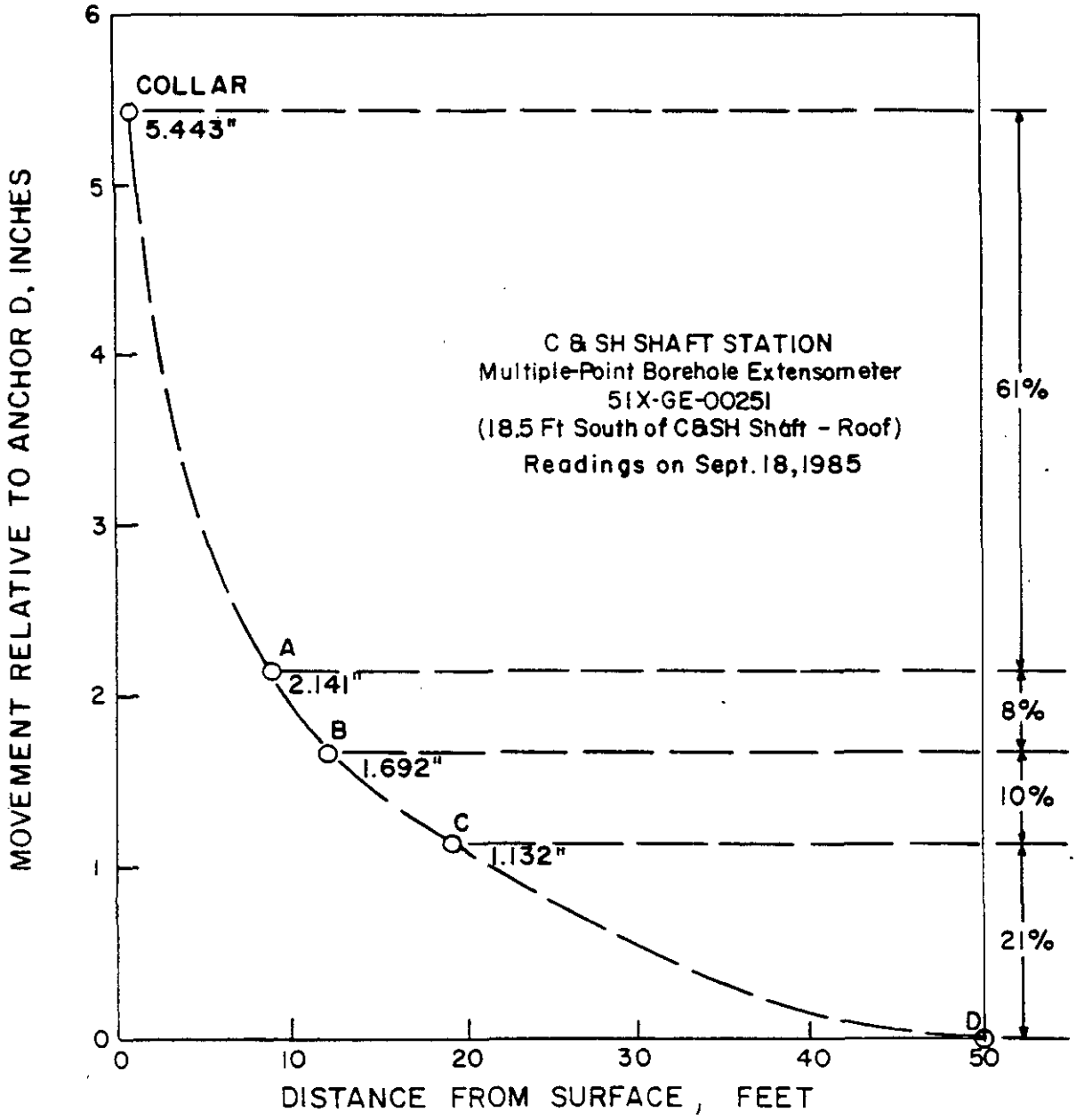

Figure 7-15

C & SH SHAFT STATION
MOVEMENT DISTRIBUTION ALONG ROOF EXTENSOMETER 51X-GE-00251

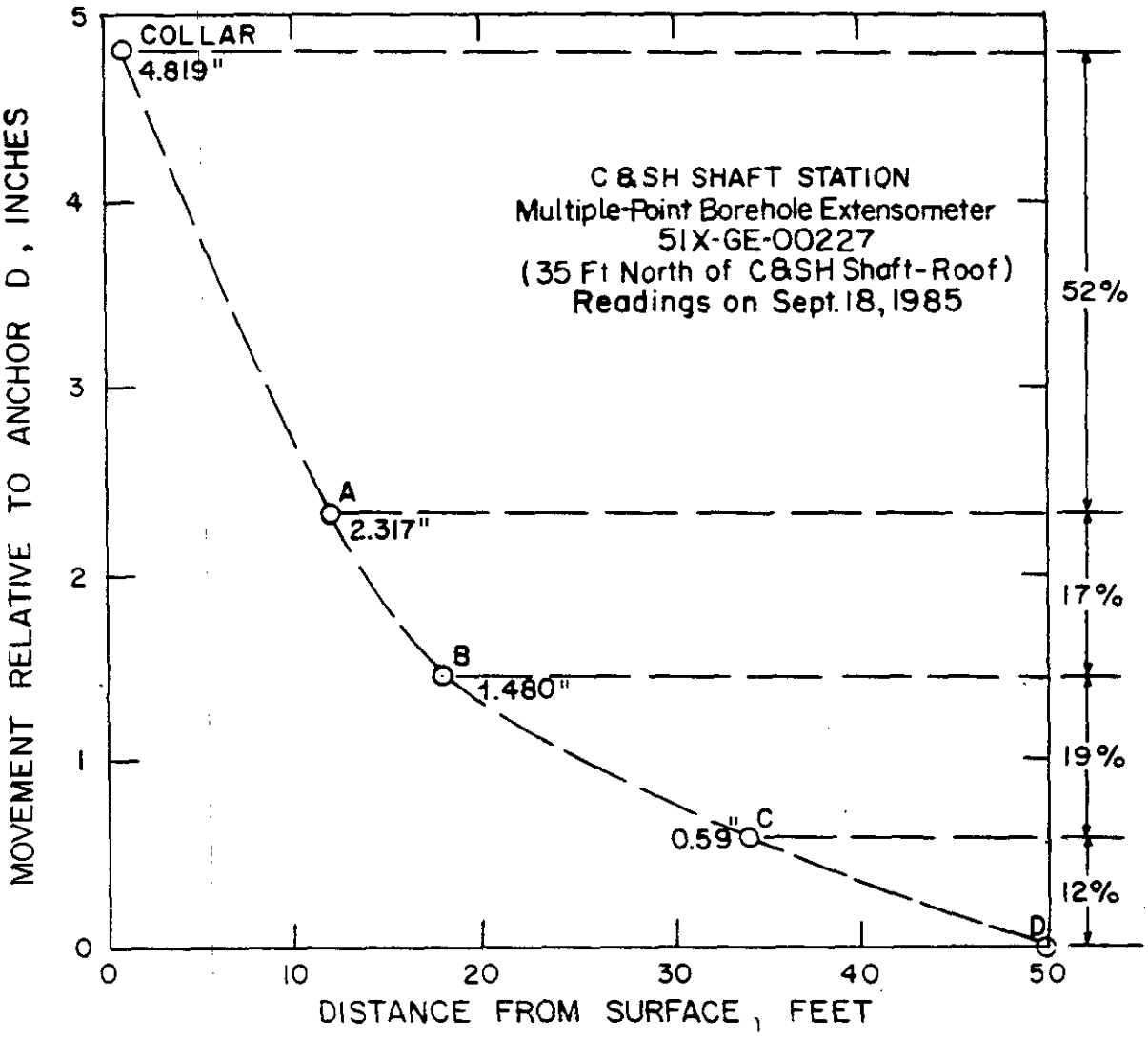

Figure 7-16

C & SH SHAFT STATION
MOVEMENT DISTRIBUTION ALONG ROOF EXTENSOMETER 51X-GE-00227

7.3.3.1 Lined Section

The water pressure on the shaft liner to date has been less than the hydrostatic design pressure. The prediction of future water pressures behind the liner is difficult due to the reasons discussed in subsection 7.3.2.1. The lower potentiometric surface and lack of hydraulic continuity along the rock/liner interface may prevent the ground water from reaching the design hydrostatic head. In addition, leaks around the piezometers and possibly obstructed filters may cause the measurements to be somewhat less than the actual pressure conditions.

Figure 7-17 shows that if the water pressure does reach the design hydrostatic pressure, the liner will remain stable based on its design factor of safety. The figure shows that the pressure capacity of the liner far exceeds the design hydrostatic pressure. This pressure was determined based on water level data obtained at the site during preliminary design activities. The data indicated that the highest potentiometric surface in the Rustler formation beneath the site occurred at a depth of approximately 250 feet below the ground surface. This data was later confirmed by investigations conducted in the site vicinity by the U.S. Geological Survey (USGS) (ref. 7-9). It is not expected that this potentiometric surface will be exceeded during the 25-year operating life of the facility. If any external water were to infiltrate along the rock/liner interface to form a column of water that would exceed the hydrostatic head contained in the design bases, the stability and safety of the steel liner would still not be compromised based on the design factor of safety.

7.3.3.2 Shaft Key

The results of the shaft key analysis indicate that after concrete is placed against the shaft wall it shrinks away from the wall at a rate greater than the rate of salt creep, resulting in a separation between the concrete and the salt. The rate of concrete shrinkage decreases with time and continuous salt creep eventually results in the salt

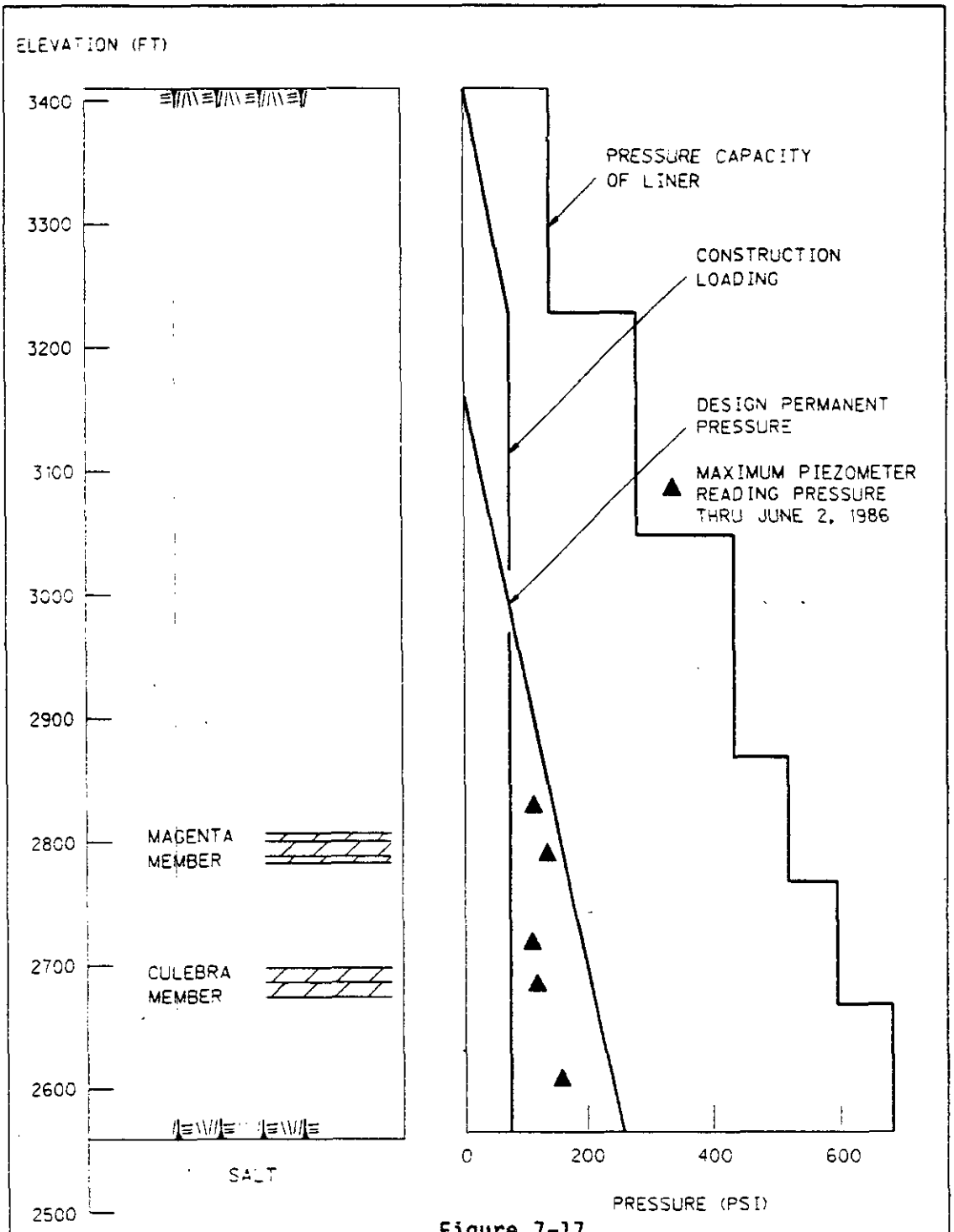

Figure 7-17

C & SH SHAFT LINER
LATERAL PRESSURE COMPARISON

contacting the concrete again. The interactive pressure between the concrete and the salt will then gradually increase due to continuous salt creep.

In the key area, the shaft wall radial and tangential stresses (Figures 7-18 and 7-19, respectively) were plotted as a function of distance from the centerline of the shaft for a typical section immediately after excavation of the shaft and for 1 year and 25 years after concrete placement. As expected, the radial stresses in the salt are initially relieved near the opening but begin increasing after the salt comes in contact with the concrete. Further away from the opening, the stresses trend toward the overburden pressure.

The tangential stresses in the salt 3 days after excavation show an elastic response which gives very high values near the opening. The stresses are relieved near the opening from the time the salt starts to creep until it contacts the concrete. After contact is made, and for the remainder of the 25 year analysis period, the stresses in the salt and concrete key increase. There exists a discontinuity of stress at the concrete/salt interface which is primarily due to differences in their material properties. Like the radial stresses, the tangential stresses approach the overburden pressure with increasing distance from the opening.

At 25 years, the radial stresses, which are equal to the lateral pressures on the salt face of the key, will increase to an average value of 275 psi. At the same time, the maximum hoop stress at the inside face of the concrete key has an approximate value of 1,000 psi, with an average value across the key of about 825 psi. Figures 7-20 and 7-21 show the predictions for average lateral pressures and average hoop stresses, respectively. A lateral pressure capacity in the key of 833 psi, based on an allowable hoop stress controlled by a concrete compression of 3,000 psi, results in a factor of safety of approximately three.

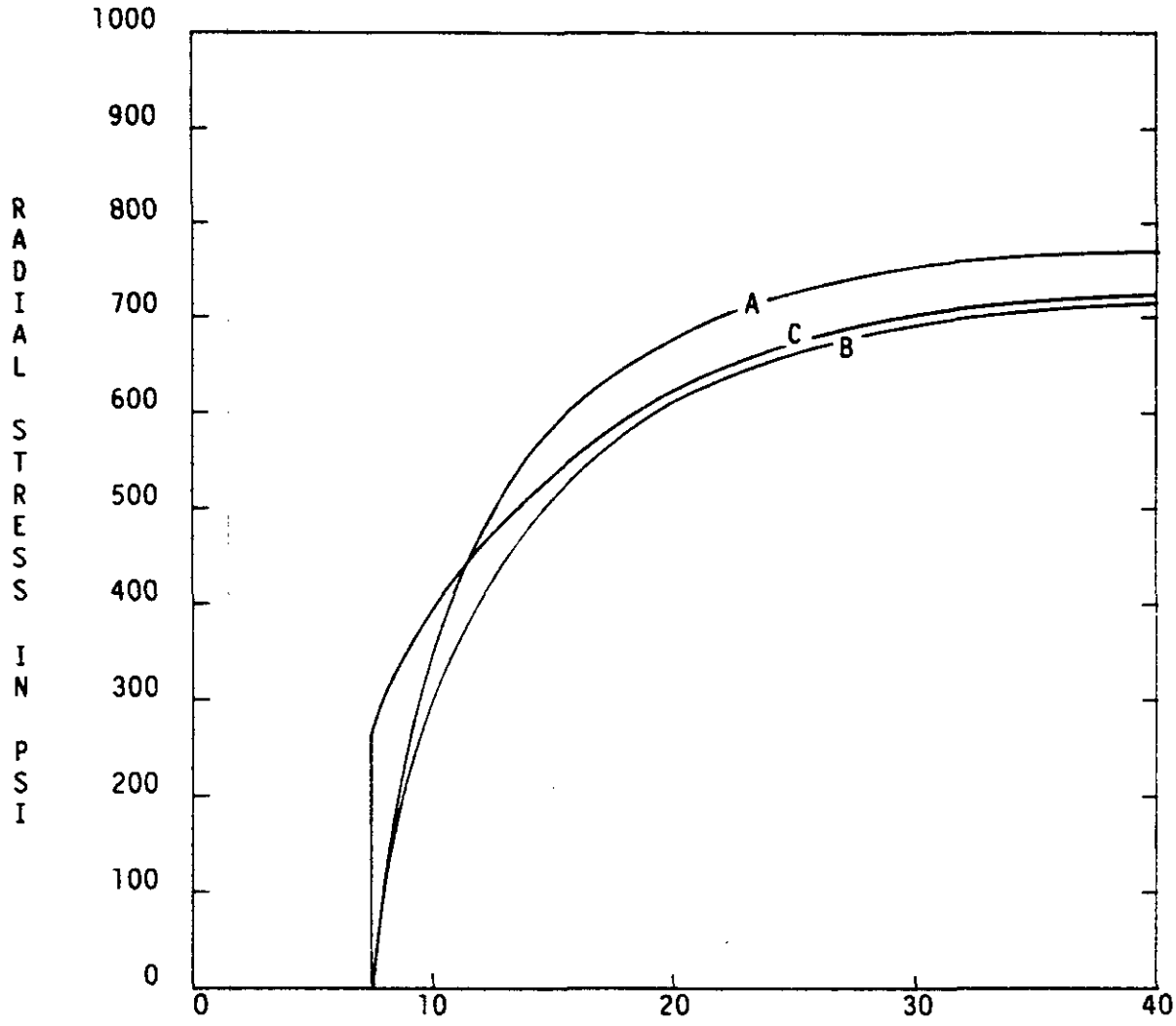

A – IMMEDIATELY AFTER EXCAVATION
B – ONE YEAR AFTER CONCRETE PLACEMENT
C – 25 YEARS AFTER CONCRETE PLACEMENT

Figure 7-18

C & SH SHAFT KEY
RADIAL STRESS DISTRIBUTION

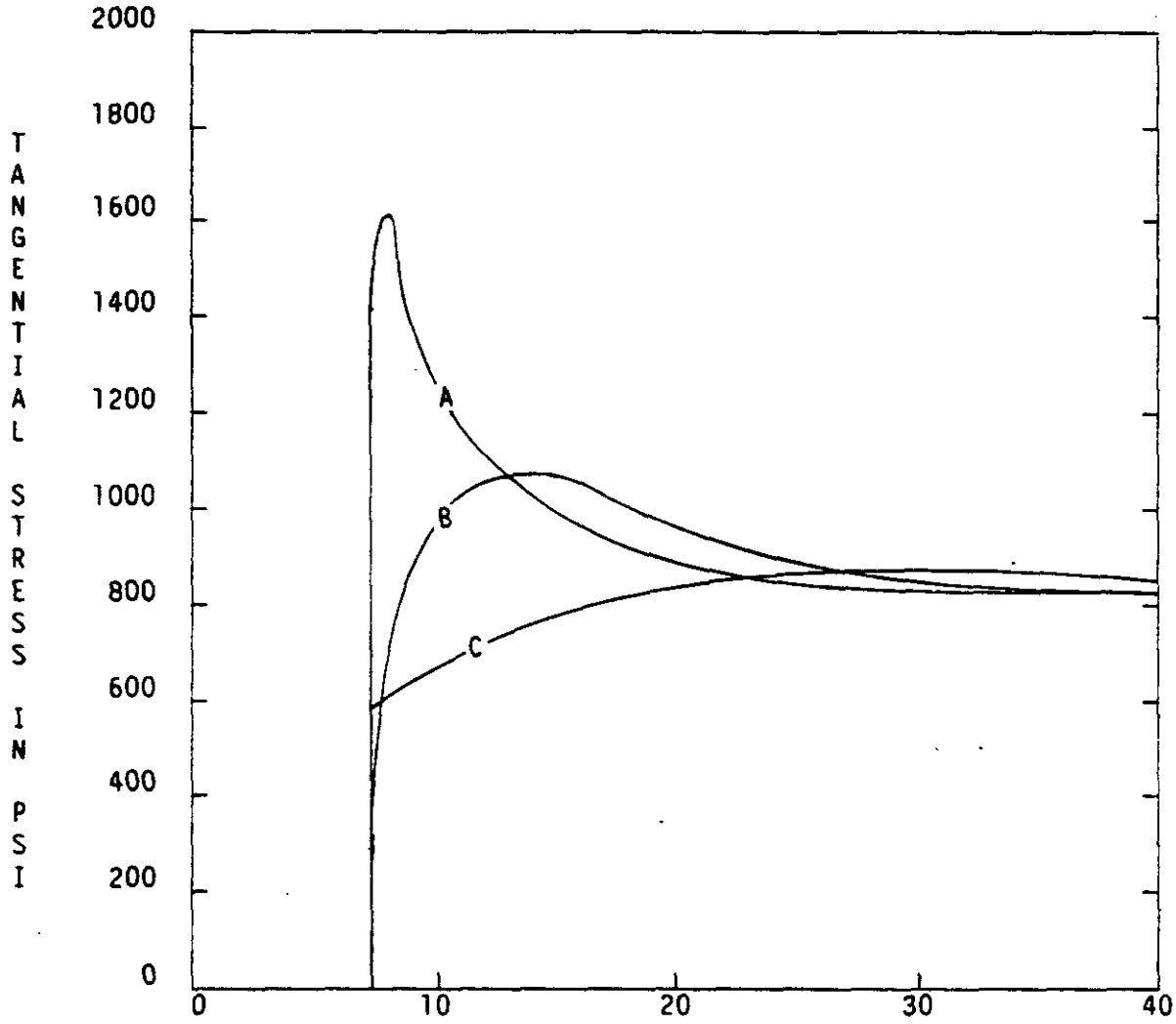

A – IMMEDIATELY AFTER EXCAVATION
B – ONE YEAR AFTER CONCRETE PLACEMENT
C – 25 YEARS AFTER CONCRETE PLACEMENT

Figure 7-19

C & SH SHAFT KEY
TANGENTIAL STRESS DISTRIBUTION

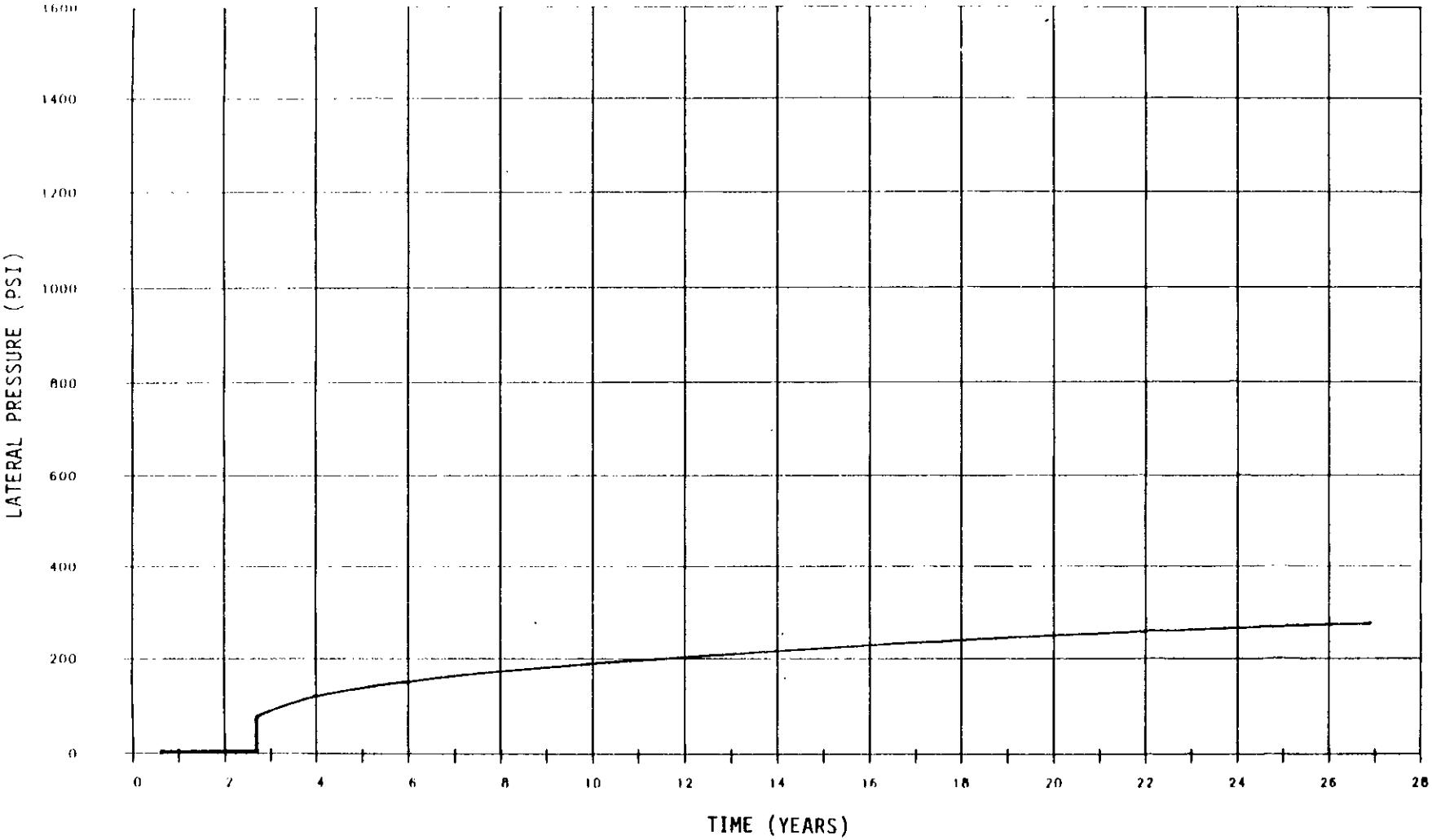

Figure 7-20

C & SH SHAFT KEY
LATERAL PRESSURE PREDICTION

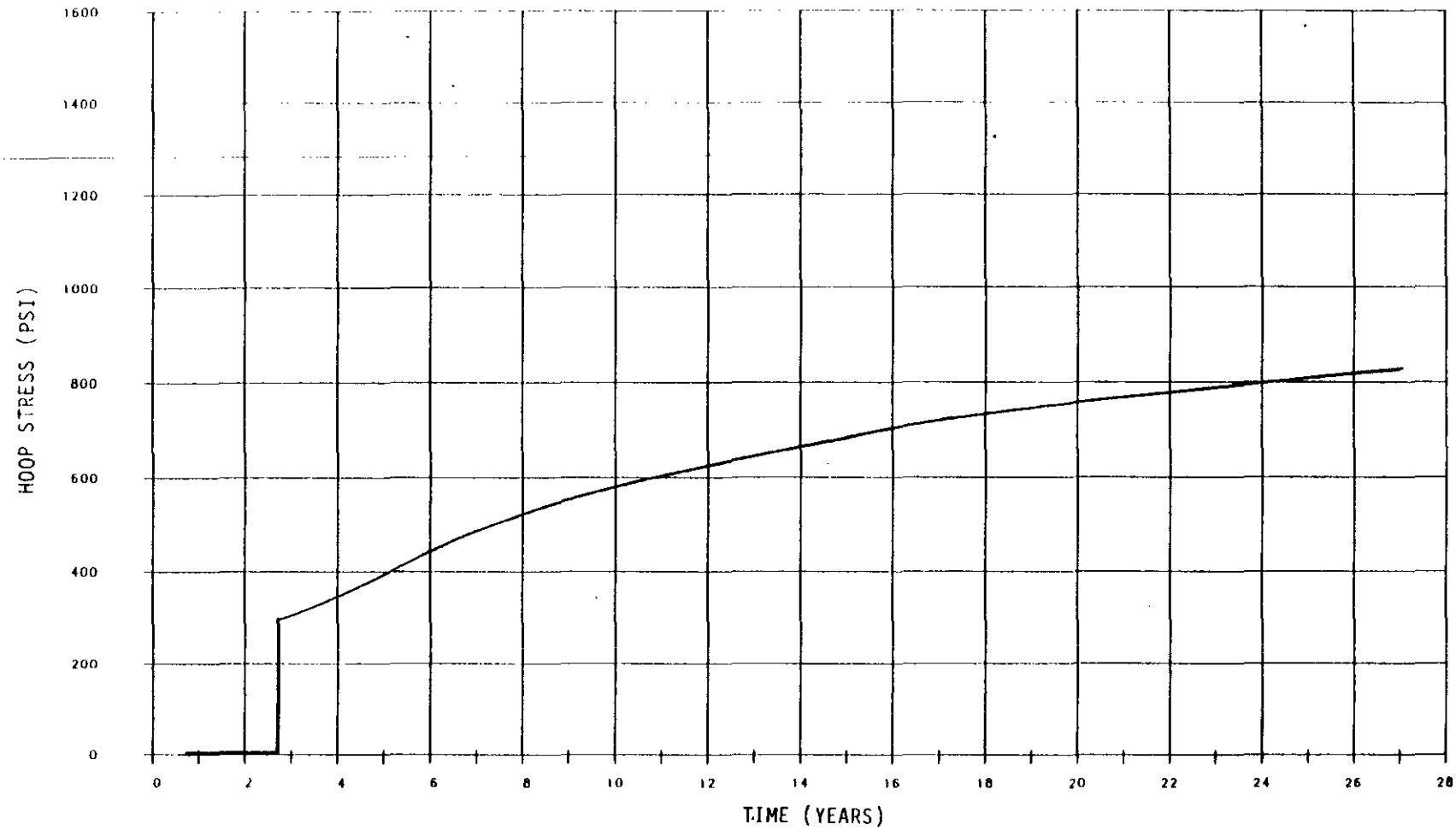

Figure 7-21

C & SH SHAFT KEY
HOOP STRESS PREDICTION

The average diametric closure of the key at 27 years is expected to be about 0.1 inch with a maximum value of 0.175 inch, or about half the predicted value for the salt in the unlined section immediately below the key (Figure 7-22). The average diametric closure of the unlined section immediately below the key at 27 years varies from 0.03 inch for the anhydrite bed to 0.38 inch for the argillaceous halite layer. Figure 7-23 shows the diametric closure predictions for both the concrete key and the salt in the adjacent shaft wall.

7.3.3.3 Unlined Section

Extrapolation of In Situ Responses. Convergence point measurements are too few to be used for the extrapolation of future in situ responses in the unlined section of the shaft. Thus, the readings of collar movements of multiple-point borehole extensometers must be used for this extrapolation. Because the extensometer collars are recessed 1 foot into the wall, and the readings are referenced to the deepest anchor which is also moving, extrapolation of collar movement will not produce an exact estimate of the movement of the shaft surface.

The maximum collar movement occurs at multiple-point borehole extensometer 37X-GE-00208 at a depth of 2,057 feet (elev. 1353 feet) (Figure 7-3). As discussed earlier, and as shown on Figure 7-9, the collar movement is affected by seasonal temperature fluctuations. However, if we consider only the later portion of the curve, its slope is approximately 0.125 inch/year between June 1984 and June 1985. Assuming this rate to be constant for another 22 years, the additional radial movement of the collar will be nearly 3 inches. Thus, the effective diameter of the unlined shaft will be reduced by nearly 6 inches.

Replication of In Situ Responses. Figures 7-24 and 7-25 show the radial and tangential stress distributions relative to the overburden stress at different times. Figure 7-24 indicates that the zone where radial stresses are affected increases in size with time while Figure 7-25 indicates that tangential stresses are only affected within an approximately constant radius of 60 feet.

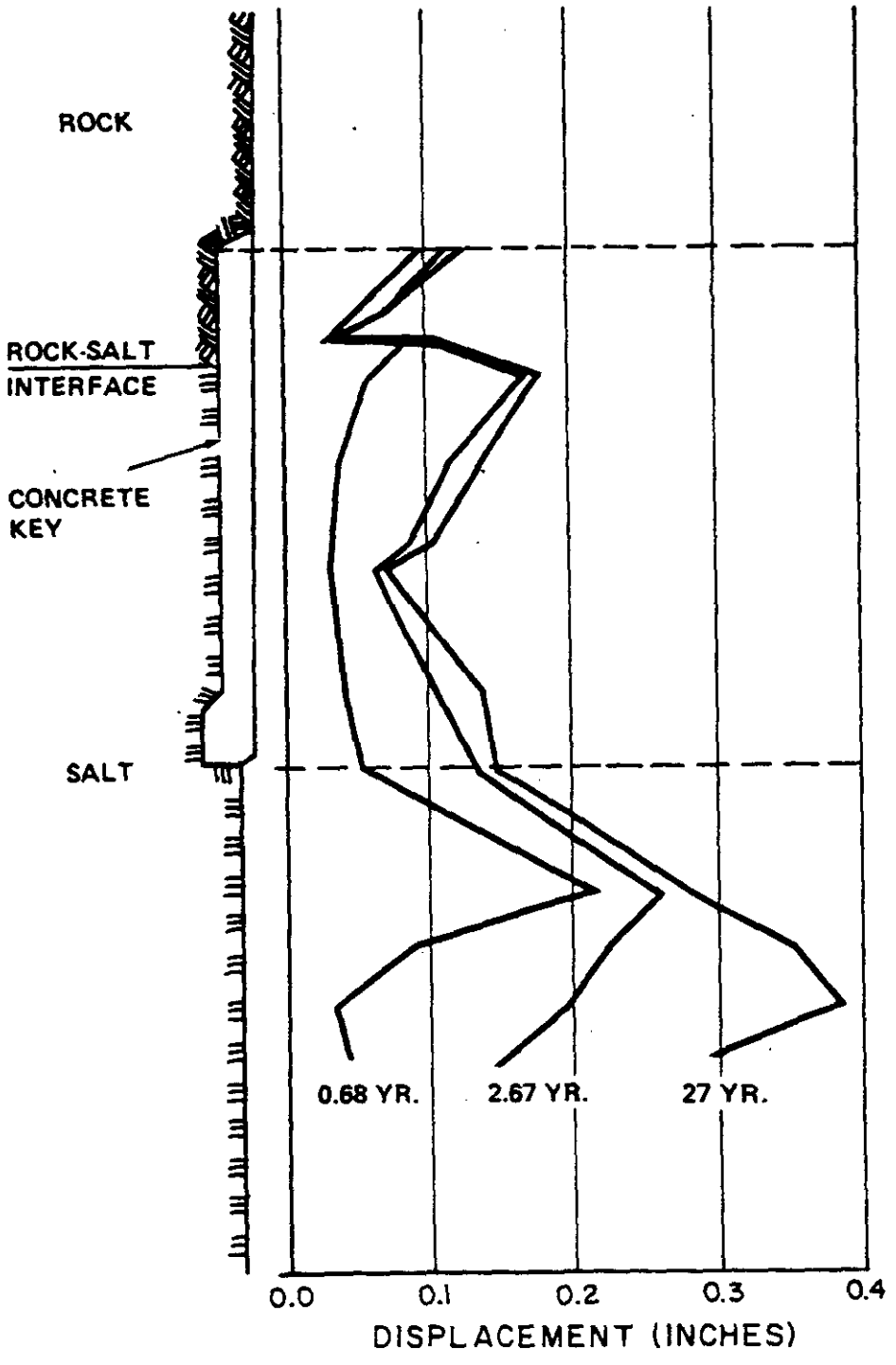

Figure 7-22

C & SH SHAFT KEY
DIAMETRIC CLOSURE

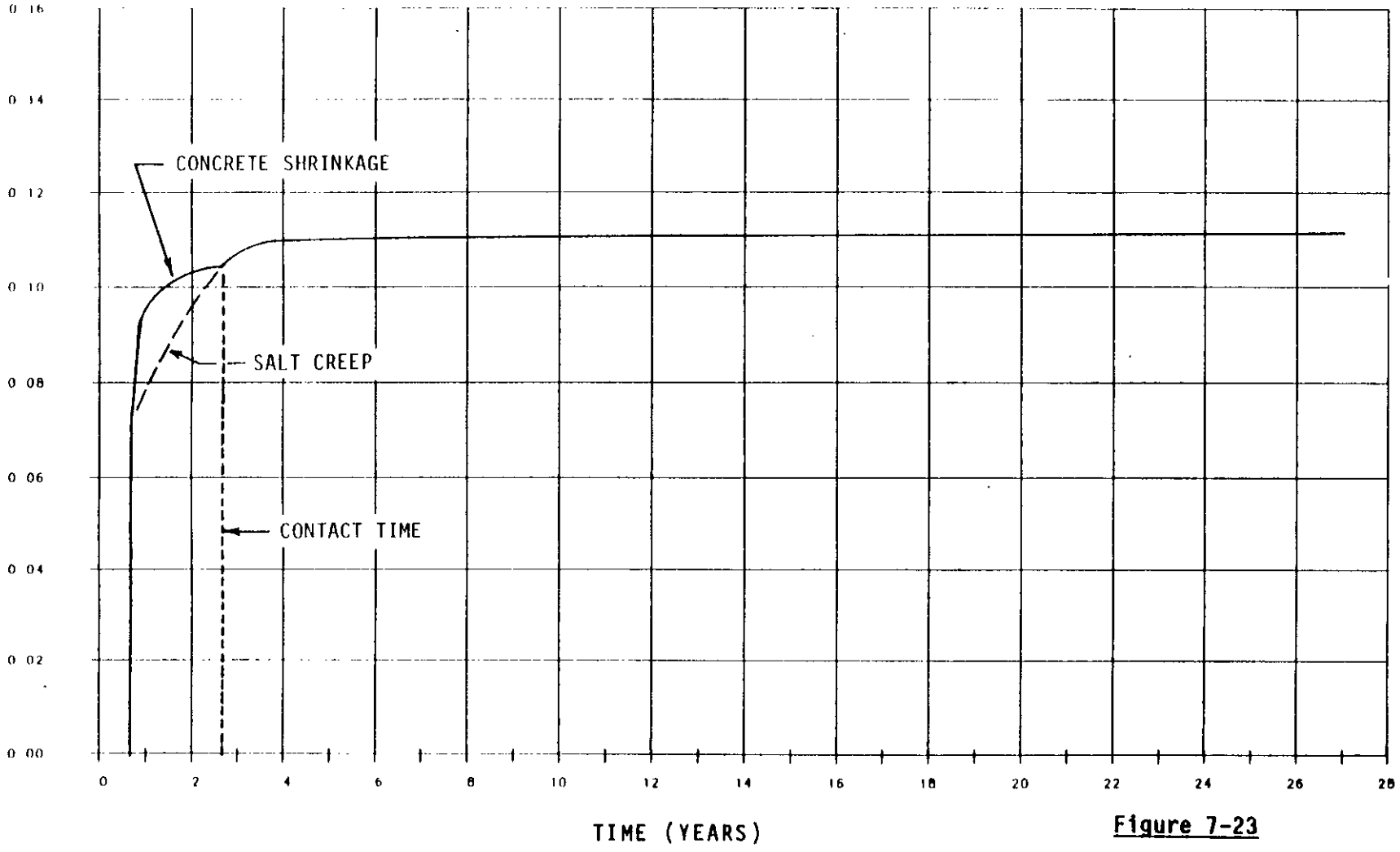

Figure 7-23

C & SH SHAFT KEY
DIAMETRIC CLOSURE PREDICTION

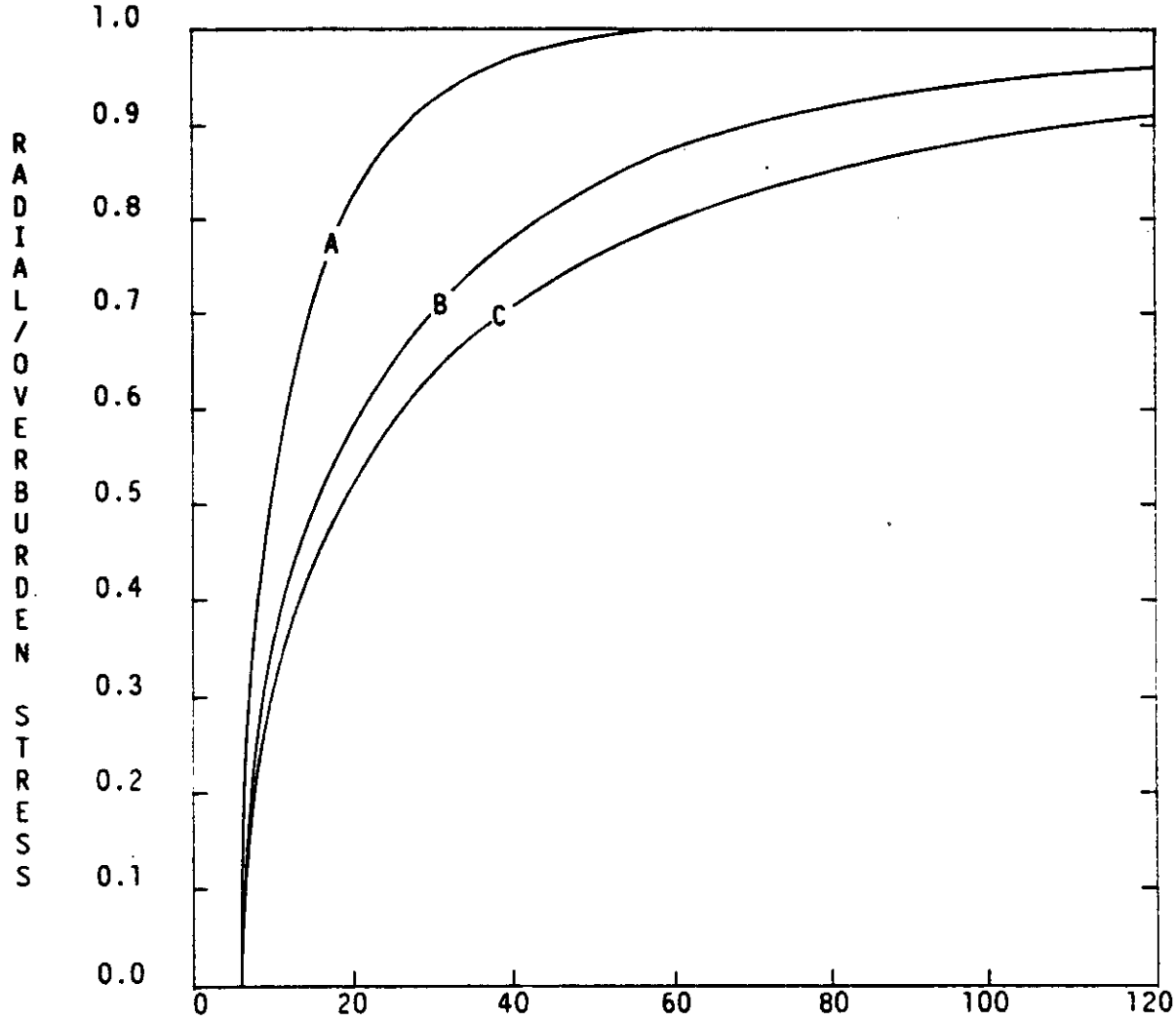

A – IMMEDIATELY AFTER EXCAVATION
B – ONE YEAR AFTER EXCAVATION
C – 15 YEARS AFTER EXCAVATION

Figure 7-24

C & SH SHAFT UNLINED SECTION
RADIAL STRESS DISTRIBUTION AT ELEVATION 1353

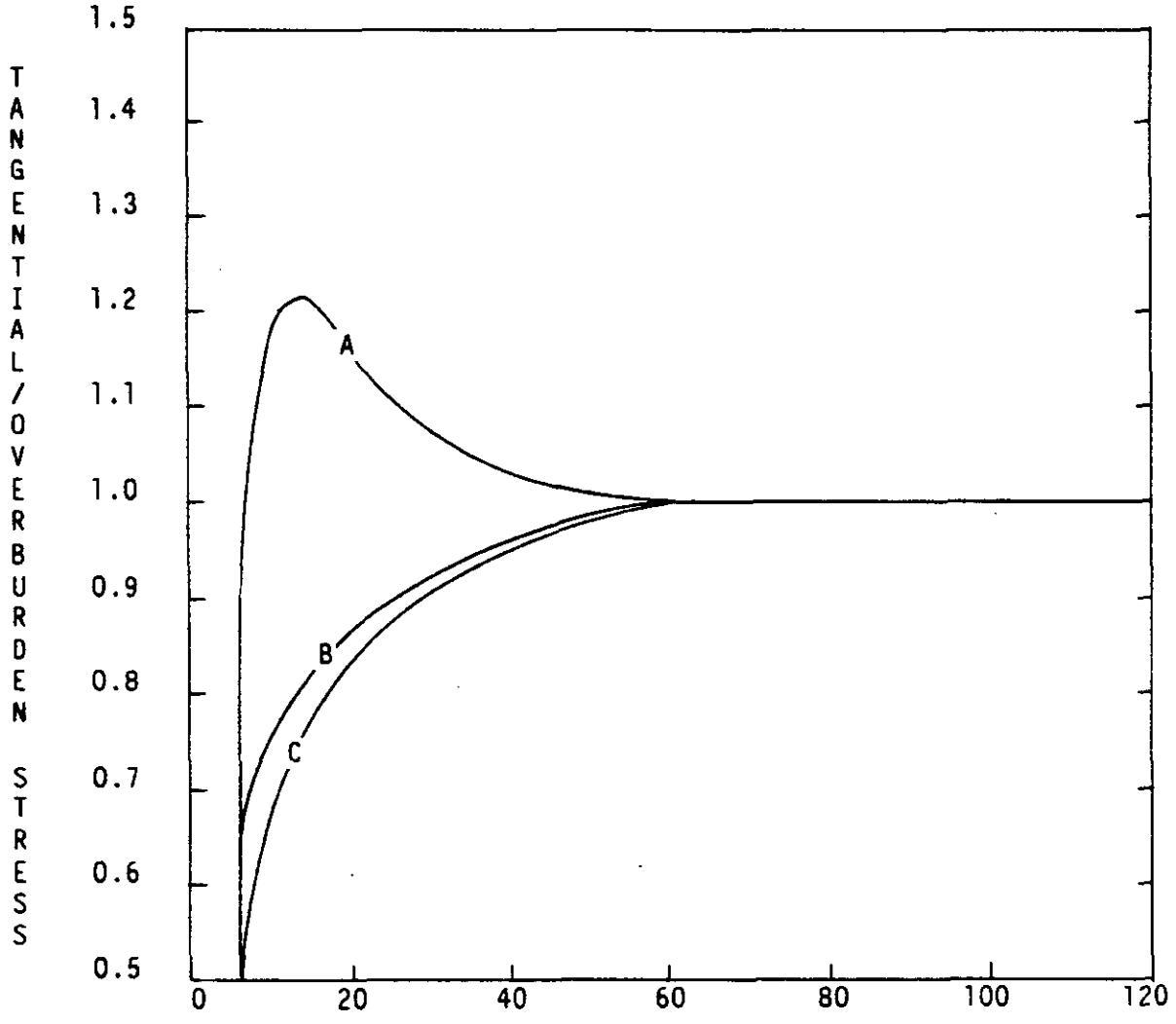

A – IMMEDIATELY AFTER EXCAVATION
B – ONE YEAR AFTER EXCAVATION
C – 15 YEARS AFTER EXCAVATION

Figure 7-25

C & SH SHAFT UNLINED SECTION
TANGENTIAL STRESS DISTRIBUTION AT ELEVATION 1353

Figure 7-26 shows the ratio of radial displacements at various distances from the shaft centerline relative to the radial displacement of the shaft wall at different times. Based on this figure, the ratio of the displacements between each extensometer anchor point and the shaft wall can be determined. This figure indicates that the extensometer collar readings relative to the deepest anchor will reach about 84 percent of the actual radial displacement of the shaft wall 15 years after excavation.

Figure 7-27 illustrates the effective creep strain distribution in the shaft at a depth of 2,057 feet (elev. 1353 feet) at selected times after excavation. The magnitude of effective strain at the shaft wall at 15 years approaches a value of approximately 0.03.

Figure 7-28 shows diametric closure versus depth at different times. The response curves are drawn relative to the time the initial instrument readings were made. The response indicated by the curve to the left of the vertical axis corresponds to the computed response which took place between excavation and the initial instrument reading. The relative response between October 1982 and June 1984 is correct regardless of the time offset. Varying the time offset in effect shifts the position of all other response curves relative to the vertical axis. The diametric closure prediction at a depth of 2,057 feet is shown on Figure 7-29.

7.3.3.4 Shaft Station

Figure 7-15 shows that, for roof extensometer 51X-GE-00251 in the C & SH shaft station, the relative movement between the collar and anchor A, expressed as a percentage of the collar reading, has remained practically constant for the last 2 years. Thus, provided that no failure of the mechanical-anchor rock bolts occurs, the closure rate of the roof is expected to stabilize. It is assumed that no new excavation will occur close to the station. If additional excavation is performed, the rate of closure between the roof and floor and between the walls may be accelerated.

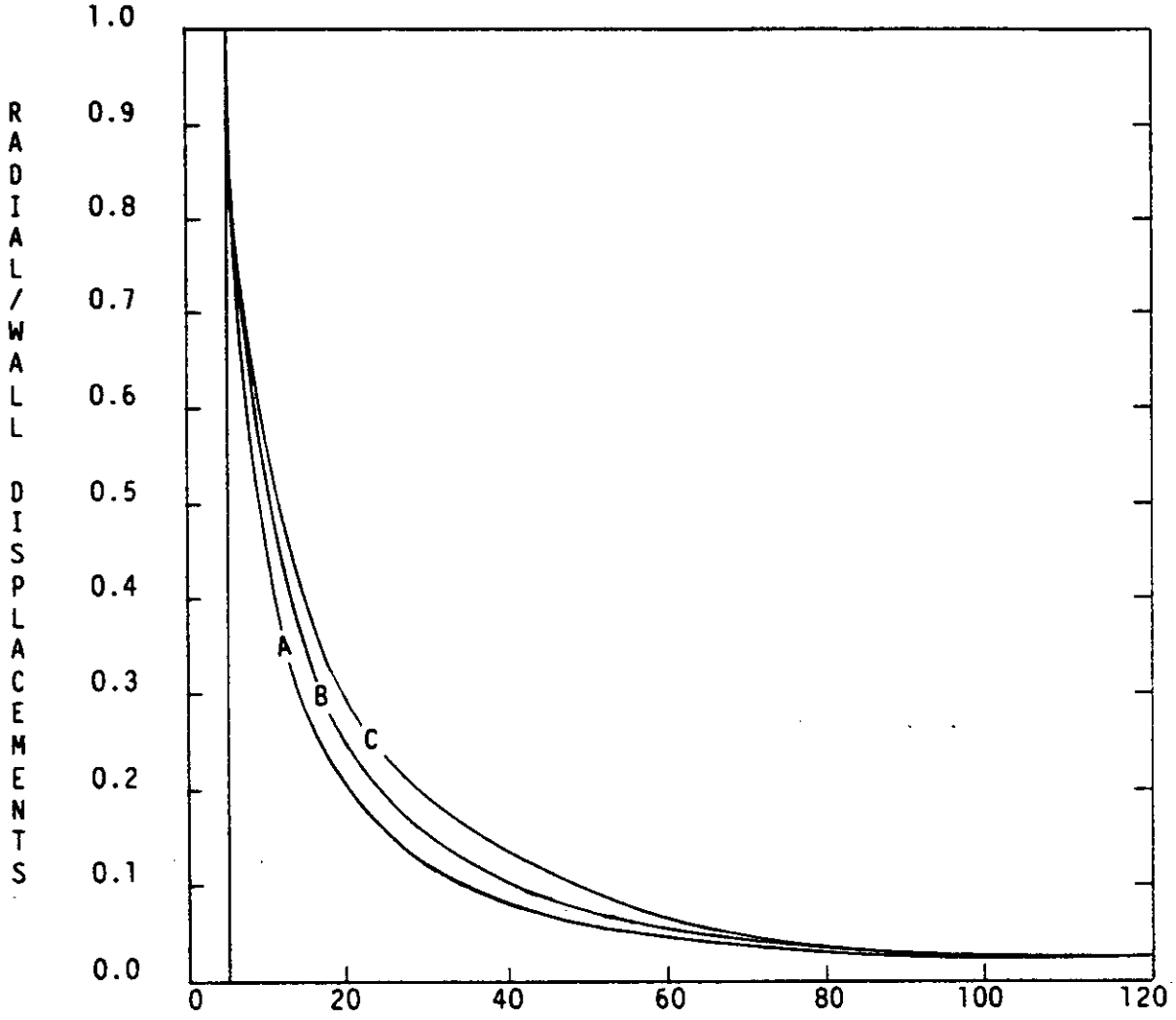

A – IMMEDIATELY AFTER EXCAVATION
B – ONE YEAR AFTER EXCAVATION
C – 15 YEARS AFTER EXCAVATION

Figure 7-26

C & SH SHAFT UNLINED SECTION
RADIAL DISPLACEMENT DISTRIBUTION AT ELEVATION 1353

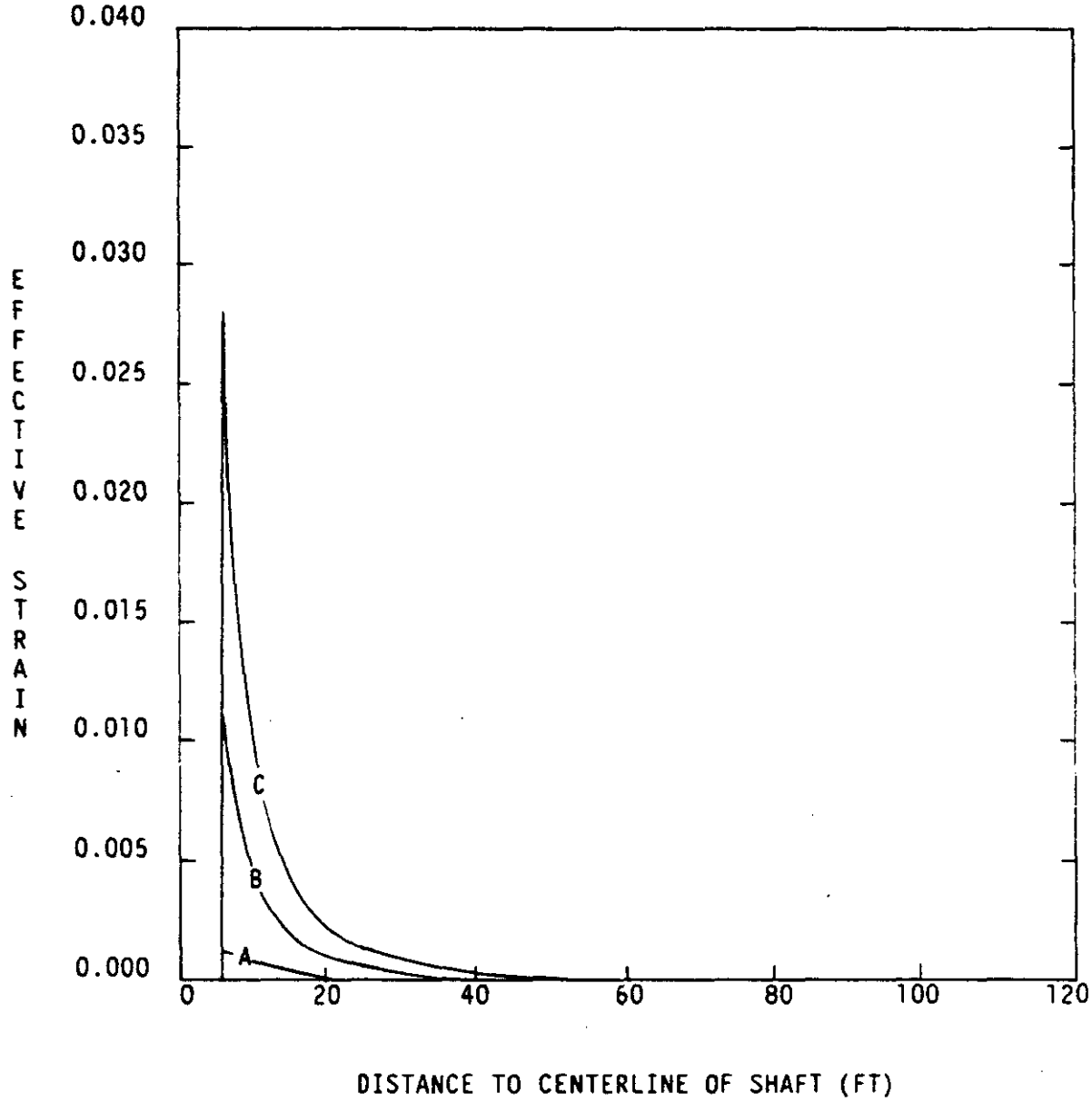

A – IMMEDIATELY AFTER EXCAVATION
B – ONE YEAR AFTER EXCAVATION
C – 15 YEARS AFTER EXCAVATION

Figure 7-27

C & SH SHAFT UNLINED SECTION
EFFECTIVE CREEP STRAIN DISTRIBUTION AT ELEVATION 1353

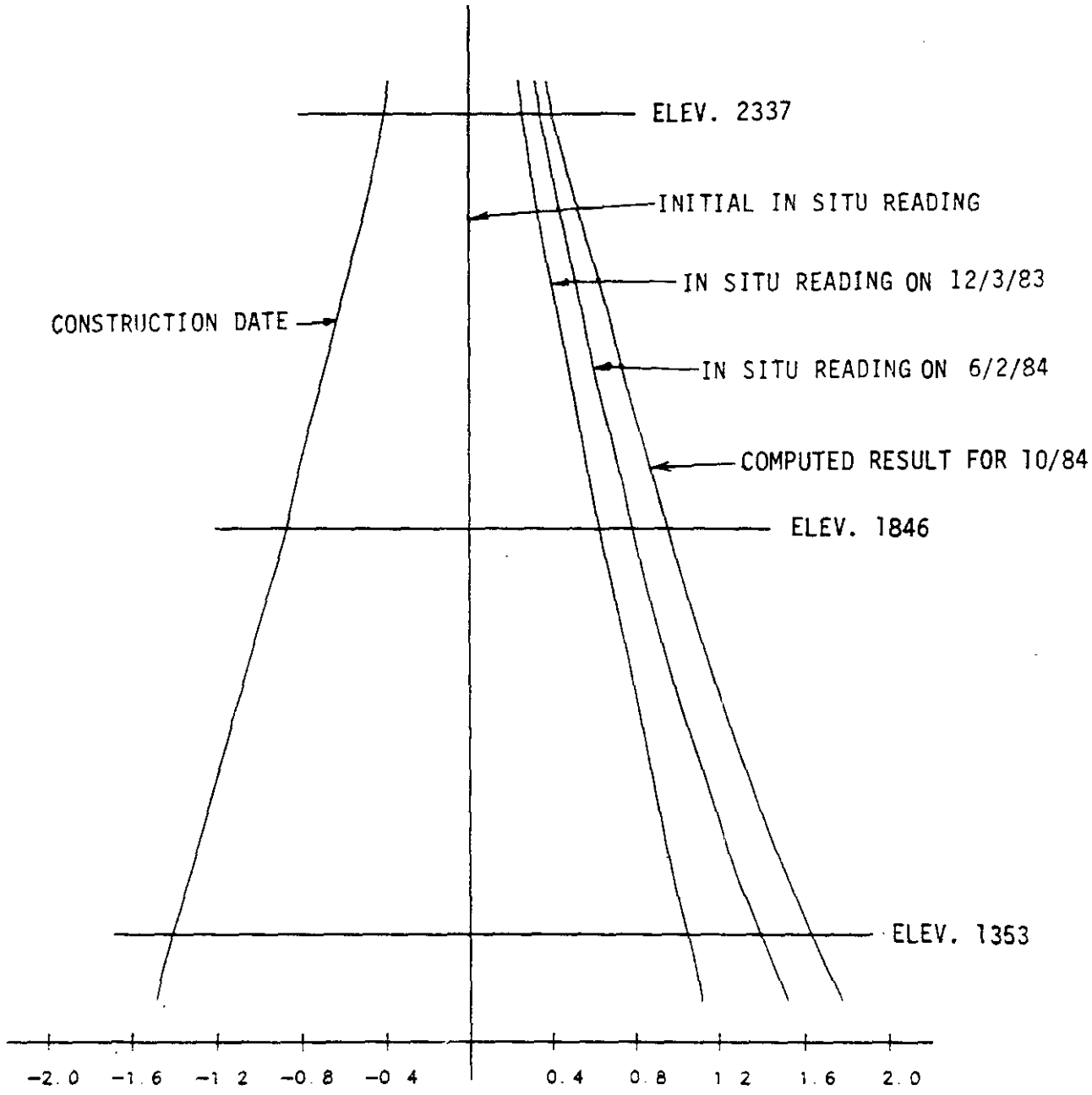

Figure 7-28

C & SH SHAFT UNLINED SECTION
RELATIVE DIAMETRIC CLOSURE

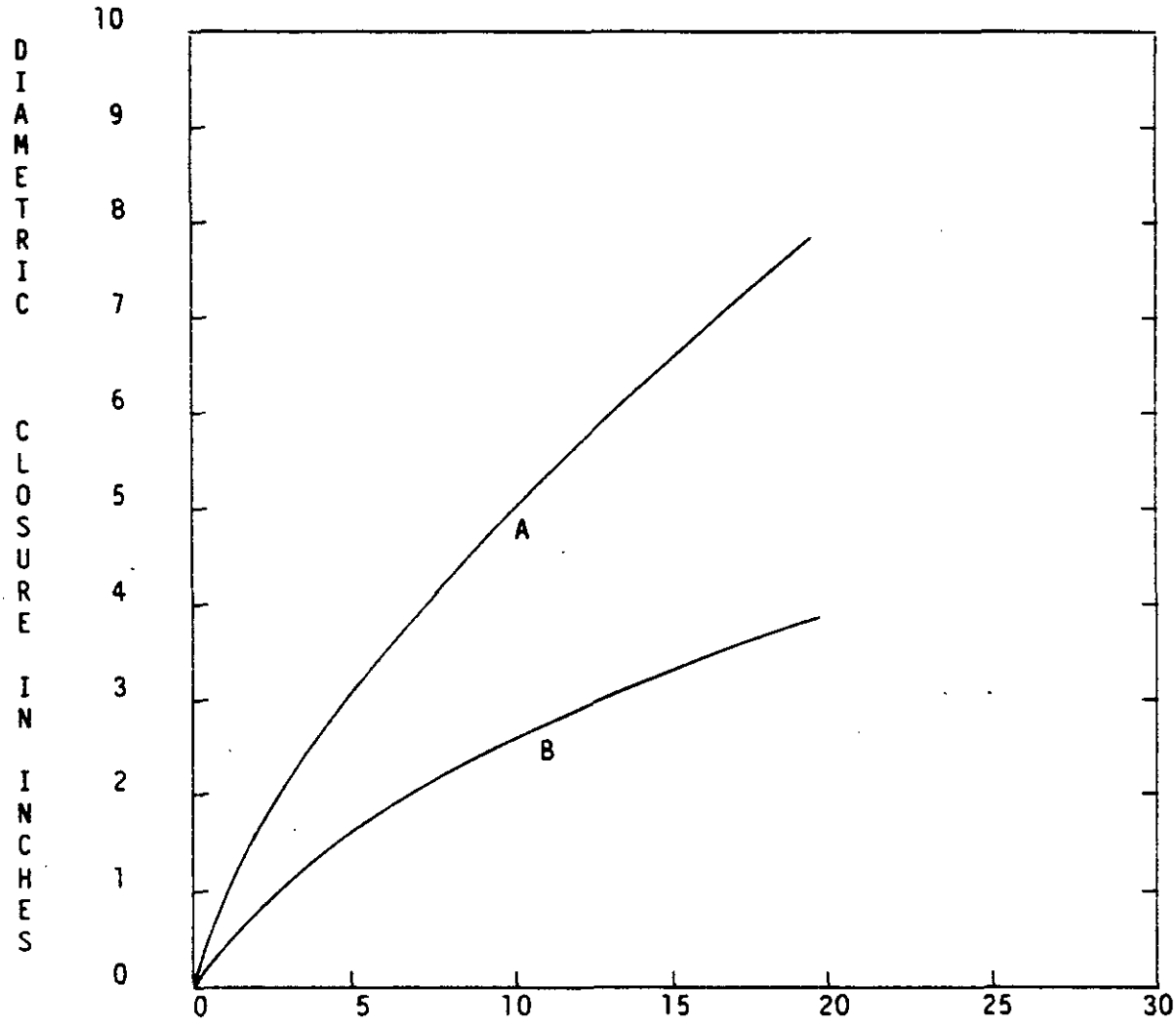

A – NORTH 17°40' WEST- MAJOR AXIS
B – NORTH 72°20' EAST- MINOR AXIS

Figure 7-29

C & SH SHAFT UNLINED SECTION
CLOSURE PREDICTION AT ELEVATION 1353

The rock bolts and wire mesh in the station roof will control spalling and stabilize the roof to provide a safe working environment but will not control salt creep. Although separations and fracturing have developed in the salt surrounding the shaft station, they exist on a much smaller scale than those observed in Test Room 3. They are expected to continue to develop throughout the operating life of the facility.

The total measured roof-to-floor closure in the C & SH shaft station was approximately 10 inches on September 16, 1985, nearly 3 1/4 years after the completion of excavation. The measured wall-to-wall closure over the same period was about 6 inches. Actual closure values are higher because the initial readings were taken nearly 260 days after the station was excavated. The average rate of roof-to-floor closure over the measurement period is approximately 3.89 inches/year. Assuming this rate will be constant throughout the operating life of 25 years, an additional roof-to-floor closure of about 8 feet is expected. Since the wall-to-wall closure is approximately 60 percent of the roof-to-floor closure, the additional wall-to-wall closure is expected to be nearly 5 feet.

7.4 CONCLUSIONS AND RECOMMENDATIONS

Design validation requires a determination of the compatibility of the design criteria, design bases and design configurations used in the reference design. Therefore, the following conclusions and recommendations address those criteria identified as applicable to the C & SH shaft in Chapter 2, Table 2-1, and the design basis elements presented in this chapter, Table 7-1. Other conclusions and recommendations that are a product of the design validation process are also presented.

7.4.1 Conclusions

Validation of the C & SH shaft reference design is based on a comparison of the applicable elements contained in the Design Criteria

and Design Bases documents with in situ conditions. These documents contain the requirements that the C & SH shaft must meet in terms of shaft stability, deformation, water pressure, water control, and shaft station stability and deformation.

Observations made during shaft inspections have not detected any signs of deterioration or instability. Due to its design pressure capacity, the liner is expected to remain stable even if the water pressure exceeds the design hydrostatic pressure.

The design basis assumption that the hydrostatic pressure begins 250 feet below the ground surface is suitable. Piezometer measurements indicate that the hydrostatic pressure is currently much less than the design basis pressure. These measurements are of sufficient accuracy to indicate that an anomalously high hydrostatic condition does not exist.

The design basis requirement that the key be designed to resist lateral pressure from the salt equal to 75 percent of the overburden pressure, approximately 640 psi, is suitable. The shaft key analysis indicates that the lateral pressure on the key at the end of 25 years will be approximately 275 psi. The lateral pressure capacity of the key is 833 psi. This provides for a factor of safety of about three. The analysis further shows that the maximum diametric closure expected for the key at the end of the operating period is only 0.175 inch. If the plastic flow or creep properties of the concrete were included in the analysis, the results would indicate that the design pressure would not be reached until after the 25-year operating life of the facility.

Based on the computed vertical, horizontal and effective stresses in the unlined section, the magnitude of stresses immediately adjacent to the opening decreases with time as the stress arch around the opening migrates away. The maximum stress occurs immediately after excavation and is followed by relaxation due to creep behavior. The stresses will, therefore, not cause a future stability problem in the unlined section of the C & SH shaft.

The analyses show the locations of effective creep strain concentrations in the unlined section of the shaft at different times. It is predicted that the maximum effective creep strain will not exceed 0.05 at the end of the operating life of the shaft. Based on the effective creep strain limit discussed in Chapter 6, the structural stability of the C & SH shaft will remain within required safety limits during its operating life.

The analyses also predict that the diametric closure near the bottom of the shaft at the end of its operating life will be approximately 10 inches along the major axis of principal strain, approximately 18 degrees from the longitudinal direction of the shaft tubular steel supports (buntons). Based on the predicted deformations and closures, the unlined section of the shaft will meet the requirements stated in the design criteria. The diameter of approximately 12 feet in the unlined section will allow for salt creep over the operating life, as required by the design bases. However, based on the design configuration of the C & SH shaft, the connections at both ends of some buntons do not provide sufficient allowance for longitudinal adjustment.

The C & SH shaft reference design complies with the criteria that require control of ground-water flow. This conclusion is made despite the fact that considerable instrumentation damage has been caused by water flow. This water has seeped into the shaft through holes cut in the liner for piezometer installation or is a result of direct rainfall. The piezometer leakage problem has been addressed and will receive additional corrective attention during a future shaft renovation. The rainwater does not reach the facility level in any significant or measureable quantity.

The chemical water seal just below the key piezometers is probably breached. The lowest water seal in the key is functioning properly. The water draining from the telltale drains has a local source. Therefore, it is concluded that there is no solutioning of the salt behind the key.

The C & SH shaft station exhibits the highest degree of deterioration in the underground facility. This is considered to be the result of the effects of blasting for initial excavation of the station. The station roof has been stabilized by rock bolting and no further significant deterioration is expected. However, removal of the 3-foot thick salt beam between the roof and clay G may be required for safety reasons in the future. Closure will continue at a rate of 3.89 inches/year vertically and 2.33 inches/year horizontally. Total closure after 25 years will be on the order of 8 feet vertically and 5 feet horizontally. This closure will require that the station roof or floor, and walls be trimmed periodically to maintain the design dimensions.

Separation and fracturing in the salt is expected to continue in the station roof and beneath the floor. Both closure and fracturing in the station will necessitate periodic maintenance during its operating life in order to maintain safety as well as the required clearances for equipment and operations.

The reference design for the C & SH shaft is validated based on the preceding discussions. The reference design complies with the design criteria and design bases. Except for instrument repair and maintenance, no modifications are required to the shaft reference design. The C & SH shaft will perform its functions as required during the operating life of the facility.

7.4.2 Recommendations

Based on the results of design validation, the following recommendations are made with respect to the C & SH shaft:

(1) Water behind the shaft key is undesirable and should be monitored carefully. If the volume of water behind the key increases, or if water starts flowing from beneath the key, past the lower water seal, it may become necessary to inject grout above the top water seal in the key. Grout should not

be placed behind the key (below the top seal) unless absolutely necessary. If this cannot be avoided, the grout must be a chemical gel (or other non-rigid grout) and must be compatible with both the existing water seal material and with the Plugging and Sealing Program requirements.

(2) Based on the results of design validation of the C & SH shaft, it is recommended that, during inspection of the shaft furnishings, the bunton connections should be inspected for closure allowance. If the allowance is insufficient, corrective action should be taken to provide for additional closure.

(3) The observation holes drilled in the roof of the shaft station to monitor displacements and separations, and in the floor to monitor fracturing, should be maintained. Continued observations of conditions in these holes will be valuable in assessing the safety and stability of the station.

CHAPTER 8
WASTE SHAFT

8.1 INTRODUCTION

The waste shaft provides the connection between the surface waste handling facilities and the underground storage level. A discussion of shaft construction was presented in Chapter 3 and geologic characterization of the shaft stratigraphy was presented in Chapter 6. This chapter presents discussions of the design criteria and design bases pertaining to the waste shaft. It documents the collection of waste shaft geotechnical data, its analysis and evaluation, and presents predictions of future shaft behavior. Conclusions and recommendations are presented based on a comparison of the results of the design validation process with the shaft reference design.

8.2 DESIGN

This section presents the design criteria and design bases used to develop the reference design for the waste shaft. The design configuration of the shaft is discussed in Chapter 3, subsection 3.3.2.

8.2.1 Design Criteria

The design criteria for the waste shaft are the same as those for the C & SH shaft. The criteria requiring validation are indicated in the listing of abridged criteria presented in Chapter 2, Table 2-1, and are discussed in Chapter 7.

The design criteria requiring evaluation for design validation of the waste shaft are:

(1) shaft shall be designed to be structurally stable;

(2) shaft shall be designed to accommodate salt creep;

(3) ground-water flow into the shaft shall be controlled;

(4) underground openings (i.e. waste shaft station) shall be designed to accommodate deformation; and

(5) underground openings shall be stable.

8.2.2 Design Bases

The Design Basis, Waste Shaft (ref. 2-15) was the primary document used as a guide for waste shaft design. The major elements of this basis are summarized in this subsection. Only a few of these elements must be evaluated or have a direct impact on design validation. These particular elements are presented in Table 8-1.

The design bases specify that the waste shaft shall be designed to transport personnel, materials and radioactive waste. It shall also serve as an intake shaft for a small volume of air during normal operations and as an escape route during emergency operations.

The shaft shall be lined with unreinforced concrete from the bottom of its collar in the waste handling building to the top of the shaft key at the rock/salt interface. The liner shall be permanent and shall protect against spalling, fallout and deterioration of the rock in the shaft wall. It shall also prevent water seepage into the shaft.

The shaft liner shall be designed in compliance with applicable ACI Codes. A load factor of 1.4 shall be used for designing the concrete liner. The specified concrete compressive strength shall be 5,000 psi. No lateral rock pressure shall be assumed for design of the shaft liner. Hydrostatic pressure shall be considered to start at 250 feet below the ground surface and extend to the rock/salt interface at the top of the key. The water pressure shall be considered to increase 0.437 pounds per square inch (psi) for each foot of depth.

At water-bearing zones, the shaft shall be enlarged and liner plate installed to provide pressure relief and drainage space behind the liner during concrete placement and curing. Drainage pipes and

Table 8-1

VALIDATION ELEMENTS OF WASTE SHAFT DESIGN BASES

(1)	Shaft liner Hydrostatic pressure is considered to start at 250 feet below the ground surface and extend to the top of the key.
(2)	Shaft key Design lateral pressure shall be 50 percent of the vertical pressure due to soil, rock and salt overburden.
(3)	Unlined section Provide 20-foot diameter to allow for future salt creep deformation.

temporary hoses shall be installed to control water inflow prior to placement of the concrete liner. When the concrete liner has attained adequate strength, the area behind the liner plate shall be grouted to preclude deterioration of the dolomite and mudstone in the water-bearing zones.

The shaft key at the bottom of the concrete liner shall be constructed of reinforced concrete keyed into the rock and salt strata. A chemical water seal shall be placed behind the top and bottom of the key to prevent the migration of water. After the completion of shaft excavation and construction of the concrete liner and key, permanent piping from water collection rings to the shaft station shall be installed. Water from the collection rings shall be piped to a tank in the shaft station and then transported to the surface. The piping shall include inspection and clean-out fittings. Inspection and cleaning of the water collection rings and drainage piping shall be performed as necessary.

A load factor of 1.7 shall be applied to the design loading used for the concrete in the shaft key. The key shall be designed to resist lateral pressure generated by salt creep. The design lateral pressure shall be 50 percent of the total vertical pressure due to the soil, rock and salt overburden.

Below the key, the shaft shall be excavated 20 feet in diameter to allow for future salt creep deformation. Rock bolts and wire mesh shall be installed in this unlined section of the shaft in order to provide a structurally stable salt surface.

A shaft station shall be excavated at the storage level. The shaft shall extend below the storage level to such a depth as required by the hoisting equipment and sump. The use of rock bolts and wire mesh shall be dictated by the condition of excavated surfaces as well as code requirements. The roof, walls and floor shall be checked periodically for loose salt in accordance with applicable codes. The tolerance for

excavation of roof, floor and wall surfaces shall be no greater than plus 6 inches. In no case shall the finished cross section dimensions be less than the design dimensions.

Geomechanical instruments shall be installed to measure water pressure behind the shaft liner, salt creep pressure behind the key, and radial convergence in the unlined section of the shaft. The types of instruments installed shall be piezometers, pressure cells, radial convergence points and extensometers.

The shaft, including the liner, key, unlined section, station and furnishings, shall be inspected at 1 month intervals, or as required by applicable codes, to detect cracking, corrosion, deterioration and water intrusion.

8.3 DESIGN VALIDATION PROCESS

The design validation process for the waste shaft consists of analytical calculations, finite element modeling, and the analysis of data collected from geomechanical instruments installed in the C & SH and waste shafts. The in situ material parameters of salt determined from C & SH shaft instrumentation data were used to analyze the closure behavior of the waste shaft. For the shaft station, the in situ measurement data obtained from the C & SH shaft station were used to predict future closure behavior. The following subsections present information pertaining to validation of the waste shaft reference design.

8.3.1 Data Collection

Data collection in the waste shaft has consisted of geologic mapping, visual observations and geomechanical instrumentation measurements. Data obtained from the geologic mapping were presented in Chapter 6. The following subsections discuss the field observations and the geomechanical instrumentation in the shaft.

8.3.1.1 Field Observations

Waste shaft inspections have been concerned primarily with water seepage through the concrete liner, salt incrustation on the surface of the liner, dissolution in the shaft sump and the results of the liner grouting program.

Water seepage through the waste shaft liner has occurred since construction. As discussed in Chapter 3, subsection 3.4.2, grouting during construction behind the steel liner plate at both the Magenta and Culebra members did not completely prevent water from entering the shaft. It was estimated that the total water seepage through the liner was approximately 0.5 gallons per minute (gpm). A remedial grouting program (ref. 3-3), conducted from August 11 through August 25, 1984, reduced the seepage to about 0.015 gpm as measured in October 1984. Subsequent inspections in February and June 1985 determined that fresh water had begun seeping through cracks and construction joints in the liner from zones within and above the grouted area. The highest level of water seepage was occurring at a depth of only 60 feet below the shaft collar. Because this is higher than the potentiometric surface of ground water in the Magenta and Culebra members, the source of the seepage was probably rainwater and construction water contained in the backfill around the shaft collar and in the underlying Gatuna sandstone. This is based on the fact that heavy rains in the late summer of 1984 left substantial quantities of water ponded in the waste-handling building excavations and in the remnant of the SPDV ventilation shaft drilling fluid reserve pit.

The initial rate of this renewed seepage could not be measured because the PVC drainpipe had been broken in several places. Subsequent repair of the drainpipe has permitted the rate of water inflow to be measured on a regular basis. The measurements are obtained by timing the flow of water from the drainpipe into a calibrated bucket. These measurements do not consider the small amount of uncontrolled "fly water" that falls down the inside of the shaft. The initial measurement, in January 1986, was 0.47 gpm. The measurements, are

plotted on Figure 8-1 and show a generally decreasing trend in the flow rate. This trend may be influenced by three factors. First, the water contained in the backfill and sandstone has slowly drained into the shaft. Second, the rate of evaporation increases as the outside air temperature increases, thus reducing the amount of water reaching the drains. Both of these conditions are temporary. A series of rainstorms could recharge the backfill and sandstone, and evaporation will decrease with cooler winter temperatures. Heavy rains in June 1986 may have been responsible for the increased flow detected by the late June reading. The third factor influencing the flow trend is the possibility that the water collection rings and the drainpipe may be partially blocked by debris. This would result in reduced water flow through the drainpipe and an increase in the amount of unmeasureable fly water.

Although there has been limited access to the waste shaft since August 1984, several inspections of the shaft and sump have been made. One inspection was made on February 21, 1985, at which time some instrumentation damage was observed. In addition, the PVC drainpipe was observed to have been broken in several locations. Appreciable salt incrustation was noted on the surface of the concrete liner and on many of the instrumentation boxes and cables. This incrustation was primarily attributed to salt dust from the underground excavation adhering to the damp shaft walls during the period since September 1984 when the waste shaft was used as an exhaust shaft. A small percentage of this salt incrustation was also attributed to water seepage through the liner.

On June 16, 1985, another inspection of the waste shaft was made to within 60 feet of the shaft station. The shaft ventilation had been changed from upcast to downcast after the February inspection. Very little salt incrustation was present on the concrete liner and only a small amount was present in places on the wire mesh. Fresh water entering the shaft through the liner, from approximately 60 feet below the collar, was running down the liner. Although much of the liner was

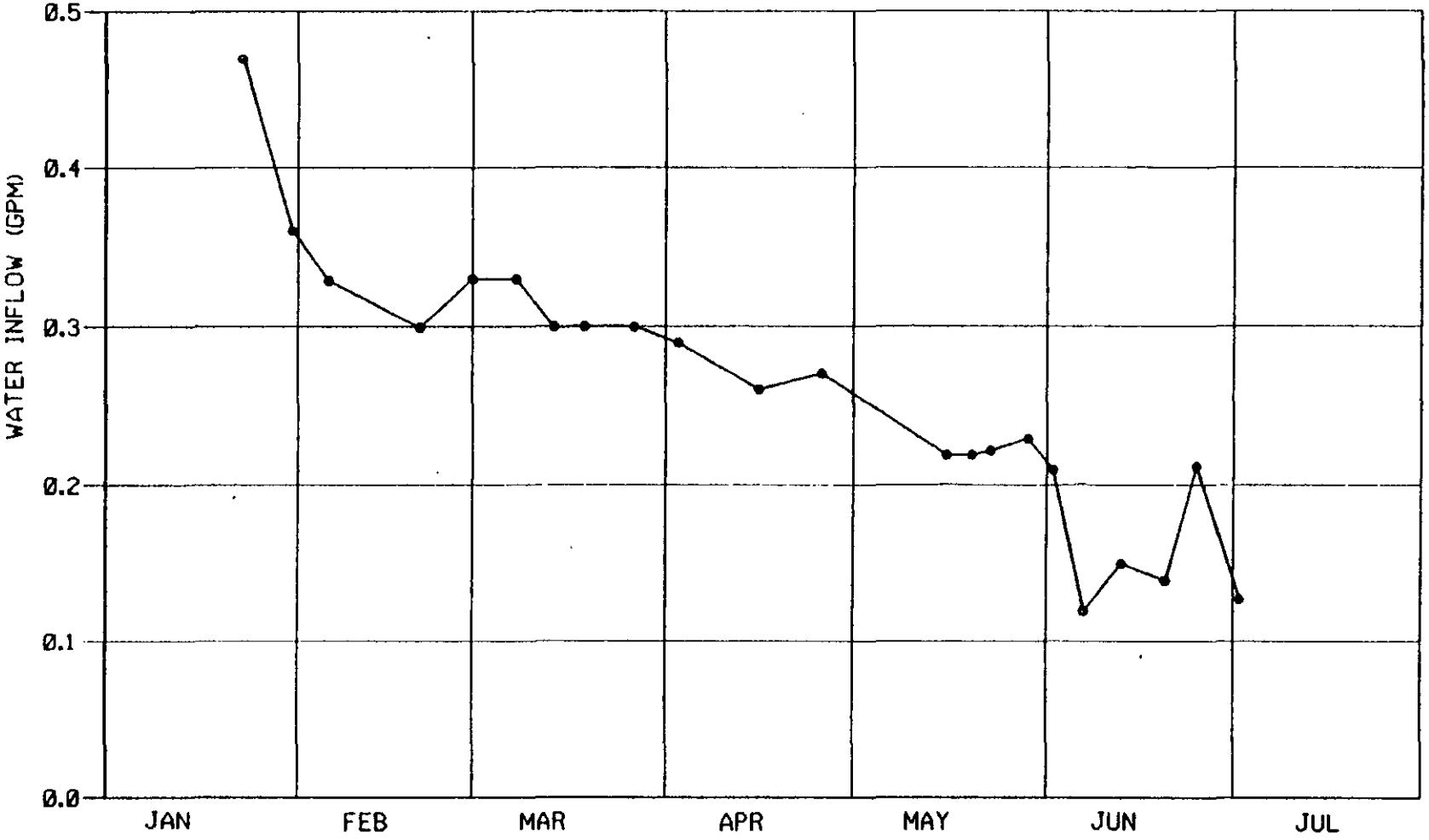

Figure 8-1

WASTE SHAFT
WATER INFLOW MEASUREMENTS

observed to be wet, the water rings were not full. This water appeared to have dissolved the salt incrustation observed in the February 1985 inspection. Cracks were common in the liner to within 60 feet of the collar. The PVC drainpipe damage had not been repaired. No water was seen draining from below the concrete key. The shaft sump contained water to within 60 feet of the shaft station floor. This water was a combination of rainwater, construction water and ground water. It was pumped out in September 1985.

On December 1, 1985, another inspection of the waste shaft was made. The PVC drainpipe was still broken or disconnected at several levels. The water rings were plugged and overflowing. There appeared to be an increase in water flow into the shaft, most noticeably at the Culebra member. An approximately 1/8- to 1/4-inch thickness of salt had been deposited on the liner below the Culebra.

On December 11, 1985, an inspection of the waste shaft sump was made. During this inspection, and a subsequent inspection on December 12, 1985, MB-139 was observed closely. The clay along the lower contact was distinct and no separations were noted. Although the upper contact could not be distinguished behind a covering of wire mesh, MB-139 could be seen quite well and appeared to be intact and undisturbed. One small fracture, approximately 2 feet long and 1/2 inch wide was observed on the west side of the shaft approximately 1 foot above the lower contact.

An anhydrite bed 61 to 66 feet below the station floor was also observed during this inspection. A zone of dissolution was present along the upper contact of this layer in the northwest to southeast half of the shaft. The dissolution occurred partially within the anhydrite bed. The maximum void width of approximately 0.7 foot occurred on the south-southwest side of the shaft and extended approximately 18 feet south into the salt. The zone of dissolution pinched out going around the shaft in either direction away from the area of maximum opening. There did not appear to be any disturbance of

the strata overlying or underlying this zone anywhere around the shaft and no voids or disturbance of the anhydrite existed on the opposite side of the shaft. The upper contact of the anhydrite with the overlying halite did not exhibit any irregularities. From the physical evidence available, it appeared that this feature was the result of localized dissolution. No dissolution of the anhydrite was observed. The dissolved material was probably a soluble evaporite mineral representing a facies change within the Salado formation. The dissolution appeared to have resulted from the previously discussed water which had been standing in the sump. The level of this water was measured at 60 feet from the shaft station floor prior to its being pumped out in September 1985. The shaft wall below the water line exhibited no significant deterioration due to the standing water. However, some sloughing of an anhydrite layer 71 to 75 feet below the shaft station floor and widening of the shaft near the bottom of the sump was evident. The shaft wall exhibited a glazed surface which probably resulted from minor dissolution of the salt surface.

A shaft inspection was conducted on July 24, 1986. The inspection team mapped the location of cracks in the concrete liner and any associated seepage. They also mapped the location of leaking construction joints. This mapping indicates that additional cracks have developed in the liner since mapping was conducted prior to the August 1984 grouting program. The shaft was found to be considerably drier than during the 1984 mapping program. Many of the new cracks mapped may have existed in 1984 but were masked by the water on the shaft walls. Also, salt precipitates now enhance the outline of the cracks. The inspection also revealed that recent construction work inside the shaft has resulted in some instrument cable and junction box damage and in breakage of the previously repaired PVC drainpipe.

The waste shaft station has shown little deterioration since it was enlarged from the SPDV ventilation shaft station dimensions. Visual surveys are performed approximately every 3 months by site geologists. The results of these inspections are documented in the GFDRs. Only

minor spalling along the station walls has occurred. Vertical fractures similar to those found in the drifts and test rooms have developed at intersection corners. The roof, although showing no visible evidence of deterioration, has been covered by wire mesh and rock bolts for safety purposes. During the July 1986 shaft inspection, some separation at clay G was observed on the east and west sides of the shaft. The separation was a maximum of 3/4 inch wide at the shaft surface and decreased away from the shaft. No separation was observed at clay H.

Minor separations and fracturing in MB-139 and in the overlying halite have been observed in the station floor. A dish-like fracture zone similar to that found in Test Room 2 is present, but has developed on a much smaller scale. Inspection of MB-139 in the shaft sump, and evidence from boreholes drilled in the station floor, show that the marker bed and the overlying halite are, for the most part, intact.

8.3.1.2 Geomechanical Instrumentation

The waste shaft geomechanical instrumentation is similar in design to that of the C & SH shaft. The shaft contains 12 vibrating-wire piezometers, 4 pressure cells, 9 multiple-point borehole extensometers, and 3 sets of radial convergence points. Figure 8-2 shows the instrument locations in the waste shaft and Figure 8-3 shows details of the key instrumentation.

As in the C & SH shaft, all of the geomechanical instruments, except the convergence points, are monitored remotely. The instruments are connected to the surface datalogger that polls all of the remotely-read underground instruments on a scheduled basis.

The 12 piezometers were installed on September 7 and 8, 1984, after the 6-foot diameter SPDV ventilation shaft had been enlarged to become the 20-foot to 23-foot diameter waste shaft. The water that could exert pressure on the liner is expected to come from the two water-bearing members in the Rustler formation. The Magenta dolomite member occurs

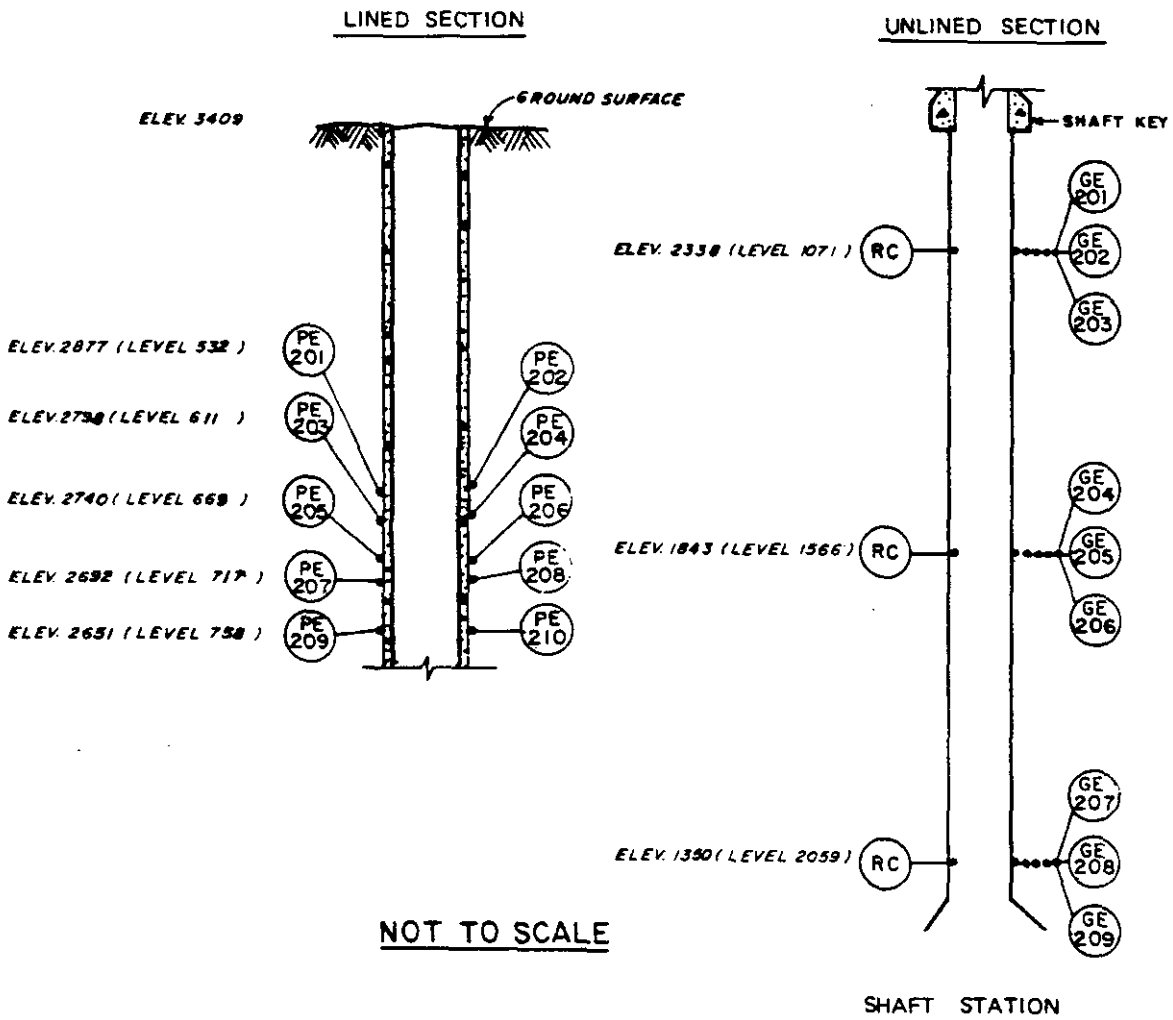

LEGEND

- (PE) PIEZOMETER
- (RC) CONVERGENCE POINTS
- (GE) EXTENSOMETER

NOTES

1. PC'S AT EACH LEVEL CONSIST OF FOUR POINTS.
2. THE TERM "LEVEL" IS AN APPROXIMATE DEPTH IN FEET FROM THE SHAFT COLLAR AT ELEVATION 3409 FT MSL
3. SEE FIGURE 8-2 FOR DETAILS OF SHAFT KEY INSTRUMENTATION.

Figure 8-2

WASTE SHAFT
INSTRUMENTATION

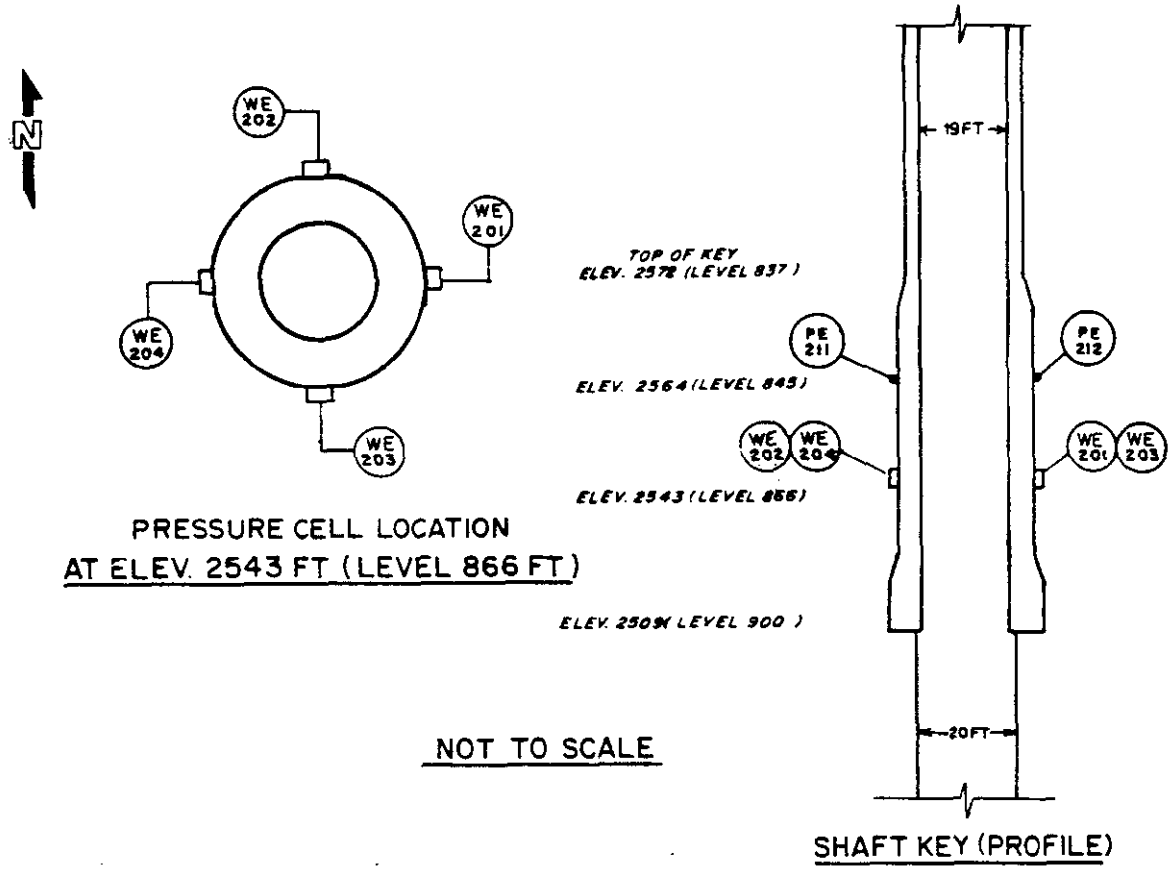

LEGEND

(WE) - PRESSURE CELL

(PE) - PIEZOMETER

NOTES:

1. THE TERM "LEVEL" IS AN APPROXIMATE DEPTH IN FEET FROM THE SHAFT COLLAR AT ELEVATION 3409 FT MSL
2. PRESSURE CELLS LOCATED AT CONCRETE-ROCK INTERFACE.

Figure 8-3

WASTE SHAFT KEY
INSTRUMENTATION

from a depth of 596 feet to 621 feet (elev. 2813 to 2788 feet) and the Culebra dolomite member from a depth of 706.5 feet to 728.5 feet (elev. 2702.5 to 2680.5 feet). Two piezometers are at each of the following elevations: 2877, 2798, 2740, 2692, 2651 and 2564 feet (Figures 8-2 and 8-3). The piezometers are located on opposite sides of the shaft, one at N60°E and the other at S60°W. Piezometer readings are shown on the data plots in Appendix J.

The four pressure cells are located in the waste shaft key between the salt of the shaft wall and the concrete comprising the key. The pressure cells were installed at a depth of 866 feet (elev. 2543 feet). The four cells are spaced 90 degrees apart around the shaft at the north, east, south, and west positions (Figure 8-3). Initial pressure cell readings were taken on April 6, 1984. The waste shaft key concrete was placed between March 23 and April 3, 1984. Pressure cell data plots are also presented in Appendix J.

The extensometers and convergence points were installed only in the unlined section of the shaft below the key. These instruments, whose locations are shown on Figure 8-2, were installed after enlargement of the shaft to its final dimensions.

The nine multiple-point borehole extensometers were installed between August 31 and September 5, 1984, 3 to 5 months after the completion of shaft enlargement. Three extensometers each are located at three elevations in the unlined section of the shaft: 2338, 1843 and 1350 feet (Figure 8-2). The extensometers are spaced 120 degrees apart around the shaft. Plots of the readings are presented in Appendix J.

A set of radial convergence points, consisting of four points each, is located at each of the same elevations as the extensometers. The convergence points were installed immediately after enlargement of the shaft. Due to interference by shaft furnishings, it was not possible to set the convergence points at 90 degrees from each other. The set of convergence points at a depth of 1,071 feet consists of two points

on each side of the shaft conveyance furnishings. The two points were set 44 degrees apart. At the other two depths the two points on each side of the shaft are set 53 degrees apart. Convergence point readings were obtained from April through June 1984 and are plotted in Appendix J. However, their performance is considered poor and erratic. The readings have been affected by salt incrustation on the convergence point eyebolts and extensions. Convergence point readings were discontinued when the temporary waste shaft hoist was decommissioned on September 12, 1984. The convergence points will be inaccessible until approximately December 1986, when the permanent waste shaft hoist is installed.

Geomechanical instruments were installed in the SPDV ventilation shaft station in late 1982. The instrumentation consisted of three multiple-point borehole extensometers and two sets of convergence points as shown on Figure 8-4. When the shaft was enlarged to become the waste shaft, the station was also enlarged and the original instruments were destroyed. Two extensometers were then installed in the enlarged shaft station. Both of these extensometers are in the roof, one on either side of the waste shaft (Figure 8-5).

8.3.2 Analysis and Evaluation

Analysis of the waste shaft data and its evaluation against reference design parameters has been divided into four elements: the concrete-lined section of the shaft; the shaft key; the unlined section; and the shaft station. This division is based on the different in situ and design conditions in each of these areas.

8.3.2.1 Lined Section

Engineering mechanics principles were used to design the concrete liner against elastic buckling. Both axial and flexural stresses were considered in the design. Permissible stress values were those used for structural plain concrete (ref. 8-1) utilizing the ultimate strength design method. Since there are no significant salt strata in

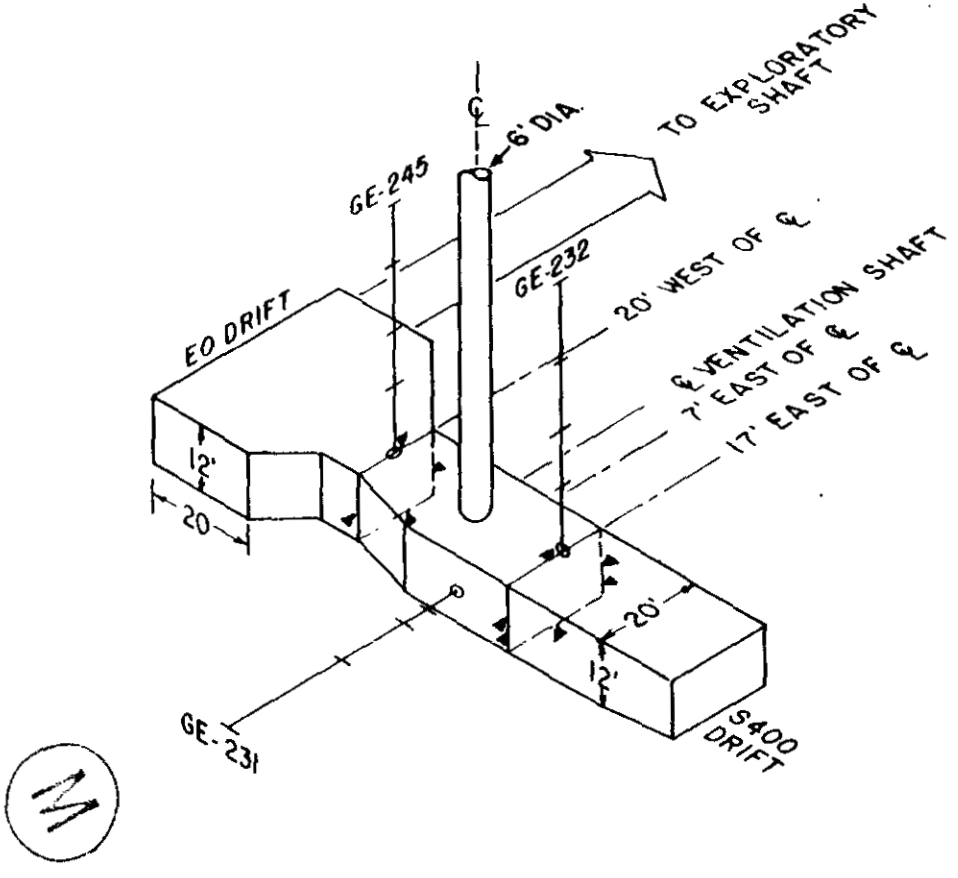

EXPLANATION

ANCHOR — COLLAR

GE EXTENSOMETER

RC RADIAL CONVERGENCE POINT

N

10 0 10 20 30 FEET

SCALE

Figure 8-4

SPDV VENTILATION SHAFT STATION
INSTRUMENTATION

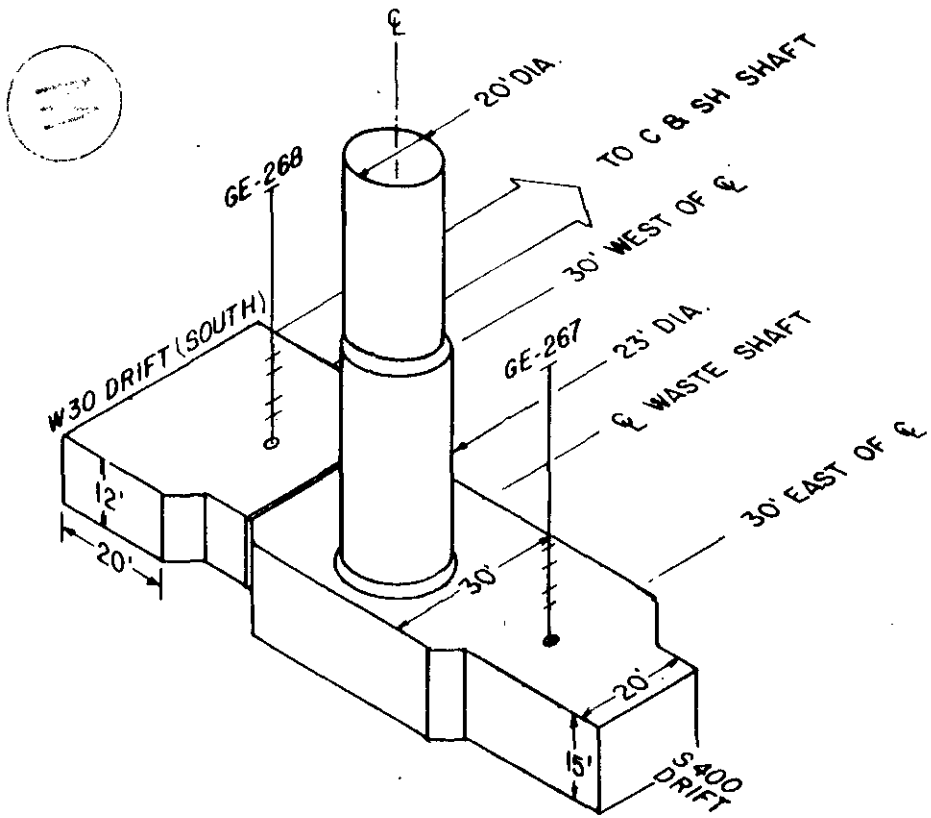

EXPLANATION

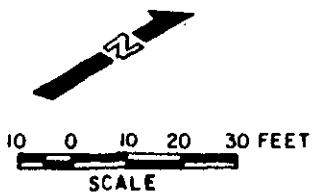

NOTES:

1. PREVIOUSLY IDENTIFIED AS THE SPDV VENTILATION SHAFT STATION.
2. INITIAL INSTRUMENTATION WAS DESTROYED IN JUNE 1984. EXTENSOMETERS GE-267 AND GE-268 WERE INSTALLED AFTER STATION ENLARGEMENT.

Figure 8-5

WASTE SHAFT STATION INSTRUMENTATION

the rock surrounding the liner, rock creep and the resulting rock pressure against the liner were assumed to be negligible. Hydrostatic pressure acting from a depth of 250 to 844 feet was used in the design based on the applicable design basis element (Table 8-1).

Additional stresses in the liner due to initial imperfections in roundness and grouting pressures were also considered. For stress calculations, an initial imperfection of 1 inch was assumed in the roundness of the liner. In place of the local water pressures, grouting pressures 1.3 times the ground-water pressure were assumed to act over one-sixth of the circumference of the liner. Due to localized effects, a 20 percent increase in the allowable concrete stress was assumed due to the short-term loading of the grouting pressure.

The external pressure capacities and corresponding closure limits (maximum diametric changes) for different thicknesses of the liner are:

Depth (feet)	Liner Thickness (inches)	Pressure Capacity (psi)	Closure Limit (inches)
27 to 462	10	216	0.165
462 to 580	14	370	0.215
580 to 762	18	523	0.251
762 to 837	20	598	0.266

The intent of the shaft piezometers is to monitor the pressure exerted on the liner by water from the Rustler formation. These data would indicate if the design hydrostatic pressure from the design basis was suitable.

Table 8-2 summarizes the variation in measured water pressures behind the liner at different times. Figure 8-6 shows the average reading on September 18, 1985, for each piezometer pair plotted against shaft depth. For comparison, the hydrostatic design pressure for the liner through this interval is also shown.

The measured pressures at this time are lower than the design pressure for two apparent reasons. First, water seepage through cracks and

Table 8-2

WASTE SHAFT LINER AND KEY
SUMMARY OF MEASURED WATER PRESSURES (psi)

PIEZOMETER NO. 31X-PE-00

Date of Reading	201	202	203	204	205	206	207	208	209	210	211	212
	Elev. 2879		Elev. 2798		Elev. 2740		Elev. 2692		Elev. 2651		Elev. 2564	
Dec. 26, 1984	-1	0	16	20	-7	-8	77	93	65	76	13	11
May 16, 1985	-2	0	11	16	12	-15	79	95	58	84	8	10
June 27, 1985	*	0	13	19	*	-16	78	95	*	91	11	12
Sep. 18, 1985	*	1	17	26	*	-14	99	115	*	107	19	22
Dec. 18, 1985	*	-3	-3	-2	*	-3	47	51	*	27	4	8
Mar. 16, 1986	*	-3	2	6	*	-13	*	63	*	47	5	12
June 13, 1986	*	0	10	15	*	-20	*	85	*	74	18	19

* Piezometer not functioning.

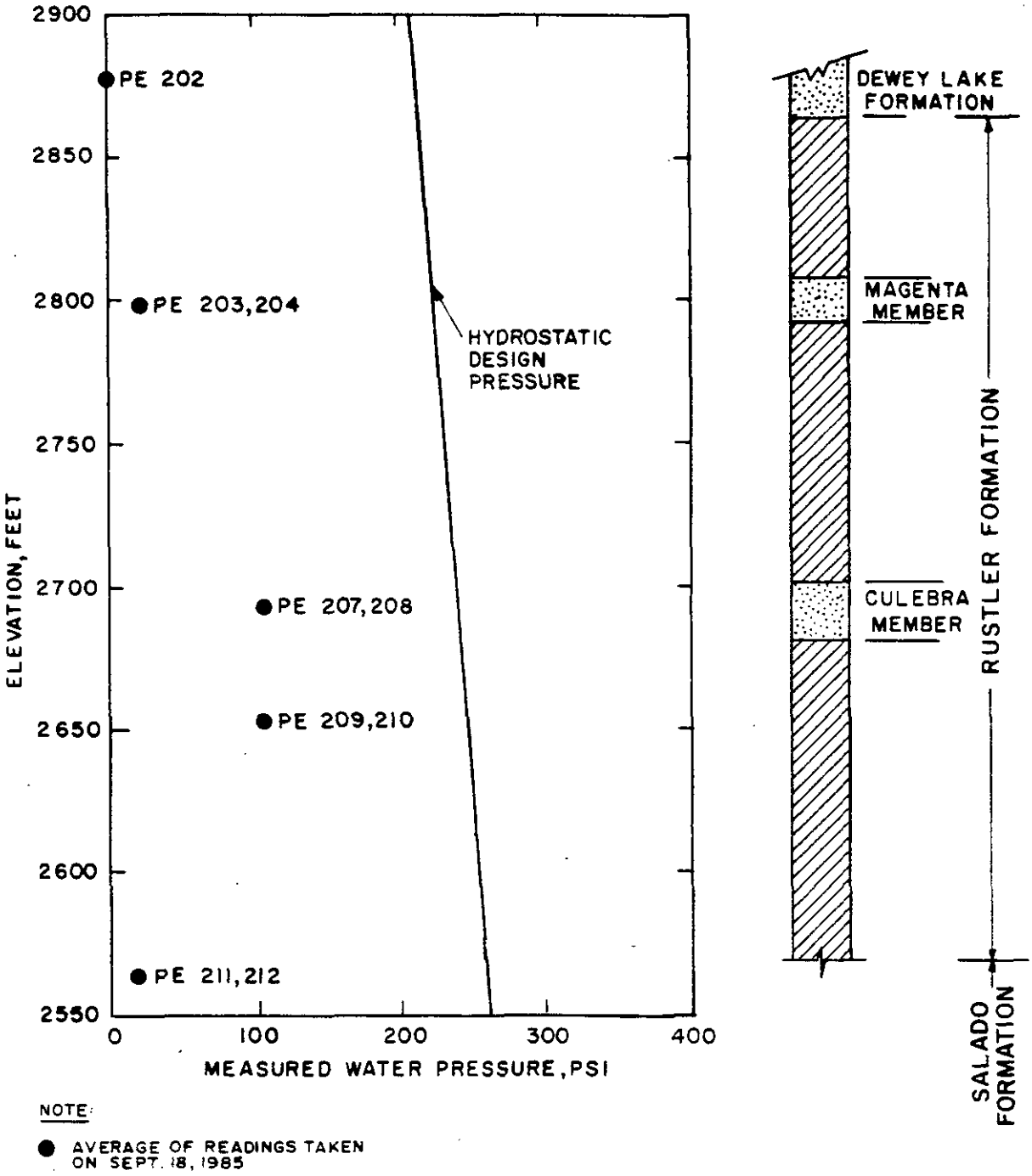

M

Figure 8-6

WASTE SHAFT LINER
WATER PRESSURE MEASUREMENTS

construction joints in the liner has not allowed the water to build up to its full hydrostatic head. This means that the piezometers are not measuring the full pressure that might be expected against the liner if the leaks were sealed. Second, the low pressure readings, and especially the variation in readings, suggest that hydraulic continuity is incomplete along the rock/liner interface. It is possible that water from the Culebra has been isolated, or at least restricted, in its vertical extent. This is suggested by the distribution of pressures shown on Figure 8-6.

The pressure distribution of the piezometers is also shown on Figure 8-7. These readings, however, are the maximum pressure values measured for each piezometer elevation. The figure also shows the design hydrostatic pressure distribution for the entire liner and its pressure capacity. The pressure capacity provides a significant factor of safety over the design hydrostatic pressure.

8.3.2.2 Shaft Key

Due to lithostatic pressure, the salt formation behind the shaft key tends to creep over time. The result is a buildup of inward pressure against the concrete key. The concrete key was designed to withstand a lateral pressure equal to 50 percent of the vertical overburden pressure (approximately 60 ksf) for at least 25 years after its construction. This reduction in lateral pressure from 75 percent of the overburden pressure for the C & SH shaft to 50 percent for the waste shaft was based on the results of the analysis of data obtained from the C & SH shaft (Chapter 7).

A nonlinear finite element analysis was utilized to simulate the long-term creep interaction of the salt and the concrete key. The analysis was performed using the MARC Finite Element Program discussed in Chapter 6. The material properties of the finite element model simulated the creep behavior of the salt via a power law (equation C.4-6 in Appendix C) provided in the analysis.

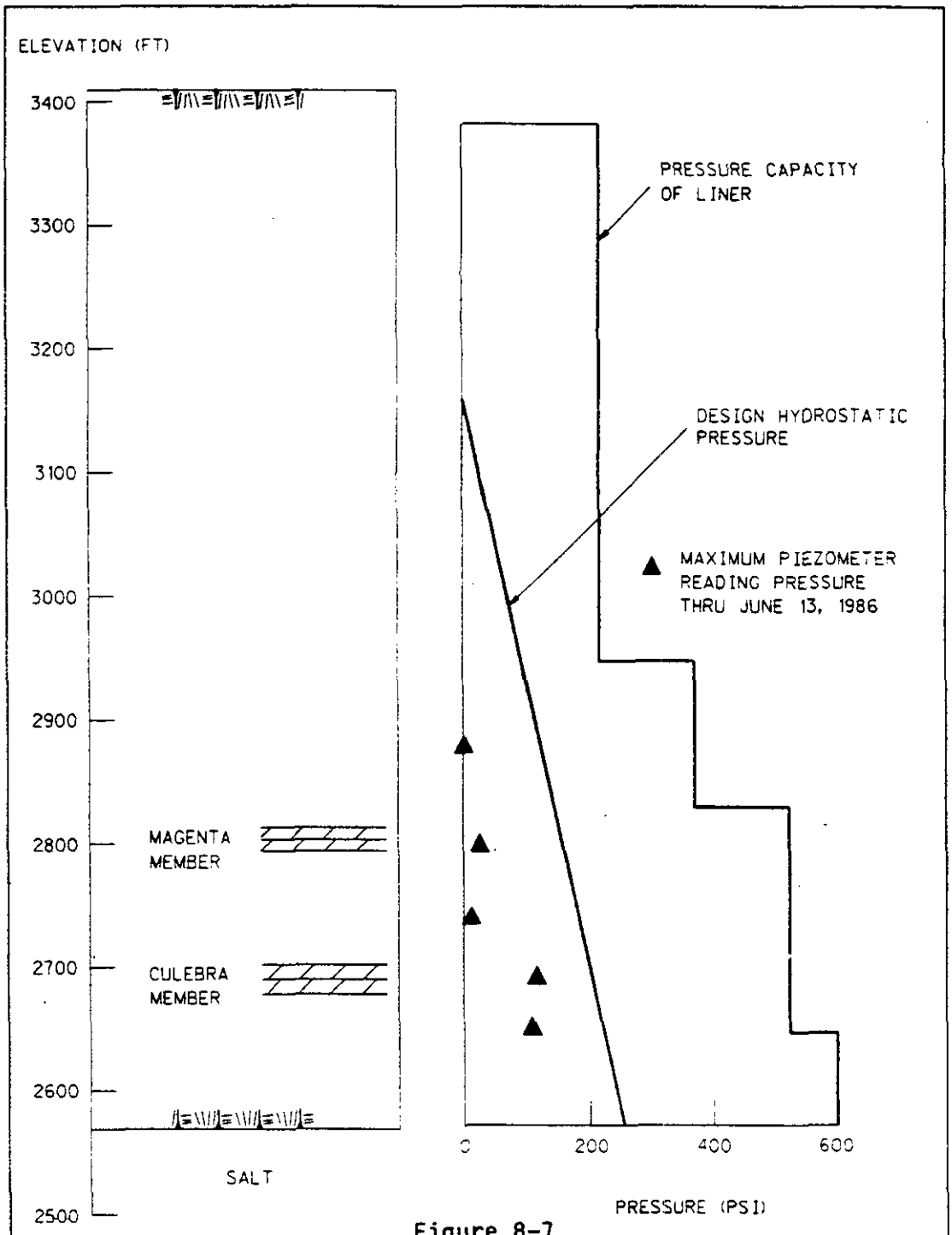

Figure 8-7

WASTE SHAFT LINER
LATERAL PRESSURE COMPARISON

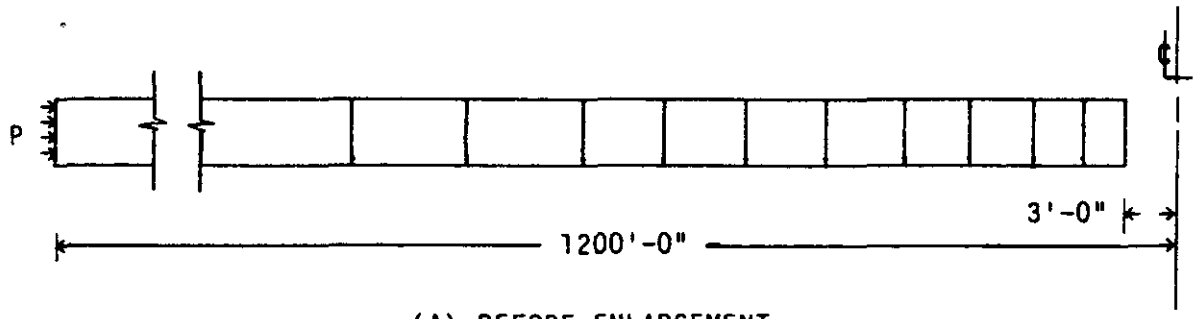

(A) BEFORE ENLARGEMENT

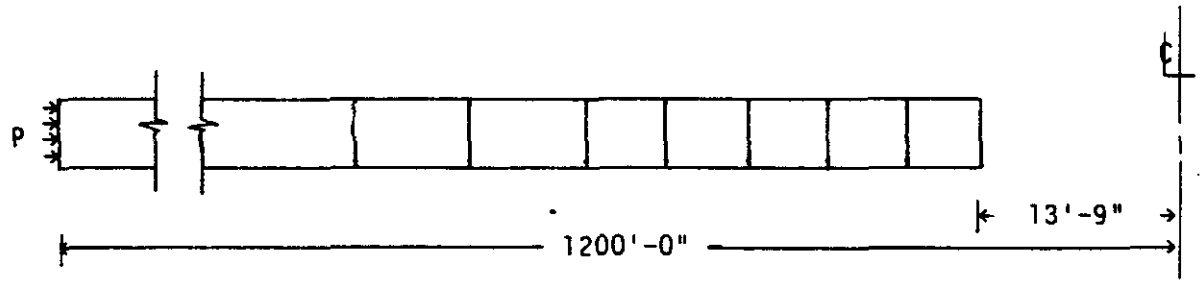

(B) AFTER ENLARGEMENT

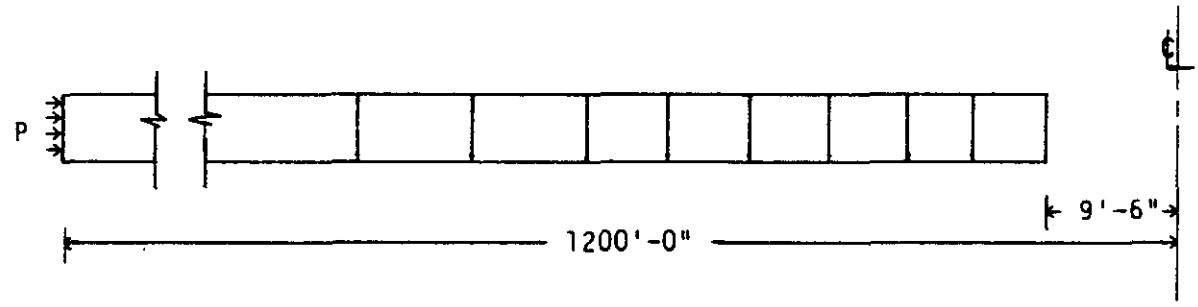

(C) AFTER CONCRETE CONSTRUCTION

Figure 8-8

WASTE SHAFT KEY
FINITE ELEMENT MODEL

Model Simulation. Unlike the more sophisticated analysis of the C & SH shaft key (which employed a multi-layered, axisymmetric finite element model), the finite element model for the waste shaft key and surrounding salt consists of a single layer of quadrilateral, axisymmetric ring elements as shown on Figure 8-8. Because only the lateral flexural stiffness of the shaft key was considered in the finite element model, and not its longitudinal flexural stiffness, the analysis provides conservative results. Also for conservatism, the shrinkage effect of the concrete was not taken into account in this analysis.

An inner element of the model, shown on Figure 8-8, represents a segment of the concrete key. In order to simulate the time interval between shaft excavation and concrete placement for the key, this element was not tied to the surrounding salt deposits. All depth-dependent input values, such as overburden stresses, were computed for a depth of 892 feet, low in the key, where such values are at a maximum. Because halite is the most dominant material in the rock around the shaft key, its properties were used for the model elements. Halite is also the material at the base of the shaft key where lateral pressure is at a maximum.

The following analytical procedure was used to perform a creep analysis of the waste shaft key:

(1) Initially, lateral forces were applied outwardly against the inside surface of the shaft. This simulates the condition prior to excavation of the original 6-foot diameter shaft.

(2) Lateral forces were applied inwardly against the outer vertical boundary of the model. The magnitude of these forces were based on the lateral earth pressure, equal to 892 feet of overburden, computed for the key elevation of 2517 feet.

(3) Internal stresses were applied in each element to represent the initial lithostatic stress state.

(4) All nodes of the model were restrained against vertical displacement.

(5) Subsequently, outward lateral forces against the inside surface of the shaft were removed to simulate excavation of the original 6-foot diameter shaft.

(6) A creep analysis was performed on the salt deposits surrounding the 6-foot diameter shaft until that time when the shaft diameter was enlarged and the concrete for the key was placed (795 days).

(7) The three innermost ring elements were detached (tie constraints removed) from the model to represent the enlargement of the shaft. A concrete ring element (tie constraints added to the model) then replaced the three salt elements just removed to model the concrete key.

(8) A second creep analysis was performed using this new model and a creep time representing 28 years after placement of the concrete key.

The stratigraphy in the upper section of the waste shaft is similar to that in the C & SH shaft. The creep parameters determined from in situ salt behavior in the C & SH shaft were, therefore, assumed to be valid for correlating analytical results of the waste shaft from normalized time to real time. The secondary creep parameter C was found to equal 5.70×10^{-21} $ksf^{-4.9}$ sec^{-1}. Because early in situ measurements were not available for the C & SH shaft, the primary creep parameters A and z were determined from in situ data from the horizontal drifts and were found to be 3.2 and 1.1×10^{-7} sec^{-1}, respectively.

Seepage Evaluation. The structural integrity of the shaft key is not totally dependent upon salt creep. The stability of the key, and consequently the shaft liner, can be compromised by water dissolving the salt surrounding the key. Water is prevented from seeping from the upper water-bearing zones down into the salt around the key primarily by two chemical water seals. The key configuration, including the seals, is described in Chapter 3.

The number of piezometers in the key are not sufficient to conclusively support an evaluation of seepage. However, the distribution of water pressure behind the liner and key provides an indication that there is probably no hydraulic continuity along the rock/liner interface. This is especially evident at the lowermost water-bearing zone at a depth of 717 feet (elev. 2692 feet). Here, water pressures are over 100 psi. The next lower level of piezometers, at a depth of 758 feet (elev. 2651 feet), also indicate pressures of about 100 psi. However, the lowest level of piezometers, in the shaft key, reflect pressures of less than 25 psi.

The telltale drains in the waste shaft key could not be located during the July 1986 inspection. Assuming they were constructed as designed, they may be covered by a thin veneer of concrete formed during concrete placement. A seep was noted on one side of the shaft at the approximate design level of the telltales. Inspection of the base of the key determined that no water was seeping from behind the key. This indicates that ground water is not bypassing the lower water seal between the key and the surrounding halite.

8.3.2.3 Unlined Section

The structural behavior of the unlined section of the waste shaft was also computed by a nonlinear creep analysis using the MARC Finite Element Program (ref. 6-8). The objective of the analysis was to compute the actual structural behavior by utilizing applicable in situ data from the C & SH shaft and the horizontal drifts, and to verify the design adequacy of the unlined section of the shaft.

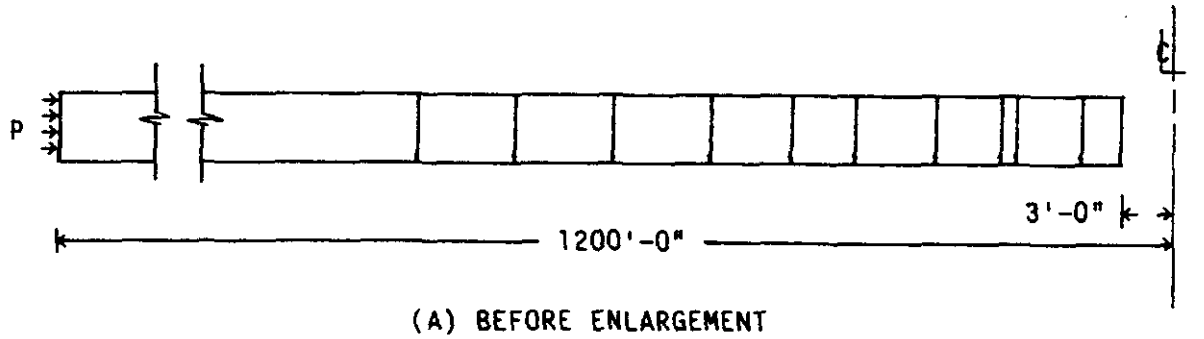

(A) BEFORE ENLARGEMENT

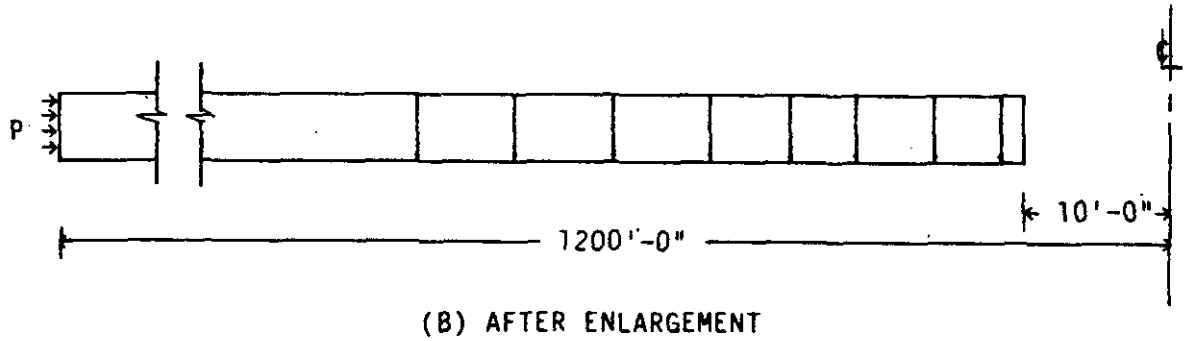

(B) AFTER ENLARGEMENT

Figure 8-9

WASTE SHAFT UNLINED SECTION
FINITE ELEMENT MODEL

Model Simulation. The finite element model used for the unlined section of the waste shaft utilizes a single horizontal row of 70 quadrilateral axisymmetric ring elements. The model, shown on Figure 8-9, has its upper and lower horizontal boundaries restrained against vertical movement and a constant uniform lithostatic pressure, equal to 2,059 feet of overburden, applied to its outside vertical boundary. The same lithostatic pressure was initially applied to the inside vertical boundary as well; however, that pressure was later removed from the inside boundary to simulate the drilling of the original 6-foot diameter shaft.

The analysis simulates the salt creep until that time when the 6-foot diameter shaft was enlarged to its present 20-foot diameter. The shaft enlargement was simulated in the model by removing those ring elements that were located within the 20-foot diameter shaft opening. With the enlarged shaft configuration, simulated salt creep for another 28 years was analyzed.

Determination of Creep Parameters. Because the stratigraphy beneath the WIPP site is fairly uniform, the values of the creep parameters for the unlined section of the waste shaft were assumed to be identical to those values calculated at the corresponding elevations of the C & SH shaft. In addition, the C & SH shaft was drilled at a much earlier date than was the waste shaft; therefore, more in situ geomechanical instrument measurements were available for the C & SH shaft. The values of the creep parameters for the C & SH shaft were determined by correlating analytical results with extensometer readings obtained from a depth of 2,057 feet (elev. 1353 feet) in the shaft. The creep parameters C, A and z for the C & SH shaft were found to be 1.30×10^{-21} $ksf^{-4.9}$ sec^{-1}, 3.2 and 1.1×10^{-7} sec^{-1}, respectively. Chapter 7 presents specific details on how the creep parameters were evaluated for the C & SH shaft.

8.3.2.4 Shaft Station

The analysis of closure and stability of the waste shaft station is based upon closure measurements in the C & SH shaft station. This is due to the limited amount of geomechanical instrumentation data available from the waste shaft station for the reasons discussed in subsection 8.3.1. The following discussion presents a brief comparison of the two shaft stations.

The waste shaft station cross-section dimensions are 15 feet high and 30 feet wide. These dimensions are comparable to those of the C & SH shaft station. However, the C & SH shaft station was excavated by drilling and blasting while the waste shaft station was excavated using a mining machine. The density of rock bolts in the roof of the C & SH shaft station is much greater than that in the waste shaft station. Also, the roof of the C & SH shaft station close to the shaft is approximately 3 feet below clay G, while clay G at the waste shaft station is nearly 8 feet above the roof. Thus, closure analysis of the waste shaft station using measurement data from the C & SH shaft station will be conservative.

The dimensions of the waste shaft station are also comparable to those of the test rooms and storage rooms. Computational analysis of the storage rooms (Chapter 12) predicts that failure will occur in MB-139, below the floor, due to gradual stress buildup. Similar behavior is expected to occur in MB-139 beneath the waste shaft station.

8.3.3 Prediction of Future Behavior

This subsection presents predictions of future behavior for the various elements of the waste shaft including the lined section, the shaft key, the unlined section and the shaft station.

8.3.3.1 Lined Section

The cracks in the concrete-lined section of the shaft are primarily the result of normal tension cracking occurring during the restrained

shrinkage of plain concrete. The cracks are not detrimental to the liner's structural integrity but sealing by grouting will be required to meet the design criteria regarding ground-water control.

Although the rate of water flowing into the waste shaft has been minor, the total volume of flow has resulted in the lowering of the potentiometric surface around the shaft. Other activities have also affected the potentiometric level in the vicinity of the shafts. Most notably, SNL pumping tests in borehole H-3 in late 1985 lowered the potentiometric surface approximately 40 feet (A.R. Lappin, SNL, personal communication). Due to the unknown effect of current and future hydrologic studies at the WIPP, it is difficult to predict the magnitude of future water pressure on the liner. However, two statements can be made concerning this water pressure:

(1) The piezometer data present a valid indication of water pressures behind the liner. Although this data cannot be used for predicting future pressures, continuous monitoring of these instruments will reflect current pressures and indicate short-term trends. This information can be compared with the design basis pressure distribution (Figures 8-6 and 8-7) to evaluate liner stability.

(2) Following the next grouting program in the waste shaft, if all water seepage through the liner has been stopped, it is possible that the potentiometric surface could return to its highest level determined during preliminary design activities. Assuming complete hydraulic continuity behind the liner, this condition would result in a pressure distribution equal to that of the hydrostatic pressure used for liner design. This condition would be within the design limits.

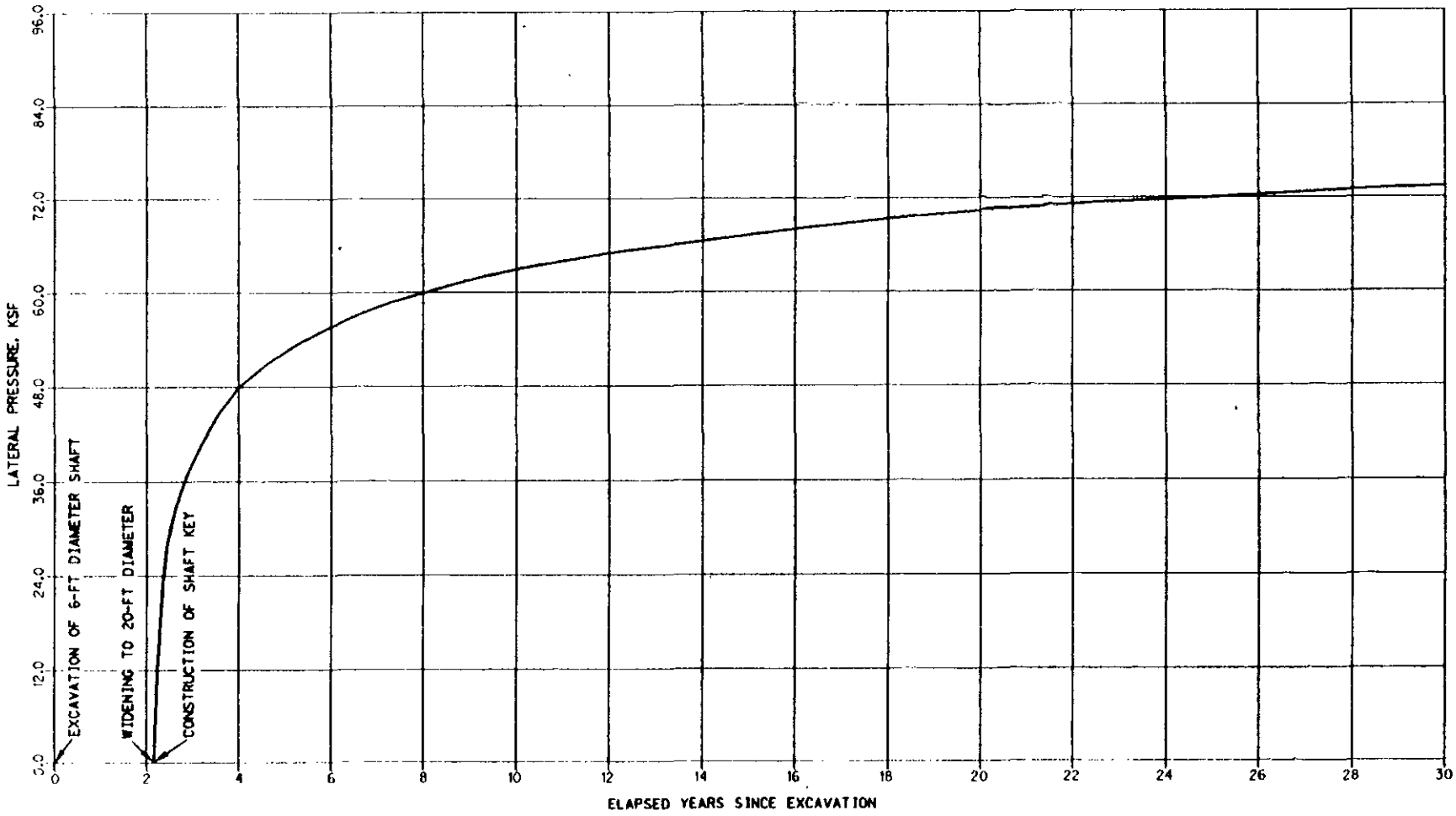

Figure 8-10

WASTE SHAFT KEY
LATERAL PRESSURE PREDICTION

8.3.3.2 Shaft Key

Figure 8-10 shows the predicted lateral pressure curve for the concrete key based on the finite element analysis. The key was designed as a compression cylinder in accordance with the strength design method for reinforced concrete (ref. 7-5) using an ultimate hoop stress of 4.25 ksi (0.85 f'_c). Using the design basis load factor of 1.7 for lateral loads, the maximum allowable hoop stress in the concrete key is 2.50 ksi, which results in an allowable lateral rock pressure of 148 ksf based on the diameter of the key. The design basis lateral pressure design requirement is approximately 60 ksf. Figure 8-10 shows a lateral pressure on the shaft key of approximately 72 ksf at the end of the 25-year shaft operating life. If the shrinkage and creep properties of the concrete were taken into account in the finite element analysis, the lateral pressure would actually be less than 72 ksf at 25 years.

The reinforced concrete of the shaft key is expected to exhibit cracks due to shrinkage. These are tensile cracks due to the reinforcement restraining the concrete from shrinking. The cracks are not considered significant because they are common to most reinforced concrete structures.

8.3.3.3 Unlined Section

Figures 8-11 and 8-12 show the radial and tangential (hoop) stress distributions relative to the overburden stress for different times in the unlined section of the waste shaft. Figure 8-11 shows the zone around the shaft opening where radial stresses are affected and indicates a decrease in magnitude over time. The computational results depicted on Figure 8-12 indicate that tangential stresses are only affected within a radius of approximately 120 feet.

Figures 8-13 and 8-14 show the effective stress and effective creep strain distributions in the unlined section of the waste shaft. The effective stress in the shaft wall at 25 years is approximately 140 ksf

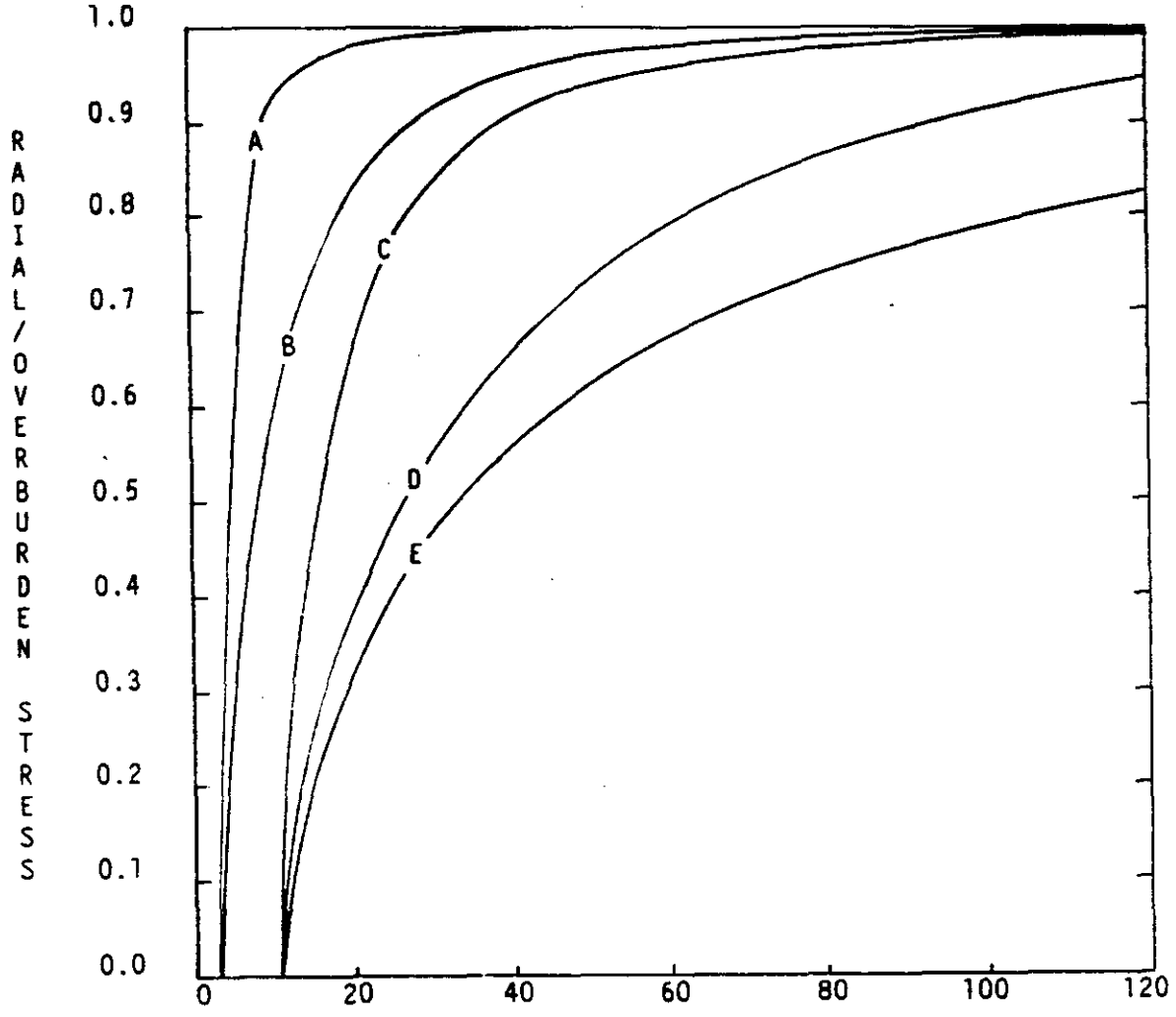

A - IMMEDIATELY AFTER EXCAVATION OF 6-FT DIAMETER SHAFT
B - IMMEDIATELY BEFORE WIDENING TO 20-FT DIAMETER
C - IMMEDIATELY AFTER WIDENING TO 20-FT DIAMETER
D - ONE YEAR AFTER WIDENING OF SHAFT
E - 25 YEARS AFTER WIDENING OF SHAFT

Figure 8-11

WASTE SHAFT UNLINED SECTION
RADIAL STRESS DISTRIBUTION AT ELEVATION 1350 FEET

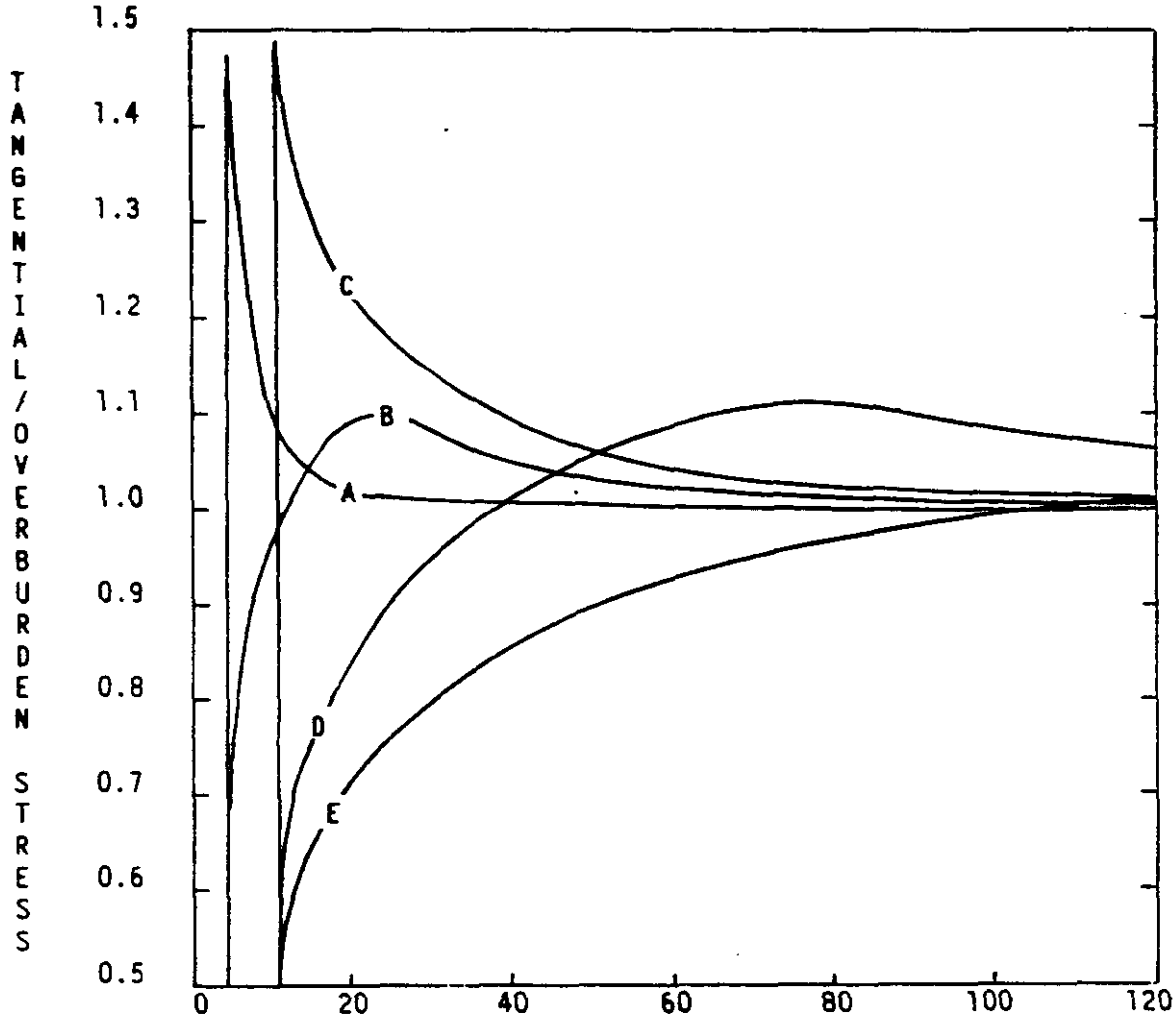

A - IMMEDIATELY AFTER EXCAVATION OF 6 FT-DIAMETER SHAFT
B - IMMEDIATELY BEFORE WIDENING TO 20 FT-DIAMETER
C - IMMEDIATELY AFTER WIDENING TO 20 FT-DIAMETER
D - ONE YEAR AFTER WIDENING OF SHAFT
E - 25 YEARS AFTER WIDENING OF SHAFT

M

Figure 8-12

WASTE SHAFT UNLINED SECTION
TANGENTIAL STRESS DISTRIBUTION AT ELEVATION 1350 FEET

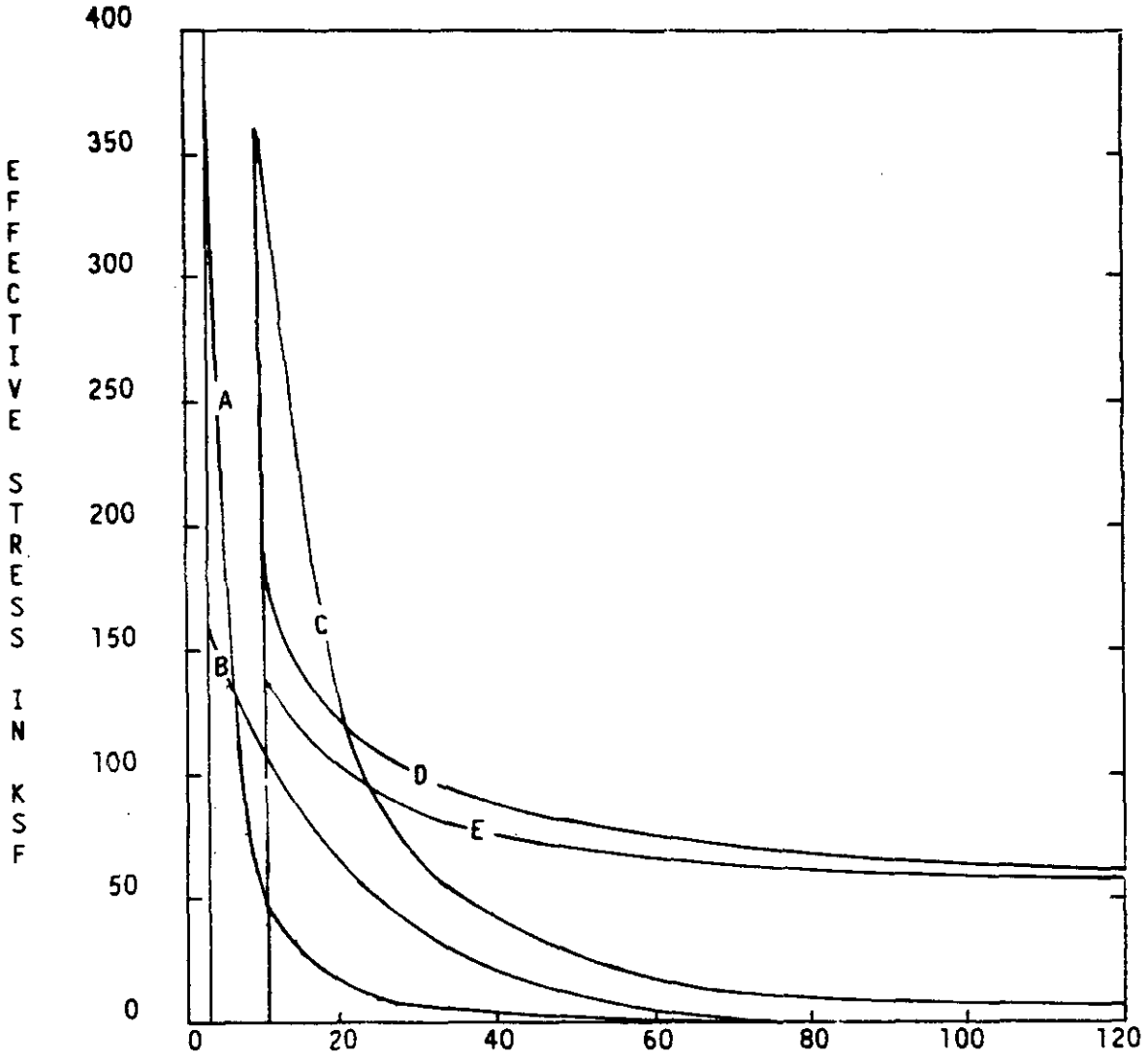

A - IMMEDIATELY AFTER EXCAVATION OF 6-FT DIAMETER SHAFT
B - IMMEDIATELY BEFORE WIDENING TO 20-FT DIAMETER
C - IMMEDIATELY AFTER WIDENING TO 20-FT DIAMETER
D - ONE YEAR AFTER WIDENING OF SHAFT
E - 25 YEARS AFTER WIDENING OF SHAFT

Figure 8-13

WASTE SHAFT UNLINED SECTION
EFFECTIVE STRESS DISTRIBUTION AT ELEVATION 1350 FEET

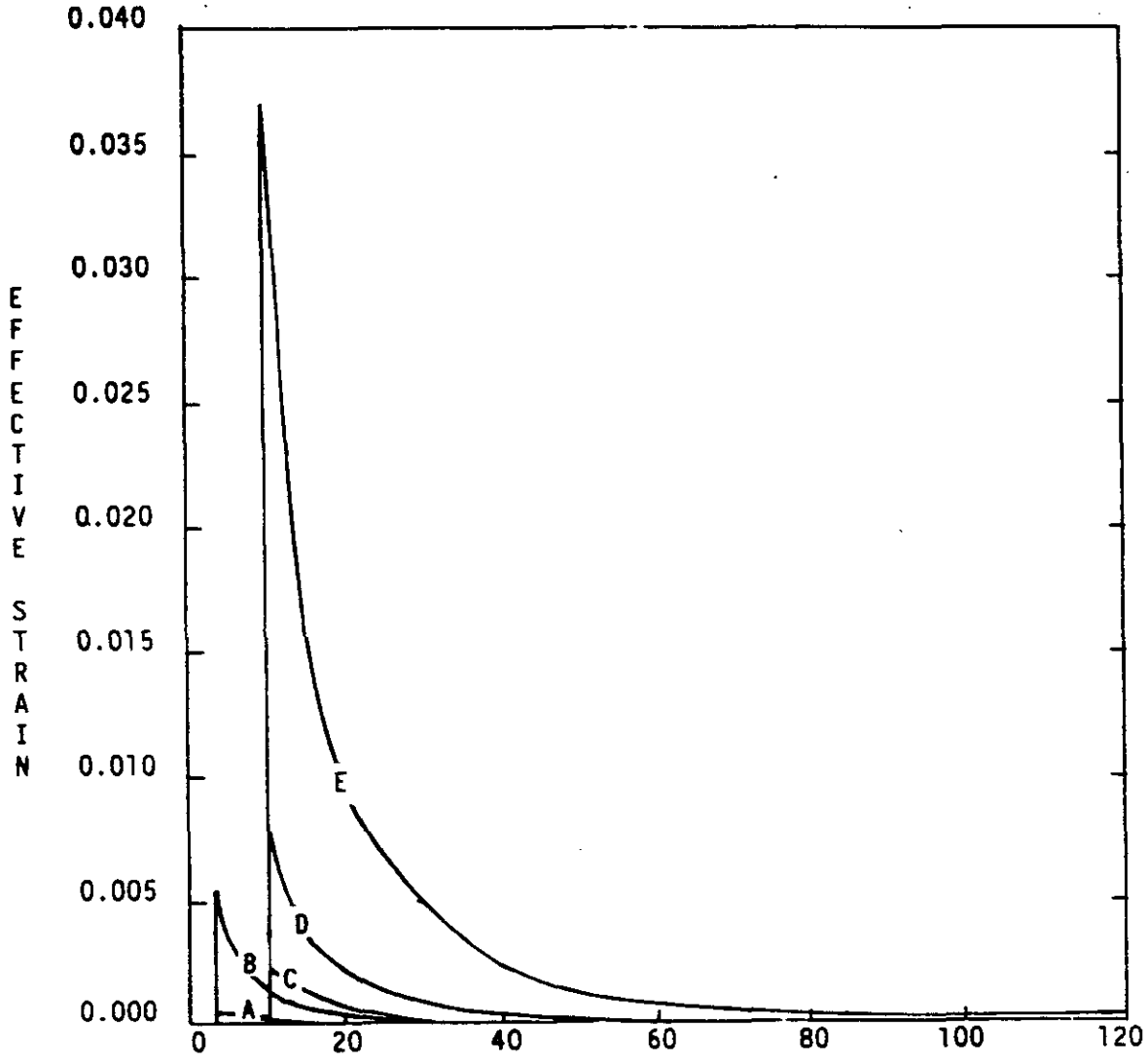

A - IMMEDIATELY AFTER EXCAVATION OF 6-FT DIAMETER SHAFT
B - IMMEDIATELY BEFORE WIDENING TO 20-FT DIAMETER
C - IMMEDIATELY AFTER WIDENING TO 20-FT DIAMETER
D - ONE YEAR AFTER WIDENING OF SHAFT
E - 25 YEARS AFTER WIDENING OF SHAFT

M

Figure 8-14

WASTE SHAFT UNLINED SECTION
EFFECTIVE CREEP STRAIN DISTRIBUTION AT ELEVATION 1350 FEET

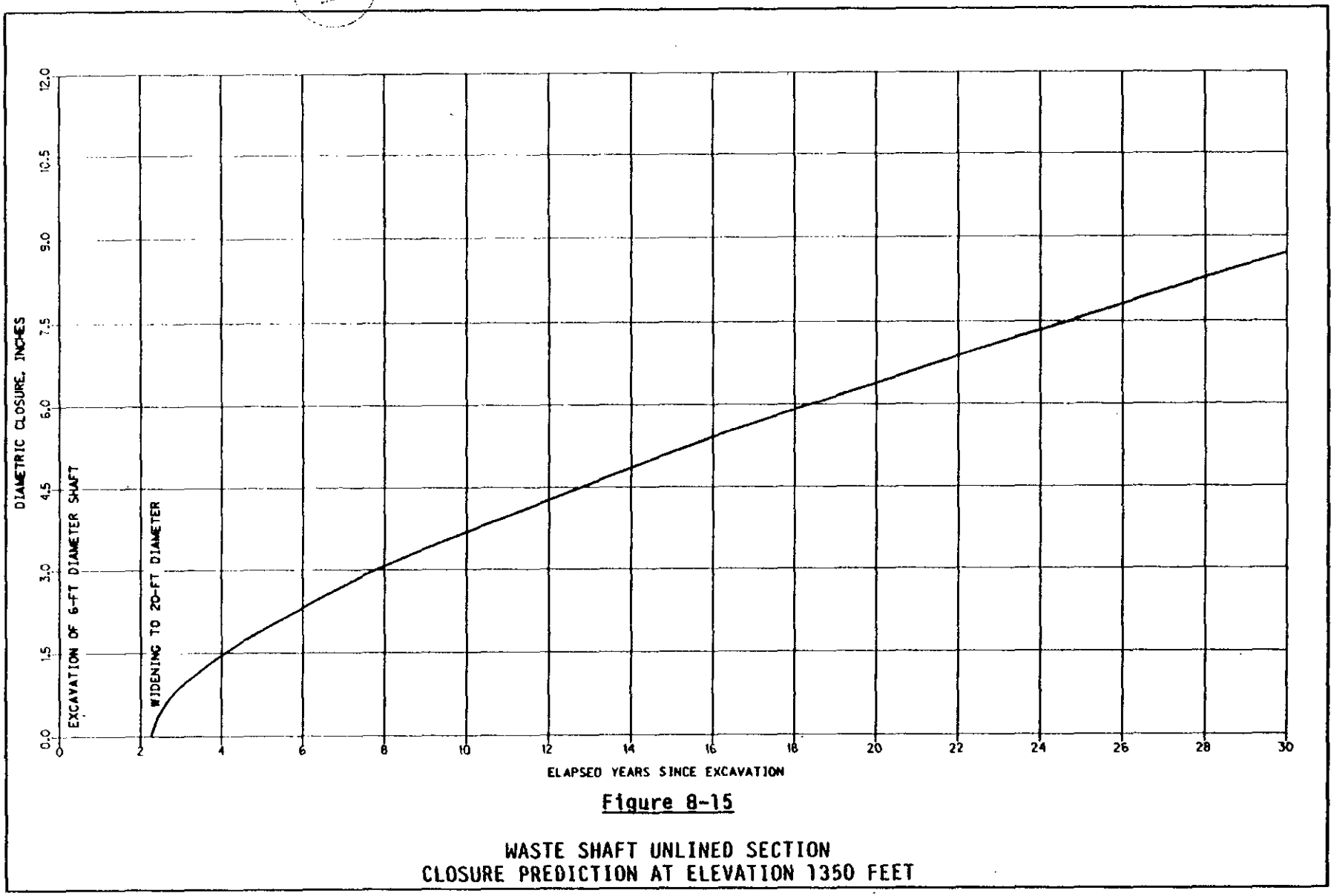

Figure 8-15

WASTE SHAFT UNLINED SECTION
CLOSURE PREDICTION AT ELEVATION 1350 FEET

while the effective creep strain in the shaft wall at 25 years reaches a value of approximately 0.037.

Figure 8-15 contains the prediction of diametric closure for the unlined section of the waste shaft at a depth of 2,059 feet (elev. 1350 feet). This figure shows a diametric closure of approximately 7 1/2 inches over the 25-year operating life of the shaft.

8.3.3.4 Shaft Station

Closure in the waste shaft station is predicted using measurement data from the C & SH shaft station. The measured roof-to-floor closure in the C & SH shaft station was approximately 10 inches on September 16, 1985, over 3 years after the completion of excavation. The measured wall-to-wall closure is greater than 6 inches over the same time period. However, the initial readings were taken nearly 260 days after the station was excavated; therefore, the actual closure magnitudes will be higher. The average rate of roof-to-floor closure over the measurement period was approximately 3.89 inches/year. Using this value as a constant closure rate over the plant operating life of 25 years, an additional roof-to-floor closure of about 8 feet is expected to occur. The wall-to-wall closure over the same period is expected to be approximately 60 percent of the roof-to-floor closure, or about 5 feet. Actual closure may be lower as discussed in subsection 8.3.2.4.

8.4 CONCLUSIONS AND RECOMMENDATIONS

Design validation requires an assessment of the compatibility of the design criteria, design bases and design configurations used for the reference design. The following conclusions and recommendations address those design elements identified in Section 8.2. Other conclusions and recommendations resulting from the design validation process are also presented.

8.4.1 Conclusions

The design criteria require that all of the shafts are to be stable. Shaft stability has been evaluated using analytical calculations,

finite element modeling and in situ data analysis. The shaft liner is considered stable because the water pressure exerted on it has remained significantly below the design hydrostatic pressure. If the water pressure increases to the design hydrostatic pressure, as may be expected if the leaks are sealed by additional grouting, liner stability will not be compromised. The pressure capacity of the liner sufficiently exceeds the design hydrostatic pressure.

Based on existing evidence, the cracks in the liner and key do not present a structural problem. The unreinforced concrete liner is expected to function as intended, provided that the existing cracks and construction joints are grouted and contact grouting is performed at the rock/liner interface. Consolidation grouting of the surrounding rock may also be necessary to achieve a dry shaft.

The shaft key was designed to withstand a design basis lateral pressure equal to 50 percent of the overburden pressure (approximately 60 ksf). The finite element analysis determined that the lateral pressure on the key at the end of the facility operating life will be approximately 72 ksf. Although this value is higher than the design lateral pressure, the key is expected to remain stable throughout its operating life because the allowable lateral rock pressure is 148 ksf. This is twice the lateral pressure predicted and provides a sufficient margin of safety. Furthermore, if the shrinkage and creep properties of the concrete were taken into account in the analysis, the lateral pressure would be less than 72 ksf.

The analytical results for the waste shaft, presented in Section 8.3, show the calculated redistribution of stresses around the shaft due to the effects of creep. Based on the computed vertical, horizontal and effective stresses in the unlined section, the magnitude of stresses immediately adjacent to the opening decreases with time as the stress arch around the opening migrates away. The maximum stress occurs immediately after excavation and is followed by relaxation due to creep behavior. Therefore, the stresses will not cause a future stability

problem in the waste shaft except in the anhydrite bed (MB-139) below the floor of the shaft station. Gradual buildup of stress in this bed may result in floor heave and fracturing.

The analysis shows the locations of effective creep strain concentrations for selected times in the unlined section. Based on these predicted values of effective creep strain and the strain limit discussed in Chapter 6, the waste shaft will remain structurally stable over its planned 25-year operating life.

The analysis predicts that diametric closure in the unlined section of the waste shaft will be approximately 7 1/2 inches over its 25-year operating life. Based on the predicted deformations and closures, the waste shaft will meet the requirements stated in the design criteria and the 20-foot diameter unlined section will provide sufficient operating clearance to allow for salt creep.

The design criteria requires that no uncontrolled ground water reach the facility level via the shafts. The majority of water seeping through cracks and construction joints in the liner is collected in three water-collection rings and directed to the underground facility where it is disposed. Only minor amounts of uncontrolled fly water reach the facility level. This water has a negligible impact and does not affect validation of the criterion regarding ground water reaching the facility level.

Shaft inspections have determined that only one minor seep occurs in the key and that no water seepage occurrs from the base of the key. This supports the conclusion that the water seals are functioning, that no water is seeping along the concrete/salt interface, and that no salt dissolution is occurring behind the concrete key. The installation technique for the waste shaft water seals was improved over that used for the C & SH shaft water seals (Chapter 3).

The zone of dissolution observed in the shaft sump wall is not considered to be detrimental to the operation of the facility. The

material was dissolved differentially by standing water in the sump resulting from construction activities. It is not the result of any geologic discontinuity or process. This zone will not produce any structural problems in construction of the waste shaft facilities.

The waste shaft station is expected to undergo roof-to-floor closure at a rate of 3.89 inches/year. However, this rate has been obtained by using the C & SH shaft station instrument data. The actual closure rate may be lower. Additional heave and fracturing in the salt beneath the floor, as well as in MB-139, is expected to occur. Some remedial work will be required to maintain the required roof-to-floor clearance for operational equipment and activities.

The reference design for the waste shaft is considered to be validated in accordance with the objectives of the design validation program based on the analyses, evaluations and predictions of future behavior presented in this chapter. With one exception, the waste shaft reference design complies with the design criteria and the design bases. The criterion that stipulates that shaft liner design shall prevent ground-water flow into the shaft has not been met. The rate of water currently seeping into the waste shaft is not considered to be detrimental to the stability of the shaft or to its functional purpose. However, the criteria will be satisfied when additional remedial grouting has been performed. No modifications to the shaft reference design will be required.

8.4.2 Recommendations

Based on the results of design validation, the following recommendations with respect to the waste shaft are made:

(1) Due to the limited in situ data base, validation of the waste shaft key and unlined section relies on numerical modeling utilizing creep parameters derived from the C & SH shaft in situ data. It is recommended that the modeling be repeated, prior to the first receipt of waste, using the latest in situ

data from the waste shaft. This analysis should be repeated periodically for comparison and verification of in situ data against design parameters.

(2) Grouting should be performed to completely seal the waste shaft liner. This should include contact grouting behind the liner and grouting of shrinkage cracks and construction joints. Consolidation grouting may also be required. Qualified personnel should inspect the shaft at regularly scheduled intervals. The liner should be checked for leaks after grouting has been completed. The key should be checked for water seeping from behind the key at its base. If any seepage is detected it may become necessary to grout the area above the upper water seal. If possible, grout should not be placed behind the key below the upper seal. However, should grouting behind the key become necessary, the grout must be a chemical gel (or other non-rigid grout) and must be compatible with both the existing water seal material and with the requirements of the Plugging and Sealing Program.

(3) The dissolution zone in the waste shaft sump should be filled with a salt-compatible cement mortar.

(4) Because waste shaft station closure is based on C & SH shaft station data, and because of the importance of the waste shaft station in general, vertical convergence points or meters should be installed at selected locations and measurements taken periodically. These data should then be analyzed to obtain better estimates of station closure.

CHAPTER 9
EXHAUST SHAFT

9.1 INTRODUCTION

This chapter presents information on design validation of the exhaust shaft. Included are discussions of its design, the design validation process, and conclusions and recommendations pertaining to validation of the reference design.

9.2 DESIGN

This section presents the design criteria and design bases used to develop the reference design for the exhaust shaft. The design configuration of the shaft is discussed in Chapter 3, subsection 3.3.3.

9.2.1 Design Criteria

The design criteria for the exhaust shaft are identical to those for the other two shafts. The criteria requiring validation are indicated in the listing of abridged criteria presented in Chapter 2, Table 2-1, and are discussed in Chapter 7.

The design criteria requiring evaluation for design validation of the exhaust shaft are:

(1) shaft shall be designed to be structurally stable;

(2) shaft shall be designed to accommodate salt creep; and

(3) ground-water flow into the shaft shall be controlled.

9.2.2 Design Bases

The design bases are the detailed design requirements developed from the design criteria. The primary design basis document for the exhaust shaft is the Design Basis, Exhaust Shaft (ref. 2-16). The major elements of the design bases are the same as those for the waste shaft,

except for the items discussed in the next paragraph. The elements that require evaluation or that have a direct impact on design validation are presented in Table 9-1.

In addition to adhering to the design basis elements discussed previously for the waste shaft, the exhaust shaft shall be designed to connect the facility level with the exhaust filter building at the ground surface. The exhaust shaft shall be used to remove air from the underground development level during construction and storage operations. The entire shaft shall be inspected utilizing a closed-circuit television camera that shall be lowered from the top of the shaft. Unlike the design bases for the other two shafts, the exhaust shaft design basis does not require the installation of geomechanical instrumentation.

9.3 DESIGN VALIDATION PROCESS

As discussed in Chapter 5, design validation of the exhaust shaft has been achieved by data collection, its analysis and evaluation, and the prediction of future behavior. Data collection activities have included geologic mapping and visual observations of the exhaust shaft wall. Although geomechanical instruments have been installed in the shaft, no data was available for design validation due to the late date of installation.

Computational analyses for the exhaust shaft were performed in the same manner as those for the waste shaft. The finite element analyses of the shaft key and unlined section used the material parameters for salt obtained from the C & SH shaft and horizontal drift analyses. The results of the analyses were then used to predict future behavior.

9.3.1 Data Collection

Data collection in the exhaust shaft was on a much smaller scale than in the other two shafts. Geologic mapping was conducted in the shaft to verify the stratigraphy. This mapping is discussed in detail in Chapter 6. Visual inspections and observations in the shaft were

Table 9-1

VALIDATION ELEMENTS OF EXHAUST SHAFT DESIGN BASES

(1)	Shaft liner Hydrostatic pressure should be considered to start at 250 feet below the ground surface and extend to the top of the key.
(2)	Shaft key Design lateral pressure shall be 50 percent of the vertical pressure due to soil, rock and salt overburden.
(3)	Unlined section Provide 15-foot diameter to allow for future salt creep deformation.

sporadic due to limited access. The following discussion presents those observations which affect design validation.

9.3.1.1 Field Observations

Exhaust shaft construction was completed on January 15, 1985. Initial of the lined section of the shaft was performed on January 30, 1985. At that time water seepage through cracks and construction joints in the liner was observed. Seepage into the shaft was measured at 0.35 gallons per minute (gpm).

Subsequent inspections of the exhaust shaft liner were made in February and May 1985 to observe its condition and to evaluate the need for grouting to reduce water seepage. The first occurrence of moisture on the liner was observed 25 feet below the shaft collar. The majority of water seepage was occurring between approximate depths of 569 feet and 759 feet (elev. 2840 feet and 2650 feet). Below a depth of 759 feet the entire shaft liner was wet, making it difficult to determine the exact source of seepage. Some salt accumulation was observed on the liner below the Culebra water-bearing member. The May 1985 inspection generally revealed a 1/4- to 3/8-inch thickness of salt incrustation in this area with some local accumulation up to 4 inches in thickness.

Salt accumulation at two telltale drain holes, at a depth of 857 feet (elev. 2552 feet) on the northeast and east sides of the shaft key, had resulted in the almost complete plugging of these holes. The six other drain holes had minor salt accumulation. The bottom of the key had salt stalactites hanging from the concrete but no flow of water under the concrete was observed. There was no evidence of any dissolution of salt at the concrete/salt contact.

A cement/chemical grouting program was conducted in the exhaust shaft from June 1 through July 31, 1985. An inspection of the exhaust shaft liner was made on July 30, 1985. The liner was appreciably drier than it had been prior to grouting, especially below the Culebra member. One collar pipe, for future piezometer installation at a depth of 616

feet (elev. 2793 feet), was weeping and one pipe, at a depth of 722 feet (elev. 2687 feet), was dripping. This water constituted the majority of the total seepage into the shaft. Weeping from random cracks above a depth of 617 feet appeared to be of the same magnitude as before grouting. The water ring at the base of the shaft key was relatively dry. New telltale drain holes at a depth of 870 feet (elev. 2539 feet) were all dry. Several of the original drain holes, at 857 feet, and several new holes, at a depth of 855 feet (elev. 2554 feet), were weeping slightly. No evidence of seepage at the concrete key/salt contact was observed. The grouting program reduced water seepage into the exhaust shaft to an essentially non-measurable quantity.

Cursory inspections of the exhaust shaft made during the installation of geomechanical instruments in November and December 1985 indicated no appreciable change in the condition of the shaft liner since the July 1985 inspection.

A second grouting program was conducted in the exhaust shaft during August, September and October, 1986. The program was performed at this time to reduce the possible need for grouting in the future when shaft access will be limited. The grouting was conducted on a smaller scale than in the earlier program. It consisted of injecting grout through existing sleeves from the top of the salt in the key are to the top of the Magenta member. Grouting was also performed, as required, above the Magenta through sleeves in the liner. The results of the grouting were not available at the time of publication of this report.

9.3.1.2 Geomechanical Instrumentation

The original exhaust shaft design contained no provision for the installation of geomechanical instrumentation based on the assumption that rock behavior would be similar to that in the waste shaft. However, it was subsequently decided that geomechanical instrumentation should be installed to obtain shaft-specific behavior information for later use in the shaft sealing program.

Instrument locations in the exhaust shaft were based on waste shaft instrument locations. Twenty-one piezometers, 4 pressure cells and 9 extensometers have been installed in the exhaust shaft. The instrument installation was completed on December 27, 1985, 385 days after the completion of shaft excavation. All exhaust shaft instruments are monitored remotely by the datalogger.

9.3.2 Analysis and Evaluation

The analysis and evaluation of the constructed exhaust shaft has been performed using direct observation data and geomechanical instrumentation readings from the C & SH and waste shafts. This analysis and its evaluation against reference design parameters was performed for the three major sections of the shaft: the lined section; the shaft key; and the unlined section.

The adequacy of the exhaust shaft reference design was evaluated based on a complete spectrum of geomechanical behavior including stress, strain and deformation over the planned operating life of 25 years. The analyses used creep parameters computed from the C & SH shaft and the 8 x 25-foot drifts as well as hydrostatic pressures from the waste shaft.

9.3.2.1 Lined Section

Analyses were performed for the unreinforced concrete liner in the exhaust shaft. However, because no instrumentation data from this shaft were available, the analyses were based on data obtained from the C & SH and waste shafts.

The structural analysis and design of the exhaust shaft were performed using engineering mechanics principles and design bases similar to those used for the waste shaft as described in Chapter 8. For example, both axial and flexural stresses were considered in the design of the concrete liner, with permissible stress values taken as those used for structural unreinforced concrete (ref. 8-1) utilizing the ultimate

strength design method. Loads considered in the design of the concrete liner included a hydrostatic pressure assumed to act from a depth of 250 to 844 feet; a grouting pressure equal to 1.3 times the ground-water pressure acting over one-sixth of the circumference of the liner; and stresses due to an initial imperfection of 1 inch in the roundness of the liner. Since there is no major salt strata surrounding the liner, no significant creep will occur and rock pressures against the liner were assumed to be negligible.

Based on its finished dimensions, the computational results show that the external pressure capacities and corresponding closure limits (maximum diametric changes) for different thicknesses of the exhaust shaft liner are:

Depth (feet)	Liner Thickness (inches)	Pressure Capacity (psi)	Closure Limit (inches)
15 to 500	10	320	0.140
500 to 740	14	513	0.175
740 to 844	16	611	0.190

Since no measurements of the finished liner diameter were taken during construction, the actual closure is not available for comparison.

Figure 9-1 shows the relationship between the hydrostatic design pressure and the pressure capacity of the liner. The hydrostatic pressure is identical to that used for design of the waste shaft. Because the exhaust shaft liner also has water seeping through cracks and construction joints, the hydrostatic pressure is expected to behave in the same manner as discussed for the waste shaft in Chapter 8. That is, the design hydrostatic pressure is not expected to be reached until the shaft liner is completely sealed. When the design hydrostatic pressure is reached, the liner will have a factor of safety greater than two, based on the liner pressure capacity.

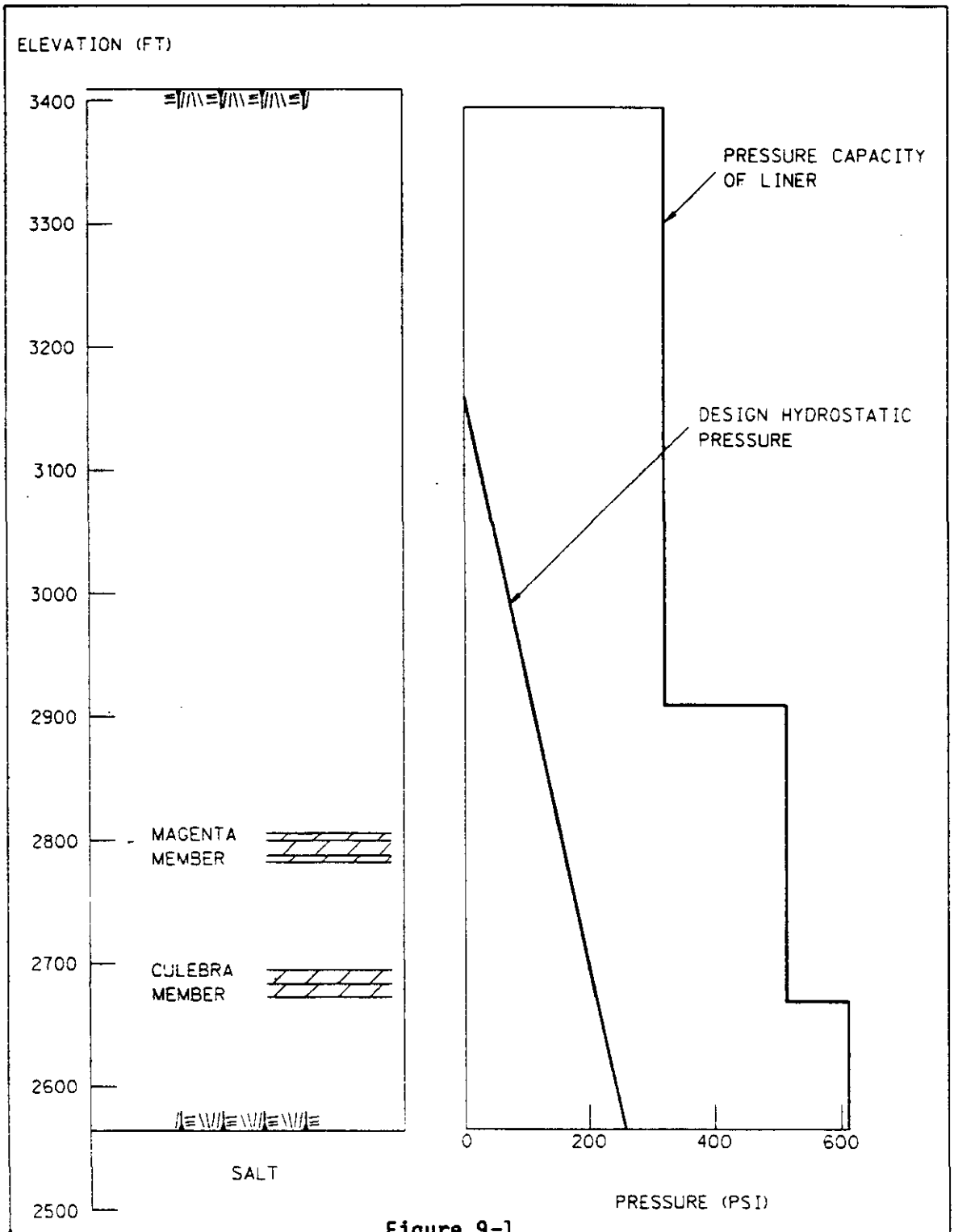

Figure 9-1

EXHAUST SHAFT LINER
LATERAL PRESSURE COMPARISON

9.3.2.2 Shaft Key

The exhaust shaft key was designed to withstand a lateral pressure equal to 50 percent of the vertical overburden pressure or about 60 ksf. A nonlinear finite element analysis, similar to that performed for the waste shaft key described in Chapter 8, was used to simulate the long-term creep interaction of the salt and the concrete key. The creep behavior of the salt was simulated using a power law (equation C.4-6 in Appendix C). For conservatism, the shrinkage effects and creep of the concrete were not taken into account in the analysis.

Model Simulation. The finite element model for the exhaust shaft key and surrounding salt consists of a single layer of quadrilateral axisymmetric ring elements as shown on Figure 9-2. An inner element of the model represents a segment of the concrete key; however, this element is not tied to the surrounding salt deposits until that time when the concrete for the shaft key is actually placed. All depth dependent input values, such as overburden stresses, initial lithostatic state, etc., were computed based on a depth of 891.5 feet, low in the key, where such values are at a maximum. Halite is the prevalent material present at the base of the shaft key and its properties were used for the parameters modeling the salt deposits surrounding the key.

The analytical procedure used to perform the creep analysis for the exhaust shaft key was similar to that used for the waste shaft key analysis described in Chapter 8. However, in the finite element model for the exhaust shaft, the key diameter was enlarged to 21 feet with a finished inside diameter of 14 feet.

9.3.2.3 Unlined Section

The structural behavior of the unlined section of the exhaust shaft was also computed using the MARC Finite Element Program discussed in Chapter 6. The analysis computed the actual structural behavior by utilizing applicable in situ data from the C & SH shaft and the horizontal drifts.

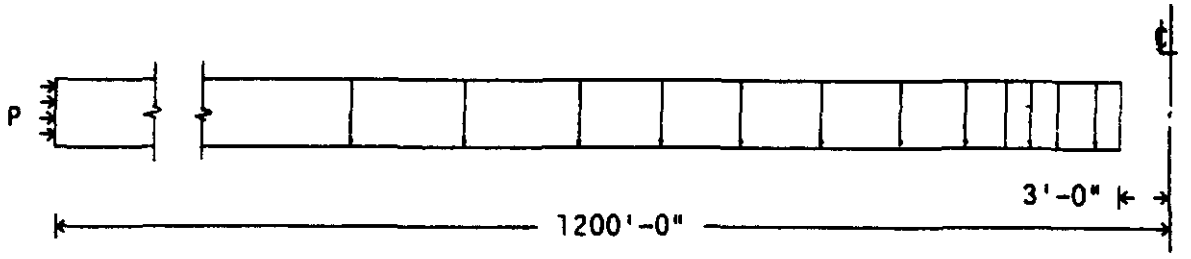

(A) BEFORE ENLARGEMENT

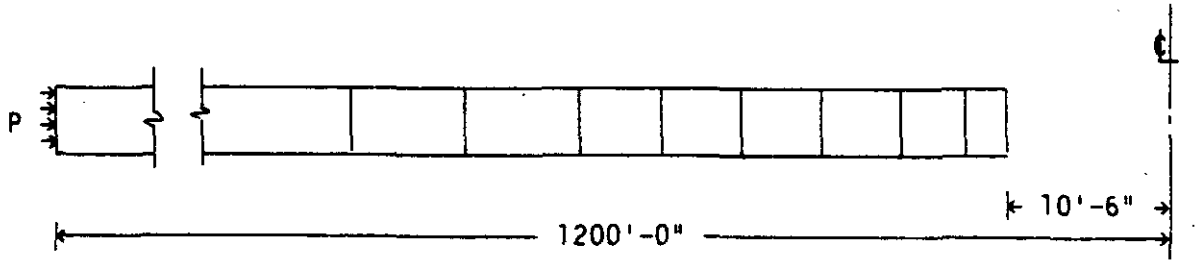

(B) AFTER ENLARGEMENT

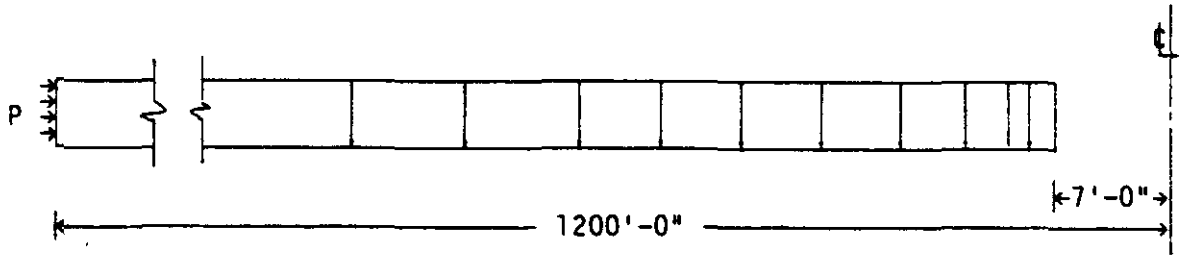

(C) AFTER KEY PLACEMENT

Figure 9-2

EXHAUST SHAFT KEY
FINITE ELEMENT MODEL

M

Model Simulation. The finite element model used for the unlined section of the exhaust shaft utilizes a single horizontal row of 70 quadrilateral axisymmetric ring elements. The model, shown on Figure 9-3, has its upper and lower horizontal boundaries restrained against vertical movement and has a constant lithostatic uniform pressure, equal to 2,066 feet of overburden, applied to its outside vertical boundary. The same lithostatic pressure was initially applied to the inside vertical boundary; however, that pressure was later removed from the inside boundary to simulate the drilling of the 6-foot diameter pilot bore.

The analysis simulates the salt creep until that time when the 6-foot diameter hole was enlarged to its present 15-foot diameter. The shaft enlargement is simulated in the model by removing those ring elements which are located within the newly-excavated 15-foot diameter. With the enlarged shaft configuration, simulated salt creep for another 25 years was analyzed.

Determination of Creep Parameters. Since the stratigraphy surrounding the C & SH shaft is similar to that surrounding the exhaust shaft, the creep parameters determined from the in situ salt behavior in the C & SH shaft were assumed to be valid for correlating analytical results for the exhaust shaft from normalized time to real time. The secondary creep parameter C for the C & SH shaft was found to equal 5.70×10^{-21} $ksf^{-4.9}$ sec^{-1}. Since early in situ measurements were not available for the C & SH shaft, the primary creep parameters A and z were determined from in situ data from the horizontal drifts and were found to be 3.2 and 1.1×10^{-7} sec^{-1}, respectively.

Chapter 7 presents specific details on the computation of the secondary creep parameter C from the C & SH shaft. Chapter 10 presents the computation of the primary creep parameters A and z from the drifts.

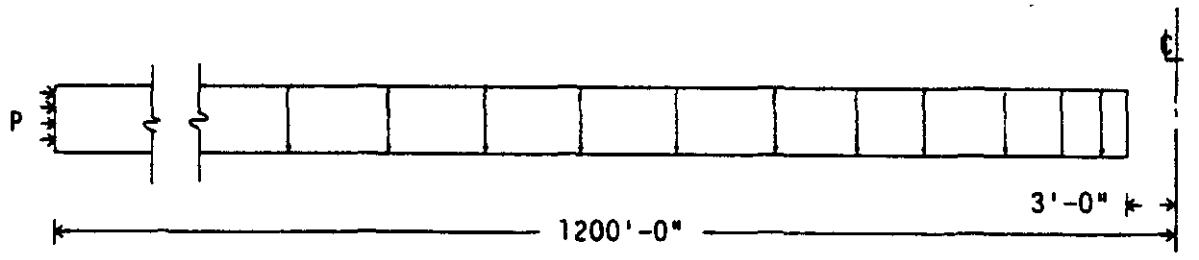

(A) BEFORE ENLARGEMENT

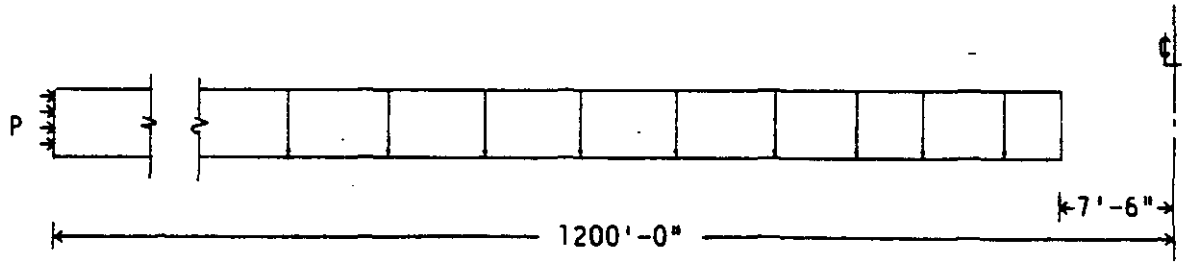

(B) AFTER ENLARGEMENT

Figure 9-3

EXHAUST SHAFT UNLINED SECTION
FINITE ELEMENT MODEL

9.3.3 Prediction of Future Behavior

This subsection presents the results of the analysis and evaluation of the exhaust shaft. Predictions of future behavior for the lined section, key and unlined section are discussed.

9.3.3.1 Lined Section

The cracks in the concrete liner of the exhaust shaft are primarily tension cracks formed during restrained shrinkage we described in Chapter 8 with respect to the waste shift liner. These are neither unusual nor unexpected. Grouting of the cracks, as well as the leaking construction joints, will be required to meet the design criteria regarding ground-water control.

As discussed in Chapter 7, subsection 7.3.3.1, there is no reason to expect that the potentiometric surface at the WIPP site will exceed the design basis depth of 250 feet below the ground surface over the operating life of the facility. In the future, the recently installed piezometers will permit monitoring of the actual water pressure on the liner. Even if the water pressure rises to the design pressure, the pressure capacity of the liner will provide a sufficient margin of safety.

9.3.3.2 Shaft Key

The elapsed time from the drilling of the 6-foot diameter pilot bore to its widening to 21 feet in the key area and construction of the concrete key was approximately 316 days. Figure 9-4 shows the predicted lateral pressure curve for the concrete key based on the finite element analysis. The key was designed as a compression cylinder in accordance with the strength design method for reinforced concrete (ref. 7-5) using an ultimate hoop stress of 4.25 ksi. Using a load factor of 1.7 for lateral loads, the maximum allowable hoop stress in the key is 2.50 ksi. This hoop stress results in an allowable lateral rock pressure of 154 ksf based on the diameter of the key. Figure 9-4 shows a lateral pressure on the key of approximately 72 ksf

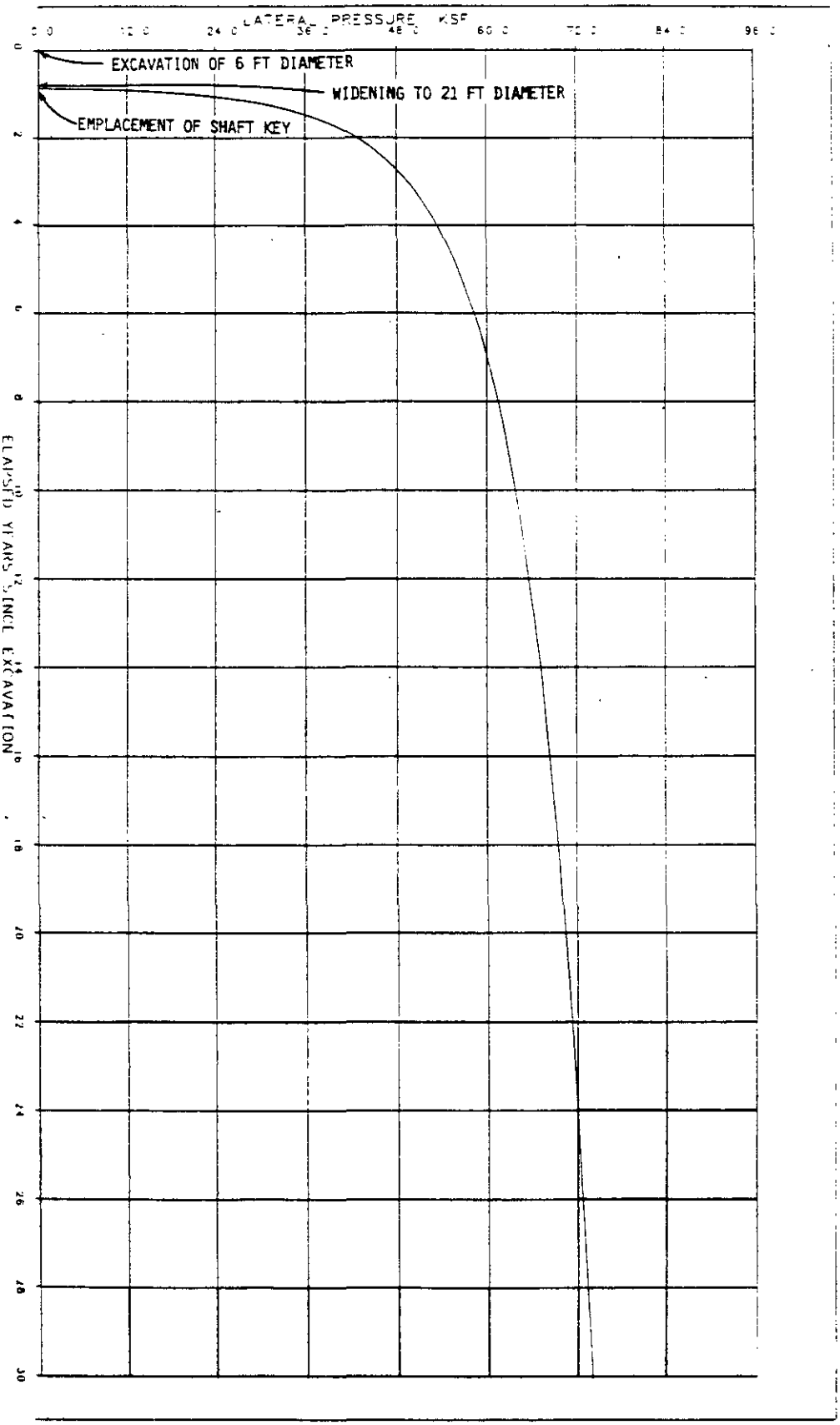

Figure 9-4

EXHAUST SHAFT KEY
LATERAL PRESSURE PREDICTION

at 25 years. Although higher than the design basis lateral pressure of 60 ksf, this value is about 50 percent of the allowable lateral pressure. In addition, the lateral pressure would actually be less than 72 ksf if concrete shrinkage and creep were taken into account in the finite element analysis.

Although no shrinkage cracks have been found in the reinforced concrete in the key, their presence would not be unexpected. They are common to most reinforced concrete structures and should not be of major concern.

9.3.3.3 Unlined Section

Figures 9-5 and 9-6 show predictions for radial and tangential (hoop) stress distributions relative to the overburden stress at different times for the unlined section of the exhaust shaft. Figure 9-5 shows the zone around the shaft opening where radial stresses are affected and their decrease in magnitude over time. The computational results indicate that tangential stresses are affected only within a radius of approximately 120 feet.

Figures 9-7 and 9-8 show predictions of the effective stress and effective creep strain distributions in the unlined section of the exhaust shaft. The magnitude of the effective stress in the shaft wall at 25 years approaches 140 ksf while the effective creep strain reaches a value of approximately 0.037.

Figure 9-9 shows approximately 6 inches of diametric closure in the unlined section of the exhaust shaft at a depth of 2,066 feet (elev. 1343 feet) over the 25-year operating life of the shaft.

9.4 CONCLUSIONS AND RECOMMENDATIONS

Design validation of the exhaust shaft requires an assessment of the compatibility of the design criteria, design bases and design configurations used for the reference design. The following discussion presents conclusions and recommendations regarding validation of the

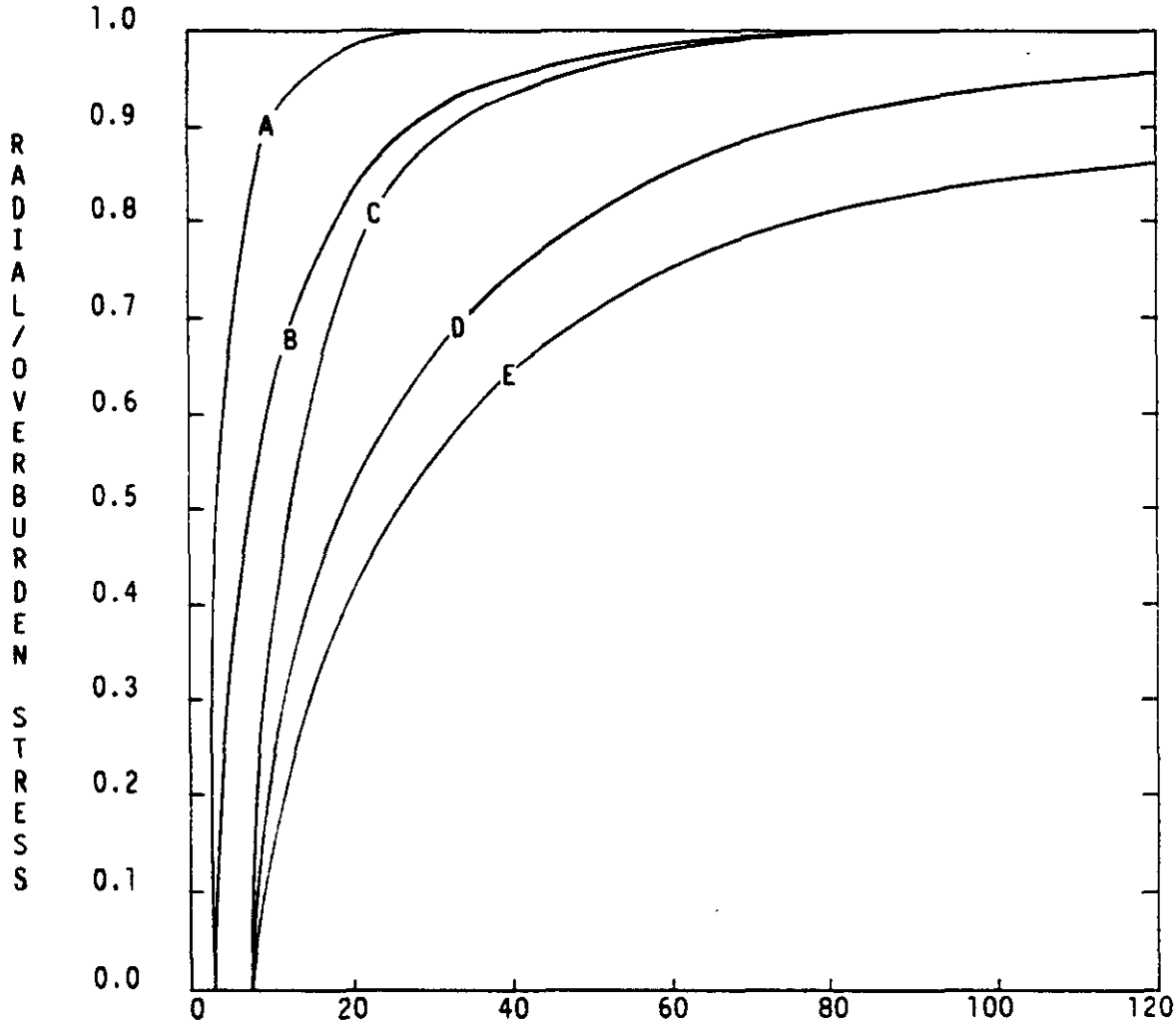

A - IMMEDIATELY AFTER EXCAVATION OF 6-FT DIAMETER SHAFT
B - IMMEDIATELY BEFORE WIDENING TO 15-FT DIAMETER
C - IMMEDIATELY AFTER WIDENING TO 15-FT DIAMETER
D - ONE YEAR AFTER WIDENING OF SHAFT
E - 25 YEARS AFTER WIDENING OF SHAFT

M

Figure 9-5

EXHAUST SHAFT UNLINED SECTION
RADIAL STRESS DISTRIBUTION AT ELEVATION 1343 FEET

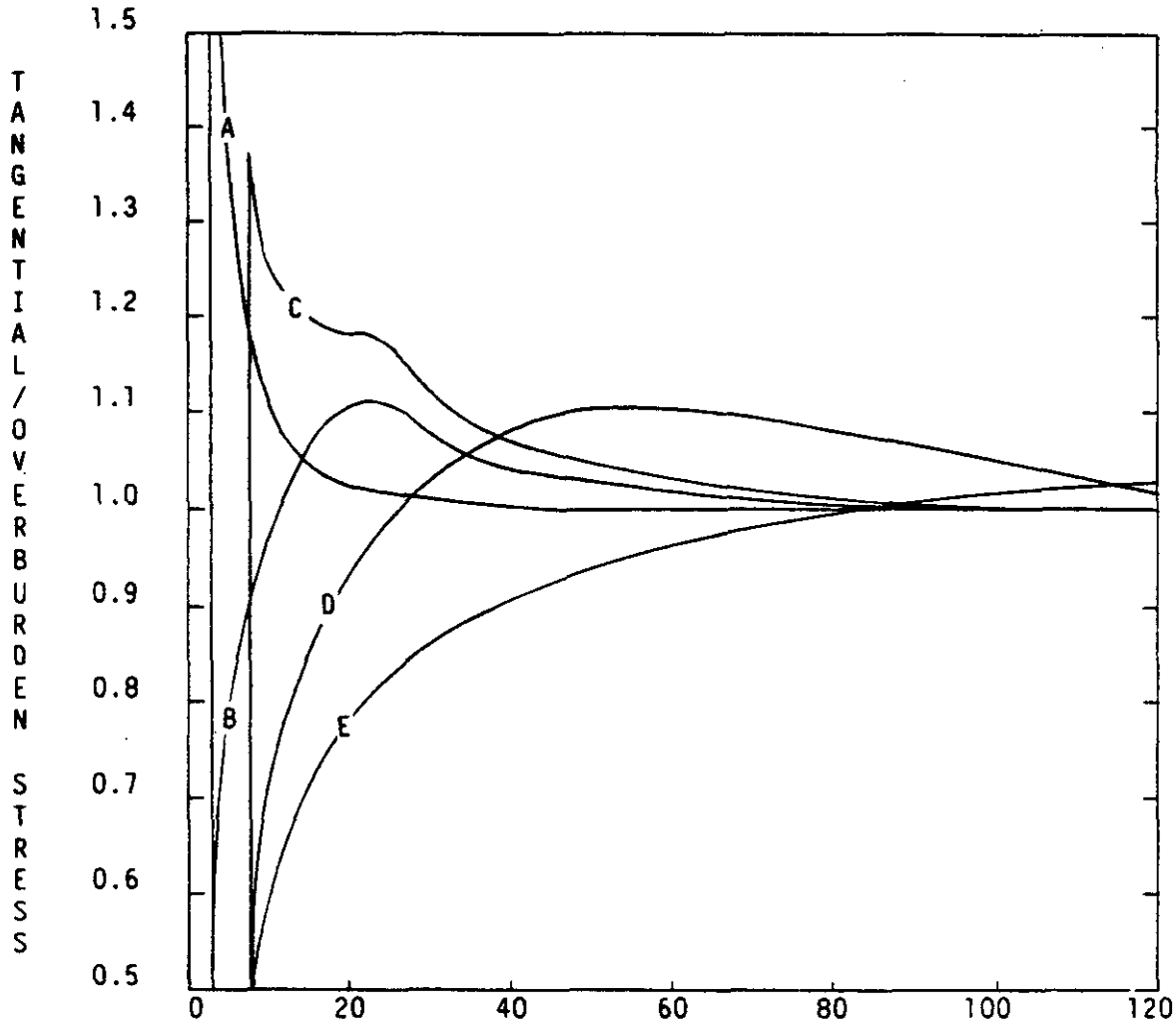

A - IMMEDIATELY AFTER EXCAVATION OF 6-FT DIAMETER SHAFT
B - IMMEDIATELY BEFORE WIDENING TO 15-FT DIAMETER
C - IMMEDIATELY AFTER WIDENING TO 15-FT DIAMETER
D - ONE YEAR AFTER WIDENING OF SHAFT
E - 25 YEARS AFTER WIDENING OF SHAFT

Figure 9-6

EXHAUST SHAFT UNLINED SECTION
TANGENTIAL STRESS DISTRIBUTION AT ELEVATION 1343 FEET

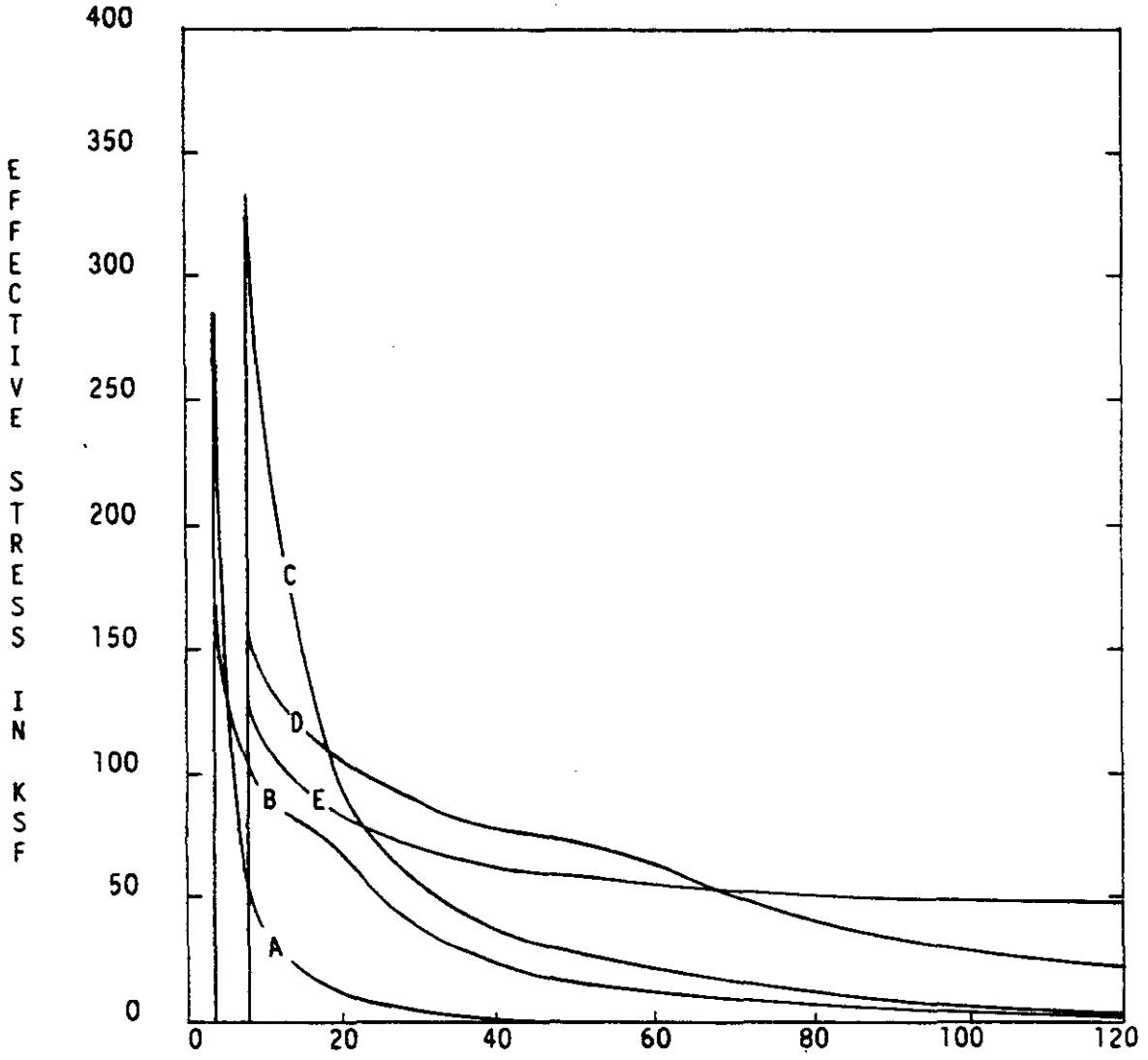

A - IMMEDIATELY AFTER EXCAVATION OF 6-FT DIAMETER SHAFT
B - IMMEDIATELY BEFORE WIDENING TO 15-FT DIAMETER
C - IMMEDIATELY AFTER WIDENING TO 15-FT DIAMETER
D - ONE YEAR AFTER WIDENING OF SHAFT
E - 25 YEARS AFTER WIDENING OF SHAFT

Figure 9-7

EXHAUST SHAFT UNLINED SECTION
EFFECTIVE STRESS DISTRIBUTION AT ELEVATION 1343 FEET

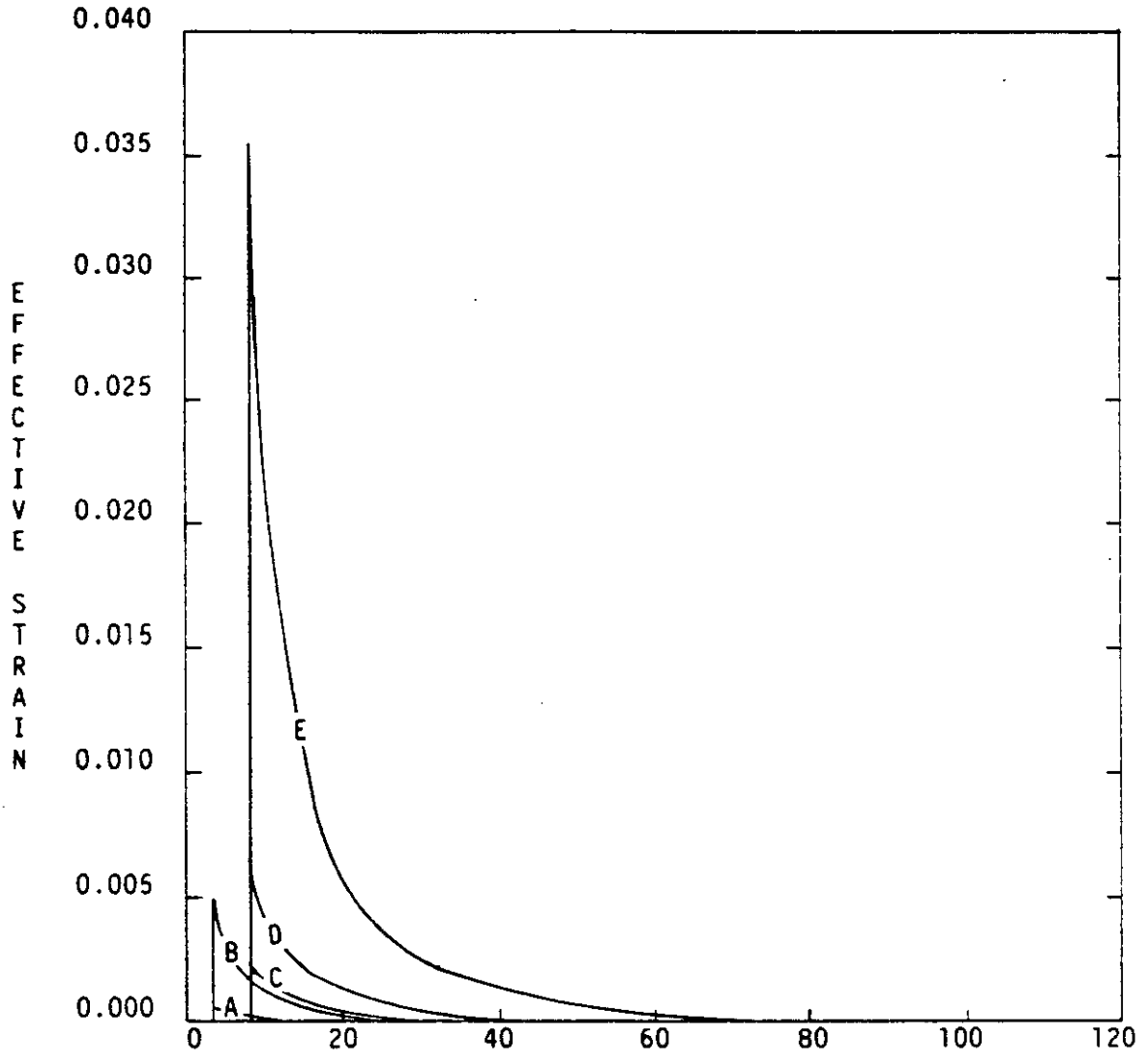

A – IMMEDIATELY AFTER EXCAVATION OF 6-FT DIAMETER SHAFT
B – IMMEDIATELY BEFORE WIDENING TO 15-FT DIAMETER
C – IMMEDIATELY AFTER WIDENING TO 15-FT DIAMETER
D – ONE YEAR AFTER WIDENING OF SHAFT
E – 25 YEARS AFTER WIDENING OF SHAFT

Figure 9-8

EXHAUST SHAFT UNLINED SECTION
EFFECTIVE CREEP STRAIN DISTRIBUTION AT ELEVATION 1343 FEET

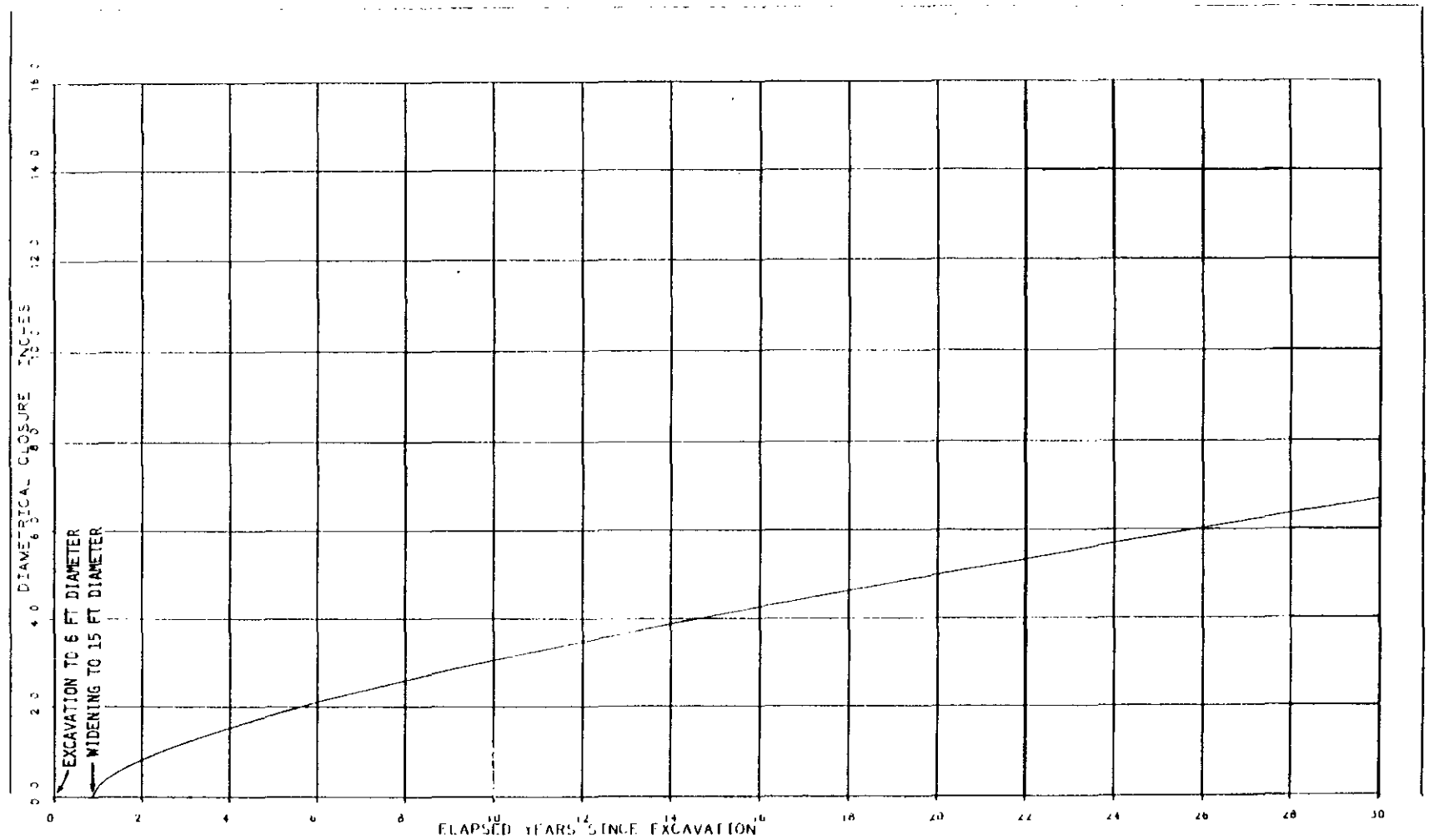

Figure 9-9

EXHAUST SHAFT UNLINED SECTION
CLOSURE PREDICTION AT ELEVATION 1343 FEET

exhaust shaft design as they pertain to the design elements identified in Section 9.2. These design elements stipulate the requirements that the exhaust shaft must meet in terms of shaft stability, deformation, water pressure and water control. Other conclusions and recommendations that are a product of the design validation process are also presented.

9.4.1 Conclusions

The stability of the exhaust shaft has been evaluated using analytical calculations, finite element modeling and analysis of data from the C & SH and waste shafts. The conclusions regarding shaft stability are the same as those for the waste shaft. The water pressure exerted on the shaft liner is currently less than the design hydrostatic pressure. If the hydrostatic pressure increases to its design limit, the liner will remain stable because its pressure capacity exceeds the design hydrostatic pressure by a factor greater than two. The cracks in the liner are not expected to result in any structural instability.

Analytical results show that the lateral pressure on the shaft key at the end of the 25-year operating life will be approximately 72 ksf. Although this pressure exceeds the design basis lateral pressure of 60 ksf, the allowable lateral pressure on the key is 154 ksf, or more than twice the predicted lateral pressure at 25 years. This provides a sufficient margin of safety against failure. If concrete shrinkage and creep were taken into account in the analysis, the margin of safety would be even greater.

The analytical results also show the redistribution of stresses around the unlined section of the shaft due to the effects of salt creep. Based on the computed vertical, horizontal and effective stresses in the unlined section, the magnitude of stresses immediately adjacent to the opening decreases and the stress arch around the opening migrates away with time. The maximum stress occurs immediately after excavation and is followed by relaxation due to creep behavior. Therefore, the stresses will not cause a future stability problem in the unlined

section of the shaft. The analysis shows the locations of effective creep strain concentrations at different times around the opening in the unlined section. Based on the predicted values of effective creep strain and the strain limit discussed in Chapter 6, the exhaust shaft will remain structurally stable within the limits required for safety during its operating life.

The analysis also predicts that the maximum diametric closure in the unlined section at the end of the operating period will be approximately 6 inches. Based on the predicted deformations and closures, the exhaust shaft will meet the requirements stated in the design criteria. The design basis requirement that the 15-foot diameter unlined section allow for salt creep over its operating life will be met.

As in the waste shaft, water is entering the exhaust shaft through cracks and construction joints in the concrete liner. The amount of water seepage was greatly reduced by grouting conducted after construction. The small amount of water still reaching the open shaft quickly evaporates in the upcast flow of exhaust air. While the exhaust fans are operating, no water reaches the underground facility level. The water seals behind the shaft concrete key appear to be functioning as intended at the bottom of the key. No water is seeping from the concrete/salt interface. There is no evidence of salt dissolution behind the key.

The reference design for the exhaust shaft has been validated in accordance with the objectives of the design validation program, based on the analyses, evaluations and predictions of future behavior presented in this chapter. With one exception, the exhaust shaft reference design complies with the design criteria and the design bases. The criterion that the liner shall prevent ground-water flow into the shaft has not been met. However, the water currently seeping into the shaft is not considered to be detrimental to shaft stability or function. No modifications to the exhaust shaft reference design are required.

9.4.2 Recommendations

Based on the results of design validation, recommendations similar to those for the waste shaft are made for the exhaust shaft:

(1) Validation of the exhaust shaft key and unlined section relied on analysis and modeling using in situ data from the C & SH and waste shafts. It is recommended that the numerical modeling be repeated, prior to the first receipt of waste, using in situ data from the exhaust shaft instruments. This analysis should be repeated periodically for the comparison of in situ data against design parameters.

(2) The exhaust shaft should be inspected by qualified personnel at regularly scheduled intervals. The liner should be inspected for renewed seepage and grouting performed if an amount of water considered sufficient to affect the liner's stability or functional purpose is observed. The key should be inspected for water seeping from behind the key at its base. If any is detected, grout should be injected above the top water seal. Grout should not be placed behind the key below the top seal. If this cannot be avoided, the grout must be a chemical gel (or other non-rigid grout) and must be compatible with both the existing water seal material and with the requirements of the Plugging and Sealing Program.

CHAPTER 10
DRIFTS

10.1 INTRODUCTION

This chapter presents the results of validation of the reference design for the underground drifts. Discussions are presented on the reference design, data collected from the openings, its analysis and evaluation, and predictions of future behavior. Conclusions and recommendations pertaining to the reference design are presented based on the results of the validation process.

The term drifts includes all horizontal underground openings except the shaft stations, test rooms, and storage area rooms and their associated drifts. Discussions of the shaft stations are presented in Chapters 7 and 8. Discussions of the test rooms, storage rooms and storage area drifts are presented in Chapters 11 and 12.

The largest drifts planned for the underground facility were initially excavated 8 feet high and 25 feet wide. These drifts have been or will be enlarged to 12 feet high. The present 12-foot high, 25-foot wide drifts were excavated earlier than most of the smaller drifts and, therefore, have the longest history of in situ data collection. Because these 12 x 25-foot drifts are the largest to be excavated, they also have the most critical dimensions. Consequently, the analyses, evaluations and predictions are based primarily on these larger drifts. The smaller drifts and rooms are, therefore, considered to be validated as a result of the validation of the larger 12 x 25-foot drift reference design.

10.2 DESIGN

This section presents the design criteria and design bases used to develop the reference design of the drifts.

10.2.1 Design Criteria

The design criteria established for the design of the WIPP underground facility are discussed in Chapter 2 and summarized in Table 2-1. Table 2-1 presents the major criteria affecting underground design, including such items as waste receipt rate, type of waste, backfill requirement, etc. Those criteria requiring evaluation of their suitability for design validation are indicated in Table 2-1. The remaining criteria contained in the Design Criteria document (ref. 2-7) do not require evaluation.

Three of the indicated criteria pertain directly to the drift reference design. The first criterion states that the underground openings shall be designed to provide structurally stable excavations and pillars. "Stable" is defined in the criteria document to mean that deformations of excavations and pillars are to remain within the limits required for structural function, ventilation and safety. The second criterion states that the underground opening reference design shall provide maximum stability for the excavated rooms and drifts. The third criterion stipulates that the underground excavation shall be designed to accommodate creep closure and maintain the minimum dimensions required for the operating life of the opening. Not only are these criteria to be evaluated for their suitability, but the reference design configurations based on them must also be evaluated. These reference design configurations were discussed in Chapter 3.

10.2.2 Design Bases

The design bases comprise the second level of the design documents. They outline specific design requirements that were followed in designing the final drift configurations. Only those design bases that apply directly to the underground drift configurations are discussed in this subsection. The Design Basis, Underground Excavations (refs. 2-9 and 2-18), Design Basis, Underground Shops and Facilities (ref. 2-20), and Design Basis, Geomechanical Instrumentation (ref. 2-17) should be referred to for details of the appropriate design bases used for the underground drifts. None of these design bases contained elements

pertaining specifically to the drifts that required evaluation during the validation program. Those bases that required evaluation for validation pertain only to the storage area drifts and are discussed in Chapter 12.

The design bases specify that excavation within the shaft pillar area shall be the minimum required to meet the operational and safety requirements of the waste storage level. The area extraction ratio was, therefore, kept below 15 percent in this area.

The maximum tolerance for excavation of the roof, floor and walls shall be plus six inches. In no case shall the finished dimensions be less than those specified by the design. The minimum vertical dimension for equipment clearances used to meet this basis was 11 feet.

Supports for underground workings shall comply with Federal and New Mexico codes. The use of rock bolts and wire mesh in specific areas shall be determined by mine conditions and code requirements. Entry roofs, walls and floors shall be checked periodically for loose salt in accordance with applicable codes. Methods of locating gas or brine accumulations shall be implemented, such as drilling holes ahead of the excavation and testing for the presence of gas.

A geomechanical instrumentation system shall be installed to provide in situ measurement data for design verification or modification and for subsequent operational planning. In addition, the instrumentation system shall monitor stress change, closure and creep to provide a record of the structural stability of the drifts and to provide early warning of abnormal conditions for operational safety.

Deformation measurements in the drifts shall be measured as a function of horizontal and vertical closure. Salt creep and stress distributions around the drifts and at intersections shall also be measured.

The instrumentation shall provide the primary detection of changes in structural behavior. Visual observations shall follow any detected abnormal strain, pressure or deformation for evaluation of the safety of the underground working places. In addition, a program shall be provided for periodic visual inspection of all underground working places.

10.3 DESIGN VALIDATION PROCESS

Validation of the reference design of the underground drifts includes the collection of data and the presentation of results based on its analysis and evaluation. The results of the design validation process are used to present conclusions regarding the compatibility of the design criteria, design bases and design configurations, and recommendations for modifications, if any. This section presents the data collected and predictions of future drift behavior based on analysis and evaluation of the data.

10.3.1 Data Collection

Data pertaining to the underground drifts was collected from various sources. Geologic data was acquired from geologic mapping and core drilling. These data verified the stratigraphic continuity at the facility level and are discussed in detail in Chapter 6. Data were also acquired from periodic visual inspections and from geomechanical instrumentation. Collection of these data are described in the following subsections.

10.3.1.1 Field Observations

Various aspects of underground behavior are evaluated by qualitative observations and documentation. Visual inspections of the drifts include observations of their general surface conditions in response to stress redistribution and creep. These conditions include shallow spalls from the roof and walls, especially at their intersection; and vertical fracturing in the pillars, both at corners and parallel to the walls. In addition to visual inspections, other techniques are used. Boreholes are surveyed using video cameras and displacements,

separations and fracturing of geologic strata surrounding the boreholes are detected using a simple probe. Surveys of underground conditions have been performed at least once every 3 months. Each survey is documented in a GFDR beginning with the February 1984 edition (refs. 4-12 through 4-19).

Recently, a special program was conducted to determine the effect of excavation induced deformation on the salt strata surrounding the facility level. An array of boreholes was drilled into the roof and floor at 30 locations in the drifts and test rooms during May through July 1986. These arrays are shown on Figure 10-1. These boreholes were used to locate separations and fractures in the halite and anhydrite near the horizontal underground openings. This Excavation Effects Program was instigated after the discovery of significant fracturing beneath the southern half of Test Room 3 (Room T). The objectives of this excavation effects study were to determine if fracturing of this magnitude has occurred anywhere else and to investigate existing conditions at selected localities throughout the facility.

The documented field observations can be separated into four categories: roof and wall spalling; pillar fracturing; roof displacements and separations; and floor displacements, separations and fracturing.

Roof and Wall Spalling. During and immediately after excavation, a sounding survey of the roofs of all drifts was performed. Each survey identified areas of potential instability, such as drummy or slabby salt. Remedial work was accomplished immediately and included scaling, additional excavation, or rock bolting. Comprehensive sounding surveys were also performed in every underground opening in July 1983 and November 1984. The behavior of the roof and walls is documented in the table entitled "Condition of Roof and Walls" in each GFDR.

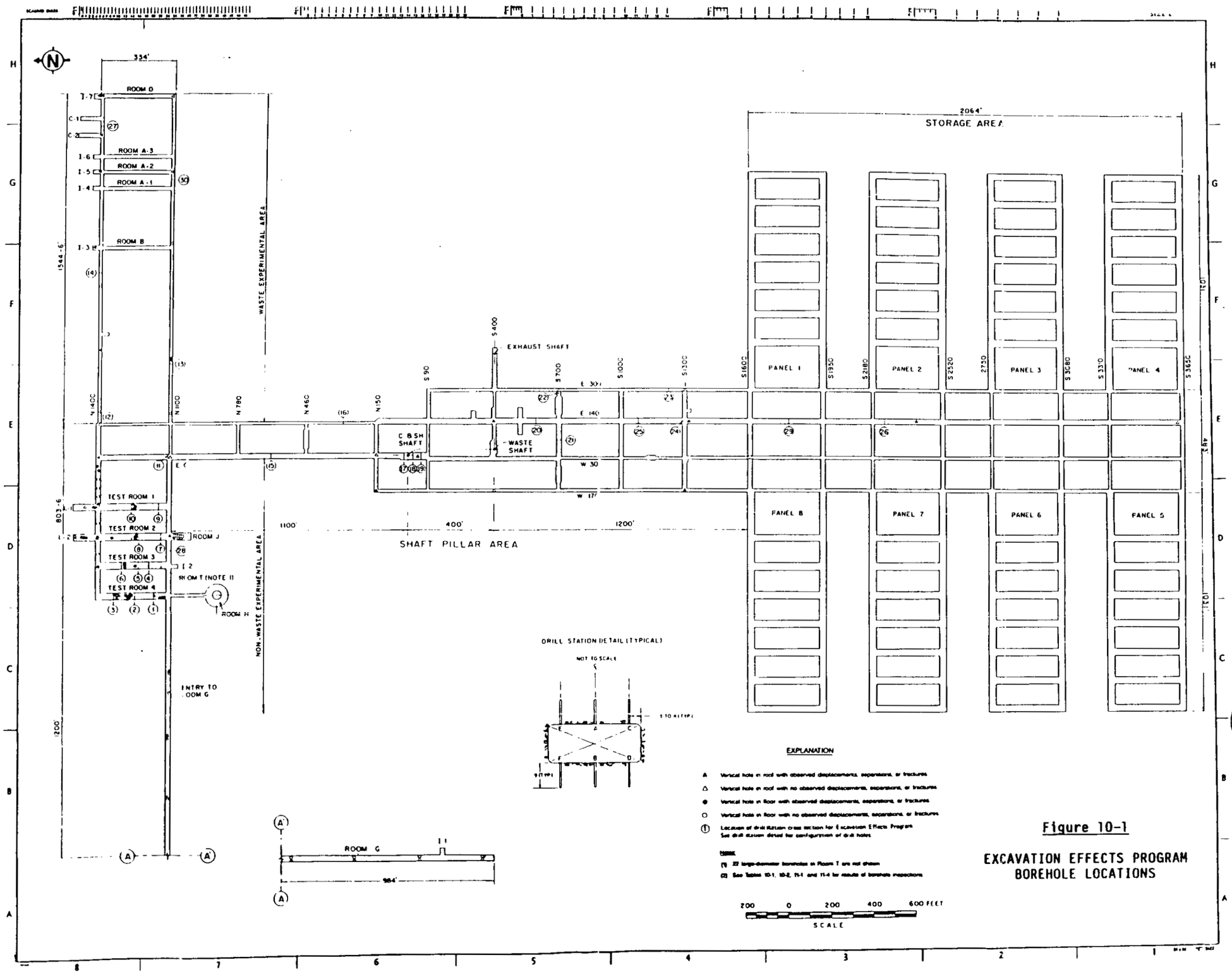

Figure 10-1

EXCAVATION EFFECTS PROGRAM
BOREHOLE LOCATIONS

Pillar Fracturing. Vertical fractures have developed in the corners formed by drift intersections. These fractures began appearing about 3 to 6 months after excavation. Site geologists have monitored the growth of these fractures and have included their observations in the GFDRs.

Vertical fractures parallel to the drift walls have been detected in several horizontal boreholes. These fractures were not present at the time of drilling. They were first observed in May 1986 and occur within 1 to 2 feet of the wall surface.

Roof Displacements and Separations. Horizontal displacements and vertical separations have been detected in some open boreholes in the drifts during the past 2 years. Periodic inspections of all accessible boreholes in the drifts have been made since September 1985. The results of these inspections in the roof holes are presented in Table 10-1.

Visual inspections were conducted directly or remotely using a video camera and/or probe. The probe used was described in Chapter 7, subsection 7.3.1.4. Depths to displacements and separations were measured with a tape measure. Relative horizontal displacements were measured where possible or estimated.

The recently conducted Excavation Effects Program consisted of drilling numerous arrays of 1 7/8-inch and 3-inch diameter holes at selected locations along the drifts (Figure 10-1). The holes were drilled approximately 9 feet into the roof and floor and inspected using a probe. The results of the inspection of these holes are presented in Table 10-2.

The N1100 and N1420 drifts were excavated eastward to E1680 in early 1984. These drifts incline upward to the experimental area. The roofs of both drifts intersect anhydrite beds "a" and "b". Slabby rock at the intersection was removed by the mining machine and rock bolts

Table 10-1

DRIFTS
RESULTS OF INSPECTION OF VERTICAL BOREHOLES IN ROOFS

Hole	Date Completed	Hole Size (in.)	Depth (ft)	Approximate Location	Observed Condition*
DH-01	2-10-84	3	50.8	N1424/E439.5	None
DH-03	2-7-84	3	48.8	N1112/E444	D
DH-03A	3-12-84	3	49.9	N1112/E450.5	D
DH-05	3-9-84	3	51.0	N1463/E972	D
DH-07	2-22-84	3	49.8	N1112/E976.5	None
DH-09	3-14-84	3	51.1	N1432/E1332.5	None
DH-11	3-6-84	3	50.9	N1112/E1332.5	None
DH-13	3-28-84	3	13.8	N1424/E1690	D, S
DH-13A	3-29-84	3	49.0	N1425/E1691	D, S
DH-13B	4-5-84	3	21.0	N1425/E1695	D, S
DH-15	3-21-84	3	51.0	N1104/E1688.5	None
DH-17	1-19-84	3	52.0	N1104/E1688	None
DH-19	1-21-84	3	51.6	N1107/E206.5	None
DH-21	2-27-84	3	50.4	N1421/E786	None
DH-23	2-15-84	3	51.0	N1112/E781	None
DH-25	3-30-84	3	51.8	N1422/E1510	D, S
DH-27	7-27-84	3.5	50.5	N1107/W682	None
DH-29	7-25-84	3.5	50.4	N1099/W982	None
DH-29A	9-12-84	3.5	35.0	N1099/W987	None
DH-31	7-19-84	3.5	50.5	N1099/W1282	None

* D = displacement; S = separation; F = fracturing

Table 10-1 (continued)

DRIFTS
RESULTS OF INSPECTION OF VERTICAL BOREHOLES IN ROOFS

Hole	Date Completed	Hole Size (in.)	Depth (ft)	Approximate Location	Observed Condition*
DH-31A	7-24-84	3.5	49.2	N1099/W1280	None
DH-31B	9-12-84	3.5	4.9	N1099/W1261	None
DH-33	7-18-84	3.5	50.5	N1099/W1582	None
DH-33A	9-13-84	3.5	4.1	N1099/W1570	None
DH-35	1-27-85	3.5	52.0	N1102/W1882	None
DH-37	1-26-85	3.5	51.5	N1101/W2182	None
DH-39	1-24-85	3.5	50.7	N1101/W2482	None
DH-41	1-24-85	3.5	49.9	N1101/W2782	None
DH-205	2-18-83	3	50.7	N1410/E0	None
DH-211	12-19-82	3	50.0	S1320/E163	None
DH-219	1-14-83	3	51.0	S2422/E162	None
DH-227	1-28-83	3	51.7	S3656/E147	None
DH-301	8-30-84	3.5	50.8	N150/W170	D
DH-303	9-4-84	3.5	51.4	S400/W170	None
DH-313	7-10-84	3	19.6	S1300/E300	None
DH-313A	7-12-84	3	50.2	S1300/E299	None
DH-315	9-6-84	3.5	50.3	S1300/W170	D
DH-317	7-6-84	3	50.1	S1600/W33	None
DH-317A	7-6-84	3	5.0	S1600/W30	None
DH-317B	9-7-84	3.5	51.0	S1597/W30	None
DH-319	9-10-85	3.5	51.1	S700/E300	None

Table 10-1 (continued)

DRIFTS
RESULTS OF INSPECTION OF VERTICAL BOREHOLES IN ROOFS

Hole	Date Completed	Hole Size (in.)	Depth (ft)	Approximate Location	Observed Condition*
OH-2	8-83	4	20	S410/E147	None
OH-3	8-83	4	20	Room 2 centerline	S, F
OH-4	8-83	4	20	N1110/W365	S
OH-6	8-83	4	20	N1110/W5	None
OH-7	8-83	4	20	S70/E0	D, S, F
OH-8	8-83	4	20	N140/E0	None
OH-9	2-84	4	15.4	N1433/W232	S, F
OH-10	2-84	4	21.0	N1420/W218	D
OH-11	2-84	4	19.7	N1433/W365	None
-	-	5	10	Room L1 centerline	None
L2PU-02	-	5	9.2	Room L2 centerline	None

Table 10-2

EXCAVATION EFFECTS PROGRAM

BOREHOLE INSPECTION SUMMARY

SECTION	OPENING DIMENSIONS (HxW-FT)	EXCAVATION - DATE	LOCATION	DATE DRILLED	DATE INSPECTED	OBSERVED CONDITIONS					
						ROOF HOLES			FLOOR HOLES		
						E	A	C	F	B	D
11	12x25	2/83 (FLOOR LOWERED 4 FT 12/83)	N110, W02	5/30/86	6/02/86	C	NONE	C (POSSIBLY CLAY G)	C	S, C	C
12	12x14	2/83	N1430, E140	6/05/86	6/10/86	S, C	C	C	S, C	S	S(?), C
13	8x14	1/84	N810, E439	6/20/86	6/30/86	D *	NONE	NONE	NONE	NONE	NONE
14	12x14	2/84	N1430, E875	6/06/86	6/10/86	S	S(?)	S	S(?)	C	S(?)
15	12x25	2/83 (FLOOR LOWERED 4 FT 12/83)	N626, W02	6/20/86	6/30/86	NONE	C	S, C	C	S, C	C
16	8x14	2/83	N305, E147	7/15/86	7/18/86	NO ROOF HOLES			NONE	C	C
17	12x32	10/82	C&SH SHAFT STATION - N028	5/30/86	6/02/86	C	NONE	F	NONE	S, F	NONE
18	17x35	6/82	C&SH SHAFT STATION - S024	6/04/86	6/04/86	C	S, F	F	S	NONE	S
19	15x35	6/82	C&SH SHAFT STATION - S056	6/03/86	6/04/86	F, C	F	F	F, C	C	C
20	14x25	12/82 (FLOOR LOWERED 5/84)	S592, E155	7/10/86	7/11/86	NONE	NONE	NONE	S, C	NONE	NONE
---	15x35	6/82	C&SH SHAFT STATION - ELECTRICAL SUBSTATION	6/05/86	6/06/86					X	Y
										S, C	S, C
21	12x20	7/85	S700, E66	7/08/86	7/09/86	NONE	NONE	NONE	NONE	S	C (POSSIBLY CLAY E)
22	12x14	5/84; 7/84	S700, E300	7/08/86	7/09/86	NONE	NONE	NONE	C	NONE	NONE
23	12x14	7/84	S890, E229	7/09/86	7/10/86	NONE	NONE	C	NONE	C	C
24	12x20	12/82; 6/85; 6/84	S1300, E155	7/09/86	7/10/86	NONE	NONE	NONE	NONE	NONE	NONE

Table 10-2 (continued)

EXCAVATION EFFECTS PROGRAM
BOREHOLE INSPECTION SUMMARY

SECTION	OPENING DIMENSIONS (HxW-FT)	EXCAVATION DATE	LOCATION	DATE DRILLED	DATE INSPECTED	OBSERVED CONDITIONS					
						ROOF HOLES			FLOOR HOLES		
						E	A	C	F	B	D
25	12x25	12/82 (FLOOR LOWERED 5/84)	S829, E155	7/9/86	7/10/86	NONE	NONE	NONE	C	C	C
26	8x25	1/83	** S2205, E154	7/16/86	7/18/86	NO ROOF HOLES			NONE	NONE	C
27	12x14	3/84	** N430, E555	7/17/86	7/18/86	NO ROOF HOLES			NONE	NONE	C
28	12x20	3/83 (FLOOR LOWERED 4/83)	** N110, W432	7/16/86	7/18/86	NONE	NO HOLE	NONE	NONE	NO HOLE	C
29	12x25	12/82 (FLOOR LOWERED 8/85)	** S1700, E155	7/10/86	7/17/86	C	NONE	NONE	NO FLOOR HOLES		
30	8x14	2/84	** N110, E1303	7/17/86	7/18/86	C	NO HOLE	NONE	C	NO HOLE	NONE

* EXISTING HOLE.
** LOCATION APPROXIMATE. NOT SURVEYED.

EXPLANATION

D = HORIZONTAL DISPLACEMENT. FOUND ONLY IN PREVIOUSLY DRILLED HOLES. DISPLACEMENT APPEARS TO DEVELOP WITH TIME FOLLOWING HOLE DRILLING.

S = VERTICAL SEPARATION. PROBE NAIL PENETRATES HOLE WALL SURFACE. VERTICAL SEPARATIONS RANGE FROM APPROXIMATELY 1/16 INCH TO 6 INCHES.

F = FRACTURE ZONE. PIECES OF HALITE COMMONLY PICKED OUT OF ZONE BY PROBE NAIL.

C = PROBE NAIL CATCHES ON HOLE WALL SURFACE BUT DOES NOT PENETRATE. INDICATES POSSIBLE SEPARATION OF LESS THAN 1/16 INCH. OCCURENCES AT KNOWN CLAY LAYERS ARE NOT INDICATIVE OF SEPARATION AND ARE NOT INCLUDED IN THIS TABLE.

NOTES:

1. SECTION LOCATIONS AND HOLE CONFIGURATIONS ARE SHOWN ON FIGURE 10-1.
2. HOLES WERE DRILLED VERTICALLY USING A JACK-LEG DRILL.
3. NOMINAL HOLE DEPTH IS 9 FEET BUT SOME HOLES ARE SHORTER DUE TO LOW DRIFT ROOF OR DRILLING DIFFICULTIES.
4. ONE ROOF AND ONE FLOOR HOLE OF EACH ARRAY WERE GENERALLY DRILLED 3 INCHES IN DIAMETER TO ACCOMODATE USE OF BOREHOLE CAMERA IF DESIRED. OTHER HOLES WERE DRILLED 1-7/8 INCHES IN DIAMETER. EXISTING HOLES WERE USED WHERE POSSIBLE.
5. OBSERVATIONS WERE MADE USING A PROBE CONSISTING OF A NAIL ATTACHED PERPENDICULAR TO THE END OF A ROD.
6. HOLES AT SECTION 13 WERE DRILLED TO ONLY 6- OR 6.5-FT DEPTH DUE TO LOW DRIFT ROOF. NO ROOF HOLES WERE DRILLED AT SECTIONS 16 OR 26 DUE TO LOW DRIFT ROOF.
7. POSSIBLE SEPARATIONS IN FLOOR HOLES AT SECTION 25 ARE PROBABLY AT CLAY E.

and wire mesh were installed. Several fractures in the roof brow at these anhydrites have been observed.

A portion of the N140 crosscut between W170 and E140 has been excavated above clay G. An inspection of this area in June 1986 showed some minor vertical separation, on the order of 1/8 inch, as well as some squeezing out of clay G. No fractures in the underlying halite were observed.

Floor Displacements, Separations and Fracturing. Fracturing has developed beneath the floor in some locations. These fractures occur in the halite above MB-139 and sometimes extend into MB-139. The most prominent fracturing at present is beneath Test Room 3, as discussed in Chapter 11.

As with the roof boreholes, observations were accomplished using both video equipment and a probe. The results of floor hole inspections conducted through July 1986 in accessible boreholes are presented in Table 10-3. Results of the Excavation Effects Program are included in Table 10-2.

10.3.1.2 Geomechanical Instrumentation

An extensive system of geomechanical instruments has been installed in the underground drifts (Figure 10-2) to provide in situ data on the deformational behavior of these openings. The majority of the instruments were installed during the SPDV Program and therefore have been monitored for over three years. Additional instrumentation was installed after the SPDV program was completed.

Instrumentation in the drifts consists of radial convergence points and multiple-point borehole extensometers. The convergence points consist of pairs of eyebolts anchored in the salt of the roof, floor and walls of the drifts as well as at corners of intersections. The closure of the opening is measured between a pair of convergence points using a tape extensometer. The borehole extensometers are the sonic-probe type

Table 10-3

DRIFTS
RESULTS OF INSPECTION OF VERTICAL BOREHOLES IN FLOORS

Hole	Date Completed	Hole Size (in.)	Depth (ft)	Approximate Location	Observed Condition*
DH-36	1-26-85	3.5	51.5	N1102/W1882	None
DH-38	1-26-85	3.5	47.5	N1101/W2182	None
DH-40	1-25-85	3.5	51.0	N1101/W2482	None
DH-42	1-23-85	3.5	51.2	N1101/W2782	None
DH-42A	1-25-85	3.5	40.5	N1101/W2789	None
DH-228	1-28-83	3	50.4	S3656/E147	None
OH-13	2-84	4	9.5	N1433/W232	S, F
OH-14	2-84	4	9.7	N1433/W365	D, S, F
JV-01	9-85	36	8	Room J	None
JV-02	9-85	36	8	Room J	None
JV-03	9-85	36	8	Room J	None
JV-04	9-85	36	8	Room J	None
JV-05	9-85	36	8	Room J	None
JV-06	9-85	36	8	Room J	None
JV-07	9-85	36	8	Room J	None
JV-08	9-85	36	8	Room J	F
JV-09	9-85	36	8	Room J	None
L2X-01	1-85	30	12	Room L2	None
L2PD-01	-	5	13.0	Room L2 centerline	D, S, F
-	-	5	11.3	Room L2 centerline	S, F

* D = displacement; S = separation; F = fracturing

Table 10-3 (continued)

DRIFTS
RESULTS OF INSPECTION OF VERTICAL BOREHOLES IN FLOORS

Hole	Date Completed	Hole Size (in.)	Depth (ft)	Approximate Location	Observed Condition*
-	-	16	10.3	Room L2 centerline	D, S
NPD-03	1-86	5	9.3	N1420, east of Test Room 1	None
NPD-04	1-86	5	9.5	N1420, east of Test Room 1	None
NPD-05	1-86	5	9.6	N1420/Room L1	None
NPD-06	1-86	5	9.5	N1420/Room L1	None
NPD-07	1-86	5	9.0	N1420/Room L2	S, F
NPD-08	1-86	5	12.0	N1420, east of Test Room 1	S
NPD-11	1-86	5	8.9	N1420, between Test Rooms 2 and 3	None
NPD-12	1-86	5	9.0	N1420, between Rooms L1 and L2	None

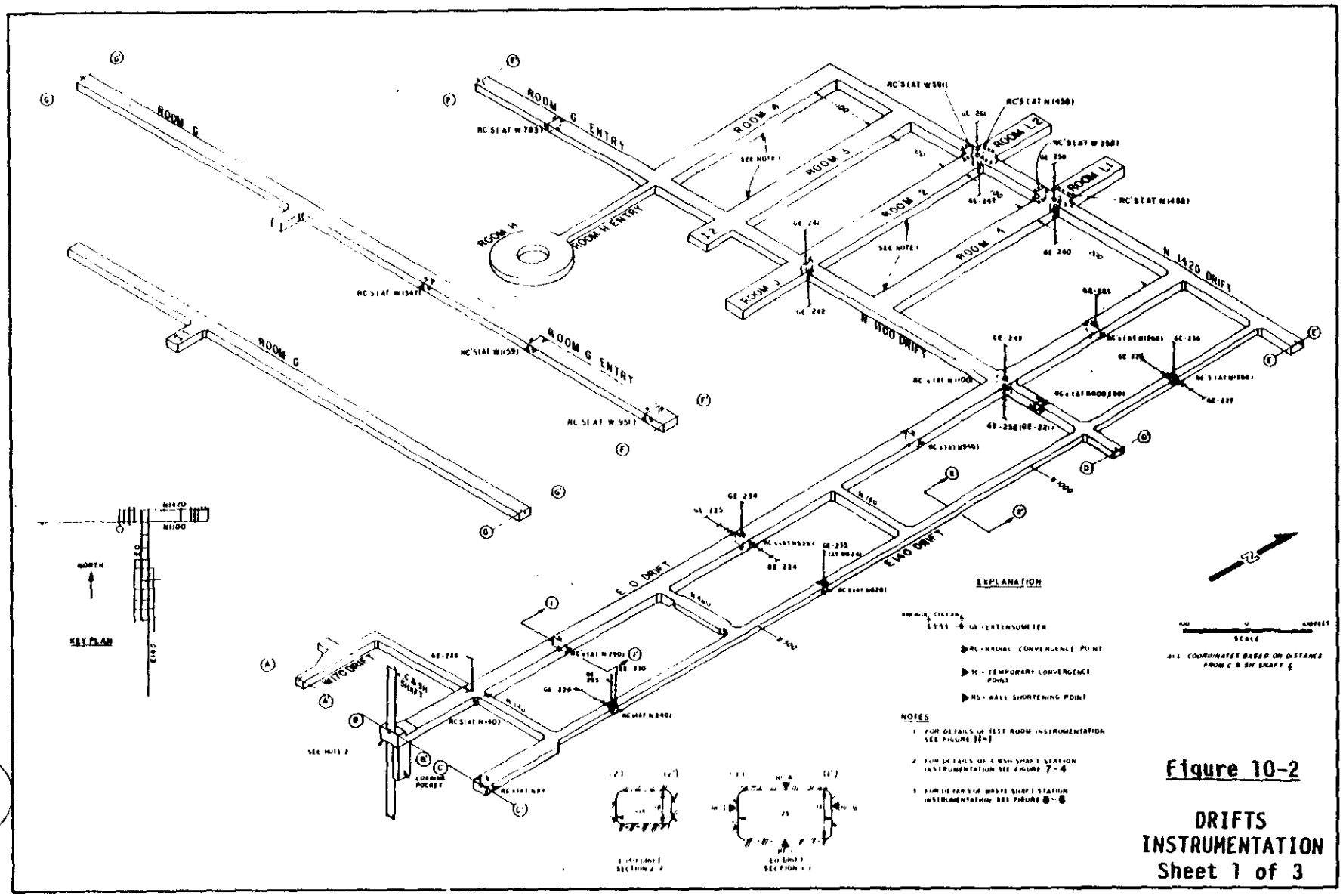

Figure 10-2

DRIFTS INSTRUMENTATION
Sheet 1 of 3

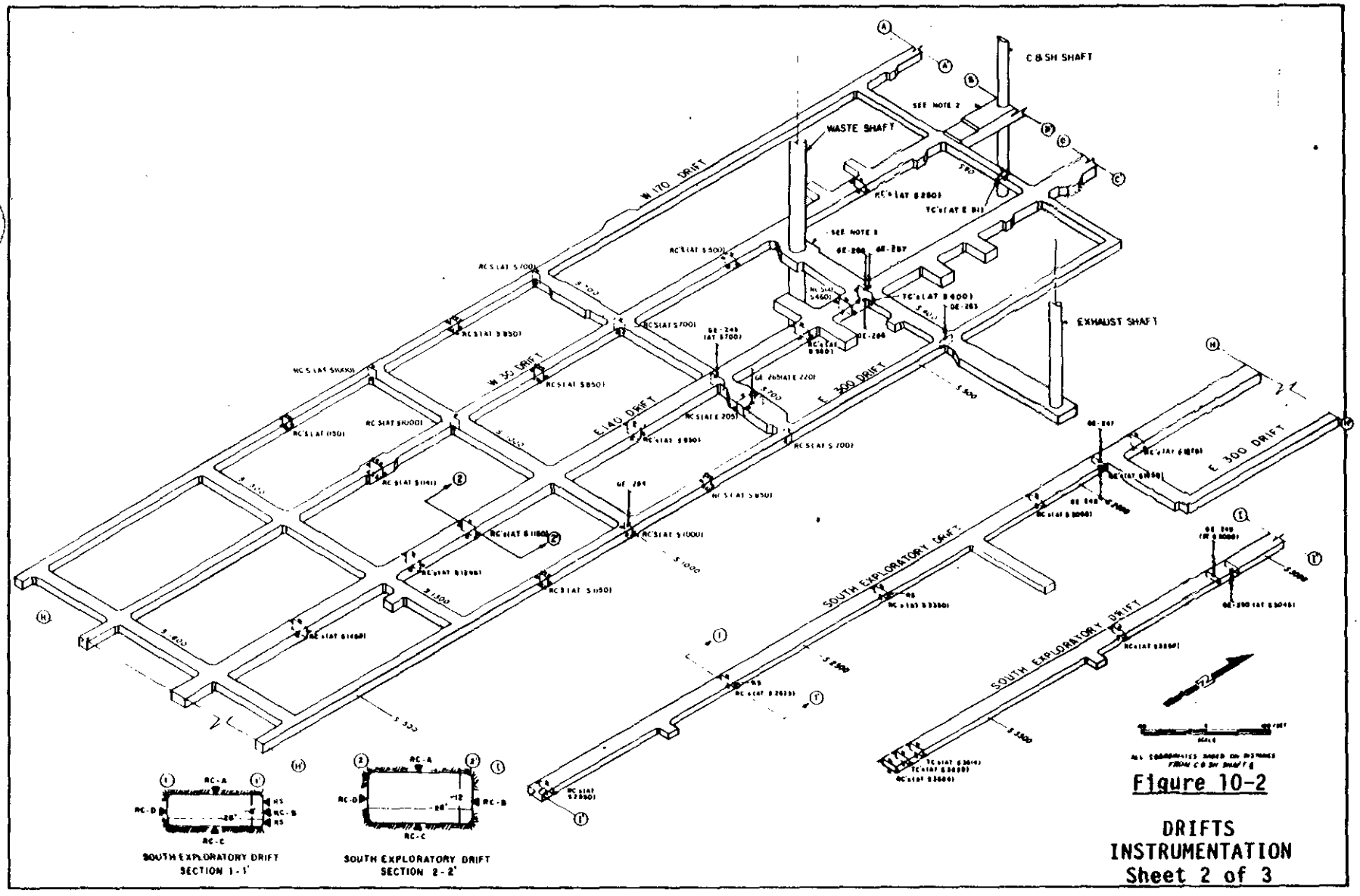

Figure 10-2

DRIFTS
INSTRUMENTATION
Sheet 2 of 3

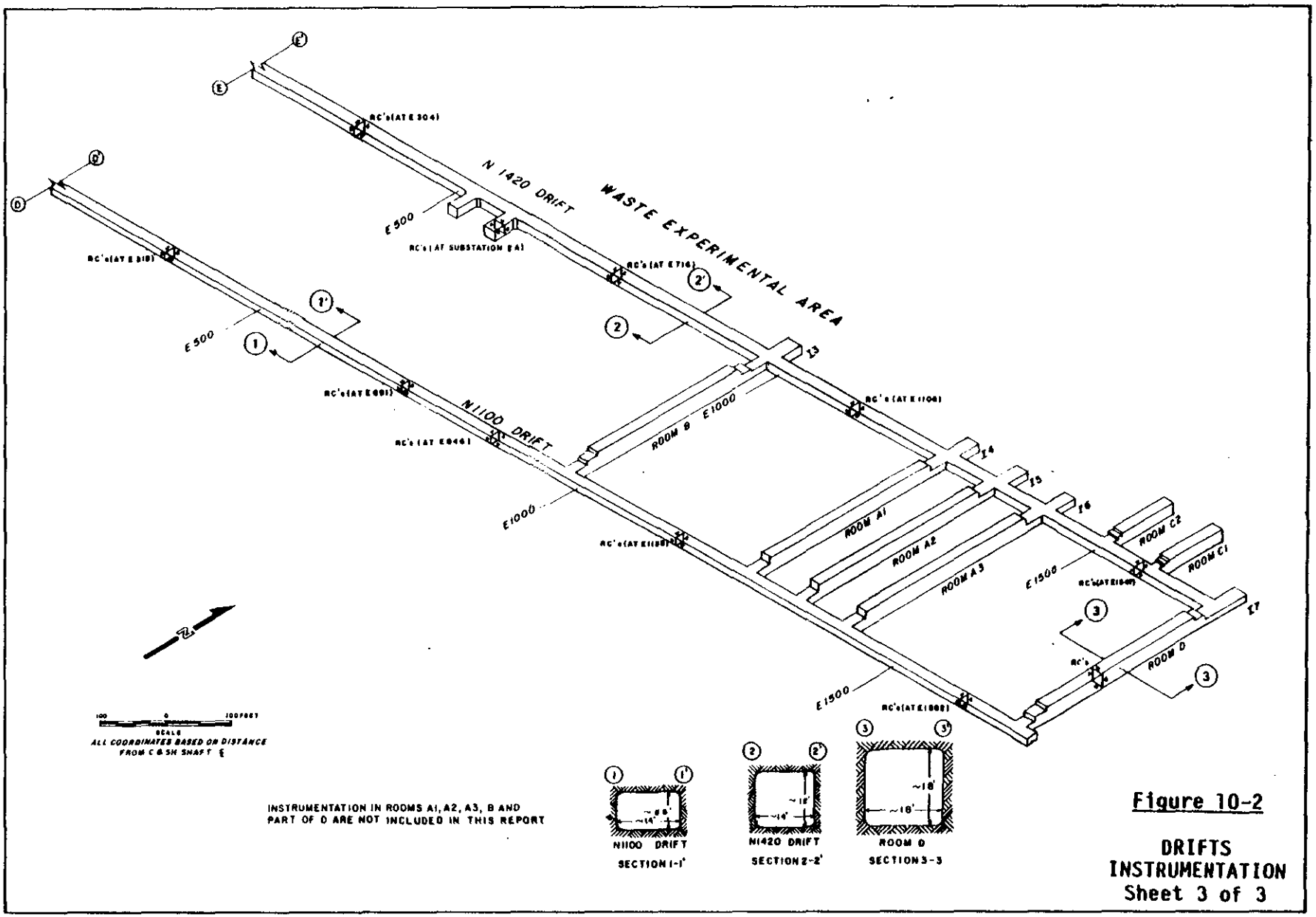

Figure 10-2

DRIFTS INSTRUMENTATION Sheet 3 of 3

with stainless steel anchor rods and expansion-ring anchors. Two-anchor, four-anchor and five-anchor extensometers have been installed. Anchor depths vary with locality and site-specific stratigraphy. Recent data plots for the drift instruments are presented in Appendix J.

No stressmeters were installed in either the halite or anhydrite surrounding the drift openings. A program to develop reliable stressmeters for use in halite was begun but abandoned when other WIPP participants initiated similar programs. The results of their programs indicate that measurements using modified stressmeters are not yet sufficiently reliable to be considered for design validation. Therefore, numerical modeling was relied upon to analyze stress changes with time in the halite and anhydrite around the openings. The reliability of the readings from the two stressmeters installed in MB-139 beneath Test Room 2 is discussed in Chapter 11.

The underground instrumentation system has had a complex history. All extensometers have been reset at least once because salt creep moved the anchor-rod magnets beyond the initial 2-inch measurement limit. Convergence points were frequently damaged by construction activities and were regularly replaced. Extensometers were also damaged during construction; some were replaced and others were abandoned. The operational history of the instruments is presented in each issue of the GFDRs.

10.3.2 Analysis and Evaluation

The in situ data collected and observations made during the design validation process were analyzed and evaluated to determine the effects of salt behavior on the drift excavations. Closure data were analyzed and a model simulation was performed for a typical 8 x 25-foot wide drift. An option for lowering the floor 5 feet was incorporated into the model for subsequent analysis of the drifts in the storage area. The results of the analysis of the larger drifts are presented in Chapter 12.

10.3.2.1 Observed Conditions

Evaluation of observed conditions is a qualitative process. It represents the assessment of qualified geologists and engineers and is an important component of the analysis and evaluation of measured responses and structural calculations.

Roof and Wall Spalling. Changes in roof and wall conditions occur slowly. Drummy areas detected during the original soundings have not enlarged significantly. These drummy areas occur in clear halite and are not associated with any noticeable clay deposits. Separations occur along planes of weakness, probably created by the orientation of crystal faces. Few new slabby areas have developed. For an unknown reason, more slabby areas developed in the roof of the E140 drift south of the waste shaft during excavation than in any other underground area. These areas have shown little, if any, growth.

Wall spalling is even more subdued. The most noticeable spalling occurs in the argillaceous halite unit and associated clay seam (geologic map unit 4 and clay F) near the intersection of the wall and roof. This area has exhibited slowly deteriorating conditions and requires occasional scaling. This spalling of map unit 4 and the squeezing out of associated clay F is most noticeable in the N1420 drift north of the test rooms and along the E140 drift south of the waste shaft. Spalling results from room closure and is related to the percentage of argillaceous material in the halite and to the proximity of the roof intersection. Similar behavior associated with anhydrite "b", anhydrite "a" and clay I has been observed in the walls of the drifts and test rooms in the waste experimental area. Some minor squeezing of clay G, clay H and clay I has occurred where these clays are exposed along drift walls. Relative motion along these clays similar to clay F is exhibited by the lower section of the wall moving into the excavation relative to the upper section. Some spalling of map unit 0 has also been noted along the E140 drift south of approximately S2500.

Pillar Fracturing. The vertical fractures that have developed in the pillar corners occur throughout the underground facility. They are particularly prominent in corners that were not beveled during excavation. The fractures range in width from closed to about 2 inches and extend into the salt essentially perpendicular to the surface.

The fractures grow steadily with time as the halite responds to deformation around the opening. Pillar corner fractures are the most obvious manifestation of pillar shortening in the drifts and rooms. These fractures will continue to grow and the corners will continue to deteriorate, with increasing spalling as a result. This behavior is expected and poses no stability problems, but it will require monitoring and maintenance throughout the operating life of the facility.

Vertical fractures have developed in the walls of the drifts parallel to the longitudinal drift axis. The fracture openings range from closed to 1/16 inch in width. The fractures have been detected in some boreholes where they occur within 2 feet of the wall surface. This type of fracturing is typical of underground excavations and probably represents tension fractures developed due to stress relief.

Roof Displacements and Separations. Clay G and clay H, above the roof of the facility level drifts, and clay I, above the roof of the drifts in the experimental area, have exhibited displacements and separations. Table 10-1 presents the results of observations made through July 1986 in 58 open boreholes. Twenty of these holes exhibited positive evidence of the occurrence of displacements and/or separations. Sixteen of these holes are at intersections. The vertical separations range from closed to 1/4 inch in width, and the horizontal displacements are up to 1 inch wide.

An additional 32 holes in 11 arrays were drilled in the roof at various facility level drift locations during the Excavation Effects Program (Figure 10-1). Of these, four arrays were drilled at intersections. Three additional arrays were drilled in the roof of drifts in the waste experimental area.

Inspection of the recently drilled holes using a probe indicate that minimal separation has occurred at the intersections and along the drifts. The size of the opening as well as the elapsed time since its excavation do not appear to have a significant effect on this phenomenon. Although the E140 drift south of the waste shaft was excavated early in construction and has the largest opening dimensions (12 x 25 feet), only minimal separations, less than 1/16 inch wide, were detected.

No separations were detected at clay G in the drift hole arrays, and the separations in the halite were usually less than 1/16 inch. There appears to be about 1/8 inch of separation at clay I in the array at E875 in the N1420 drift. This is consistent with observations made in previously drilled holes in the waste experimental area.

The observed displacements and separations immediately above the facility drifts appear to be normal deformational behavior. As the deviatoric stress around the underground openings increases following excavation, the surrounding salt will deform. The clay seams are zones of weakness that provide slip planes for salt movement during lateral loading. Movement is generally represented by the halite section below the clay seams moving into the excavation relative to the section above.

Floor Displacements, Separations and Fracturing. Minor displacements, separations and fracturing have occurred beneath the floor of the drifts. Table 10-3 presents the results of observations made in 34 open boreholes through July 1986. Ten of these holes exhibited displacements, separations or fracturing. Displacements up to 3/4 inch wide and separations up to 1/2 inch wide have been observed in boreholes at the intersection of Test Room 1 and Room L1, as well as at the intersection of Test Room 2 and Room L2. These are large, four-way intersections with 20 x 33-foot dimensions. Some displacements, separations and fracturing were also detected in three open boreholes in Room L2. Only two holes in the N1420 drift east of Test Room 1 exhibited separations, less than 1/8 inch wide. No other separations

have been detected in any other open boreholes in the N1420 drift or Room G. Only closed fractures were observed in the 30-inch diameter hole (L2X-01) in Room L2 (Figure 10-3). These fractures, many coated with clay, appeared to have originated prior to room excavation.

Nine small-diameter holes were drilled in the floor of the 35-foot wide S700 crosscut and inspected using a probe. These holes were drilled to determine the depth to MB-139 as well as to determine if any fractures were present. Fracture zones up to 1 inch wide were encountered in two locations in the halite above MB-139. Only one borehole contained a hairline fracture within MB-139.

During September 1985, nine 36-inch diameter holes were drilled in the floor of Room J, a 33-foot wide room, to accommodate structural steel columns. Only one near-horizontal fracture, less than 1/32 inch wide, was encountered in the halite above MB-139 in hole JV-8. No fractures were found in the other holes in Room J.

One fracture has been detected in the floor of the E140 drift south of the waste shaft. This fracture was observed while the drift was being enlarged from 8 feet to 12 feet high from April through June 1984. The fracture was about 18 inches below the original floor in halite and extended from approximately S1859 to S1871. Separation ranged from 1/16 inch to 1/2 inch and was associated with some clay. It curved upwards toward the floor at its northern and southern limits.

The results of the Excavation Effects Program indicate that minimal separations occur beneath the floor of the drifts and intersections. As determined from the roof holes, the size of the opening and elapsed time since excavation do not appear to have any effect on the occurrence of separations in the salt beneath the floor. No fracture zones were detected in any of the holes and separations where encountered, ranged from less than 1/16 inch to 1/8 inch wide. As with the older open boreholes, the Excavation Effects Program holes show evidence of separations within MB-139, at clay E and in the overlying halite.

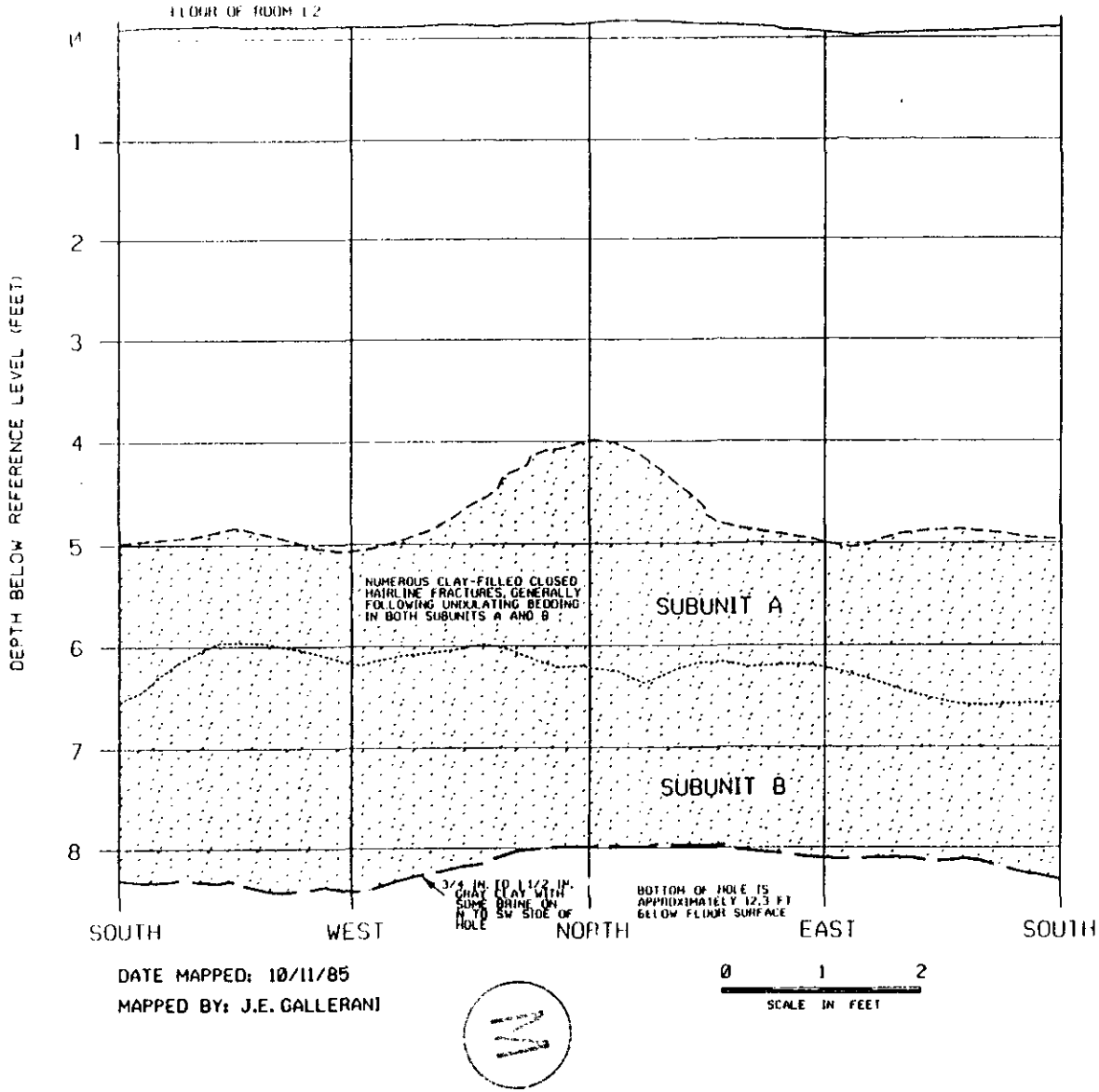

EXPLANATION

- HALITE
- MARKER BED 139
- UPPER CONTACT OF MB-139
- UPPER CONTACT OF SUBUNIT B
- CLAY E (LOWER CONTACT OF MB-139)
- FRACTURE TRACE
  DISTINCT FRACTURES, USUALLY CLOSED WITHIN A FEW INCHES OF THE BOREHOLE WALL.
- FRACTURE ZONE
  ZONE OF FRACTURED SALT BOUNDED BY DISTINCT FRACTURES.
- SMALL FRACTURE
  CLOSED HAIRLINE FRACTURES, USUALLY FORMING FRACTURE ZONES LESS THAN ONE INCH WIDE.
- (1/2) APPROXIMATE WIDTH OF SEPARATION, IN INCHES. SEPARATIONS ARE MEASURED WITHIN THE OPENING, 12 INCHES FROM BOREHOLE WALL.

NOTES:

1. BOREHOLE IS 30 INCHES IN DIAMETER.
2. MAPPING WAS PERFORMED FROM INSIDE THE HOLE. ALL FEATURES WERE MEASURED FROM AN UNSURVEYED REFERENCE LINE.
3. MAPPING WAS PERFORMED AT A SCALE OF 1 INCH EQUALS 1 FOOT.

Figure 10-3

DRIFTS
GEOLOGIC LOG OF HOLE L2X-01

The floor hole array in the N1420 drift at E875 encountered a slight separation of approximately 1/16 inch, coincident with a clay seam at a depth of about 8 1/2 feet. MB-139 at this location is about 22 feet below the floor.

Brine was encountered during the drilling of the central hole in the array at S700/E66 and continued to flow from the hole for several days after the completion of drilling. The hole encountered several separations up to 1/16 inch wide between a depth of 7.4 and 7.7 feet. No separations were detected in the other holes of this array. Brine has been encountered at several other hole array locations but no significant separations were detected in the holes.

The observations made to date indicate that fracturing in the drift floors is minimal. This includes observations of the E140 drift, which was one of the earliest excavations made during the SPDV Program. No fractures of the magnitude found in Test Room 3 (Chapter 11) have been detected in any of the drifts. Displacements, separations and fracturing beneath the floor is expected to continue in the future.

10.3.2.2 Closure Behavior at Selected Stations

Analyses were performed at selected stations to study roof-to-floor and wall-to-wall closure. Analysis was also performed to study the effect of floor lowering on closure.

Roof-to-Floor Closure. Until May 1984, the E140 drift south of the waste shaft was unique in that there were neither crosscuts nor nearby parallel drifts. However, in May and June 1984 the floor of the drift was lowered by 4 feet and new drifts and crosscuts were added between stations N140 and S1620. These two operations have resulted in an increase in closure rates for this portion of the drift. Since both operations occurred concurrently, it is difficult to isolate their effects on closure. However, it has generally been observed that any far field disturbance has only a short-term effect on the closure, and

that the closure rate, after a momentary increase, decays to its pre-perturbation rate pattern.

If we assume that the closure at station E140/S1879 is not measurably affected by the additional excavations performed north of station S1620, this station can then represent the closure of an infinitely long opening in a geologically uniform formation. However, because the convergence points were installed nearly 4 days after the completion of excavation, the roof-to-floor closure versus elapsed time curve was extrapolated backwards by fitting an equation in the form of

$$t = t_1 \, (1 + R(t)/R_1)^3 \qquad (10\text{-}1)$$

where: R(t) is the instrument reading at elapsed time t since the end of excavation; and

R_1 is the regression parameter, equal to total closure at elapsed time t_1 since the end of excavation.

This equation indicates that at t equal to 0, the slope of the closure curve is infinite. This is not true because the slope at t equal to 0 is finite but large.

Based on the results of the regression analysis, the value of R_1 was determined to be 1.97 inches. However, the curve-fitting was not very good, probably because excavation at the instrument location was done in two stages making it difficult to assign the value for t_1. Because the shape of the early part of the closure versus time curve is not smooth, the estimated value of t_1 is approximate.

Figure 10-4 compares the measured closure with the adjusted curve at station E140/S1879 using the results of the regression analysis. The reading of roof-to-floor closure on August 26, 1985, was 5.84 inches and the adjusted value is 7.81 inches. Note that this station is nearly 230 feet from the boundary location north of which the floor was lowered 4 feet. It is likely that the excavation had some effect on

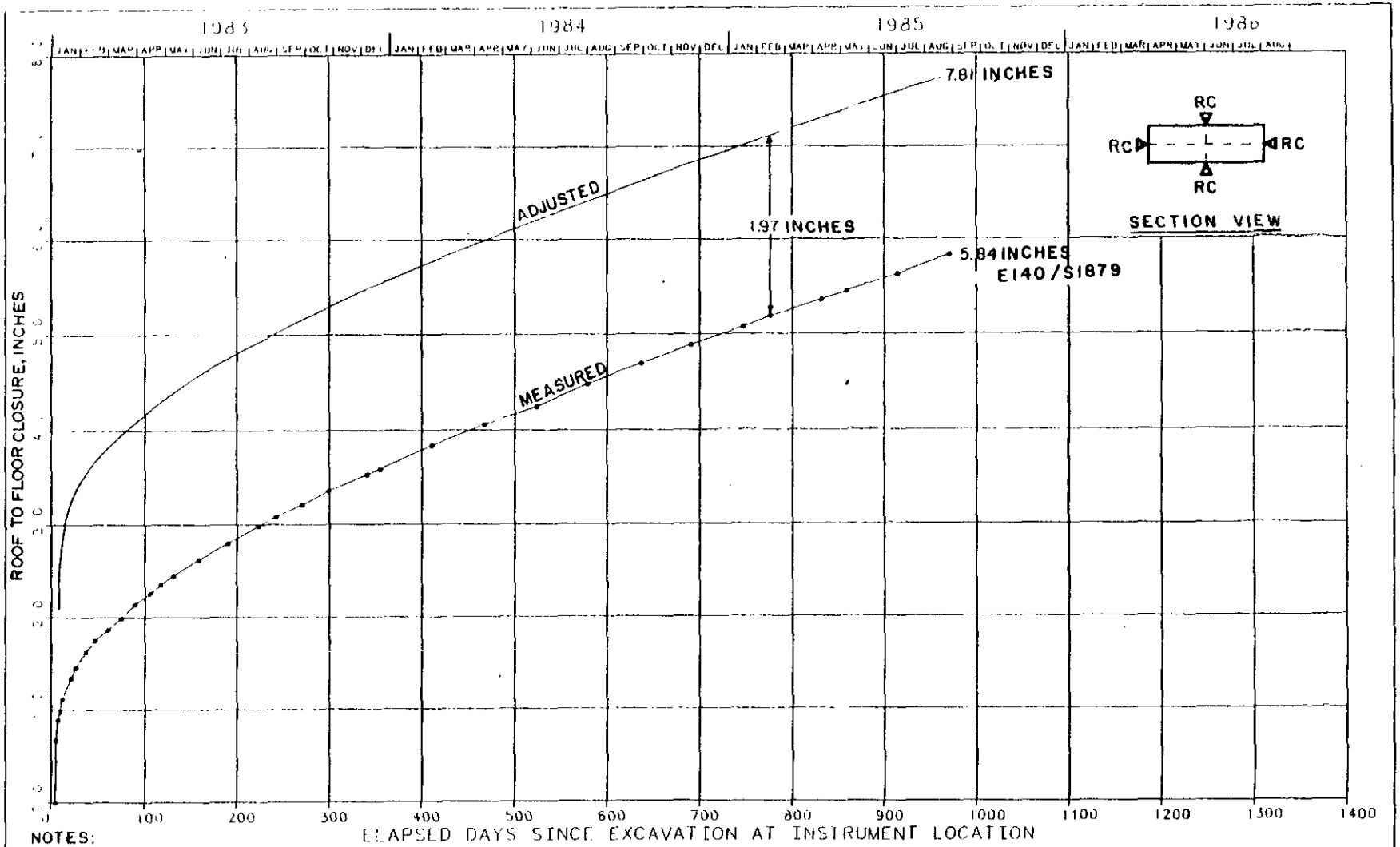

NOTES:

1. EXCAVATION DIMENSIONS = 8FT X 25FT
2. ADJUSTED CURVE OBTAINED USING THE RESULTS OF REGRESSION ANALYSIS

Figure 10-4

DRIFTS
COMPARISON OF MEASURED CLOSURE WITH REGRESSION CURVE AT E140/S1879

the closure at this station, although Figure 10-4 does not clearly show such an effect. The convergence points at this location have since been destroyed.

Figure 10-5 shows the central roof-to-floor closure at E140/S1246. The roof-to-floor convergence points were installed nearly 14 days after excavation at this location. This figure shows the effect that lowering the floor 4 feet has on the closure. In addition, the E300 drift excavation passed this location on August 21 and 22, 1984. The effect of lowering the floor, though, masks the effects of the adjacent excavation. As of August 26, 1985, the roof-to-floor closure of the 12 x 25-foot drift was 4.18 inches. The initial reading was taken on July 11, 1985, 1 day after the floor was lowered. Because the closure rate is very high at the early stages, actual roof-to-floor closure is greater than 4.18 inches.

Relationship Between Roof-to-Floor Closure and Drift Dimensions. Convergence points have been installed at various stations in underground drifts having different cross section dimensions. Some of the drifts, especially the E140 drift south of S1600, are isolated, while most of the other drifts have nearby parallel drifts and crosscuts. The closure behavior of these drifts is affected not only by the opening dimensions but also by the presence of adjacent openings. Differences in creep properties of the salt may also be responsible for differences in creep behavior. In addition, the closure behavior is affected by the 4- to 5-foot lowering of the drift floor.

Figure 10-6 shows measured roof-to-floor closure at selected stations in drifts with different cross section dimensions. Because measurements were not made immediately after the opening was excavated, the closure values were normalized to the values at approximately 10 days after the completion of excavation at the respective instrument station. As shown on this figure, the maximum closure and closure rate occur in drifts with opening dimensions of 12 x 25-feet. Because the

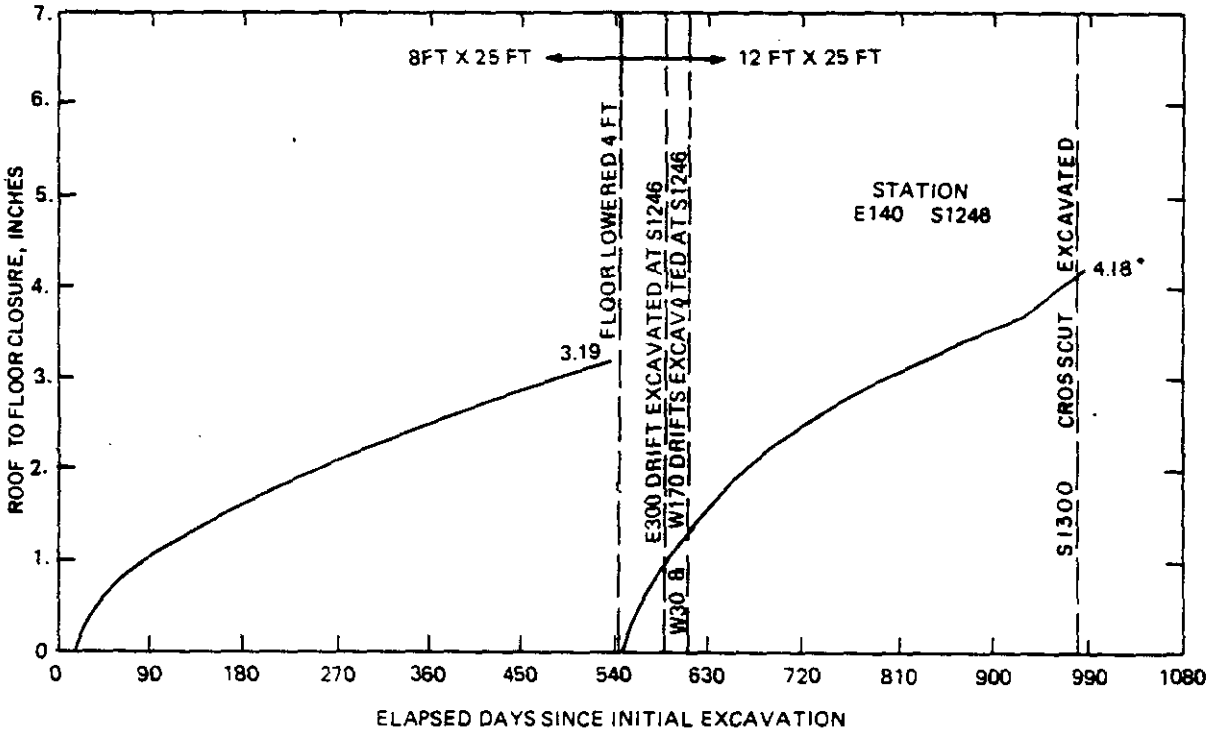

*MEASUREMENT ON AUGUST 26, 1985.

Figure 10-5

DRIFTS
EFFECT OF FLOOR LOWERING AND ADJACENT EXCAVATIONS
ON CLOSURE AT E140/S1246

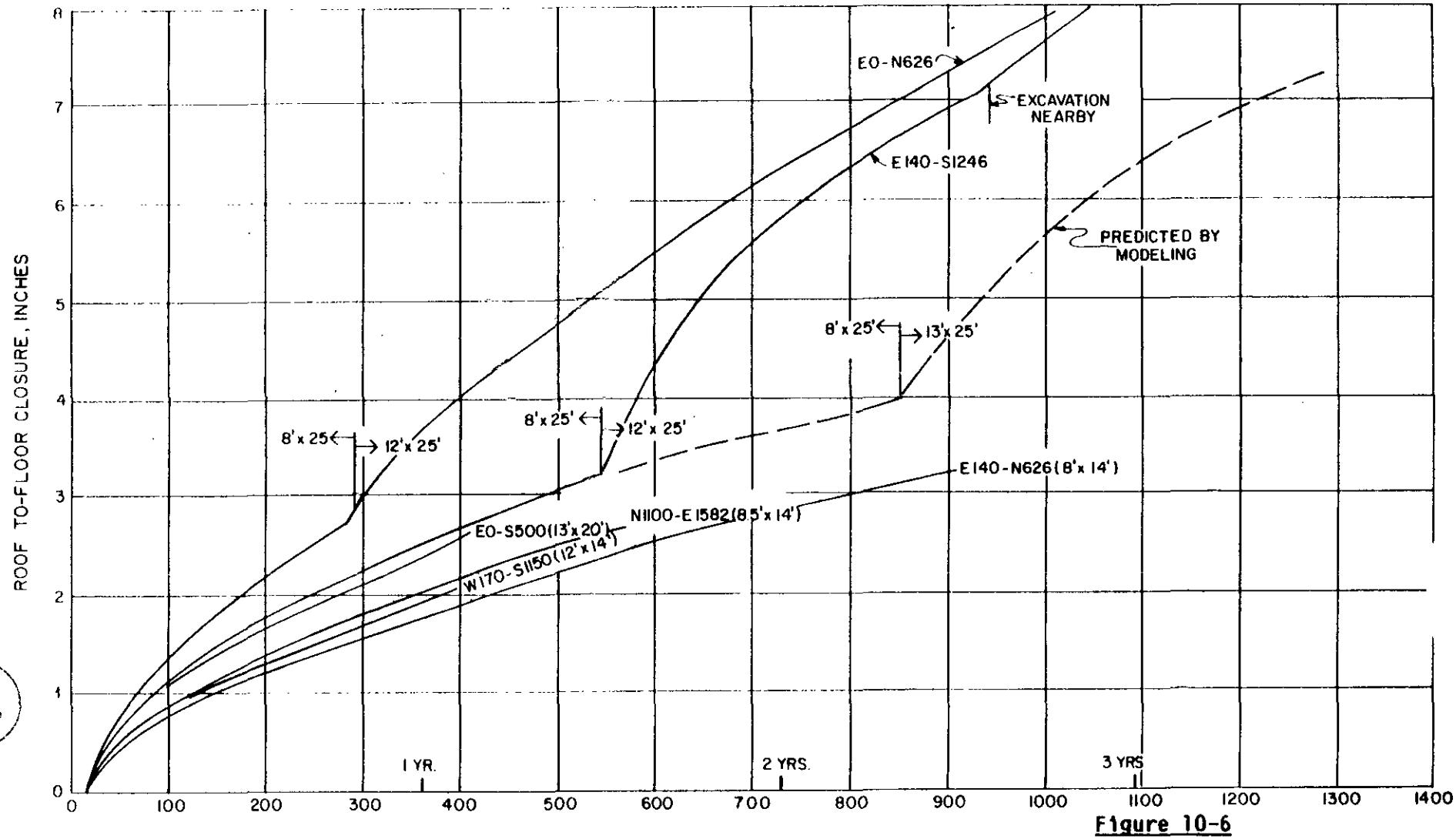

Figure 10-6

DRIFTS
COMPARISON OF ROOF-TO-FLOOR CLOSURE IN DRIFTS WI
DIFFERENT DIMENSIONS

drifts in the storage area will have cross section dimensions of 13 x 25 feet, the modeling analysis discussed in this chapter and in Chapter 12 focuses on predicting the behavior of the 13 x 25-foot drift opening for the operating life of 25 years.

The effect of lowering the floor 4 feet at instrument stations E0/N626 and E140/S1246 is to increase the closure rate permanently. Although the floor lowering was performed at different times at these stations, the steady state rate after excavation appears to be nearly the same. However, if the floor lowering is performed at a much later date following the initial excavation, it is likely that the total closure may be somewhat decreased. The closure behavior at these two stations is influenced by the presence of nearby parallel drifts and crosscuts, as well as likely differences in the creep properties of the salt.

Figure 10-6 also shows the predicted roof-to-floor closure of an infinitely long, single drift with cross section dimensions of 13 x 25 feet. This closure was obtained by modeling and is discussed in Chapter 12. The approximate steady state closure rate at E0/N626 and E140/S1246 is 2.00 inches/year. The steady state closure rate predicted for the infinitely long, single drift is 1.60 inches/year. The nearly 25 percent difference in these rates is probably due to the presence of adjacent drifts and crosscuts. This value compares well with the value of 30 percent obtained from modeling as discussed in subsection 10.3.3.3.

Figure 10-7 presents a comparison of the predicted closure of a 13 x 25-foot drift with the observed behavior of a 12 x 25-foot drift at E0/N626. The closure for the 13 x 25-foot drift was obtained by increasing the closure rate obtained from modeling the infinitely long, single drift by 30 percent. The roof-to-floor closure at E0/N626 does not include the values before the floor was lowered by 4 feet. This comparison indicates that it is reasonable to increase the closure rate of a single, infinitely long, 13 x 25-foot drift by 30 percent to account for the presence of adjacent parallel drifts and crosscuts.

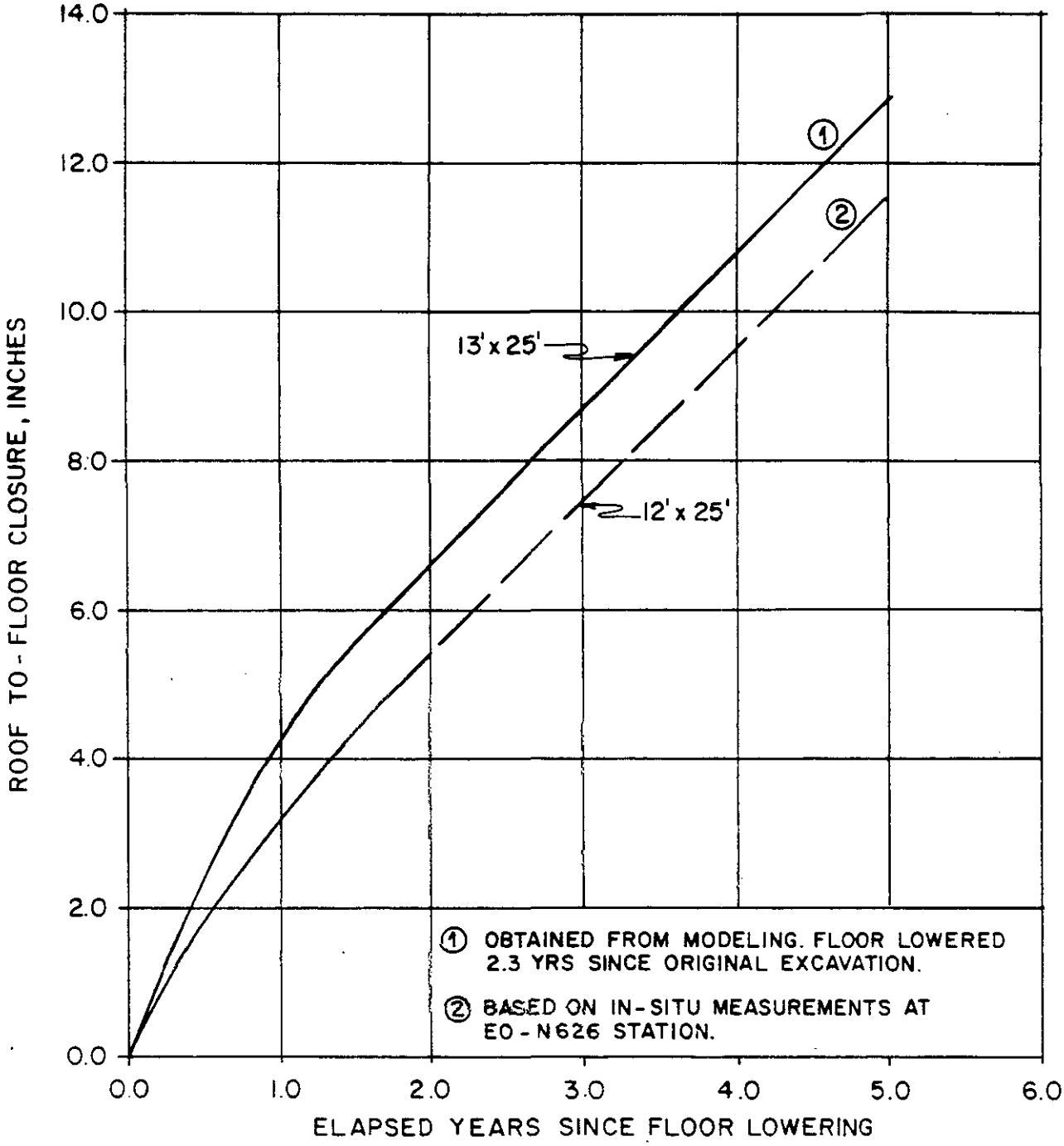

Figure 10-7

DRIFTS
COMPARISON OF PREDICTED AND OBSERVED
ROOF-TO-FLOOR CLOSURE

Wall-to-Wall Closure. The wall-to-wall convergence points at the S1246 station were installed immediately after the original excavation at this location was completed. When the cross section dimensions were 8 x 25 feet, the measurements were close to the true wall-to-wall closure at midheight of the instrument location. On June 30, 1984, the wall-to-wall closure was 5 inches for an elapsed time period of 564 days. After the floor was lowered, a new set of wall-to-wall convergence points was installed. The additional wall-to-wall closure was 3.31 inches through August 26, 1985.

Comparison of Roof-to-Floor to Wall-to-Wall Closures. Table 10-4 summarizes the closure of the E140 drift for locations south of S1620. Until August 1985, these locations were unique in that there were no crosscuts and no nearby parallel drifts at the time of the analysis. The cross section dimension was 8 x 25 feet. The maximum measured roof-to-floor closure of 5.19 inches was at station S1879. Stations S3614, S3639 and S3664 are influenced by the end constraints of the drift which terminates at about S3664.

Effect of Adjacent Drifts. Table 10-5 compares closure in the drifts at S1150. Because the initial readings were not taken immediately after the station location was excavated, the comparison is approximate. Note that, for the E140/S1150 station, the original cross section dimensions were 8 x 25 feet until June 8, 1984, and that no convergence points existed at this location prior to lowering the floor. The closure values at E140/S1150 are the maximum, not only because the opening dimensions are the largest, but also because the opening had already existed for nearly 550 days before the floor was lowered 4 feet. It is also likely that there is mutual influence between the openings.

Effect of Floor Lowering. The E0 drift between N140 and N1420 was increased in height from 8 feet to 12 feet (by lowering the floor) from November 9, 1983, through January 9, 1984. The closure readings increased rapidly as excavation approached the measurement stations but

Table 10-4

E140 DRIFT SOUTH OF S1620
SUMMARY OF MEASURED CLOSURE
(CROSS SECTION DIMENSIONS = 8 x 25 feet)

Instrument Location	Time-lag between end of excavation and initial reading (days) R-T-F*	W-T-W*	Convergence point reading (inches) Feb. 12, 1985 R-T-F*	W-T-W*
E140/S3664	14	0	1.70	1.48
E140/S3639	0	0	4.07	3.24
E140/S3614	0	0	4.49	3.72
E140/S3250	11	11	4.13	2.97
E140/S2950	10	10	4.19	3.18
E140/S2625	6	6	4.43	3.59
E140/S2350	9	9	4.33	3.44
E140/S2066	8	8	4.32	3.40
E140/S1879	4	2	5.46	4.00

* R-T-F = roof-to-floor
W-T-W = wall-to-wall

Table 10-5

COMPARISONS OF CLOSURE IN DRIFTS AT S1150

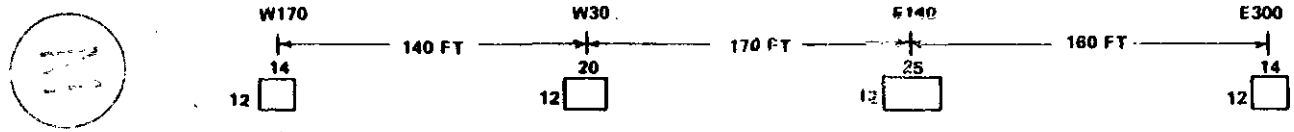

	W170/S1150	W30/S1141	E140/S1150	E300/S1150
INSTRUMENT LOCATION				
DATE OF EXCAVATION	AUGUST 21, 1984	AUGUST 21, 1984	JUNE 8, 1984*	JULY 23, 1984
DATE OF INITIAL READING				
CENTRAL ROOF-TO-FLOOR	AUGUST 23, 1984	AUGUST 22, 1984	JUNE 14, 1984	JULY 26, 1984
CENTRAL WALL-TO-WALL	AUGUST 23, 1984	AUGUST 22, 1984	JUNE 14, 1984	JULY 26, 1984
DATE OF LATEST READING FOR BOTH ROOF-TO-FLOOR AND WALL-TO-WALL CONVERGENCE POINTS	SEP. 16,1985	SEP. 16, 1985	AUG. 26, 1985	SEP. 30, 1985
CLOSURE (IN.)				
CENTRAL ROOF-TO-FLOOR	2.46	3.10	3.61	2.18
CENTRAL WALL-TO-WALL	2.62	2.76	3.03	2.35

* FLOOR LOWERED BY 4 FT ON JUNE 8, 1984. DIMENSIONS WERE 8 FT X 25 FT BEFORE JUNE 8, 1984. CROSS DRIFTS S1100 AND S1300 EXCAVATED IN AUGUST, 1985.

dropped rapidly to, or slightly above, the pre-excavation rate. The floor lowering has affected the salt material above the roof of the openings to distances of at least 30 feet.

Figure 10-8 shows the relationship of the movement rates for the collar and two intermediate anchors of roof extensometer 51X-GE-00243 at the E0/N1100 intersection. The figure shows that the movement rate of the collar and these anchors increased due to floor lowering but then began decreasing until March 1984 (about 400 days after the initial excavation). The rate then began increasing again from March until August 1984 (about 550 days after the initial excavation). Because excavation activities were performed in the area of this instrument at this time, it is possible that parting at the clay seams above the roof was occurring at an increasing rate.

Figure 10-9 shows the movement rates of the collar and anchors of roof and wall extensometers at E0/N626. The collar movement rate of the east wall extensometer appears to be somewhat less than that of the west wall extensometer. It was also observed that floor lowering has affected the closure behavior of pillars as far as 25 feet from the opening. Similarly, roof behavior has been affected, probably up to at least 30 feet above the roof.

The height of the E140 drift remained at 8 feet during floor lowering in the E0 drift between N140 and N1420. However, excavation performed in the E0 drift appears to have affected the closure behavior of the E140 drift. Figure 10-10 shows the movement rates of the collar and anchor A for roof extensometer 51X-GE-00235 at E140/N624. The collar movement rate was decreasing monotonically until late December 1983. However, it appears to have increased around January 1984. Assuming the instrument was functioning properly and there was no anomalous behavior of clay seams in the roof of the E140 drift, excavation in the E0 drift may have influenced salt behavior as much as 150 feet from the E0 drift.

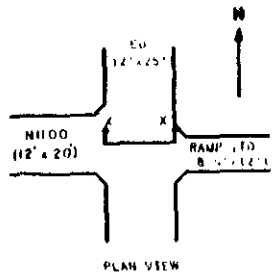

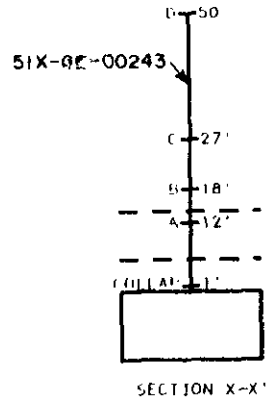

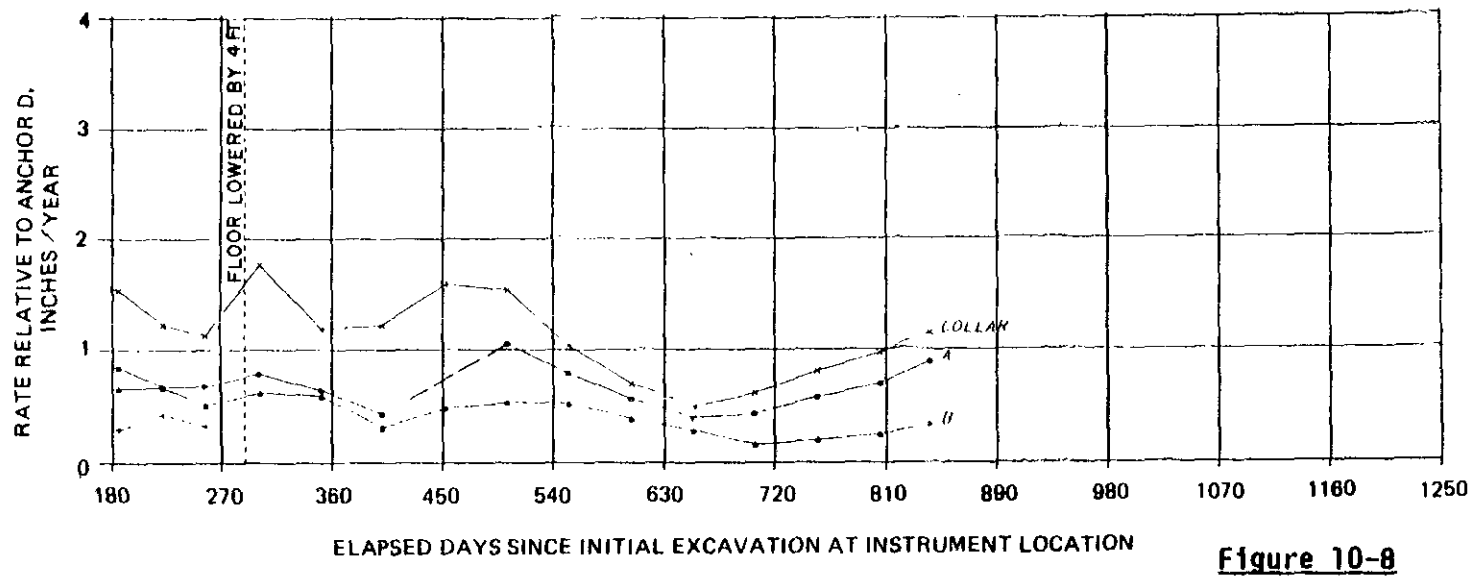

NOTE: RATE CALCULATED FOR MINIMUM INTERVALS OF 30 DAYS.

Figure 10-8

DRIFTS
EFFECT OF FLOOR LOWERING ON ROOF BEHAVIOR AT EO/N1100 INTERSECTION

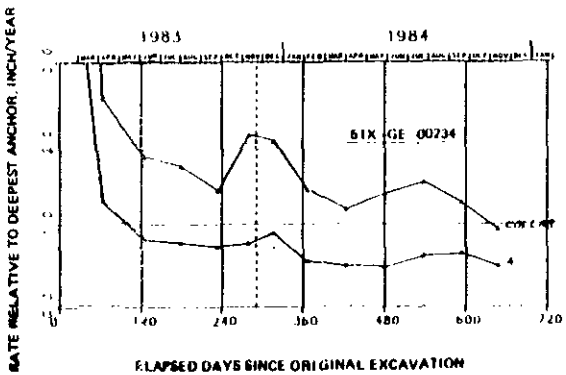

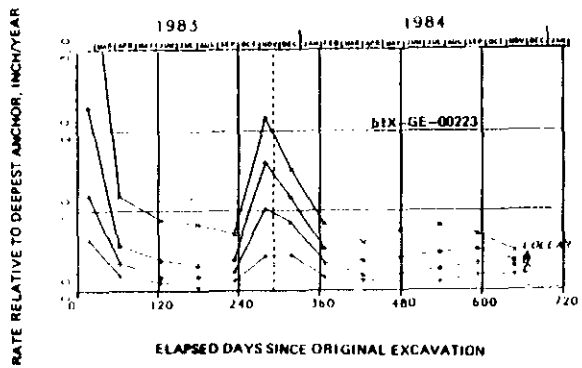

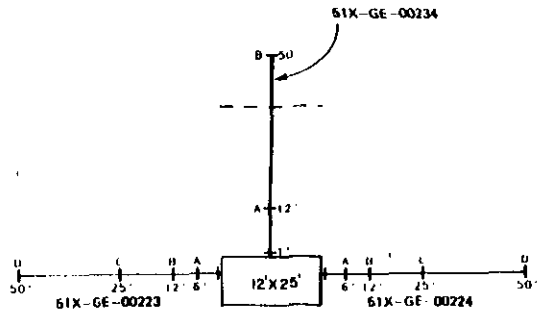

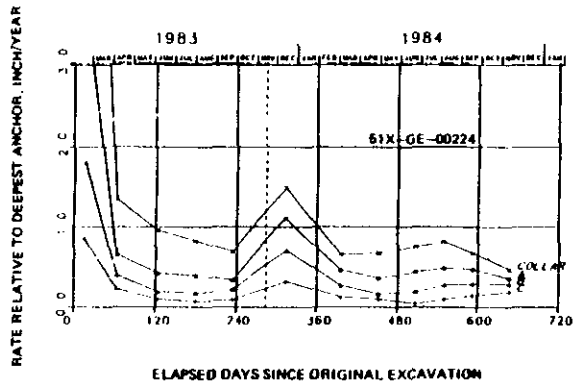

NOTE

VERTICAL DASHED LINE INDICATES TIME WHEN THE FLOOR WAS EXCAVATED FOUR FEET.

Figure 10-9

DRIFTS
EFFECT OF FLOOR LOWERING ON CLOSURE AT EO/N626

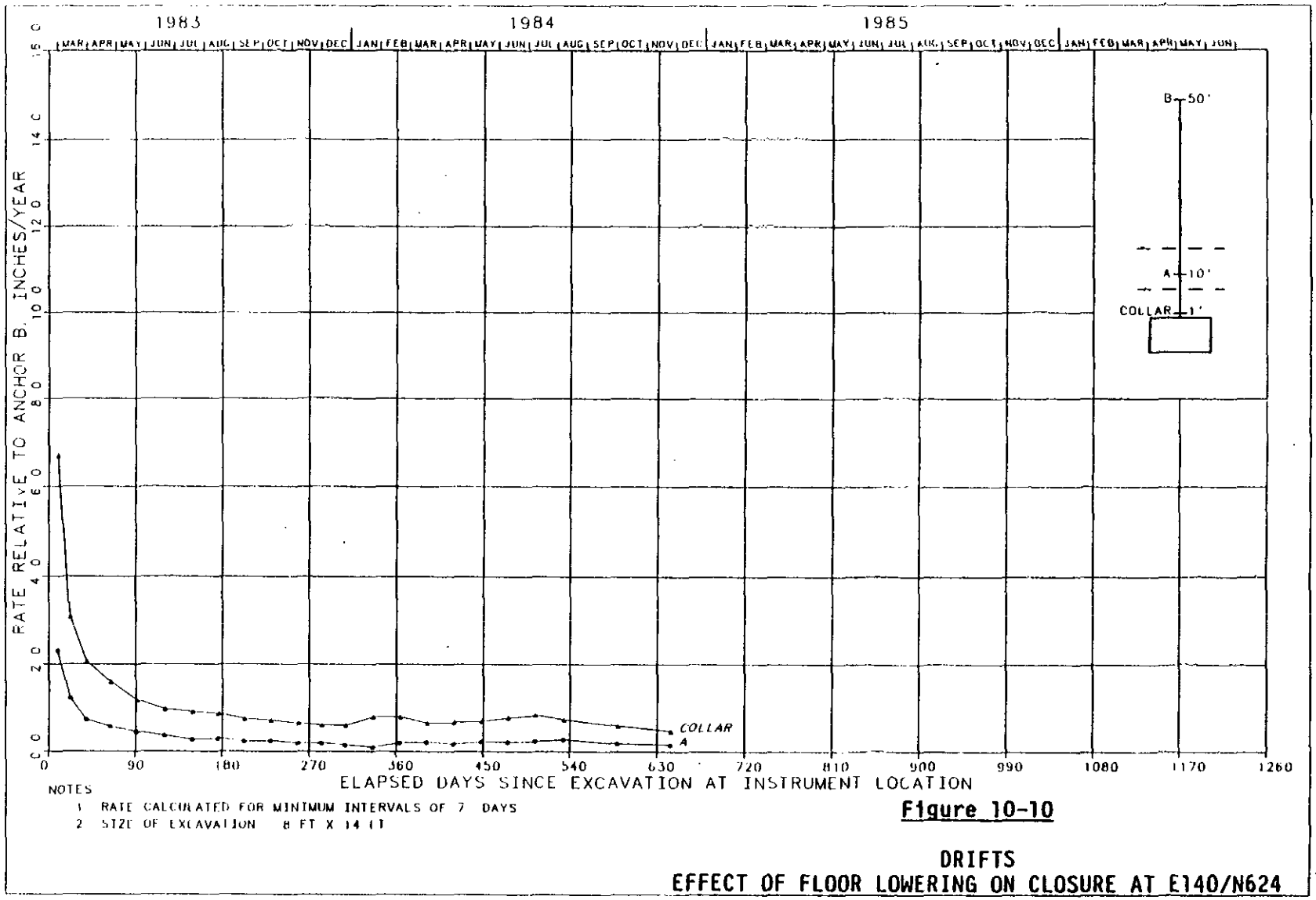

Figure 10-10

DRIFTS
EFFECT OF FLOOR LOWERING ON CLOSURE AT E140/N624

Observations of the effect of floor lowering on closure behavior are summarized below:

(1) The closure reading at an instrument station increases rapidly as floor excavation approaches the station and decreases rapidly to, or slightly above, the pre-excavation closure rate as excavation passes the instrument station.

(2) Floor lowering affects creep behavior of the salt above the roof of the openings to depths of at least 30 feet. This effect is short-lived, however, extending over a period of only a few months.

(3) Although the floor of the E140 drift north of the C & SH shaft was not lowered for most of its length, excavation performed in the E0 drift appears to have affected the E140 drift closure.

The movement rates of the anchors of extensometer 51X-GE-00243 at the E0/N1100 intersection increased and then decreased between March and August 1984. Because no excavation activity took place at this time in the vicinity of the instrument station, it was assumed that the clay seams above the roof may have been parting at an increasing rate. Figure 10-8 shows the variation in closure rates for the collar and anchor points with time. The rates of the collar and anchor movements have subsided and are probably returning to their pre-perturbation values. For comparison, the rates of collar and anchor movements of floor extensometer 51X-GE-00258 are shown on Figure 10-11. The rates of movements of the collar and intermediate anchors have a similar trend as the roof extensometer over the same time period. However, this extensometer was damaged due to mining operations on February 8, 1985. Since then, the readings have remained anomalous.

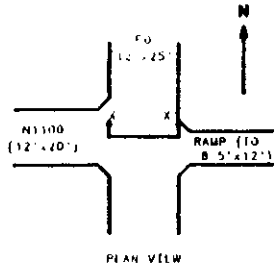

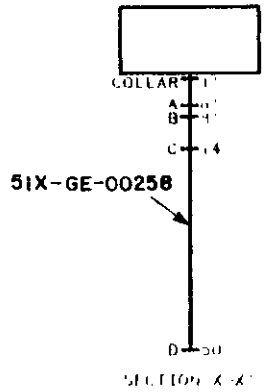

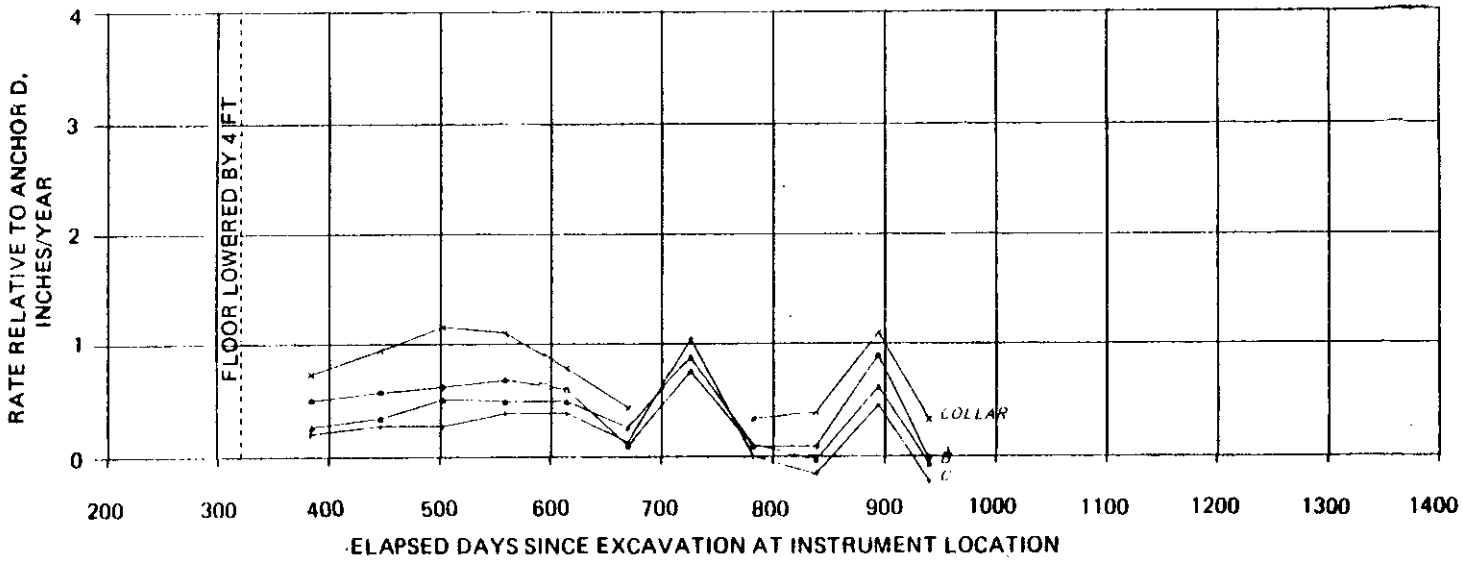

NOTE: RATE CALCULATED FOR MINIMUM INTERVALS OF 30 DAYS.

Figure 10-11

DRIFTS
RATE OF FLOOR HEAVE AT EO/N1100

10.3.2.3 Model Simulation

A finite element model utilizing an engineering approach was used to simulate the behavior of an 8 x 25-foot drift. The method described in Appendix C was used to mathematically simulate the in situ behavior of the drifts by determining the creep parameters C, A, and z. The following discussion describes the numerical modeling and the utilization of in situ data for the drifts. Also discussed are simulations of the effect of adjacent parallel and perpendicular drifts.

Utilization of Reference Stratigraphy. The reference stratigraphy described in Chapter 6 was used in the analysis. The reference level representing the elevation of clay G is 2,129.40 feet below the ground surface, based on the core hole log at station E140/S1960. Because the finite element method lends itself well to multiple layer analysis in which distinct material properties can be accounted for, the MARC General Purpose Finite Element Program (ref. 6-8) was used.

Structural Characterization. Figure 10-12 shows the finite element model used to predict closures, stresses and deformed shapes as a function of time for an 8 x 25-foot opening. The model consists of 122 plane strain elements with 21 gap/friction link elements modeling the clay seams and an option for lowering the floor 5 feet. The top and bottom boundaries of the model are at depths of 2,045.00 feet and 2,245.00 feet, respectively, below the ground surface. The drift roof, drift floor before lowering, and drift floor after lowering are at depths of 2,128.70, 2,136.70, and 2,141.70 feet, respectively, below the ground surface. The roof beam is 8.10 feet thick and the final floor level is 4.39 feet above MB-139.

Only anhydrite layers with thicknesses greater than 1 foot were included in the model. Calculations showed that most anhydrite layers less than 1 foot thick failed at vertical stresses less than 1 percent of the overburden pressure. Therefore, because their contribution to the stiffness of the model would be insignificant, they were not included.

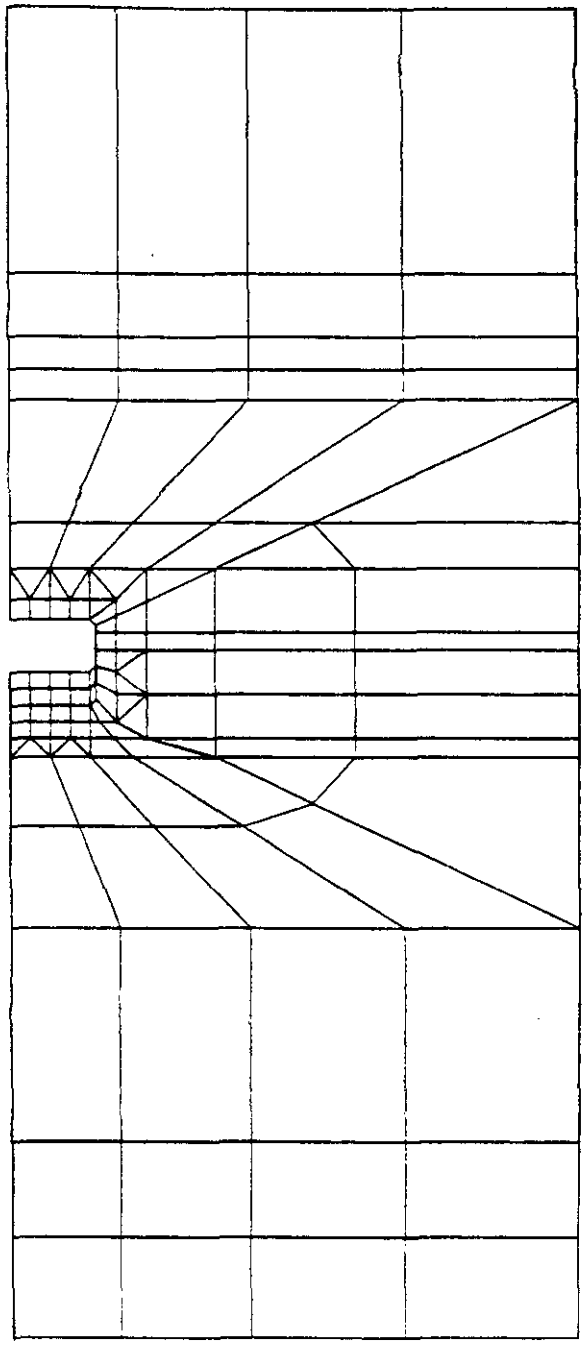

Figure 10-12

DRIFTS
FINITE ELEMENT MODEL - BEFORE FLOOR LOWERING

Clay seams in the model were limited to two above and two below the drift opening. The justification for this is twofold: first, reference 5-4 states that "90 percent of the drift closure measured with ten active slidelines could be captured with four slidelines, two directly above and two directly below the drift"; second, previous analyses have shown that, at locations representative of the more distant clay seams, the shear force is considerably less than the normal force; therefore, any slippage along these clay seams would be negligible compared to that along seams closer to the opening and they need not be included in the model. To simplify the analysis of this model, a coefficient of friction equal to 0.0 was assumed for the gap/friction elements modeling the clay seams.

The lateral boundaries of the model are 82 feet apart. and were established based upon vertical axes of symmetry with regard to adjacent drifts. The upper and lower boundaries of the model were based upon experience from previous analyses and were extended far enough in both directions so that the difference between vertical and horizontal stresses at each point of the boundaries would be within 10 percent of the vertical stresses. Horizontal restraints were assumed for the lateral boundaries while vertical restraints were assumed for the lower boundary of the model. Stress boundary conditions were utilized for the upper boundary.

Element sizes were established to make them proportional in size to the estimated stress gradient across each element. In addition, the orientations of the elements were established in order to have the radiating mesh coincide with the assumed principal stress axes. These aspects of the model were designed to enhance the overall efficiency of the analysis.

Consideration of Drift Opening. The drift openings were originally excavated to 8 x 25 feet. Further development trimmed an additional 4 feet from the floor to provide a 12 x 25-foot opening in the shaft pillar area. To provide continuous response histories from initial

excavation through the floor lowering period, special considerations were provided for modeling the opening.

Determination of Creep Parameters. Data from ten different locations along the E140 drift from S550 to S3250 were reviewed and one representative location was selected to calculate creep parameters for the drifts and for use in predicting closures and stress distributions.

Figure 10-13 shows the correlated roof-to-floor and wall-to-wall in situ data curves from the selected location, as well as the predicted closure based on the calculated creep parameters.

Transformation of Time Domains. Having determined the values of C, A and z to be 1.40×10^{-21} $ksf^{-4.9}$ sec^{-1}, 3.2 and 1.1×10^{-7} sec^{-1}, respectively, the normalized time at which the floor lowering was scheduled to take place was determined by transforming 7.25×10^{7} sec (or 2.3 years) to normalized time using equation C.4-17 in Appendix C.

The normalized time which corresponds to the scheduled real time for drift floor lowering was determined to be 1.4205×10^{-13} $ksf^{-4.9}$ or 418 time increments from the start of the program. Accordingly, the drift height was changed at the end of increment 418, and the analysis continued until a total real time of approximately 5 years was reached.

Effect of Parallel Drifts. The extraction ratio at a particular location is dependent upon the arrangement of the drifts and pillars. Therefore, the effect that the extraction ratio has on structural responses can be determined by considering the effect of adjacent drifts. Two different cases were considered in the analysis. One case assumes the adjacent drifts are parallel to the drift being analyzed while the other case assumes adjacent drifts are perpendicular to the drift being analyzed.

To simplify and minimize the computational effort, a multiple drift model was used for the analysis of the 8 x 25-foot drift. For this

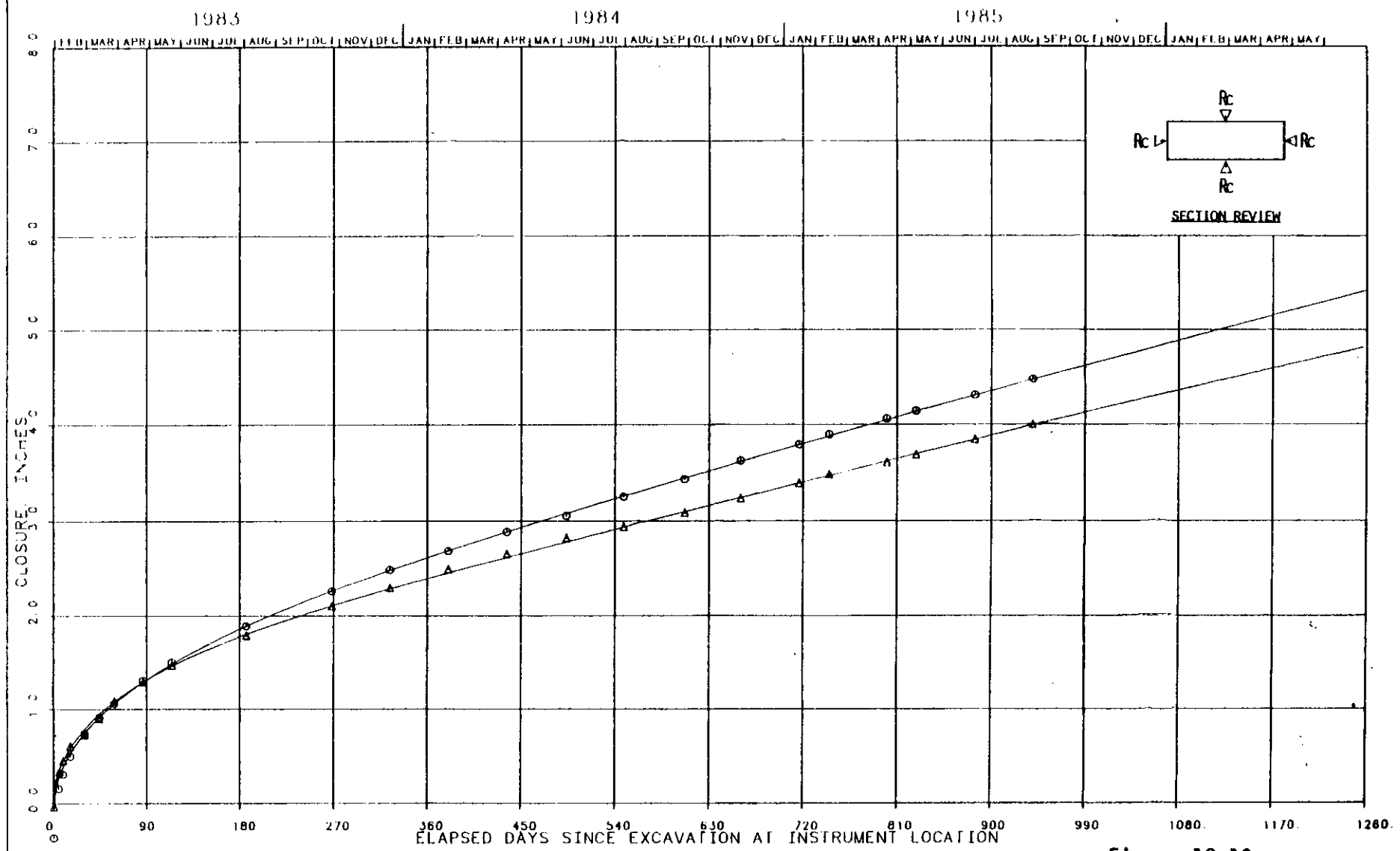

Figure 10-13

DRIFTS
CORRELATED CLOSURE HISTORIES

model, the drift was assumed to be located between an infinite number of parallel drifts, with each having identical cross sections and pillar widths. Two-dimensional analyses using this model were performed assuming a state of plane strain. The boundary displacement conditions at the centerline of the pillar were assumed to be restrained in the horizontal direction but free in the vertical direction. Under these assumptions, this mathematical model can more accurately simulate the geologic conditions in the future when adjacent drifts will exist rather than at the present time when only a single drift exists. Computational results for the parallel drifts are presented in subsection 10.3.3. Parallel drifts with different dimensions and spacings can be incorporated into the present mathematical model and corresponding structural responses can be computed.

Effect of Perpendicular Drifts. Ideally, a three-dimensional analysis is required for the case when the drifts are not parallel to each other. However, the structural responses can be approximated based on the two-dimensional analysis described in this section.

Additional drifts which intersect perpendicular to the drift in question increase the average overburden pressure in the pillar. The two-dimensional analysis of parallel drifts has indicated that the vertical stresses initially increase sharply in the pillar area adjacent to the opening. Over time, salt creep reduces this stress peak as the stresses are redistributed over the width of the pillar. Eventually, the vertical stress level becomes nearly uniform over most of the pillar width.

The total overburden load in the pillar is equal to the average vertical stress multiplied by the pillar support area. Because this total overburden load remains constant before and after the excavation of perpendicular drifts, the average vertical pressure is inversely

proportional to the support area. This increased average vertical stress can, therefore, be expressed as:

$$\bar{\sigma}_r = \bar{\sigma}_i \, W_t/W_2 \qquad (10\text{-}2)$$

where: $\bar{\sigma}_r$ is the average vertical stress of a rectangular pillar, i.e., pillar within a gridwork of intersecting drifts;
$\bar{\sigma}_i$ is the average vertical stress of an infinitely long pillar, i.e., pillar without the perpendicular drifts;
W_t is the distance between the center lines of the perpendicular drifts; and
W_2 is the pillar width in the perpendicular direction, i.e., W_t minus the width of the perpendicular drift.

After the excavation of additional drifts in the perpendicular direction, the restraints at the new wall boundaries are released. Consequently, the distribution of effective stress in the pillar changes. Actual distribution of the effective stresses can be obtained through a three-dimensional computational analysis. However, a two-dimensional analysis can be used to estimate the stress distribution.

A two-dimensional analysis can neither model the restraint conditions nor predict out-of-plane displacements that occur at the boundary of the perpendicular drifts. As a result, the vertical stress distribution from the two-dimensional analysis is assumed to represent a plane some distance from the perpendicular drifts where the actual behavior more closely represents the plane strain condition. The accuracy of this assumption depends upon the distance between the plane being analyzed and the perpendicular drift. In all cases, the results of a two-dimensional analysis represent a lower bound on the effects of perpendicular drifts.

The pillar dimensions are identified as W_1 for the width of the pillar between parallel drifts and W_2 for the width of the pillar

between perpendicular drifts. For an infinitely long pillar, which can be considered as a rectangular pillar with W_1/W_2 equal to zero, the vertical stress distribution of the drift to the center of the pillar can be determined from a two-dimensional analysis. The distribution of the vertical stress $\sigma_i(y)$, shown at the top of Figure 10-14, is symmetrical with respect to the centerline of the pillar and stabilizes within several months after excavation.

For a square pillar, which can be considered as a special case of the rectangular pillar with W_1/W_2 equal to one, the vertical stress distribution should be symmetrical with respect to the two centerlines and two diagonals of the pillar. This is shown graphically in the middle of Figure 10-14, where the x-axis is assumed to be along the drift axis. Assuming the vertical stress distribution $\sigma_s(x,y)$ from the center of the pillar to any of the four walls is the same as the stress distribution $\sigma_i(y)$ across the width of the infinite pillar, the ratio of the average vertical stresses between the square and the infinite pillars can then be estimated from equation 10-3:

$$\frac{\bar{\sigma}_s}{\bar{\sigma}_i} = \frac{\int_0^{W/2} \int_{-x}^{+x} \sigma_s(x,y)\, dydx}{\int_0^{W/2} \int_0^{W/2} \sigma_i(y)\, dydx} \qquad (10\text{-}3)$$

where: $\bar{\sigma}_i$ is the average vertical stress for the infinitely long pillar;

$\bar{\sigma}_s$ is the average vertical stress for the square pillar;

$\sigma_i(y)$ is the vertical stress distribution for the infinitely long pillar; and

$\sigma_s(x,y)$ is the vertical stress distribution for the square pillar.

Based on the computational results from the previous analyses, the average vertical stress of a square pillar is estimated to be 15 percent higher than that for the infinitely long pillar. At the WIPP

facility level, most of the pillars have a rectangular shape. As shown at the bottom of Figure 10-14, a rectangular pillar can be separated into regions which are assumed to act either as an infinite or square pillar. By using a weighted area method, the following equation expresses the effect of varying the pillar's aspect ratio on the average vertical stress:

$$\bar{\sigma}_r = (1 + 0.15 \frac{W_1}{W_2}) \bar{\sigma}_i \qquad (10\text{-}4)$$

where: $\bar{\sigma}_r$ is the average vertical stress for the rectangular pillar.

The corresponding change in pillar shortening is proportional to the ratio of $\bar{\sigma}_r$ to $\bar{\sigma}_i$, raised to some power, with an exponent not exceeding n, where n is the exponent in the power law expression for the creep behavior. Subsection 10.3.3.3 presents the results using equation 10-4.

10.3.2.4 Bay Strains

Strains around an opening in salt vary with space and time. Although, it is difficult to measure these strains directly, they can be inferred from the measurements of anchor displacements of multiple-point borehole extensometers. Relative movements between anchors will provide an approximate distribution of strain along the axis of the extensometer. If these relative displacements are normalized over the spacing between the anchors, then these normalized relative displacements are termed "bay strains". The bay strain will be closer to the true strain provided that the spacing between anchors is small and that the deformation varies linearly with spacing between anchors. Bay strains are useful in detecting any anomalous behavior in salt around an opening such as that influenced by discontinuities, clay seams, or the effect of local stress concentrations.

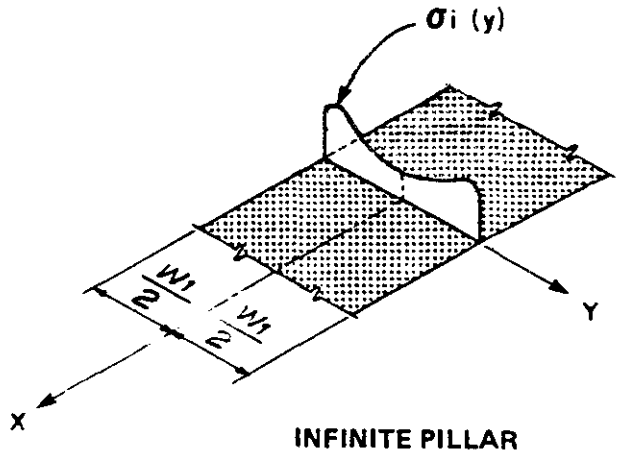

INFINITE PILLAR

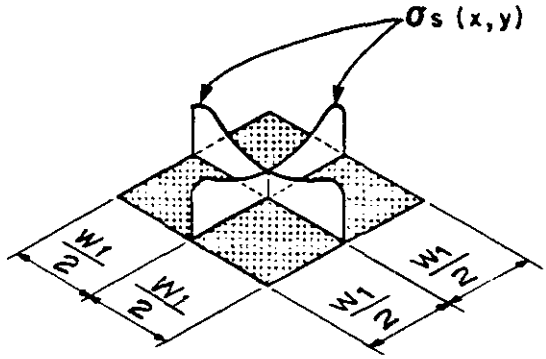

SQUARE PILLAR

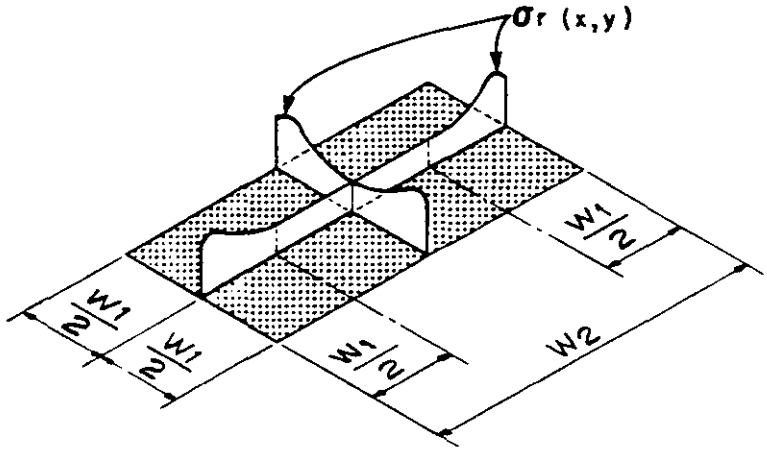

RECTANGULAR PILLAR

Figure 10-14

DRIFTS
VERTICAL STRESS DISTRIBUTIONS IN VARIOUS PILLARS

Figure 10-15 shows the variation of bay strains with elapsed time since completion of excavation for floor extensometer 51X-GE-00242. This extensometer is located at the intersection of Test Room 2 and the N1100 drift. The sudden increase in the bay strains may not be related to salt behavior and is apparently related to system measurement. Thus, it is likely that the maximum average bay strain in the first 6 feet of salt in the floor is no more than 1 percent. The analysis of bay strains in the floor of the drifts in other locations indicates that the maximum average bay strain generally occurs in the first 6 feet (collar to anchor A) in either the roof or the floor. Figures K-36 to K-45 in Appendix K show the variation of bay strains with elapsed time since excavation.

Figure 10-16 shows the rate of bay strains for extensometer 51X-GE-00242. The overall trend is that the rates decrease with time and are currently less than 0.5 percent/year. Figures K-46 to K-55 in Appendix K summarize the variation of strain rates with time.

The decreasing trend in the rates of bay strain with time is an indication that the salt in the roof and floor of the drifts is currently stable.

10.3.3 Prediction of Future Behavior

The results of the analysis of the 8 x 25-foot drift have been categorized as follows:

(1) Effective stresses and effective creep strains immediately after initial excavation; immediately before and after floor lowering; and 5 years after initial excavation.

(2) Principal stresses immediately after initial excavation; immediately before and after floor lowering; and 5 years after initial excavations.

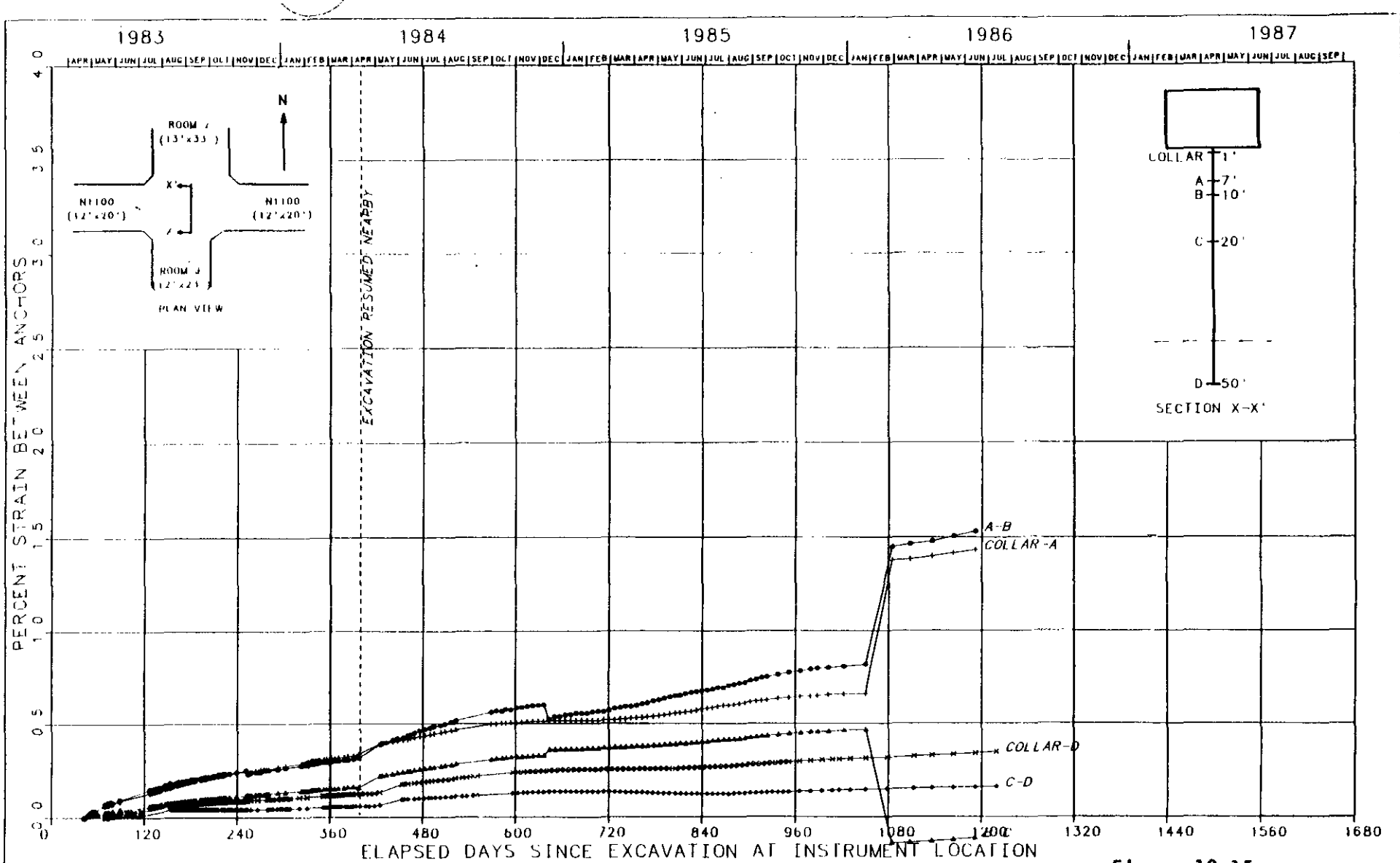

Figure 10-15

DRIFTS
STRAIN VERSUS TIME SINCE EXCAVATION
N1100/TEST ROOM 2 INTERSECTION

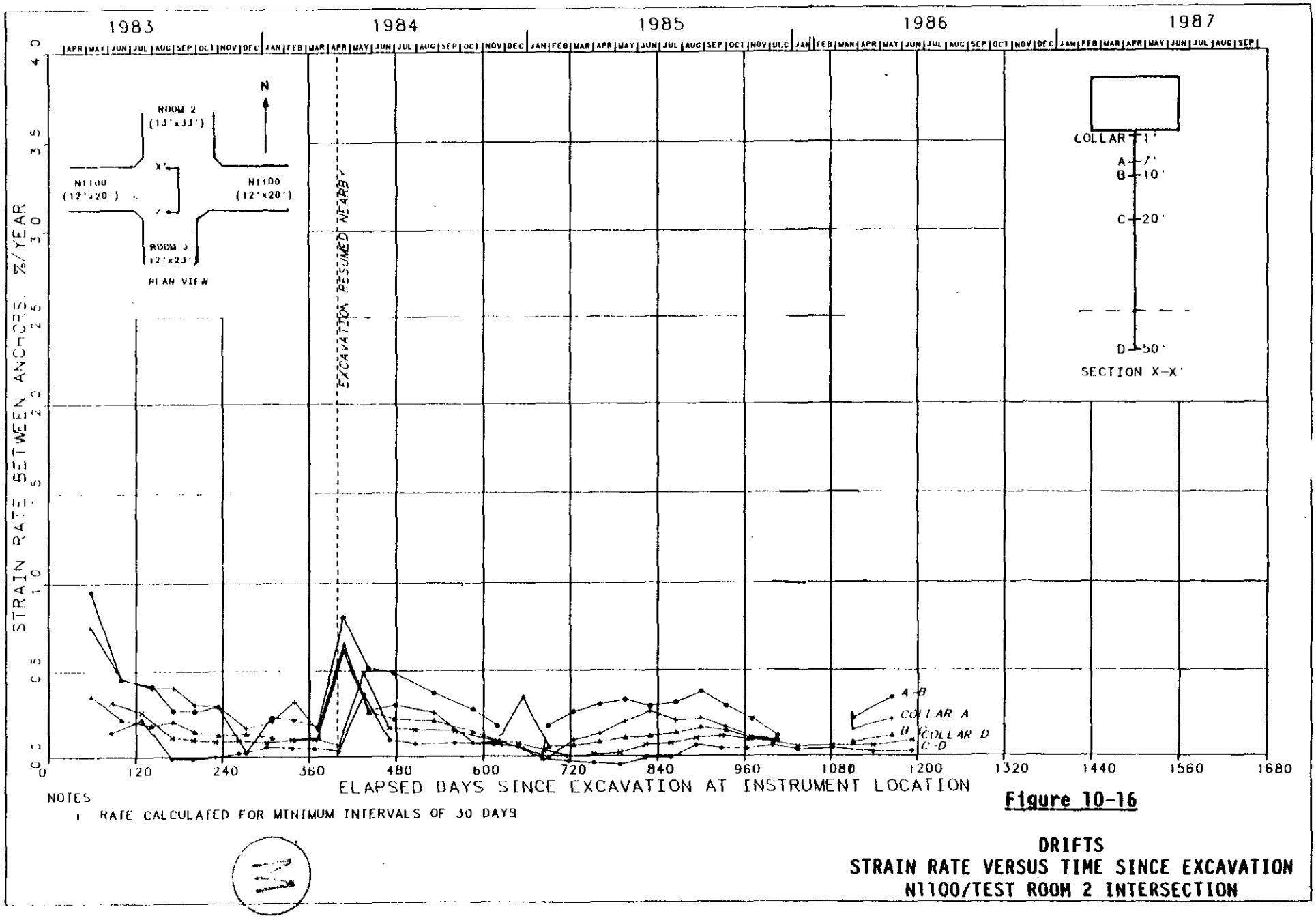

NOTES

1. RATE CALCULATED FOR MINIMUM INTERVALS OF 30 DAYS

Figure 10-16

DRIFTS
STRAIN RATE VERSUS TIME SINCE EXCAVATION
N1100/TEST ROOM 2 INTERSECTION

(3) Deformed drift shapes immediately before floor lowering and 5 years after initial excavation.

10.3.3.1 Effective Stresses

Figures 10-17 and 10-18 show the distribution of effective stresses in each of the elements of the mesh located near the midheight of the finite element model. The contours are numbered with integers from 1 to 10 with each contour interval representing an effective stress increment of 100 ksf. As time passes, the plots show the effective stresses becoming more concentrated in the anhydrite layer. That is, more energy in the form of strain energy is transferred from the creeping halite and argillaceous halite layers to the anhydrite.

10.3.3.2 Principal Stresses

The principal stress plots (Figures 10-19 and 10-20) show that, immediately after excavation, the magnitudes of the predicted principal stresses are relatively large in the corners of the drift and in the anhydrite layer. As the salt creeps, the principal stresses concentrate in the anhydrite layer near the centerline of the drift.

10.3.3.3 Deformation and Closure

A mesh showing the deformed drift shape is presented on Figure 10-21. This mesh shows the outline of the original, undeformed drift in dashed lines while the deformed shape at the corresponding creep time is shown in solid lines.

The deformed shape immediately before floor lowering shows significant vertical deflection (downward) in the roof area of the drift. The drift floor has heaved upward only slightly and the walls have begun to creep inward.

Effects Due to Extraction Ratio. An analysis was performed to simulate the effect on the response of the drift due to a change in the extraction ratio. A change in the extraction ratio is caused by

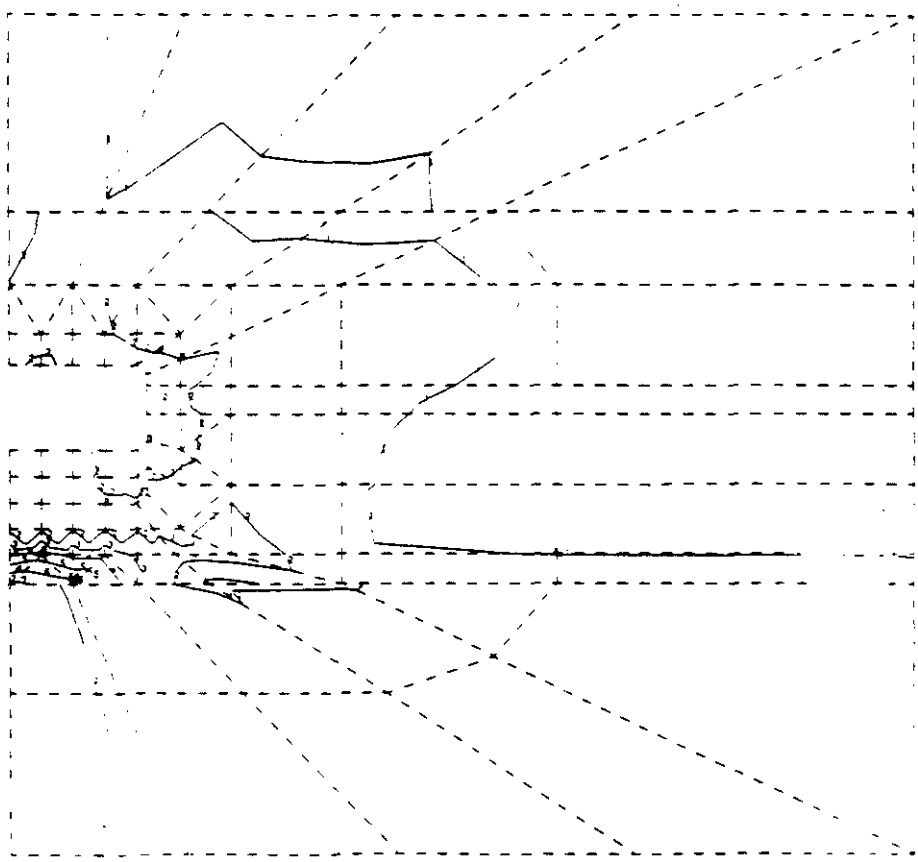

EXPLANATION OF CONTOUR LINES

1 = 100 KSF
2 = 200 KSF
3 = 300 KSF
4 = 400 KSF
5 = 500 KSF
6 = 600 KSF
7 = 700 KSF
8 = 800 KSF
9 = 900 KSF
10 = 1000 KSF

NOTE:
KSF = Kips per square foot.

Figure 10-17

DRIFTS
EFFECTIVE STRESS DISTRIBUTION IMMEDIATELY AFTER EXCAVATION

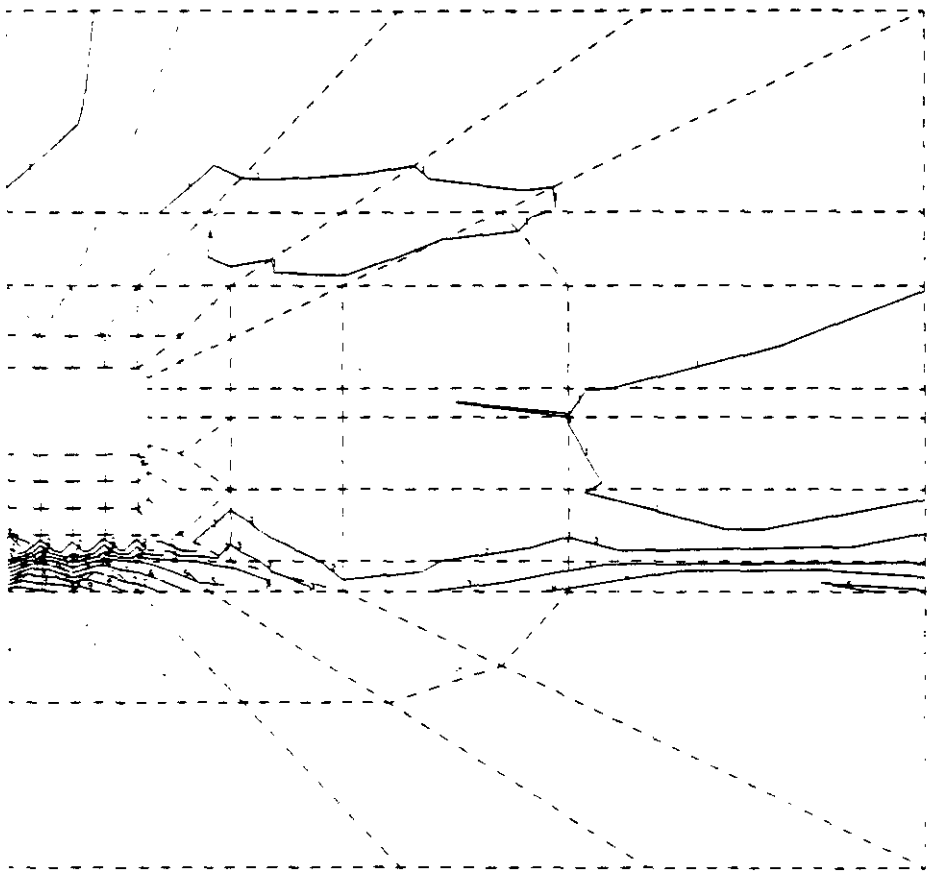

EXPLANATION OF CONTOUR LINES

1 = 100 KSF
2 = 200 KSF
3 = 300 KSF
4 = 400 KSF
5 = 500 KSF
6 = 600 KSF
7 = 700 KSF
8 = 800 KSF
9 = 900 KSF
10 = 1000 KSF

NOTE:
KSF = Kips per square foot

Figure 10-18

DRIFTS
EFFECTIVE STRESS DISTRIBUTION IMMEDIATELY BEFORE FLOOR LOWERING

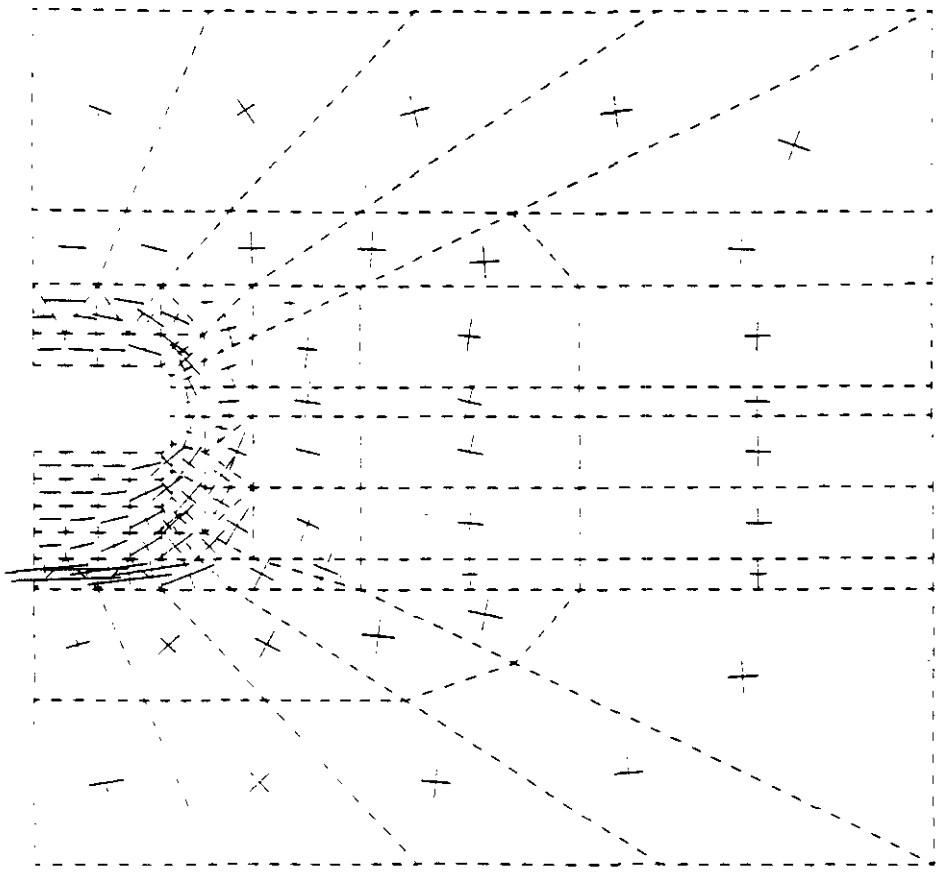

Figure 10-19

DRIFTS
PRINCIPAL STRESSES IMMEDIATELY AFTER EXCAVATION

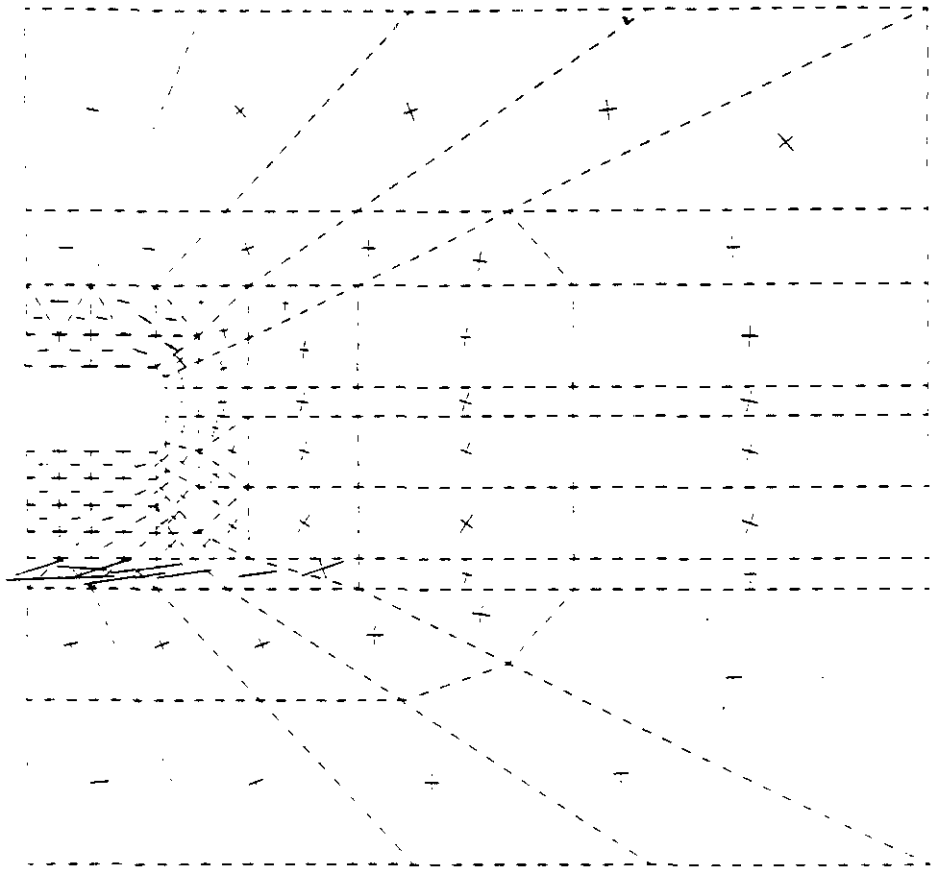

Figure 10-20

DRIFTS
PRINCIPAL STRESSES IMMEDIATELY BEFORE FLOOR LOWERING

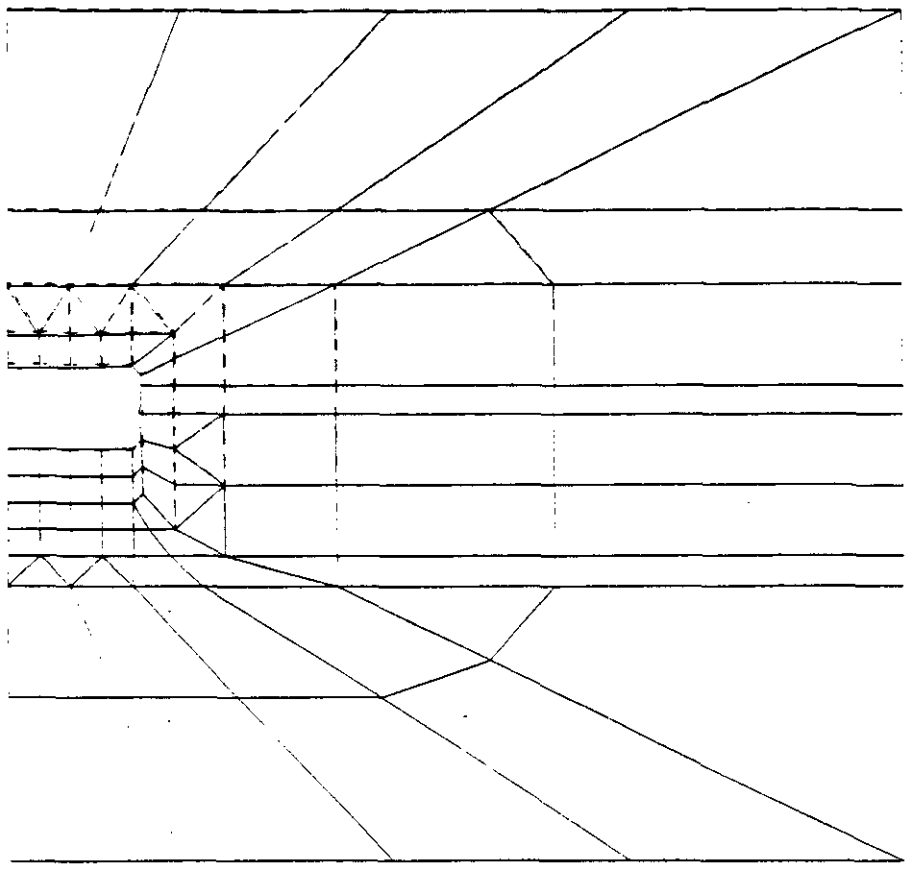

Figure 10-21

DRIFTS
DEFORMED SHAPE IMMEDIATELY BEFORE FLOOR LOWERING

excavation in adjacent or remote areas. The effect due to excavation in adjacent areas was simulated by modifying the finite element model used in the analysis. The difference is essentially a comparison of a single drift to a set of intersecting multiple drifts. Developing a single drift model which accurately represents the behavior of the infinite pillar requires assuming a width for the model. Therefore, to examine the effect of pillar width on analytical results, a 139-foot wide model similar to the one shown on Figure 10-12 was used as a base case and was later widened to 278 feet. Each model consists of an 8 x 25-foot drift.

Figures 10-22 and 10-23 show comparisons of the closure behavior for the two different pillar widths. Because the width of the model is expected to affect the vertical stresses, both the pillar shortening and roof sag components of closure are included. The top graph in both figures indicates that by halving the pillar width to that of the northern area spacing the roof-to-floor closure increases by about 15 percent.

The effects on pillar shortening due to increased overburden stress from the perpendicular drifts can be seen on the middle graph in Figure 10-22. Comparison of the infinite pillar with and without perpendicular drifts indicates a 15 percent increase in pillar shortening due to the presence of the intersecting drifts. Comparing the curves for the narrow pillar in the top two graphs indicates that pillar shortening contributes approximately half of the total closure response. The 15 percent increase in the pillar shortening then corresponds to a 7 1/2 percent contribution in total closure. This is also true for the total closure rate. The combined effects of single versus multiple drifts and multiple parallel drifts versus an intersecting gridwork account for about a 24 percent difference in the total closure rate.

The effects of releasing the boundary constraints at the perpendicular drift wall can be estimated by the use of equation 10-4. For the

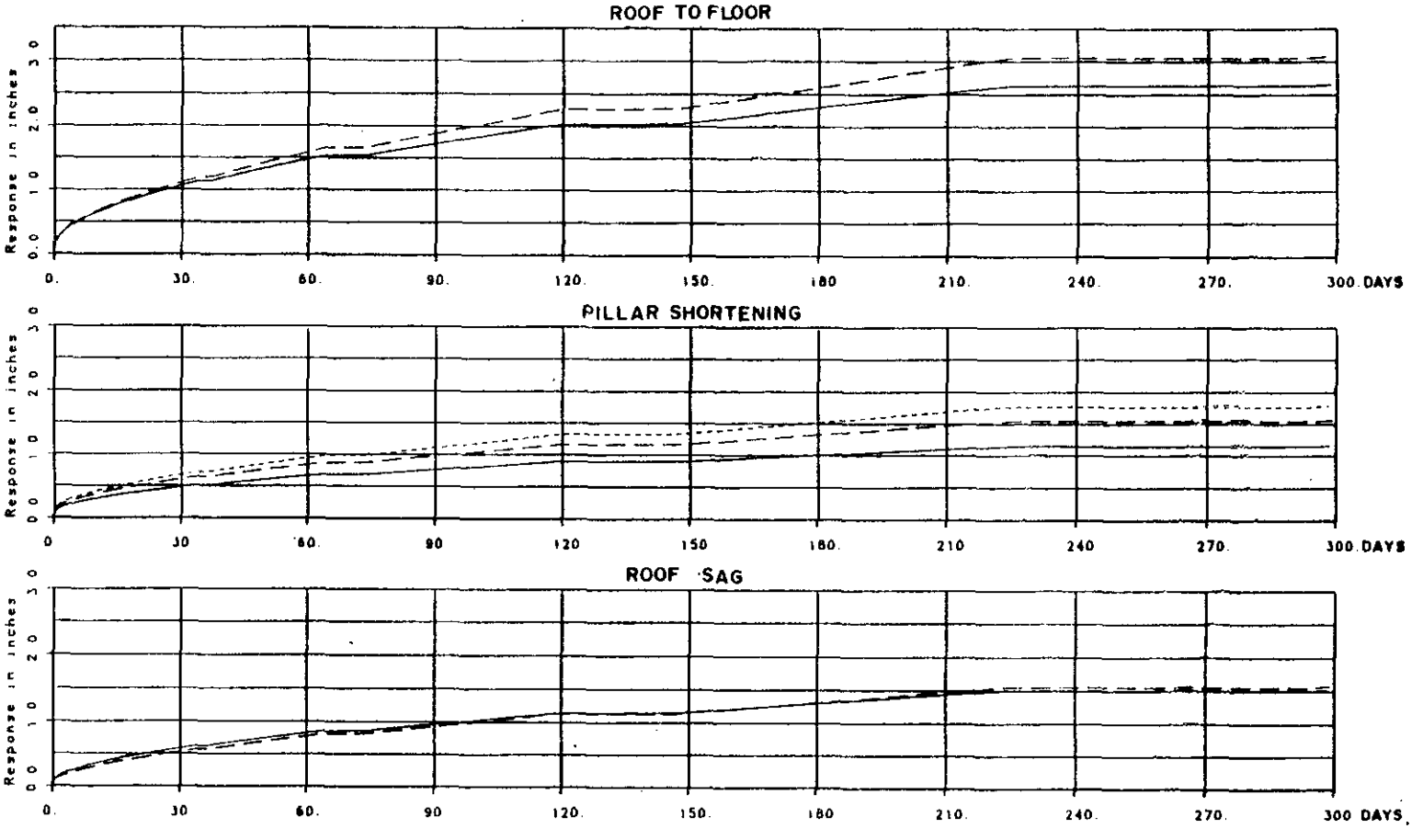

Wide Pillar ——————————

Narrow Pillar — — — — — — — — — —

Narrow Pillar with Perpendicular Drift ----------

Figure 10-22

DRIFTS
COMPARISON OF CLOSURE COMPONENT RESPONSES

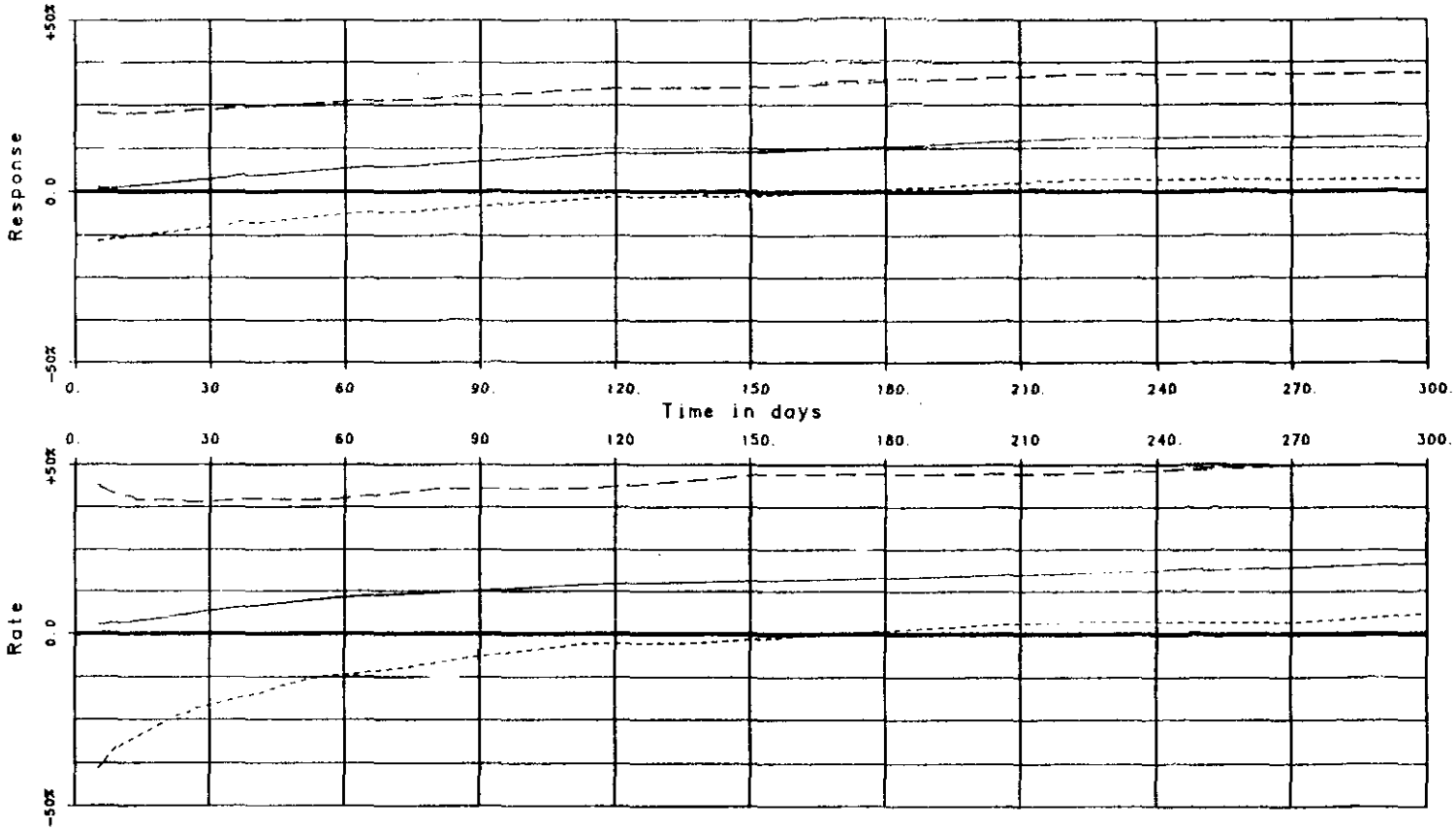

Figure 10-23

DRIFTS
CLOSURE EFFECTS DUE TO PILLAR WIDTH

northern area where the W_1/W_2 ratio is approximately 0.4, the average effective stress is increased by about 6 percent. If the pillar shortening rate is proportional to the square of the increase in average effective stress in the pillar, the boundary release accounts for a 12 percent increase in pillar shortening. As described in the previous paragraph, this 12 percent increase in pillar shortening rate corresponds to about a 6 percent increase in the total closure rate. This factor, combined with the previously described effects, yields about a 30 percent difference in the total closure rate. This compares well with the value presented in subsection 10.3.2.2.

The roof sag component of closure is shown in the bottom graph of Figure 10-23. Figure 10-22 shows the comparison of the closure components of the narrow model relative to the wide model which is equivalent to comparing multiple parallel drifts to a single drift. As this figure indicates, the behavior differences appear to stabilize after about 200 days.

10.3.3.4 Effectiveness of Numerical Modeling

The creep parameters C, A and z were determined using roof-to-floor and wall-to-wall closure data. The effectiveness of the numerical modeling which uses one set of measured data to predict with reasonable accuracy other variables such as stress and strain needs to be verified to infuse confidence in the numerical modeling procedure. Besides, such a comparison will enable testing the adequacy of the basic creep level as well as assumptions regarding the statigraphy assumed for the model.

The 8 x 25-foot drift south of S2180 was isolated until July 1986 and different sets of creep parameters were determined by numerical modeling using roof-to-floor closure data from various convergence point measurements. In situ roof-to-floor closure data for stations south of S2180 indicate that the drift behaves essentially like an infinitely long isolated opening except at the very end of the E140 drift. This affords an opportunity to compare the measured relative displacements in the roof as well as in the floor at one instrument

location with the values obtained from numerical modeling which used roof-to-floor closure data from measurements at some other instrument location to "back calculate" the creep parameters.

Figure 10-24 compares the measured relative displacement between the collar and anchor D of extensometer 51X-GE-00247, in the roof at E140/S1950, with the values obtained from the numerical modeling. The calculated value is the relative vertical displacement of two nodes comparable to the positions of the collar and anchor D of the extensometer. The parameters C, A and z were obtained using roof-to-floor closure data from the instrument location at E140/S1879. The agreement is reasonable because the slopes of both the measured and calculated relative displacements are nearly identical. Figure 10-25 similarly compares the measured relative displacement in floor extensometer 51X-GE-00248 at E140/S1950 with the calculated values from the same numerical modeling. The slope of the in situ curve is 28 percent steeper than the calculated value. This is probably because the numerical model assumes that the anhydrite layer in the floor of the drift as linearly elastic with infinite strength. This may not be true if the anhydrite has pre-existing fractures, and thus may not be able to absorb the heave from the salt below.

Figure 10-26 compares the measured wall-to-wall closure at E140/S1879 with the calculated wall-to-wall closure from the results of the same numerical modeling. The average slope of the curve from numerical modeling is nearly 43 percent steeper than the slope of the curve from measurement data.

10.4 CONCLUSIONS AND RECOMMENDATIONS

The following subsections present conclusions pertaining to validation of the drift reference design and recommendations for design modifications. These are based on a comparison of the design criteria, design bases and reference design configurations with the results of the analysis and evaluation of data collected during the design validation process.

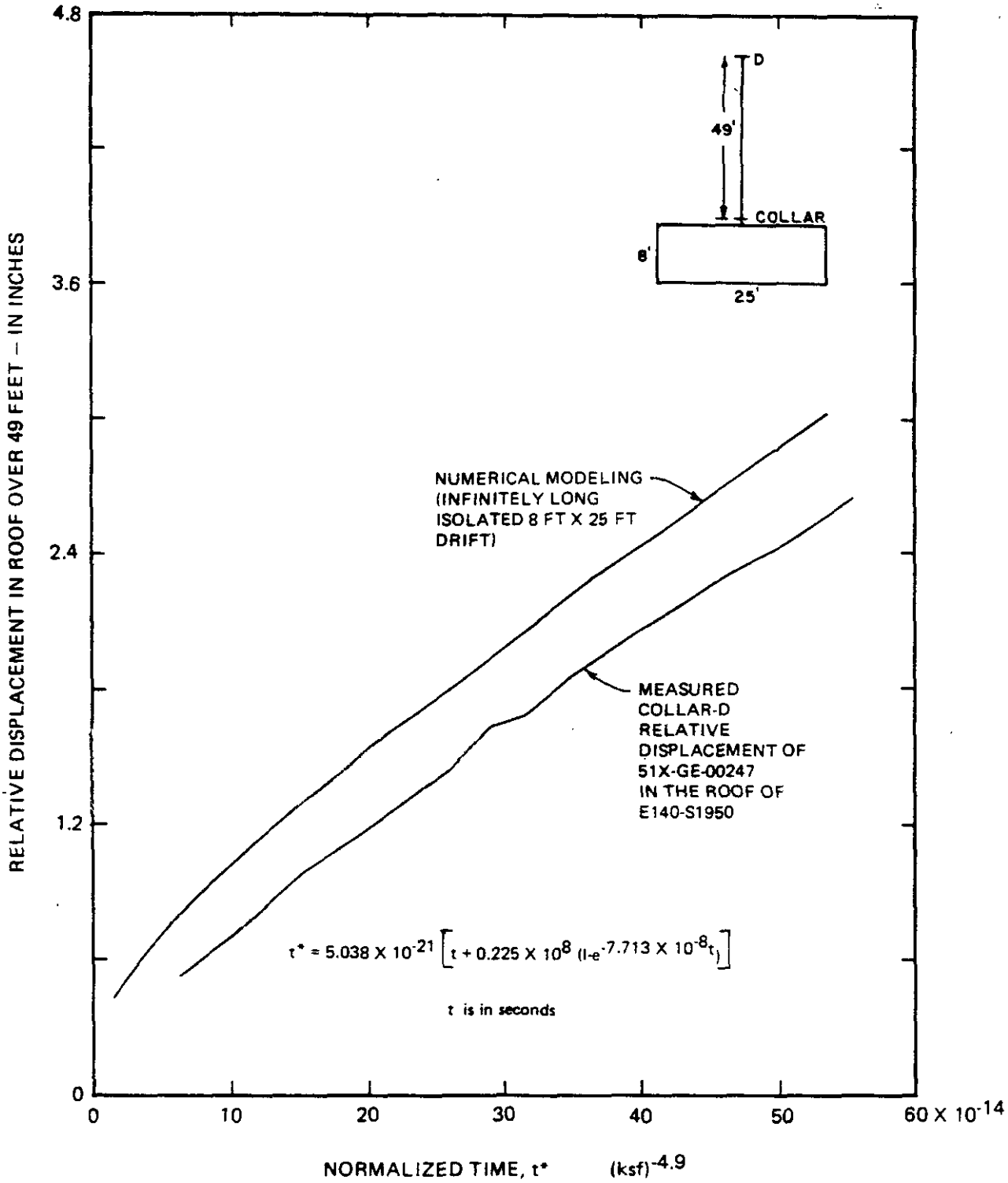

Figure 10-24

DRIFTS
NUMERICAL MODELING VERSUS IN SITU MEASUREMENT
DATA FROM ROOF EXTENSOMETER

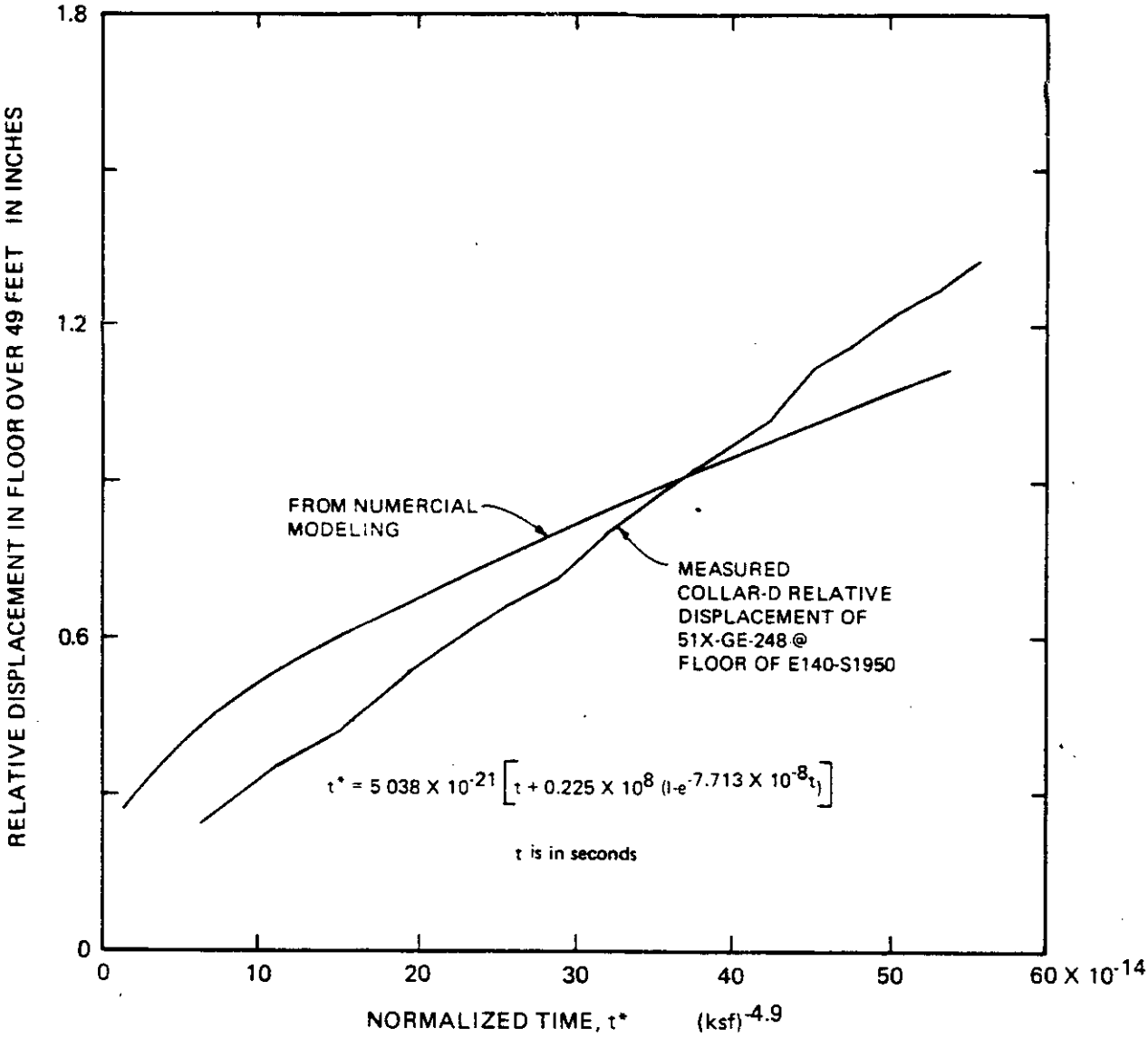

Figure 10-25

DRIFTS
NUMERICAL MODELING VERSUS IN SITU MEASUREMENT
DATA FROM FLOOR EXTENSOMETER

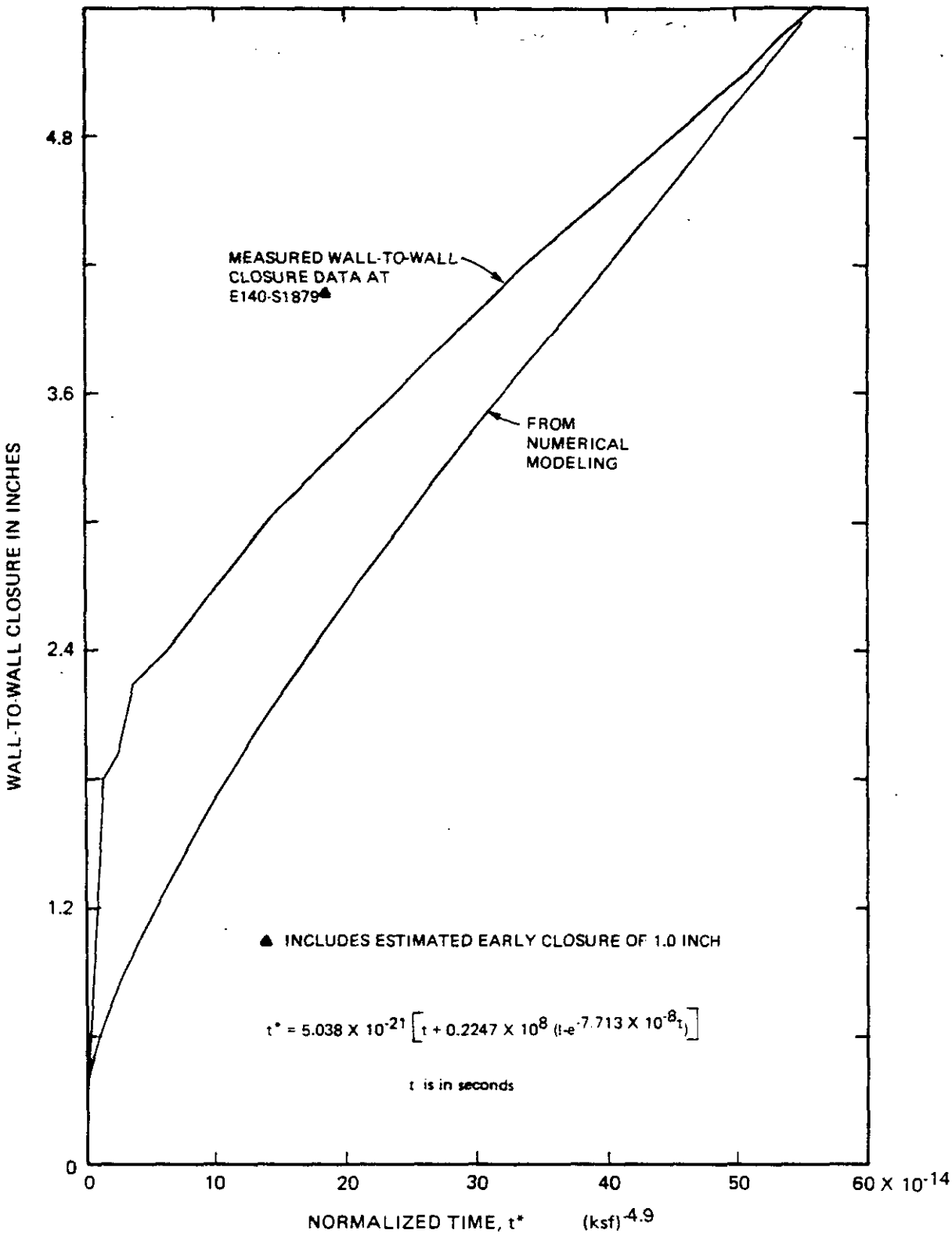

Figure 10-26

DRIFTS
NUMERICAL MODELING VERSUS MEASURED WALL-TO-WALL CLOSURE
AT E140/S1879

10.4.1 Conclusions

The evaluation of field observations and analytical results shows that the design criteria were appropriate for design of the horizontal openings. The three criteria identified as requiring specific evaluation, that the drifts remain within the required structural limits, provide maximum stability, and maintain the minimum required dimensions, were determined to be suitable. The reference design for the horizontal openings is therefore validated.

Spalling from the roof and walls of the drifts and fracturing and spalling at pillar corners will continue. Displacements and separations at clay seams above the roof may slowly increase. This deformational behavior is expected and can be controlled by scaling and rock bolting as necessary.

The average bay strains determined from the relative displacements of extensometer anchors 3 years after drift excavation are within 1 percent. The strain rates as well as the closure rates decrease with time indicating that the drifts are stable. Based on the projections of closure rates, the drifts will continue to be stable.

Fracturing beneath the floor of the drifts is minor and has nowhere developed to near the degree as that beneath the floor of Test Room 3. If additional fracturing develops in the future beneath the drifts, it is also expected to be minor. Based on experience in local potash mines, this type of fracturing is not expected to cause stability or operational problems.

The comparison of measured closure behavior in drifts with different dimensions indicates that the maximum closure and closure rate will occur in 12 x 25-foot drifts. The closure rates are affected by the presence of nearby parallel drifts and crosscuts as well as differences in salt properties. Based on available measurement data and the results of modeling analyses, the closure rate in the 13 x 25-foot

storage area drifts may be 30 percent greater than that of a single, infinitely long drift with the same dimensions (Chapter 12).

Analyses of salt behavior around the 25-foot wide drifts has determined the redistribution of stresses due to the effect of creep. Based on the computed vertical, horizontal and effective stresses, the stress which develops immediately after excavation is followed by relaxation due to creep behavior. According to the analyses, stress should not cause future stability problems in the drifts.

The analyses have also determined the locations of effective creep strain concentrations around the drifts at different times. Based on the predicted values of effective creep strain and the strain limit discussed in Chapter 6, the drifts will remain within the structural stability limits required, with respect to catastrophic failure, during the facility operating life. Minor spalls from the roof and wall surfaces are expected to occur. Analysis of observations in mines and discussion with mine personnel indicates that the surfaces of the drifts may start to deteriorate more rapidly after about 15 years. Increased maintenance will then be required.

10.4.2 Recommendations

Based on the results of design validation of the drifts, it is recommended that all drifts be inspected frequently for operational clearance and safety. If the clearance is insufficient, the drifts must be trimmed to the required dimensions. Trimming the floor to increase drift height is preferred over trimming the roof. Over the 25 year operating life, the roof should not be trimmed more than 12 inches for drifts 25 feet wide or less. Trimming the roof more than 12 inches would make the beam of salt too thin and increase the possiblity of a roof fall. Further trimming must be accomplished from the floor even though this will decrease the thickness of the salt above MB-139. Scaling and rock bolting should be performed where

necessary for safety purposes. Periodic inspection of accessible open boreholes should be performed to monitor the occurrence and behavior of displacements, separations and fracturing in the salt above the roof and beneath the floor of the drifts.

CHAPTER 11
TEST ROOMS

11.1 INTRODUCTION

The four test rooms comprise a panel with a configuration similar to that designed for the waste storage area. The test rooms were instrumented, observed and analyzed in order to evaluate the potential behavior of the storage rooms. This chapter presents the results of data collection activities in the test rooms and the analysis and evaluation of the data with respect to the behavior of the excavated rooms. The information presented here will be used in Chapter 12 to predict the future behavior of the storage rooms and to validate their reference design.

11.2 DESIGN

The test rooms represent a portion of the storage room reference design configuration. The purpose of the test rooms is to provide geotechnical information that can be used to predict the potential behavior of the storage rooms. Because they were excavated to permit validation of the storage room reference design, and will not be used for permanent storage, the test rooms were not specifically addressed in the Design Criteria document. The design criteria apply to the configuration of the storage rooms and, therefore, only indirectly to the configuration of the four-room test panel.

No Design Basis documents were developed specifically for the test rooms. Only two Design Basis documents (refs. 2-9 and 2-18) contain elements pertaining to the test rooms. These elements specify that test rooms shall be provided to verify underground conditions as required by the SPDV Program and that their dimensions shall be 33 feet wide, 13 feet high and 300 feet long. All other design bases that require evaluation are applicable to the storage rooms rather than to the test rooms.

The test room panel is the experimental model for the storage ... Validation of the test panel reference design configuration is not required. The test room data and analyses presented in this chapter are the bases for validation of the storage rooms. Predictions of the future behavior of the storage rooms based on these data analyses are presented in Chapter 12.

11.3.1 Data Collection

Data collection in the test rooms consisted of the accumulation of geotechnical data from geologic mapping, core drilling, observations of deformational behavior and geomechanical instrument measurements. Geologic mapping and core drilling were performed in the four test rooms. The stratigraphy defined by the mapping and core logging is discussed in Chapter 6. Observations of in situ behavior and data from the geomechanical instrumentation program are presented in the following subsections.

11.3.1.1 Field Observations

Some aspects of test room behavior can only be evaluated by visual observation. Visual inspections of the rooms include observations of their general surface conditions in response to stress redistribution and salt creep. These conditions include small spalls from the roof and walls, especially at their intersection, and vertical fracturing at pillar corners and along the walls in response to pillar shortening.

Field observations include other qualitative and quantitative techniques in addition to visual inspections of excavation surfaces. Boreholes are surveyed using video cameras. Horizontal displacements and vertical separations of the geologic strata surrounding boreholes are determined using a probe, as described in Chapter 7, subsection 7.3.1.4. Wall surfaces of large diameter holes are mapped by a geologist.

A qualitative determination of the conditions of the test rooms is made

by site geologists during an inspection of the rooms at least once every 3 months. These inspections have been documented in each GFDR starting with the February 1984 edition (refs. 4-12 through 4-19). Detailed descriptions of observed test room behavior are contained in each of these reports.

As discussed in Chapter 10, an Excavation Effects Program was conducted throughout the underground facility during May through July 1986. This program was conducted to further characterize near-field deformation above and below the facility level. Ten arrays of boreholes were drilled in the roof and floor of the test rooms. The locations of the arrays are shown on Figure 10-1 in Chapter 10.

The results of some of these observations are used in conjunction with the results of numerical analysis and in situ measurement data to quantify the structural behavior of the test rooms. The documented field observations can be separated into four categories: roof and wall spalling; pillar fracturing; roof displacements and separations; and floor displacements, separations and fracturing.

Roof and Wall Spalling. A sounding survey of the roof of each test room was conducted during and immediately after excavation. Only a few areas of drummy rock were discovered and these were either removed or rock bolted.

The rooms have exhibited only minimal spalling over a period of 3 years since their excavation. The drummy areas originally found in the roofs have not grown noticeably, but some additional areas have been discovered by subsequent roof soundings. Additional scaling and rock bolting have been performed in most of these areas. The most noticeable spalling is associated with the argillaceous halite unit (geologic map unit 4, Appendix G, Figures G-1 through G-4) high on the test room walls. This spalling is generally continuous but shallow. Some spalling from the roof close to the walls has also been observed within the past year that has required support by rock bolts in selected areas.

Fracturing. [illegible] formed by the intersection of drifts with [illegible] the fractures have separations that range from essentially closed to about 2 inches wide. They generally extend into the rock perpendicular to the rock surface for an unknown distance. All corners of the test rooms show fracturing and consequent spalling. The fractures first appeared in the pillar corners about 3 to 6 months after excavation. They started as thin, hairline fractures and have steadily grown in length, width and presumably depth. Each of the GFDRs document this gradual development of the fractures. Scaling of these corners has been performed periodically.

Vertical fracturing has developed in the pillars parallel to the room walls. This fracturing is relatively minor and, to date, has been observed only in Test Rooms 3 and 4. The fracturing has been detected in horizontal boreholes drilled into the walls and occurs within approximately 2 feet of the wall surface. The fractures range from closed to about 1/32 inch wide.

Roof Displacements and Separations. Inspections of open boreholes in the test room roofs were conducted using a video camera and/or probe. The video camera produces high-resolution, color videotapes that are useful in identifying horizontal displacements and vertical separations. The probe is used in conjunction with a tape measure to determine the location and amount of movement in the boreholes. As in other areas of the underground facility, expected horizontal and vertical movements of the geologic strata surrounding the boreholes have been observed or measured in the test rooms. These observations are summarized in Table 11-1.

Ten arrays of boreholes were drilled in the test rooms in May 1986 as part of the Excavation Effects Program. These holes were used for additional investigation of test room roof displacements and separations. Each hole was inspected using a probe. Table 11-2 presents a summary of the results of this study.

Table 11-1

TEST ROOMS 1 THROUGH 4
RESULTS OF INSPECTION OF VERTICAL BOREHOLES IN ROOFS

Hole	Date Completed	Hole Size (in.)	Depth (ft)	Approximate Location	Observed Condition*
IG-205	4-17-83	3	56	Room 1; 1 ft from west wall	D
IG-206	4-15-83	3	52	Room 1; 1 ft from east wall	D
IG-203	3-26-83	3	52	Room 2; 1 ft from west wall	D
IG-204	3-83	3	52	Room 2; 1 ft from east wall	D
OH-3	8-83	4	20	Room 2 centerline	S, F
P4X-26	10-83	5	52.1	Room 4; N1360/W630	None
P4X-30	12-83	4	50.9	Room 4; N1360/W630	S
-	-	6	8	Room 4; N1360/W639	D, F
-	-	5	$9\pm$	Room 4 center; N1176	S(?)

* D = Displacement; S = Separation; F = Fracturing

Table II-2

EXCAVATION EFFECTS PROGRAM
BOREHOLE INSPECTION SUMMARY

SECTION	OPENING DIMENSIONS (HxW-FT)	EXCAVATION DATE	LOCATION	DATE DRILLED	DATE INSPECTED	OBSERVED CONDITIONS					
						ROOF HOLES			FLOOR HOLES		
						E	A	C	F	B	D
1	13x33	4/83	ROOM 4, N1175	5/15/86	5/15/86	C	S(?) *	C(?)	D, S *	C	S, C
2	13x33	4/83	ROOM 4, N1264	5/16/86	5/16/86	C(?)	NONE	C	NONE	C	S
3	13x33	4/83	ROOM 4, N1361	5/16/86	5/16/86	NONE	D *	NONE	NONE	D, S, F *	S
4	13x33	4/83	ROOM 3, N1198	5/15/86	5/15/86	NONE	NONE	S	NONE	S	S
5	13x33	4/83	ROOM 3, N1243	5/15/86	5/15/86	NONE	NONE	NONE	S, F (USED ROOM 3 LARGE DIAMETER HOLES)		
6	13x33	4/83	ROOM 3, N1312	5/15/86	5/15/86	S	C	NONE	D, S, F (USED PREVIOUSLY DRILLED HOLES MB-FI-01 THROUGH 03)		
7	13x33	3/83	ROOM 2, N1147	5/21/86	5/22/86	NONE	NONE	C	C	F, C	NONE
8	13x33	3/83	ROOM 2, N1231	5/21/86	5/22/86	F	F	NONE	S	S, F, C	F
9	13x33	4/83	ROOM 1, N1159	5/21/86	5/22/86	C	F	NONE	C	S, C	NONE
10	13x33	4/83	ROOM 1, N1275	5/21/86	5/22/86	F	S, F, C	NONE	C	S	S, C

* EXISTING HOLE.

EXPLANATION

D = HORIZONTAL DISPLACEMENT. FOUND ONLY IN PREVIOUSLY DRILLED HOLES. DISPLACEMENT APPEARS TO DEVELOP WITH TIME FOLLOWING HOLE DRILLING.

S = VERTICAL SEPARATION. PROBE NAIL PENETRATES HOLE WALL SURFACE. VERTICAL SEPARATIONS RANGE FROM APPROXIMATELY 1/16 INCH TO 6 INCHES.

F = FRACTURE ZONE. PIECES OF HALITE COMMONLY PICKED OUT OF ZONE BY PROBE NAIL.

C = PROBE NAIL CATCHES ON HOLE WALL SURFACE BUT DOES NOT PENETRATE. INDICATES POSSIBLE SEPARATION OF LESS THAN 1/16 INCH. OCCURENCES AT KNOWN CLAY LAYERS ARE NOT INDICATIVE OF SEPARATION AND ARE NOT INCLUDED IN THIS TABLE.

NOTES:

1. SECTION LOCATIONS AND HOLE CONFIGURATIONS ARE SHOWN IN CHAPTER 10, FIGURE 10-1.
2. HOLES WERE DRILLED VERTICALLY USING A JACK-LEG DRILL.
3. NOMINAL HOLE DEPTH IS 9 FEET BUT SOME HOLES ARE SHORTER DUE TO LOW DRIFT ROOF OR DRILLING DIFFICULTIES.
4. ONE ROOF AND ONE FLOOR HOLE OF EACH ARRAY WERE GENERALLY DRILLED 3 INCHES IN DIAMETER TO ACCOMODATE USE OF BOREHOLE CAMERA IF DESIRED. OTHER HOLES WERE DRILLED 1-7/8 INCHES IN DIAMETER. EXISTING HOLES WERE USED WHERE POSSIBLE.
5. OBSERVATIONS WERE MADE USING A PROBE CONSISTING OF A NAIL ATTACHED PERPENDICULAR TO THE END OF A ROD.

Floor Displacements, Separations and Fracturing. Horizontal displacements, vertical separations and fracturing have been observed beneath the floor of the test rooms in boreholes. They have been observed to occur in MB-139 and in the overlying halite. Geologic maps of Test Room 3 (Room T) boreholes are presented in Appendix G, Figures G-10 through G-31. A summary of the results of the inspection of all small-diameter boreholes drilled in the floor of the test rooms is presented in Table 11-3. The inspections were accomplished using video equipment and/or a probe.

The only prominent exposure of floor fracturing is in the 36-inch diameter boreholes drilled in the floor of the south half of Test Room 3 (Room T). A total of 22 holes were drilled in this area during September and November 1985 for the erection of structural steel columns. A drilling summary is presented in Table 11-4. The holes are approximately 7.2 feet deep. The bottom of many of the holes coincides with the occurence of clay E at the base of MB-139. The remaining holes were terminated above the base of the marker bed.

The holes were logged on a 360 degree foldout at a scale of 1 inch to 1 foot. All features were measured from a level reference line which was later surveyed to determine elevations. Fracture traces, fracture zones and hairline fractures, in addition to lithologic contacts, were logged. A fracture trace is a distinct fracture surface exposed on the wall of the borehole. Fracture traces shown on the logs, unless otherwise noted, are closed within a few inches of the wall surface. A fracture zone is an area on the wall bounded by distinct fractures. Rock within the zone is broken by numerous smaller fractures spaced less than 1 inch apart. The fractured rock is commonly broken out very close to the wall surface of the borehole due to drilling, but becomes closed within 1/2 to 2 inches of the wall surface. Locally, the zone is open or partially filled with drill cuttings. At a distance of 12 inches from the borehole, the cumulative vertical separation measured over the length of the hole varies from less than 1/4 inch to 6 inches. The hairline fractures are closed fractures usually found

...ROUGH 4

RESULTS OF INSPECTION OF VERTICAL BOREHOLES IN FLOOR

Hole	Date Completed	Hole Size (in.)	Depth (ft)	Approximate Location	Observed Condition*
IG-202	4-18-83	3	52	Room 1; 1 ft from west wall	D
GE-269	1-86	3	55	Room 1 centerline	S, F
IG-201	3-26-83	3	52	Room 2; 1 ft from west wall	D
NG-254	3-84	6	7	Room 2 centerline	None
GE-270	1-86	3	55	Room 2 centerline	S, F
2NPD-01	2-86	5	8.9	Room 2; N1370	S, F
MB-FI-01	12-85	4	12.0	Room 3; N1309	D, S, F
MB-FI-02	12-85	4	12.0	Room 3; N1309	D, S, F
MB-FI-03	12-85	4	12.0	Room 3; N1309	D, S, F
GE-271	1-86	3	55	Room 3 centerline	S, F
P4X-06	1983	5	9.0	Room 4; N1369/W625	D, S, F
P4X-25	10-83	5	50.2	Room 4; N1360/W630	D, S, F
P4X-27	10-83	5	51.1	Room 4; N1360/W630	D, S, F
P4X-29	10-83	5	49.5	Room 4; N1360/W630	D, S, F
P4X-31	11-83	5	50.4	Room 4; N1360/W630	D, S, F
P4X-81	11-83	16	-	Room 4	D, S, F
P4X-83	12-83	16	6.1	Room 4	S, F
P4X-84	1-84	36	9.5	Room 4	D, S, F

* D = Displacement; S = Separation; F = Fracturing

Table 11-4

TEST ROOM 3 (ROOM T)
SUMMARY OF DRILLING

Hole	Date Completed	Drilling Fluid	Communication During Drilling*
TV-01	10-25-85	Brine**	---
TV-02	10-28-85	Air	---
TV-03	11-05-85	Air	TV-07, TV-14 through 75° dipping fracture. TV-15 through fractures in halite close to surface on east side. Surface fracture close to east wall 25 feet south of TV-03. No communication to TV-13. TV-17, TV-12.
TV-04	11-08-85	Air	---
TV-05	11-20-85	Air	---
TV-06	11-13-85	Air	---
TV-07	10-29-85	Air	TV-12
TV-08	11-19-85	Air	---
TV-09	11-21-85	Air	---
TV-10	11-14-85	Air	TV-13, TV-14, TV-17, TV-15, TV-06, TV-11
TV-11	11-11-85	Air	---
TV-12	9-17-85	Air	---
TV-13	10-09-85	Air	TV-12, TV-15
TV-14	10-11-85	Air	TV-15
TV-15	9-23-85	Air	TV-19
TV-16	9-30-85	Air	TV-19, TV-20

TEST ROOM 3 (ROOM T)
SUMMARY OF DRILLING

Hole	Date Completed	Drilling Fluid	Communication During Drilling*
TV-17	10-15-85	Air	---
TV-18	10-02-85	Air	---
TV-19	9-20-85	Air	---
TV-20	9-25-85	Air	TV-19 along main fracture zone on north-northeast side.
TV-21	10-18-85	Air	---
TV-22	10-19-85	Air	TV-19 along main fracture zone on north-northeast side. TV-20 along main fracture zone on west side.

* Communication is indicated by drilling dust emanating from connected holes and detected by driller or geologist.

** Source of brine encountered in TV-01 is clay E at base of MB-139. Driller noted that this clay and about 4 inches of the overlying anhydrite were moist in many holes.

within fracture zones less than 1 inch wide. Some of these appear to be pre-excavation features within MB-139.

Additional small-diameter boreholes were drilled into the test room floors as part of the Excavation Effects Program. The 10 arrays summarized in Table 11-2 include three floor holes at each array. These holes were drilled primarily to determine if the fracturing observed in the 22 large-diameter holes in Test Room 3 extends to other areas beneath the test rooms.

11.3.1.2 Geomechanical Instrumentation

Geomechanical instrumentation in Test Rooms 1 through 4 initially consisted of 19 borehole extensometers, 16 horizontal inclinometers, 6 vertical inclinometers, 4 sets of convergence points, 2 convergence meters, and 2 rigid-inclusion vibrating-wire stressmeters (Figure 11-1). These instruments, with the exception of the inclinometers and convergence points, were connected to the datalogger system on May 13, 1983.

Due to failure for various reasons, some instruments in the test rooms had to be replaced. Those instruments replaced include both stressmeters in Test Room 2 and the extensometers in the floor of Test Rooms 1, 2 and 3. The history of instrument performance and maintenance is discussed in the GFDRs.

Figure 11-2 shows the instruments in each test room and the excavation dates at the instrument locations. Because the excavation of each test room required about 10 days to complete, it was difficult to assign a single date of excavation for some instrument locations. Table 11-5 presents the dates of excavation used for plotting and analysis of the test room data.

11.3.2 Analysis and Evaluation

This section discusses the analysis and evaluation of the results of

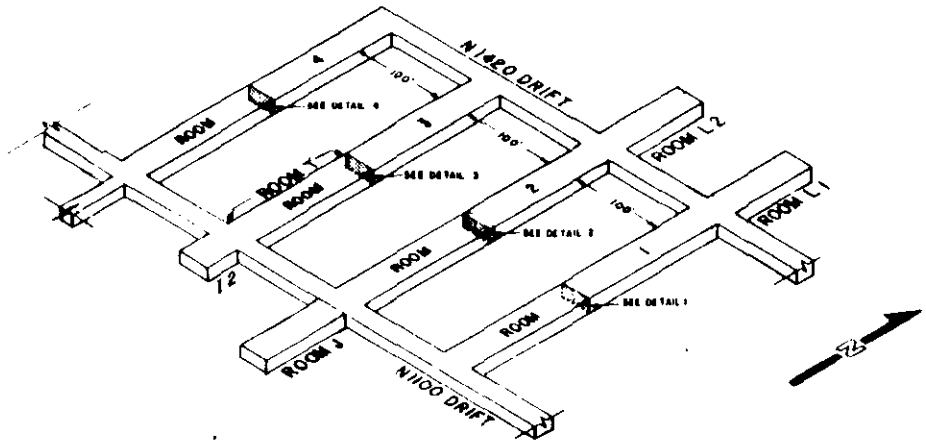

ALL COORDINATES BASED ON DISTANCE FROM C@SH SHAFT ℄

(FOR DETAILS 1, 2, 3, & 4)

EXPLANATION

- IG INCLINOMETER
- CE CONVERGENCE METER
- GE EXTENSOMETER
- RC RADIAL CONVERGENCE PI
- SG STRESSMETER (RIGID INCLU

NOTE

1 EXTENSOMETERS GE 269, GE 270 AND GE 271 REPLACED GE-230, GE-218 AND GE-210, RESPECTIVELY.

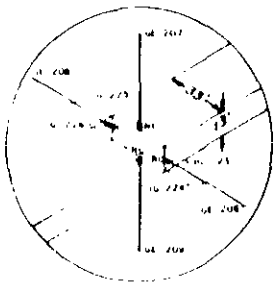

ROOM 4
INSTRUMENTATION LOCATION
DETAIL 4

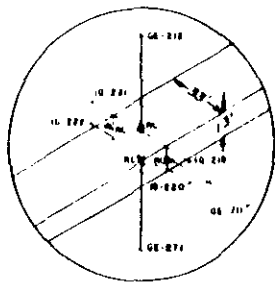

ROOM 5
INSTRUMENTATION LOCATION
DETAIL 3

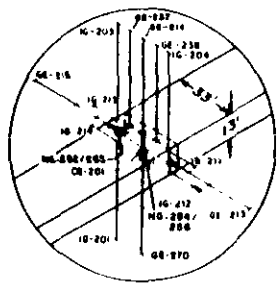

ROOM 2
INSTRUMENTATION LOCATION
DETAIL 2

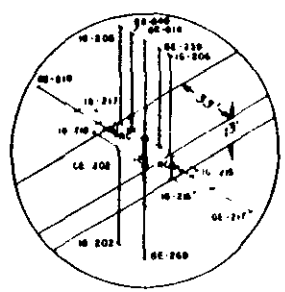

ROOM 1
INSTRUMENTATION LOCATION
DETAIL 1

Figure 11-1

TEST ROOMS INSTRUMENTATI

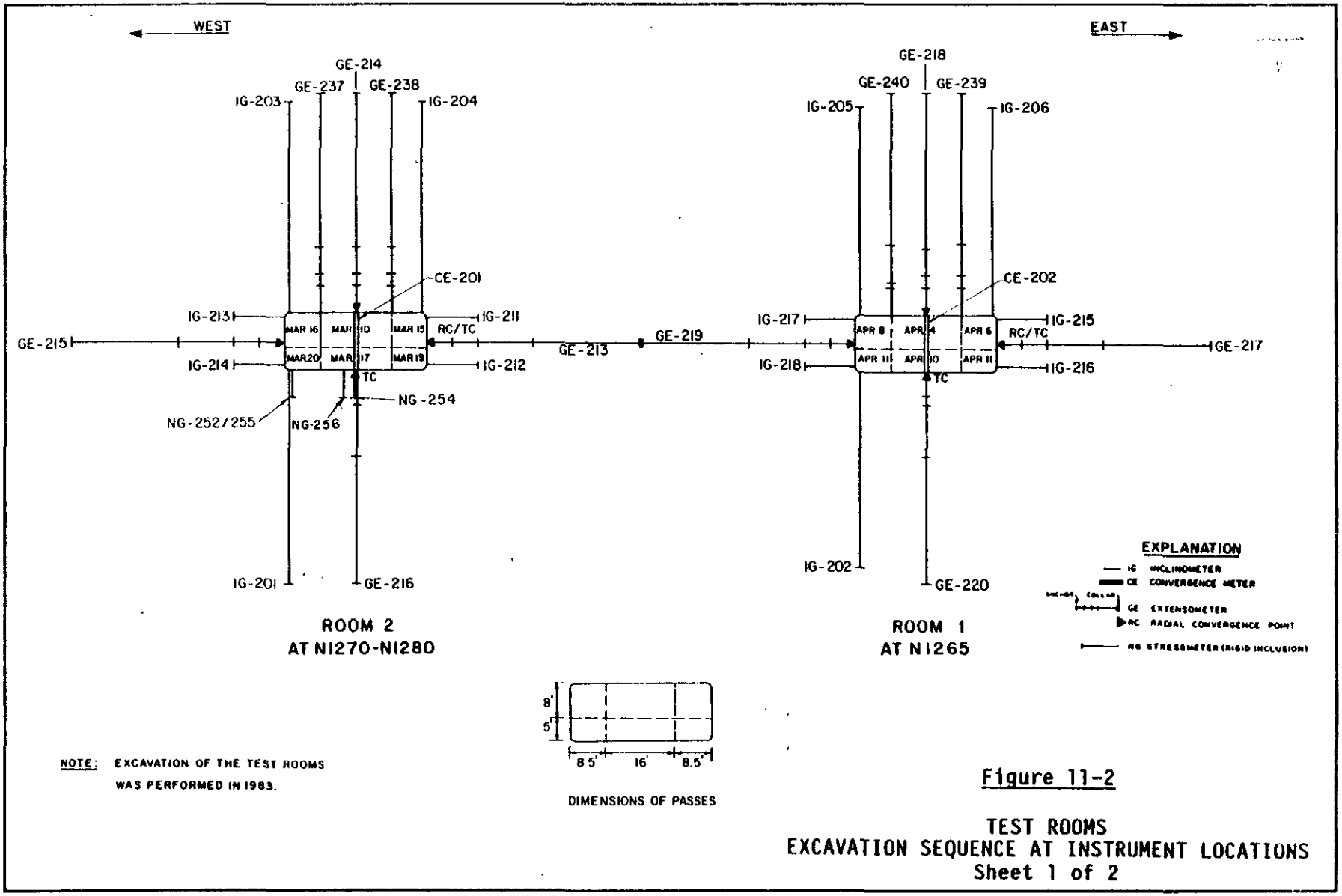

Figure 11-2

TEST ROOMS
EXCAVATION SEQUENCE AT INSTRUMENT LOCATIONS
Sheet 1 of 2

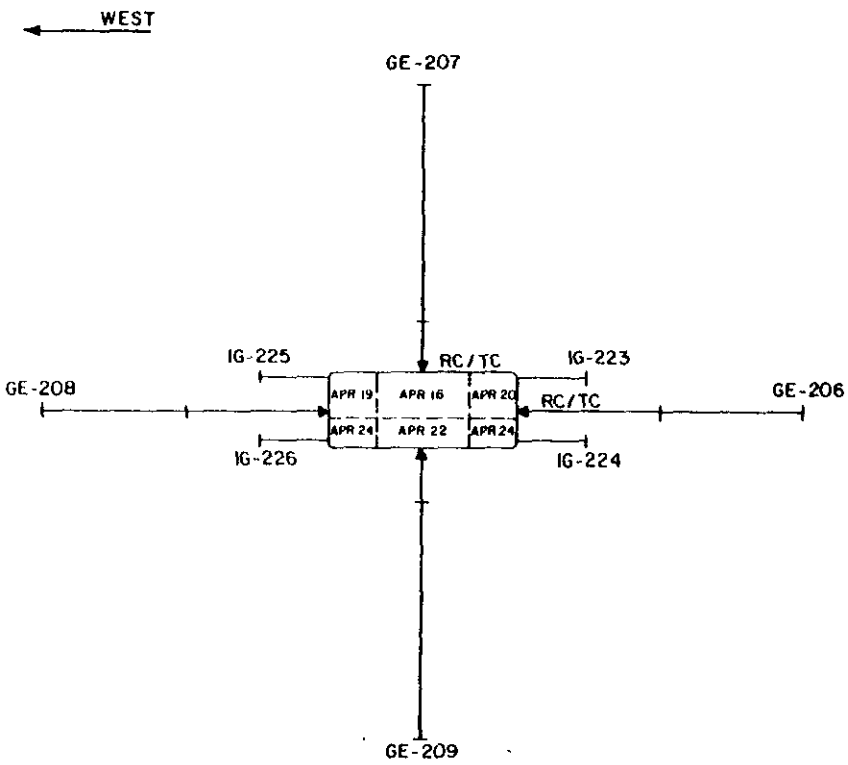

ROOM 4
AT N1275

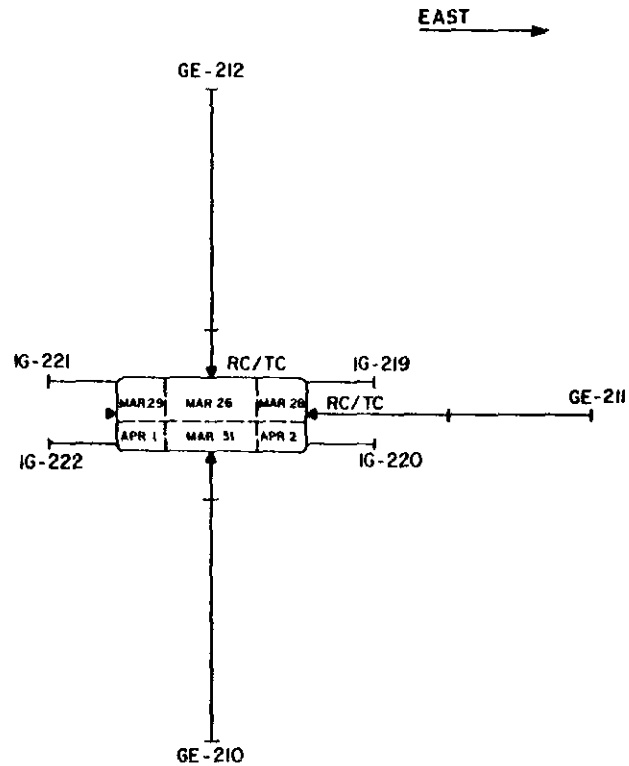

ROOM 3
AT N1265

DIMENSIONS OF PASSES

NOTE: EXCAVATION OF THE TEST ROOMS WAS PERFORMED IN 1983

Figure 11-2

TEST ROOMS
EXCAVATION SEQUENCE AT INSTRUMENT LOC.
Sheet 2 of 2

Table 11-5

TEST ROOMS
ASSUMED EXCAVATION DATES FOR DATA ANALYSIS

Type of Instrument/Location	Instrument Designation	Assumed Date of Excavation Room 1	Room 2	Room 3	Room 4	Basis for Selection
Convergence meters	51X-CE-00202 51X-CE-00201	Apr. 7, 1983	Mar. 13, 1983			Average of dates for upper and lower center passes.
Roof extensometers - center	51X-GE-00218 51X-GE-00214 51X-GE-00212 51X-GE-00207	Apr. 4, 1983	Mar. 10, 1983	Mar. 26, 1983	Apr. 16, 1983	Date for upper center pass.
Floor extensometers - center	51X GE-00220 51X-GE-00216 51X-GE-00210 51X-GE-00209	Apr. 10, 1983	Mar. 17, 1983	Mar. 31, 1983	Apr. 22, 1983	Date for lower center pass.
Roof extensometers - east side	51X-GE-00239 51X-GE-00238	Apr. 5, 1983	Mar. 13, 1983			Average of dates for upper center and upper east passes.
Roof extensometers - west side	51X-GE-00240 51X-GE-00237	Apr. 6, 1983	Mar. 13, 1983			Average of dates for upper center and upper west passes.
Wall extensometers - east side	51X-GE-00217 51X-GE-00213 51X-GE-00211 51X-GE-00206	Apr. 6, 1983	Mar. 15, 1983	Mar. 28, 1983	Apr. 20, 1983	Date for upper east pass.
Wall extensometers - west side	51X-GE-00219 51X-GE-00215 51X-GE-00208	Apr. 8, 1983	Mar. 16, 1983		Apr. 19, 1983	Date for upper west pass.

Table 11-5 (continued)

TEST ROOMS
ASSUMED EXCAVATION DATES FOR DATA ANALYSIS

Type of Instrument/Location	Instrument Designation	Assumed Date of Excavation Room 1	Room 2	Room 3	Room 4	Basis for Selection
Wall shortening points - east side	IG 215-216 RS IG 211-212 RS IG 219-220 RS IG 223-224 RS	Apr. 8, 1983	Mar. 17, 1983	Mar. 30, 1983	Apr. 22, 1983	Average of dates for upper and lower east passes.
Wall shortening points - west side	IG 217-218 RS IG 213-214 RS IG 221-222 RS IG 225-226 RS	Apr. 9, 1983	Mar. 18, 1983	Mar. 30, 1983	Apr. 21, 1983	Average of dates for upper and lower west passes.
Wall-to-Wall convergence points - near roof	IG 211-213 TC IG 219-221 TC		Mar. 15, 1983	Mar. 28, 1983		Average of dates for upper east and west passes.
Wall-to-Wall convergence points - near floor	IG 212-214 TC IG 220-222 TC		Mar. 19, 1983	Apr. 1, 1983		Average of dates for lower east and west passes.
Wall-to-Wall permanent convergence points - center	Room 1 RC Room 2 RC Room 3 RC Room 4 RC	Apr. 7, 1983	Mar. 15, 1983	Mar. 29, 1983	Apr. 19, 1983	Average of dates for upper east and west passes.
Roof-to-Floor permanent convergence points - center	Room 3 RC Room 4 RC			Mar. 28,1983	Apr. 19, 1983	Average of dates for upper and lower center passes.

Table 11-5 (continued)

TEST ROOMS
ASSUMED EXCAVATION DATES FOR DATA ANALYSIS

Type of Instrument/Location	Instrument Designation	Assumed Date of Excavation Room 1	Room 2	Room 3	Room 4	Basis for Selection
Wall-to-Wall temporary convergence points - center	Room 1 TC	Apr. 7, 1983				Average of dates for upper east and west passes.
	Room 2 TC		Mar. 15 1983			
	Room 3 TC			Mar. 29, 1983		
	Room 4 TC				Apr. 19, 1983	
Roof-to-Floor temporary convergence points - center	Room 1 TC	Apr. 7, 1983				Average of dates for upper and lower center passes.
	Room 2 TC		Mar. 13, 1983			
	Room 3 TC			Mar. 28, 1983		
	Room 4 TC				Apr. 19, 1983	
Floor stressmeters - west corner	51X-NG-00252		Mar. 20, 1983			Date for lower west pass.
	51X-NG-00255		Mar. 20, 1983			Date for lower west pass.
Floor stressmeters - center	51X-NG-00254		Mar. 17, 1983			Date for lower center pass.
	51X-NG-00256		Mar. 17, 1983			Date for lower center pass.

Notes:

(1) The "Elapsed Days Since Excavation" shown on the data plots in Appendix J were calculated using this "Assumed Date of Excavation".

(2) See Figure 11-2 for the excavation sequence at the center of the test rooms.

(3) The dates of excavation for individual inclinometers were not used for plotting.

field observations and numerical modeling of the test rooms using in situ measurement data are also presented. In addition, regression analyses of the closure rate obtained from the closure measurements were also performed. The fitted equations were used to supplement the prediction of closure behavior in the storage rooms and are discussed in Chapter 12.

11.3.2.1 Observed Conditions

Roof and Wall Spalling. Minor spalling from the roof in the test rooms, resulting in shallow drummy areas, has occurred as expected. Drummy areas usually occur within 3 to 6 inches of the roof in areas of clear halite not associated with any noticeable clay. Separations occur along local planes of weakness in the halite, probably created by the orientation of crystal surfaces. This same phenomenon occurs in the drifts. Drummy areas have been identified immediately after excavation and additional areas have developed since that time. These later-occurring drummy areas appear to develop primarily along the roof within several feet of the walls.

Spalling along the walls of the test rooms is a result of local stress concentrations and the low tensile properties of salt. It is also related to the percentage of argillaceous material in the halite and to the proximity of floor and roof intersections. The squeezing of clay F at the upper contact of geologic map unit 4 is associated with the spalling phenomenon. Minor spalling is also associated with map unit 0, near the floor.

Pillar Fracturing. Vertical fracturing in the pillars is the expected result of room deformation and stress concentrations. The fractures that have developed in the walls of the test rooms, parallel to the rooms, are considered to be tension fractures resulting from stress relief. Fractures detected in boreholes drilled in the upper portion of geologic map unit 4 are related to the spalling occurring in this unit.

Horizontal inclinometers in the test room walls show both upward and downward vertical movement toward the center of the wall (Appendix J, Figures J-320 through J-335). Although no displacements have been observed, the inclinometer data indicate that the salt has moved toward the central horizontal axis of the room. This movement, due to vertical compressive stress and salt creep, is discussed further in subsection 11.3.2.2. Tensile stresses resulting from this salt creep and pillar shortening have caused fractures to lengthen and widen and new fractures to develop. Fracturing is more prominent at pillar corners that were not beveled to the 4 x 4-foot design.

Fracturing parallel to the room walls will continue to occur. Spalling and local failure will also continue at pillar corners and will require periodic maintenance.

Roof Displacements and Separations. The displacements observed in various open boreholes in the test room roofs are the result of deformation around the openings. The halite at the storage horizon is interrupted by anhydrite beds and thin clay layers. These layers, particularly anhydrite "b" and the underlying clay G, are directly associated with the displacements observed in the test room roofs.

Lateral displacement in the salt above the test rooms is similar to that detected above the drifts. The halite bounded by the roof and clay G moves toward the room center relative to the upper layers of salt. The movement is, however, not exactly symmetrical about the room centerline. This is confirmed by inclinometer readings in the roof of Test Rooms 1 and 2 which show that the lateral movement of the salt close to the roof is greater to the west than to the east (Appendix J, Figures J-316 through J-319). However, this trend is reversed at about 32 feet above the roof of the test rooms. The halite comprising the lower roof beam is subjected to horizontal compressive stresses resulting in shear along clay G and possible vertical separation as the beam moves downward. Some casing deformations have also been observed within 1 foot of the hole collar of the roof inclinometers. The

re[illegible]ve [illegible] and is probably due to the near surface halite resisting the shear movement along clay G.

Movement within the halite below clay G, opposite to that found elsewhere, has been observed in one borehole in Test Room 4. This may be the result of movement along existing planes of weakness in the halite or of the resistance of the halite to shear movement along clay G.

The current results of the Excavation Effects Program indicate that minimal separation or fracturing has occurred at clay G or in the underlying halite above the test room roofs. In Test Rooms 3 and 4, separations less than 1/16 inch wide have been observed. No separation has been observed at clay G. In the array of holes comprising Section 5 in Table 11-2, above the 36-inch diameter holes in the floor of Test Room 3 (Room T), no separations or fracturing were detected. In hole C of Section 4 in Test Room 3, two 1/4-inch vertical separations were found within 1 foot of the roof. These fractures resulted from roof spalling.

Similar small separations were observed in the roof of Test Rooms 1 and 2. Also, fracture zones (in one case 2.4 inches wide) were detected in the halite below clay G in the center hole of three of the four arrays.

Floor Displacements, Separations and Fracturing. The only prominant display of fracturing observed throughout the entire WIPP underground facility during design validation has been in the area of the 36-inch diameter holes drilled in the floor in the south half of Test Room 3 (Room T). Cross sections of the room floor through these holes are presented in Appendix G, Figures G-33 and G-34. Two distinct fracture zones are evident. The first is a dish-shaped zone that angles 10 to 20 degrees downward from near the room walls, intersects MB-139, and flattens near the room center. This zone is most pronounced along the series of holes shown on Figure G-34. In the

northern cross section (Figure G-33), this fracture zone is evident in the holes west of the room centerline but is not present in the holes east of the centerline. In both sections, this upper fracture zone "daylights" at the floor surface or pinches out before reaching the room pillars.

A second fracture zone, dipping approximately 50 to 60 degrees from horizontal and exposed in the holes closest to the room walls, occurs below the upper fracture zone. This lower zone is more regular and planar than the upper zone. With the exception of one hole, this lower zone occurs entirely within MB-139 and is more developed on the west side of the room.

In addition to the two major fracture zones, some subhorizontal fracturing is present just above clay E at the base of MB-139. This fracturing is most evident in the holes closest to the room centerline. No separations along clay E were observed in any of the holes.

Communication between holes during drilling was observed and is described in Table 11-3. During the drilling of hole TV-03, drilling dust was observed coming up through a surface fracture close to the east wall, 25 feet south of the hole location.

A series of measuring pins were installed in two open holes, TV-03 and TV-19, in late January 1986 to monitor movements within the holes. The pins were installed in MB-139 and in the overlying halite and straddle the fracture zones. Measurements taken until the holes became inaccessible in June 1986 indicated that some small-scale dilation was occurring in both of the holes.

The fractures observed beneath the floor of Test Room 3 are directly related to the excavation geometry and the stratigraphy. Some fractures within MB-139 may have been pre-existing but have opened since room excavation.

[illegible] inch diameter holes were drilled in the north half of Test Room 3 to determine if fracturing is occuring there. These holes were drilled to a nominal depth of 12 feet below the floor. A thin fracture zone was detected within 1 1/2 feet of the floor in two of the holes and minor fracturing was detected in MB-139 in all of the holes. This fracturing is significantly less developed than that observed in the south half of Test Room 3.

The 22 large-diameter holes in Test Room 3 were drilled late in 1985. They are, therefore, too recent to document any lateral displacements along the observed fractures. However, other older floor boreholes do indicate relative displacement. In Test Room 4, boreholes P4X-06, P4X-25, P4X-27, P4X-29 and P4X-31 all show multiple displacements and vertical separations (Table 11-2). These are primarily within MB-139 and exhibit up to 2 inches of lateral displacement and up to 1/2 inch of vertical separation. These five holes are near the room centerline. The relative movement of the multiple displacements observed is complicated and does not follow the simpler interpretation of the roof displacements. The most significant displacements in all of the holes have taken place closest to the floor surface and, in all cases, the salt above the fracture has moved east relative to the underlying salt. Inclinometers IG-202 and IG-201, in Test Rooms 1 and 2, also exhibit similar relative displacement. Both of these inclinometers are on the west side of their respective test rooms. The marker bed and the overlying salt have moved east towards the room centerline relative to the underlying salt. Movement is apparently along clay E and is approximately 3/4 inch.

Although no detailed investigation of the salt beneath the test room pillars has been performed, the Test Room 3 fracture mapping indicates that it is unlikely that fractures extend beneath them to any significant extent. Neither of the two fracture zones identified can be traced into the pillars. The upper fracture zone pinches out prior to reaching the walls or daylights at the floor surface. The lower fracture zone cannot be traced beyond the hole walls, but it is not

suspected of continuing beneath the pillars. One small diameter hole was drilled at an angle into each of the walls of Test Room 3 in May 1986. Except for a localized clay break at a depth of 3.2 feet, there was no evidence of separation.

Fractures and separations have been observed in four large-diameter holes drilled in the floor in the south end of Test Room 4. Fractures were observed in these holes during drilling in November 1983 and January 1984. The fracturing was minor, however, with no separations observed. One hole became inaccessible soon thereafter. Fractures in the other holes have been observed to increase in number and to exhibit separation (Table 11-2). Fractures occur in the marker bed and in the overlying halite. Because two of the holes have restricted access, monitoring of the fractures is difficult. Borehole P4X-84, in the southwest corner of Test Room 4, was mapped in February 1986 and the results are shown in Appendix G, Figure G-32. The separations and displacements in P4X-84 over the 2 year period since excavation are small in comparison to those in the floor holes in the south half of Test Room 3.

A low-angle fracture in the floor of Test Room 2 was observed in August 1985. An inspection in June 1986 showed that it extended from approximately N1242 to N1208. This fracture daylights at the floor surface, 1.5 feet to 6 feet from the west wall, and extends 2 feet below the floor surface toward the east. Approximately 8 to 10 inches of separation is present along this fracture, and approximately 25 square feet of floor in the vicinity of this fracture sounds drummy.

As part of the Excavation Effects Program, a series of holes were drilled in each of the test rooms to determine the extent of floor fracturing and for future monitoring of this phenomenon. Existing boreholes, such as those in Test Rooms 3 and 4, were utilized where possible. The locations of the holes are shown on Figure 10-1 in Chapter 10. These holes were inspected using a probe and the results are summarized in Table 11-2. The holes exhibited some fractures and

The dish-shaped profile observed in the floors in Test Room 3 was also found in some of the hole arrays, although on a much smaller scale. It was most pronounced in several of the holes close to the room walls where separations were estimated to be a maximum of 6 inches. In other locations, the separation ranged from 1/8 inch to 3 inches. Within MB-139, fractures and separations found in the central holes of the Test Room 1 array ranged from approximately 1/8 inch to 3 inches. For other hole arrays, the maximum separations were 1/2 inch and, again, these were found in the central holes.

Horizontal displacements and vertical separations have been observed in various small-diameter boreholes in the test room floors. Horizontal displacements up to 2 1/2 inches and vertical separations estimated to be up to 1/2 inch wide were present in some of these holes. Multiple displacements in single boreholes were also present. The horizontal displacements and vertical separations found in many of the holes are within MB-139 or coincide with the lower contact of this unit. These displacements and separations have developed since room excavation, although some of them may have developed along pre-existing planes of weakness in the marker bed.

In addition to observations made in open boreholes, ground-penetrating radar and gas permeability testing have been conducted in some of the test rooms. A radar survey was conducted in Test Rooms 2 and 3. The radar method has some limitations. It appears to be effective in locating the first reflector such as a fracture or clay seam beneath the floor, but the structure below this is not easily distinguished. MB-139 is readily defined on the records but fractures within it cannot be discerned.

Zones of relatively high permeability have been found to develop immediately beneath the floor of the test rooms and beneath the intersections of Test Rooms 1 and 2 with the N1420 drift. There also appears to be a slight increase in permeability, relative to background values, within MB-139 and immediately beneath the floor of the N1420

drift between Test Rooms 1 and 2. Some increase in permeability also appears to occur in MB-139 near the center of the pillar between Test Rooms 2 and 3. This data is only preliminary, however, because only one hole intersecting MB-139 beneath the pillar has been drilled and tested for permeability.

Gas tracer measurements performed along the centerline in the north half of Test Room 2 and across the N1420 drift to Room L2 indicate the existence of fracturing beneath the floor. A video survey of the boreholes used for the tracer tests shows the presence of fracture zones and separations mainly within MB-139. Holes tested along the N1420 drift, except at intersections, show little increase in background permeability. A video survey of these holes did not show any separations or fracturing.

In summary, subhorizontal fracturing has developed beneath the test room floors. The majority of this fracturing occurs as single fractures or thin fracture zones within MB-139 and the overlying halite. Horizontal displacements ranging up to 2 inches and separations generally ranging up to 1/2 inch have been measured in small diameter boreholes. Separations up to 6 inches have been observed locally. Only the south half of Test Room 3 (Room T) in the WIPP underground facility has exhibited extensive fracturing beneath the floor.

The Excavation Effects Program was designed in part to determine if fracturing similar to that occurring beneath the floor of Test Room 3 has developed in other areas of the facility. The results of this program show that, although small-scale fracturing is occurring beneath all of the test rooms, no other areas of fracturing have developed on the same order of magnitude as that in Test Room 3. The fracturing occurring beneath the floor of Test Room 3 appears to have existed prior to drilling. The stress changes induced by the size and number of holes drilled in this area probably exacerbated the existing fractures.

Roof-to-Floor Closure. Figure 11-3 shows the relationship between measured roof-to-floor closure and the elapsed time since excavation of the four test rooms, as determined from convergence meter and convergence point data. Because of differences in time-lag between the end of excavation and the time of the initial readings, the relative positions of these curves are deceptive. For analysis purposes, the roof-to-floor closure that occurred before installation of the convergence instruments was determined using equation 10-1 in Chapter 10.

In addition, part of the measurement data from the temporary convergence points were added to the permanent convergence instrument data to obtain approximate values of the actual roof-to-floor closure. Table 11-6 shows roof-to-floor convergence point readings and adjusted closure magnitudes for the test rooms. Item 7 in this table shows the approximate roof-to-floor closure obtained by adding suitable portions of the temporary convergence point readings to the readings of the permanent convergence instruments.

It is apparent that the fracturing observed in the floor of the test rooms, and vertical separations in the roof, have contributed to the total roof-to-floor closure. However, based on measured cumulative vertical separations in September 1985, the contribution of floor fracturing to the total roof-to-floor closure is not more than 1 inch.

The total estimated closure (item 9 in Table 11-6) includes the values of early closure estimated by using equation 10-1 in Chapter 10. Based on the indicated additive values, the maximum roof-to-floor closure of approximately 16 1/2 inches through June 1986 occurs in Test Rooms 2 and 3. Test Room 4 has undergone the least roof-to-floor closure. Figure 11-4 shows the adjusted roof-to-floor closure values as a function of time.

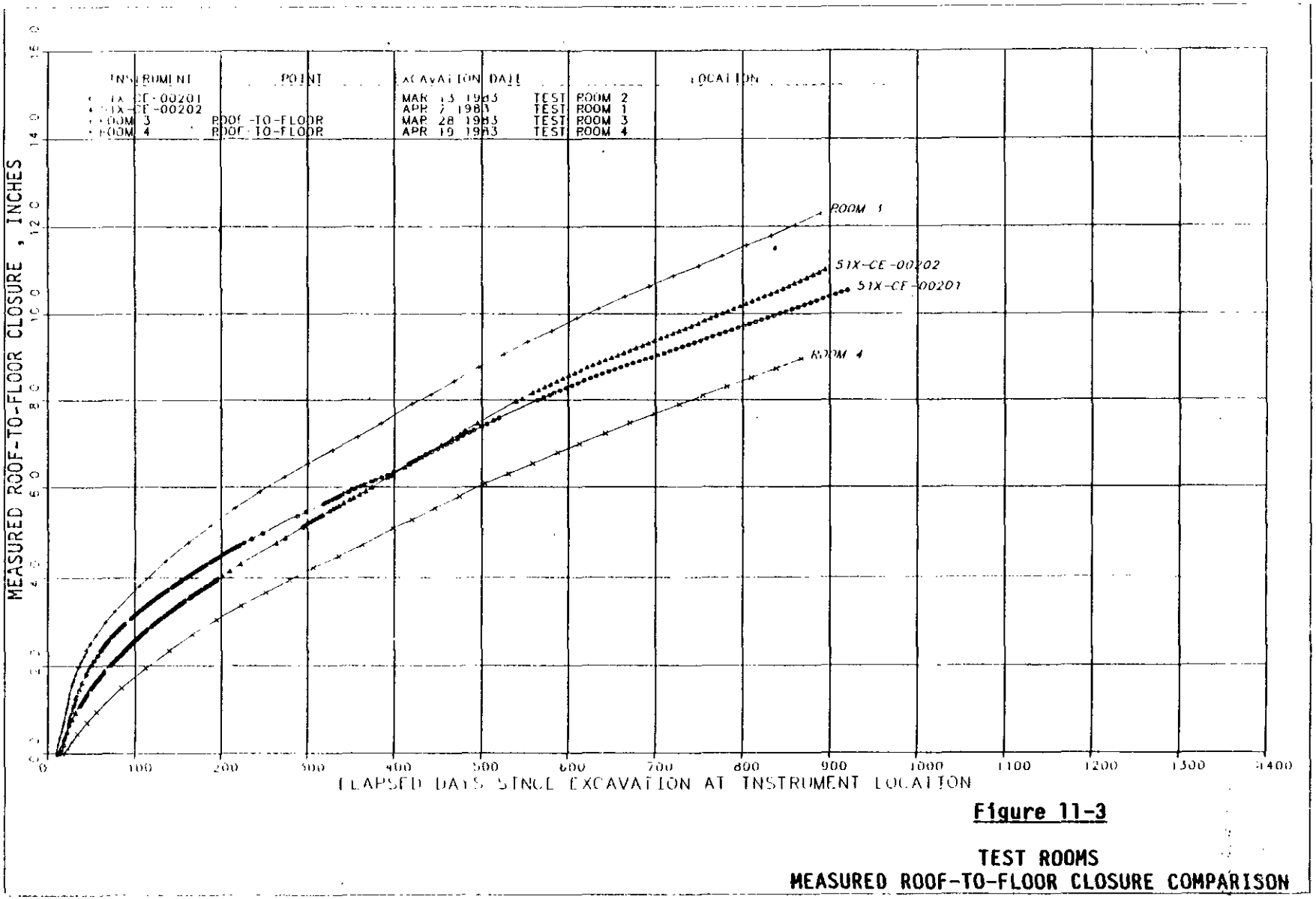

Figure 11-3

TEST ROOMS
MEASURED ROOF-TO-FLOOR CLOSURE COMPARISON

Table 11-6

TEST ROOMS
ROOF-TO-FLOOR CLOSURE COMPARISONS

Description	Test Room 1	2	3	4
(1) Excavation period	April 3-13 1983	March 9-20 1983	March 24-April 3 1983	April 15-25 1983
(2) Date of first reading of temporary convergence (TC) points	April 12, 1983	March 21, 1983	April 4, 1983	April 26, 1983
(3) Date of first reading of permanent convergence (RC and CE) instruments	April 20, 1983	March 29, 1983	April 7, 1983	May 6, 1983
(4) Reading of TC points (inches) on date indicated	0.84 April 20, 1983	0.88 March 28, 1983	0.40 April 7, 1983	0.45 May 5, 198
(5) Reading of RC and CE instruments (inches) on date indicated	13.11 June 13, 1986	12.20 June 13, 1986	13.83 April 28, 1986	10.62 April 28
(6) Total elapsed days of combined TC and RC measurements [Date for (5) - Date for (2)]	1157	1179	1120	1098
(7) Total measured closure (inches) [(4) + (5)]	13.95	13.08	14.23	11.0
(8) Estimated closure (inches) by regression analysis for the period of (2) - (1)	2.39	3.72	2.17	1.3
(9) Total estimated closure (inches) [(7) + (8)]	16.34	16.80	16.40	12.39

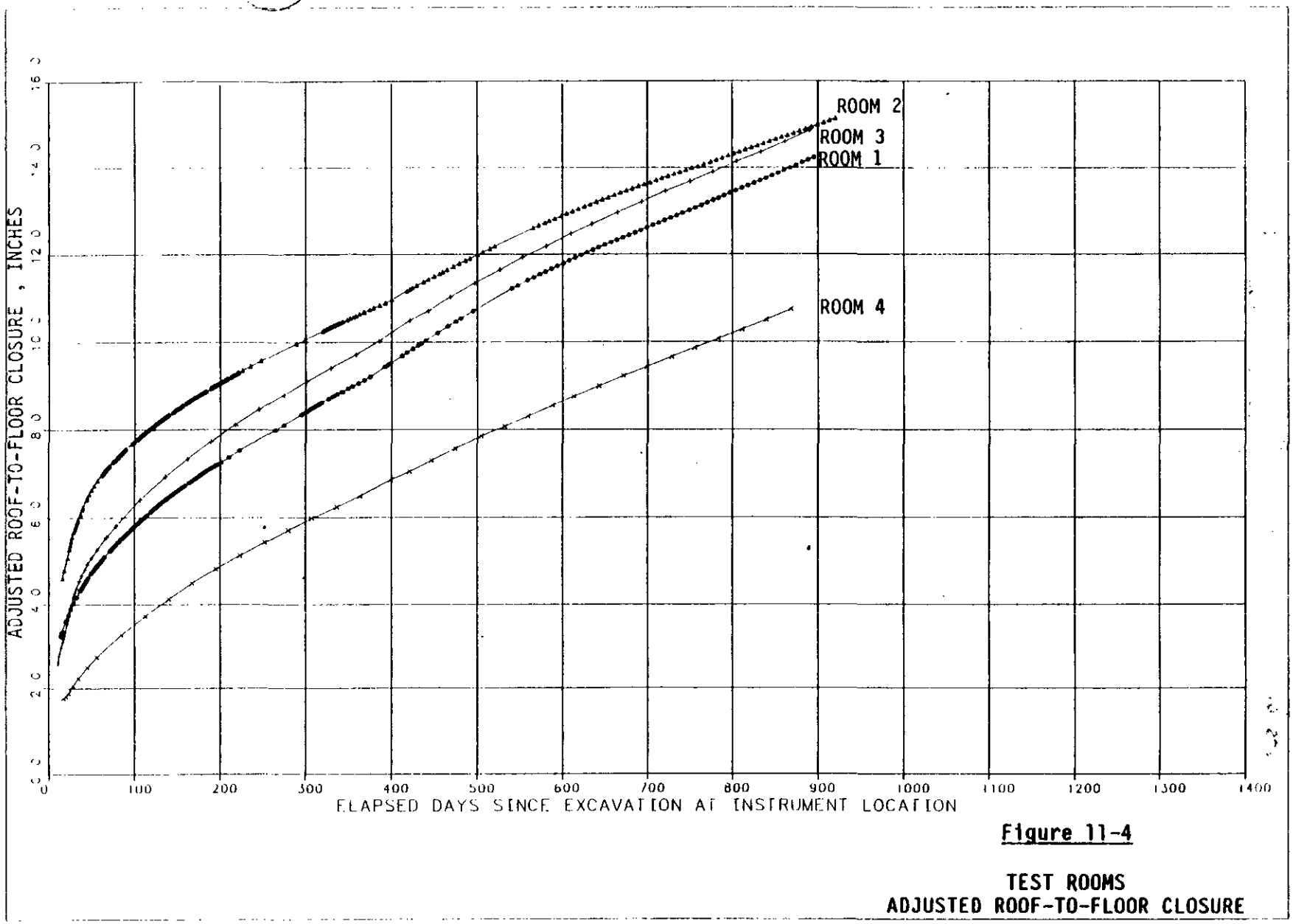

Figure 11-4

TEST ROOMS
ADJUSTED ROOF-TO-FLOOR CLOSURE

Figure 11-4 shows that [illegible] except for occasional [illegible] disturbances from nearby excavations. Provided there are no additional perturbations in and around the test rooms, it is likely that the rate of closure will reach a steady state value. It is possible to get an estimate of the rate of closure using either a phenomenological rheological model or an empirical model that is essentially a curve-fitting procedure. Both methods have been attempted. Numerical methods using the phenomenological approach are discussed in Chapter 5.

Closure rates rather than measured closure are used in the empirical approach because measured closure is not absolute. Early closure measurements are not available because the instruments could not be installed immediately after excavation. However, the calculation of closure rates is not affected by the lack of early measurements. The closure rates are calculated by assuming a linear relationship between closure and elapsed time over a short interval. This time interval has been arbitrarily chosen as a minimum of 7 days.

Because it is expected that the closure rate will initially be relatively high and then decrease to a steady rate, the following equation was used:

$$C(t) = \frac{A}{t^n} + C_c(1 - e^{-at}) \qquad (11\text{-}1)$$

where: $C(t)$ is the closure rate at elapsed time t after excavation;
A, a and n are constants which depend upon the deformation characteristics of the salt, initial stress regime and dimensions of the opening; and
C_c is the steady state closure rate.

The value of C(t) is obtained by arbitrarily choosing a time interval of not less than 7 days. If R_i is the closure reading at calendar time t_i and R_{i+1} is the closure reading at t_{i+1}, then

$$C(t) = \frac{R_{i+1} - R_i}{\Delta t} \qquad (11\text{-}2)$$

where: $\Delta t = (t_{i+1} - t_i) \quad \geq 7 \text{ days}$ (11-3)

The value of t is defined as:

$$t = \frac{t_i + t_{i+1}}{2} \qquad (11\text{-}4)$$

A regression analysis, which is the fitting of an equation like 11-1 to the set of [C(t),t] data points, was performed using NLIN, a commercially available statistical software package (ref. 11-1). The general method used to estimate the constants, herein called the regression parameters, was to minimize the sum of the squares of the differences between the actual measured values and the values predicted by the proposed equation.

Equation 11-1, a nonlinear equation, cannot be converted into linear form. The statistical software NLIN employs iterative methods that attempt to find least-square estimates for nonlinear models. The methods commonly employed are the Gauss-Newton technique and the Marquardt compromise technique (ref. 11-2). However, the requisite partial derivatives of the equation with respect to the parameters must be specified. In many cases, the Marquardt compromise, which is considered to work well in many circumstances, gives a better estimate and provides quicker convergence of the values of the regression parameters. However, nonlinear regression analyses may not always result in good estimates of the regression parameters. In addition, the analysis tacitly assumes that the regressor variables are measured without error. Thus, the observations, which in this case are the values of C(t), were not weighted.

Figure [illegible] roof-to-floor closure rates for Test Room 1 calculated by equation 11-1 to the values calculated using the fitted equation 11-2. The data used was obtained during the first year following the completion of excavation. The regression analysis showed that, for all practical purposes, equation 11-1 could be simplified as

$$C(t) = \frac{A}{t^n} + C_c \qquad (11\text{-}5)$$

because the value of 'a' obtained from the regression analysis was large enough to make the term e^{-at} comparatively negligible. The fitted equation for the roof-to-floor closure data in Test Room 1 has the form

$$C(t) = \frac{206.58}{t^{0.84}} + 2.24(1-e^{-5.27t}) \text{ inches/year} \qquad (11\text{-}6)$$

where: t is the elapsed time in days since excavation.

However, as shown by equation 11-5, equation 11-6 can be approximated as

$$C(t) = \frac{206.58}{t^{0.84}} + 2.24 \text{ inches/year} \qquad (11\text{-}7)$$

The method used was the Marquardt compromise technique. The coefficient of determination is 0.99.

The analysis was repeated later using roof-to-floor closure data at 980 days (2.68 years) after the completion of excavation. The regression equation was

$$C(t) = \frac{211.16}{t^{0.85}} + 2.44 \text{ inches/year} \qquad (11\text{-}8)$$

The steady state closure rate determined using the first year of data only is 9 percent less than the rate determined by using 2.68 years of

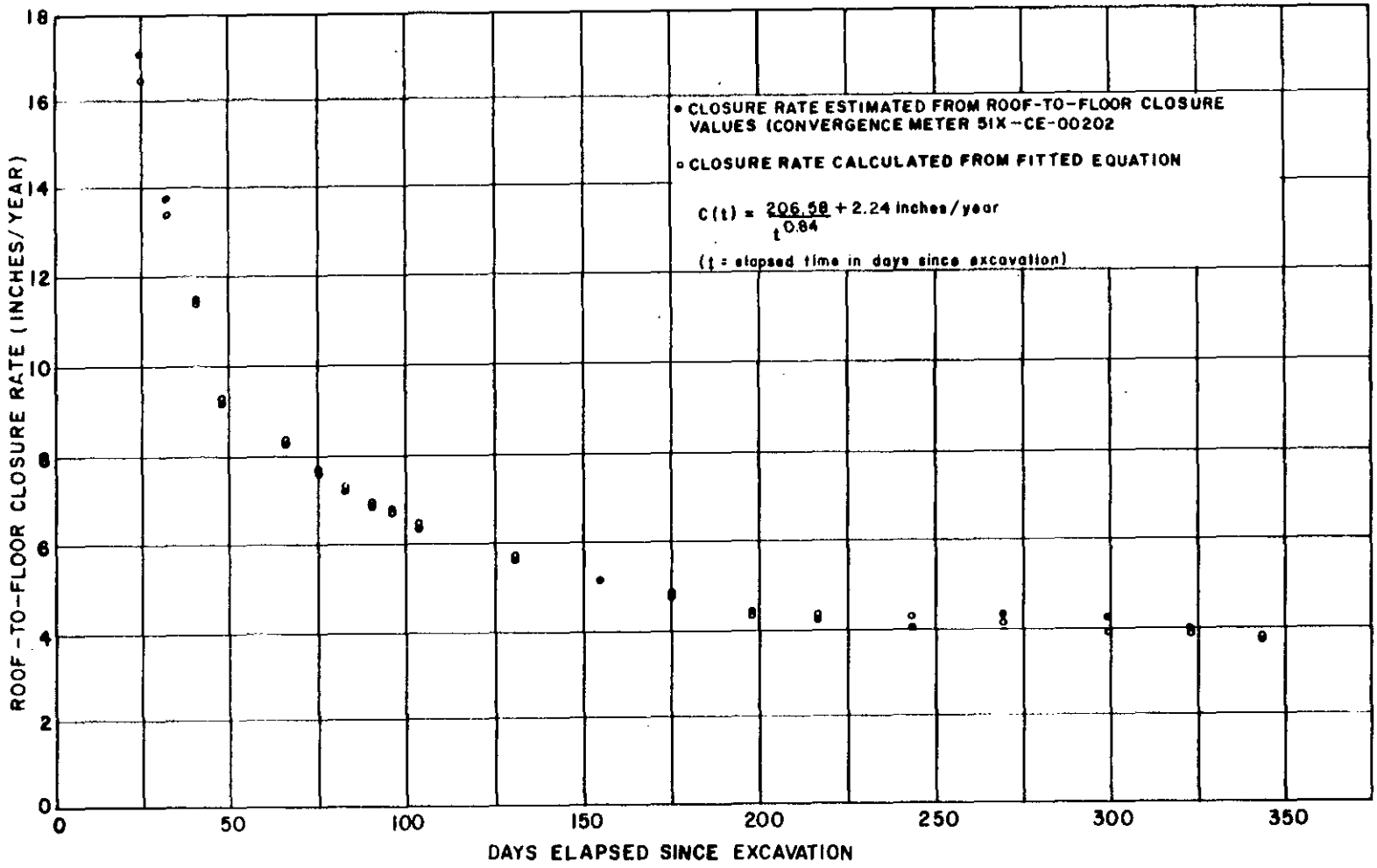

Figure 11-5

TEST ROOM 1
REGRESSION ANALYSIS OF ROOF-TO-FLOOR CLOSURE

measurement data, up to

1986, gave

$$C(t) = \frac{208}{t^{0.85}} + 2.40 \text{ inches/year} \qquad (11\text{-}9)$$

Equations 11-7, 11-8 and 11-9 show the consistency of the regression parameters for different input data sets.

Figure 11-6 shows the predicted roof-to-floor closure rate for Test Room 1 as a function of elapsed time in years using equation 11-9. Based on equation 11-7, the roof-to-floor closure rate at the end of 25 years is expected to be approximately 2.34 inches/year. Using equation 11-8, it will be 2.53 inches/year or 2.49 inches/year using equation 11-9.

Figures 11-7 through 11-10 show the fitted curves based on roof-to-floor closure rates calculated from equation 11-2, using data up to June 1986. To get an approximate idea of the roof-to-floor closure for periods of time greater than 1 year since the completion of excavation, equation 11-7 was integrated with respect to time between the limits of 1 year and time t_2 (in years) to yield

$$R(t) = 0.78(t_2^{0.147} - 1) + 0.20(t_2 - 1) \qquad (11\text{-}10)$$

Figure 11-11 shows the predicted roof-to-floor closure in feet for Test Room 1 (excluding that which has occurred in the first year after excavation) as a function of time in years. According to this prediction, 25 years after excavation this value will be 5.34 feet. A similar analysis using equation 11-9 gave a value of 5.3 feet.

Table 11-7 is a summary of the results of the nonlinear regression analyses for the roof-to-floor closure rates in the test rooms using 3 years of measurement data. The parameters contained in this table are applicable for an elapsed time expressed in years. For Test Room 4, the regression analysis using only the permanent convergence point data did not produce satisfactory results. The analysis was

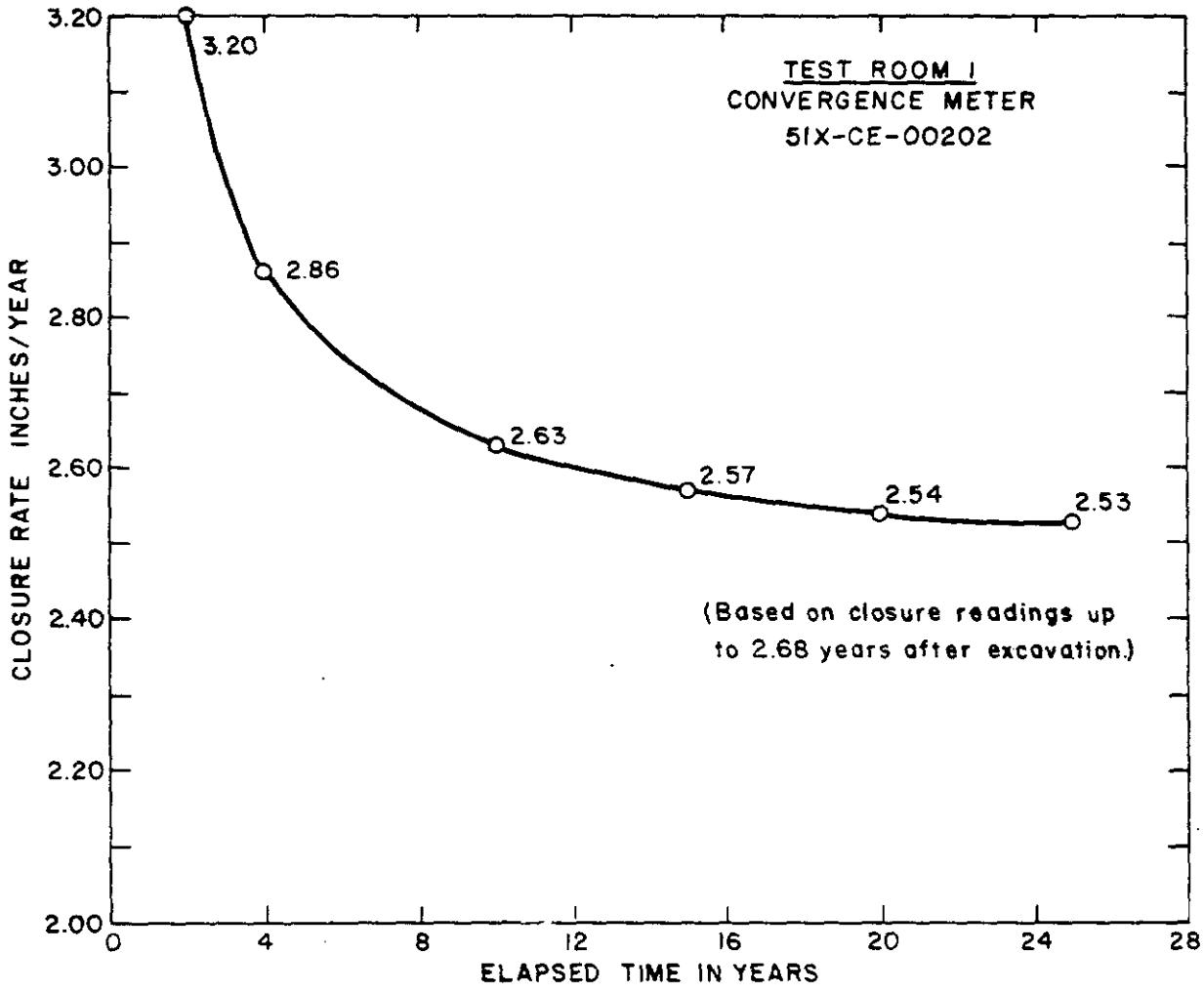

Figure 11-6

TEST ROOM 1
PREDICTED ROOF-TO-FLOOR CLOSURE RATE

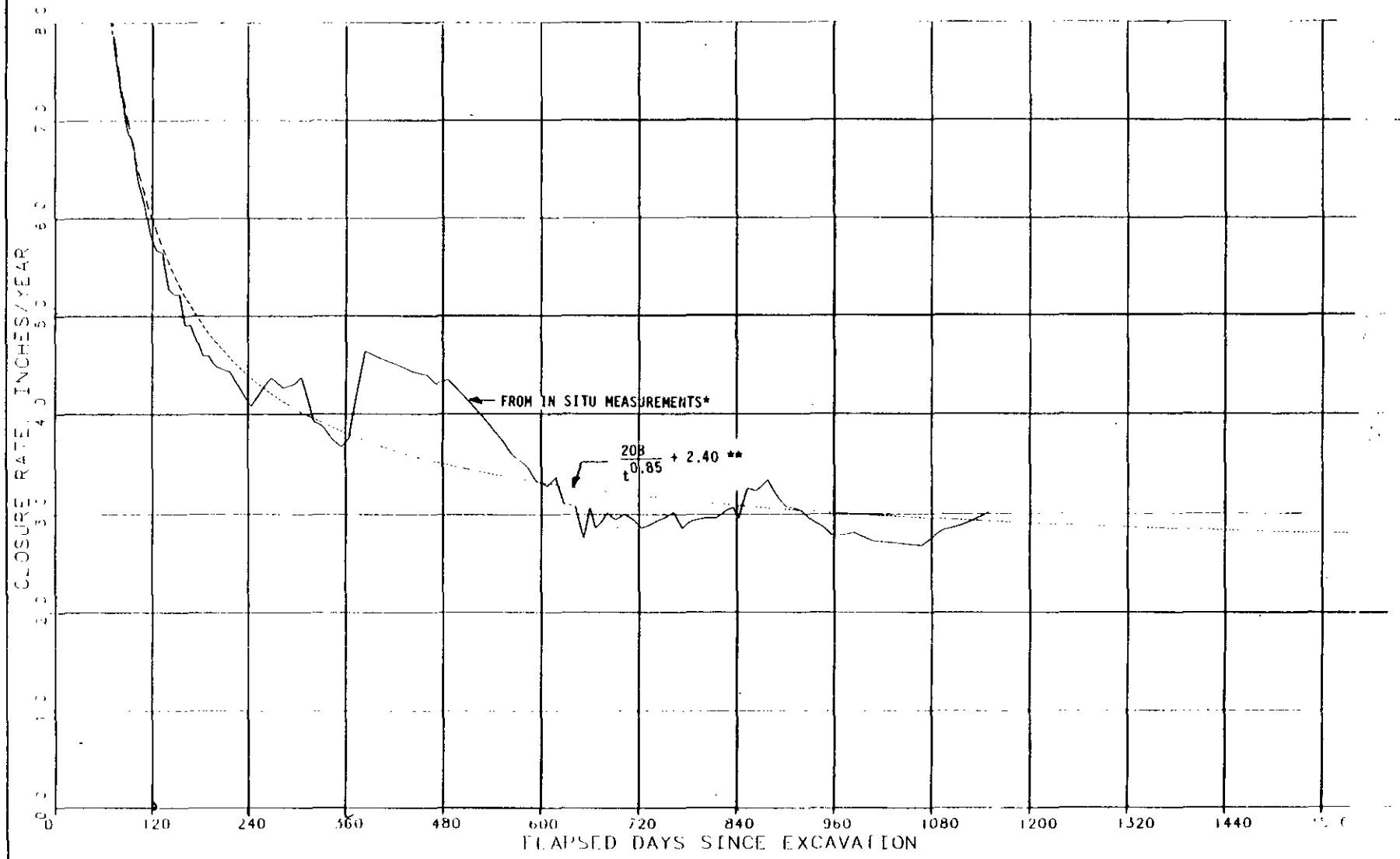

* RATE CALCULATED FOR TIME INTERVAL ≥7 DAYS.

** REGRESSION ANALYSIS OF IN SITU DATA UP TO JUNE 1986.

Figure 11-7

**TEST ROOM 1 ROOF-TO-FLOOR CLOSU
RESULTS OF REGRESSION ANALY**

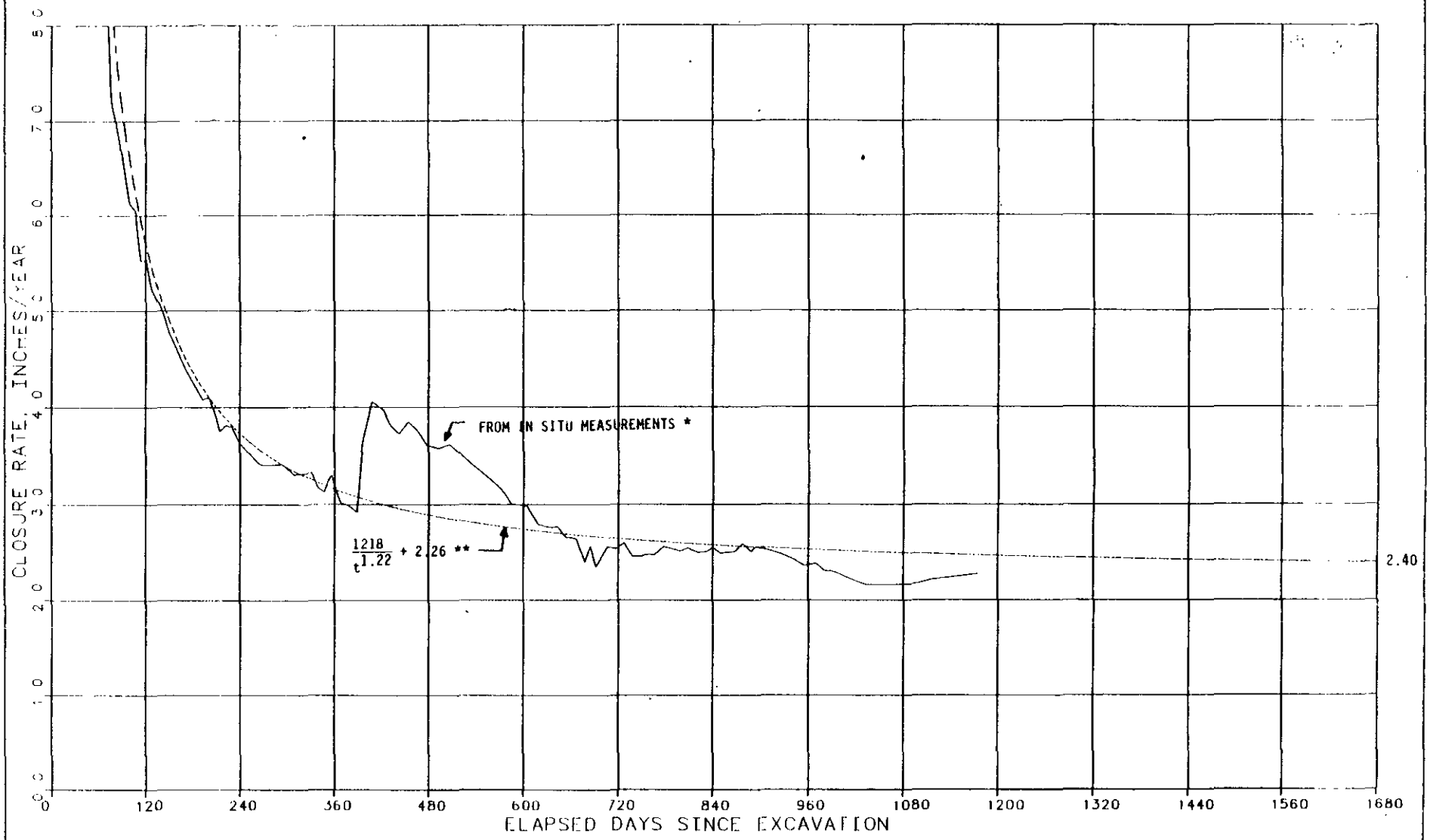

* RATE CALCULATED FOR TIME INTERVAL ≥7 DAYS.

** REGRESSION ANALYSIS OF IN SITU DATA UP TO JUNE 1986.

Figure 11-8

TEST ROOM 2 ROOF-TO-FLOOR CLOSURE RATE RESULTS OF REGRESSION ANALYSIS

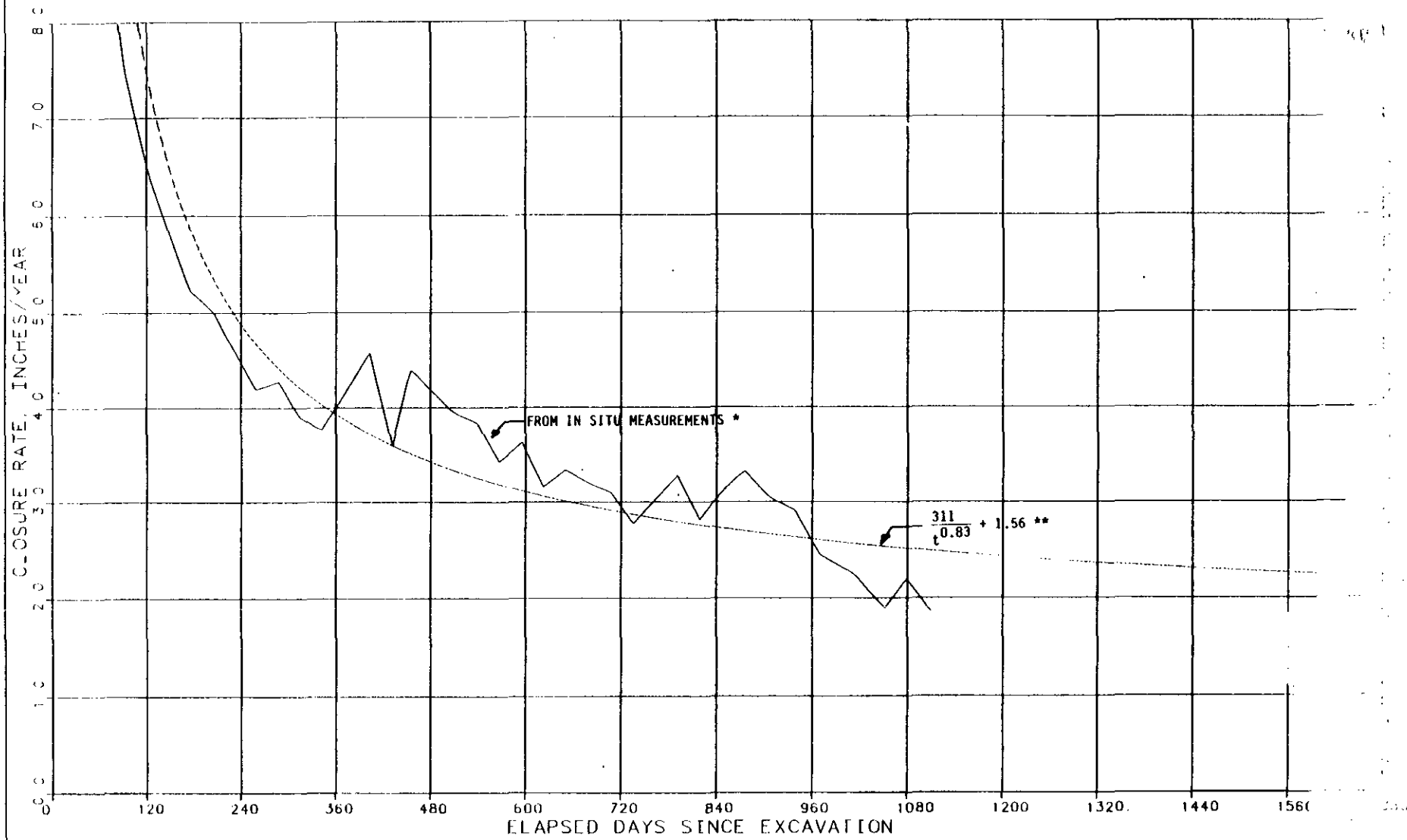

* RATE CALCULATED FOR TIME INTERVAL ≥7 DAYS.

** REGRESSION ANALYSIS OF IN SITU DATA UP TO JUNE 1986.

Figure 11-9

TEST ROOM 3 ROOF-TO-FLOOR CLOSURE RESULTS OF REGRESSION ANALYSIS

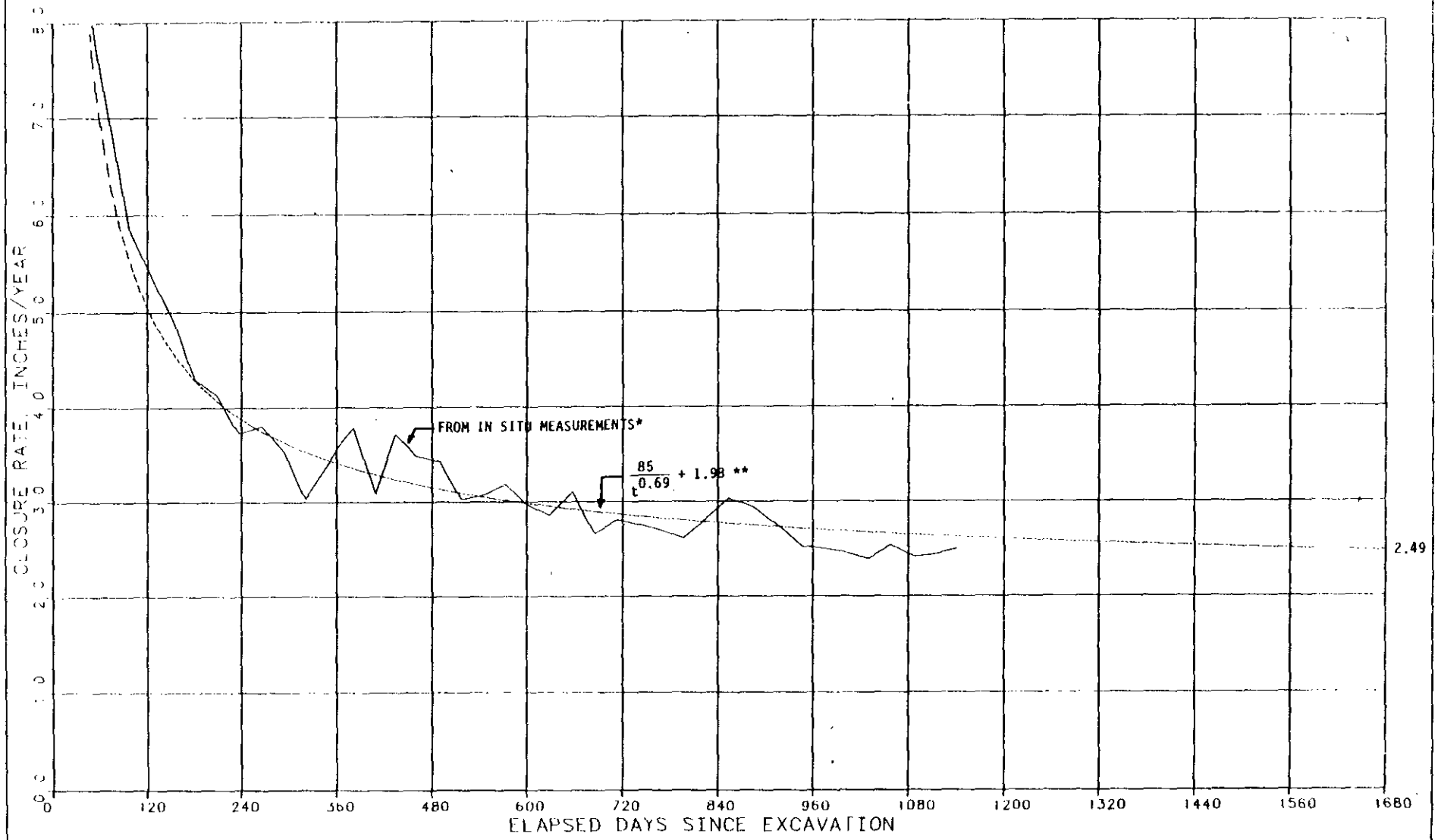

* RATE CALCULATED FOR TIME INTERVAL ≥7 DAYS.

** REGRESSION ANALYSIS OF IN SITU DATA UP TO JUNE 1986.

Figure 11-10

TEST ROOM 4 ROOF-TO-FLOOR CLOSURE RATE RESULTS OF REGRESSION ANALYSIS

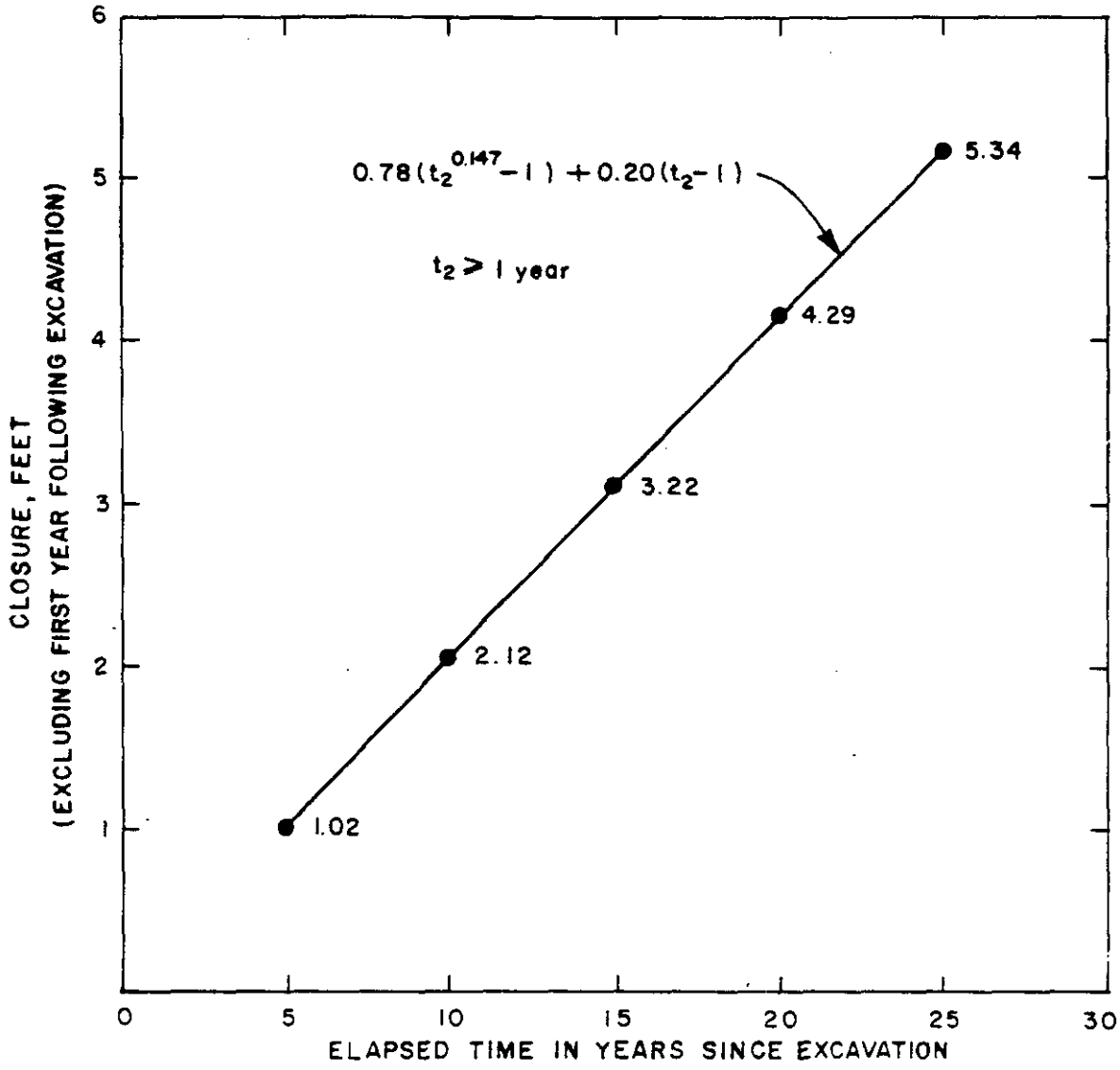

Figure 11-11

TEST ROOM 1
PREDICTED ADDITIONAL ROOF-TO-FLOOR CLOSURE

TEST ROOMS
SUMMARY OF RESULTS OF REGRESSION ANALYSES
FOR ROOF-TO-FLOOR CLOSURE RATES

Description	Test Room 1	2	3	4*
Regression Parameters**				
A	208	1218	311	85
n	0.85	1.22	0.83	0.69
C_c	2.40	2.26	1.56	1.98
r^2	0.99	0.98	0.94	0.97

Note: Analyses based on data obtained through June 1986.

* Data used for regression analysis includes data from temporary convergence points.

** Equation is: $C(t) = \frac{A}{t^n} + C_c$

where: C(t) is closure rate in inches/year;
A and n are constants;
t is elapsed time in days; and
C_c is steady state closure rate.

r^2 is the coefficient of determination.

repeated with [illegible] produced good results. The [illegible] of the regression analysis of roof-to-floor closure rates discussed in this subsection are used in Chapter 12 to define the bounds on the roof-to-floor closure rates for the storage rooms.

Wall-to-Wall Closure. Figure 11-12 summarizes the measured wall-to-wall closure magnitudes for the test rooms. Because of the lack of early measurements, the relative positions of the individual curves are not absolute. Table 11-8 presents an estimate of the actual wall-to-wall closure for the four test rooms. The approach is similar to the one used for estimating the actual roof-to-floor closure values. The maximum wall-to-wall closure occurs in Test Room 3 and is about 13 inches. The minimum wall-to-wall closure is about 9 inches in Test Room 4.

The regression analysis of wall-to-wall closure rates for Test Room 1, using measurement data up to June 1986, shows that the equation has the form

$$C(t) = \frac{202}{t^{0.94}} + 1.75 \text{ inches/year} \qquad (11\text{-}11)$$

where: t = elapsed time in days since excavation.

Comparing equation 11-11 with equation 11-9, the long-term wall-to-wall closure rate will be 73 percent of the roof-to-floor closure rate.

Table 11-9 is a summary of the results of the regression analyses for the wall-to-wall closure rates in Test Rooms 1 through 4. The closure rate values determined from temporary convergence point readings were included in the analysis of Test Room 2. The fitted curves for Test Rooms 2 and 3 are relatively poor. Figures 11-13 through 11-16 show the fitted equations for the wall-to-wall closure rate versus elapsed time curves for Test Rooms 1 through 4.

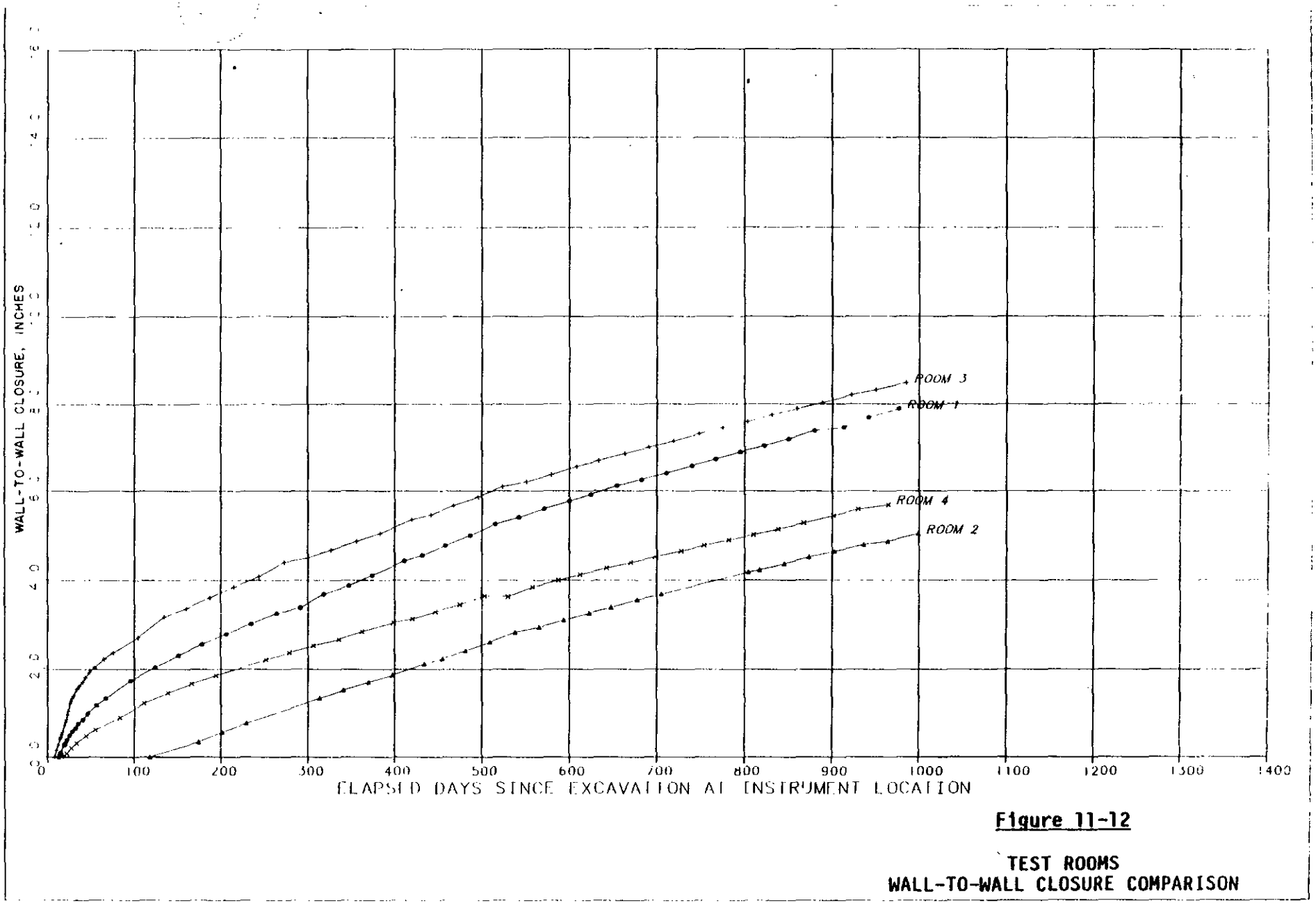

Figure 11-12

TEST ROOMS
WALL-TO-WALL CLOSURE COMPARISON

Table 11-8

TEST ROOMS
WALL-TO-WALL CLOSURE COMPARISONS

Description	Test Room 1	2	3	4
(1) Excavation period	April 3-13 1983	March 9-20 1983	March 24-April 3 1983	April 15-25 1983
(2) Date of first reading of temporary convergence (TC) points	April 9, 1983	March 21, 1983	March 31, 1983	April 21, 19
(3) Date of first reading of permanent convergence (RC) points	April 20, 1983	July 12, 1983	April 7, 1983	May 6, 198
(4) Reading of TC points (inches) on date indicated	1.58 April 20, 1983	3.36 July 12, 1983	1.42 April 7, 1983	1.48 May 5, 1983
(5) Reading of RC points (inches) on date indicated	8.82 June 16, 1986	5.82 June 16, 1986	9.24 June 16, 1986	6.39 June 16, 198
(6) Total elapsed days of combined TC and RC measurements [Date for (5) - Date for (2)]	1166	1151	1176	1151
(7) Total measured closure (inches) [(4) + (5)]	10.40	9.18	10.66	7.87
(8) Estimated closure (inches) by regression analysis for the period of (2) - (1)	1.79	2.51	2.16	1.42
(9) Total estimated closure (inches) [(7) + (8)]	12.19	11.69	12.82	9.29

Table 11-9

TEST ROOMS
SUMMARY OF RESULTS OF REGRESSION ANALYSES
FOR WALL-TO-WALL CLOSURE RATES

Description	Test Room 1	2*	3	4
Regression Constants**				
A	202	222	231	1766
n	0.94	0.79	0.83	1.81
C_c	1.75	0.30	0.74	1.88
r^2	0.96	0.95	0.92	0.99

Note: Analyses based on data obtained through June 1986.

* Data used for regression analysis includes data from temporary convergence points.

** Equation is: $C(t) = \frac{A}{t^n} + C_c$

where: C(t) is closure rate in inches/year;
A and n are constants;
t is elapsed time in days; and
C_c is steady state closure rate.

r^2 is the coefficient of determination.

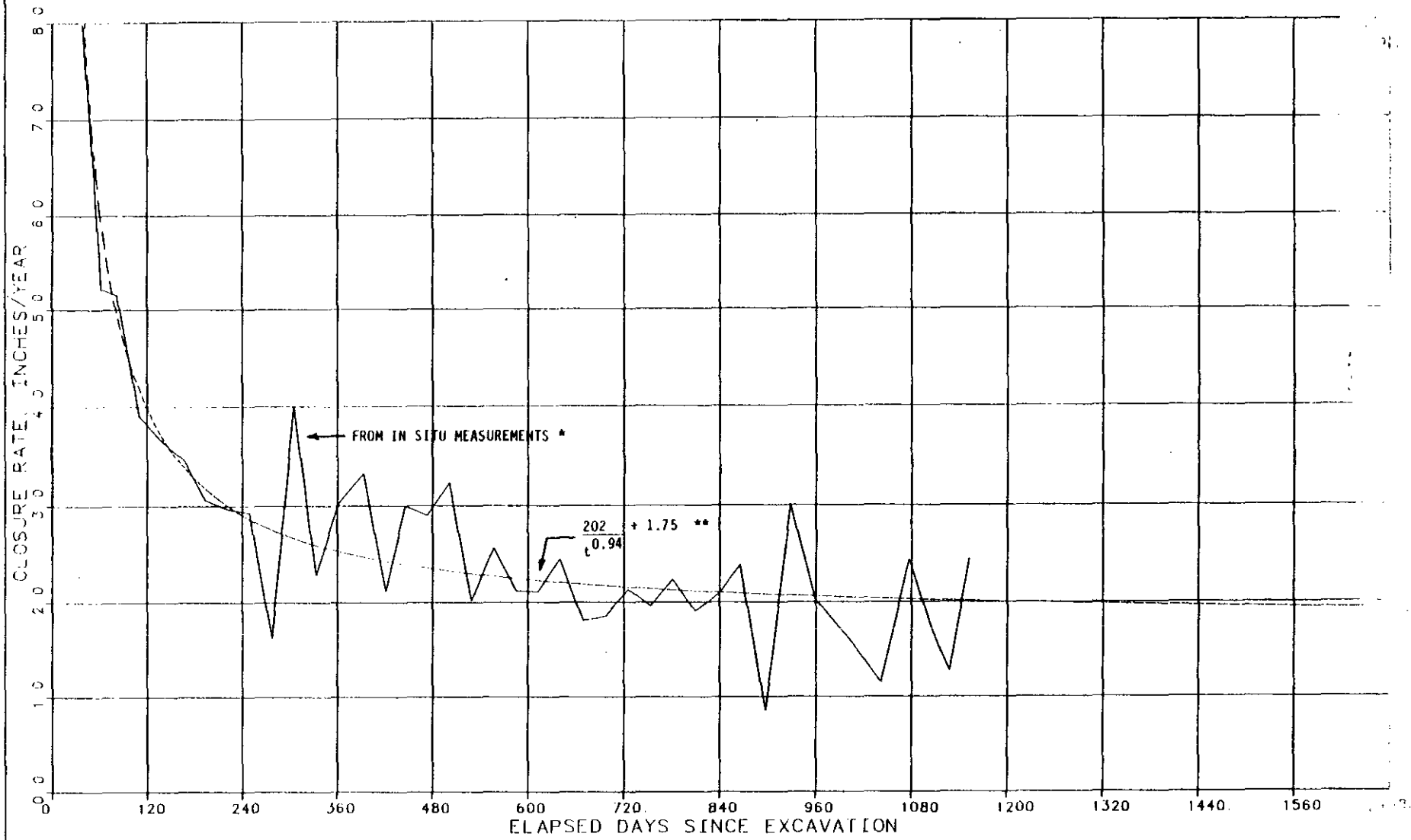

* RATE CALCULATED FOR TIME INTERVAL ≥7 DAYS.

** REGRESSION ANALYSIS OF IN SITU DATA UP TO JUNE 1986.

Figure 11-13

TEST ROOM 1 WALL-TO-WALL CLOSURE
RESULTS OF REGRESSION ANALYS

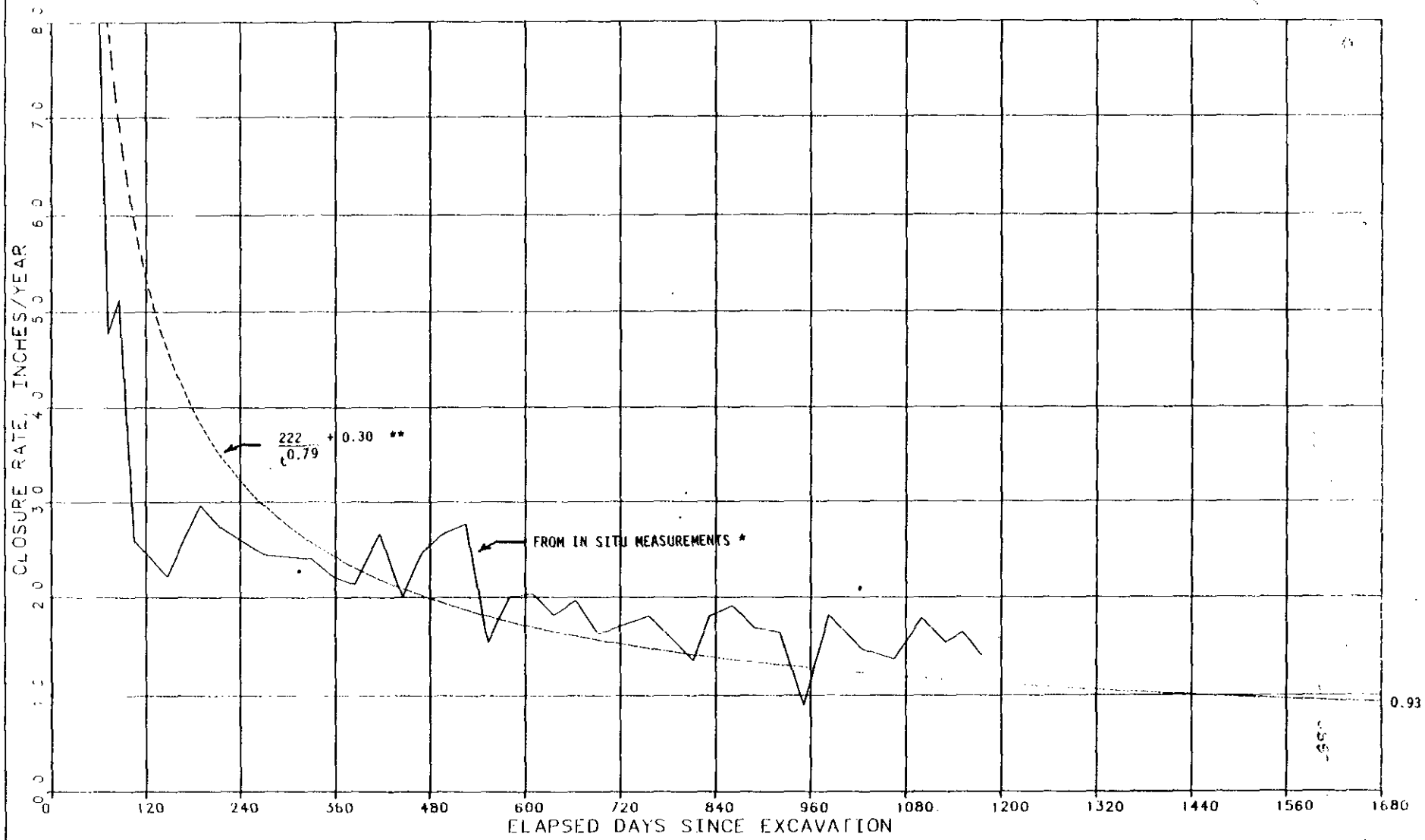

* RATE CALCULATED FOR TIME INTERVAL ≥7 DAYS.

** REGRESSION ANALYSIS OF IN SITU DATA UP TO JUNE 1986.

Figure 11-14

TEST ROOM 2 WALL-TO-WALL CLOSURE RATE RESULTS OF REGRESSION ANALYSIS

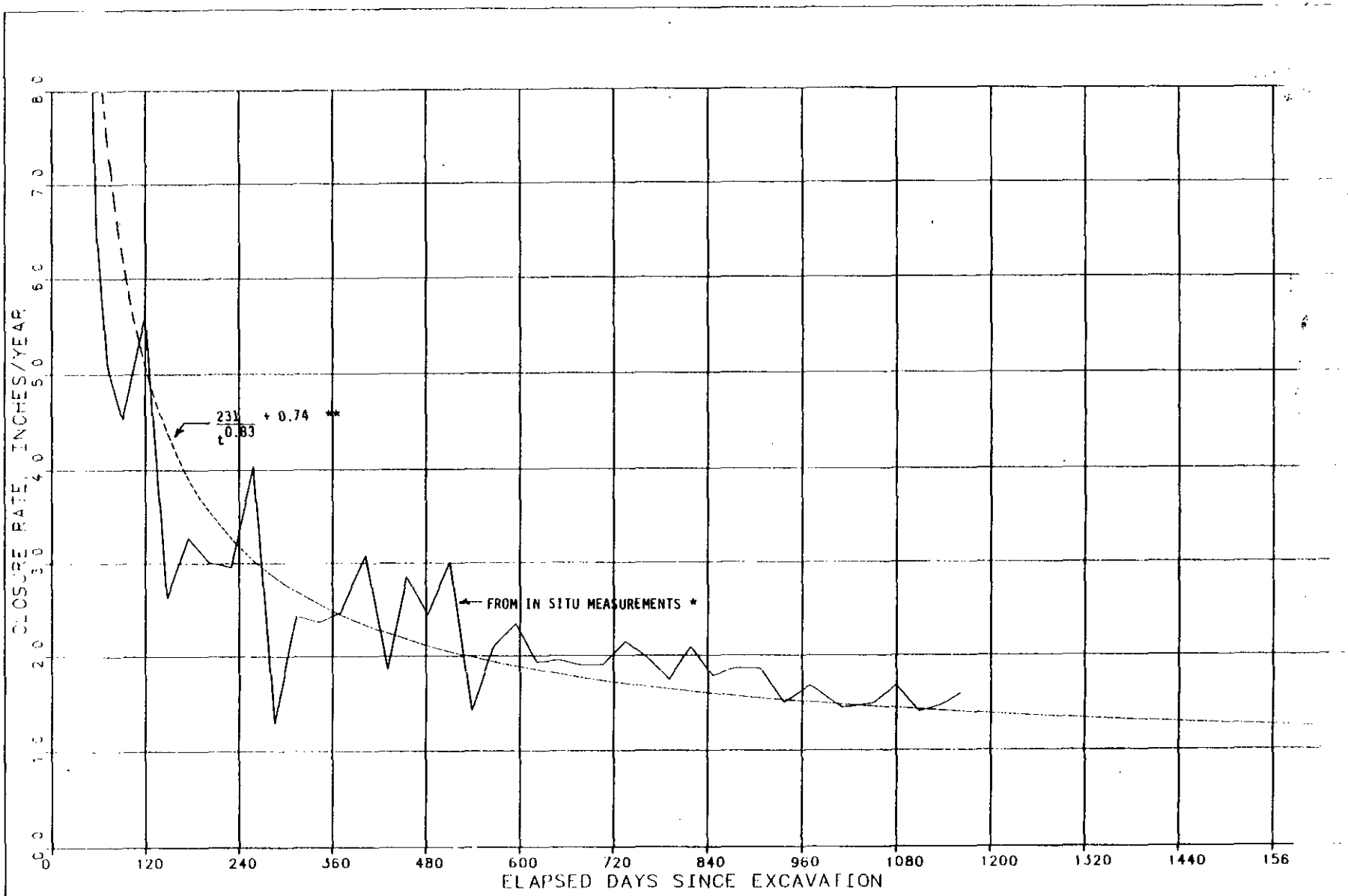

* RATE CALCULATED FOR TIME INTERVAL ≥7 DAYS.

** REGRESSION ANALYSIS OF IN SITU DATA UP TO JUNE 1986.

Figure 11-15

TEST ROOM 3 WALL-TO-WALL CLOS
RESULTS OF REGRESSION ANAL

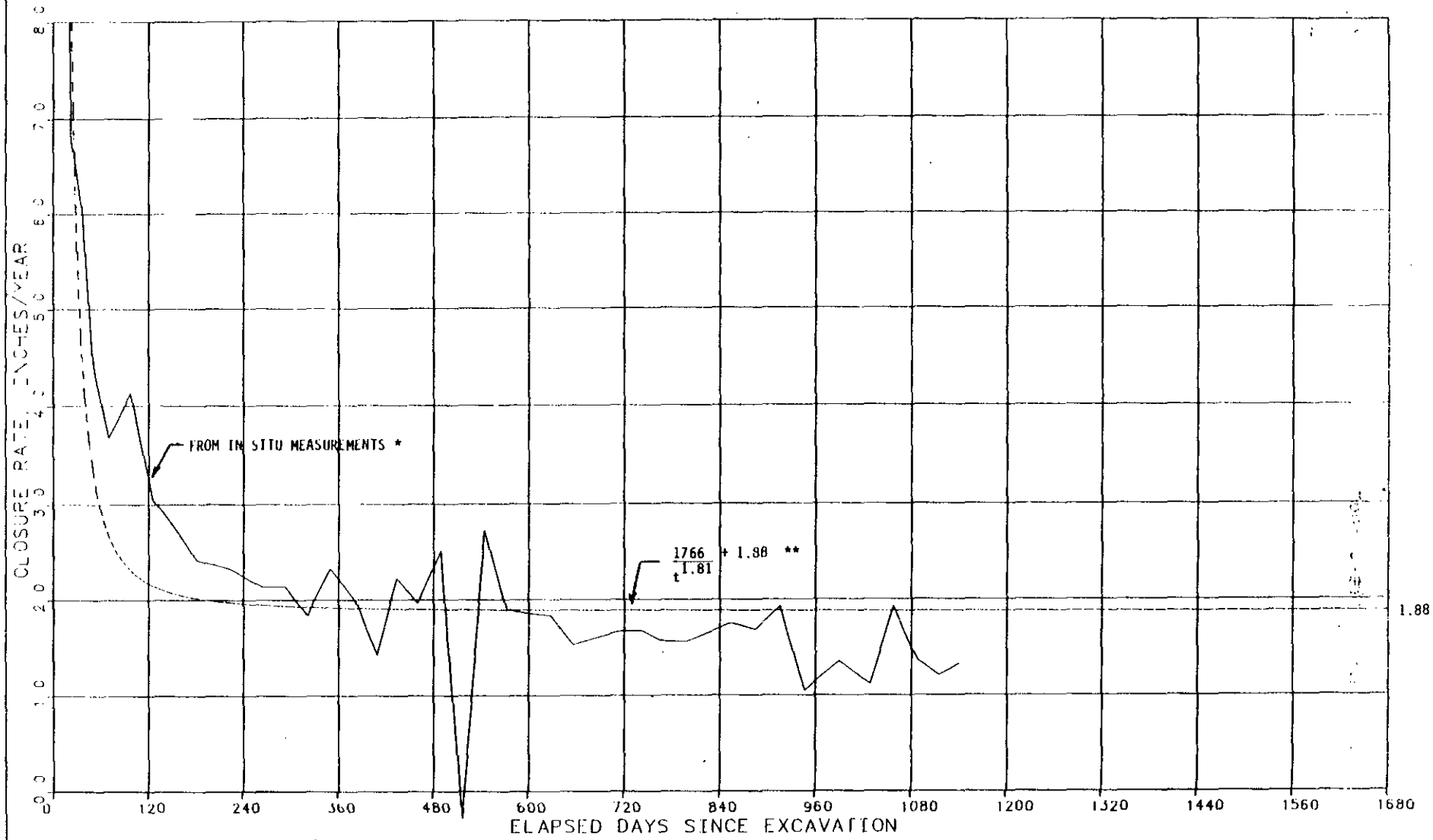

* RATE CALCULATED FOR TIME INTERVAL ≥7 DAYS.

** REGRESSION ANALYSIS OF IN SITU DATA UP TO JUNE 1986.

Figure 11-16

TEST ROOM 4 WALL-TO-WALL CLOSURE RATE
RESULTS OF REGRESSION ANALYSIS

Summary of the collar multiple-point borehole extensometers in the test rooms. Because the extensometers could not be installed as soon as the excavation was completed, the collar readings do not reflect absolute closure. The table also shows the sum of the collar movements from both the east and west walls in each of the rooms except Test Room 3, which has no extensometer in the west wall. The last two columns of this table permit a comparison of the sum of the collar movements with wall-to-wall convergence point readings. Ideally, providing the salt is homogeneous, the central vertical lines of the pillars between Test Rooms 1 and 2 and Test Rooms 2 and 3 should be lines of symmetry with zero lateral strain. The deepest anchor at 50 feet for extensometers 51X-GE-00213 and 51X-GE-00215 should be expected to undergo negligible displacement. Therefore, the sum of the collar movements for Test Rooms 2 and 3 should be approximately the same as the wall-to-wall convergence point readings. As shown in Table 11-10, this is the case for Test Room 2. Exact equivalence is difficult to obtain because the collars of the extensometers are recessed into the wall by variable amounts and the time-lag between the end of excavation and the date of initial reading is not the same for the extensometers and the convergence points.

Comparison of Roof-to-Floor to Wall-to-Wall Closure Rates. Table 11-11 presents recent roof-to-floor and wall-to-wall closure rates for the test rooms. The rates were calculated using convergence point readings with a time interval of approximately 1 month. Based on these readings, the average wall-to-wall closure rate is approximately 68 percent of the roof-to-floor closure rate.

11.3.2.3 Deformation

An indication of the deformation of the salt around the test rooms may be obtained by comparing inclinometer measurements around a room. Figure 11-17 shows the cumulative measurements from the four wall inclinometers located around Test Room 3 through March 6, 1985. The inclinations are measured along the plane of the cross section.

Table 11-10

TEST ROOMS
WALL EXTENSOMETER COLLAR MOVEMENTS VERSUS CONVERGENCE POINT READINGS

Test Room	Extensometer	Location	Readings on June 13, 1986 (inches)	Sum of East & West Readings (inches)	Wall-to-Wall Convergence Point Readings on June 16, 1986 (inches)
1	51X-GE-00217	East wall	3.16	7.36	8.82*
	51X-GE-00219	West wall	4.20		
2	51X-GE-00213	East wall	4.95	9.52	9.18**
	51X-GE-00215	West wall	4.57		
3	51X-GE-00211	East wall	4.17	-	9.24*
	-	West wall	-		
4	51X-GE-00206	East wall	3.26	5.95	6.39*
	51X-GE-00208	West wall	2.69		

* From (5) in Table 11-8.
** From (7) in Table 11-8.

Table 11-11

TEST ROOMS
CLOSURE RATE COMPARISONS

Description of Closure Location	Test Room 1	2	3	4
Roof-to-Floor				
Reading/Date	12.88/May 16, 1986	12.03/May 16, 1986	13.65/Mar. 24, 1986	10.39/Mar. 24, 19
Reading/Date	13.11/June 13, 1986	12.20/June 13, 1986	13.83/Apr. 28, 1986	10.62/Apr. 28, 19
Difference in readings	0.23 inch	0.17 inch	0.18 inch	0.23 inch
Time interval	28 days	28 days	27 days	27 days
Rate ($\dot{V}$)	3.00 inch/yr	2.22 inch/yr	2.43 inch/yr	3.10 inch/yr
Wall-to-Wall				
Reading/Date	8.63/May 19, 1986	5.72/May 19, 1986	8.90/Mar. 24, 1986	6.09/Mar. 24, 1
Reading/Date	8.82/June 16, 1986	5.82/June 16, 1986	9.03/Apr. 28, 1986	6.22/Apr. 28, 19
Difference in	0.19 inch	0.10 inch	0.13 inch	0.13 inch

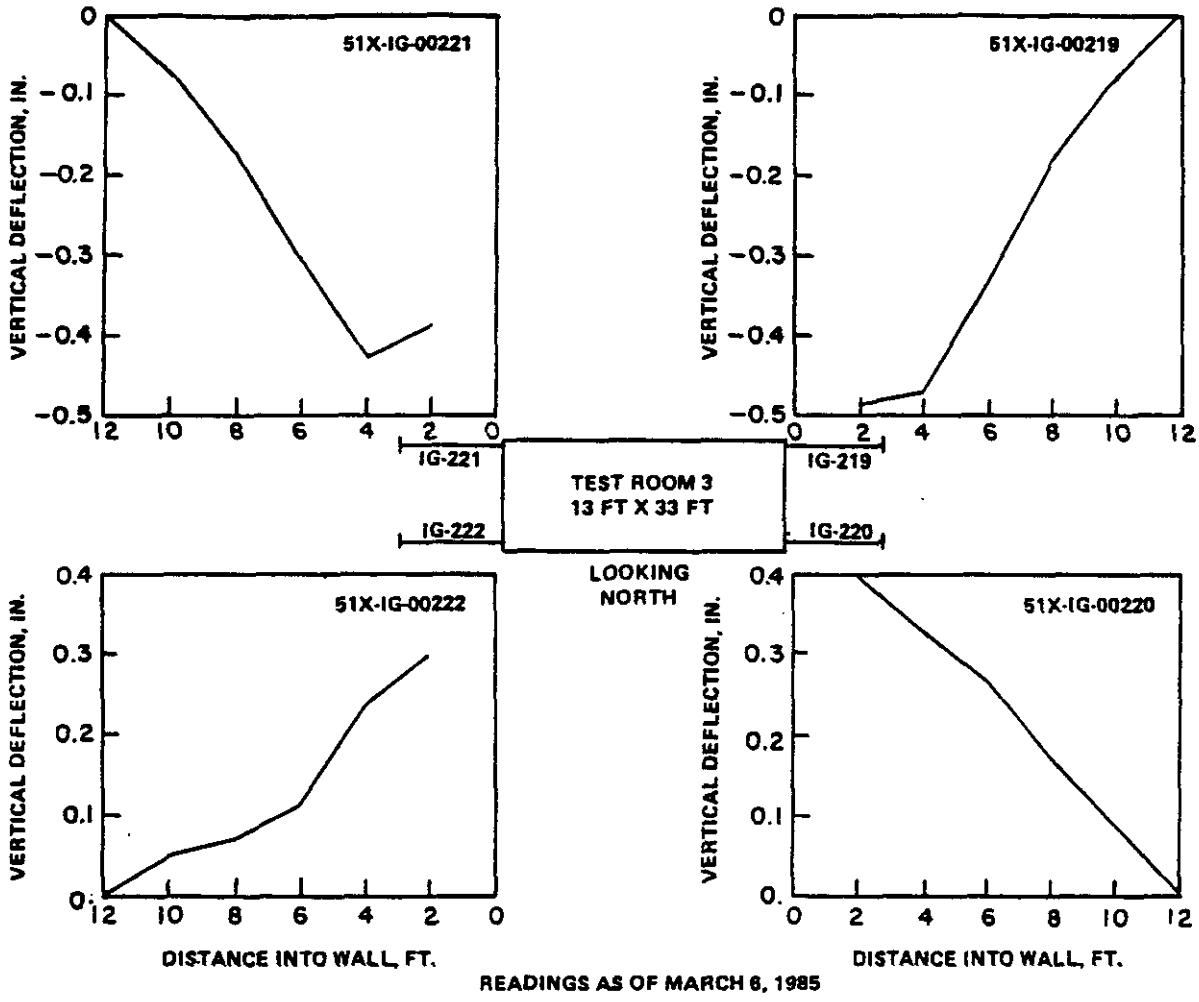

Figure 11-17

TEST ROOM 3
WALL INCLINOMETER BEHAVIOR

Figure 11-[illegible] shows [illegible] March 6, 1985. The initial readings from these inclinometers were taken 9 to 15 days after the completion of excavation in the test room. The current readings indicate that the maximum relative vertical deflection is on the order of 1 inch over a length of 12 feet.

The inclinometers near the roof show vertical downward deflection while those near the floor indicate upward deflection. This indicates that the central multiple-point borehole extensometers located in the walls of the test rooms probably undergo negligible vertical deflection.

11.3.2.4 Bay Strains

Relative movements between anchors of the multiple-point borehole extensometers will provide an approximate distribution of salt deformation around the excavated openings. The relative displacements are normalized over the spacing between anchors and are termed "bay strains". The bay strain is approximately the average axial strain between any two anchor points and will be closer to the true strain provided that the spacing between the anchors is small and that the deformation varies linearly with the spacing between the anchors. Bay strains are useful in detecting any anomalous behavior in the salt around an opening, such as that influenced by discontinuities, clay seams, or the effect of local stress concentrations.

Figure 11-19 shows the strain between the collar and anchor A for the roof extensometers in Test Room 1. The distance between the collar and anchor A is 5 feet. The maximum strain occurs at the east and west sides of the roof of the test room and is equal to approximately 4 percent through June 1986. Although the roof sag, as depicted by collar movement, is higher at the center of the rooms than at the sides, the bay strain is higher at the sides than at the center. As discussed in subsection 11.3.2.5, the numerical modeling also indicates higher strain at the roof and wall intersections. Figure 11-20 shows the vertical strain rates for these same extensometers. The rates are

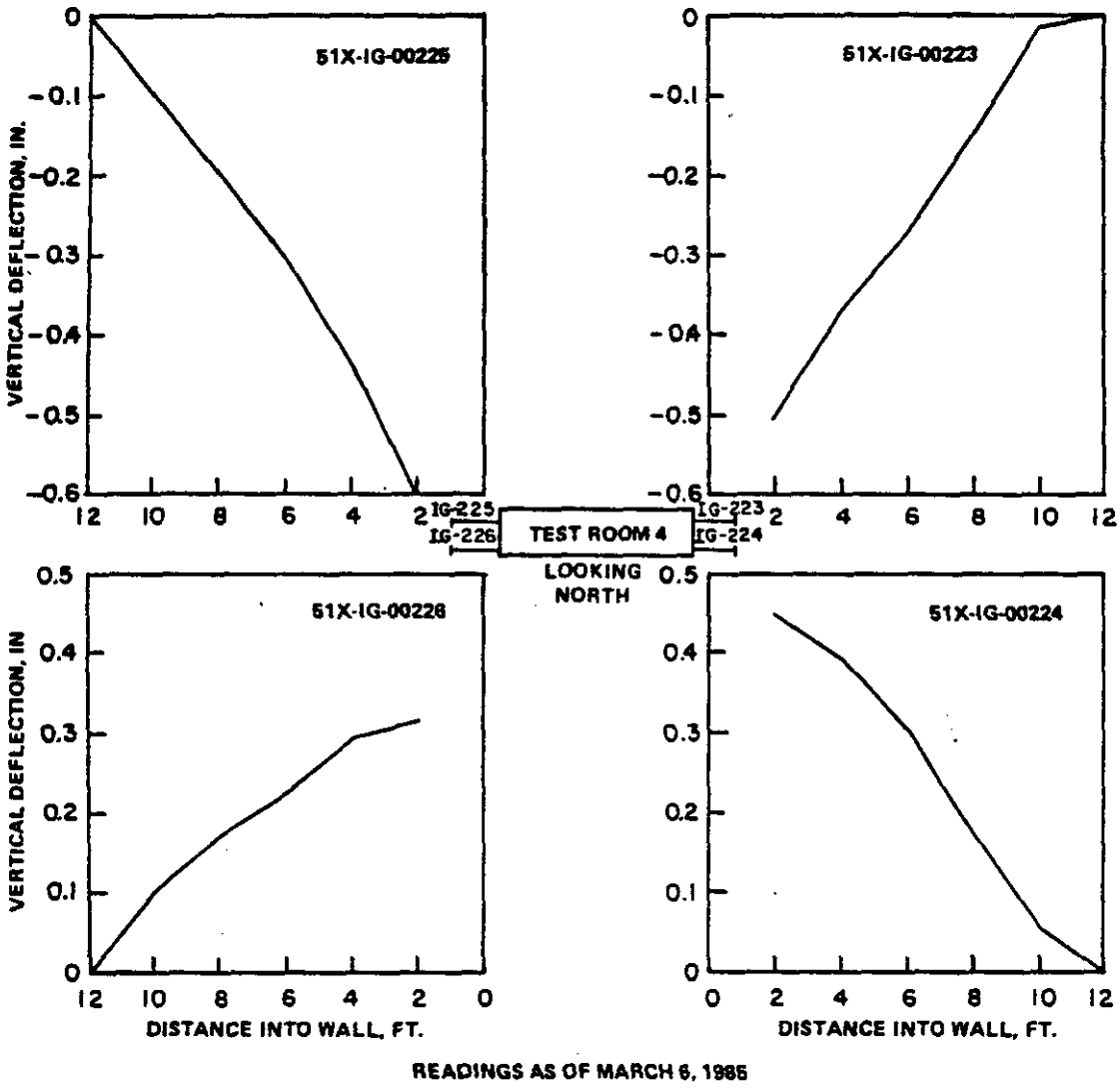

Figure 11-18

TEST ROOM 4
WALL INCLINOMETER BEHAVIOR

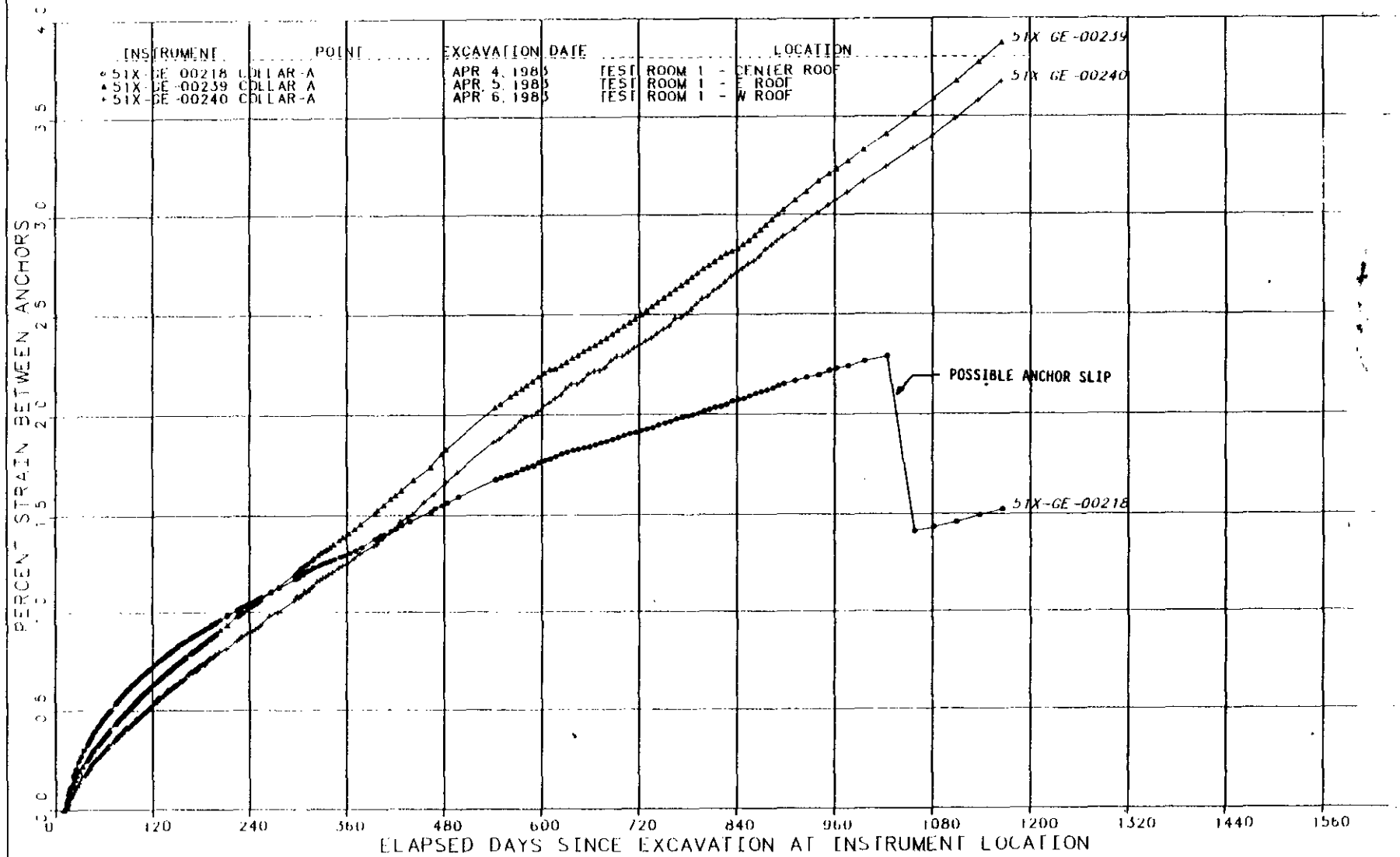

Figure 11-19

TEST ROOM 1 ROOF EXTENSOMETER STRAIN VERSUS TIME SINCE EXCA

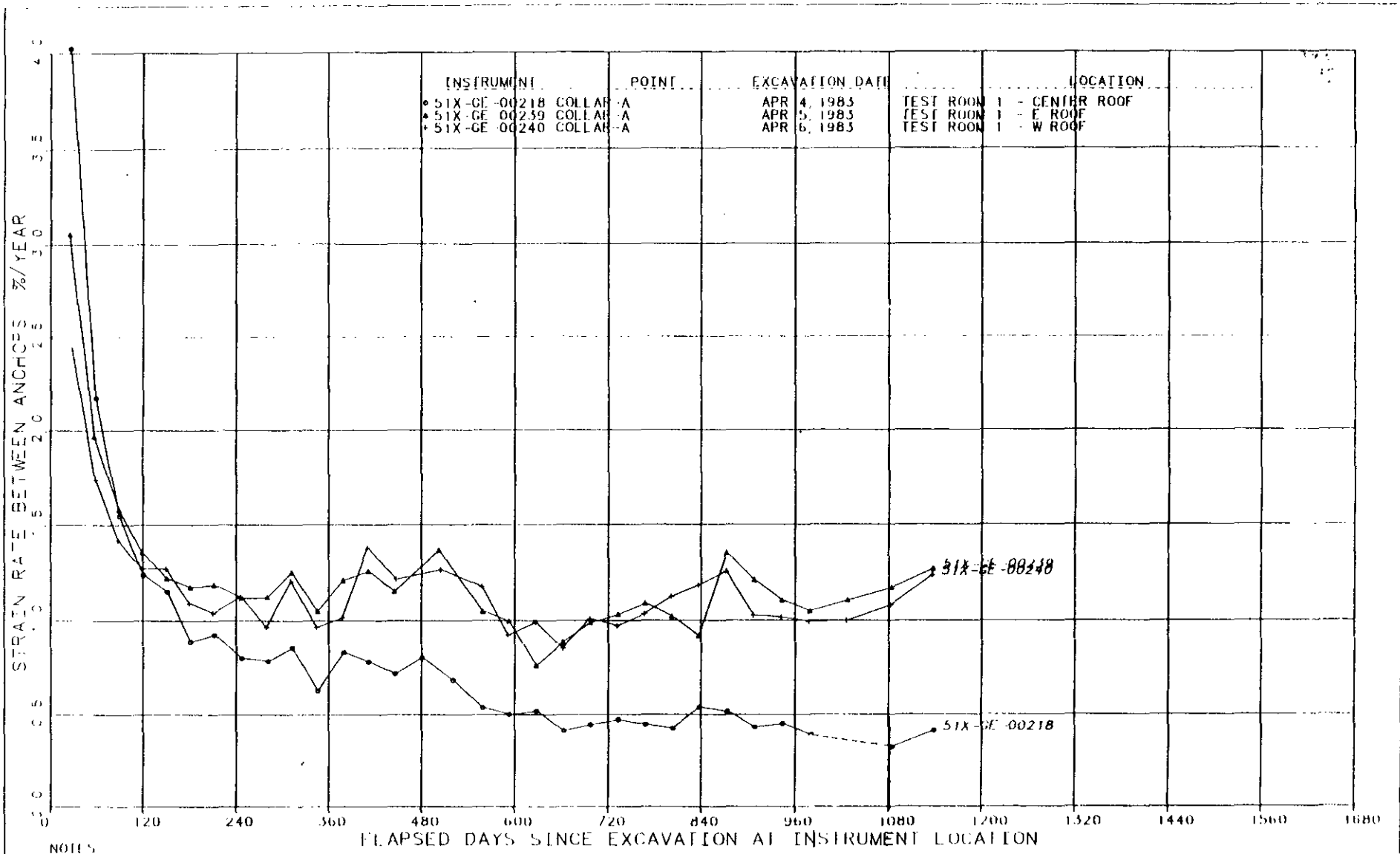

NOTES

1 RATE CALCULATED FOR MINIMUM INTERVALS OF 30 DAYS

Figure 11-20

TEST ROOM 1 ROOF EXTENSOMETERS
STRAIN RATE VERSUS TIME SINCE EXCAVATION

...ne strains, the ...rain ... are higher close to the pillars.

Figures K-37 through K-46 in Appendix K show the bay strains in percent as a function of elapsed time since excavation for all of the test rooms. To monitor more closely the separation across the clay seam at the base of anhydrite "b", the spacing between anchors A and B in Test Rooms 1 and 2 is 1 foot. Currently, the maximum strain occurs between anchors A and B on the west side and central part of the roof in Test Room 1, and is on the order of 5 percent. Because the anchors are not equally spaced, and the deformation varies nonlinearly with the distance along the anchor, a comparison of bay strain between successive anchors may be misleading.

Figures K-47 through K-56 in Appendix K show the strain rate plots for all of the roof and floor extensometers. In general, the strain rate is decreasing with time, except for floor extensometer 51X-GE-00210 in Test Room 3 where, for anchor A, the strain rate increased with time until the extensometer failed (Figure K-42). The decreasing trend in the strain rates is an indication that the salt above the roof and below the floor is currenty stable and will remain stable based on the projected decreasing rate.

11.3.2.5 Model Simulation

As discussed in Chapter 5, Section 5.3, numerical analyses using creep constants obtained from laboratory tests did not provide a good correlation with in situ measured closure. Therefore, an engineering approach using curve fitting methods was employed. The finite element method was used to simulate the behavior of the test rooms and to determine stress distributions. The effects of material properties and the proximity to other rooms were considered for incorporation into the model. The reference stratigraphy used in the model and the material properties of the geologic layers are described in Chapter 6. The constitutive equations used in the analyses, particularly the governing creep equations, are presented in Appendix C. Using the procedures

described in Chapter 5, Section 5.4, in situ roof-to-floor closure data through June 30, 1985, were correlated with the finite element responses to determine the values of creep parameters C, A and z for each test room. In order to eliminate the effect of excavation sequence on computation of the creep parameters, only in situ data taken after the completion of all test room excavation activities were utilized. The average values of these parameters for the four test rooms were then used to predict the responses of the future storage rooms as described in Chapter 12.

Figure 11-21 shows the finite element model for the test room panel based on the reference stratigraphy. The model has 363 nodes and consists of 270 plane strain elements, with gap/friction link elements modeling a clay seam at a depth of 2,104.87 feet. A friction coefficient of 0.4 was used for a member property of the gap/friction link elements. MB-139 was modeled as an elastic layer from a depth of 2,130.36 to 2,133.18 feet. The top and bottom boundaries of the model are at depths of 1,978.5 feet and 2,250.0 feet, respectively. The roof and floor of the room are at depths of 2,112.56 feet and 2,125.56 feet, respectively.

Two openings were incorporated in the finite element model to simulate differences resulting from the proximity of inner and outer rooms. These openings were modeled using height and width dimensions of 13 feet and 33 feet respectively. The boundary on one side of the model was taken as the vertical axis of symmetry for the center pillar and consists of horizontal restraints. The boundary on the other side of the model also utilized horizontal restraints. These boundaries were established based on experience from previous analyses and were extended far enough so that the effects of the boundaries on the structural responses were minimal. Stress boundary conditions were used at the top and bottom of the finite element model. A single vertical restraint at the lower left corner of the model was used to eliminate any rigid body modes in the model.

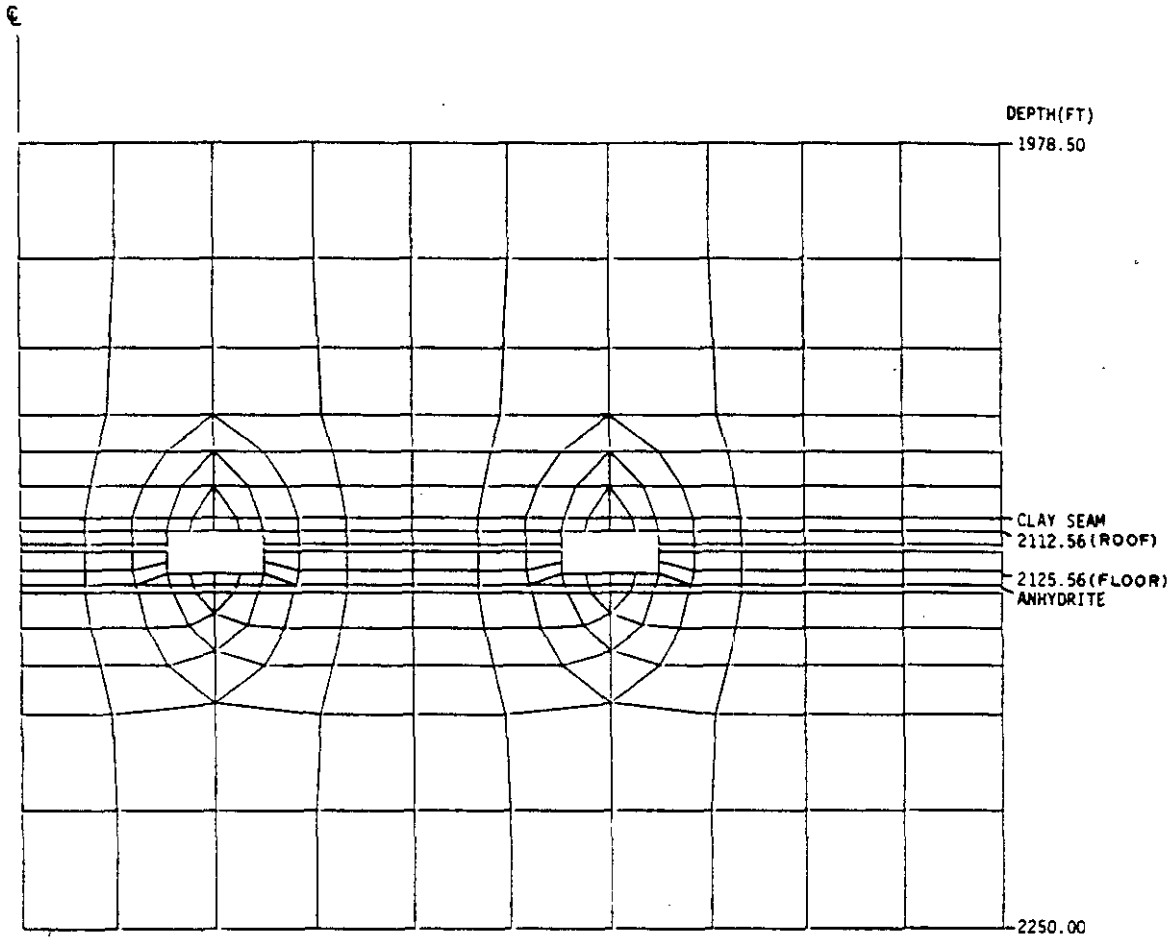

Figure 11-21

TEST ROOMS
FINITE ELEMENT MODEL

Element sizes were proportioned to minimize the stress gradients across each element. In addition, elements were oriented to have the mesh radiating from the opening of the model to be commensurate with estimated orientations of the principal stress axes. These aspects of the model were designed to increase the overall efficiency of the analyses.

Computation of In Situ Responses and Creep Parameters. The test room analyses were performed using the procedures described in Chapter 6 and the MARC General Purpose Finite Element Program (ref. 6-8). Time steps used in the analyses were within the specified tolerances recommended by the MARC Program. The analysis was performed in several stages with each stage containing between 50 and 100 integration steps. After completing each stage, the corresponding real time was computed to determine the required number of integration steps for the subsequent runs.

Figures 11-22 through 11-25 show the correlations of in situ and analytical roof-to-floor closures for Test Rooms 1 through 4. The in situ roof-to-floor closure data for Test Rooms 1 and 2 are from convergence meter readings while the measurements for Test Rooms 3 and 4 are from convergence points. Table 11-12 shows the individual creep parameters C, A and z for all four test rooms determined by numerically correlating the in situ roof-to-floor closure data. The table also shows the mean values of the creep parameters for three test room combinations.

Similarly, Figures 11-26 through 11-29 show the correlations of in situ and finite element wall-to-wall closures for Test Rooms 1 through 4. The in situ wall-to-wall closure data for Test Rooms 1, 3 and 4 are from permanent convergence points while the data from Test Room 2 consists of both temporary and permanent convergence point measurements. Table 11-13 shows the individual creep parameters C, A and z for all four test rooms determined by numerically correlating the in situ wall-to-wall closure data. The table also shows the mean values of the creep parameters for three test room combinations.

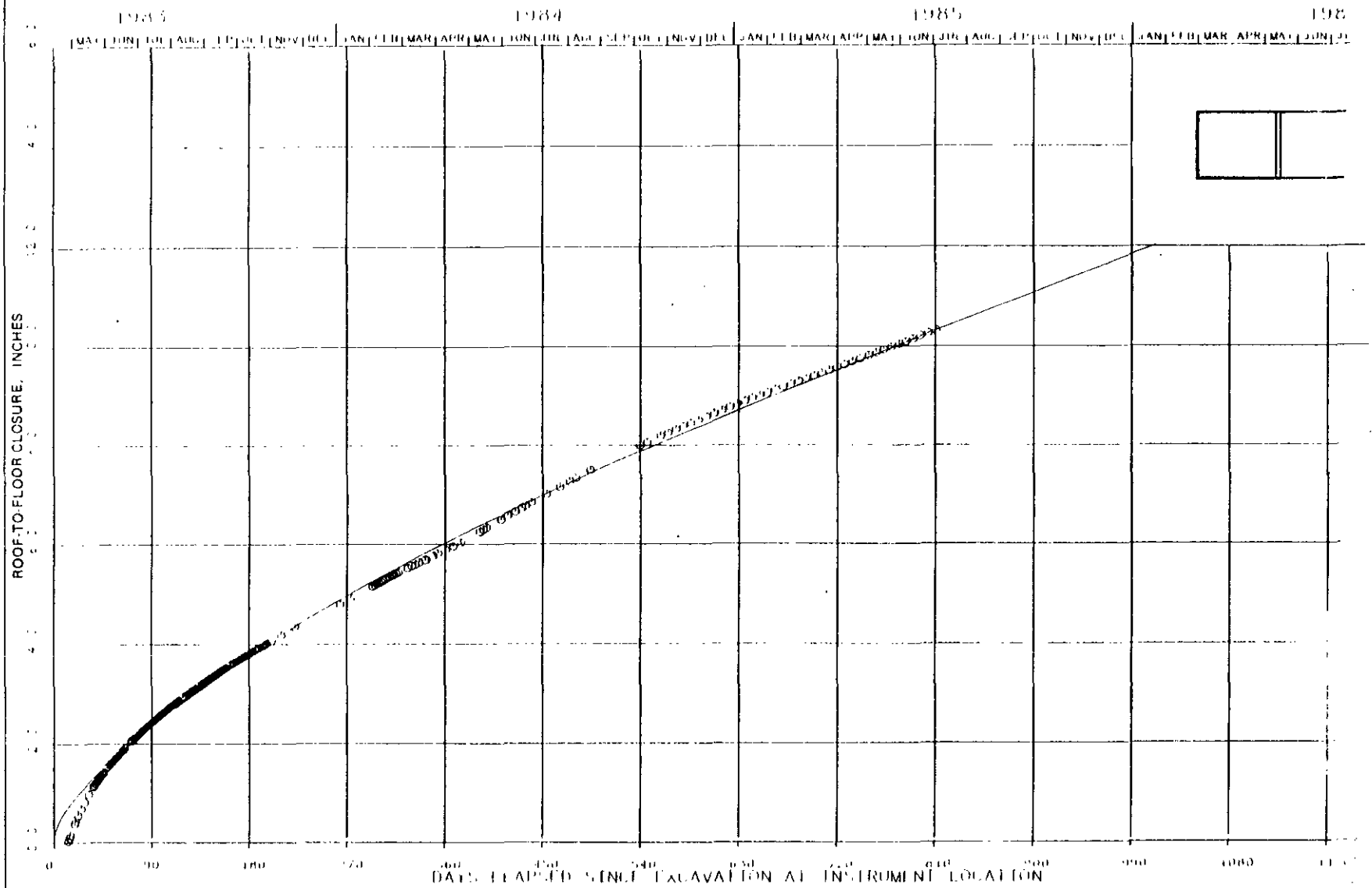

Figure 11-22

TEST ROOM 1
ROOF-TO-FLOOR CLOSURE HISTOR

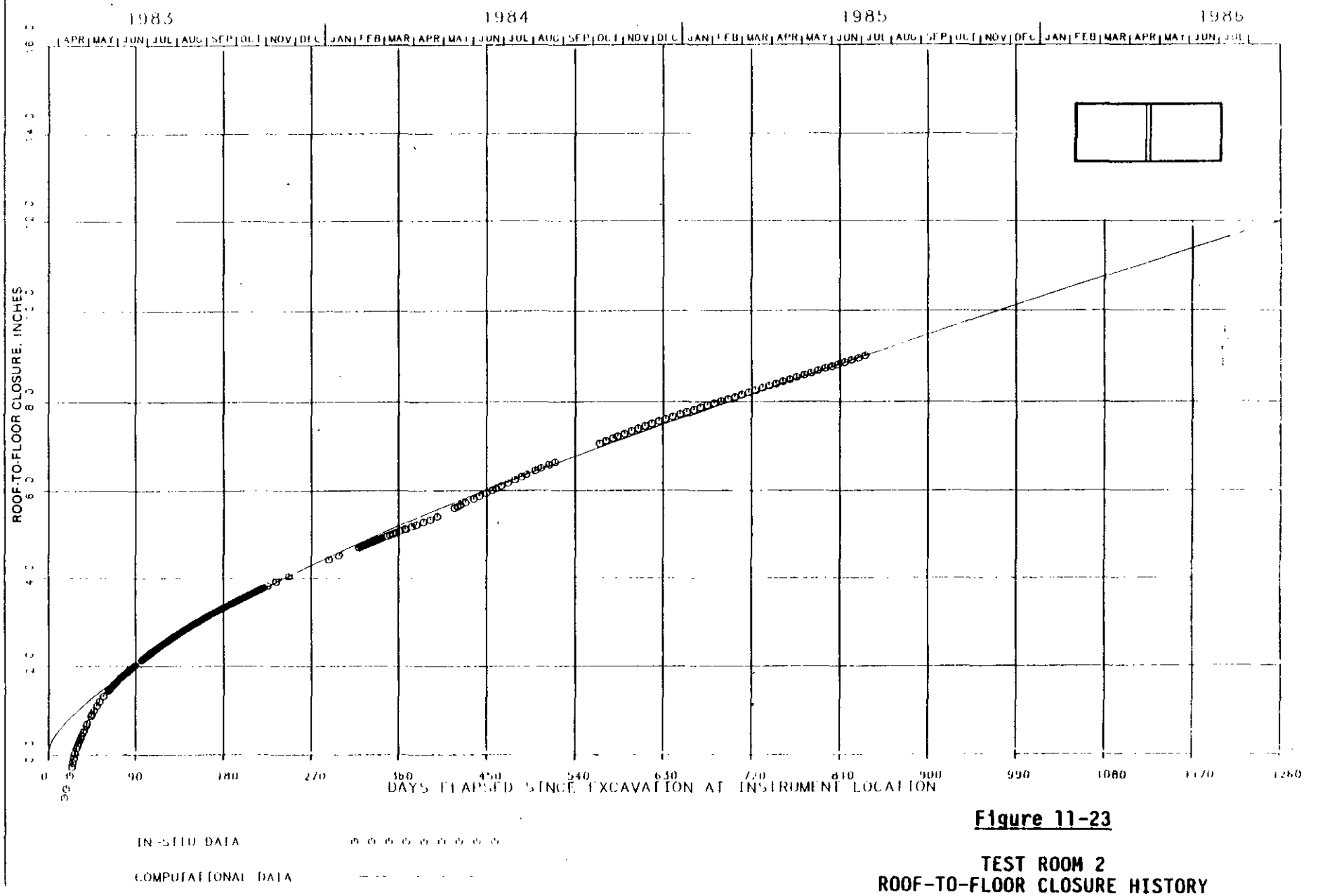

Figure 11-23

TEST ROOM 2
ROOF-TO-FLOOR CLOSURE HISTORY

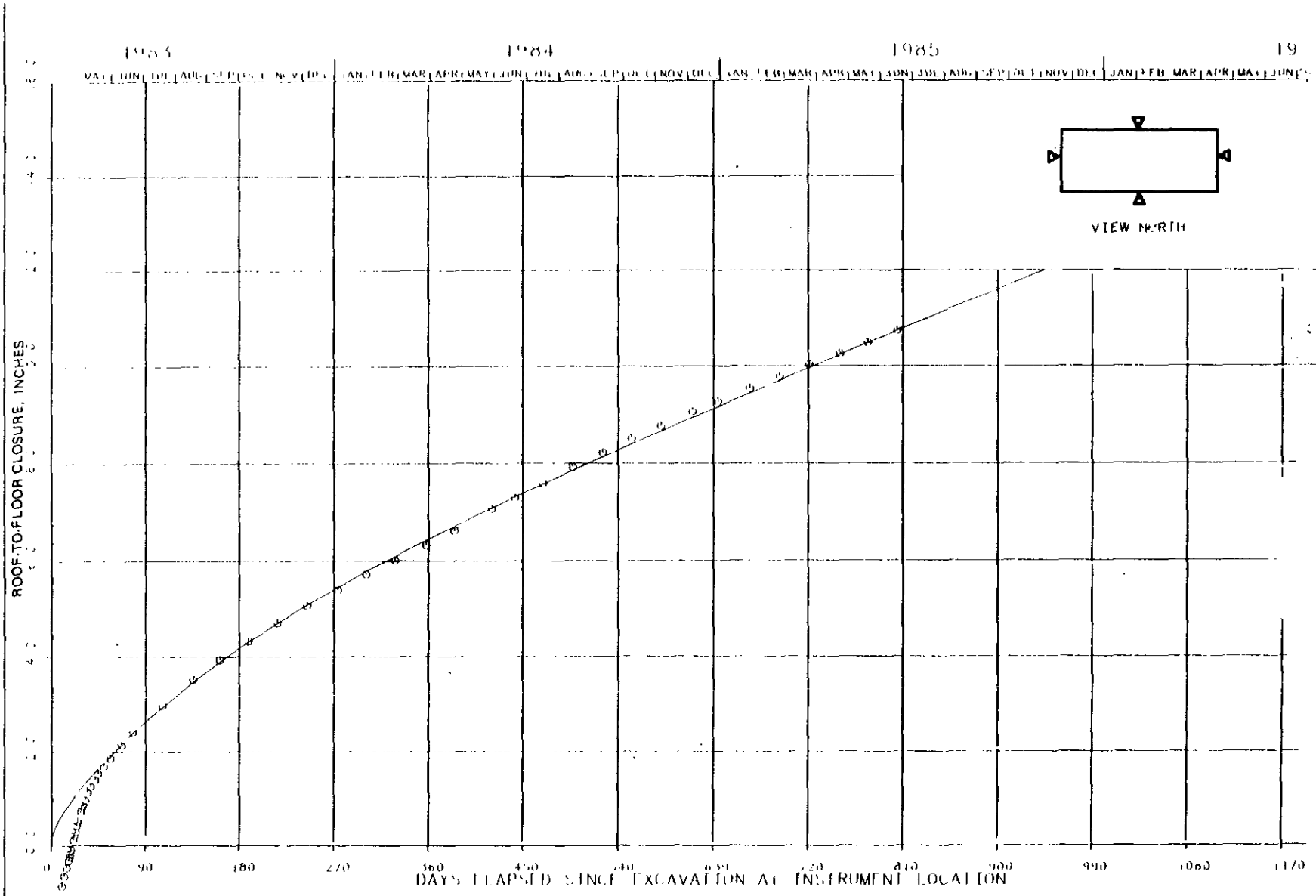

Figure 11-24

TEST ROOM 3
ROOF-TO-FLOOR CLOSURE HISTO

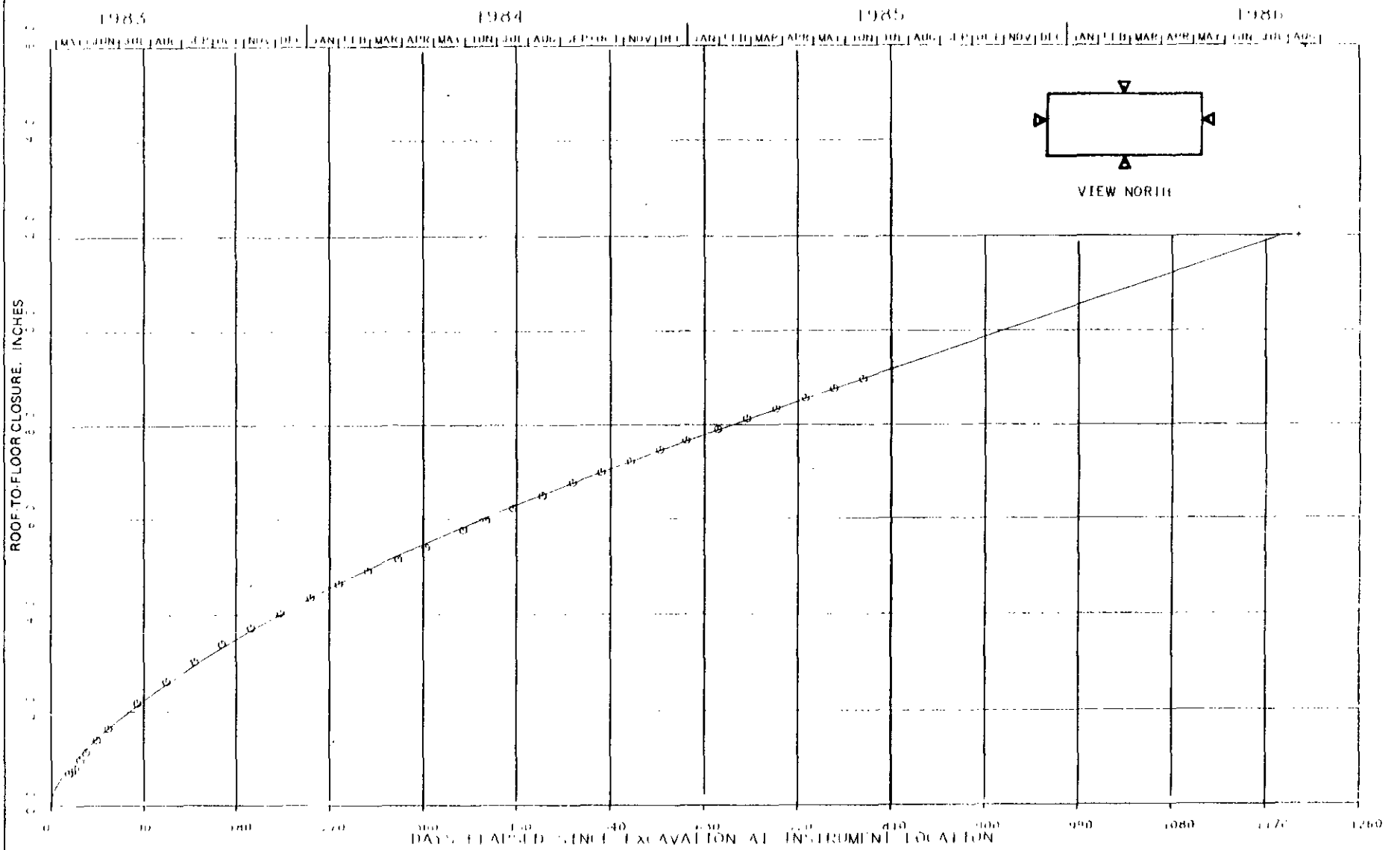

Figure 11-25

TEST ROOM 4
ROOF-TO-FLOOR CLOSURE HISTORY

TEST ROOM CREEP PARAMETERS
DETERMINED FROM ROOF-TO-FLOOR CLOSURES

Test Room	C ($ksf^{-4.9}sec^{-1}$)	A	z (sec^{-1})
1	3.103×10^{-21}	1.593	4.670×10^{-8}
2	1.919×10^{-21}	1.712	4.782×10^{-8}
3	2.516×10^{-21}	2.077	7.268×10^{-8}
4	2.813×10^{-21}	1.712	5.572×10^{-8}
Mean $\bar{X}$ (Rooms 1 thru 4)	2.588×10^{-21}	1.774	5.573×10^{-8}
Mean $\bar{X}$ (Rooms 1 & 4)	2.958×10^{-21}	1.653	5.121×10^{-8}
Mean $\bar{X}$ (Rooms 2 & 3)	2.218×10^{-21}	1.895	6.025×10^{-8}

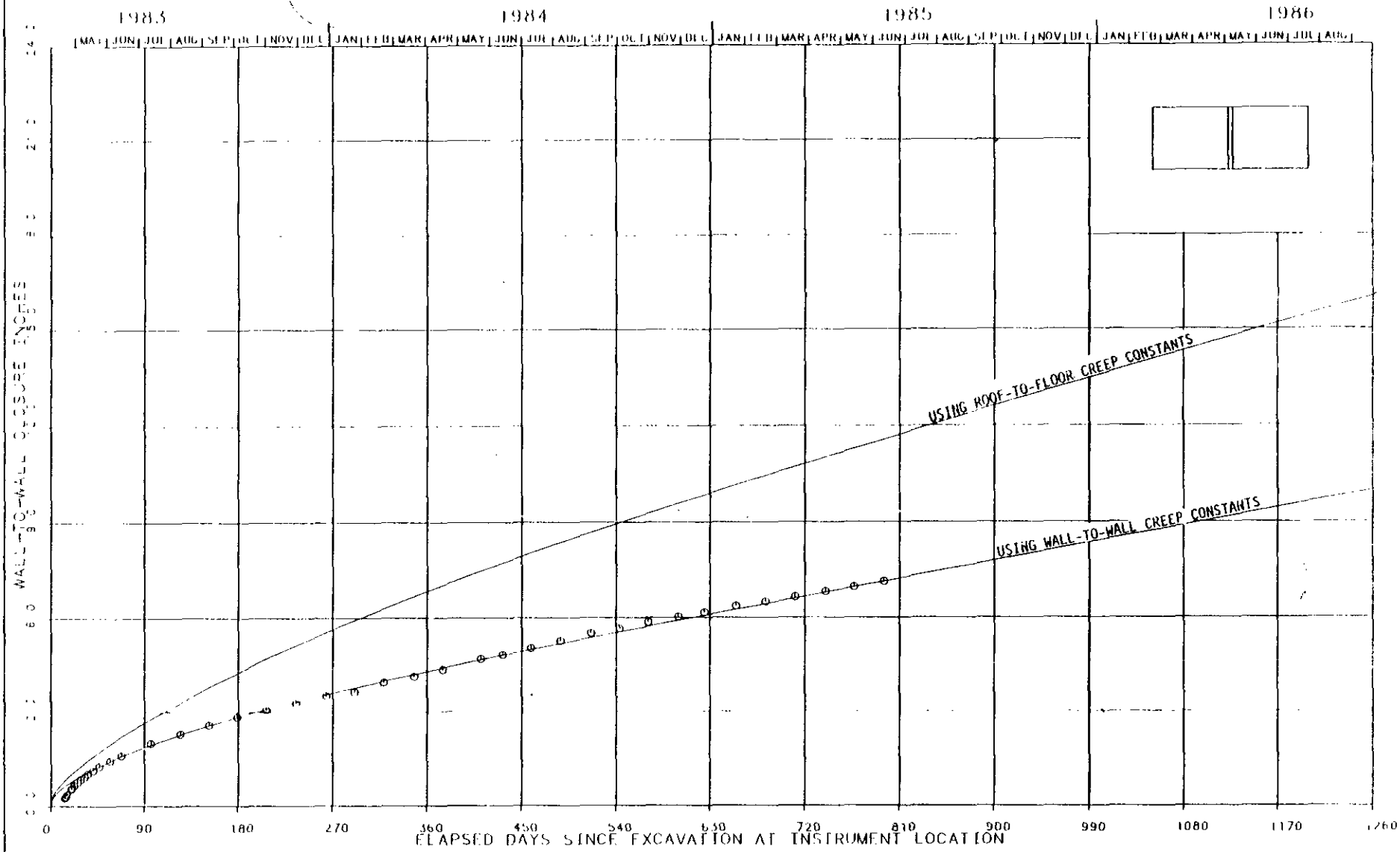

Figure 11-26

TEST ROOM 1
WALL-TO-WALL CLOSURE HISTORY

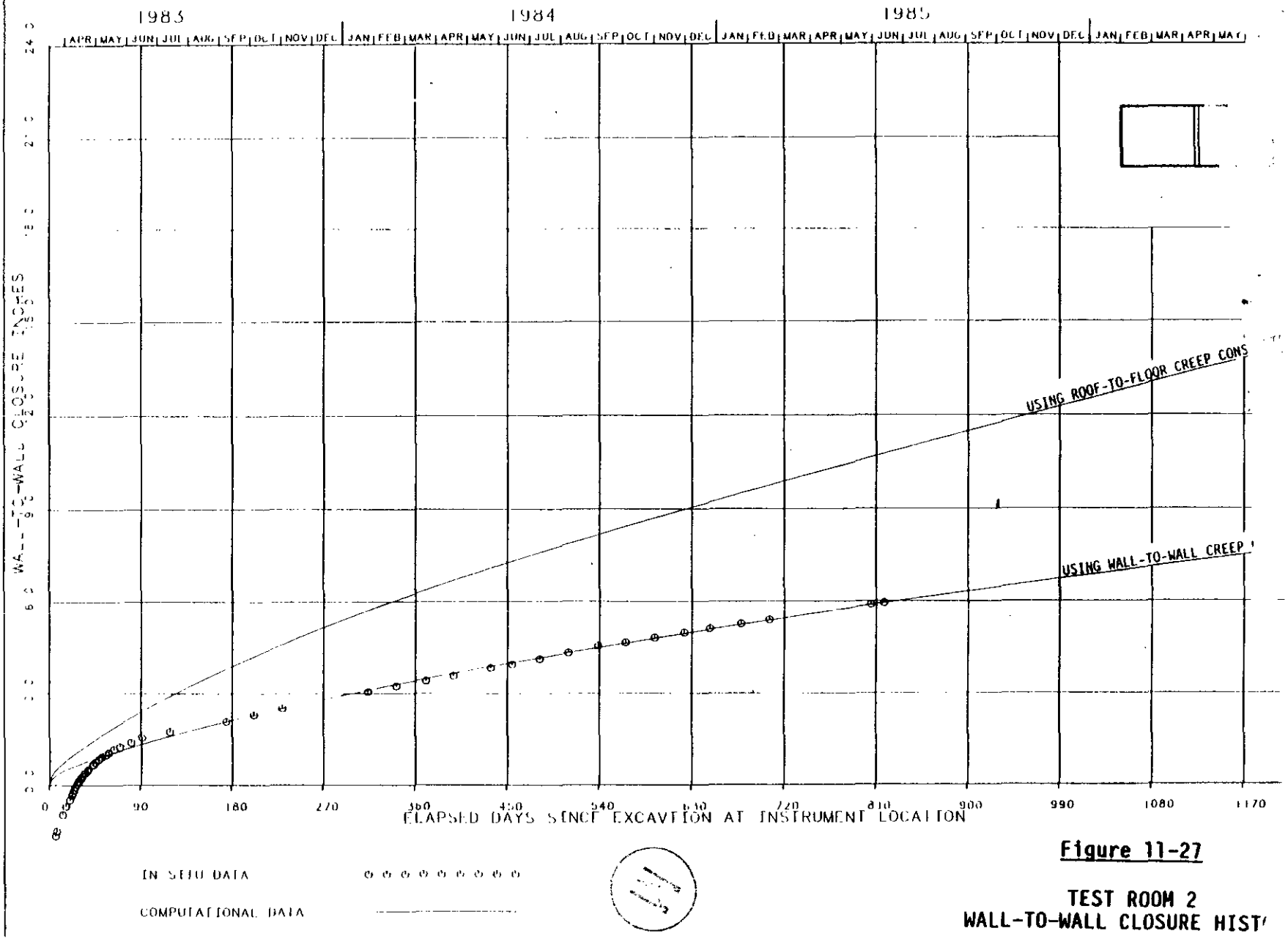

Figure 11-27

TEST ROOM 2
WALL-TO-WALL CLOSURE HIST

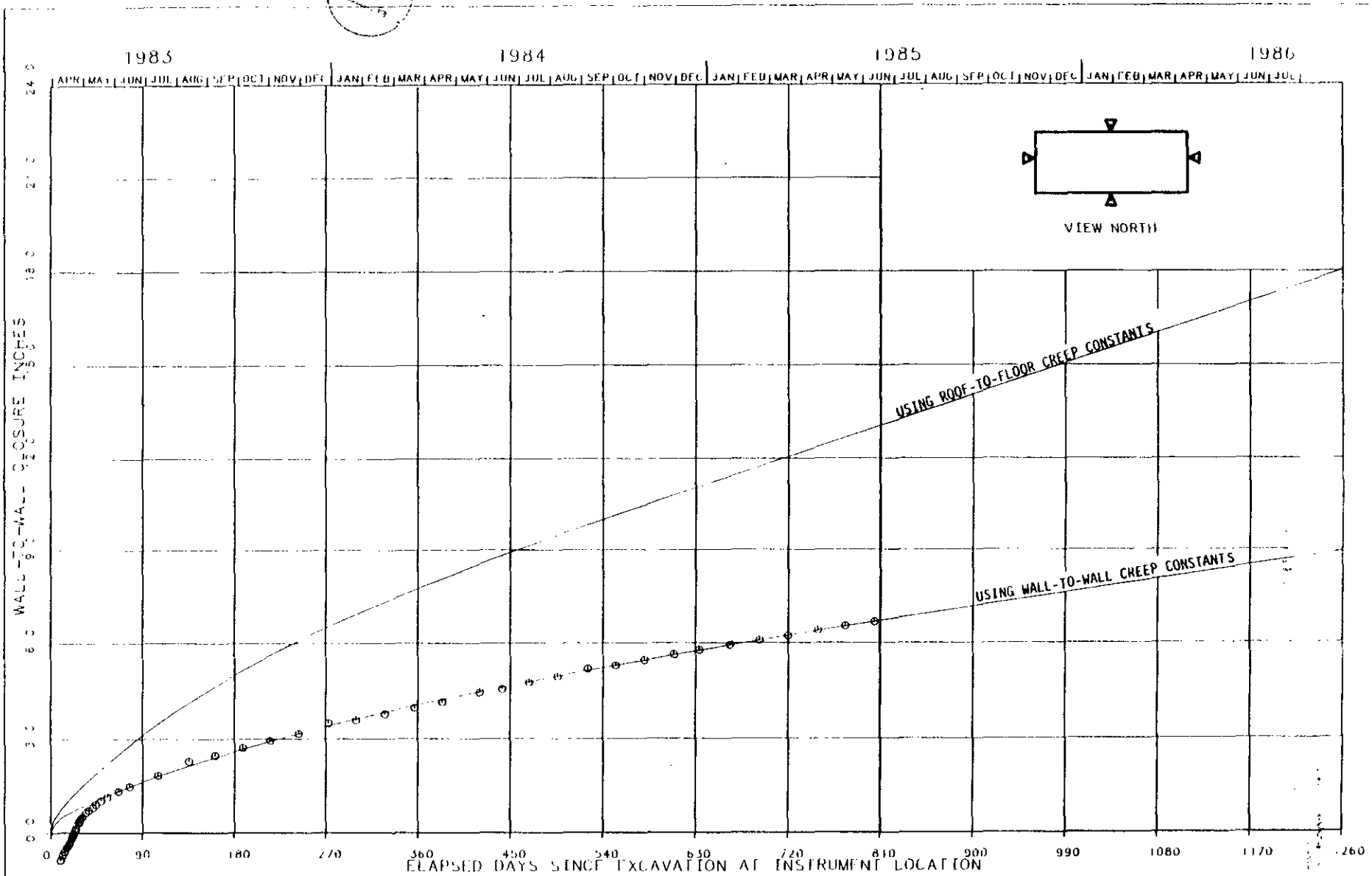

Figure 11-28

TEST ROOM 3
WALL-TO-WALL CLOSURE HISTORY

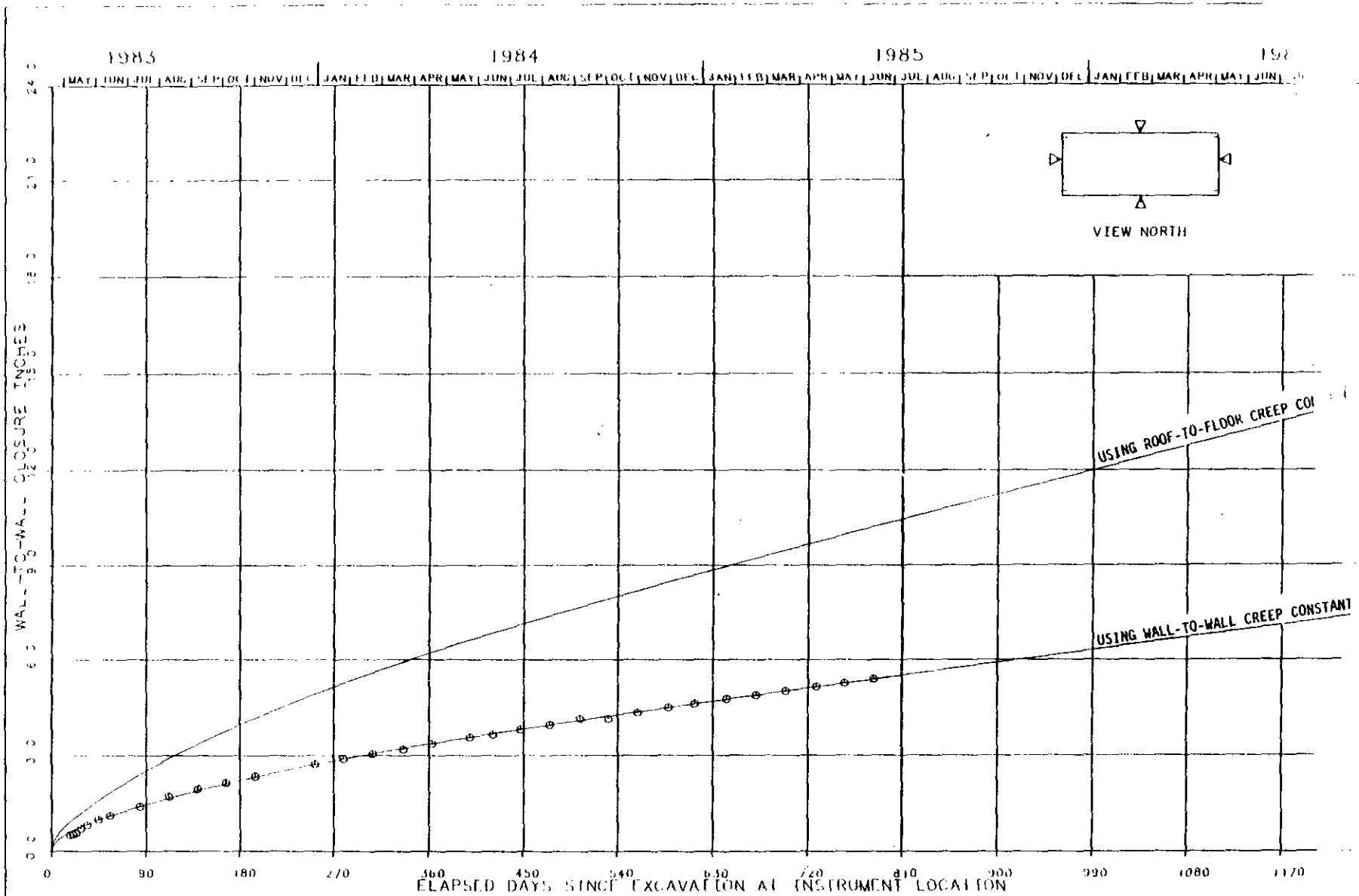

Figure 11-29

TEST ROOM 4
WALL-TO-WALL CLOSURE HIST

Table 11-13

TEST ROOM CREEP PARAMETERS
DETERMINED FROM WALL-TO-WALL CLOSURES

Test Room	C ($ksf^{-4.9}sec^{-1}$)	A	z (sec^{-1})
1	2.054×10^{-21}	1.502	6.810×10^{-8}
2	0.850×10^{-21}	1.630	2.476×10^{-8}
3	1.095×10^{-21}	1.920	4.464×10^{-8}
4	1.444×10^{-21}	1.419	5.276×10^{-8}
Mean $\bar{X}$ (Rooms 1 thru 4)	1.361×10^{-21}	1.618	4.757×10^{-8}
Mean $\bar{X}$ (Rooms 1 & 4)	1.749×10^{-21}	1.461	6.043×10^{-8}
Mean $\bar{X}$ (Rooms 2 & 3)	0.973×10^{-21}	1.775	3.470×10^{-8}

[illegible] and 11-30, the creep [illegible] the test rooms using roof-to-floor closure values vary slightly from the values obtained using wall-to-wall closure values. To illustrate these variations, the upper curves on Figures 11-26 through 11-29 show the wall-to-wall finite element responses using creep parameters determined from roof-to-floor numerical correlations. The discrepancy may be partly due to material anisotropy of the salt which is not taken into account in the constitutive relationship for the salt. However, the most important contributor to the discrepancy may be the behavior of the clay seams and anhydrite beds. The model also does not include the complete effects of anisotropic creep behavior due to the combination of different layers in the actual stratigraphy. This behavior, due to anisotropic geometry, can be shown using a simple one-dimensional model similar to the one used by Branstetter et. al. (ref. 11-3). Consider a block of halite containing N horizontal layers with equal thickness. The creep law for each of the layers is assumed to be

$$\dot{\varepsilon}_c = f_i(t)\sigma^{-n} \qquad i = 1, 2, \ldots\ldots N \qquad (11\text{-}12)$$

The equivalent vertical creep function computed by considering only the creep relation in the vertical direction can be expressed as

$$f_v(t) = \frac{\sum_{i=1}^{N} f_i(t)}{N} \qquad (11\text{-}13)$$

However, the equivalent horizontal creep function computed by considering only the horizontal direction becomes

$$f_h(t) = \left[\sum_{i=1}^{N} f_i(t)^{-\frac{1}{n}} \right]^{-n} N^n \qquad (11\text{-}14)$$

It was found that, for any problem in which $f_i(t)$ varies, the value of the equivalent creep function in the horizontal direction, based on

equation 11-14, is lower than the value in the vertical direction, based on equation 11-13.

Replication of in situ creep behavior by the finite element model would require extensive research into the existing constitutive equations and perhaps modification of the MARC Finite Element Program. It is believed that the present methodology can adequately predict the roof-to-floor and wall-to-wall closures within acceptable engineering accuracy and that further work into anisotropic creep behavior is not justified for design validation.

One method of determining the structural adequacy of the salt is by using the effective strain. Model simulation of Test Room 2 behavior showed that the effective strain reached a maximum value at the intersections of the walls with the roof and floor. As discussed in subsection 11.3.2.4, bay strains in the vertical direction, determined from roof and floor extensometer data, are on the order of 5 percent through June 1986. Field observations of the test room walls have not found any structural failure at these strain values. Occasional minor, shallow spalls are a continuing occurrence, especially along the upper portion of geologic map unit 4.

Based on the results of the model simulation of Test Room 2, the maximum effective strain at the roof and wall intersection will be 6 percent about 15 years after excavation. The corresponding average vertical strain over a 2-foot thickness of salt will be 15 percent. However, effective strain is not directly measurable. At best, only vertical or horizontal strains can be determined from multiple-point borehole extensometer measurements. A comparison of the predicted vertical strain with the vertical strain determined from the relative displacement between the collar and anchor A of the roof extensometers has been made. Because the collar and anchor A are 5 feet apart, the strain calculated from the relative displacements will be an average value. Similarly, the strain from three elements spanning the collar to anchor A interval were summed and averaged for comparison.

shows the [illegible] the roof and wall intersection. Although [illegible] is expressed in terms of t*, the relationship between t* and the real time t is approximately linear. The strain determined from the collar to anchor A readings indicates that the rate is currently decreasing with time.

Figure 11-31 shows the relationship for the center of the roof. This rate is also decreasing with time, even though the numerical analysis shows a constant rate.

11.3.2.6 Effectiveness of Model Simulation

The procedure discussed in the previous subsection and in Chapter 5 used roof-to-floor closure data for the test rooms to calculate the creep parameters C, A and z. Extrapolation of creep behavior was then accomplished using these derived creep parameters.

The numerical analysis gives the displacements of nodal points and stresses within the elements. The effectiveness of the model used can be checked by comparing measurement data other than roof-to-floor closure with the magnitude predicated by the model. For example, relative displacements between anchor points in multiple-point borehole extensometers may be compared with predicted relative displacements between appropriate nodes of the model. Such a comparison will be helpful to assess the effectiveness of model simulation.

Because a symmetrical two-room model representing four rooms was used for model simulation, the relative displacement between the collar and the deepest anchor of the central roof extensometers in Test Rooms 1 and 4 were calculated for an interval of 60 days, and the average value determined. The real time t was converted to the normalized time t* using equation C.4-17 in Appendix C. This is because the numerical analysis was performed in terms of the normalized time. The vertical displacements of appropriate nodes in the finite element model, which approximately duplicate the collar and the deepest anchor of the roof extensometers, were compiled. If the nodes did not exactly match the

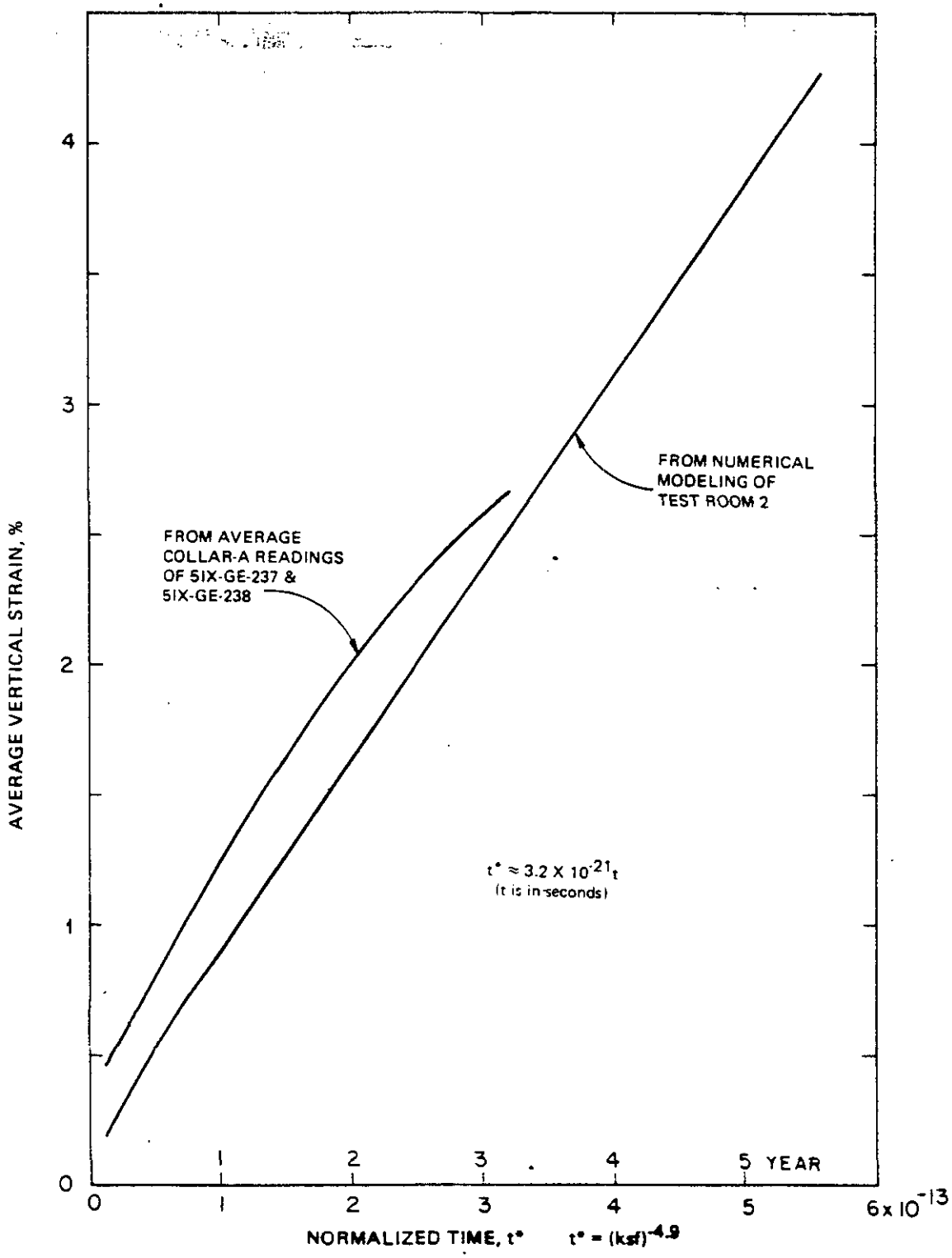

Figure 11-30

TEST ROOM 2
VERTICAL STRAIN AT ROOF AND PILLAR CORNER

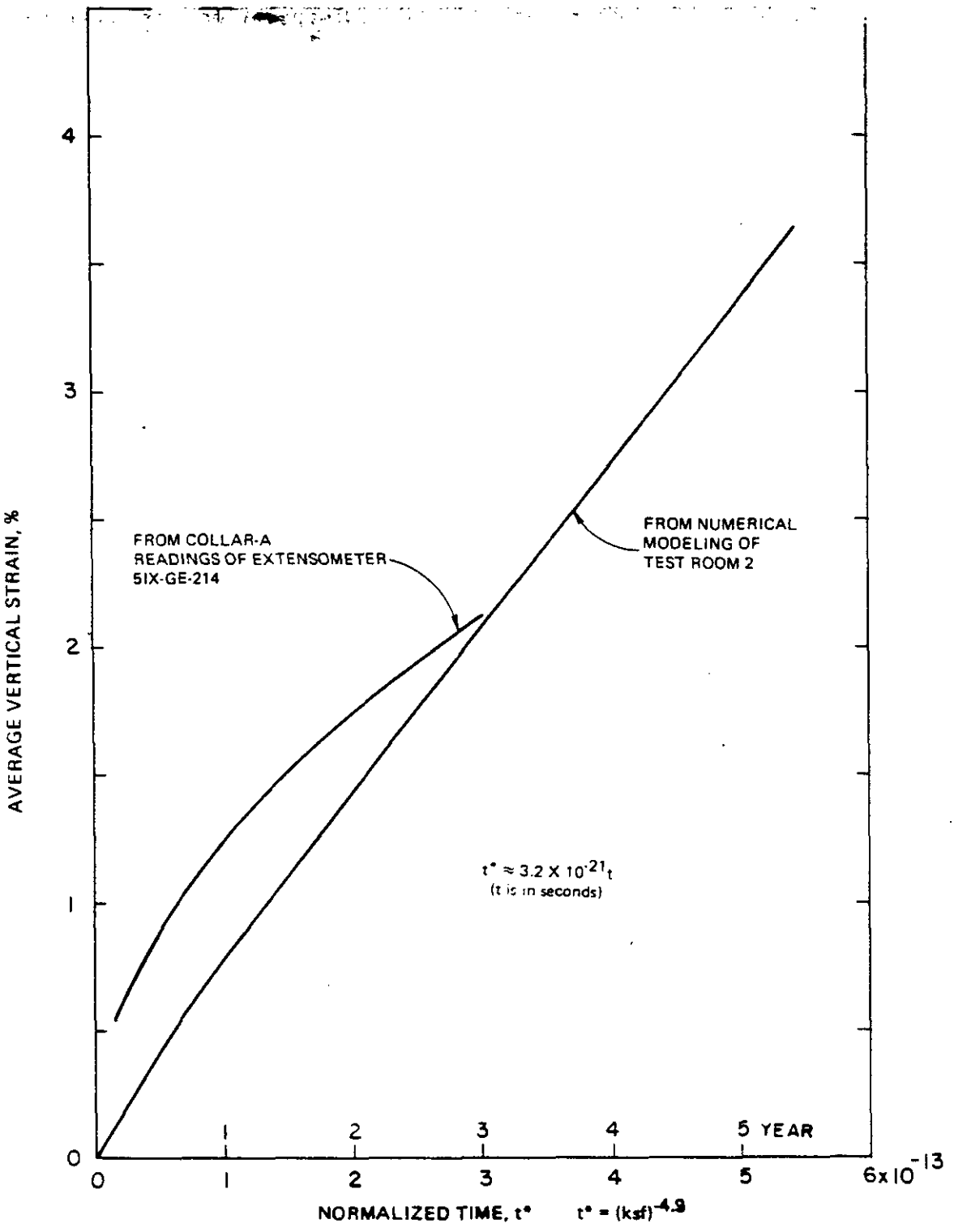

Figure 11-31

TEST ROOM 2
VERTICAL STRAIN AT ROOF CENTER

location of the deepest anchor, then linear interpolation was used to determine the displacement of salt at the required location.

Figure 11-32 compares the average relative displacement between the collar and the deepest anchor for the central roof extensometers 51X-GE-00207 and 51X-GE-00218, with the relative displacement between appropriate nodal points computed from the numerical model. A normalized time t* of 37.07×10^{-14} is equivalent to an elapsed time of nearly 3 years since the completion of excavation at the instrument location. The discrepancy between the measured and calculated relative movements is nearly 2 inches in 3 years.

For large values of t, the normalized time is approximately proportional to the real time, since the exponential term in equation C.4-17 in Appendix C approaches unity. For large values of t* (and t), the calculated relative displacement rate will be approximately 44 percent higher than the measured relative displacement rate if the current rate is maintained. A similar analysis was made for Test Rooms 2 and 3. Figure 11-33 compares the measured values with the values obtained from numerical modeling. The discrepancy in this case is 27 percent with respect to the measured value at nearly 3 years of elapsed time.

A comparison of salt heave measurement data from a floor extensometer in Test Room 4 was made with the values computed from numerical modeling. Figure 11-34 shows the results of this comparison. The numerical model underestimates the salt heave in the floor by approximately 70 percent of the measured value. This discrepancy is probably due to the assumption in the model that MB-139, 4.8 feet below the floor, is elastic and has infinite strength. Measurements from the floor extensometer and observations of fracturing indicate that MB-139 cannot be strictly considered as elastic. As discussed in subsection 11.3.2.1, borehole P4X-84 indicates the presence of lateral displacements and vertical separations in MB-139 beneath the floor of Test Room 4. This indicates that stresses in parts of the anhydrite bed may have reached the failure state.

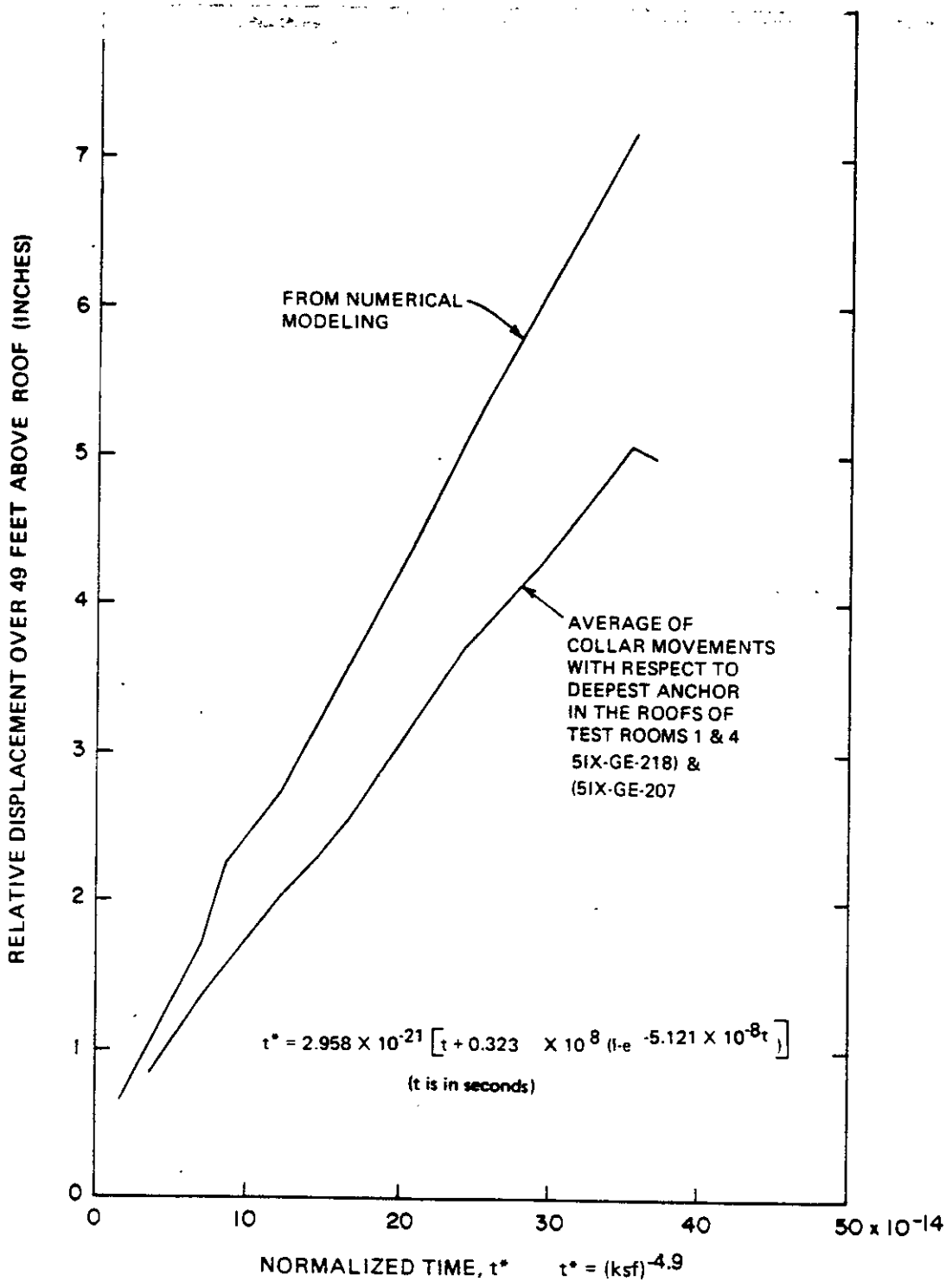

Figure 11-32

TEST ROOMS 1 AND 4 ROOF EXTENSOMETERS
NUMERICAL MODELING VERSUS IN SITU MEASUREMENT DATA

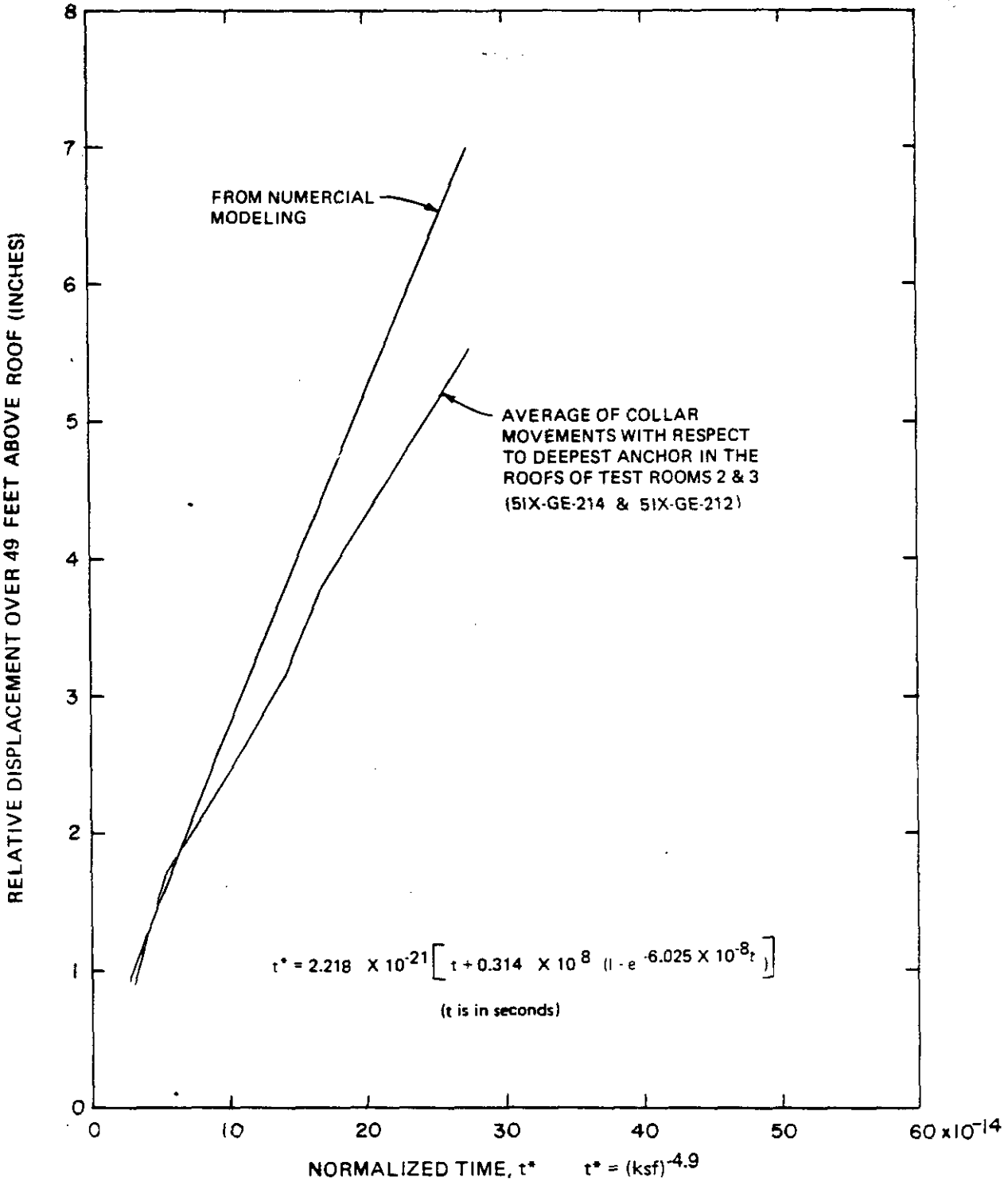

Figure 11-33

TEST ROOMS 2 AND 3 ROOF EXTENSOMETERS
NUMERICAL MODELING VERSUS IN SITU MEASUREMENT DATA

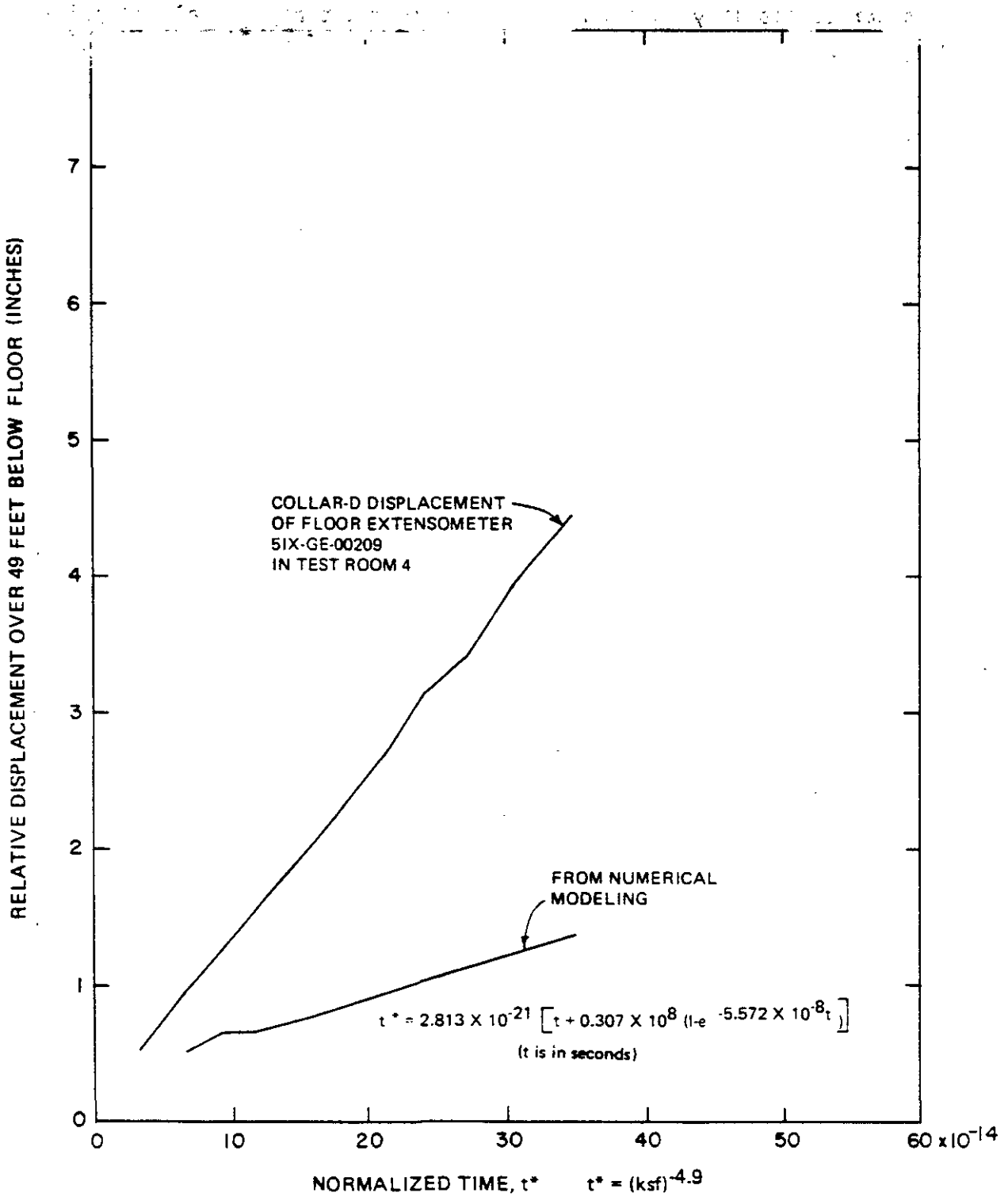

Figure 11-34

TEST ROOM 4 FLOOR EXTENSOMETER
NUMERICAL MODELING VERSUS IN SITU MEASUREMENT DATA

Another possibility is that the fractures might have developed prior to excavation of the test rooms (ref. 6-6). In either case, assumptions of linear elasticity for the anhydrite bed become untenable. Modifications to the material characterization of this anhydrite material will be required to better represent its deformational behavior.

The basic philosophy of the model simulation developed in this report is that in situ measurement data are utilized to back calculate the creep parameters of the salt mass with the attendant discontinuities such as clay seams and anhydrite beds. For the model simulation technique, the in situ roof-to-floor closure data have been used to extract the creep parameters and predict future behavior using these creep parameters. This is because the roof-to-floor closure is deemed critical to evaluate the adequacy of the room dimensions for the effective storage and retrieval of waste. The discussions in the previous paragraphs indicate that there are discrepancies between measured and predicted quantities for variables other than roof-to-floor closure, such as deformations within the salt mass. Such discrepancies are not due exclusively to any inadequacy of the numerical modeling procedure but are also due to differences in the actual and assumed stratigraphy, variations in creep parameters with space and time, and inadequate representation of the stress-strain behavior of the anhydrite bed. However, it has been demonstrated that the model can predict, with sufficient accuracy for engineering purposes, the roof-to-floor closure behavior of the test rooms. A similar model simulation analysis was made for wall-to-wall closure and independent creep parameters were developed. Extrapolation of wall-to-wall closure with time was achieved using these creep parameters. This model simulation technique using in situ data was employed because the more detailed approach using material properties derived from laboratory tests may not produce more accurate results, as discussed in Chapter 5, subsection 5.4.3.

The reference design was based on computations for a single room rather than for multiple rooms. It was assumed that, with a low extraction ratio, the rooms with 100-foot pillars would not have as much early interaction as that which has developed in the four-room test panel. In Figure 11-35 the two lower curves show the computational results of roof-to-floor closure predictions for a 13 x 33-foot room using creep constants obtained from laboratory tests. The bottom curve represents the computational results from reference 11-4, dated August 1982, while the middle curve represents the updated result from reference 11-5, dated March 1985, which used revised creep parameters and an updated reference stratigraphy. In situ closure data for all four test rooms, including adjustments for their early closure, are plotted on the same figure for comparison. Interaction effects may be partly responsible for the discrepancy.

11.4 CONCLUSIONS AND RECOMMENDATIONS

11.4.1 Conclusions

The determination of the closure behavior of the WIPP underground openings using creep constants derived from laboratory experiments underestimated the actual closure. The measured roof-to-floor closure in the test rooms has exceeded 12 inches in the 3 years since the end of their excavation. This does not comply with the design criteria vertical closure allowance of 12 inches in 5 years.

Average vertical strains at roof and wall intersections, as determined from extensometer readings, were close to 3 percent in June 1986 and the strain rate was decreasing. Maximum vertical strain by numerical modeling occurs at roof and wall intersections and compares well with the value determined from in situ measurements.

Spalling from the roofs and walls, and fractures in the pillars and at pillar corners have been observed. Displacements and minor separations have been observed at clay seams and in the underlying halite in

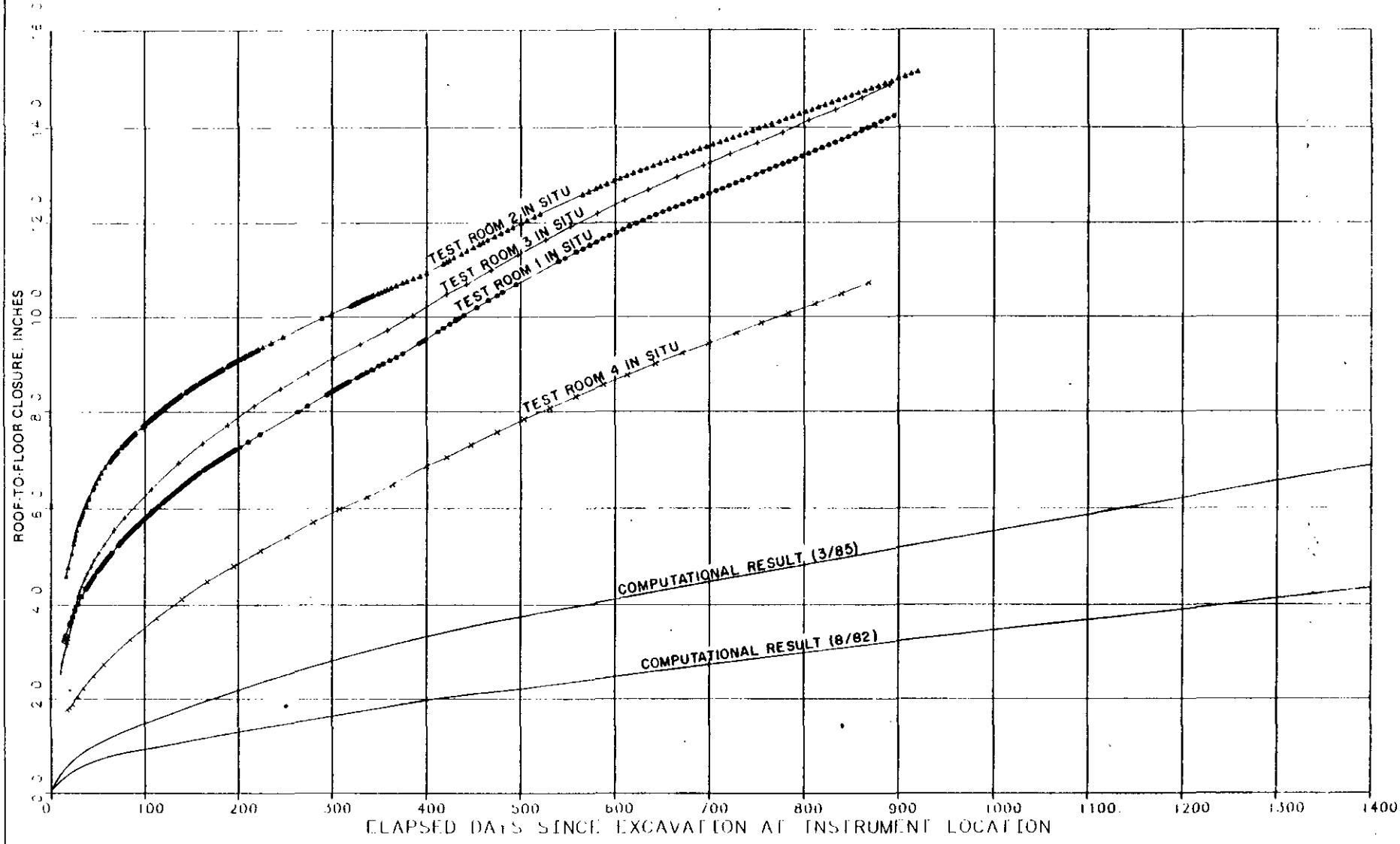

Figure 11-35

TEST ROOMS
COMPARISON OF LABORATORY VERSUS IN SITU DATA

trate the roofs. hese continue. Periodic maintenance of the roof and wall surfaces will be required.

Floor fracturing is well developed in the south half of Test Room 3 (Room T). Floor fracturing also occurs to a minor degree in the other test rooms and in a few areas in the drifts. Because the prominent floor fracturing occurring in Test Room 3 has not been found in any other rooms or drifts, it is considered to be anomalous to the underground facility. It is possible that the number and size of the 22 large-diameter holes in Test Room 3 exacerbated the pre-existing fractures. If floor fracturing occurs in the storage rooms, it is not expected to cause any operational or storage problems. As discussed in Chapter 3, Section 3.2, the WIPP project participants agreed, in a meeting on February 13, 1986, that the underground conditions do not require moving the facility level (ref. 3-2).

11.4.2 Recommendations

Observations and geomechanical instrumentation measurements should continue in the test rooms. Because they are the models for the determination of storage room behavior, trimming, rock bolting and other maintenance in the test rooms should be kept to the minimum required for safety, and the rooms allowed to deform.

It is recommended that Test Room 2, in particular, be preserved. It is the only test room that has not been physically altered. This room will then serve as a model for the storage rooms as they will exist prior to waste emplacement. Test Room 2 should not be trimmed or supported except as anticipated for the storage rooms. Additional instrumentation may be installed and small-diameter holes should be drilled in the roof and floor to observe the development of displacements, separations and fracturing. Large-diameter drilling should be prohibited and the room should be closed to all other activities. Continued observations of Test Room 2 behavior will

provide valuable data on anticipated storage room performance for the period between room excavation and the emplacement of waste.

A program of drilling, testing and geologic mapping should be continued to determine the development and extent of fracturing beneath the test room floors. When this has been determined, several monitoring stations should be established to document the behavior of the fractures. This program should also include monitoring roof displacements and separations. Arrays of small-diameter holes should be drilled in a few locations in each test room as soon as possible to document movement above the roof. However, drilling in Test Room 2 should be kept to a minimum.

Additional efforts are needed to refine constitutive laws for the creep behavior of salt as well as the representation of stratigraphy. The stress-strain-time behavior of anhydrite beds should be more accurately represented.

CHAPTER 12
STORAGE AREA

12.1 INTRODUCTION

The storage area encompasses all rooms, drifts and crosscuts that will be used for the permanent storage of CH and RH TRU wastes. The storage area is located south of the waste shaft station, from S1600 to S3664 (see Chapter 1, Figure 1-2, and this chapter, Figure 12-1, for location and layout). The storage area is arranged to provide a system in which CH and RH TRU wastes can be efficiently and safely handled and stored. A panel of four full-scale test rooms was excavated to determine the adequacy of the opening configuration and dimensions (Chapter 11). Evaluation of in situ data from these test rooms were utilized to predict the closures of, and stresses and strains around, the future storage area rooms and drifts.

This chapter presents information on the reference design of the storage area rooms and drifts, the design validation process, conclusions regarding the suitability of the reference design based on the findings of the validation process, and recommendations for modifications to the storage area design configurations that will, if implemented, result in a validated reference design.

12.2 DESIGN

This section presents the design criteria, design bases and reference design configurations that were used for the WIPP storage area rooms and drifts.

12.2.1 Design Criteria

The Design Criteria, RMC-IIA, for the storage area (ref. 2-8) is summarized in Chapter 2, Table 2-1. This table presents the major criteria that governed the WIPP underground opening reference design, including those criteria that require evaluation as part of the design validation process. The following discussion presents a description of

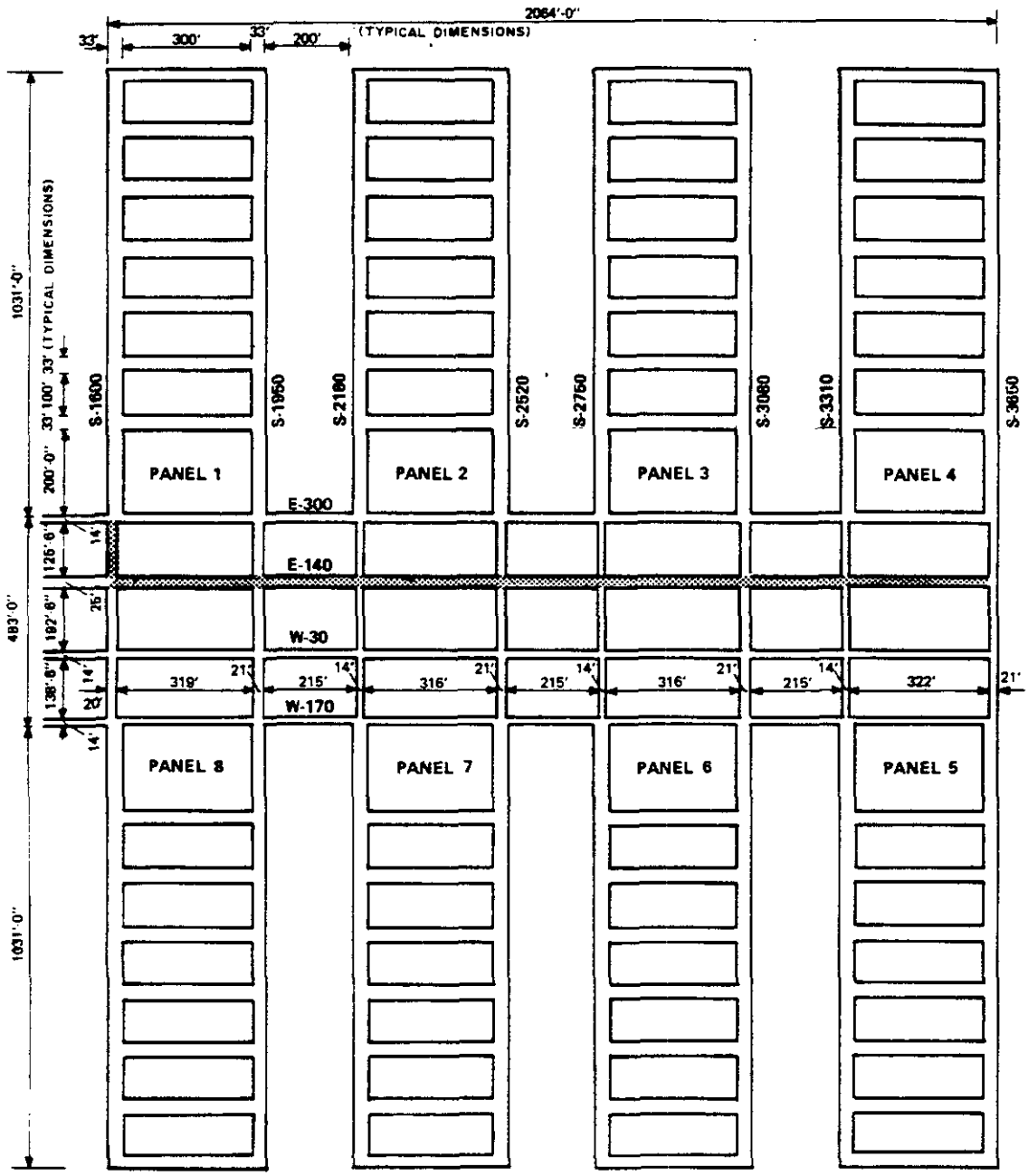

Figure 12-1

STORAGE AREA
REFERENCE DESIGN PLAN

the three design criteria pertaining to the storage area that require evaluation for validation of the reference design.

The first criterion requires that the excavation dimensions of the storage area rooms and drifts include an allowance for creep closure sufficient to prevent container breaching by creep-induced stresses during the retrievability period. The second criterion states that each storage room shall allow for salt creep and shall be sized to minimize breaching of the CH waste containers for a period of 10 years. The third criterion states that the underground storage rooms and access drifts shall be designed to be compatible with the waste transport vehicle, with the waste container sizes, shapes, weights, and stacking configurations, and with the waste handling and backfilling equipment requirements.

Other criteria that apply to the storage area reference design also apply to the drifts and were discussed in Chapter 10.

12.2.2 Design Bases

The design bases describe the specific dimensional requirements used to develop the reference design for the storage area drift and room configurations (Figures 12-2 and 12-3). The Design Basis, Underground Excavations (ref. 2-18) contains the bases used for the storage area reference design. The major elements from this Design Basis document are summarized in the following discussion. Although other design bases were also used, they did not have a direct impact on design validation. The specific design bases requiring evaluation during the validation process are presented in Table 12-1.

The design bases specify that the reference design shall provide an underground storage area in which CH and RH TRU wastes can be efficiently handled and stored. The reference design of the waste storage area shall permit simultaneous storage of CH and RH TRU wastes. To the extent possible, the configuration of the storage area shall minimize haulage distances for excavated salt and waste storage.

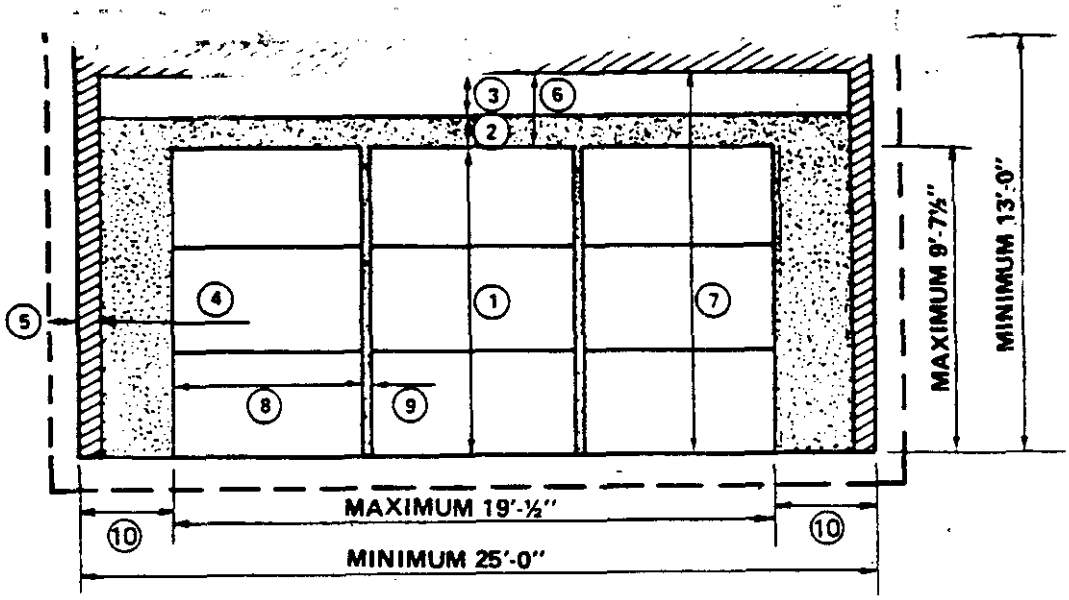

EXPLANATION

(1) HEIGHT OF WASTE PACKAGES STACKED THREE HIGH: 9'-7 1/2" FOR BOXES; 9'-0" FOR SIX PACKS.

(2) SALT COVER: 1' TO 2'; LEVEL OF SALT IS MAINTAINED AT 10'-8" ABOVE THE FLOOR.

(3) VENTILATION SPACE: 1'-4" MINIMUM UNTIL ROOM OR PANEL IS FILLED AND PLUGGED.

(4) SALT CREEP ALLOWANCE: 1'-0" ROOF; 4 1/2" EACH WALL (ASSUMED TO BE ADEQUATE FOR 5 YEARS).

(5) CONSTRUCTION TOLERANCE: +6". THE CONTRACTOR MUST MAINTAIN THE MINIMUM ROOM DIMENSIONS.

(6) BACKFILLING CONVEYOR CLEARANCE: 2'-4" ABOVE WASTE PACKAGES.

(7) HEADROOM: 12'-0" FOR CH BOXES AND RH TRANSPORTER.

(8) WASTE PACKAGE WIDTH: 6'-2 1/2" FOR BOXES; 6'-1 1/2" FOR SIX PACKS.

(9) STACKING TOLERANCE: 2 1/2" BETWEEN WASTE PACKAGES.

(10) SALT BACKFILL: 3'-0" BETWEEN WASTE PACKAGES AND WALL.

Figure 12-2

STORAGE AREA
DRIFT REFERENCE DESIGN DIMENSIONS

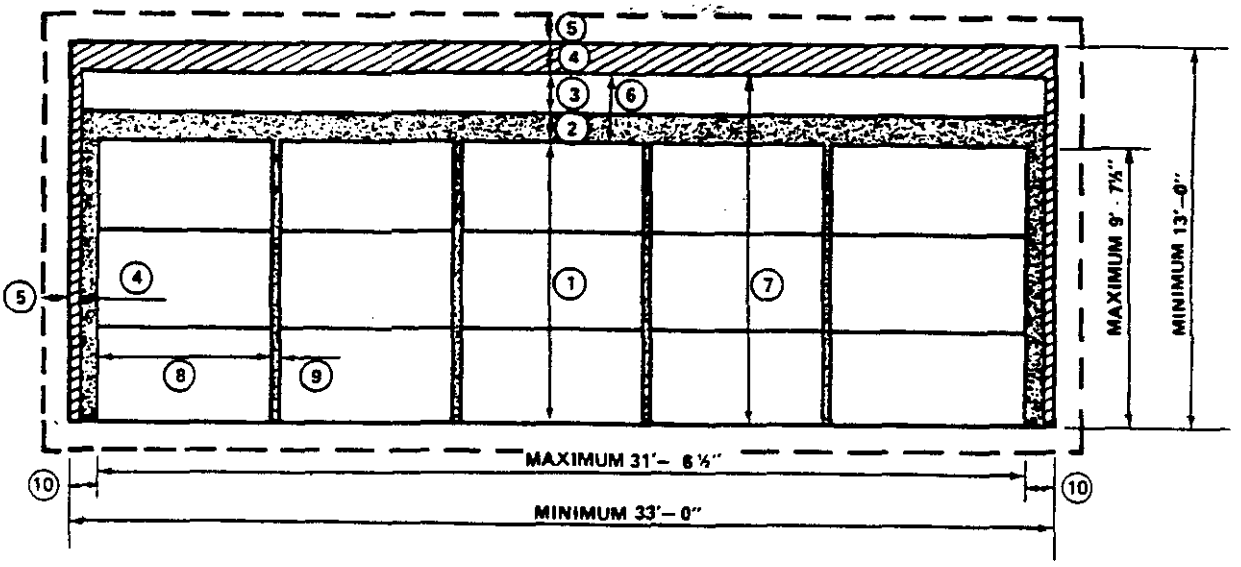

EXPLANATION

(1) HEIGHT OF WASTE PACKAGES STACKED THREE HIGH: 9'-7 1/2" FOR BOXES; 9'-0" FOR SIX PACKS.

(2) SALT COVER: 1' TO 2'; LEVEL OF SALT IS MAINTAINED AT 10'-8" ABOVE THE FLOOR.

(3) VENTILATION SPACE: 1'-4" MINIMUM UNTIL ROOM OR PANEL IS FILLED AND PLUGGED.

(4) SALT CREEP ALLOWANCE: 1'-0" ROOF; 4 1/2" EACH WALL (ASSUMED TO BE ADEQUATE FOR 5 YEARS).

(5) CONSTRUCTION TOLERANCE: +6". THE CONTRACTOR MUST MAINTAIN THE MINIMUM ROOM DIMENSIONS.

(6) BACKFILLING CONVEYOR CLEARANCE: 2'-4" ABOVE WASTE PACKAGES.

(7) HEADROOM: 12'-0" FOR CH BOXES AND RH TRANSPORTER.

(8) WASTE PACKAGE WIDTH: 6'-2 1/2" FOR BOXES; 6'-1 1/2" FOR SIX PACKS.

(9) STACKING TOLERANCE: 2 1/2" BETWEEN WASTE PACKAGES.

(10) SALT BACKFILL: 8 3/4" BETWEEN WASTE PACKAGES AND WALL.

Figure 12-3

STORAGE AREA
ROOM REFERENCE DESIGN DIMENSIONS

(1) Operational requirements

a. The storage area rooms, drifts and crosscuts shall be designed to allow for retrieval of all CH and RH waste stored for a period of up to 5 years after the initial emplacement of each waste species.

b. Excavation dimensions in the waste storage area shall be to a uniform height of 13 feet.

(2) Essential features

Provide 1 foot vertical and 9 inches horizontal allowance for creep closure to maintain the minimum design dimensions up to 5 years after initial emplacement.

(3) Safety design requirements

A minimum opening of 16 inches shall be left at the top of the rooms and drifts for air passage above the waste and backfill.

Construction and storage operations shall be physically separated and performed during different shifts.

Each storage room is to be filled with waste containers consisting of six-packs of CH TRU waste storage drums and/or boxes of CH TRU waste. The containers shall be stacked three high and five wide, stored with their longest dimension across the opening. A 2 1/2-inch stacking tolerance shall be allowed between waste packages. All rooms, drifts and crosscuts in the storage area may be used to store CH waste containers stacked three high. For this reason, excavation shall be to a uniform height of 13 feet throughout the waste storage area.

The underground storage area shall provide for the horizontal emplacement of 1,000 RH canisters. The RH canisters, nominally 10 feet long and 26 inches in diameter, shall be stored in the salt pillars. Emplacement holes shall be perpendicular to the walls, approximately midway between the floor and ceiling and evenly spaced laterally. Canister spacing shall be based on the assumption that the average heat output per canister will be 60 watts or less. Thermal loading in the RH waste storage area shall not exceed 10 kilowatts (kw) per acre. Allowing 12 inches for salt creep, RH waste emplacement machinery shall be designed to operate in an effective room height of 12 feet, including all required clearances.

The storage area floor shall be approximately 2,150 feet below the ground surface. The final level of the excavations shall be as determined by the DOE Contracting Officer.

Four parallel entries shall be provided from the shafts to the waste storage area. These entries shall provide separate channels for air intake and exhaust, salt removal, and waste storage.

Excavation dimensions shall include an allowance for salt creep of 1 foot in the vertical direction and 9 inches in the horizontal direction for all rooms for up to 5 years. The tolerance for excavation of roof,

...ater than pl... ... the finished cross section dimensions be less than design dimensions.

Provision shall be made for the expansion of the storage area within the boundaries of Zone II (Chapter 1, Figure 1-1) if required in the future. The area extraction ratio in the storage area shall not exceed 25 percent.

The stored CH TRU waste packages shall be covered with a layer of salt backfill (3/8 inch or less in grain size) for fire protection. The volume of stored CH TRU waste in any one compartment without a vertical fire barrier shall be limited to a maximum of 500,000 cubic feet. For ventilation above the backfilled waste, a minimum opening of 16 inches shall be provided.

No personnel may work in air that has passed over the stored CH TRU waste. However, personnel may work in air that has passed through an opening where RH TRU waste has been emplaced provided that canister holes have been sealed with plugs. Personnel may not work in air that has passed through openings where RH TRU waste is being emplaced.

12.2.3 Design Configuration

The reference design of the storage area was developed in accordance with the design criteria and the design bases. The design configuration is based on the stratigraphy determined from borehole ERDA-9 and on salt creep performance determined from laboratory tests on core extracted from ERDA-9. The ERDA-9 exploratory hole was the only hole within the underground development area which was permitted to penetrate the Salado formation to the underground facility horizon.

The storage area reference design configuration (Figures 12-1, 12-2 and 12-3) consists of eight panels with seven rooms each. The rooms are 13 feet high, 33 feet wide and 300 feet long. The panel entries are also 13 feet high and 33 feet wide. The rooms are separated in each panel

by 100-foot wide pillars and the panels are separated by 200-foot wide pillars. The test rooms discussed in Chapter 11 were designed to be the same size as the storage rooms. The test rooms were constructed to monitor salt performance, permit observations of opening stability, and to permit validation of the storage room reference design.

The reference design provides for the storage of CH waste in one room while RH waste is stored in another room. Emplacement of RH waste canisters into horizontal holes is depicted on Figure 12-4. After the RH waste canisters are emplaced in the walls of the storage room a shield plug is placed in the wall sleeve. When the emplacement of RH waste canisters is completed in the storage room, CH waste can be stored in the same room. During the 5-year demonstration period, the RH waste canisters are stored in steel sleeves in the first room of Panel 1. During permanent storage, they are emplaced in pillars throughout the storage area as dictated by the receival rate of the waste.

The RH waste canisters (with a heat output of 60 watts or less) are placed in horizontal holes spaced so that the local storage area thermal loading does not exceed the design basis limit of 10 kw/acre. For the reference design, and for this report, the thermal effects on storage room behavior were not considered significant. The reference design for RH waste is subject to the results of the ongoing WIPP experimental program.

The reference design configuration also defines stacking configurations and tolerances for ventilation, backfill and salt creep. These tolerances are shown on Figures 12-2 and 12-3 for the storage area drifts and rooms, respectively. In order to meet these requirements, the reference design configuration incorporates a reference operating procedure. This procedure is based on the waste receipt rates, emplacement rates, and retrieval rates stipulated by the design criteria. This operating procedure is part of the storage room reference design and is incorporated in construction package EP-01X.

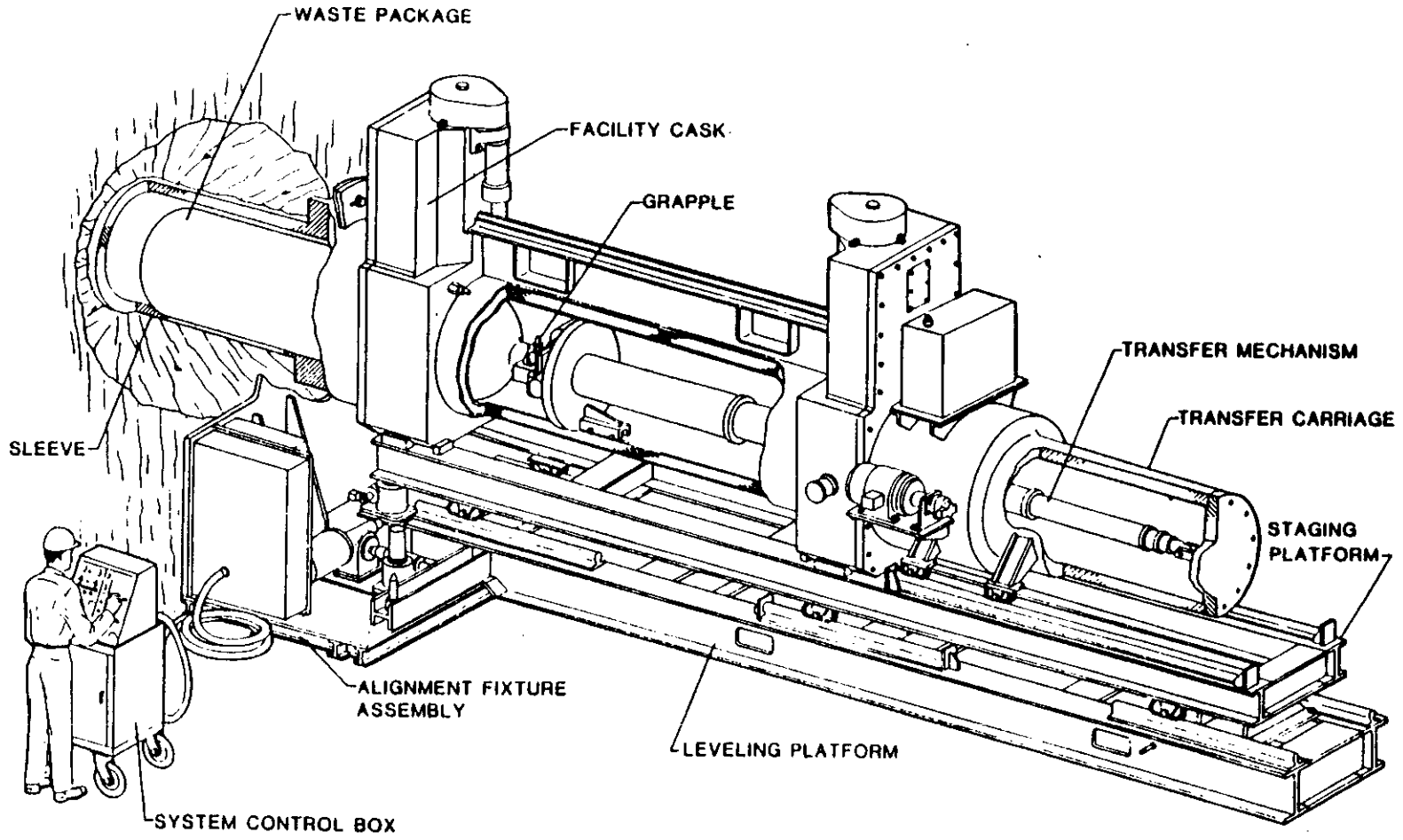

Figure 12-4

STORAGE AREA
HORIZONTAL EMPLACEMENT OF RH WASTE

This package contains the design documents that will be used to operate the WIPP.

12.3 DESIGN VALIDATION PROCESS

The design validation process for the storage area consists of the evaluation of numerical modeling and data analysis from the drifts and test rooms (Chapters 10 and 11) and its application to the reference design of the storage area drifts and rooms. The predicted future performance of the storage area openings was compared to the performance of existing openings having comparable dimensions. This was then used as the upper bound for validating the reference design.

12.3.1 Data Collection

Geomechanical instrumentation data collected from the test rooms were used to compute the creep parameters of the surrounding salt. Geologic mapping and drill cores from the underground facility were used to confirm the stratigraphy of the storage area. Test room instrumentation data and the computation of creep parameters are presented in Chapter 11. Chapter 6 presents information on the geologic mapping, drill cores and development of the reference stratigraphy.

The geomechanical instruments in the test rooms have provided deformation measurements and response data on the excavated openings. Periodic visual inspections of the rooms have provided observational data with which to further evaluate the response of the surrounding salt. Geologic mapping and core drilling in the E140 drift south of the waste shaft have provided information on the stratigraphy in the storage area.

12.3.2 Analysis and Evaluation

12.3.2.1 Storage Rooms

Analysis and evaluation of the storage room reference design have been performed using data collected from the test rooms. The adequacy of

The design was [illegible] behavior, including stress, strain and [illegible], which could be expected to occur over the operating life of each room. The operating life is defined as the period of time from initial excavation of the room until retrieval operations are completed, if the decision to retrieve is made, or until the storage operation for each panel is completed.

Evaluation of the geologic mapping and drill cores from the E140 drift south of the waste shaft has confirmed the continuity of the stratigraphy 50 feet above and below the storage area (refs. 4-1 and 4-2).

Based on an engineering approach (Chapter 5), numerical analyses were performed based on creep parameters determined from test room data and the stratigraphy surrounding the facility level. Because the extrapolation of the in situ closure data for the drifts and test rooms indicates that more than four rooms in a storage panel could influence the total closure and overall creep rate, a mathematical model was developed to estimate the upper bound responses. This requires assuming an infinite array of equally spaced storage rooms such that the centerline of a typical room and the centerline of any one of its pillars form axes of symmetry. In addition, the rooms were assumed to be infinitely long.

Figure 12-5 shows the finite element model that was used to determine the responses for an infinite array of infinitely long storage rooms. The model has 94 nodes and consists of 59 plane strain elements, with gap/friction link elements having a friction coefficient of 0.4 to model a clay seam. Because test room creep parameters are used in predicting the responses of the storage rooms, this model uses the same comparative element sizes and external loads as those used in the test room model described in Chapter 11, Section 11.3. The boundaries on both sides of the model were taken as vertical axes of symmetry to represent the pillar centerlines and consist of horizontal restraints.

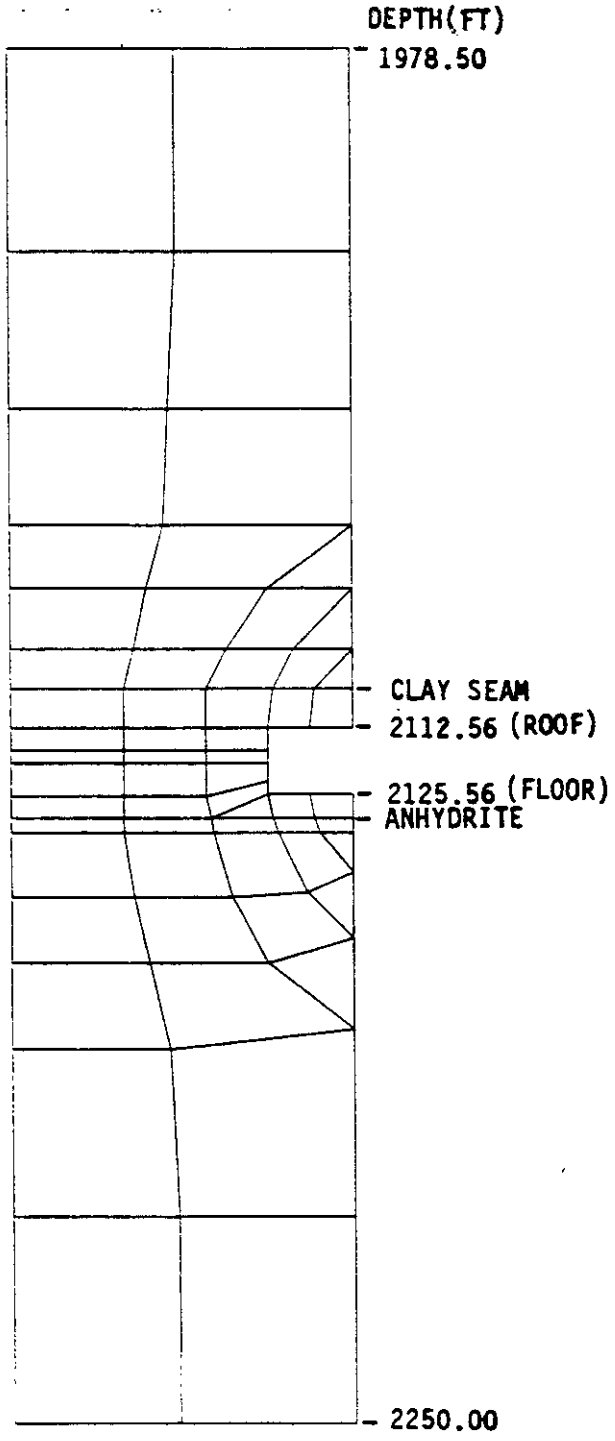

Figure 12-5

STORAGE AREA
ROOM FINITE ELEMENT MODEL

anhydrite bed, and the [illegible] room are based on the reference stratigraphy and are identical to those used in the test room finite element model.

The analyses were performed using the MARC General Purpose Finite Element Program discussed in Chapter 6. The average values of the creep parameters were derived from test room roof-to-floor and wall-to-wall in situ closure data. Using these computed creep parameters, previously presented in Chapter 11, Tables 11-10 and 11-11, the predicted future responses of the storage rooms were computed. The results of the analyses are presented below.

12.3.2.2 Storage Area Drifts

Analysis and evaluation of the 13 x 25-foot drift design for the storage area have been performed using data collected from the existing 8 x 25-foot drifts. The same finite element model used for the 8 x 25-foot drifts (Chapter 10) was used for the larger drifts. A removable floor section extending 5 feet vertically downward from the original floor level was integrated into the model so that this group of elements could be removed at the appropriate stage in the analysis to simulate floor excavation. A coefficient of friction of 0.0 was assumed for the gap/friction elements to model a clay seam. The time between initial excavation and the subsequent floor excavation was assumed to be 2 years. Therefore, all results presented in the following subsection are directly affected by these assumptions. Figure 12-6 shows the model after removal of the floor elements.

12.3.3 Prediction of Future Behavior

12.3.3.1 Storage Rooms

Because the room size and panel configuration of the four test rooms is similar to the design of the proposed storage rooms, the behavior of the storage rooms was computed using the measured data from the test rooms, as presented in Chapter 11. The results of the storage room

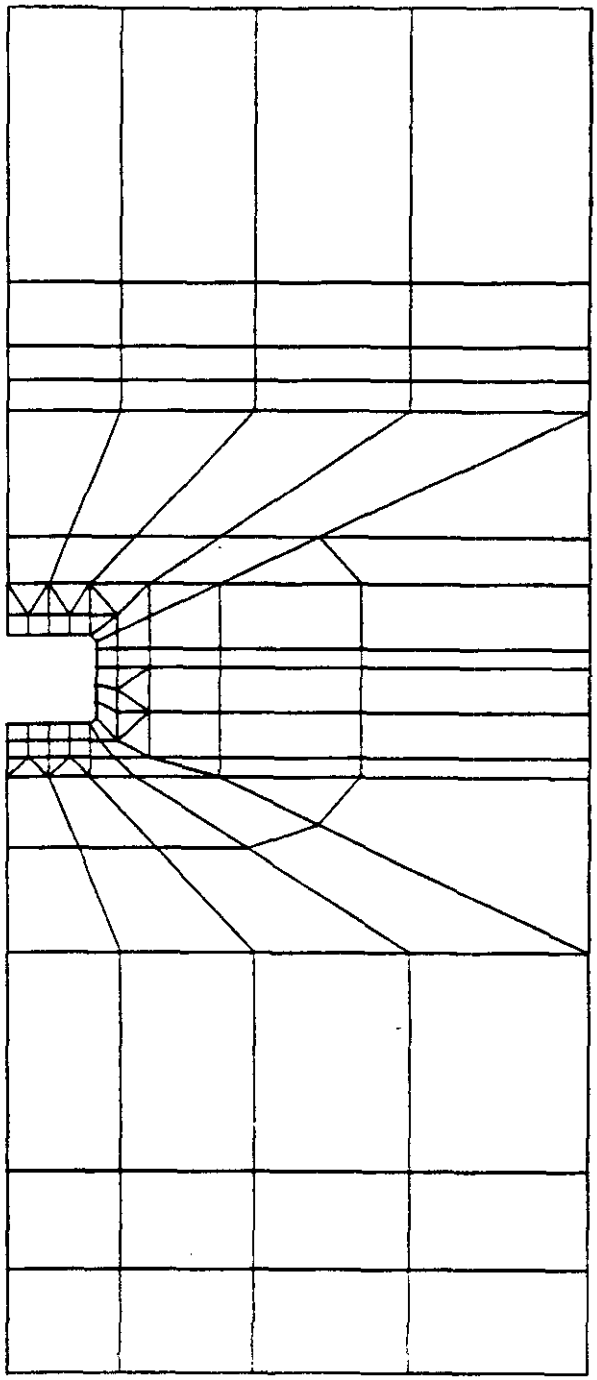

Figure 12-6

STORAGE AREA
DRIFT FINITE ELEMENT MODEL - AFTER FLOOR LOWERING

alysis [illegible] steps. These integration steps correspond to real times immediately after excavation, 1 year and 10 years after excavation. The horizontal and vertical stresses, effective stresses, effective creep strains, principal stresses and the deformed shapes were plotted at these times based on the mean value of the averaged wall-to-wall and roof-to-floor creep parameters presented in Tables 11-12 and 11-13 in Chapter 11. A closure calculation considering the effects at a room intersection was performed utilizing the values from these tables. Roof-to-floor and wall-to-wall closure predictions for the storage room were then plotted.

Horizontal and Vertical Stresses. The computed horizontal stress distributions in the storage rooms are plotted on selected elements of the finite element mesh immediately after excavation and at times of 1 year and 10 years after excavation (Figures 12-7 through 12-9). A contour interval of 250 ksf was chosen and 10 contour increments were used to span a stress range from 0 to 2,500 ksf compression.

Horizontal stresses immediately after excavation are totally compressive throughout the selected elements of the model. Most of the changes in horizontal stresses in the salt around the opening occur within the first year after excavation and remain practically constant even 10 years after excavation. The walls and the underlying anhydrite bed (MB-139), near the center of the room, have the largest compressive stresses, with values between 250 and 500 ksf compression. As the opening slowly deforms, horizontal stresses tend to become more compressive in the anhydrite bed near the room's vertical centerline. In the anhydrite bed far from the room centerline, the horizontal stresses are relatively low.

The vertical stress distribution was also plotted for time periods immediately after excavation and at times of 1 year and 10 years after excavation (Figures 12-10 through 12-12). The contour interval and stress range are the same as those used for the horizontal stress plots.

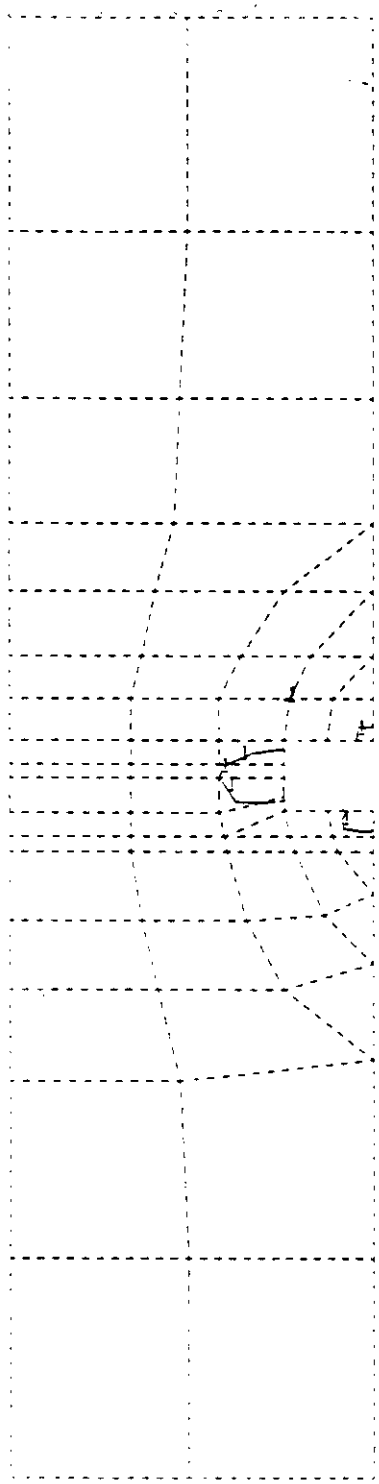

CONTOUR	σ_h(ksf)
1	250
2	500
3	750
4	1000
5	1250
6	1500
7	1750
8	2000
9	2250
10	2500

Figure 12-7

STORAGE ROOMS
HORIZONTAL STRESS DISTRIBUTION IMMEDIATELY AFTER EXCAVATION

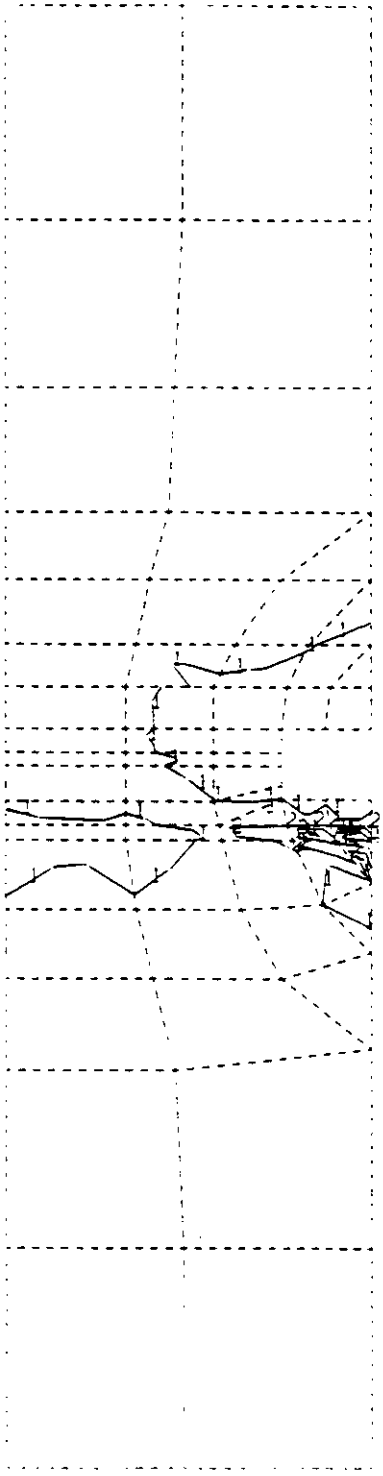

CONTOUR	σ_h(ksf)
1	250
2	500
3	750
4	1000
5	1250
6	1500
7	1750
8	2000
9	2250
10	2500

Figure 12-8

STORAGE ROOMS
HORIZONTAL STRESS DISTRIBUTION 1 YEAR AFTER EXCAVATION

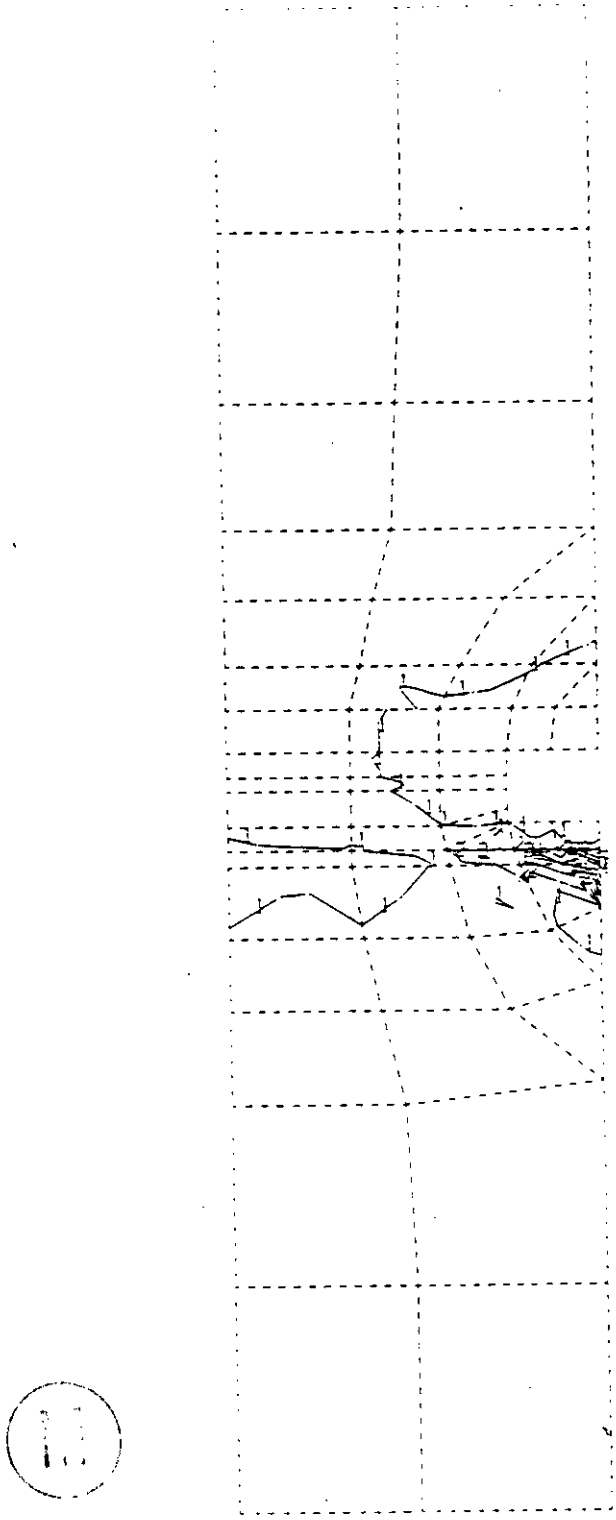

CONTOUR	σ_h(ksf)
1	250
2	500
3	750
4	1000
5	1250
6	1500
7	1750
8	2000
9	2250
10	2500

Figure 12-9

STORAGE ROOMS
HORIZONTAL STRESS DISTRIBUTION 10 YEARS AFTER EXCAVATION

[illegible] in the wall [illegible]
[illegible]ately after excavation of between 500 and 750 ksf com[illegible]
This stress is approximately twice the original lithostatic stress before excavation and clearly shows the expected stress concentrations around the opening immediately after excavation. As the opening deforms, the vertical stress is redistributed around the opening and reduced to between 250 and 500 ksf compression.

Figures 12-11 and 12-12 show very small differences from 1 year through 10 years after excavation. That is, the vertical stress is relatively constant throughout that period with most of the halite roof beam having low stress in the vertical direction. Likewise, the uppermost level of elements in the room's floor has relatively low stress in the vertical direction due to its lack of vertical confinement.

The anhydrite bed (MB-139) below the storage room is, in general, subjected to low vertical stresses; however, some compressive vertical stress is indicated under the pillars.

Effective Stresses and Effective Creep Strains. Figures 12-13 through 12-15 show the computed effective stress distribution in those elements of the finite element model near the room opening. Ten contour increments, each having an interval of 250 ksf, were chosen to span a stress range from 0 to 2,500 ksf. The effective stress plot immediately after excavation shows a relatively low stress concentration in the anhydrite bed below the floor and no stresses greater than 500 ksf in the halite beds.

At 1 year and 6.5 years after excavation, the computed effective stresses have increased and concentrated in the anhydrite bed and overlying halite. Because the anhydrite was modeled as being elastic until failure and stiffer than halite, it supports more stress, which results in a large effective stress gradient in the anhydrite. The maximum computed effective stress is 2,600 ksf, concentrated in the anhydrite bed near the room centerline.

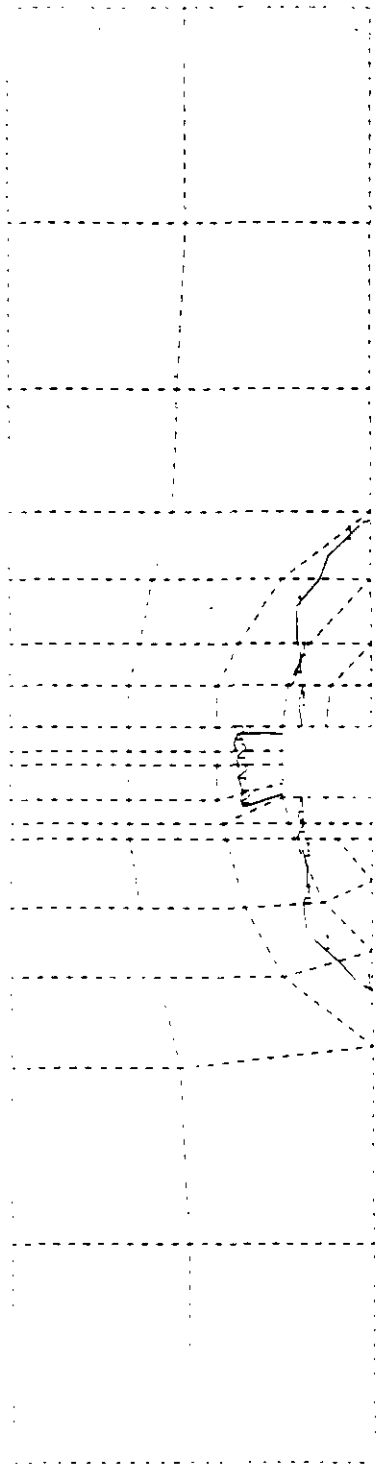

CONTOUR	σ_v (ksf)
1	250
2	500
3	750
4	1000
5	1250
6	1500
7	1750
8	2000
9	2250
10	2500

Figure 12-10

STORAGE ROOMS
VERTICAL STRESS DISTRIBUTION IMMEDIATELY AFTER EXCAVATION

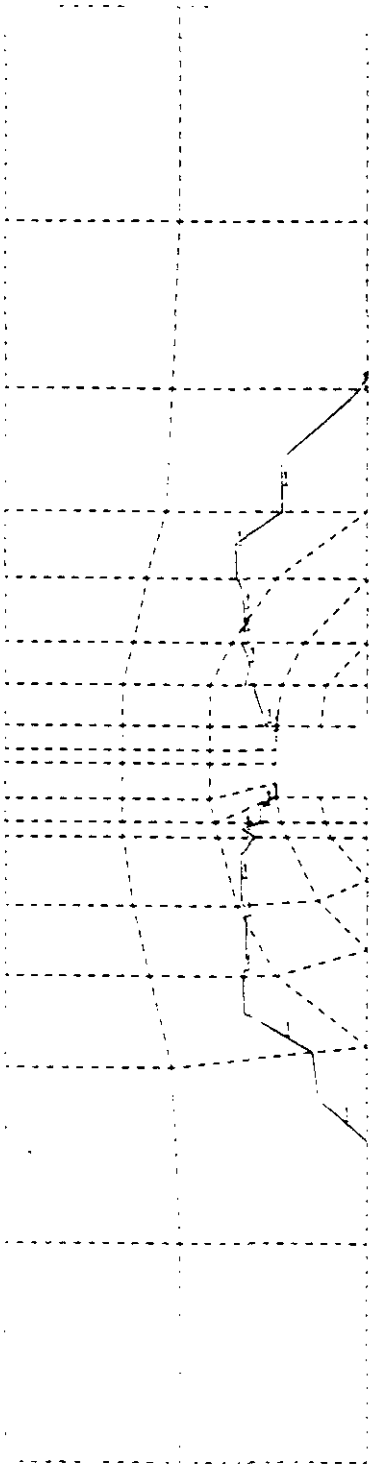

CONTOUR	σ_v(ksf)
1	250
2	500
3	750
4	1000
5	1250
6	1500
7	1750
8	2000
9	2250
10	2500

Figure 12-11

STORAGE ROOMS
VERTICAL STRESS DISTRIBUTION 1 YEAR AFTER EXCAVATION

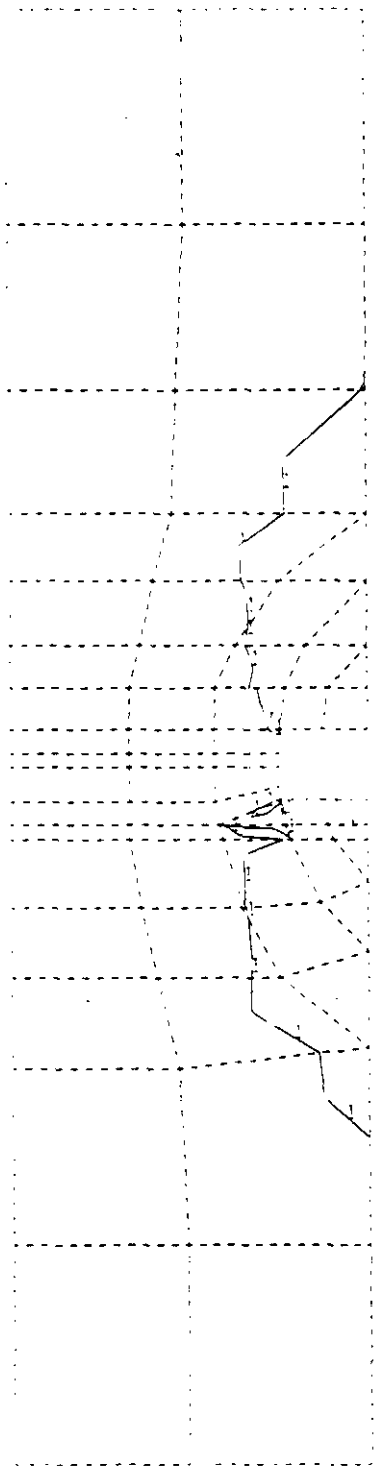

CONTOUR	σ_v(ksf)
1	250
2	500
3	750
4	1000
5	1250
6	1500
7	1750
8	2000
9	2250
10	2500

Figure 12-12

STORAGE ROOMS
VERTICAL STRESS DISTRIBUTION 10 YEARS AFTER EXCAVATION

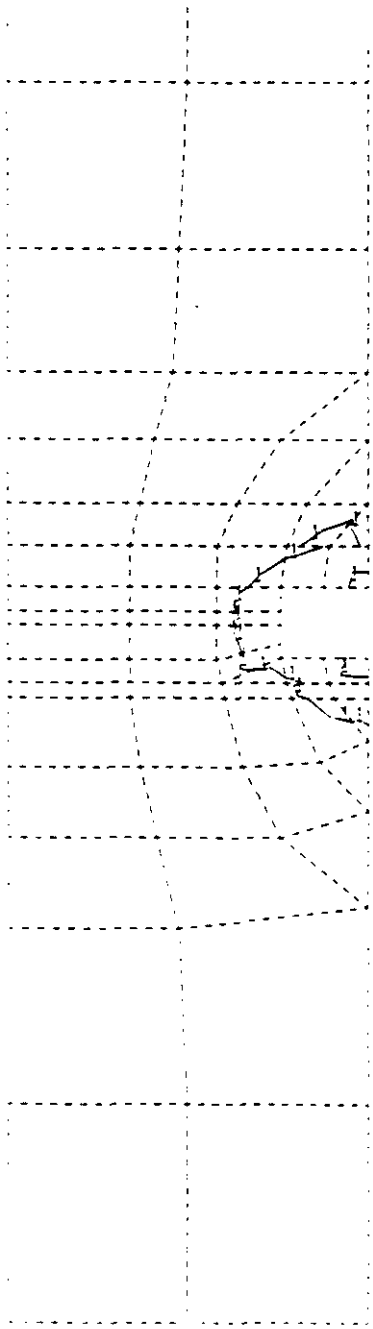

CONTOUR	$\overline{\sigma}$(ksf)
1	250
2	500
3	750
4	1000
5	1250
6	1500
7	1750
8	2000
9	2250
10	2500

Figure 12-13

STORAGE ROOMS
EFFECTIVE STRESS DISTRIBUTION IMMEDIATELY AFTER EXCAVATION

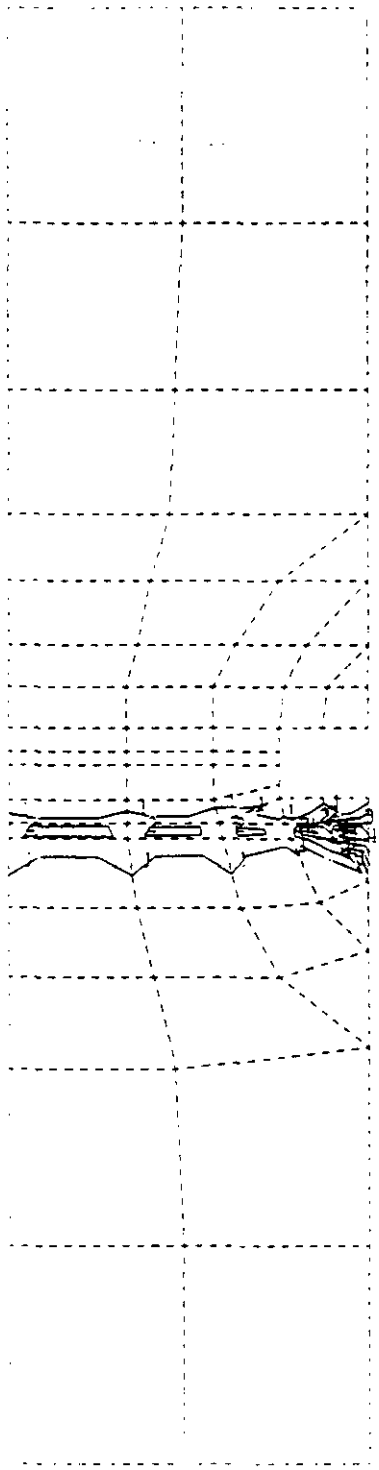

CONTOUR	$\bar{\sigma}$(ksf)
1	250
2	500
3	750
4	1000
5	1250
6	1500
7	1750
8	2000
9	2250
10	2500

Figure 12-14

STORAGE ROOMS
EFFECTIVE STRESS DISTRIBUTION 1 YEAR AFTER EXCAVATION

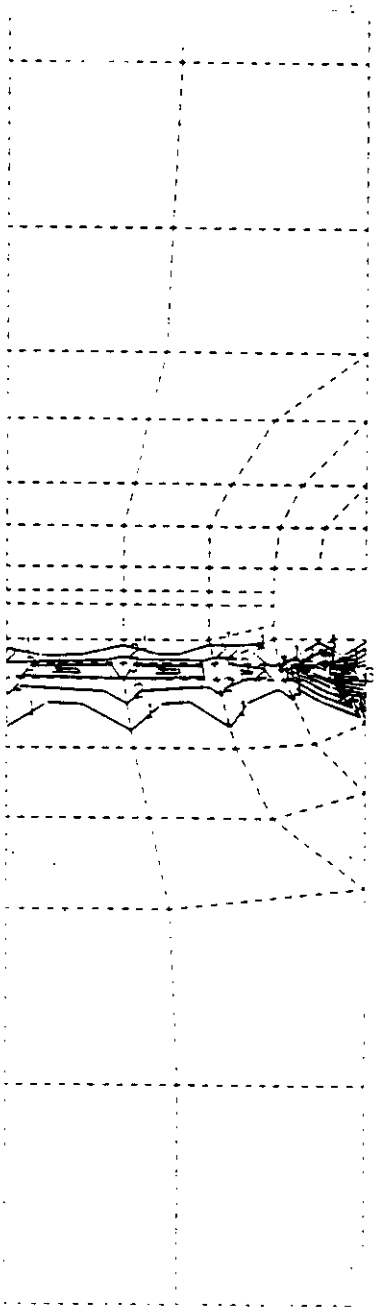

CONTOUR	$\bar{\sigma}$ (ksf)
1	250
2	500
3	750
4	1000
5	1250
6	1500
7	1750
8	2000
9	2250
10	2500

Figure 12-15

STORAGE ROOMS
EFFECTIVE STRESS DISTRIBUTION 10 YEARS AFTER EXCAVATION

Because the model does not include failure criteria for the anhydrite bed, an analysis for potential failure in this bed was performed separately. In Chapter 6, the failure criterion

$$\sqrt{J_2'} = 752 - 0.279J_1 \quad \text{(stress in ksf)} \tag{12-1}$$

was defined for the anhydrite bed based on laboratory tests. Rewriting this equation in terms of the effective stress at failure $\bar{\sigma}_f$ and the first stress invarient at failure $(J_1)_f$:

$$\bar{\sigma}_f(\text{ksf}) = 1302.5 - 0.483\,(J_1)_f \tag{12-2}$$

From the results of the numerical modeling, the average effective stress stress at a point close to the center of the room exceeds $\bar{\sigma}_f$ at about 8.5 years since excavation. This does not mean catastrophic failure will occur. Instead, there will be a redistribution of stress in the anhydrite bed which the model cannot consider.

Computed effective creep strain distributions were plotted on selected elements of the deformed mesh at 1 year and 6.5 years after excavation (Figures 12-16 and 12-17). Ten strain increments with an interval of 0.01 were used to span a strain range from 0 to 0.100.

At 1 year after excavation, effective creep strains have concentrated in the region around the room opening. At 6.5 years after excavation, the effective creep strains have further intensified around the room opening and in the region above the anhydrite bed near the room centerline.

Based on laboratory creep tests on samples of halite, a failure criterion has been proposed (equation 6-5 in Chapter 6). Based on this criterion, the failure effective strain for halite is a function of the mean normal stress intensity and reaches a maximum magnitude of nearly 16 percent at a mean stress intensity of 125 ksf.

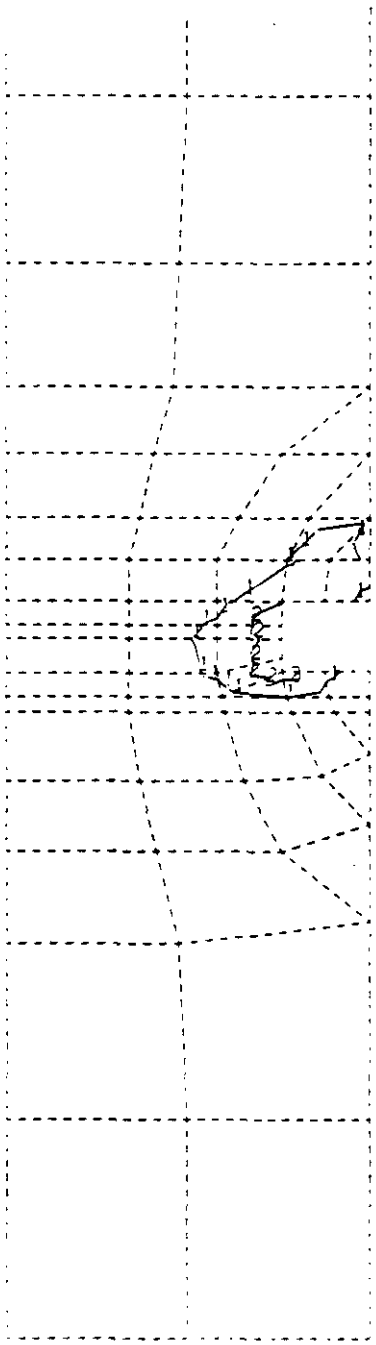

CONTOUR	$\bar{\epsilon}$
1	0.01
2	0.02
3	0.03
4	0.04
5	0.05
6	0.06
7	0.07
8	0.08
9	0.09
10	0.10

Figure 12-16

STORAGE ROOMS
EFFECTIVE CREEP STRAIN DISTRIBUTION 1 YEAR AFTER EXCAVATION

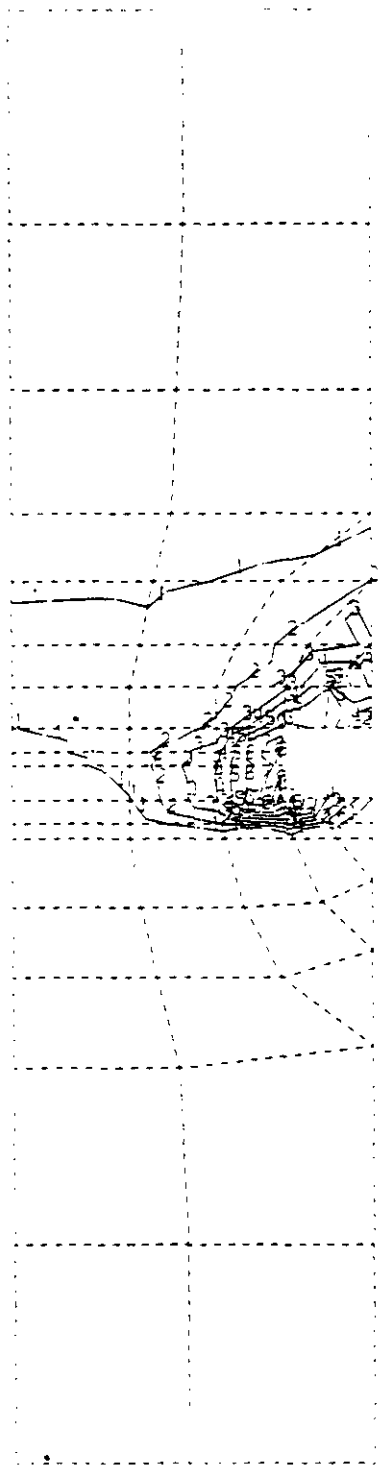

CONTOUR	$\bar{\epsilon}$
1	0.01
2	0.02
3	0.03
4	0.04
5	0.05
6	0.06
7	0.07
8	0.08
9	0.09
10	0.10

Figure 12-17

STORAGE ROOMS
EFFECTIVE CREEP STRAIN DISTRIBUTION 10 YEARS AFTER EXCAVATION

creep strain ...

..., and by linear extrapolation beyond 6.5 years, failure will be initiated in the halite about 12 years after the completion of excavation. The failure will be initiated at floor and wall intersections.

However, the numerical modeling also shows that effective strain decreases rapidly with distance away from the opening. Thus, the failure is expected to be confined very close to the opening. This will require periodic scaling and trimming.

Principal Stresses. The computed principal stresses on the plane of a section across the storage rooms are presented in a qualitative manner on Figures 12-18 through 12-20. The magnitudes of the two principal stresses are proportional to the lengths of the corresponding lines which are plotted, perpendicular to each other, at the centroid of each of the elements.

Immediately after excavation, the magnitudes of the principal stresses are relatively large in the corners of the room and in the anhydrite bed. As the room opening deforms, the principal stresses concentrate in the anhydrite bed near the room centerline.

The plots of the principal stresses also show the stress arch which forms around the room due to the transfer of loads around the room opening. The stress arch tends to become enlarged with time and migrates away from the room.

Deformation and Closure. Figures 12-18 through 12-20 also show the predicted deformed shapes of a typical storage room at different times. The dashed lines represent the outline of the deformed shape of the storage room.

Immediately after excavation, deformation starts around the opening. After 1 year of creep, the halite roof beam deforms noticeably at its

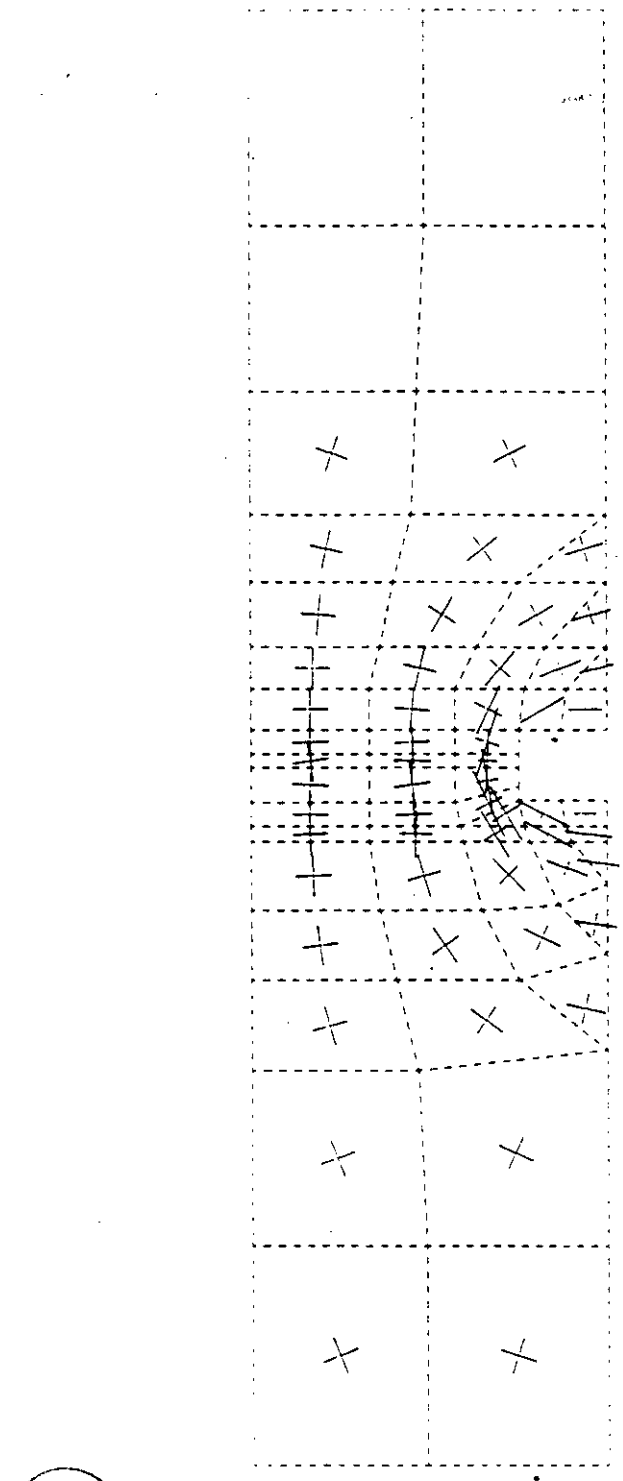

M

Figure 12-18

STORAGE ROOMS
PRINCIPAL STRESSES AND DEFORMED SHAPE
IMMEDIATELY AFTER EXCAVATION

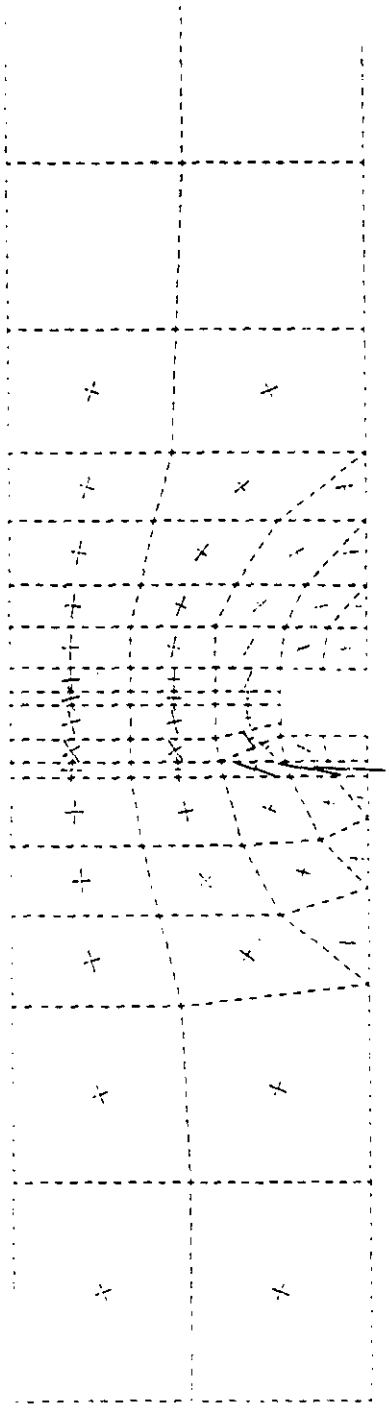

Figure 12-19

STORAGE ROOMS
PRINCIPAL STRESSES AND DEFORMED SHAPE
1 YEAR AFTER EXCAVATION

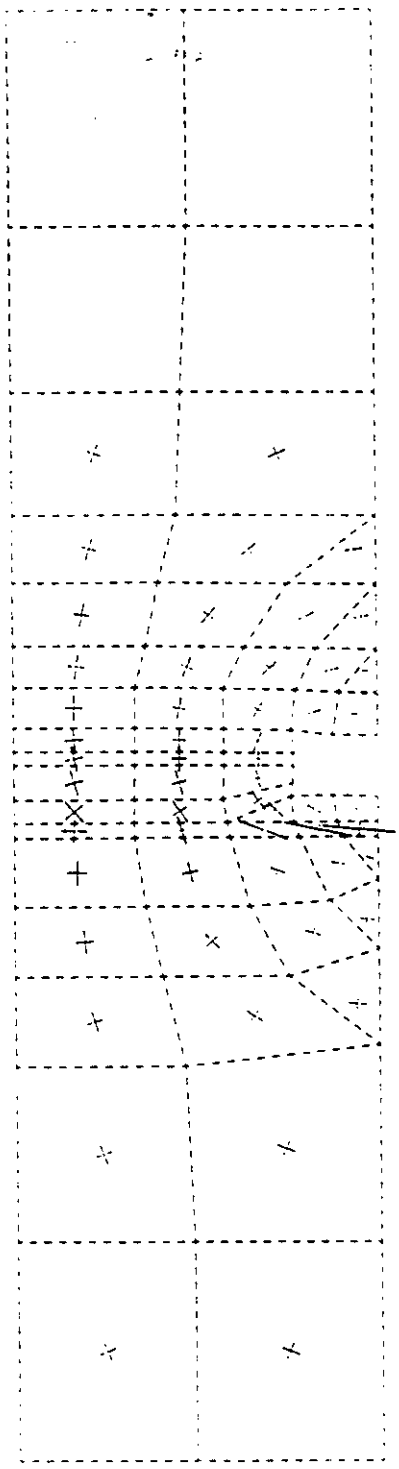

Figure 12-20

STORAGE ROOMS
PRINCIPAL STRESSES AND DEFORMED SHAPE
10 YEARS AFTER EXCAVATION

the predicted all [illegible] However, the floor heave is still very small [illegible], some slippage has occurred along the clay seams. This is graphically depicted as a slight horizontal disjointing of the lines that form the element boundaries along a clay seam.

At 6.5 years after excavation, the predicted deformed shape of the storage room shows much downward deformation in the roof beam at its centerline. The floor has heaved slightly upward, with the upward displacement being somewhat more noticeable in the center of the room. The analysis shows very little deformation in the anhydrite bed even after 10 years. Based on the small amount of floor heave, it appears that the stiff anhydrite bed diminishes the amount of floor creep by supporting a large amount of lateral pressure. However, because there is a potential for the anhydrite bed to fail locally at about 8.5 years after excavation, it may not be able to support this large amount of lateral pressure. This may result in a higher creep rate in the floor than predicted by the model.

As discussed in Chapter 11, laboratory derived creep constants underpredicted actual closure in the test rooms. Thus, back calculation of average creep parameters was made using either measured roof-to-floor or wall-to-wall closure data. The effectiveness of the model simulation techniques used to derive the creep parameters and extrapolate closure behavior were discussed in detail in Chapter 11, subsection 11.3.2.5. Because MB-139 was assumed to be linearly elastic with infinite strength, the numerical modeling underpredicted floor heave but overpredicted roof sag. However, the overall roof-to-floor closure is reasonably well predicted by the model.

In order to show the effect of geometry and extraction on the closure rate, extrapolations of the in situ closure histories for the test rooms and various size drifts, as well as the calculated roof-to-floor and wall-to-wall closures for the storage rooms were plotted for comparison (Figures 12-21 and 12-22). Similar calculations were made using the

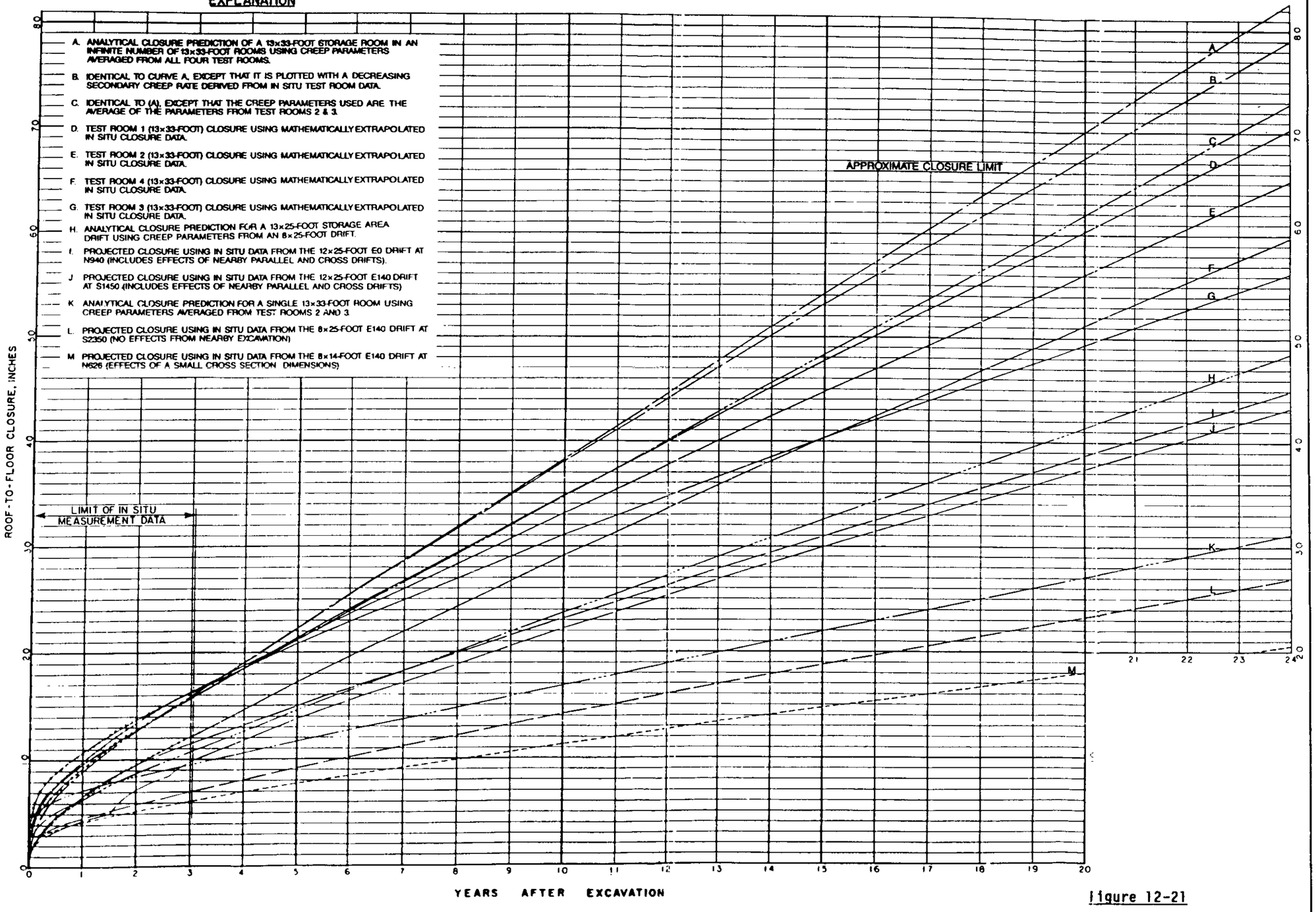

Figure 12-21

ROOF-TO-FLOOR CLOSURE
GEOMETRY AND EXCAVATION EFFECTS

EXPLANATION

A. ANALYTICAL CLOSURE PREDICTION OF A 13×33-FOOT STORAGE ROOM IN AN INFINITE NUMBER OF 13×33-FOOT ROOMS USING CREEP PARAMETERS *AVERAGED FROM ALL FOUR TEST ROOMS.*

B. IDENTICAL TO CURVE A, EXCEPT THAT IT IS PLOTTED WITH A DECREASING SECONDARY CREEP RATE DERIVED FROM IN SITU TEST ROOM DATA.

D. TEST ROOM 1 (13×33-FOOT) CLOSURE USING MATHEMATICALLY EXTRAPOLATED IN SITU CLOSURE DATA.

E. TEST ROOM 2 (13×33-FOOT) CLOSURE USING MATHEMATICALLY EXTRAPOLATED IN SITU CLOSURE DATA.

F. TEST ROOM 4 (13×33-FOOT) CLOSURE USING MATHEMATICALLY EXTRAPOLATED IN SITU CLOSURE DATA.

G. TEST ROOM 3 (13×33-FOOT) CLOSURE USING MATHEMATICALLY EXTRAPOLATED IN SITU CLOSURE DATA.

I. PROJECTED CLOSURE USING IN SITU DATA FROM THE 12×25-FOOT EO DRIFT AT N940 (INCLUDES EFFECTS OF NEARBY PARALLEL AND CROSS DRIFTS).

J. PROJECTED CLOSURE USING IN SITU DATA FROM THE 12×25-FOOT E140 DRIFT AT S1450 (INCLUDES EFFECTS OF NEARBY PARALLEL AND CROSS DRIFTS).

L. PROJECTED CLOSURE USING IN SITU DATA FROM THE 8×25-FOOT E140 DRIFT AT S2350 (NO EFFECTS FROM NEARBY EXCAVATION).

M. PROJECTED CLOSURE USING IN SITU DATA FROM THE 8×14-FOOT E140 DRIFT AT N626 (EFFECTS OF A SMALL CROSS SECTION DIMENSIONS).

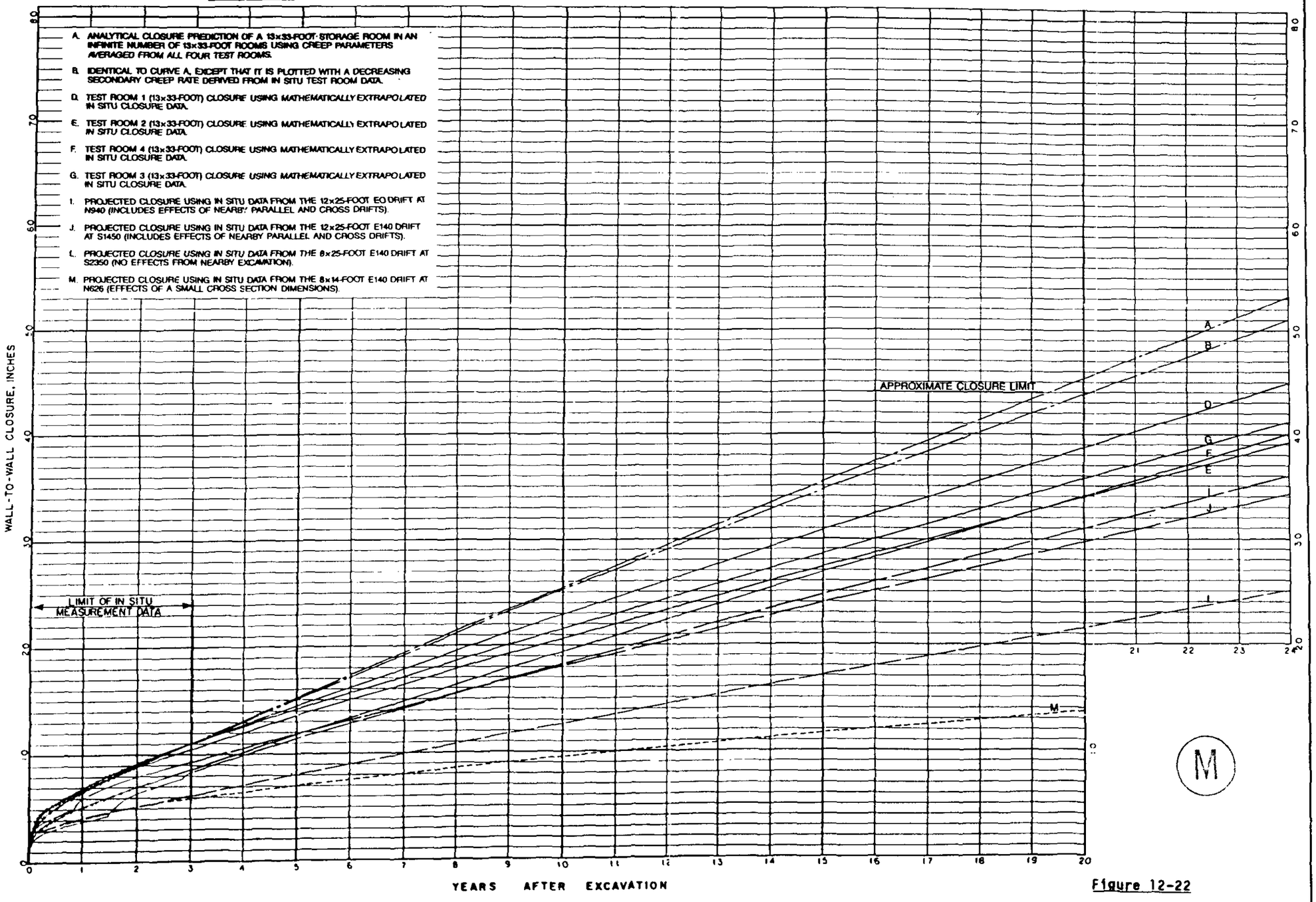

Figure 12-22

WALL-TO-WALL CLOSURE
GEOMETRY AND EXCAVATION EFFECTS

average creep parameters for the two interior 13 x 33-foot test rooms and using an infinite array of rooms to indicate the sensitivity of the value of the parameters. The same parameters were also used in the calculations of a single 13 x 33-foot room model to determine the effects of extraction on the number of rooms in an array. The descriptions of the closure curves plotted on Figures 12-21 and 12-22 are as follows:

(A) Analytical closure prediction of a 13 x 33-foot storage room in an infinite number of 13 x 33-foot rooms using creep parameters averaged from all four test rooms.

(B) Identical to curve A, except that it is plotted with a decreasing secondary creep rate derived from in situ test room data.

(C) Identical to curve A, except that the creep parameters used are the average of the constants from Test Rooms 2 and 3.

(D) Test Room 1 closure using mathematically extrapolated in situ closure data.

(E) Test Room 2 closure using mathematically extrapolated in situ closure data.

(F) Test Room 4 closure using mathematically extrapolated in situ closure data.

(G) Test Room 3 closure using mathematically extrapolated in situ closure data.

(H) Analytical closure predicted for a 13 x 25-foot storage area drift using creep parameters from an 8 x 25-foot drift.

(I) Projected closure using in situ data from the 25 x 25-foot E0 drift at N940 (includes effects of nearby parallel and cross drifts).

(J) Projected closure using in situ data from the 12 x 25-foot E140 drift at S1450 (includes effects of nearby parallel and cross drifts).

(K) Analytical closure prediction for a single 13 x 33-foot room using creep parameters averaged from Test Rooms 2 and 3.

(L) Projected closure using in situ data from the 8 x 25-foot E140 drift at S2350 (no effects from nearby excavation).

(M) Projected closure using in situ data from the 8 x 14-foot E140 drift at N626 (effects of small cross section dimensions).

As expected, the two interior test rooms (Test Rooms 2 and 3) had more closure and higher closure rates during the first year than the outer rooms (Test Rooms 1 and 4). This is due to the fact that Test Rooms 2 and 3 were excavated before Test Rooms 1 and 4. However, Test Rooms 1 and 4 exhibit higher closure rates during the secondary creep stage. This is consistent with the stress arch principle.

An evaluation of these 13 closure curves indicates that geometry and extraction ratio strongly impact the total closure in a seven-room panel within an eight-panel storage area and that the rate of closure will be faster than the extrapolated curves for a test room within the four-room test panel. For conservatism, Curve A (Figures 12-21 and 12-22) is used for storage room analysis, prediction and validation.

Curve A on Figure 12-21 represents the roof-to-floor closure prediction using the average creep parameter values for Test Rooms 1 through 4. These values were previously presented in Chapter 11, Table 11-12. In

the first year following excavation, the roof-to-floor closure curve is non-linear. The primary creep closure rate is very fast, as shown by the steeply sloped region in the first 3 months. Two and one half inches were added to the measured closure values to compensate for the lack of early closure data (Chapter 11). During secondary creep, the curve flattens and becomes approximately linear with a closure rate of approximately 3 inches per year. This closure prediction shows a closure of approximately 22 inches at 5 years after excavation and 54 inches at 15 years after excavation.

Curve A on Figure 12-22 represents the wall-to-wall closure prediction using the average creep parameter values for Test Rooms 1 through 4. These values were previously presented in Chapter 11, Table 11-13. As with the roof-to-floor closure, the wall-to-wall closure is non-linear in the first year following excavation. Again, the closure rate due to primary creep is initially very fast in the first 3 months as shown by the steep slope of the curve. Two inches were added to the measured closure values, as discussed in Chapter 11, to compensate for the lack of early closure data. The curve eventually flattens during the secondary creep phase and becomes approximately linear with a closure rate of about 2 inches per year. The wall-to-wall closure prediction shows a closure of approximately 15 inches at 5 years after excavation and 36 inches at 15 years after excavation.

When the storage rooms are fully occupied by waste and backfill material, the closure of the room will be limited by the ability of the contents to be compacted. Assuming that the volume of the waste container can be compacted by 40 percent and the volume of the backfill material by 15 percent, the roof-to-floor closure is predicted to have a maximum value of 66 inches and the wall-to-wall closure a maximum value of 44 inches. This maximum closure would occur after about 18 years for vertical closure and 19 years for horizontal closure (Figures 12-21 and 12-22). A reduction in the closure rate after the wall and roof surfaces begin compacting the backfill material and exerting pressure on the waste containers has not been considered.

Curve A ... conservative estimates of storage room closure. Therefore, values from these curves were used in evaluating the reference design against the design criteria and design bases requirements. The design bases allow up to 12 inches of closure in the first 5 years after excavation in order to maintain a 16-inch space for ventilation and backfill equipment and to maintain a 12-foot minimum clearance for storage equipment. The estimated vertical closure in 5 years using curve A is about 22 inches. This 10 inch increase over the design basis limit could be accommodated by increasing the reference design room height from 13 feet to 13 feet 10 inches. This would be satisfactory for permanent storage. Another way to accommodate the increased closure and still maintain the 16-inch ventilation space (Figure 12-3) is to eliminate the backfill or reduce its thickness covering the CH containers to 6 inches or less. Deleting the salt backfill would require a change in the design criteria.

The solution to the increased vertical closure is not so simple for permanent storage, however. If at the end of the 5-year demonstration period, a decision is made requiring the stored waste to be retrieved, the design criteria assume that it will take twice as long to retrieve waste as it took to store it. This would result in a room being an additional 10 years old before retrieval is completed. Under these circumstances, a 15-year old room would have a closure of 54 inches, based on Curve A. Assuming that a storage room was excavated to the maximum allowable height of 14 feet, the closure would be 14 inches more than could be accommodated (24 inches for closure allowance, including 12 inches allowed by the design basis and 12 inches for the increase in room height from 13 feet to 14 feet, and 16 inches for ventilation space). This would result in the backfill being compressed and in the possible crushing and breaching of the waste containers. Because this scenario does not comply with the design criteria requirements, other alternatives must be considered.

These alternatives, including modification of the design criteria, are presented in subsection 12.6.2. Two considerations must be addressed here, however, to support the recommendations. First, the 10 year maximum retrieval period assumed by the design criteria is very conservative. Should retrieval be conducted on a three shifts per day basis, rather than the assumed one shift per day, no room would be older than 7 years by the time its waste was retrieved. Based on Curve A, a 7 year old room, from the time of initial excavation, would have a closure of about 28 inches. Assuming a room was excavated to the 14-foot high maximum and allowing 24 inches for closure, the waste containers will not be crushed or breached. However, the ventilation space will be reduced to 12 inches. This could be tolerated because the maximum 28-inch closure will be at the room centerline; additional ventilation space will be gained closer to the room walls. Alternatively, the thickness of the salt backfill over the containers could be reduced or eliminated to maintain the ventilation.

The second consideration supporting the recommendations is that a reduction in room closure can be gained by modifying the excavation technique. A panel of rooms could be excavated to the reference design dimension of 13 to 14 feet high. After a year of closure, these openings will be closing at the rate determined by secondary creep. At this time the rooms could be trimmed to 14 feet high. Trimming will remove the salt that has moved into the room during the year and provide a full dimensioned room that will close at the rate determined by secondary creep. Based on an average secondary creep closure rate of 3 inches per year, the rooms would have the following predicted closures after trimming:

5 years	15 inches
7 years	21 inches
10 years	30 inches
15 years	45 inches

Should the retrieval be effected within 7 years after trimming, a

would meet all of the retrieval requirements without further modification.

In order to gain the reduced closure benefits of secondary creep, the amount of trimming must be kept to a minimum. The rooms should initially be excavated as close to the 14-foot high maximum dimension as possible. The trimming operation a year later should remove no more salt from the floor than necessary to enlarge the room height to 14 feet. This small amount of trimming will minimize the increase in closure that typically follows major re-excavation, as has already been experienced at the WIPP during floor lowering in some drifts (Chapter 10, Figure 10-6, and this chapter, Figure 12-21, Curve J). This is discussed in detail in the next subsection.

The width of the storage rooms presents similar problems. The reference design specifies a minimum room width of 33 feet and a maximum width of 34 feet. Again, Curve A on Figure 12-22 represents the most conservative estimate of horizontal closure. The design basis allows 9 inches of horizontal closure in the first 5 years (4 1/2 inches for each wall). The space between the wall and the waste containers (Item 10, Figure 12-3), for the storage area reference design, will be backfilled with loose salt.

The predicted wall-to-wall closure in 5 years, using Curve A, is about 15 inches. This closure will result in compaction of the salt backfill and possibly in the crushing and breaching of some containers. This condition is suitable for permanent storage. Should retrieval be required, the predicted closure for a 15-year old room would be 36 inches. If it is assumed that the room is excavated to its maximum dimensions, as discussed earlier, the room would be 34 feet wide with the waste containers 15 inches from each wall. This 30 inches of horizontal clearance is not adequate to meet the design criteria requirements for the crushing and breaching of containers, even if backfill were not required. In order to meet the intent of the design criteria, the reference design must be modified. The five alternatives presented in subsection 12.6.2 include modifications to accommodate this horizontal closure.

As is the case with vertical closure in the storage rooms, timing of retrieval operations and two-stage excavation can be used to reduce the wall-to-wall closure. Should three shifts per day be used during retrieval and if the rooms are a maximum of 7 years old, then wall-to-wall closure would be about 20 inches. If the storage operation is conducted on a first emplaced/first retrieved basis and retrieval is effected before a room exceeds an age of 6 years, horizontal closure would be further reduced to 18 inches. Both of these operational changes would decrease the possiblity of crushing or breaching the waste containers.

Two-stage excavation gains additional closure benefits. If a room is initially excavated to the maximum design width of 34 feet and after a year of closure trimmed to 34 feet, closure would be controlled by secondary creep. Based on a wall-to-wall secondary creep closure rate of 2 inches per year, the rooms would have the following predicted closures after trimming:

5 years	10 inches
7 years	14 inches
10 years	20 inches
15 years	30 inches

This will further minimize crushing or breaching of the waste containers.

It is expected that increasing the distance between the waste canisters and the wall by increasing the room to the maximum design width of 34 feet, thereby increasing the amount of loose salt backfill in this space, will increase the time it takes for horizontal closure to consolidate the backfill and transfer sufficient load to crush the waste canisters. This, coupled with the faster retrieval schedules discussed previously and the fact that the backfill will not be completely confined, will minimize crushing and breaching of the canisters as required by the criteria. How much it will be minimized

from in situ ... consoldiation and container stability become available.

12.3.3.2 Storage Area Drifts

The results of the analysis of the storage area drifts with dimensions of 8 x 25 feet were plotted at various integration time steps. These integration steps correspond to real times immediately after floor lowering and 5 years after initial excavation. The effective stress and effective creep strain, principal stresses, and deformed shape were plotted at these times based on the roof-to-floor creep parameters for a representative station (Chapter 10).

Effective Stresses and Effective Creep Strains. Figures 12-23 and 12-24 show the calculation for effective stress distribution in those elements of the finite element model near the drift opening. As with similar plots for the 8 x 25-foot drifts discussed in Chapter 10, each contour increment represents an effective stress interval of 100 ksf.

The plot of effective stress immediately after floor lowering shows the impact on the stress distribution as a result of the drift height modification. This change in effective stress precipitates a concomitant increase in the creep rate. This appears as a sharp but short increase in slope on the roof-to-floor closure versus time curve (Chapter 10, Figure 10-6, and this chapter, Figure 12-21, Curve J).

At the end of 5 years, the anhydrite bed shows a very large effective stress gradient from top to bottom in the vicinity of the drift floor due to the stiffness of the bed. Maximum effective stresses are in excess of 1,000 ksf.

The effective creep strains have concentrated in the region around the drift opening and intensify with time. A rough linear extrapolation of effective creep strain beyond 5 years indicates that the maximum

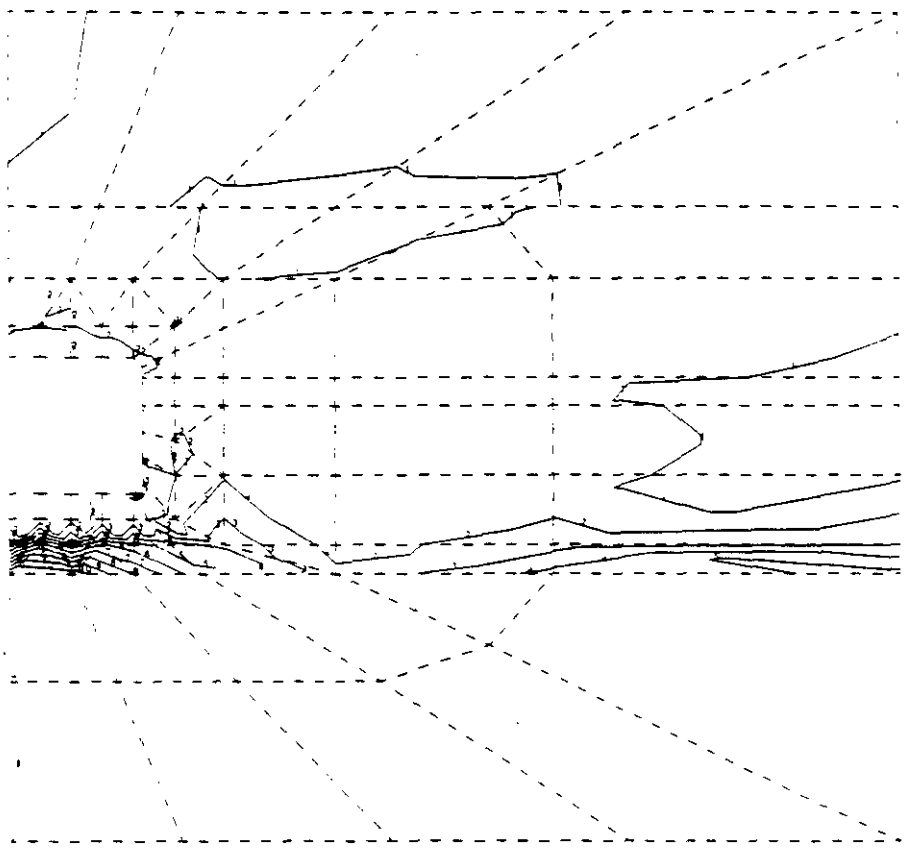

CONTOUR	$\bar{\sigma}$(ksf)
1	100
2	200
3	300
4	400
5	500
6	600
7	700
8	800
9	900
10	1000

Figure 12-23

STORAGE AREA DRIFTS
EFFECTIVE STRESS DISTRIBUTION IMMEDIATELY AFTER FLOOR LOWERING

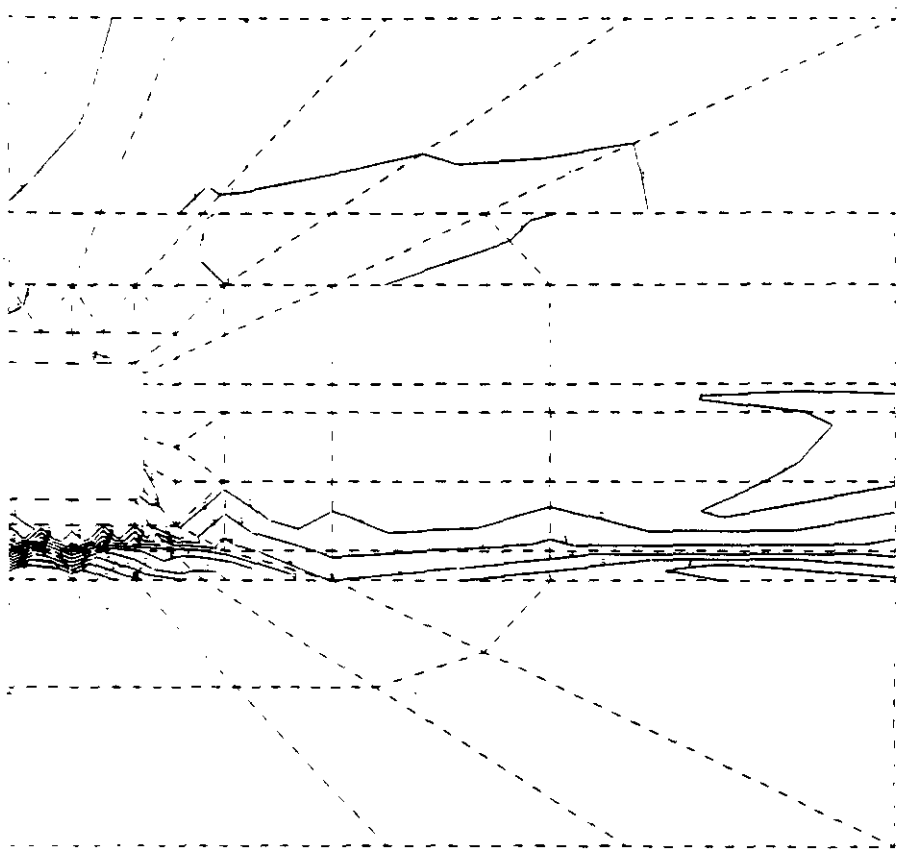

CONTOUR	$\bar{\sigma}$(ksf)
1	100
2	200
3	300
4	400
5	500
6	600
7	700
8	800
9	900
10	1000

Figure 12-24

STORAGE AREA DRIFTS
EFFECTIVE STRESS DISTRIBUTION 5 YEARS AFTER EXCAVATION

average effective creep strain may reach 16 percent at about 20 years after excavation. Based on failure criteria for halite obtained from laboratory test data (Chapter 6), failure in halite may start at about 15 percent. However, the numerical modeling indicates that the effective creep strain drops off sharply away from the opening. It is therefore expected that high effective strain would not result in a large scale failure in halite.

Principal Stresses. The plots of principal stresses (Figures 12-25 and 12-26) consistently show the "arch" pattern which develops around the drift in order to transfer loads past the drift opening. The arch is shown to migrate away from the opening with time. As expected, the magnitude of major principal stress is greater in the corners of the drift and in the underlying anhydrite bed. The anhydrite in particular is subjected to large stresses because it is the only material that has been assumed in the model to not creep; it therefore "stores" a large amount of energy in the form of elastic strain.

Deformation and Closure. Figure 12-27 shows the deformed shape 5 years after drift excavation, or approximately 3 years after floor lowering. It should be noted that, while both the roof and walls are creeping inward, the upward floor heave is small by comparison. This phenomenon is due to the stiffening effect of the underlying anhydrite bed.

The stress redistribution that occurs as a result of modifying the drift height is the driving force behind the large roof and wall deflections that are the most prominent features of the plot at 5 years. A close examination of the 5-year deformed plot shows that clay seam slippage has occurred. The most noticeable slippage has occurred in the clay seam located about 8 feet above the existing roof. Here, the maximum horizontal relative displacement across the seam is approximately 3 1/2 inches. Actual relative displacement will be lower because the clay seams have a finite friction coefficient.

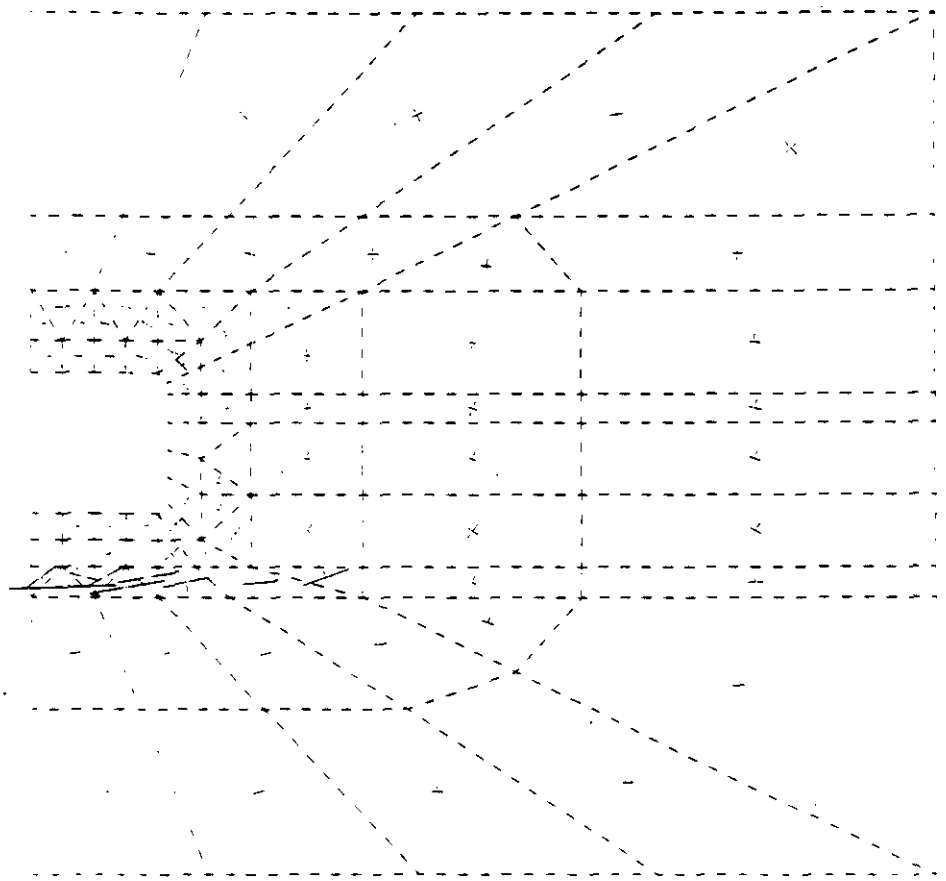

Figure 12-25

STORAGE AREA DRIFTS
PRINCIPAL STRESSES IMMEDIATELY AFTER EXCAVATION

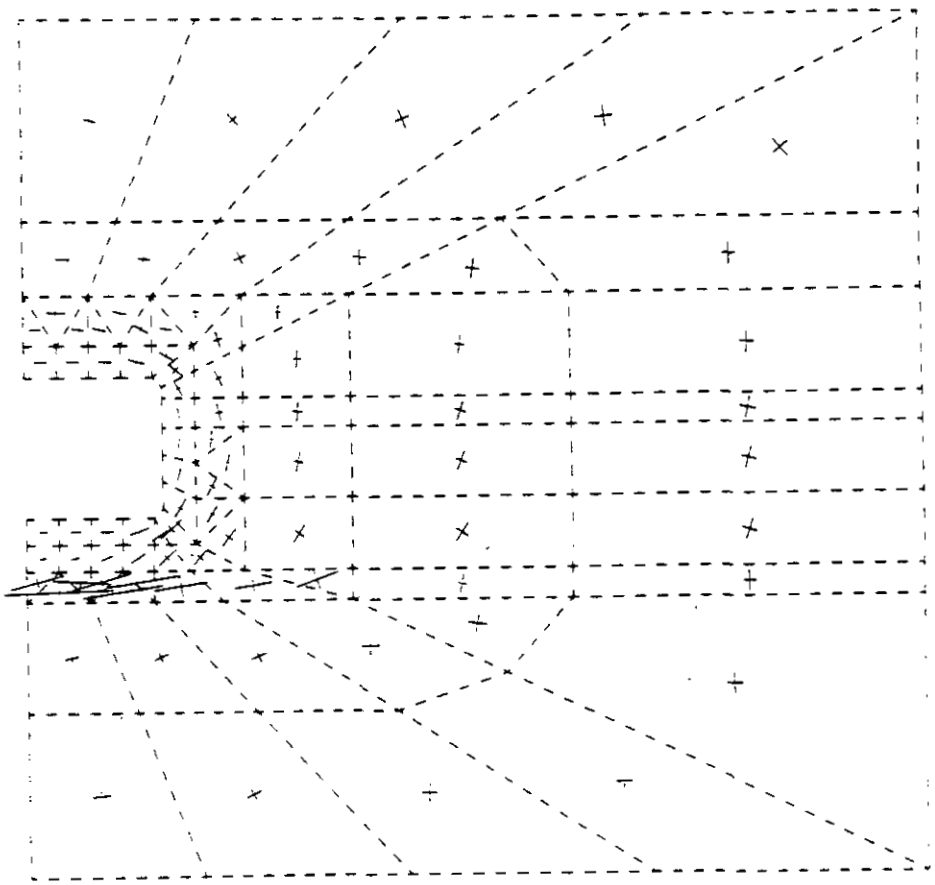

Figure 12-26

STORAGE AREA DRIFTS
PRINCIPAL STRESSES 5 YEARS AFTER EXCAVATION

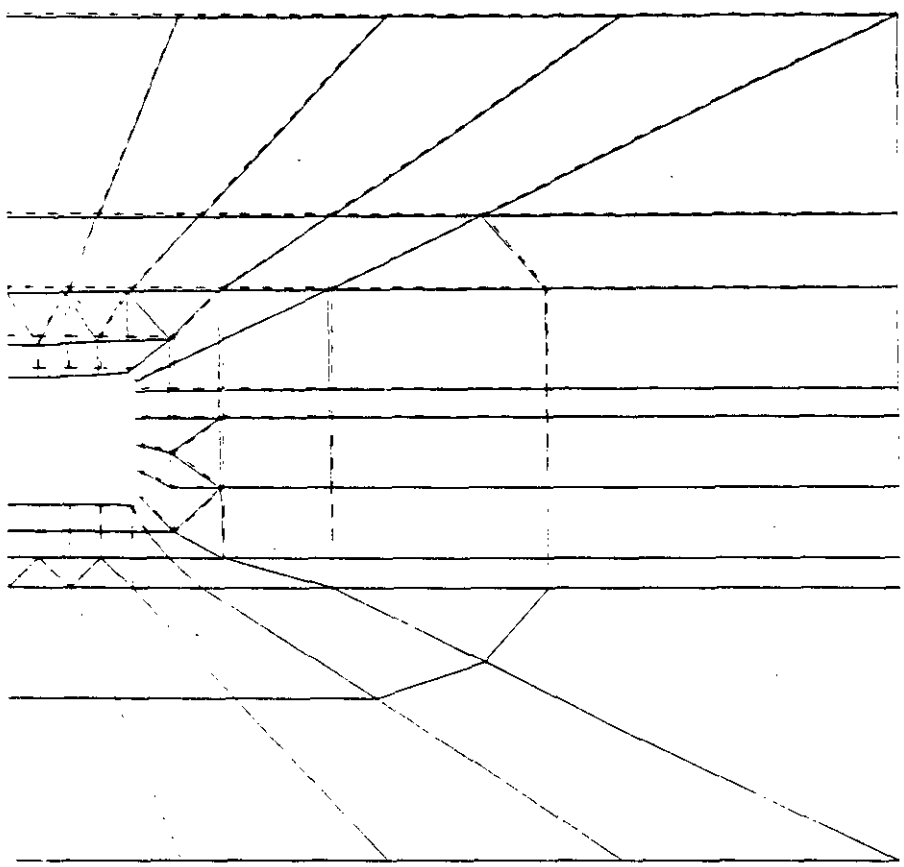

Figure 12-27

STORAGE AREA DRIFTS
DEFORMED SHAPE 5 YEARS AFTER EXCAVATION

Figure 12-28 demonstrates the effect of increasing the vertical dimension of a storage area drift at some point after initial excavation. The finite element model is calibrated with in situ data. It models an 8 x 25-foot drift that has its height increased to 13 feet by excavating an additional 5 feet from the floor. The 8 x 25-foot drift exhibits typical closure; that is, the curve shows high rate of closure during primary creep and a nearly constant closure rate during secondary creep. When the floor is lowered (in this case 2.3 years after excavation), primary creep is temporarily reinitiated. The secondary creep phase is eventually re-established, but with some difference. The slope of the curve during secondary creep after floor lowering is slightly steeper than the secondary creep prior to floor lowering. The rate of closure does not return to the initial rate, but rather reflects the new, larger dimension of the drift. In this model, the modified drift has 11 inches of vertical closure 5 years after initial excavation.

The same computation included wall-to-wall closure. The effects of floor lowering were the same as for roof-to-floor closure. After floor lowering, primary creep was reinitiated and followed by a new secondary creep phase with a slightly higher closure rate. Five years after initial excavation, the predicted horizontal closure is about 8 inches.

A rough extrapolation of the predicted roof-to-floor and wall-to-wall closures based on model simulation and resulting secondary creep closure indicates the following:

Time (Years)	Roof-to-Floor Closure at 2.0 inches/year (inches)	Wall-to-Wall Closure at 1.6 inches/year (inches)
10	20	16
15	30	24
20	40	32
25	50	40

The maximum effective strain around the drift opening reaches 6 percent about 8 years after excavation. Based on in situ observations and the

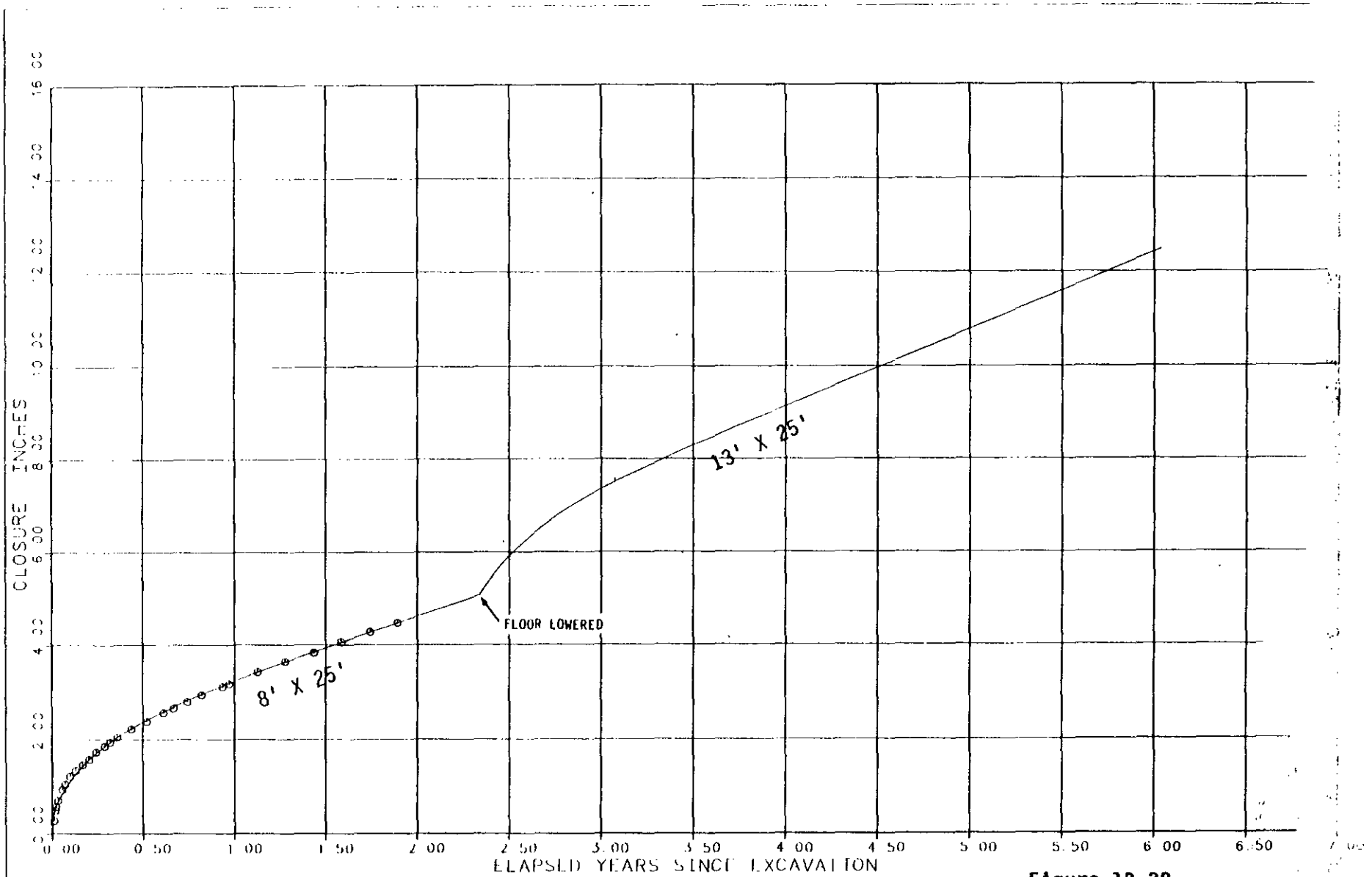

Figure 12-28

STORAGE AREA DRIFTS
ROOF-TO-FLOOR CLOSURE PREDICTION

results of modeling the test rooms, this effective strain of 6 percent may not result in instability of the drifts. However, in 15 years the effective strain at the excavation surface will exceed 10 percent locally and the roof-to-floor closure will be nearly 30 inches. According to the failure criterion, based on laboratory tests on samples of halite (Chapter 6), the halite is supposed to fail at about 16 percent effective strain. Therefore, minor surface deterioration can be expected and some trimming will be required to permit operation of the waste storage equipment. Because the effective strain decreases rapidly within the salt, trimming on the order of only a few feet may be needed after 20 years.

The storage drifts, as with the storage rooms, must accommodate greater than predicted closure. The reference design provides for waste storage in the storage area drifts only after all of the main storage rooms are filled. Since this would occur toward the end of the operating phase, waste in these drifts would not be subject to retrieval under the provisions governing the 5-year demonstration period. Waste stored in the drifts would be on a permanent basis.

Increased closure does impact waste emplacement and emplacement machinery. In the reference design, the greatest age a drift would reach before waste was emplaced would be about 15 years. At this age, based on the calculated closure for a 13 x 25-foot drift, the predicted roof-to-floor closure would be about 25 inches and the predicted wall-to-wall closure would be about 20 inches. The storage drifts would have to be trimmed to permit proper storage and equipment clearance. Similarly, the storage drifts and crosscuts less than 25 feet wide would also require trimming.

12.3.3.3 Intersections

The modeling of intersections is an expensive, three-dimensional analysis. However, to estimate closures at a storage room intersection, a simplified method can be utilized in place of a

Two-dimensional analysis [illegible] and develops the mathematical relationship [illegible] floor closure at the intersections.

When normalized time is sufficiently large, analytical results have consistently shown that room closure in the normalized time domain can be estimated by the following equation:

$$u = u^*_o + \dot{u}^*_f \, t^* \qquad \text{when: } t^* > 1x10^{-11} \text{ ksf}^{-4.9} \qquad (12\text{-}3)$$

where: $t^* = C[t + \frac{A}{z}(1 - e^{-zt})]$ is the normalized time;

u^*_o is a constant; and

$$\dot{u}^*_f = \lim_{\Delta t \to 0} \frac{\Delta u}{\Delta t^*}$$

Closure for the storage room intersections, in normalized time, was calculated using the creep parameters discussed in Chapter 11 and in situ data collected near the intersections of the N1420 drifts with Rooms L1 and L2. As expected, the closure history follows equation 12-3 when the normalized time is greater than $8.0x10^{-12}$ ksf$^{-4.9}$. The average values of u^*_o and $\dot{u}^*_f$ for Rooms L1 and L2 were calculated to be 0.0450 feet and $1.967x10^{12}$ ksf$^{-4.9}$, respectively.

After determining the values of u^*_o and $\dot{u}^*_f$, equation 12-3 can be utilized for computing the closure at a storage room intersection. Figure 12-29 shows the roof-to-floor closure prediction at a storage room intersection.

12.4 STORAGE AREA PLUGS

The design criteria require that the storage area reference design contain provisions for the isolation of the waste storage panels from each other. The reference design contains recommended locations for plugs which would provide this isolation. It does not, however,

provide a specific design for the plugs. The design of the plugs is currently under investigation by SNL (ref. 12-8).

The recommended locations for the plugs are shown on Figure 12-30. The plugs will be constructed in the entry drifts to each panel. The four main access drifts to the storage area will also contain plugs. The section of the entry drifts leading from the access drifts to the first storage room is 200 feet long. The reference design contains provisions for the construction of approximately 100-foot long plugs centered in this 200-foot section of each entry drift.

Originally, the reference design contained entry drift cross section dimensions of 13 feet high and 33 feet wide. These dimensions are the same as those for the storage room reference design and were chosen based on waste container stacking considerations. This design was modified as the result of a meeting between the DOE and all project participants (ref. 3-2). The reference design modification was based on the necessity to minimize the cross section area of the plugs while maintaining sufficient room for the excavation and waste storage equipment.

The reference design modification for the entry drifts is shown on Figure 12-31. The 100-foot long section containing the plug has been reduced in cross section to 13 feet high and 14 feet wide for the exhaust drift and 20 feet wide for the intake drift. However, the operating contractor may further modify these dimensions to accommodate equipment. The four main access drifts will retain their original cross section dimensions in the areas of the planned plugs.

The plug shown on Figure 12-31 would consist of multiple components as described in reference 12-8. These components include a central core of bentonite or bentonite-based mix, salt-brick bulkheads, and cement-based bulkheads. Prior to constructing the multiple-component plug in an entry drift, the operating contractor must investigate the disturbed zone surrounding the drift. In particular, the occurrence of any fractures within and above MB-139, beneath the floor, and any

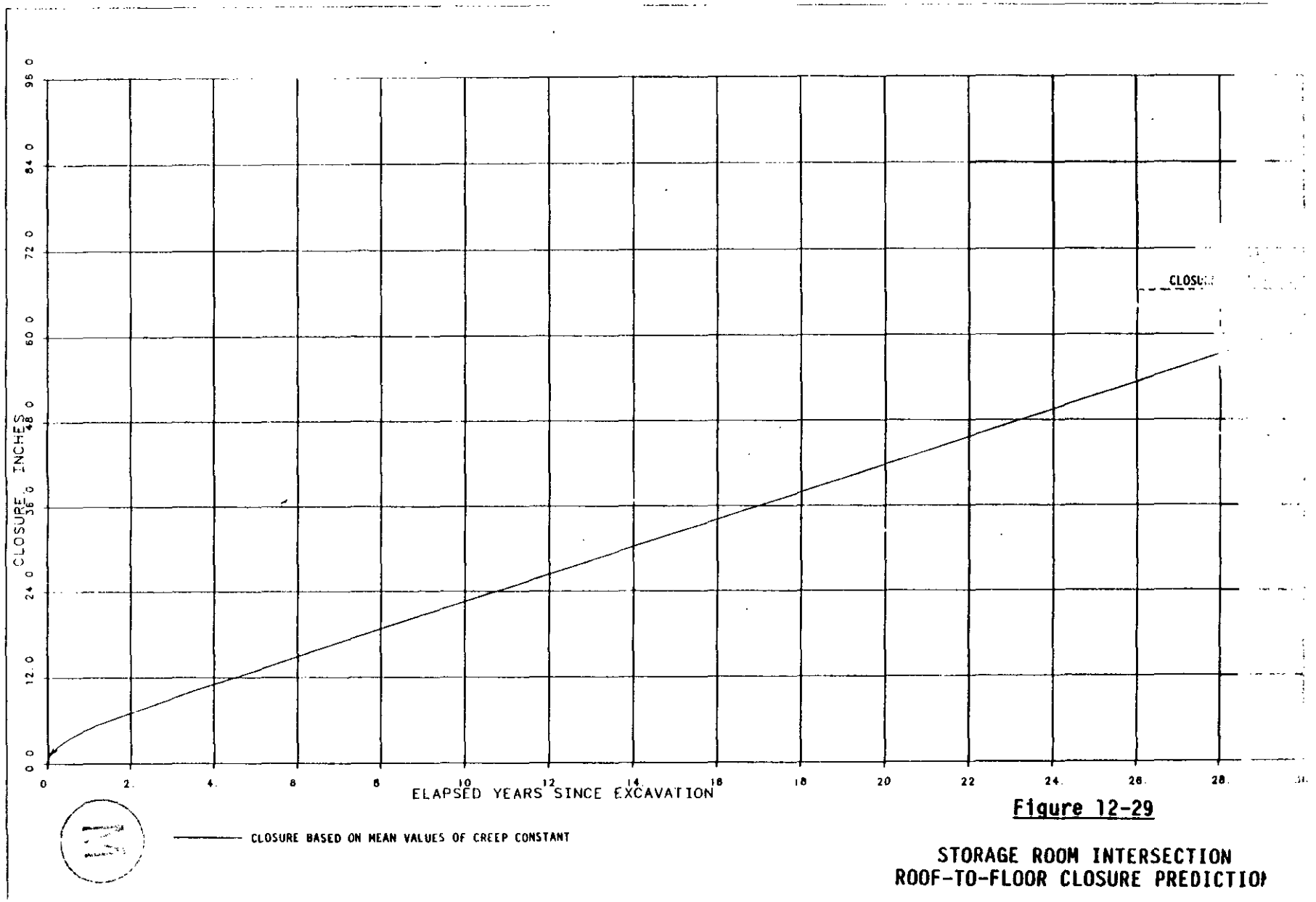

Figure 12-29

STORAGE ROOM INTERSECTION
ROOF-TO-FLOOR CLOSURE PREDICTION

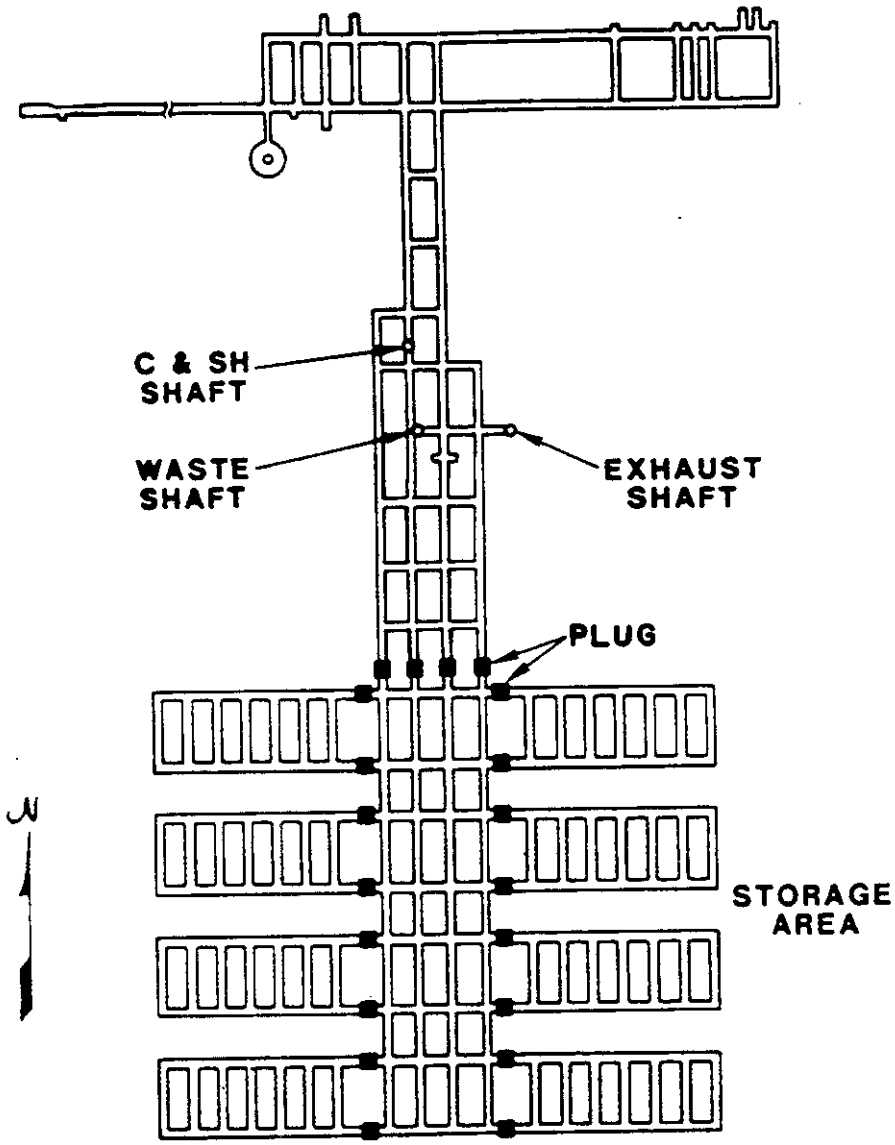

Figure 12-30

STORAGE AREA
PLUG LOCATIONS

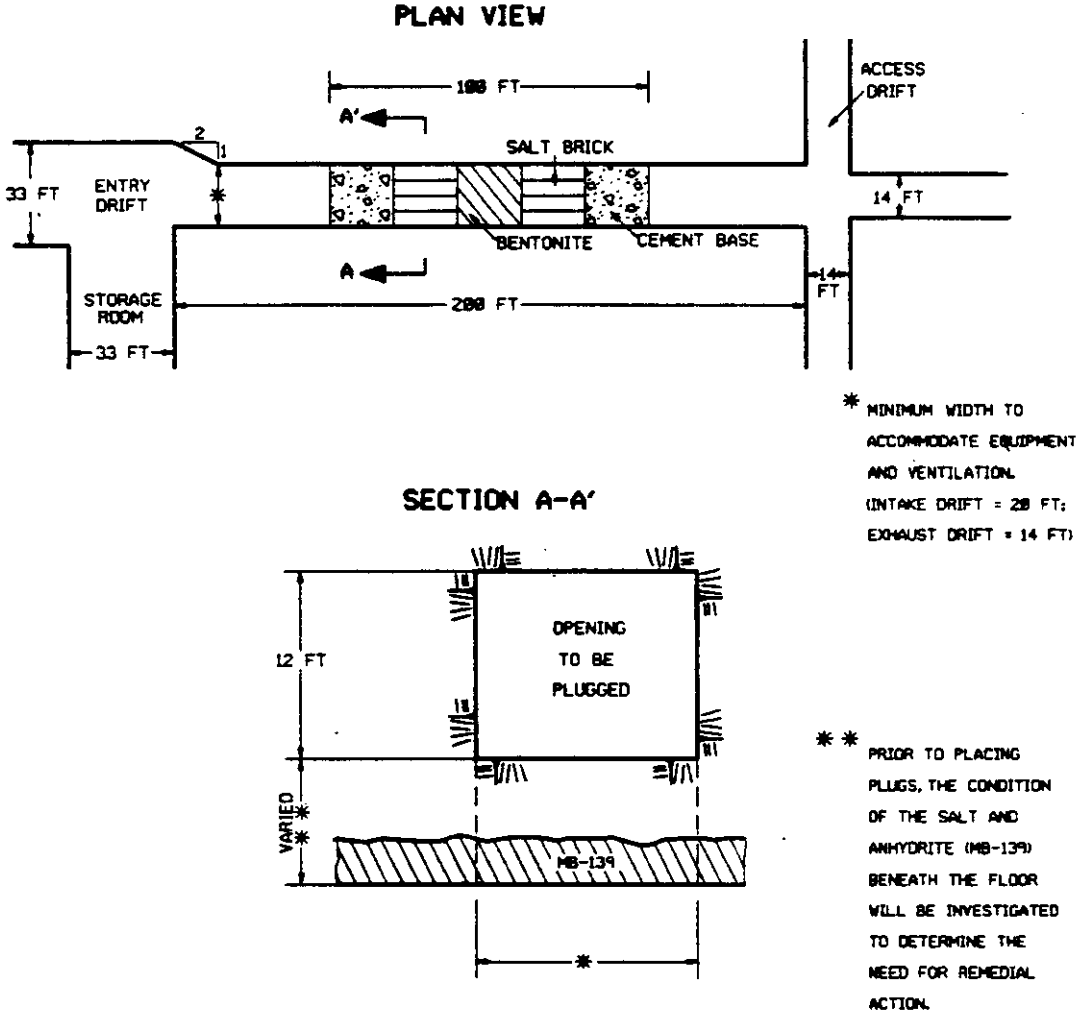

Figure 12-31

STORAGE AREA
PROPOSED PANEL PLUG REFERENCE DESIGN

separations at clay seams above the roof will need to be evaluated. If zones of unacceptable permeability are detected in the floor, the plug area should be lowered to remove the fractured zone and MB-139. Similarly, should any separations be found at clay seams above the entry drift, the roof should be excavated up through the highest seam exhibiting separation.

If the disturbed zone effects are not substantial, low-pressure grouting may be considered as an alternative remedial action. This would permit retention of the minimum cross section for the plug area. In addition, pressure grouting could be used in conjunction with excavation to treat deeper fractures, if present.

12.5 STORAGE ROOM BACKFILL

In accordance with the design criteria, the storage room reference design includes backfilling the rooms with crushed salt after waste emplacement. The storage area drift and room dimensional requirements are shown on Figures 12-2 and 12-3. The thickness of the salt backfill covering the waste packages shown on these figures is 1 to 2 feet. This is to be the thickness of the salt after placement and does not take into account backfill consolidation during room closure.

The only purpose for backfilling presented in the criteria is to provide fire protection in the storage rooms based on an accident scenario in which spontaneous ignition of the contents of a CH TRU waste container results in fire propagation to adjacent containers. Recent studies concerning the potential for spontaneous ignition in CH TRU waste containers have indicated that this is not a credible scenario. Although backfill is a design criteria requirement and therefore must be incorporated into the reference design, the results of these studies indicate that backfill will not be necessary for fire protection.

The following subsections present conclusions pertaining to validation of the WIPP storage area reference design and recommendations for design modifications to achieve validation of the reference design. These are based on a comparison of the design criteria, design bases and reference design configurations with the results of the analysis and evaluation of data collected during the design validation process.

12.6.1 Conclusions

The most significant finding of the design validation program is the difference between closure predicted from laboratory test data and the closure actually occurring in the underground facility. The storage area reference design configurations were designed before long-term in situ data were available. Closure rates were estimated using creep constants derived from the laboratory analyses of salt cores from borehole ERDA-9. These estimates resulted in the establishment of a closure limit of 12 inches in the first 5 years following excavation. Evaluation of the in situ data demonstrates that this closure limit is insufficient. The predicted closure based on laboratory analyses underestimates the actual closure at 3 years by about a factor of three (Figure 11-35). Establishing the causes for this underprediction of closure requires additional study and research and is beyond the scope of this report.

Vertical and horizontal closure demonstrated by the in situ data will not allow the reference design to meet the design criteria requirements. The waste containers will most likely be crushed and breached. Furthermore, because of the in situ closure the waste container stacking configurations and transport vehicle would not be compatible with the reference design room and drift configurations. In order for the reference design to comply with the design criteria, the storage area design configurations or the design criteria will have to be modified. Five alternative modifications are presented in the next subsection.

The analytical results for the storage area show the redistribution of stresses around the openings due to the effects of creep. Based on the computed vertical, horizontal and effective stresses, the magnitude of stresses immediately adjacent to the openings decreases and the stress arch around the openings migrates away with time. The maximum stress occurs immediately after excavation and is followed by relaxation due to creep behavior. Therefore, the stresses will not cause a future stability problem in the storage area except in MB-139, where a gradual buildup of stress may cause local failure of the anhydrite. This failure is expected to be in the form of floor slabbing and should not affect the structural performance of the openings nor hinder the waste storage operations. Investigations of the test room floors indicate that major fracturing has occurred only in the south half of Test Room 3 (Room T). All other floor fracturing has been minor.

The analysis shows the locations of effective creep strain concentrations at different times around the openings. Based on the predicted values of effective creep strain and the strain limit discussed in Chapter 6, effective creep strain may locally exceed the critical strain which is based on laboratory test data. However, this is not expected to disturb the overall structural stability within the limits required for safety during the 5-year demonstration period and permanent storage. Minor spalls and failures on the wall surfaces, similar to the ones discussed in Chapter 11, are expected to occur and can be easily identified and monitored. Scaling of these minor failures, when necessary, is considered a normal maintenance operation.

The facility stratigraphy is continuous and uniform. No anomalous conditions have been encountered that would jeopardize facility operations or waste storage integrity. The fracturing that is occurring beneath the test room floors may develop to some degree beneath the storage rooms. These fractures are not considered to be deleterious to storage room performance. There have been no occurrences of gas or brine in quantities that would adversely affect waste storage operations.

[illegible] plugs as [illegible]. The reference design [illegible] drifts contains a reduced cross section in the plug area. The minimum dimensions for the plug area will be dictated by operating requirements. The dimensions may also require alteration if disturbed zone effects are present that necessitate additional excavation.

An independent study has concluded that spontaneous combustion in the waste containers is not a credible event. In this case, crushed salt backfill will not be required for fire protection. Because it has been determined that the storage rooms will close at a rate faster than originally anticipated, deletion of the backfill requirement will provide additional allowance for vertical closure. This has favorable implications in terms of recommended modifications discussed in the next subsection.

12.6.2 Recommendations

The reference design will be validated when any of the following alternative modifications or combinations thereof are incorporated:

(1) Maintain the reference design room dimensions (13 to 14 feet high and 33 to 34 feet wide), retain the salt backfill but reduce the volume of waste to be stored and modify the waste stacking configuration in each room and entry drift (Figure 12-32). These changes would be required only during the 5-year demonstration period. Revise the criteria to require that retrieval operations be accomplished within 7 years of excavating each room. This will assure that the waste containers will not be crushed or breached. However, it will require a significant number of additional rooms during and after the demonstration period.

(2) Maintain the reference design room dimensions and the waste storage volume. Revise the criteria to delete the requirement for salt backfill and to require that if the

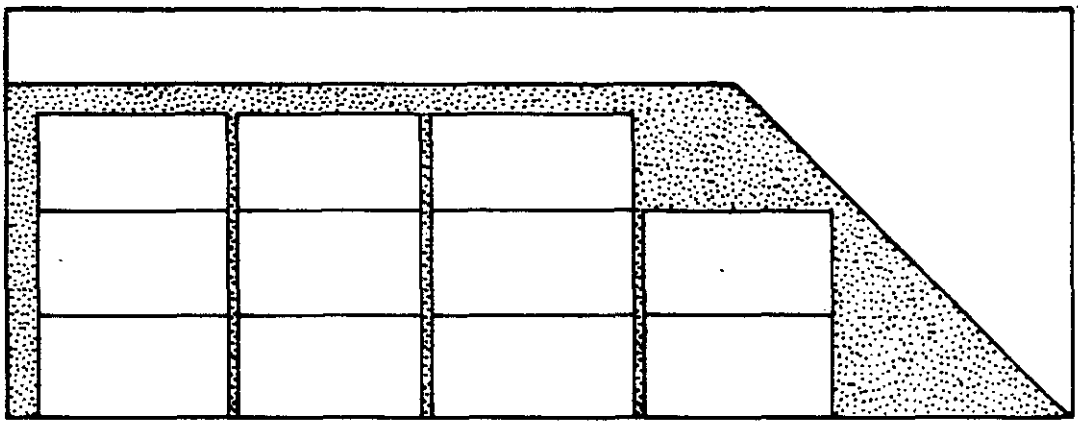

Figure 12-32

STORAGE AREA
MODIFIED WASTE STACKING CONFIGURATION

any room in which waste [illegible] years. This will preclude the possibility of crushing and/or breaching any waste containers and will make retrieval easier and more rapid. No additional rooms will be required.

(3) Maintain the reference design room dimensions, the waste storage volume, and the salt backfill. Revise the storage operations during the 5-year demonstration period so that the waste stored first can be retrieved first. Excavate the rooms to 14 x 34 feet initially and then trim them to 14 x 34 feet a year later. Rooms having waste retrieved will not be older than 6 years and the wall-to-wall closure will be approximately 12 inches. This would minimize the crushing and breaching of the waste containers. The criteria are to be revised as stated under (5) of these recommendations. However, due to the first-in/first-out recommendation, more rooms will be required during the 5-year demonstration period to accommodate the expected volume of waste. Trimming to the final dimensions will also increase operating costs. The total number of rooms required will be the same as provided by the reference design.

(4) For the 5-year demonstration period, reduce the storage room width from 33 feet to 28 feet, maintain the 13 to 14-foot height, and reduce the pillar width to 84 feet. Maintain the first room for RH emplacement at 33 feet to 34 feet wide and 13 feet to 14 feet high as provided in the reference design. Reduce the volume of waste to be stored in each room and maintain the salt backfill. Excavate the rooms to 14 x 28 feet then, after approximately 1 year, trim them to 14 x 28 feet again. Provide for first-in/first-out emplacement and retrieval during the 5-year demonstration period. This will reduce the rate of creep to approximately

the rate for the 13 x 25-foot drifts. The potential for crushing and breaching of the waste containers will be minimized and the stability should be better than that for a 33-foot wide room. The total volume of excavation will be approximately the same. If this alternative is selected, additional engineering evaluation will be required.

(5) Maintain all of the features of the reference design. That is, maintain the storage room configuration of 13 feet high and 33 feet wide, maintain the salt backfill, maintain the planned volume of waste to be stored in each room and drift, and maintain the same optimized excavation plan for the 5-year demonstration period and permanent storage. Revise the design criteria to allow crushing and breaching of the CH waste containers during the 5-year demonstration period as well as during permanent storage. Also, revise the criteria requiring a demonstration of waste package handling to include a demonstration of the retrieval of crushed and breached containers prior to receiving waste. This alternative will not only demonstrate the safe retrieval of waste if required during the 5-year demonstration period but also at any time during permanent storage.

In addition to these recommended alternative modifications, the following modifications are recommended:

(6) The drifts used for storage will have to be maintained and trimmed to provide the required equipment and storage clearances. The closure rates are not critical for storage because these drifts will be used only for permanent storage near the end of the permanent storage period.

the plugs in the

(8) Install instrumentation in the storage rooms to obtain in situ data to monitor storage room behavior.

GLOSSARY

G.1 TERMINOLOGY

Back - The roof of underground horizontal openings.

Bunton - Horizontal, tubular steel section installed in the C & SH shaft to support the wood guide rails which center the shaft conveyance as they travel in the shaft.

CH TRU waste - Contact-handled transuranic waste that is packaged so that the dose rate at the surface of the waste package is not greater than 200 millirem/h.

Closure - The gradual decrease in distance between two opposing points in an underground opening as a result of rock or salt movement.

Convergence - See "closure".

Datalogger - Computer system that collects and records the output of geomechanical instrumentation.

Design bases - Detailed requirements established from the design criteria to provide additional direction in development of the engineering design of the WIPP underground facilities.

Design configuration - Engineered design dimensions of underground facility openings based on requirements of design criteria and design bases.

Design criteria - General requirements established to govern the engineering design of the WIPP underground facilities.

Design validation - The process of confirming the WIPP underground opening reference design by determining the compatibility of the design criteria, design bases and reference design configurations using site specific information. Validation is achieved through an assessment of the condition and behavior of the underground openings, and on predictions of their future behavior, based on in situ observations and measurements.

Drummy - Term used to describe rock that sounds hollow or loose when tapped with a solid object; used especially in relation to a mine roof.

Facility level - The underground horizontal portion of the WIPP facility developed for waste storage purposes.

Floor/roof beam - The rock thickness between the floor or roof of an excavated opening and the first underlying or overlying clay seam.

Galloway - A multi-decked steel platform suspended in a shaft and raised or lowered by means of a cable hoist. It is used to transport material and personnel in the shaft, particularly during shaft outfitting.

Guide - Vertical shaft member of steel or wood which is used to center the conveyance equipment as it travels in the shaft.

Long-term monitoring - The extended acquisition and evaluation of data to determine the geomechanical response of the rock/salt to excavation. These data will supplement the R & D program.

Muck - The broken rock and other material that is removed during shaft or horizontal opening excavation.

Penecontemporaneous - Term used to indicate a geologic process that occurs concurrent with or after sediment deposition but before lithification.

Potash - Any potassium-rich rock mined and refined to produce products used in agriculture or industry.

Preliminary design validation - The process of achieving a preliminary evaluation of the underground design criteria, design bases and design configurations early in construction, primarily by visual observations of the underground openings and geomechanical instrumentation measurements.

R & D Program - The WIPP mission designed to provide a technical understanding of systems design, safety and environmental assessments for the disposal of radioactive waste from U.S. defense programs. The program includes technology development through laboratory testing of theoretical analysis and in situ testing to evaluate the techniques used to monitor the responses of materials and facility systems.

RH TRU waste - Remote-handled transuranic waste that is packaged so that the dose rate at the surface of the package is greater than 200 millirem/h but less than 100 rem/h.

Rib - The vertical wall of underground horizontal openings.

Scaling - The removal of loose rock from underground opening surfaces.

Shaft outfitting - The process of installing shaft furnishings (utilities, buntons, guides, conveyance equipment, etc.), as well as stabilizing the wall by means of rock bolts, wire mesh or lining.

Short-term monitoring - The acquisition and evaluation of data to determine the initial geomechanical response of the rock/salt to excavation.

Site and Preliminary Design Validation (SPDV) - A WIPP program consisting of two integrated subprograms, Site Validation and Preliminary Design Validation, that are defined in their individual listings.

Site characterization - The process of obtaining geotechnical data and conducting experiments to determine the suitability of the WIPP site for a research and development facility to demonstrate the safe disposal of defense-related nuclear waste.

Site validation - The process of achieving the highest practicable level of confidence in the site's suitability and overall qualification through subsurface investigations.

Slabbing - The weakening of rock fragments or segments along fractures parallel to the excavation surface.

Spud - To begin drilling a well, hole or shaft.

Spalling - The breaking loose of chips, thin slabs, or fragments from the outer surface of a rock mass.

Telltale pipe - A pipe used to monitor the effectiveness of the chemical water seals in the shaft keys. The pipe provides a pathway for water to flow through the concrete beneath the seals from the salt/concrete interface to the inside face of the concrete key.

Transuranic (TRU) waste - Radioactive waste containing transuranic elements created by the absorption of neutrons into uranium atoms.

Underground development level - See "facility level".

Underground facility horizon - The stratigraphic interval within the Salado formation, from a depth of approximately 2,100 to 2,170 feet (elev. 1240 to 1310 feet), which was selected for testing and storage of low-level nuclear waste.

G.2 ACRONYMS

ACI	American Concrete Institute
AEC	Atomic Energy Commission
BNI	Bechtel National, Incorporated
BTP	Brine Testing Program
C & SH	Construction and salt handling
CH TRU	Contact-handled transuranic
DOE	U.S. Department of Energy
FEIS	Final Environmental Impact Statement
GFDR	Geotechnical Field Data Report
GSA	Geological Society of America
GTP	Gas Testing Program
LTC	Local termination cabinet
MIIT	Material Interface-Interactions Test
MOC	Management and Operating Contractor
MSHA	Mine Safety and Health Administration
NAS	National Academy of Sciences
R & D	Research and development
RH TRU	Remotely-handled transuranic
RMC-IIA	Revised Mission Concept IIA
SAR	Safety Analysis Report
SME	Society of Mining Engineering
SNL	Sandia National Laboratories
SPDV	Site and Preliminary Design Validation
TRU	Transuranic
TSC	Technical Support Contractor
USGS	United States Geological Survey
WIPP	Waste Isolation Pilot Plant

REFERENCES

1-1 Waste Isolation Pilot Plant, Design Validation Plan, January 27, 1983, Document No. 76B510AB-000, Rev. 6, U.S. Department of Energy, WIPP Project Office, Albuquerque, New Mexico.

1-2 Letter, D.T. Schueler (DOE) to G.S. Goldstein (State of New Mexico), August 31, 1981, "Cost and Merit Evaluation for Stipulated Agreement Activities".

1-3 Waste Isolation Pilot Plant Preliminary Design Validation Report, March 30, 1983, prepared for the U.S. Department of Energy by Bechtel National, Inc., San Francisco, California.

1-4 Final Environmental Impact Statement: Waste Isolation Pilot Plant, 1980, DOE/EIS-0026, U.S. Department of Energy, Washington, D.C.

1-5 Waste Isolation Pilot Plant Safety Analysis Report, 1980, U.S. Department of Energy, WIPP Project Office, Albuquerque, New Mexico.

1-6 Matalucci, R.V., C.L. Christensen, T.O. Hunter, M.A. Molecke, and D.E. Munson, 1982, WIPP Research and Development Program: In Situ Testing Plan, SAND81-2628, Sandia National Laboratories, Albuquerque, New Mexico.

1-7 Waste Isolation Pilot Plant, Design Validation Strategy, 1986, U.S Department of Energy, WIPP Project Office, Carlsbad, New Mexico.

1-8 Site Validation Program, 1982, WIPP-DOE-116, Rev. 1, prepared for the U.S. Department of Energy by the Technical Support Contractor, Albuquerque, New Mexico.

2-1 Seward, Paul D., compiler, 1982, Abridged Borehole Histories for the Waste Isolation Pilot Plant (WIPP) Studies, SAND82-0080, Sandia National Laboratories, Albuquerque, New Mexico.

2-2 U.S. Department of Energy, 1982, Basic Data Report, Borehole WIPP-12 Deepening, TME 3148, Albuquerque, New Mexico.

2-3 _____, 1982, Basic Data Report for Borehole DOE-1, TME 3159, Albuquerque, New Mexico.

2-4 Powers, D.W., S.J. Lambert, S.E. Shaffer, L.R. Hill, and W.D. Weart, editors, 1978, Geological Characterization Report, Waste Isolation Pilot Plant (WIPP) Site, Southeastern New Mexico, SAND78-1596, Sandia National Laboratories, Albuquerque, New Mexico.

2-5 Results of Site Validation Experiments, Waste Isolation Pilot Plant (WIPP) Project, Southeastern New Mexico, 1983, Vols 1 and 2, TME 3177, prepared for the U.S. Department of Energy by the Technical Support Contractor, Albuquerque, New Mexico.

2-6 Weart, W.D., March 1983, Summary Evaluation of the Waste Isolation Pilot Plant (WIPP) Site Suitability, SAND83-0450, Sandia National Laboratories, Albuquerque, New Mexico.

2-7 Design Criteria, Waste Isolation Pilot Plant (WIPP), Site and Preliminary Design Validation (SPDV), October 1981, WIPP-DOE-72, Rev. 1, prepared for the U.S. Department of Energy by the Technical Support Contractor, Albuquerque, New Mexico.

2-8 Design Criteria, Waste Isolation Pilot Plant (WIPP), Revised Mission Concept-IIA (RMC-IIA), February 1984, WIPP-DOE-71, Rev. 4, prepared for the U.S. Department of Energy by the Technical Support Contractor, Albuquerque, New Mexico.

2-9 Waste Isolation Pilot Plant, Design Basis, SPDV Underground Excavations, November 21, 1980, D-51-W-02, Rev. 3, prepared for the U.S. Department of Energy by Bechtel National, Inc.

2-10 Waste Isolation Pilot Plant, Design Basis, Exploratory Shaft, December 16, 1980, D-31-R-03, Rev. 2, prepared for the U.S. Department of Energy by Bechtel National, Inc.

2-11 Waste Isolation Pilot Plant, Design Basis, Exploratory Shaft Furnishings and Station, December 12, 1980, D-37-S-02, Rev. 2, prepared for the U.S. Department of Energy by Bechtel National, Inc.

2-12 Waste Isolation Pilot Plant, Design Basis, Exploratory Shaft Geomechanical Instrumentation, December 3, 1980, D-32-X-01, Rev. 2, prepared for the U.S. Department of Energy by Bechtel National, Inc.

2-13 Waste Isolation Pilot Plant, Design Basis, Underground Experimental Areas, October 20, 1982, D-52-K-04, Rev. 2, prepared for the U.S. Department of Energy by Bechtel National, Inc.

2-14 Waste Isolation Pilot Plant, Design Basis, WIPP-RMC IIA (General), May 14, 1983, D-76-K-01, Rev. 7, prepared for the U.S. Department of Energy by Bechtel National, Inc.

2-15 Waste Isolation Pilot Plant, Design Basis, Waste Shaft, September 21, 1983, D-31-R-01, Rev. 8, prepared for the U.S. Department of Energy by Bechtel National, Inc.

2-16 Waste Isolation Pilot Plant, Design Basis, Exhaust Shaft, September 21, 1983, D-35-R-01, Rev. 1, prepared for the U.S. Department of Energy by Bechtel National, Inc.

2-17 Waste Isolation Pilot Plant, Design Bases, Geomechanical Instrumentation, September 1983, D-76-X-01, Rev. 6, prepared for the U.S. Department of Energy by Bechtel National, Inc.

2-18 Waste Isolation Pilot Plant, Design Basis, Underground Excavations, October 14, 1983, D-51-W-01, Rev. 6, prepared for the U.S. Department of Energy by Bechtel National, Inc.

2-19 Waste Isolation Pilot Plant, Design Basis, Design Classification, November 30, 1983, D-76-K-03, Rev. 9, prepared for the U.S. Department of Energy by Bechtel National, Inc.

2-20 Waste Isolation Pilot Plant, Design Basis, Underground Shops and Facilities, January 17, 1984, D-54-E-01, Rev. 6, prepared for the U.S. Department of Energy by Bechtel National, Inc.

2-21 WIPP Conceptual Design Report, 1977, SAND77-0274, prepared for the U.S. Department of Energy by Sandia National Laboratories, Albuquerque, New Mexico.

2-22 WIPP Title I Design Report, and supplements, 1979 and 1980, prepared for the U.S. Department of Energy by Bechtel National, Inc., San Francisco, California.

2-23 Stability Analysis of Underground Openings, RMC-II, 1981, Study Report No. 51-R-510-04, Rev. 0, prepared for the U.S. Department of Energy by Bechtel National, Inc., San Francisco, California.

2-24 Li, W.T., and C.L. Wu, May 1983, Analysis of Creep for a Nuclear Waste Storage in Salt Formation, Nuclear Technology.

2-25 Society of Mining Engineers of The American Institute of Mining, Metallurgical, and Petroleum Engineers, Inc., 1973, SME Mining Engineering Handbook, 2 Volumes, Port City Press, Baltimore, Maryland.

REFERENCES (continued)

2-26 Morgan, H.S., R.D. Krieg, and R.V. Matalucci, November 1981, Comparative Analysis of Nine Structural Codes Used in the Second WIPP Benchmark Problem, SAND81-1389, Sandia National Laboratories, Albuquerque, New Mexico.

2-27 Miller, J.D., C.M. Stone, and L.J. Branstetter, August 1982, Reference Calculations for Underground Rooms of the WIPP, SAND82-1176, Sandia National Laboratories, Albuquerque, New Mexico.

2-28 Memo from W.D. Weart (Sandia) to Distribution, July 31, 1981, "Reference Creep Law and Material Properties for WIPP".

2-29 Empirical Design Basis of Underground Salt Openings in the WIPP Project, November 12, 1979, Document No. DR-51-R-1, prepared for Bechtel National, Inc., by Shosei Serata.

2-30 U.S. Bureau of Mines, 1973, Subsidence Due to Underground Mining, Information Circular 8571.

3-1 Geotechnical Activities in the Exploratory Shaft - Selection of the Facility Interval, March 1983, TME 3178, prepared for the U.S. Department of Energy by the Technical Support Contractor, Albuquerque, New Mexico.

3-2 U.S. Department of Energy, June 30, 1986, "Project Position Regarding Subhorizontal Floor Fracturing", DOE Memo-WIPP:RAC 86:2003.

3-3 Grouting Report, Waste Shaft Lining, January 1985, Bechtel Document 31D510AA, prepared for the U.S. Department of Energy.

4-1 Geotechnical Field Data Report No. 2, November 9, 1982, "Exploratory Shaft, Exploratory Shaft Key, and Exploratory Shaft Station Instrumentation", compiled for the U.S. Department of Energy by TSC-D'Appolonia, Albuquerque, New Mexico.

4-2 Geotechnical Field Data Report No. 3, December 15, 1982, "Underground Excavation Field Instrumentation Data (shaft data not updated)", compiled for the U.S. Department of Energy by TSC-D'Appolonia, Albuquerque, New Mexico.

4-3 Geotechnical Field Data Report No. 4, January 8, 1983, "Geologic Mapping and Water Inflow Testing in the SPDV Ventilation Shaft", compiled for the U.S. Department of Energy by TSC-D'Appolonia, Albuquerque, New Mexico.

4-4 Geotechnical Field Data Report No. 5, January 18, 1983, "Geologic Mapping of Access Drifts 'Double Box' Area", compiled for the U.S. Department of Energy by TSC-D'Appolonia, Albuquerque, New Mexico.

4-5 Geotechnical Field Data Report No. 6, January 17, 1983, "Underground Excavation Field Instrumentation Data", compiled for the U.S. Department of Energy by TSC-D'Appolonia, Albuquerque, New Mexico.

4-6 Geotechnical Field Data Report No. 7, January 17, 1983, "Geologic Mapping of Exploratory Drift", compiled for the U.S. Department of Energy by TSC-D'Appolonia, Albuquerque, New Mexico.

4-7 Geotechnical Field Data Report No. 8, January 17, 1983, "Underground Excavation Field Instrumentation Data", compiled for the U.S. Department of Energy by TSC-D'Appolonia, Albuquerque, New Mexico.

4-8 Geotechnical Field Data Report No. 9, February 18, 1983, "Logging of Vertical Coreholes 'Double Box' Area and Exploratory Drift", compiled for the U.S. Department of Energy by TSC-D'Appolonia, Albuquerque, New Mexico.

4-9 Geotechnical Field Data Report No. 10, March 18, 1983, "Underground Excavation Field Instrumentation Data", compiled for the U.S. Department of Energy by TSC-D'Appolonia, Albuquerque, New Mexico.

4-10 Quarterly Geotechnical Field Data Report, July 1983, WIPP-DOE-163, compiled for the U.S. Department of Energy by TSC-D'Appolonia, Albuquerque, New Mexico.

4-11 Quarterly Geotechnical Field Data Report, October 1983, WIPP-DOE-177, compiled for the U.S. Department of Energy by TSC-D'Appolonia, Albuquerque, New Mexico.

4-12 Quarterly Geotechnical Field Data Report, February 1984, WIPP-DOE-196, compiled for the U.S. Department of Energy by Bechtel National, Inc., San Francisco, California.

4-13 Quarterly Geotechnical Field Data Report, May 1984, WIPP-DOE-199, compiled for the U.S. Department of Energy by Bechtel National, Inc., San Francisco, California.

4-14 Quarterly Geotechnical Field Data Report, August 1984, WIPP-DOE-200, compiled for the U.S. Department of Energy by Bechtel National, Inc., San Francisco, California.

4-15 Quarterly Geotechnical Field Data Report, November 1984, WIPP-DOE-202, compiled for the U.S. Department of Energy by Bechtel National, Inc., San Francisco, California.

4-16 Quarterly Geotechnical Field Data Report, March 1985, WIPP-DOE-210, compiled for the U.S. Department of Energy by Bechtel National, Inc., San Francisco, California.

4-17 Quarterly Geotechnical Field Data Report, June 1985, WIPP-DOE-213, compiled for the U.S. Department of Energy by Bechtel National, Inc., San Francisco, California.

4-18 Quarterly Geotechnical Field Data Report, September 1985, WIPP-DOE-218, compiled for the U.S. Department of Energy by Bechtel National, Inc., San Francisco, California.

4-19 Quarterly Geotechnical Field Data Report, December 1985, WIPP-DOE-221, compiled for the U.S. Department of Energy by Bechtel National, Inc., San Francisco, California.

5-1 Hansen, Francis D., November 1979, Triaxial Quasi-Static Compression and Creep Behavior of Bedded Salt from Southeastern New Mexico, SAND79-7045, Sandia National Laboratories, Albuquerque, New Mexico.

5-2 Nawcrock, W.R., and D.W. Hannum, May 1979 (revised), Intern Summary of Sandia Creep Parameters on Rock Salt from the WIPP Study Area, Southeastern New Mexico, SAND79-0115, Sandia National Laboratories, Albuquerque, New Mexico.

5-3 Krieg, R.D., January 1984, Reference Stratigraphy and Rock Properties for the Waste Isolation Pilot Plant (WIPP) Project, SAND83-1908, Sandia National Laboratories, Albuquerque, New Mexico.

5-4 Herrmann, W., W.R. Wawersik, and H.S. Lauson, November 1980, A Model for Transient Creep of Southeastern New Mexico Salt, SAND80-2172, Sandia National Laboratories, Albuquerque, New Mexico.

5-5 Jaegar, J.C., and N.G.W. Cook, 1976, Fundamentals of Rock Mechanics, Second Edition, Chapman and Hall, London.

5-6 Li, W.T., C.L. Wu, and N. Antonas, November 1982, "Salt Creep Design Consideration for Underground Nuclear Waste Storage", Proceedings of MRS 6th Int. Sym. on Scientific Basis for Nuclear Waste Management.

5-7 Primary Creep of Rock Salt, November 8, 1983, Bechtel Report 76-D-540AD-01.

6-1 McKinney, R.F., and R.S. Newton, January 3, 1983, Site Validation Field Program Plan, Rev. 1.2, prepared for the U.S. Department of Energy by the Technical Support Contractor, Albuquerque, New Mexico.

6-2 Geotechnical Activities in the Waste Handling Shaft, October 1984, WTSD-TME-038, prepared for the U.S. Department of Energy by the Technical Support Contractor, Albuquerque, New Mexico.

6-3 Jones, C.L., 1981, Geological Data for Borehole ERDA-9, Eddy County, New Mexico, U.S. Geological Survey Open-file Report 81-469.

6-4 Holt, R., and D. Powers, 1986, Geotechnical Activities in the Exhaust Shaft, DOE-WIPP-86-008, prepared for the U.S. Department of Energy by the Technology Development Department of the Management and Operating Contractor, Carlsbad, New Mexico.

6-5 Stein, C.L., September 1985, Mineralogy in the Waste Isolation Pilot Plant (WIPP) Facility Stratigraphic Horizon, SAND85-034, Sandia National Laboratories, Albuquerque, New Mexico.

6-6 Borns, D.J., September 1985, Marker Bed 139: A Study of Drillcore from a Systematic Array, SAND85-0023, Sandia National Laboratories, Albuquerque, New Mexico.

6-7 Herrmann, W., W. R. Wawersik, and H.S. Lauson, March 1980, Analysis of Steady State Creep of Southeastern New Mexico Bedded Salt, SAND-80-0558, Sandia National Laboratories.

6-8 MARC Analysis Research Corp., 1980, MARC General Purpose Finite Element Program User Information Manual, Rev. J.2-1.

7-1 American Welding Society, 1980, Structural Welding Code - Steel, AWS D1.1.

7-2 ASME Boiler and Pressure Vessel Code, 1980, Sections V, VIII and IX, American Society of Mechanical Engineers.

7-3 Timoshenko, S., and S. Woinowsky-Krieger, 1959, Theory of Plates and Shells, McGraw-Hill, New York.

7-4 Li, W.T., N. Antonas, C.L. Wu, and K. Mark, February 1983, "Salt Structural Interaction of Underground Nuclear Waste Storage", Proceedings of the Waste Management '83 Symposium, Tucson, Arizona.

7-5 American Concrete Institute, 1977, Building Code Requirements for Reinforced Concrete, ACI-318.

7-6 Antonas, N., W. T. Li, K. Mark, and C. L. Wu, May 1983, "Creep Interaction of Salt and a Concrete Ring Structure", Proceedings of ASME EMD Specialty Conference.

7-7 Geology Laboratory Results of Rock Testing, 1979, Document No. 22-4-510-04, Rev. 2, prepared for the U.S. Department of Energy by Bechtel National, Inc., San Francisco, California.

7-8 Designing for Effects of Creep, Shrinkage, Temperature in Concrete Structures, 1971, ACI Publication SP-27, American Concrete Institute, Detroit, Michigan.

7-9 Mercer, J. W., 1983, Geohydrology of the Proposed Waste Isolation Pilot Plant Site, Los Medanos Area, Southeastern New Mexico, USGS Water-Resources Investigations Report 83-4016, Albuquerque, New Mexico.

8-1 American Concrete Institute, 1972, Building Code Requirements for Structural Plain Concrete, ACI-322.

11-1 SAS Institute, Inc., 1985, SAS, Release 5.03, Cary, North Carolina.

11-2 SAS Institute, Inc., 1985, User's Guide: Statistics; Version 5 Edition, Chapter 25, The NLIN Procedure, Cary, North Carolina.

11-3 Branstetter, L.J., R. D. Krieg, and C.M. Stone, October 1982, The Effect of a Random Variation of Rock Salt Creep on Calculations of Storage Room Closure for the WIPP Project, SAND82-0024, Sandia National Laboratories, Albuquerque, New Mexico.

11-4 Miller, J. D., C. M. Stone, and L. J. Branstetter, August 1982, Reference Calculations for Underground Rooms of the WIPP, SAND82-1176, Sandia National Laboratories, Albuquerque, New Mexico.

11-5 Branstetter, L. J., March 1985, Second Reference Calculations for the WIPP, SAND83-2461, Sandia National Laboratories, Albuquerque, New Mexico.

12-1 General Design Criteria Manual for Department of Energy Facilities, June 10, 1981, draft, DOE 6430.

12-2 Physical Protection of DOE Property, September 29, 1977, IMD 6105.

12-3 Standard for Protection Against Radiation, Code of Federal Regulations, 10 CFR 20.

12-4 Requirements for Radiation Protection, Chapter 11, DOE 5480.1A.

12-5 A Guide to Reducing Radiation Exposure to As Low As Reasonably Achievable, DOE/EV/1830-T5.

12-6 Mine Safety and Health Standards - Metal and Non-Metal Underground Mines (MSHA), Code of Federal Regulations, 30 CFR 57.

12-7 New Mexico Mine Safety Code, 1981.

12-8 Stormont, J. C., November 1984, Plugging and Sealing Program for the Waste Isolation Pilot Plant (WIPP), SAND 84-1057, Sandia National Laboratories, Albuquerque, New Mexico.